Characterization of Motor Oils and Other Lubricants by High Performance Liquid Chromatography, Three-Dimensional Excitation Emission Matrices and Two-Dimensional Low Temperature Fluorescence Spectroscopy

by

KELLY A. WALSH

A dissertation submitted to the Graduate Faculty in Criminal Justice in partial fulfillment of the requirements for the degree of Doctor of Philosophy,

The City University of New York

2012

This manuscript has been read and accepted for the Graduate Faculty in Criminal Justice in satisfaction of the dissertation requirement for the degree of Doctor of Philosophy.

Dr. Thomas A. Kubic

Date

Chair of Examination Committee

Dr. Joshua Freilich

Date

Executive Officer

Dr. John A. Reffner

Dr. Nicholas D. K. Petraco

Mr. Nicholas Petraco, Sr.
Supervisory Committee

CITY UNIVERSITY OF NEW YORK

Abstract

Characterization of Motor Oils and Other Lubricants by High Performance Liquid Chromatography, Three-Dimensional Excitation Emission Matrices and Two-Dimensional Low Temperature Fluorescence Spectroscopy

By

Kelly A. Walsh

Advisor: Dr. Thomas A. Kubic

Criminals often use automobiles during the commission of crimes. Criminalists routinely analyze automotive transfer evidence, including paint, rubber and glass in order to establish an association between a suspect car and a person or object that may have come in contact with that car. Currently, there is no routine forensic method to analyze transferred automotive undercarriage residue. This feasibility study will use fluorescence spectroscopy, both room-temperature and low-temperature (77K), and HPLC, to analyze this material and will investigate the use of compiled spectral libraries to assist in determining the evidentiary value of this process for this sample set.

Automobile undercarriage residues are a complex mixture of compounds from many sources including automotive fluids, asphalt residues, exhaust particulates and tire particulates. Each of these sources may contain compounds that fluoresce when

excited with light in the ultraviolet or visible region of the electromagnetic spectrum. Given the many sources of fluorescing compounds and the effect of environmental conditions on these compounds, it is hypothesized that the two-dimensional and three-dimensional fluorescence spectrum of automobile undercarriage residues along with HPLC analysis can be used to differentiate among automobiles.

Five undercarriage locations were swabbed from ten motor vehicles. Extraction via sonication in different solvents separated each residue into fractions. These fractions were analyzed by fluorescence spectroscopy and HPLC with UV detection. The types of fluorescence spectroscopy used were emission scans, synchronous scans, excitation-emission matrices, and low-temperature fluorescence spectroscopy. Previous studies with fluorescence characterization of lubricants relied on visual examination of the spectral data to determine differences or similarities (Purcell 2002). This study will use visual examination, peak number and position, chromatographic data and spectral libraries to show similarities and differences among the samples.

The research contributes to the body of knowledge about analytical methods that may characterize a long-observed transferable material, automotive undercarriage residue, to create associations between automobiles and persons or objects. These associations can be used to help the trier-of-fact decide upon the likelihood that an automobile came into contact with a person or object. Additionally, this research makes contributions to the field of environmental science which seeks to characterize petroleum-derived organic contaminants.

Acknowledgements

I would like to gratefully acknowledge the many people whose support was critical to my work. First and foremost, I owe a debt of gratitude to my mentor, Dr. Thomas A. Kubic, for his support, guidance and for an education that is singular and invaluable. Thank you for opening your life, lab and mind to me these past years. While I may have been of some assistance to you on various projects, it was always I who was the true beneficiary of our collaborations. This work would not have been possible without your continued guidance, advice and support. Many thanks to my additional committee members, Dr. John A. Reffner, Dr. Nicolas D. K. Petraco and Mr. Nicolas Petraco, Sr. Thank you for your sharing your wisdom and continued review and support of this work.

Additional thanks are owed to Drs. Selman Berger and Lawrence Kobilinsky, both chairmen of the Science Department at John Jay College during my time there. I am grateful for the supportive setting that the science department provided me as a student, researcher and instructor. I am additionally grateful for the support I received through the CUNY Graduate Center Criminal Justice PhD program as a graduate adjunct fellow and for the continued support of the CJ forensic science specialization during the chairmanships of Dr. Todd Clear, Dr. Karen Terry and Dr. Joshua Freilich.

Thank you to my parents for their unwavering encouragement. And finally, thank you to my husband, Dan, to whom this work is dedicated.

Table of Contents

List of Figures and Tables

List of Figures and Tables (continued)

List of Figures and Tables (continued)

Introduction

The criminalist's analysis of transfer evidence can be a powerful tool to create associations. Incidents involving automobiles often yield several different types of transfer evidence. Transferred paint is primarily analyzed by light microscopy, infrared microspectrophotometry, pyrolysis gas chromatography-mass spectroscopy and scanning electron microscopy with energy dispersive X-ray spectrometry (Caddy 2001). The density, refractive index and elemental composition of transferred glass can be established. Transferred rubber is identified by attenuated total reflectance microspectrophotometry and pyrolysis gas chromatography. The results of these multi-instrumental analyses are compared to find a likelihood of association between an automobile and a person or object. Historically, this likelihood has been unquantifiable but forensic science researchers and practitioners are beginning to adopt a Bayesian approach to generating likelihood ratios (Taroni *et al*, 2010).

Missing from the list of regularly analyzed transfer evidence is automotive undercarriage residue. This material, mainly consisting of petroleum-derived products, is a complex, dynamic and easily transferable material. This study investigated the usefulness of liquid chromatography to adjust the concentration of fluorescing compounds, fluorescence spectroscopy to characterize automotive undercarriage residue and visual examination coupled with spectral library searching techniques to gauge the discriminatory power of the latter technique.

Contribution to the Field of Forensic Science and Criminal Justice

The contribution of this research to forensic science is the ability to use a long-observed transferable material, automotive undercarriage residue, to create associations between automobiles and persons or objects. These associations can be used to help the trier of fact determine the likelihood that a specific automobile came into contact with a person or object. This project illustrates the discriminatory power of transferred petroleum materials and the usefulness of fluorescence spectroscopy and high performance liquid chromatography with UV detection. This type of evidence is found in "hit and run" type vehicular crimes and in environmental crimes.

1. Vehicular Crimes

Incidents where a vehicle comes in contact with a person or object result in a several different types of transfer evidence. Glass, paint, and rubber transferred from a vehicle to person or object, and fibers and biological evidence transferred from person to vehicle are routinely analyzed to determine if contact took place. At present, the transfer of petroleum products from the vehicle to a person or object are not routinely analyzed. I suggest that automotive undercarriage residue analysis could be valuable in creating an association between a suspect car and person or object that came in contact with the underside of that vehicle. This association becomes valuable in the case of a hit-and-run incident where investigators may need to connect a suspect vehicle, not found at the scene but located at a later time, to a victim. If the victim made contact with the underside of the offending vehicle it is very likely that there was a transfer of automotive

undercarriage residue. Characterizing the fluorescing components of this residue by conducting a spectral comparison of the transferred and native materials could prove especially valuable in the efforts to associate a vehicle to a victim. This is especially true when there are no classic types of transfer evidence (e.g paint, glass) recovered or it is of little evidentiary value. In cases where the identity of the vehicle is known but the details of the collision are contested, automotive undercarriage reside may be helpful for reconstruction purposes (Purcell, 2002).

2. Environmental crimes

Oil spills on both ground and water are a much too frequent occurrence. These events have environmental, legal and financial consequences to the municipalities that detect and oversee the clean-up of the spilled petroleum products. For the fiscal year 2007 there were 527 oil spill incidents, both water and ground, in New York City (NYC DEP, 2007). Clean-up costs can vary wildly depending on such factors as type and amount of oil spilled, rate of spillage, spill location, weather, season and competence of clean-up personnel. It is not always clear, especially in heavily industrialized areas, where the spill originated and therefore what organization or company is the responsible party. Careful chemical analyses of the spilled material using chromatographic and spectroscopic methods have been successful in establishing the source of spilled petroleum materials (Zieba, 1985). This current research, despite its focus on automotive sources of transferred petroleum products, builds on the body of work regarding environmental crimes. Similar laboratory techniques can be used for environmental soil

or water samples. If this method proves to be highly discriminatory it would be extremely helpful in cases where there are hundreds of potential polluters. If culpability can be established in a greater percentage of oil spill events, then more of the clean-up costs can be shifted away from the taxpayer and onto the responsible party.

Instrumental Theory

1. Fluorescence and Phosphorescence

All electrons in an atom are represented by four quantum numbers; n, l, m_l, m_s. The principle quantum number, n, represents the energy of the orbital. The azimuthal quantum number, l, determines the shape of the orbital and the angular momentum of the electron. The magnetic quantum number, m_l, determines the orientation of the orbital in space. The spin quantum number, m_s, describes the spin of the electron and can only be represented by the values, +1/2 or -1/2(Sharma, A., Schulman, S. G., 1999).

Upon excitation with a photon, an electron goes to a higher energy state and maintains its original m_s value, the spin of that electron is still paired with the one left in the ground state and the total angular momentum is zero, S=0 therefore the multiplicity (2S+1) equals one. When multiplicity equals 1 the excited electron is in the singlet state. Fluorescence occurs when an electron is excited to a singlet state and radiatively relaxes down to the ground state. This process is short-lived, usually 10^{-9} to 10^{-7} seconds (Sharma, A., Schulman, S. G., 1999).

If an electron is excited and has the same spin quantum number as the lone electron left in the ground state then the spin direction is parallel and the total angular momentum is equal to one and the multiplicity (2S+1) equals three. When the multiplicity equals three, the excited electron is in the triplet state. Phosphoresce occurs

when an electron enters an excited triplet state and radiatively relaxes down to the ground state. This process is much longer comparatively ranging from 10^{-5} to several seconds. Any condition that inhibits radiationless relaxation, lower temperature or a rigid medium, increases the amount of observable phosphorescence. Phosphorescence in solutions is observed less often than fluorescence mainly because of the non-radiative competing processes of collisional deactivation, quenching, photochemical reactions and other energy transfer process. Competing with both fluorescence and phosphorescence are several non-radiative processes including internal conversion and vibrational relaxation (Sharma, A., Schulman, S. G., 1999).

Figure 1. A Joblonski diagram of the processes that result in luminescence.

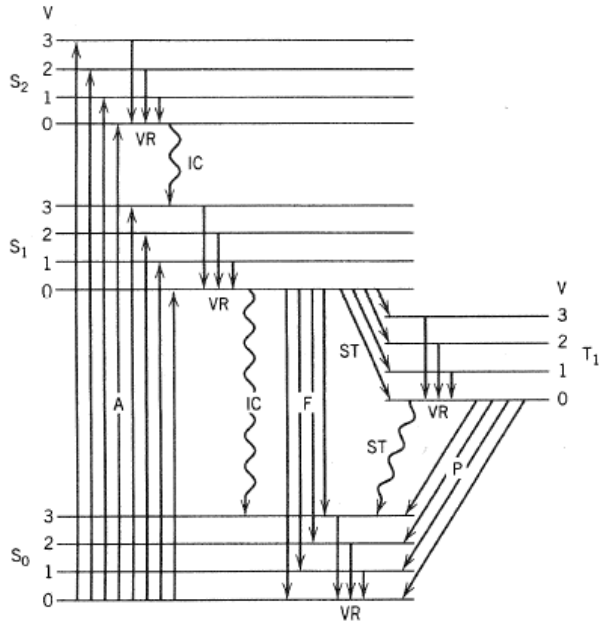

Source: Sharma and Schulman (1999)

When a molecule absorbs a photon of ultraviolet or visible wavelength, an electron is promoted to a higher energy state. This excited electron can return to the ground state through several processes. Luminescence occurs when this relaxation process results in the emission of a photon. If the electron radiatively transitions from the first singlet state back to the ground state then the emission of this photon is called fluorescence. Most observable luminescence from organic compounds comes from the excitation of an electron in a π orbital. If the electron radiatively transitions from the first triplet state to the ground state then the emission of this photon is called phosphorescence. An electron enters the first triplet state after an internal conversion from the excited singlet state. Because the transition can end on any one of the vibrational levels of the ground state, the phosphorescence band itself reflects the ground state of vibrational levels (Ingle, J. D., Crouch, S. R., 1988) (Schenk, 1973).

The excited electron may return to the ground state via non-radiative processes of internal conversion or vibrational relaxation. Whenever a non-radiative relaxation is energetically preferred over a radiative process the total amount of photons emitted by the sample will be reduced. The relationship between exciting photons and emitted photons is described as the quantum yield (Φ).

Fluorescent intensity at a specific wavelength is directly proportional to the number of photons absorbed. The non-radiative processes of intersystem crossing and

internal conversion compete with fluorescence for transition of the lowest excited singlet state electron and therefore not all potentially fluorescent molecules will return to the ground state by fluorescence. The amount of the excited molecules that fluoresce is called the quantum yield (Ingle, J. D., Crouch, S. R., 1988). Quantum yield represents the efficiency of the fluorescence emitted. The following equation states the relationship between fluorescence intensity and quantum yield (Guilbault, G. G., 1990).

$$F = [P_o(1- e^{-\varepsilon bc)}] \Phi \qquad \text{Equation 1.}$$

Where F is the fluorescence intensity, P_o is the source intensity, ε is the molar absorptivity, b is the path length, c is the concentration and Φ is the quantum yield. Guilbault states that when Eq. 1 is subjected to a McLaren (sic) expansion, the relationship between fluorescence intensity and concentration is linear when fluorophore concentrations is low and when $\varepsilon bc < 0.05$. This linearity is represented by Eq. 2.

$$F= [K\Phi P_o] \varepsilon bc \qquad \text{Equation 2.}$$

At higher concentrations, quenching causes deviations from linearity. Therefore, fluorescence spectrophotometry is a useful quantitative technique for concentrations within the linear range. Rigid structures have a much higher quantum yield than

compounds that are not rigid due to the inhibition of collisions that result in non-radiative relaxation and therefore will have a larger range of fluorophore concentrations that are linearly related to fluorescence intensity (Sharma, A., Schulman, S. G., 1999).

Fluorescence spectrometry is much more sensitive and selective than UV-Vis spectrophotometry. This makes it a very valuable technique for the analysis of very small concentrations (Schenk, 1973). Fluorescence intensity and concentration have a linear relationship only when the total absorbance of the system is below 0.05 absorbance units as measured on a UV-Vis spectrophotometer. Above this absorbance the relationship begins to plateau and could actual decrease due to the increased likelihood of solute-solute interactions.

Polycyclic aromatic hydrocarbons are highly fluorescing compounds. Polycyclic aromatic hydrocarbons (PAHs) contain the rigid aromatic structure necessary to inhibit radiationless relaxation that competes with fluorescence (Sharma, A., Schulman, S. G., 1999).

2. Effect of substituents

Any compound that allows the correct electronic transitions may fluoresce. Compounds with rigid aromatic rings are strong absorbers and are much less likely to

return to the ground state via non-radiative means, however not all aromatic systems behave in the same manner. Electron-donating groups (e.g. NH_2) bound to aromatic rings can increase fluorescent efficiency while electron-withdrawing groups (e.g. Cl^-) may quench fluorescence (Sharma, A., Schulman, S. G., 1999).

3. Effect of concentration

The same compound or mixture of compounds may exhibit differently shaped spectra at different concentrations. Shifts of the peak wavelength maxima to longer wavelengths are referred to as "red shifts." Red shifts occur at higher concentrations and not only alter peak maxima, but may result in changes in peak shape. As solute-solute interactions increase it is possible for excited molecules to aggregate with ground state molecules producing an excited dimer. This excited dimer could relax to the ground state non-radiatively, essentially quenching the fluorescence from the excited single molecule. If the excited dimer relaxes radiatively, the luminescence will be at longer wavelengths than that from the single excited molecule. This aggregation affects the shape, position and intensity of the resultant fluorescence (Sharma, A., Schulman, S. G., 1999).

Changes in the position and shape with concentration of the fluorophore are due in part to self quenching and self absorption. Self quenching occurs when energy is transferred via the collision between excited molecules. This process does not result in radiation. Because of the increased likelihood of collision, self quenching increases with

concentration and contributes to deviations from the linearity of Beer's law. At higher concentrations there is an increase in solute-solute interactions. As it does in absorbance spectroscopy, an increase in these interactions causes deviations in the linearity between concentration and intensity of fluorescent light (Sharma, A., Schulman, S. G., 1999). This study evaluated the use of chromatographic and gravimetric analysis to establish concentration. Proper concentration determination would ensure that all spectral differences and similarities seen in a comparison will be attributed to different sample composition and not different concentrations of the same composition.

Literature review

1. Early Work

Early work by the U. S. Coast Guard in the 1970's was successful in identifying the source of spilled oil using the complementary methods of fluorescence spectroscopy, IR spectroscopy, thin layer chromatography and gas chromatography. Each of these techniques is sensitive to different components in the sample. A multi-instrument approach is thorough but time consuming (Curtis, 1977).

2. SSE and VSSE

The first fluorescence spectra were made by either by keeping a constant excitation wavelength and scanning the emission wavelength range, or by keeping a constant emission wavelength and scanning the excitation wavelength range. Synchronous scan excitation (SSE) was a significant advancement. Both the excitation wavelength and the emission wavelength are scanned synchronously at a fixed wavelength interval ($\Delta \lambda$). The SSE technique usually results in more detailed spectra and therefore increased the discriminating power of fluorescence spectroscopy.

J.B.F. Lloyd addressed the evidential value of luminescence of engine oils and similar materials using synchronous scan excitation and emission fluorescence (SSE).

Lloyd was able to differentiate among samples with high molecular weight with the SSE technique (Lloyd, 1971, Part I, II, III).

SSE has been a very popular technique in the forensic analysis of transfer evidence. Rubber bumper guards and petroleum lubricants from sexual assaults were characterized by Blackledge (Blackledge 1980, 1983).

Pharr, McKinzie and Hickman used SSE to characterize gasoline, kerosene, diesel oil, asphalt and fuel oil in organic and aqueous extracts of ground water. They claimed this characterization is a "fingerprinting" technique. I find this terminology ill-fitting to describe the categorization they were successful in achieving. Any technique made analogous to fingerprint analysis should be an individualizing technique (Pharr et. al. 1992).

Patra and Mishra used SSE to classify diesel fuel, gasoline and kerosene. They actually induced the red shift seen with concentration dependent samples to characterize these materials and increase the discrimination of the technique. The wavelength shifting that the researchers used to characterize their samples is precisely why it is so important to establish a concentration for a proper comparison of samples in this study. If identical materials of different concentrations generate spectra of different shape and intensity false exclusions are probable (Patra et al, 2001).

Variable separation synchronous excitation (VSSE) was developed by Kubic, Lasher, Dwyer and Sheehan in 1983. This technique differs from SSE in that the $\Delta \lambda$ is not fixed. This advancement enabled the user to produce any cross-section of a three-dimensional total fluorescence plot between 45° and 90°. With multiple scans at different angles the three dimensional plot could be constructed. Using the VSSE technique, the researchers were able to differentiate between 61 new motor oils and 45 used motor oils, their results were presented in a two-part publication (Kubic et. al . 1983).

3. EEM and contour plots

When computers became the rule rather than the exception in data collection, three-dimensional fluorescence data representation was simplified. The three dimensions of excitation wavelength, emission wavelength and fluorescence intensity are referred to as an excitation-emission matrix (EEM). The EEM can be represented in two dimensions as a contour plot.

Early work with EEMs was done by Freegarde, Hatchard and Parker. They investigated the use of contour plots from fluorescence spectral data to differentiate oils and were successful in distinguishing among nine samples (Freegarde et. al. 1971).

In 1989 Siegel and Cheng were able to differentiate between samples of mid-range petroleum distillates, which appeared to be identical with gas chromatography, using 3D fluorescence plots (Siegel, et. al. 1989).

In 2006, Holbrook et al. at NIST investigated the effect of different corrections made to EEM spectra. The corrections significantly improve intra-laboratory data comparisons. Instrumental bias varies among instruments. This type of bias may result in "systematic errors in measured fluorescence intensity caused by the wavelength-dependent output or response of individual instrument components, such as excitation lamps, monochromator gratings, and detectors" (Holbrook, 2006). In order for laboratories to compare data collected on different instruments this instrument dependent bias needs to be corrected. Other researchers have addressed these corrections on the Varian Cary Eclipse (Holbrook, 2006) (Hall, Clow and Kenny, 2005). Since all fluorescence spectra were collected on the same instrument these corrections are not necessary for this feasibility study. The light source in the Varian Cary Eclipse is a xenon flash lamp. Since a flash lamp is only illuminated in very short period of time it has a much longer useable lifetime and is not prone to source decay. If future work aims to create a comparable data set, the 2006 Holbrook work should be consulted to inform data collection and processing.

4. Low Temperature Fluorescence Spectroscopy

Spectra collected at liquid nitrogen temperatures may show phosphorescence as well as fluorescence therefore it is most accurate to describe all low temperature work as luminescence spectrometry (Fortier, 1978).

Fortier and Eastwood, pioneers in low temperature luminescence, used this technique to differentiate among different classes of fuel oil. They noticed an increase in spectral structure and observable phosphorescence at 77K. Subtle spectral details were enhanced at liquid nitrogen temperatures. This increase in detail arises from the lack of collisional broadening and other non-radiative relaxation mechanisms that are hindered in the rigid, frozen glass. They determined that the optimum concentration for analysis is 10 to 20 ppm. This concentration gave sharp spectral structure with a good signal-to-noise ratio. These researchers, along with Hendrick, in a later article recommend the combined use of low temperature luminescence and synchronous scanning to differentiate among very similar oil samples (Fortier, 1978) (Eastwood, 1978).

In 1983, Kubic, Lasher and Dwyer, used low temperature luminescence and with variable synchronous excitation fluoremetry (VSSE) to distinguish among 61 automobile motor oils. They coupled the low temperature spectral data with room temperature spectal data to obtain complete differentiation among engine oils (Kubic, et al 1983).

In a 1998 Analytical Chemistry review article, Soper, Warner and McGown note that the publications regarding low-temperature luminescence have slowed but progress has been made in the applications of online detection in capillary electrophoresis to distinguish structurally similar analytes (Soper, et. al. 1998).

A 2006 review article compiled the literature from January 2004 to December 2005. The authors site advances using LEDs in time-resolved fluorescence of samples contaminated with crude oils, novel fluorescence sensors have been developed for the analysis of biological and chemical warfare agents, and numerous multivariate statistical analysis techniques are being applied to luminescence data. Much of the current research in the field of fluorescence spectroscopy is striving to make this technology more portable so measurements can be taken in the field. Portability is especially important to environmental chemists and hazardous material responders who work "in the field" and need fast but accurate results (Fletcher, et. al. 2006).

5. Other instrumental techniques

The only study to focus specifically on automotive chassis residue was conducted by Zieba. Zieba used IR spectrophotometry to identify the specific lubricating oils in the samples. She was most successful with fresh oil samples and less so with the undercarriage residues. She observed spectral difference among the undercarriage residue samples but could not determine if these differences were due to sample

composition or random errors or poor reproducibility of the technique. Her results show that significant changes to the class characteristics of the unused oils occur during use. Changes in lubricant chemistry brought on by mechanical and thermal stress caused observable differences in the IR spectra of the samples (Zieba, 1985).

In 2007 Reardon and his research team used high temperature gas chromatography-mass spectrometry to characterize new and used motor oils. PAH presence was investigated using extracted ion profiling and not chemical extraction. The percentage of aromatic compounds increased with the degree of oil wear. Of the different brands and grades, 32 of 34 samples were distinguished. Of the dipstick swabs 26 of the 30 samples were distinguished. All differentiation was done with visual examination of the smoothed chromatograms. The Reardon study shows that there are measurable differences in used motor oils (Reardon et. al. 2007).

To aid analysis of a more common forensic evidence type, Petraco, Gill, Pizzola and Kubic investigated the usefulness of multivariate pattern recognition procedures to distinguish among 20 liquid gasoline samples collected during casework. Their work showed that these samples could be differentiated using canonical variate analysis, orthogonal canonical variate analysis and principal component analysis with varying dimensionality requirements (Petraco et. al. 2008).

6. Sample Preparation

Kershaw and Fetzer developed an extraction procedure to analyze coal liquids by fluorescence spectroscopy. They fractionated coal liquids into oils, asphaltenes and pre-asphaltenes. Oils are soluble in n-pentane, asphaltenes are soluble in toluene and pre asphaltenes are soluble in pyridine. Pinero-Iglesias *et. al.* compared Soxhlet, ultrasonic and microwave assisted extraction techniques for the extraction of PAHs from diesel particulate matter using a standard reference material from NIST (SRM 1650). Extraction of PAHs from these types of particulates can be difficult because they form at the same time as the particles and can be adsorbed into their internal structure. The researchers found that the ultrasonic, microwave and Soxhlet extractions all had comparable recoveries of the individual PAH compounds (Kershaw et. al. 1995) (Pineiro-Iglesias et. al. 2002).

8. The Material - Automotive undercarriage residue

Automotive undercarriage residue is a complex mixture that has multiple contributing sources including motor oils and other lubricants, asphalt particles, tire particles and exhaust particles. All of these sources contain fluorescing compounds, particularly polycyclic aromatic hydrocarbons (PAHs) (Rogge, et. al 1993) (Pineiro-Iglesias et. al 2002). Logic dictates that the residues on the lowest parts of the automotive undercarriage are most likely to be transferred when the underside of an automobile comes in contact with a person or object.

Motor oil is used to inhibit metal-on-metal contact on engine parts. Motor oil is refined from crude oil and comes from the high boiling point fraction of crude oil. The base stock of motor oil comes from the lubricating portion of crude oil. This refined product contains additives to improve its performance as a lubricating agent. These additives include thickening agents, pressure additives, antioxidants, detergents, alkaline components, rust inhibitors, pour-point depressants and antifoaming agents (Motor Oil Guide, 1971) (Wilkinson, 1992). The Society of Automotive Engineers (SAE) assigns grades to motor oils based on viscosity. Some oils have two grades that reflect a changing viscosity with temperature. When stressed during use by high temperatures and mechanical movements, new compounds are formed through oxidative and other processes. These new compounds change the fluorescing characteristics of a motor oil, making the fluorescence spectrum on an oil a dynamic pattern (Kubic et al. 1983).

Road dust particulates come from many sources including vehicle exhaust, brake lining particles, road top particles, tire wear debris and settled aerosols from local combustion of fossil fuels. Rogge *et. al.* studied the organic contribution of all but the last contributor in this list and found polycyclic aromatic hydrocarbons present in all material types (Rogge et. al. 1993).

Regardless of the contributing source to the automotive undercarriage residue, only those compounds that contain fluorophores will contribute to the total fluorescence spectrum. A fluorophore is a functional group in a molecule that after photon excitation allows for the proper electronic relaxation to the ground state. The main fluorophore that will contribute the fluorescence spectrum of each sample is the aromatic ring.

Automotive undercarriage residue has multiple contributors. Of particular importance are those contributors which are dynamic in nature; the more dynamic the source, the greater the chance of individualization.

9. Importance of Concentration

It is important that a concentration of fluorescing compounds is established before final spectral characterization. Both intensity of luminescence and shape of the spectrum will change with concentration. It is imperative, for two reasons, that the concentration of the samples be established. First, comparisons of two samples with the same fluorescing compounds but different concentrations may results in a false discrimination if smaller secondary and tertiary peaks are not observed in the less concentrated sample. Second, the fluorescence exhibited by the detected compounds may shift to longer wavelengths at higher concentration. This shift may also result in false discrimination when comparing two samples of very different concentration but of common origin. False discrimination

in the method could result in false positives and false negatives if the method is applied to a questioned sample and a sample of known origin.

Some researchers have monitored and used the red shift as a way to characterize samples. Patra and Mishra investigated this concept to differentiate among different petroleum products. In their study they wanted to observe the red shifting to characterize the compounds (Patra et al 2001). Since individual compounds may not be identified, the total concentration of the compounds will be determined by measuring the total integrated area of the absorbing compounds resolved by liquid chromatography or by the mass of the extracted residues.

Methods

1. Sample Collection

Ten motor vehicles were included in this study. All ten were passenger vehicles, either sedans or sport utility vehicles, of various years, makes and models. Five undercarriage locations on each motor vehicle were sampled, including the right and left front ball joints on all vehicles along with three additional locations as detailed in Table 1.

Table .1 Vehicle Sample Set and Specific Locations

01 GMC Denali	01	Right ball joint
	02	Left ball joint
	03	Engine oil pan
	04	In front of right ball joint
	05	In front of left ball joint
02 Ford Bronco II XLT	01	Right ball joint
	02	Left ball joint
	03	Cross member
	04	Oil pan
	05	Under radiator in front of engine
03 BMW 330xi	01	Right ball joint
	02	Left ball joint
	03	Inner right joint – left of ball joint
	04	Inner left joint – right of ball joint
	05	Right joint in the back
04 Ford Taurus	01	Right ball joint
	02	Left ball joint

Table .1 Vehicle Sample Set and Specific Locations (continued)

	03	Engine oil pan
	04	Under radiator
	05	Lower part of engine block
05 Honda Accord	01	Right ball joint
	02	Left ball joint
	03	Middle strut
	04	Undercarriage Position a
	05	Undercarriage Position b
06 Mercury Marquis	01	Right ball joint
	02	Left ball joint
	03	Oil Pan
	04	Undercarriage Position a
	05	Undercarriage Position b
07 Ford Escort	01	Right ball joint
	02	Left ball joint
	03	Oil Pan
	04	Undercarriage Position a
	05	Undercarriage Position b
08 BMW 740 iL	01	Right ball joint
	02	Left ball joint
	03	Front skid guard
	04	Left frame
	05	Right bushing
09 Chevrolet Cavalier RS	01	Right ball joint
	02	Left ball joint
	03	Oil pan center
	04	In front of oil pan

Table .1 Vehicle Sample Set and Specific Locations (continued)

	05	To the right of the oil pan
10 Dodge Caravan	01	Left ball joint
	02	Right ball joint
	03	Behind radiator
	04	Oil pan
	05	Left front of cross member

Known samples have a naming scheme that reflects their original source. The generic name is "##X" where #1 equals the origin vehicle, #2 equals the origin vehicle location and X equals the known set it came from (A, B, C). For example, sample name 21A indicates that this swab came from car 2 (Ford Bronco II XLT), location 1(right ball joint) and is from known set "A."

Samples were taken with sterile cotton swabs and stored in labeled screw-capped test tubes. Each location was swabbed five times creating 5 sets of 50 samples. Additional samples of used motor oils were collected from the dipstick of each vehicle in the study. These liquid samples were used for instrumental method development due to the ease of making solutions of known w/v concentrations. These samples were not used in the known sets because they would not be representative of transferred materials as they are found on the underside of a motor vehicle. Instead, swabbed samples were taken from the bottom of vehicle oil reservoirs. Residues from the exterior of the reservoir, while they may contain used motor oils that have seeped out of the interior of the oil reservoir, they also contain road particulates and other debris. It is this exterior-pan

material that is more likely to be transferred when a person or item comes into contact with the underside of a motor vehicle.

From the five swabs taken at each location, three sets were used as the identified known samples, one set was used for extraction and instrumental method development and one set was re-labeled to produce samples of unknown origin. The unknown sample set was re-labeled by Kate Grimley, who recorded the origin of each unknown and sealed these results in a signed and dated envelope. Additionally, Ms. Grimley chose a numbering scheme that was random with respect to the origin naming scheme. Each unknown name begins with the letter "M" and is followed by a two digit number. I arbitrarily selected, without replacement, ten of these relabeled vials to be the unknowns in this study.

There were observable differences between the residue colors, textures and ease of transfer from vehicle to vehicle. In general, older vehicles yielded greater quantities of transferable undercarriage residues which were more greasy than the residues from younger vehicles. Newer vehicles, especially the BMW 330xi, yielded less material per swab and this material was grittier and less oily than that found older cars. This implies that the tendency to transfer oils and other lubricants may be a function of age, use and vehicle design.

2. Extraction Procedure

The Kershaw and Fetzer three-solvent extraction scheme was used for this study. Three fractions, oils, asphaltenes and pre-asphaltenes, were extracted from each swab using ultrasonication solvent extraction with pentane, toluene and pyridine respectively. The extraction took place inside the same screw-capped test tube used for swab storage.

The extraction technique is summarized in Table 2 below:

Table 2. Extraction Method

Extraction volume	2 aliquots of 2mL each
Temperature	Pentane – 30 ºC Toluene – 60 ºC Pyridine – 60 ºC
Sonication time	30 minutes each aliquot (1 hr total)
Centrifugation time	20 minutes for the combined aliquots.

The total sampling scheme is summarized in the Figure 2.

Figure 2. Total Sampling Scheme - Flow Chart of Sampling and Extraction Scheme for a Single Motor Vehicle

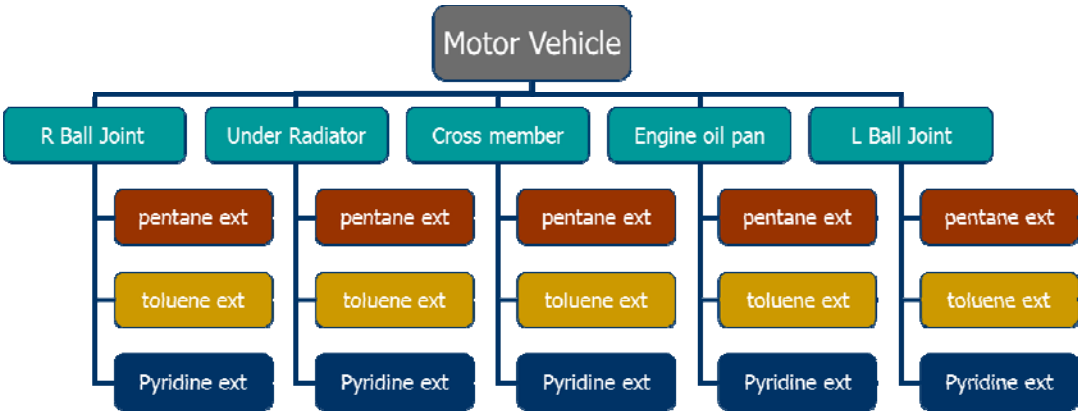

After extraction, the two aliquots were combined and filtered with successive 0.42 micron and 0.22 micron nylon syringe filters to reduce turbidity. A turbid solution can contribute to undesirable Rayleigh-Tyndell (RT) scattering. RT scattering inhibited spectral details in previous work. (Purcell 2002) After filtration, extracts were centrifuged for 20 minutes and then were gently evaporated at room temperature for at least eight hours in preweighed aluminum weighing dishes. Each dish mass was taken in triplicate and averaged. The average pre-residue mass was subtracted from the average post-residue mass to determine the actual residue mass. Residues were then quantitatively transferred to a 5 mL volumetric flask using successive washes of the dilution solvent. The concentration in w/w ppm for each undiluted solution of pentane extract was calculated using the equation below:

$$C = (g_{residue}*1000)/(\rho_{solvent}*V_{flask}/1000) \qquad \text{Eq. 2}$$

Where C equals the concentration in ppm of the undiluted solution, $g_{residue}$ is the average mass of the pentane extract residue, $\rho_{solvent}$ is the density of the solvent[1] and V_{flask} is the volume of the volumetric flask.

The undiluted solution concentrations of known samples ranged from 9600 ppm to 22 ppm. The triplicate knowns from 22A were run at no dilution, 200 ppm, 100 ppm and 50 ppm at three excitation wavelengths, 220 nm, 230, nm and 290 nm. The spectra from the samples at 100 ppm concentration produced the best results with the relative

[1] Acetonitrile for the pentane extracts and methylcyclohexane for the toluene and pyridine extracts.

intensities of each lambda max at each excitation wavelength showing agreement among the triplicate samples from the same motor vehicle location. The undiluted solutions from the triplicate samples did not exhibit the same relative ratio of fluorescence intensities for the lambda max peaks at each excitation wavelength. These variations in spectral shape and relative intensity could be due to red shift observed at higher concentrations. This result favors dilution to a common concentration over no dilution of the extract solution. This result is in agreement with previous work by Eastwood and Kubic, who in separate studies recommended bringing all solutions to a common concentration prior to spectral data collection.

Previous researchers have used a variety of sample concentrations for the fluorescence analysis of oils. Eastwood , Siegel and Kubic independently recommended 20 ppm for direct analysis of oils. Purcell, whose work was also on motor vehicle undercarriage residues used a range of 10-100 ppm. The trials done using known 22A also recommend using a concentration at or close to 100 ppm. This may differ from previous work on oils since the automotive residue may contain many more material types than straight motor oil (e.g. road dust, diesel particulates). The 100 ppm concentration is based on total residue weight and a smaller portion of that residue contributes to the overall fluorescence of the sample. Any extract solution that was at 100 ppm or lower was left undiluted. The same sample naming scheme was expanded to

represent the extract type. The letter P, T, or Y was added to the end of each sample name to denote the pentane, toluene or pyridine extract respectively.[2]

Three extraction system blanks were run. Clean swabs were subjected to the entire extraction procedure including sonication, centrifugation, filtering, evaporation and reconstitution in a solvent. The blank extracts were run on the Cary Eclipse using the room temperature fluorescence excitation emission matrix parameters and low temperature emission scan fluorescence parameters. The resulting fluorescence spectra show that none of the materials used for sample preparation (i.e. swabs, glass test tube, filters or solvents) contributed any fluorescence to the extracted sample. This illustrated in figures 3-5. Note that there is no 2nd order Rayleigh scatter exhibited in figures 3-5 because of monochrometer filter settings.

[2] Sample 22AT is the reconstituted toluene extract residue from vehicle 2 (Ford Bronco), position 2 (left ball joint), known set A.

Figure 3. Pentane Extraction Blank

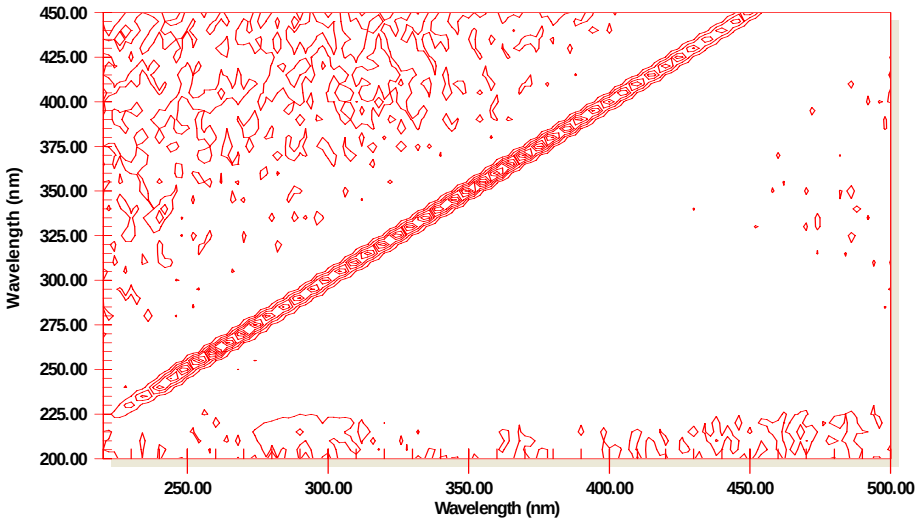

Figure 4. Toluene Extraction Blank

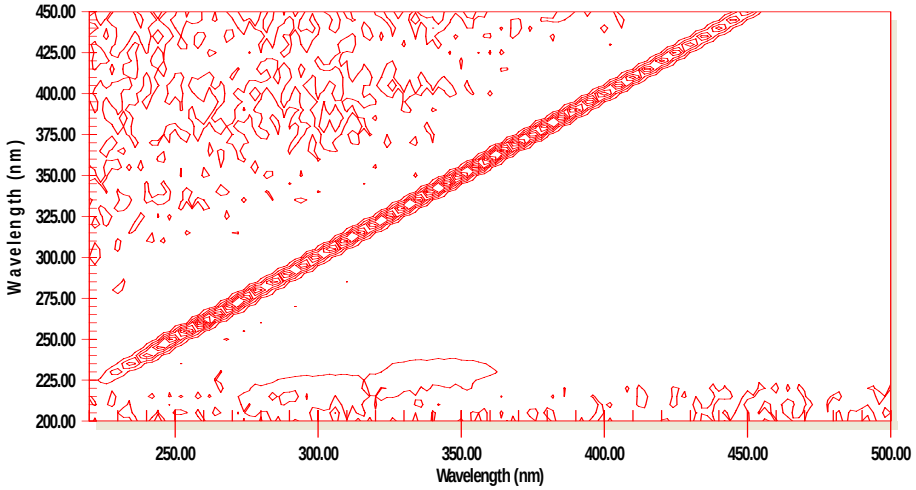

Figure 5. Pyridine Extraction Blank

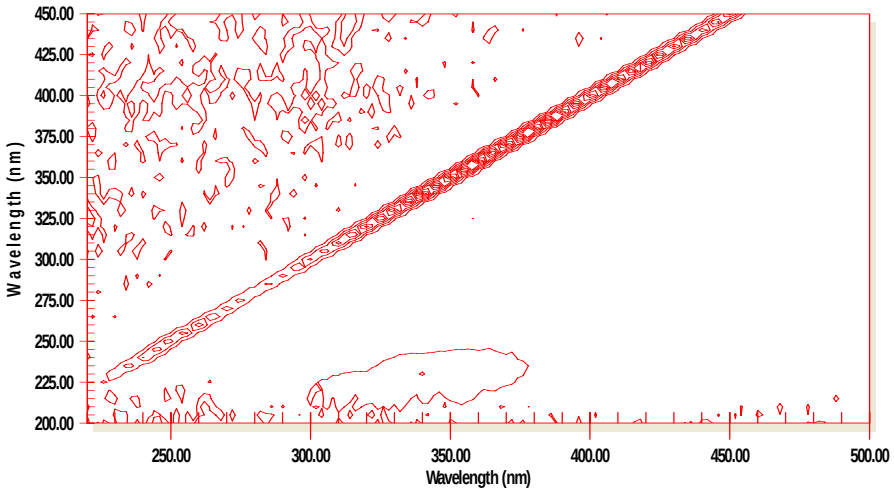

Acetonitrile and methylcyclohexane, the two solvents used for residue reconstitution and fluorescence analysis were run as blanks. There was no contribution to the observed fluorescence spectra from these two solvents. This is illustrated in figures 6 and 7. Please note that figures 6 and 7 were collected at a different emission filter setting than figures 3-5. The open setting resulted in the collection of 2nd order Rayleigh scatter.

Figure 6. Acetonitrile Blank

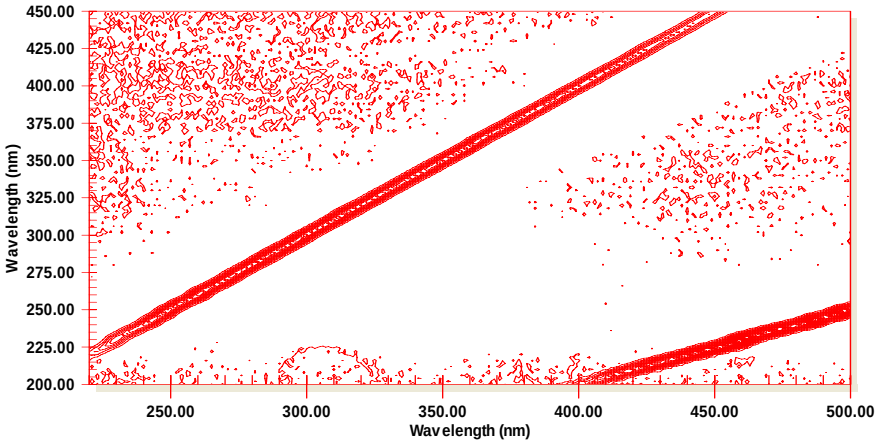

Figure 7. Methylcyclohexane Blank

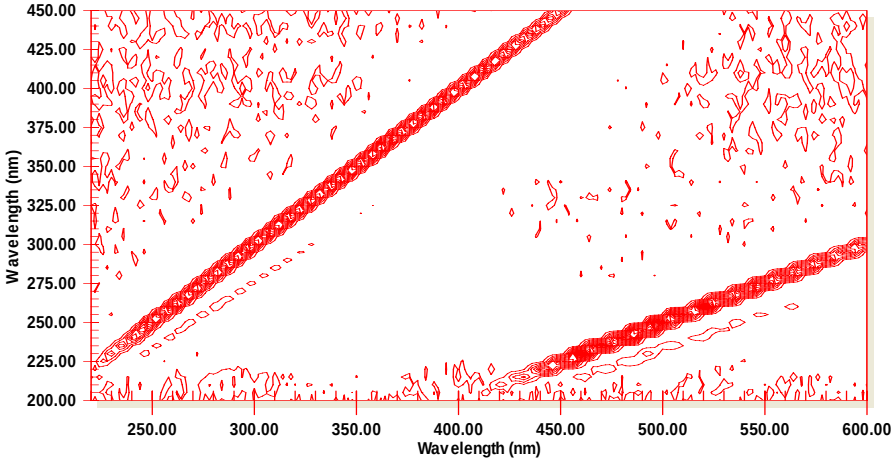

2. HPLC Method Development

Since the concentration of the fluorescing compounds in each sample will effect the peak intensity and number. It was important to determine a suitable method to create extracts of similar concentrations. Purcell's work used calculated residue weights diluted to a constant volume to create extract solutions which were then diluted to common concentrations. While he was successful at creating solutions with a common ppm

concentration, this was based on weight of all compounds extracted, and the true concentration of fluorescing compounds remained unknown. One of his recommendations for future work included using chromatographic data, specifically peak areas of a compound common to all extracts in that class to base concentration calculations on.

It was determined that HPLC was the preferred chromatographic technique. There were established methods, solvent systems and column types for the separation of polyaromatic hydrocarbons and if asphaltenes, much larger molecules with thermally labile peripheral alkyl groups, were extracted in high concentrations, this method would be preferred to gas chromatography. Additionally, HPLC has a wider variety of detector types available. It was determined that a fluorescence detector would be the best suited for this task.

Using a fluorescence detector would ensure that the compounds used to adjust the concentration exhibit fluorescence and directly influence the fluorescence excitation-emission spectra. A review of the several different commercially available fluorescence detectors was done. Funds were available through a grant from the Borough of Manhattan President's Office. I reviewed the commercially available units and obtained quotes from vendors. All necessary paperwork was submitted to the city representatives to complete the purchase. After multiple communications with representatives of the City of New York purchasing department, it became clear that the procurement process

and the hurdles encountered would delay the project timeline so much so that it became prohibitive to proceed with procurement for this study. This was indeed the case as the equipment was actually delivered in November 2010 and installation has just been completed as of this writing; almost two years after the purchasing process began. Without the ability to procure a fluorescence detector for the HPLC instrument in-house, I decided it was best to proceed with UV detector already available and installed on the HPLC. The instrument used was a Shimadzu HPLC with a SCL-10A system controller module, SIL -10A auto injector, SPD-10A UV absorbance detector. All data was collected on a HP3396A integrator.

The first of three swab extracts (pentane) was evaporated to dryness, reconstituted and brought to 5 mL total volume in acetonitrile. These undiluted solutions were analyzed via HPLC. Peaks common to all three swab extracts from a single vehicle location were identified and their areas added to create a total peak area for each known. This method is similar to that used for compounds that were historically difficult to resolve such as PCBs (Butcher *et al*, 1997).

Historically, this quantification method has been used to quantify polychlorinated biphenyl compounds analyzed by gas chromatography. Most commercial PCB production was conducted by the Monsanto Corporation and marketed under the brand name Aroclor. Packed GC columns lack the resolving ability to separate the compounds in the PCB mixture. These products were quantified using the total peak areas of selected

Aroclor peaks resolved in the chromatogram. In the method employed for this project, the peaks identified as common to each triplicate sample are analogous to the Aroclor peaks selected to represent concentration of the entire PCB sample.

3. Solvent Incompatibility

The literature most strongly supported the use of a reverse phase system for polycyclic aromatic hydrocarbons detection by HPLC. However, the aqueous solvent system and the methylcyclohexane necessary for the low temperature spectral analysis are not miscible. Since both the investigation of using chromatographic techniques and the characterization of sample fluorescence at liquid nitrogen temperatures were important parts of this project it became necessary to find a compromise. Any extract residue that was reconstituted in acetonitrile would not be able to be analyzed at low temperatures and any reconstituted in methylcyclohexane would not be analyzed by HPLC. Of the three swab extracts, pentane, toluene, and pyridine, it was expected that the toluene and pyridine extracts, if they contain asphaltenes and pre-asphaltenes as recorded by Kershaw and Fetzer, would contribute the most fluorescing components due the preponderance of aromaticity, while the oils would contribute the least due to the preponderance of unconjugated compounds. I decided to analyze the pentane extracts with HPLC and UV detections to adjust concentrations with the oils extract while reserving the other two extracts for low temperature analysis.

Table 3. HPLC Method

Isocratic Elution[3]	10:90 H2O: ACN
Flow Rate	1ml/min
Injection Volume	3 microliter
Detector λ	254 nm

The HPLC column used was a Supelco brand Supelcosil LC-PAH, 5 cm x 4.6 mm ID with 3 micrometer particles. The LC-PAH stationary phase is C-18. A guard column with the same packing material was used to prolong the life of the analytical column. Column performance was tested with three standard polyaromatic hydrocarbons listed in Table 4. Detector response linearity was tested with dilutions of phenanthrene and naphthalene in concentrations ranging from 0.019 µg /mL to 4.00 µg /mL and 0.23 µg /mL to 50 µg /mL respectively. The results are shown in Tables 6 and 7.

[3] Gradient elution was tested on dilute solutions of used waste oils. The instrument had difficulty returning to a stable baseline after the end of the gradient program. The isocratic program eliminated the baseline drift problem by maintaining a constant solvent system and ensuring complete elution of all injected compounds.

Table 4. Standard PAH Solutions

Fluorene	10 µg /mL
Naphthalene	50 µg /mL
Phenanthrene	4 µg /mL

	Inj 1	Inj 2	Inj 3	%RSD
Naphthalene				
3 µ/L inj	38257	37947	44751	9.5290
Phenanthrene				
6/µL inj	75879	75810	75483	0.27936
Fluorene				
6/µL inj	75377	75901	75568	0.35071

Table 5. HPLC Detector Linearity - Phenanthrene

Compound	µg/mL	average peak area
Phenanthrene	4.00000	640978
standard dilution 1	0.66700	111696
standard dilution 2	0.11100	22414
standard dilution 3	0.01850	6415
standard dilution 4	0.00309	ND

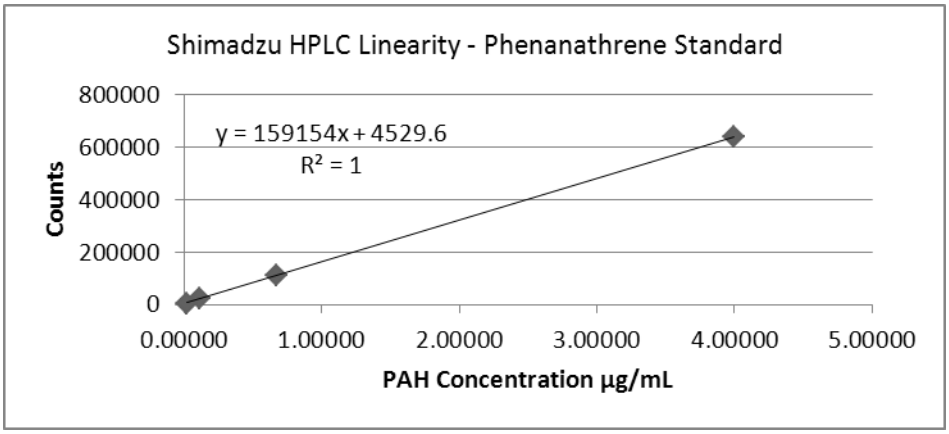

Table 6. HPLC Detector Linearity - Naphthalene

Compound	µg/mL	average peak area
Naphthalene	50.0000	635958
standard dilution 1	8.3330	89891
standard dilution 2	1.3890	16974
standard dilution 3	0.2315	3383
standard dilution 4	0.0386	ND

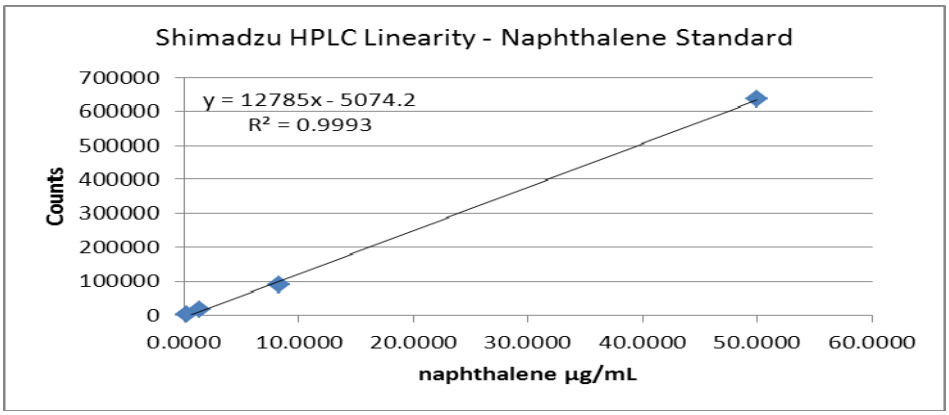

Chromatograms for all triplicate samples from the fifty motor vehicle undercarriage locations were collected. Figure 8 shows the reproducibility of the chromatograms among samples of common motor vehicle origin.

Figure 8. Chromatograms from triplicate swabs of Vehicle 1 Location 3 (13).

13A

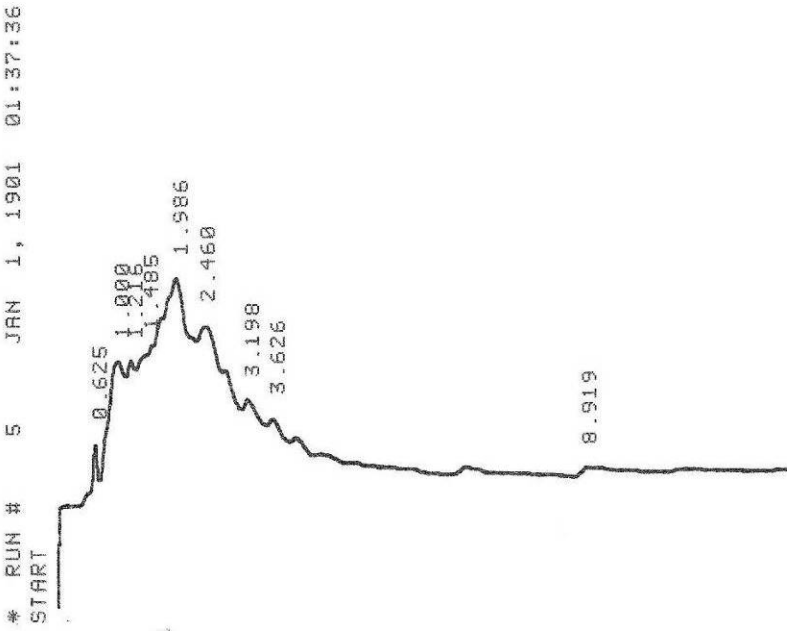

13B

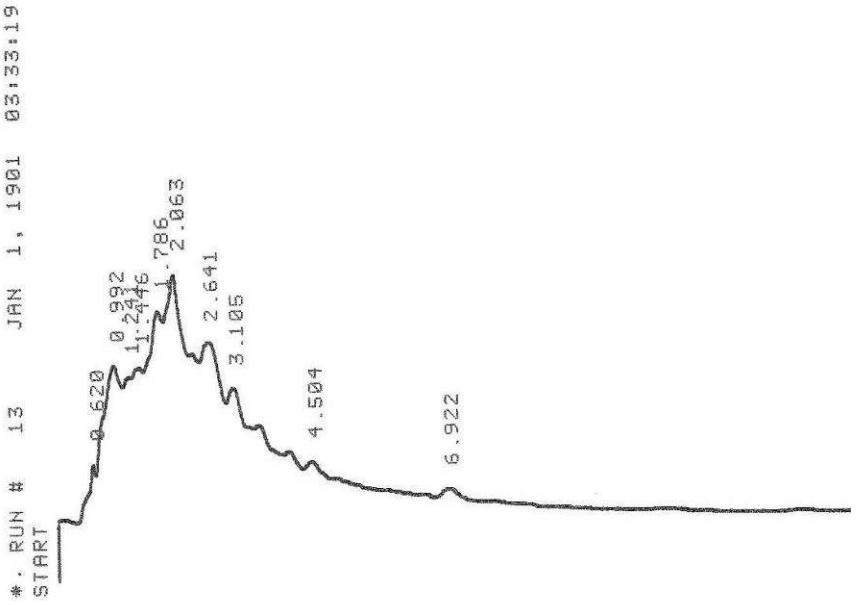

Figure 8. Chromatograms from triplicate swabs of Vehicle 1 Location 3 (13) continued

13C

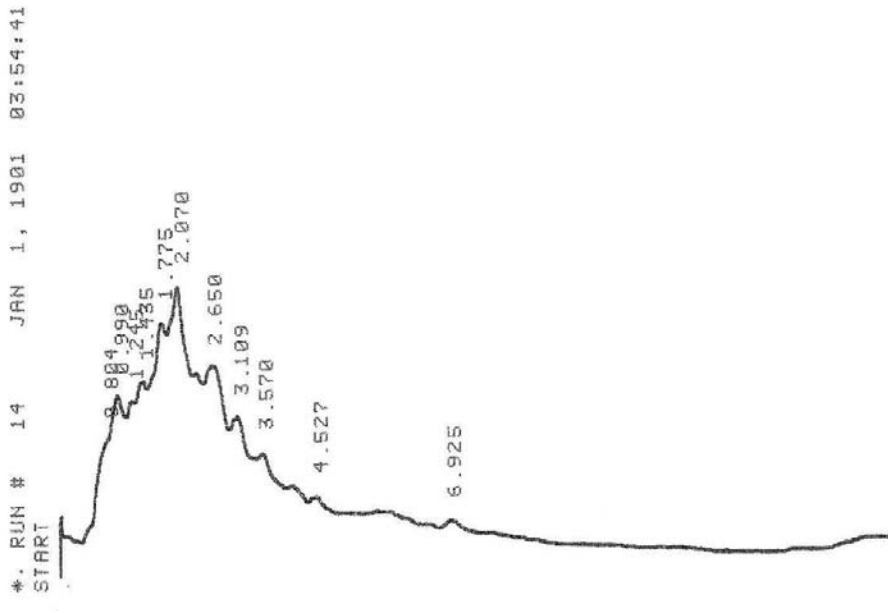

4. Cary Eclipse Instrumentation

All fluorescence spectral measurements were made on a Varian Cary Eclipse Fluorescence Spectrometer. It has a xenon flash lamp source and an extended range (200 nm – 900 nm) photomultiplier tubes, both sample and reference. Wavelength selection is accomplished with two grating monochrometers. The xenon flash lamp and signal processing technology makes the Cary Eclipse nearly immune to room light contamination. The Cary Eclipse was designed with the detector located at 90 degrees from the source. This geometry limits detection of unscattered photons from the source lamp. (Ingle, Crouch)

The Cary Eclipse software contains a validation function that tests the wavelength accuracy of the excitation and emission monochrometer and the spectral bandwidth accuracy of the excitation and emission slits.

Stray light is monitored by taking the ratio of the intensity of scattered light detected by the sample PMT at a wavelength which is at the very edges of the excitation wavelength (i.e. in the excitation wavelength is set to 350 nm this test will measure at 371 nm) The ratio must be between -0.0005 and 0.0005 a.u. to pass the test. The Raman band of water is measured at 350 nm and 300 nm and was used to test the sensitivity of the instrument. Wavelength reproducibility is measured by repeatedly measuring the wavelength at the 541.92 nm Xe lamp peak for 10 scans and calculating the difference between the extremes of the wavelengths measured. The difference must be less than 0.2 nm to pass. Wavelength accuracy is also tested using lines from the Xe source. Peaks must be within 0.5 nm of the line at 541.92 nm and 1.0 nm of the 260.54 nm line in order to pass. Initial execution of these validation tests show that the Cary Eclipse was performing within the desired parameters as set by the manufacturer.

Table 7. Instrument Validation Tests preset by Varian. Results from a 16 day period.

Varian Validation Tests		*1*	*2*	*3*	*4*	*5*	*RSD*
	Expected values	nm	nm	nm	nm	nm	
WL Accuracy Ex. Mono (Xe) (nm)	*541.92*	542.01	542.08	541.93	541.93	541.92	0.012823
	260.54	260.92	260.92	260.84	260.84	260.83	0.017567
WL Accuacy Em. Mono (Xe)	*541.92*	542.15	542.02	541.86	541.04	541.86	0.080174
	260.61	260.61	260.54	260.38	259.53	260.38	0.16732
Spectral BW Acc. Ex. Slit (nm)	*1.5*	1.651	1.667	1.664	1.751	1.766	3.188
	2.5	2.478	2.473	2.539	2.51	2.546	1.341
	5	5.336	5.345	5.386	5.321	5.339	0.456
Spectral BW Acc. Em. Slit (nm)	*1.5*	1.077	1.024	1.121	1.159	1.151	5.077
	2.5	2.423	2.394	2.454	2.428	2.377	1.249
	5	5.154	5.168	5.231	5.316	5.249	1.254
	10	10.434	10.375	10.273	10.29	10.37	0.64094
	20	20.697	20.521	20.555	20.539	20.62	0.35088
		a.u.	a.u.	a.u.	a.u.	a.u.	
Stray Light (a.u.)		0.00034	0.00034	0.00031	0.0003	0.00031	5.8
Raman H2O Sensitivity Ex.350 nm (#:1)		1325	1536	1405	1336	1474	6.375
Raman H2O Sensitivity Ex.500 nm (#:1)		863	892	889	900	828	3.36

During the course of data collection these quality assurance tests and spectral analysis of naphthalene and anthracene in fluorescent polymer blocks were run trimonthly in order to ensure that the instrument was functioning correctly.

Figure 9. Anthracene/Naphthalene Polymer Block Standard – Single EEM.

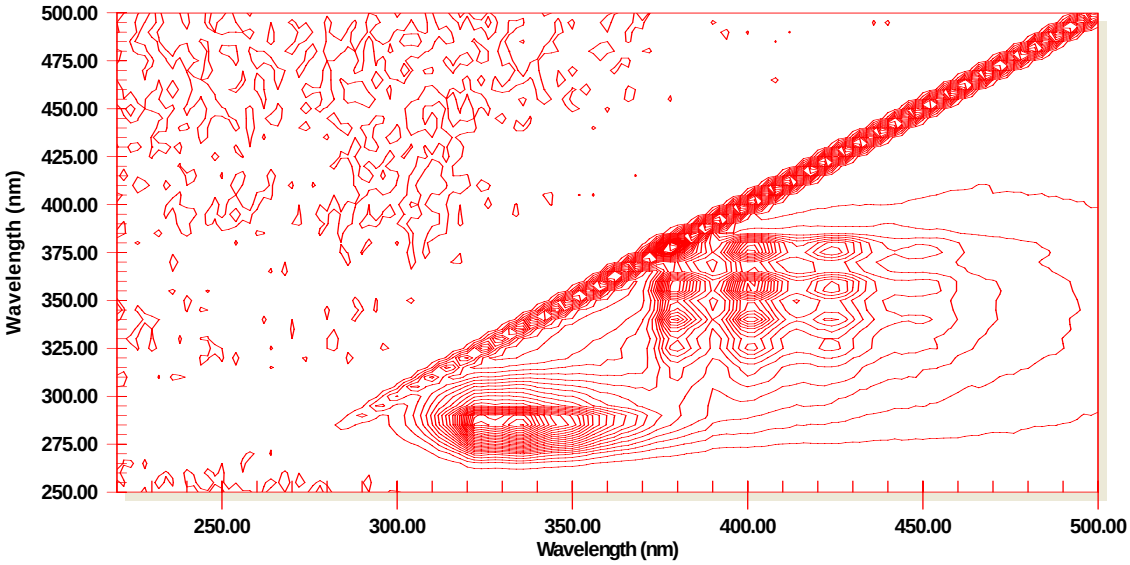

Table 7. Anthracene/Naphthalene Polymer Block Standard – Intensity and Emission values. I=Intensity

	Ex 290				Ex 320		Ex 360	
Date	Peak λ 1	I	Peak λ 2	I	Peak λ	I	Peak λ	I
5-Feb-09	324.00	249.61	336.00	248.70	401.07	97.916	402.00	250.53
20-Feb-09	324.00	243.30	336.00	241.60	402.00	93.765	402.00	238.46
27-Feb-09	324.00	245.27	336.00	244.00	402.00	84.058	402.00	204.29
2-Mar-09	324.00	248.41	336.00	249.90	402.00	86.710	402.00	207.45
16-Mar-09	324.00	242.02	336.00	283.25	402.00	85.040	402.00	199.78
31-Mar-09	324.00	238.62	336.00	239.42	402.00	85.148	402.00	196.99
9-Apr-09	324.00	239.05	335.07	244.82	402.00	85.421	401.07	183.19
15-Apr-09	324.00	239.25	335.07	238.47	401.07	84.830	401.07	191.79
28-Apr-09	324.00	242.48	335.07	241.79	401.07	85.385	402.00	194.26
% RSD	0	1.6461	0.13852	5.5522	0.11576	5.5297	0.10207	10.786

Figure 10. Anthracene/Naphthalene Polymer Standard – Excitation 290 nm. All scans Each color represents a single scan taken on one of the dates listed in Table 7. Scans from all dates are represented.

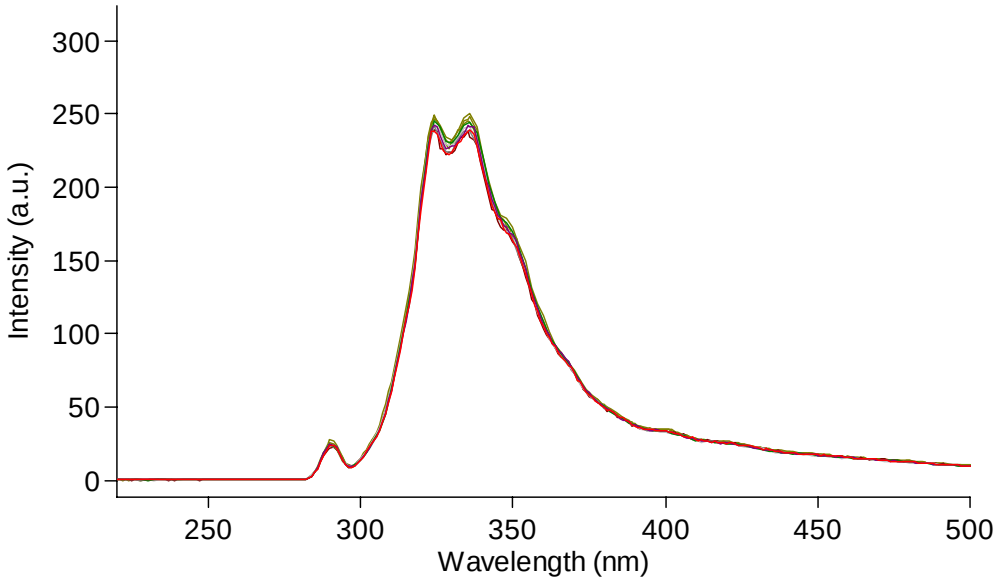

Figure 11. Anthracene/Naphthalene Polymer Standard – Excitation 320 nm. All scans. Each color represents a single scan taken on one of the dates listed in Table 7. Scans from all dates are represented

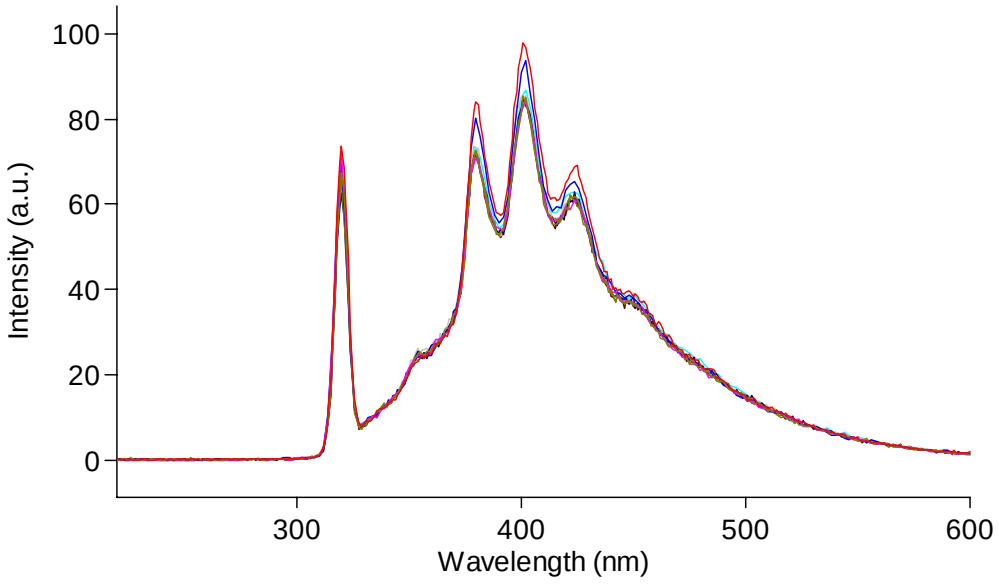

Figure 12. Anthracene/Naphthalene Polymer Standard – Excitation 360 nm. All scans. Each color represents a single scan taken on one of the dates listed in Table 7. Scans from all dates are represented.

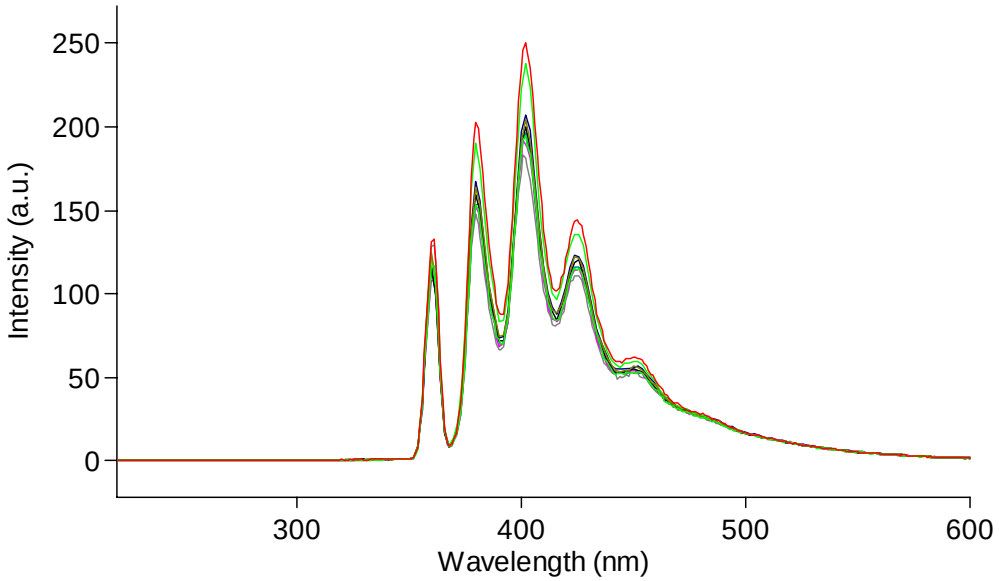

Data Collection

Excitation Emission Matrix Room Temperature Fluorescence

One sample from each vehicle undercarriage location was selected for room temperature excitation emission matrix fluorescence spectral data collection. Table 8 shows the instrument settings for this data collection. The EEM spectra from known samples collected are listed shown in the Appendices C-E.

Table 8. Cary Eclipse Setting for Room Temperature Excitation Emission Matrix Data Collection

Excitation Start	200 nm
Excitation Stop	500 nm
Emission Range	220-600nm[4]
Data Step[5]	5 nm
Ex Slit	5 nm
Em Slit	5 nm
Scan Rate	1200 nm/min
Data Interval[6]	2.0 nm
Averging Time	0.1 sec
Ex Filter	Auto
Em Filter	Auto[7]
PMT	Medium (600 V)

[4] The emission range for EEM data went from 220-600. No peaks were observed past 400 nm. The scale was reset to 220-400 nm during data processing to improve the presentation of EEM spectral detail.

[5] In an excitation emission scan, the *Data Step* is the amount that the excitation monochrometer moves prior to the next scan. It is the distance between the slices that form the EEM.

[6] The *Data Interval* determines the size of the steps between each data point in the emission range.

[7] For the pentane and some of the toluene extracts, this filter was set to "Open." This setting resulted in the collection of secondary RT scatter at wavelengths from 440 nm and above. Data processing with the Excel macro removed these peaks. The emission filter setting "Auto" is recommended for future work.

1. Parameter Selection

The excitation wavelength range was chosen based on previous work with this sample type and with direct analysis of motor oils (Purcell 2002) (Fortier and Eastwood 1978). Most organic molecules fluorescence at excitations below 500 nm. (Schenk 1973) And since the majority of the fluorescence observed is expected to be from polycyclic aromatic hydrocarbons, this excitation range is sufficient to capture these data.

Slit widths for the excitation and emission monochrometers were chosen based on previous work (Purcell 2002). The spectral resolution would have been improved with smaller slits however, there was concern about losing information from more weakly fluorescing samples. Since this resolution was sufficient for successful sample discrimination and known-unknown association in a previous study and in this work, produced EEM spectra with sufficient detail to collect the main points of comparison (i.e., the excitation and emission wavelengths of the peak fluorescence) the same slit widths were adopted for room temperature data collection for this work.

Varian claims the Cary Eclipse is capable of scanning at speeds up to 24,000 nm/min without exhibiting peak shifts. However at such a high scanning rate finer secondary spectral features may be lost. Trials with sample 41A established that a scan rate of 1200 nm/min, when compared to a scan rate of 600 nm/min, would produce spectra with no peak shift from the slower scan rate and sufficient secondary spectral detail in an EEM. This is illustrated in the Figures 13 and 14 below. The EEMs of 41A at both 600 nm/min and 1200 nm/min exhibit the same number of peaks at the same positions and all secondary spectral detail is the same. Scan rate, averaging time and data

interval are all inter-related on the Cary Eclipse. When set to the 1200 nm/min the Cary automatically sets the data interval to 2.0 nm. At this interval the noise observed at excitation wavelengths below 225 nm was reduced.

A PMT settings of medium (600 V) and high (800 V) were tested on 17 samples of known origin from 6 different motor vehicle locations. For the room temperature data collection, the PMT setting at 800 V produced many fluorescence spectra with intensities that exceed the range of the PMT. This problem was not observed with at the 600 V setting.

The use of spectral smoothing, specifically Savitzy-Golay, was considered. Setting the instrument to smooth during collection would not have allowed the collection of the raw, unsmoothed data. Attempts to smooth after collection would be extremely time consuming. Each EEM is constructed with 60 emission scans and each would have to be separately opened, smoothed and then all 60 would be reassembled in a matrix. Considering that the main data points for the comparison of spectra, the emission and excitation wavelengths of the peaks, would not be improved with smoothing, it was decided that the collection of raw but noisier data was preferable to smoothed.

Figure 13. Known 41A at Scan rate 1200 nm/min

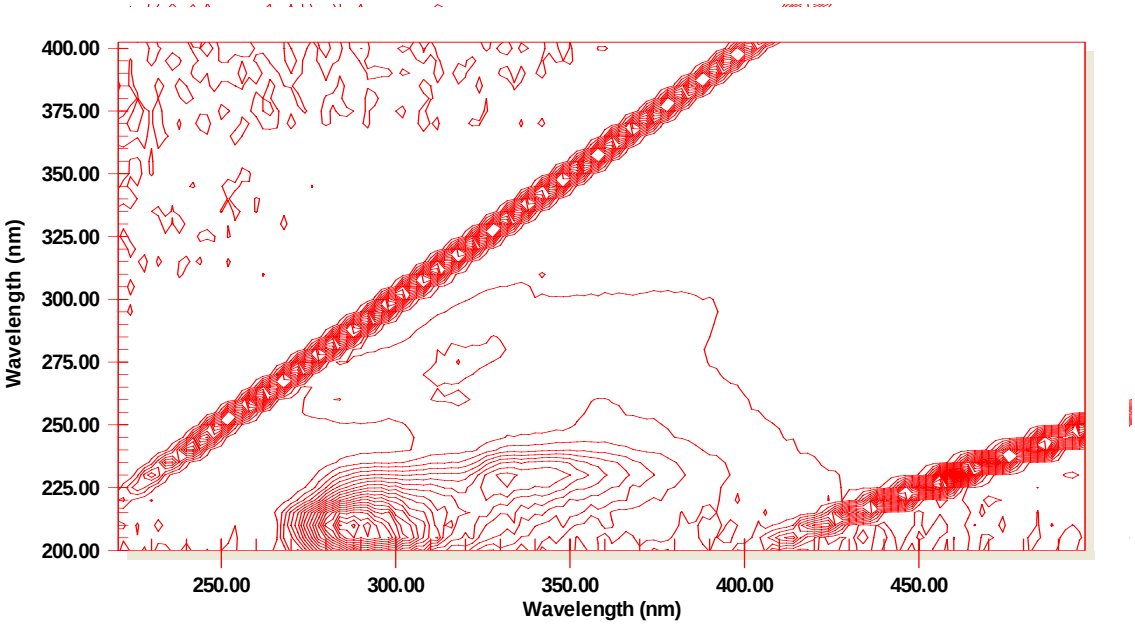

Figure 14. Known 41 A at Scan rate 600 nm/min

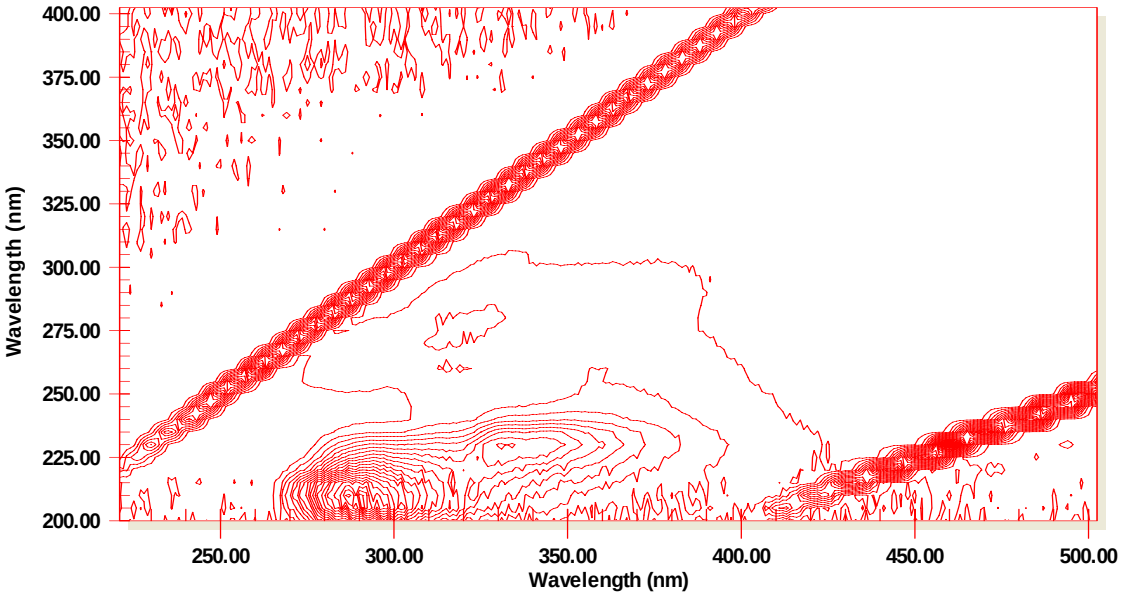

At the slower scan rate, and smaller data interval (1nm), figure 14 does exhibit smoother contour lines, especially in the excitation wavelength regions above 250 nm.

Below an excitation wavelength of 250 nm, the smaller data interval also captures more of the noise at this wavelength region were a xenon source is less intense. Since most of the peaks from these undercarriage residues samples occur at these low excitation wavelengths, the increased resolution provided by the smaller data interval did not outweigh the increased difficulty in finding peak maxima below excitation 250nm. Therefore, the faster scan at 1200nm with the larger data interval was preferred for the EEM data collection.

2. EEM Spectral Processing

The primary and secondary Raleigh Tyndall (RT) scattering observed and in previous work by Purcell was thought to be caused by turbid solutions. Turbidity can cause this type of elastic scattering because light is physically deflected from the small particles suspended in solution. However, the intensity of the RT scattering was relatively constant. Samples from the previous work were filtered once through 0.44 micron syringe filters and the results were normalized to the largest peak intensity. As a result the RT scattering looked very large on spectra that had very weak fluorescence intensity. Filter settings can eliminate collection of second order RT scattering. The emissions filter was sent to "Auto". These settings were used on most of the toluene extract solutions and all of the pyridine extract solutions. To generate accurate contour plots the RT scatter must be removed so that the Grams software does not include these peaks when scaling the contour slices. Contour plots are made by taking the total fluorescence intensity range and dividing it into a pre-determined number of sections.

The more sections the software is asked to create the more contour lines will appear on the plot. If the RT scatter is the most intense peaks in the data set, the actual fluorescence emission will be divided into less contour slices than the analyst may intend. This effect is most damaging for weakly fluorescing spectra that are more 'dwarfed' by the intense RT scattering.

A Varian representative sent an application development language (ADL)[8] program that was to stagger the starting wavelength on the emission monochrometers to avoid collecting any RT scatter. Instead of all emission scans beginning at the same wavelength this program purported to stagger the start wavelength of the emission monochrometer. For example, the first excitation wavelength 200 nm with emission scanning from 220 nm to 600 nm would collect no RT scatter because there was never a time when excitation wavelength = emission wavelength but when the excitation wavelength moved above 220 nm the emission scan would start at a longer wavelength (e. g. 240 nm) thereby cutting out the RT scatter. This program never performed as advertised. The file as-sent would not upload because of syntax problems. I edited the format into one readable by the ADL shell. After several more edits to the ADL code a single EEM spectra was collected successfully. However attempts to display this file as a contour plot resulted in repeated crashes of the Cary Eclipse program. These experiences

[8] The application development language (ADL) is a programming language, similar to BASIC, that is used by the Cary Eclipse software.

led to the decision to collect the EEM files without real-time efforts to avoid collecting RT scatter.

This scatter was removed post data collection by a customized Excel macro program. The excel macro is designed to replace intensity values with a zero value in key places where first and second order RT scatter is found. The macro deletes every intensity value where the emission wavelength is less than or equal to the excitation wavelength minus 5nm. Since fluorescence emission does not usually occur at wavelengths higher in energy than the excitation wavelength, no important spectral data is lost in this deletion. Any fluorescence due to the anti-stokes shift, where the emission is at shorter wavelengths than the excited radiation, will not be removed by this macro if it occurs at wavelengths 5 nm shorter than the excitation radiation. Peaks from anti-stokes shifting are usually much less intense than RT scatter peaks and are not necessary to remove from the data set because they do not overwhelm the spectral data.

This is repeated for intensity values at positions 2x the previous wave to delete 2nd order RT scatter. This had the largest impact on contours created from samples with weak fluorescence intensity where the RT scattering has the most obscuring power. The effect of this program is illustrated in Figures 15 and 16. Figure 16 shows that after removal of the RT scatter, three additional low intensity peaks are displayed by the contour plotting function.

Figure 15. 83BT Before Rayleigh-Tyndell scatter removal. Each color represents an excitation scan at a difference excitation wavelength.

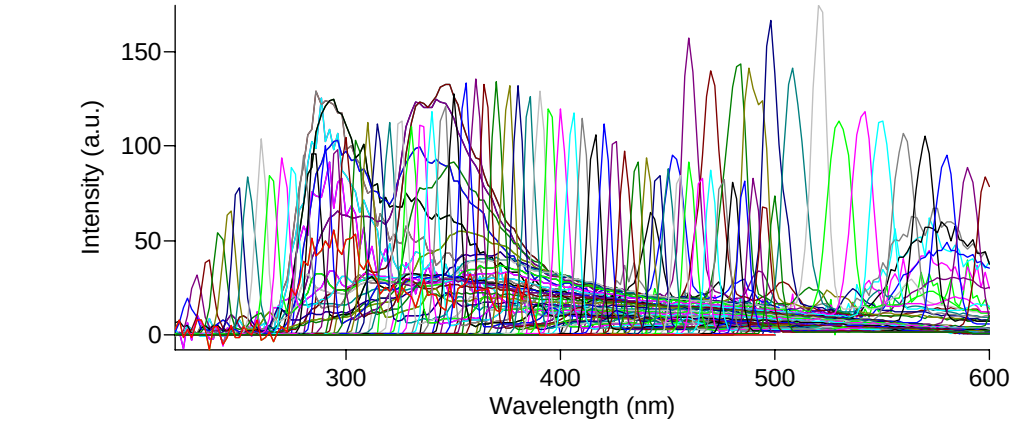

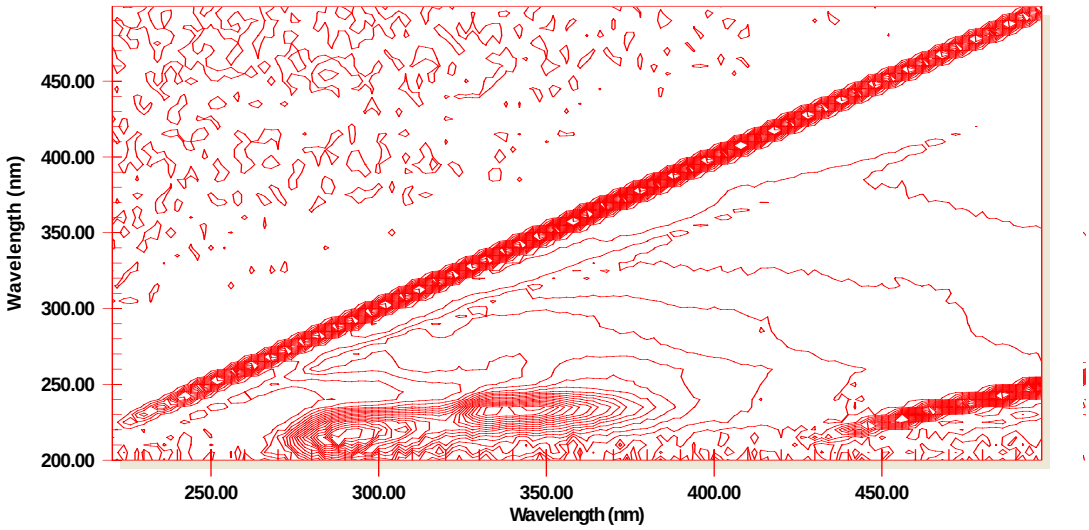

Figure 16. 83BT After Rayleigh-Tyndell Scatter Removal. Each color represents an excitation scan at a difference excitation wavelength.

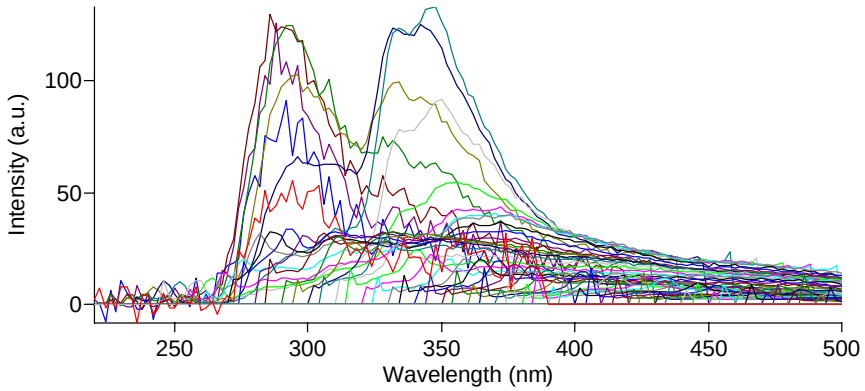

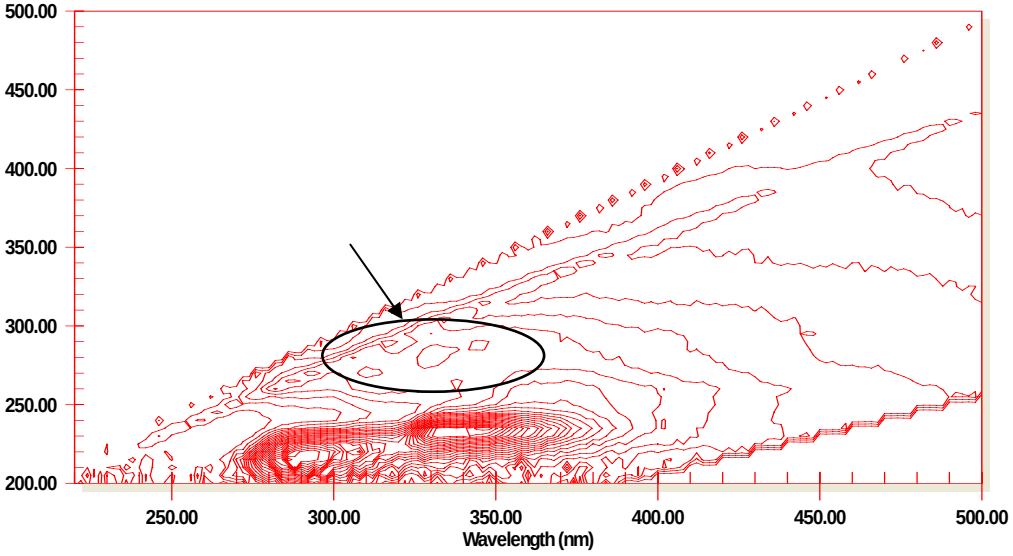

3. Low Temperature Fluorescence

Development of the Low Temperature Fluorescence Apparatus

In order to achieve the decreased temperatures needed to generate more detailed spectra I used an apparatus designed to freeze the solutions in liquid nitrogen temperature, 77K. There are several challenges associated with this process and that

must be overcome in order to generate useful spectra, most notably, maintaining frost-free sample windows and producing clear and crack-free frozen samples.

4. Apparatus

The original design supplied by Varian was inoperable. The Dewar itself had no cap and was to remain open to the atmosphere when filled with liquid nitrogen. This would not work as the freezing agent would evaporate before the completion of a single EEM, run which can take upwards of 20 minutes. Without a cap to support it, the sample tube was supposed to sit in the bottom of the Dewar and rest on the side of the reservoir resulting in a tube that was at an angle and other than normal to ground. Test scans showed that this angled tube resulted in increased Raleigh-Tyndell scatter that was most likely due to the excitation beam meeting the sample tube surface at an angle other than perpendicular.

5. Design Modifications

A cap similar to the Farand design was necessary to slow the evaporation of the liquid nitrogen and to position the tube normal to the excitation beam.

Figure 17. Farand Dewar cap with quartz-tipped glass sample tube.

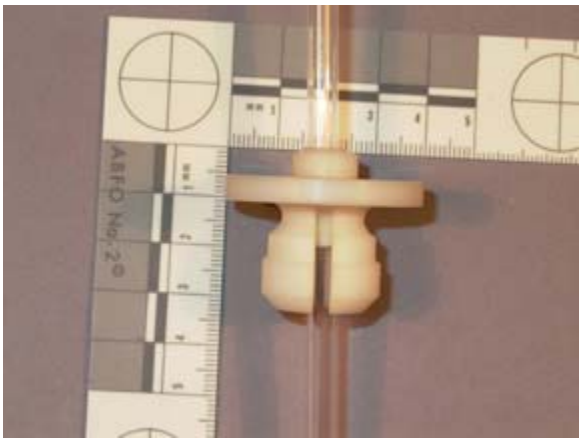

Figure 18. Farand Dewar cap top view showing vent holes.

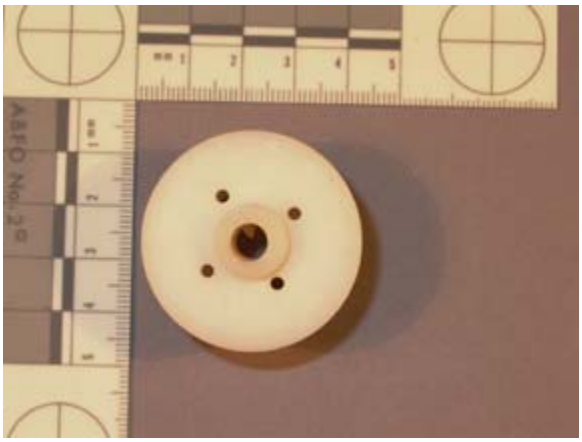

The Varian Dewar was taller than the top of the sample compartment and wider than the original Farand design[9]. To make room for this a new top was supplied with a hole cut in

[9] The Farand Dewar owned by Dr. Thomas A. Kubic is 4.3 cm OD while the Dewar supplied by Varian is 7.7 cm OD.

the top. This top was a solid piece and therefore the Dewar and the support apparatus had to be inserted into the instrument through the hole itself.

This was extremely awkward and eliminated any possibility of ensuring that the Dewar support and the quartz bottom aligned with the source. The sample tubes supplied were quartz NMR tubes with an extremely small inner diameter (3mm) and a height less than that of the Dewar itself. This limited the amount of liquid nitrogen allowable in the reservoir because it could not be higher than the top of the tube. In order to solve these issues a memorandum was drafted and sent to the vendor requesting the lid be split in two to and a cap for the Dewar. Photographs and dimensions of the original Farand cap and Dewar, measurements of the new Dewar and desired tube specifications and material preferences were sent to guide the production. Work proceeded once these modified products were delivered.

After adoption of the split lid, longer tubes and sample cap work continued on apparatus. One of the main differences between the original Farand design and the Varian design was that the Farand Dewar sat in an enclosed metal collar with inlet and exit ports for purging gas. Clearance between the collar and Dewar was not more than 5 mm. This reduced the amount of empty space around the container thereby requiring a slower stream of purge gas to ensure a dry environment. A dry environment is necessary because any moisture will freeze on the surface of the cold Dewar as white snowy ice; a

highly scattering beam-blocking coating. The better the vacuum in the Dewar walls the less likely this was to occur but it must still be avoided.

The Cary Eclipse has a large open sample compartment. While this is good for fitting in a variety of accessories it is not good for low temperature analysis. Extra space was reduced by introducing black paper-covered Styrofoam blocks to the sides of the container.

4. Final Design of the Low Temperature Apparatus.

A series of modifications to the interior of the sample compartment were tested to allow for the driest environment with the slowest flow of dry N_2 gas. Determination of the necessary modifications was an iterative process. As each design element was adopted or altered, the relative humidity (RH) of the sample compartment was monitored using a relative humidity meter. Monitoring would begin with the sample compartment at equilibrium with the laboratory RH and continue as the flow of dry nitrogen gas was delivered from the flow meter manifold. RH data was collected once every minute until the sample compartment interior reached a stable baseline. These data sets were used to identify the sample compartment design that would allow for the fastest drop in RH and the lowest sustainable RH at equilibrium.

The final design of the low temperature apparatus include a quartz-tipped liquid nitrogen Dewar held in a fixed position by an adjustable frame. Two nozzles attached to the frame delivered a steady, but adjustable stream of dry nitrogen gas to the tip of the Dewar to prevent frost formation. The nitrogen gas was supplied by the headspace of the liquid nitrogen tank and the flow was regulated by a custom built manifold of flow meters.

Figure 19. Flow Manifold[10]

Front View

Back View

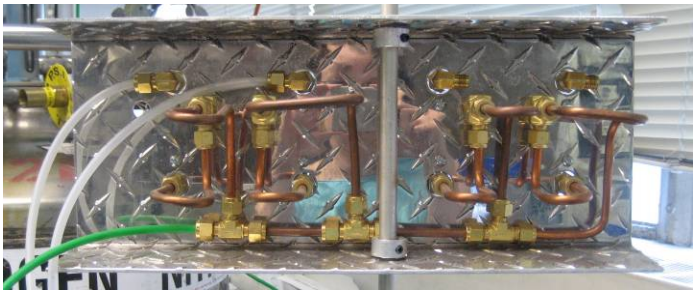

[10] As designed by Dr. Thomas A. Kubic and assembled by the author.

Styrofoam blocks, covered with black paper, were cut to fit the chamber shapes were used to limit the empty space in the sample chamber. All exterior seams on the instrument sample compartment were covered with masking tape to reduce the exposure to humid air. The Dewar was accessed through a split top with a black cap. This set-up allowed access to the Dewar bell to refill with liquid nitrogen and to remove and insert sample tubes without exposing the quartz sample tip to humid air.

Figure 20. Quartz Tipped Dewar

Figure 21. Cary Eclipse sample compartment with Dewar housing.

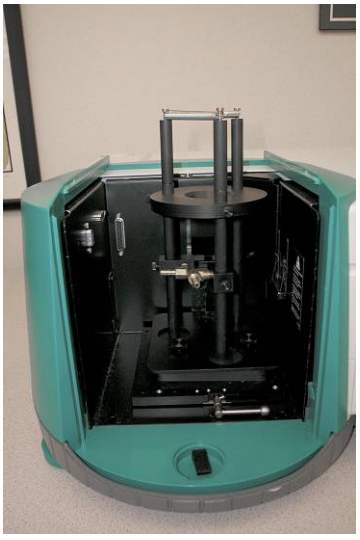

Despite all efforts to limit chamber humidity it was still necessary to keep the flow of dry nitrogen high (1L/min) and to monitor the sample chamber humidity with a relative humidity sensor with digital display. This final design would keep the quartz tip of the Dewar frost free for up to 10 hours and allow the user to do multiple quartz tube sample changes and liquid nitrogen refills. The illustration of this final design are shown in the figures below.

Figure 22. Modified interior for LT Fluorescence (Shown with cuvette holder, Dewar housing not pictured).

Figure 23. Operational View of Low Temperature Set-Up

Careful selection of sample solvent can protect against the effects of a highly scattering solid. Previous work by Kubic and Sheehan found that methylcyclohexane will freeze to a clear solid. When cooled slowly through gradual immersion, a clear frozen glass is obtained. This is shown in Figure 24.

Figure 24. Clear freeze of methylcyclohexane

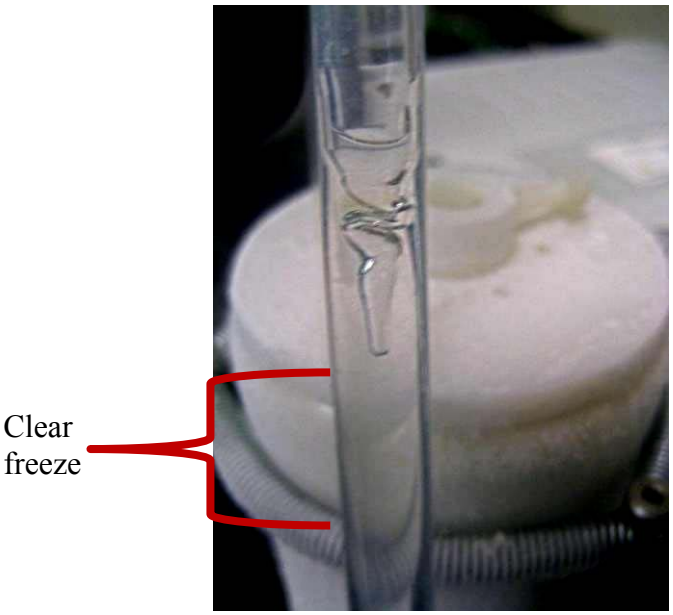

The total data set for low temperature scans of the samples from known vehicle locations equaled 5,400 data files. The ensemble averaged scans (16 single scans of the same sample at the same excitation wavelength averaged automatically) at excitations 235 nm and synchronous scan at Δ 70 nm exhibited the most consistently intense spectra of all the low temperature data collected. Therefore, these two data sets were chosen to examine the usefulness of using spectral library searching for making correct origin associations among transferred vehicle undercarriage residues. Instrumental settings for low temperature fluorescence data collection are shown below in Table 9.

Table 9. Cary Eclipse Settings for Low Temperature Data Collection

Excitation Wavelengths for Toluene extracts (nm)	220, 235, 275
Excitation Wavelengths for Pyridine extracts (nm)	220, 275, 290
Delta setting for Synchronous Scanning	70, 105
Ex Slit	10nm Round
Em Slit	1.5 nm
Scan Rate	600 nm/min
Data Interval	1.00 nm
Averging Time	0.1 sec
Ex Filter	Auto
Em Filter	Auto
PMT	High (800 V)

Because a smaller emission slit was chosen for the low temperature scans, the PMT voltage was changed to High (800 V) to compensate for the decreased spectral bandwidth and total signal. The scan rate and data interval were decreased in order to enhance the resolution gains expected from the lower temperature analysis.

Several deltas were considered for the scans at synchronous settings. Previous work with oils recommended synchronous scanning be performed between Δ 20nm and 30 nm (Lloyd 1971) (VoDinh 1978). Initial runs of oils at Δ23nm, Δ70 nm, Δ90 nm, Δ105 nm at room temperature showed inconsistent results at the four deltas, with the greatest intensity observed at Δ23 nm and Δ70 nm. However, when the extracts from known motor vehicle locations were scanned at liquid nitrogen temperatures there was an overall drop in fluorescence intensity. A review of the room temperature EEMs showed that each known sample exhibited the most intense peaks at an emission wavelength

range between 280 nm to 290 nm (Ex. 220 nm) and a second group of peaks in an emission wavelength range of 330 nm to 340nm (Ex225 nm). Concerned that any Δ setting that did not intersect these peaks would show little-to-no fluorescence emission, I chose to proceed with the settings Δ70 nm and Δ105 nm. Ultimately, this may have been a redundant since these spectral characteristics were already being captured by individual excitation scans.

6. Fluorescence procedure

Low Temperature data collection occurred as a series of scans at three predetermined excitation wavelengths and two Δ λ in synchronous scanning mode. The wavelengths were chosen after review of the EEM matrices determined the areas of most intense fluorescence. Single scans and the average of 16 scans were captured for each excitation wavelength. Figure 25 below shows the increase in signal to noise that results from scan averaging. All analysis was done using the ensemble averaged scan produced from 16 successive excitation scans averaged together. Although spectral details varied among samples, Figure 26 below shows the typical result for the low temperature data collection. Low temperature fluorescence data was collected on all triplicate samples for each motor vehicle undercarriage location.

Figure 25. Low Temperature Data Collection

Single Scan

22BT

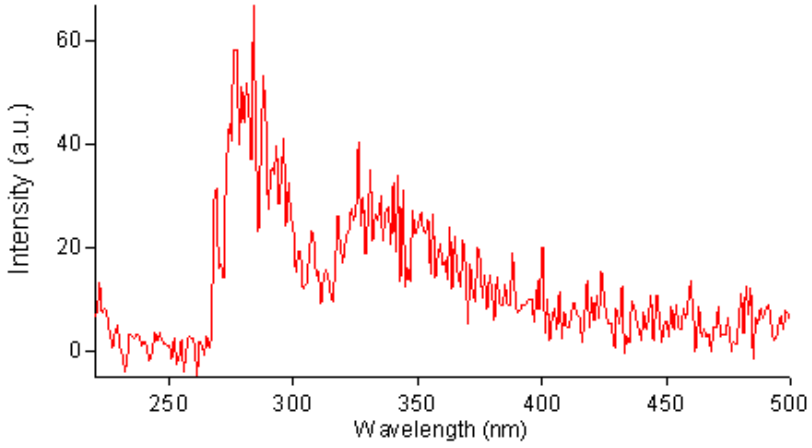

16 scans averaged - 22BT

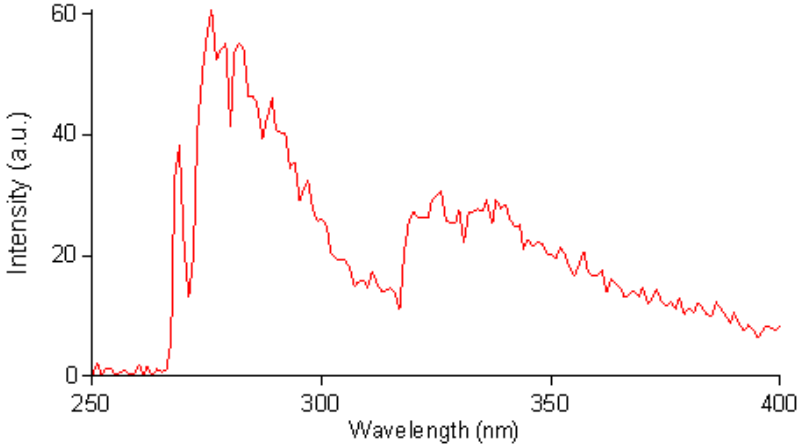

Figure 26. Low Temperature Scans – Full Data Set

24AT

Ex. 220 nm

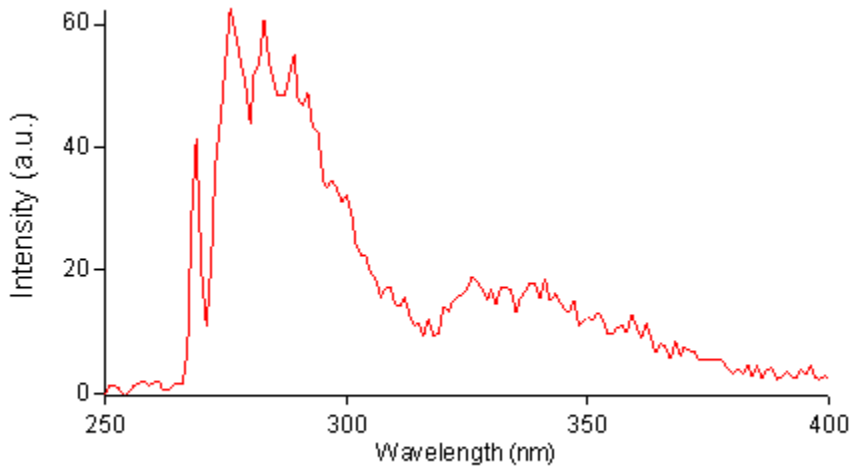

Ex 235 nm

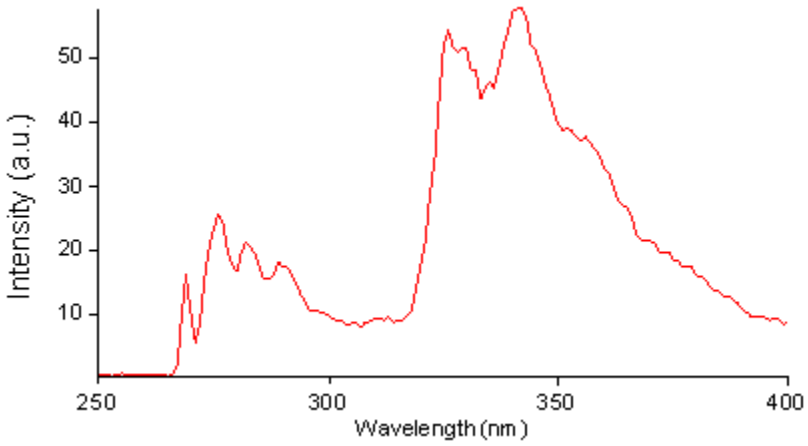

Figure 26. Low Temperature Scans – Full Data Set (continued)

Synch Δ 70

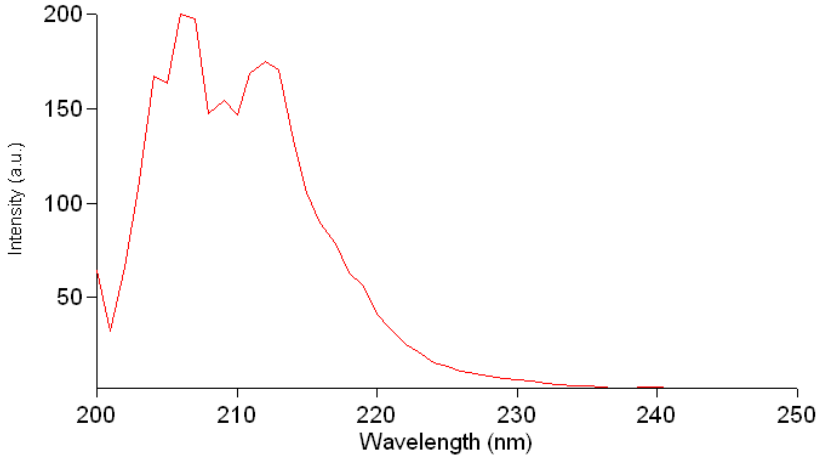

Synch Δ 105

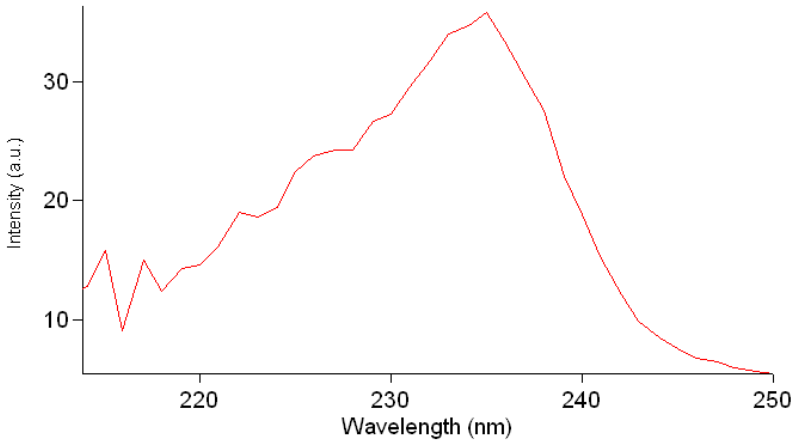

The emission wavelength range for the synchronous scans is 50 nm (200nm – 250 nm).

At this scale and data interval (1nm) it creates a jagged spectral appearance.

Figure 27. 51CT in Dewar at Room Temperature Ex. at 220 nm.

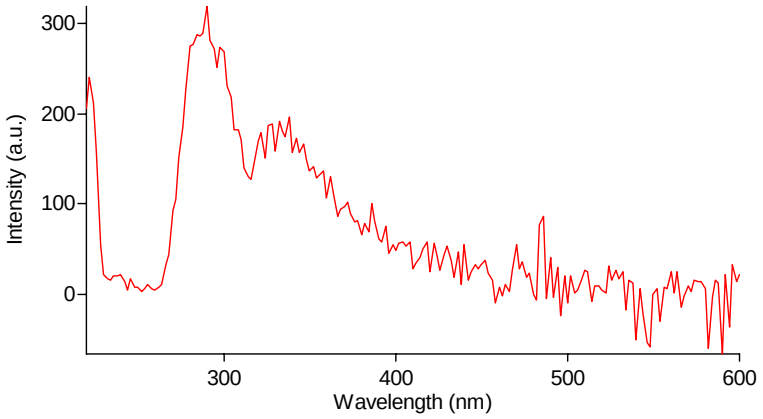

Figure 28. 51 CT in Dewar at 77 K Ex. at 220 nm.

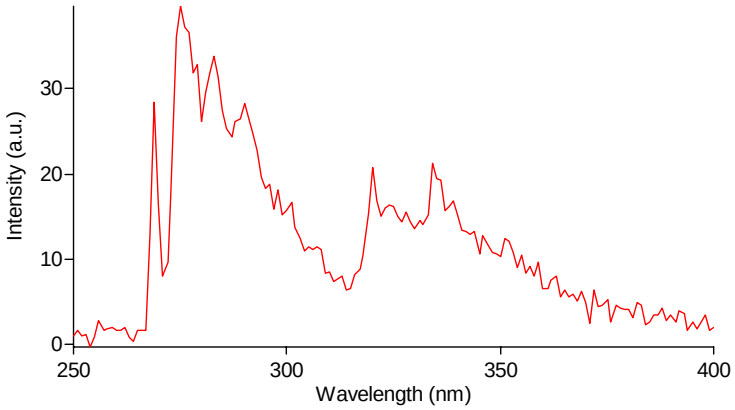

Spectral libraries were constructed using Grams Spectral ID software. All spectra collected at low temperature were converted individually into Grams files with the file extension ".spc". Three libraries were constructed using the emission scans of the toluene

extracts collected at excitation wavelengths 220 nm and 235 nm and with synchronous scan taken at Δ 70 nm. This extract type and these parameters yielded the most consistently intense spectra in the data set. All samples of unknown origin at these excitation and synchronous settings were searched against the libraries.

The Grams Spectral ID software allows for several types of library searches. All searches conducted for this study were correlation searches. The correlation setting uses an algorithm that centers the unknown and the library data about their means before a vector dot product is calculated (Grams/AI Help Resource). This means that the library and unknown spectra do not have to be normalized prior to searching. Upon searching, the unknown and the library entries are ranked by their hit quality index (H. Q. I.) this value represents the numeric rank of each comparison. The H.Q.I. values lie from zero for the best possible match to 1.000 to the worst. The closer the H.Q.I. is to zero, the better the hit.

Results

1. General Material Characteristics

There were observable differences between the residue colors, textures and ease of transfer from vehicle to vehicle. In general, older vehicles yielded greater quantities of transferable undercarriage residues which were more greasy than the residues from younger vehicles. Newer vehicles, especially the BMW 330xi, yielded less material per swab and this material was grittier and less oily than that found older cars. This implies that the tendency to transfer oils and other lubricants may be a function of age, use and vehicle design.

2. General Fluorescence Characteristics

In all fractions the most intense fluorescence was observed at excitations within the wavelength range of 200nm – 250nm. In the excitation wavelength range of 200nm-225nm it was common to find 1 or 2 peaks at emission wavelengths of 285-295 nm. Peaks found in this region of the EEM were labeled “Group A” peaks. In the excitation wavelength range of 225nm-250nm, and 2 additional peaks at emission wavelengths of 334nm and 345nm were observed. Peaks in this region of the EEM were labeled “Group B” peaks. The most intense fluorescence was usually observed in either the Group A or Group B region. All peaks found at excitations above 250nm are described as Region C peaks. While these were usually less intense than the peaks in Group A and B, it was in the Group C region where most of the variation from among samples was found. See Figure 29 below for a graphical representation of this peak grouping.

Figure 29. Region A, B, and C Excitation – Emission Regions. (Item 22A, pentane extract)

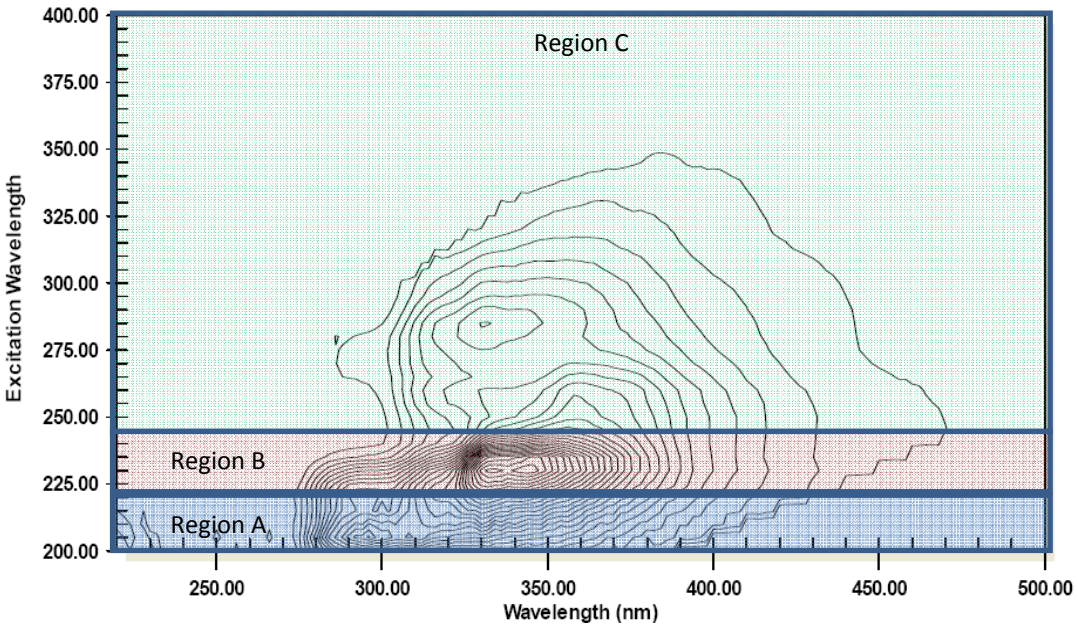

EEM spectra from the pentane and toluene extracts were grouped according to the number of peaks in each group and the excitation/emission λs all peaks present in Group C. After sorting with pentane extracts only, there were 22 unique groups, the largest with 11 vehicle locations and the smallest with 1. Results of this pentane extract peak classification are shown in Table 10.

Table 10. Classification with Pentane Extract EEM Spectra.

ND=None Detected.

Pentane Extract Groups	Sample	No. of Peaks in Group A	No. of Peaks in Group B	No. of Peaks in Group C	Group C Peak 1 (Ex., Em.) nm	Group C Peak 2 (Ex., Em.) nm	Group C Peak 3 Ex., Em.) nm
Group 1	84	1	0	1	258, 283	ND, ND	ND, ND
	72	1	0	1	264, 290	ND, ND	ND, ND
	32	1	0	1	265, 293	ND, ND	ND, ND
	33	1	0	1	269, 312	ND, ND	ND, ND
Group 2	55	1	0	3	266, 304	295, 380	295, 390
Group 3	52	1	1	1	260, 286	ND, ND	ND, ND
	53	1	1	1	266, 300	ND, ND	ND, ND
	81	1	1	1	260, 283	ND, ND	ND, ND
	M19	1	1	1	260, 282	ND, ND	ND, ND
	93	1	1	1	269, 309	ND, ND	ND, ND
	63	1	1	1	291, 383	ND, ND	ND, ND
	54	1	1	1	296, 387	ND, ND	ND, ND
Group 4	M6	1	1	2	260, 283	282, 330	ND, ND
Group 5	101	1	2	0	ND, ND	ND, ND	ND, ND
Group 6	71	1	2	1	268, 312	ND, ND	ND, ND
	64	1	2	1	273, 309	ND, ND	ND, ND
	M46	1	2	1	276, 326	ND, ND	ND, ND
	82	1	2	1	277, 325	ND, ND	ND, ND
	62	1	2	1	280, 324	ND, ND	ND, ND
	65	1	2	1	280, 328	ND, ND	ND, ND
	92	1	2	1	280, 330	ND, ND	ND, ND
	102	1	2	1	280, 329	ND, ND	ND, ND
	M28	1	2	1	280, 328	ND, ND	ND, ND
	21	1	2	1	282, 332	ND, ND	ND, ND
	22	1	2	1	284, 330	ND, ND	ND, ND
Group 7	M36	1	2	2	272, 305	281, 331	ND, ND
Group 8	74	1	3	1	275, 314	ND, ND	ND, ND
Group 9	91	2	0	2	261, 288	278, ND	308, ND
	34	2	0	2	270, 295	270, ND	309, ND
	104	2	0	2	280, 305	286, 356	ND, ND

Table 10. Classification with Pentane Extract EEM Spectra. (continued)

Group 10	85	2	1	1	260, 385	ND, ND	ND, ND
	41	2	1	2	262, 288	270, 321	ND, ND
	94	2	1	1	265, 337	ND, ND	ND, ND
	105	2	1	1	268, 301	ND, ND	ND, ND
	31	2	1	1	269, 312	ND, ND	ND, ND
	42	2	1	1	273, 323	ND, ND	ND, ND
	M29	2	1	2	279, 293	279, 310	ND, ND
	23	2	1	0	ND, ND	ND, ND	ND, ND
Group 11	75	2	2	0	ND, ND	ND, ND	ND, ND
	51	2	2	0	ND, ND	ND, ND	ND, ND
Group 12	83	2	2	1	271, 319	ND, ND	ND, ND
	24	2	2	1	275, 321	ND, ND	ND, ND
	13	2	2	1	276, 334	ND, ND	ND, ND
	103	2	2	1	276, 308	ND, ND	ND, ND
	12	2	2	1	278, 323	ND, ND	ND, ND
	43	2	2	1	280, 330	ND, ND	ND, ND
	M12	2	2	1	280, 328	ND, ND	ND, ND
	M24	2	2	1	280, 330	ND, ND	ND, ND
Group 13	11	2	2	2	260, 326	280, 328	ND, ND
	14	2	2	2	260, 296	282, 330	ND, ND
	73	2	2	2	274, 315	295, 377	ND, ND
Group 14	44	2	3	2	280, 308	281, 354	ND, ND
Group 15	45	2	3	0	ND, ND	ND, ND	ND, ND
Group 16	15	3	2	1	279, 323	ND, ND	ND, ND
Group 17	95	3	1	2	274, 313	260, 371	ND, ND
Group 18	61	3	1	1	281, 328	ND, ND	ND, ND
Group 19	25	4	1	2	254, 332	282, 328	ND, ND
Group 20	35	4	0	1	275, 310	ND, ND	ND, ND
Group 21	M10	4	2	2	256, 322	277, 322	ND, ND
Group 22	M40	4	2	1	275, 317	ND, ND	ND, ND

The same process was used with the EEM spectra obtained from the toluene extracts. After sorting with the toluene extracts only, there are 25 unique groups, the largest with 5 vehicle locations and the smallest with 1. Results of this classification are shown in Table 12 .

Table 11. Classification with Toluene Extract EEM Spectra

Toluene Extract Groups	Sample	No. of Peaks in Group A	No. of Peaks in Group B	No. of Peaks in Group C	Group C Peak 1 (Ex., Em.) nm	Group C Peak 2 (Ex., Em.) nm	Group C Peak 3 (Ex., Em.) nm
Group 1	105	1	1	1	260, 281	ND, ND	ND, ND
	M46	1	1	1	262, 308	ND, ND	ND, ND
	43	1	1	1	281, 333	ND, ND	ND, ND
	M36	1	1	1	281, 333	ND, ND	ND, ND
	22	1	1	1	287, 350	ND, ND	ND, ND
Group 2	M29	1	1	0	ND, ND	ND, ND	ND, ND
Group 3	33	1	1	2	260, 285	283, 336	ND, ND
	44	1	1	2	261, 284	282, 338	ND, ND
	15	1	1	2	262, 319	284, 332	ND, ND
	55	1	1	2	264, 288	285, 338	ND, ND
	21	1	1	2	286, 330	287, 350	ND, ND
Group 4	83	1	1	3	367, 311	280, 332	286, 346
Group 5	M10	1	2	0	ND, ND	ND, ND	ND, ND
Group 6	104	1	2	1	258, 281	ND, ND	ND, ND
	M40	1	2	1	262, 285	ND, ND	ND, ND
	101	1	2	1	275, 233	ND, ND	ND, ND
	13	1	2	1	282, 337	ND, ND	ND, ND
	75	1	2	1	285, 338	ND, ND	ND, ND
Group 7	M19	1	3	2	260, 287	280, 379	ND, ND
	54	1	3	2	262, 282	289, 380	ND, ND
Group 8	65	1	2	2	264, 340	282, 334	ND, ND
	102	1	2	2	268, 341	284, 331	ND, ND
	74	1	2	2	270, 314	277, 330	ND, ND
Group 9	63	1	2	3	259, 280	286, 331	290, 347
	41	1	2	3	263, 287	263, 338	285, 341

Table 11. Classification with Toluene Extract EEM Spectra (continued)

Group 10	11	2	1	1	267, 292	ND, ND	ND, ND
	14	2	1	1	267, 392	ND, ND	ND, ND
Group 11	35	2	1	2	260, 287	284, 338	ND, ND
	42	2	1	2	262, 288	284, 338	ND, ND
	71	2	1	2	259, 380	285, 340	ND, ND
	72	2	1	2	257, 282	285, 340	ND, ND
Group 13	82	2	1	4	256, 318	261, 329	261, 349
Group 14	84	2	1	1	284, 337	ND, ND	ND, ND
	85	2	1	1	282, 323	ND, ND	ND, ND
	103	2	1	1	258, 280	ND, ND	ND, ND
Group 15	92	2	1	2	262, 285	284, 335	ND, ND
	M28	2	1	2	270, 346	276, 352	ND, ND
Group 16	M12	2	1	0	ND, ND		
Group 17	23	2	2	1	295, 427	ND, ND	ND, ND
	24	2	2	1	280, 331	ND, ND	ND, ND
	34	2	2	1	270, 292	ND, ND	ND, ND
	45	2	2	1	266, 288	ND, ND	ND, ND
	95	2	2	1	262, 375	ND, ND	ND, ND
Group 18	31	2	2	2	265, 288	275, 330	ND, ND
	51	2	2	2	266, 288	288, 347	ND, ND
	53	2	2	2	262, 285	286, 340	ND, ND
	62	2	2	2	264, 288	285, 340	ND, ND
Group 19	M24	2	3	0	ND, ND	ND, ND	ND, ND
Group 20	73	3	1	0	ND, ND	ND, ND	ND, ND
Group 21	52	3	1	1	262, 288	ND, ND	ND, ND
	81	3	1	1	282, 338	ND, ND	ND, ND
Group 22	32	3	1	3	269, 285	281, 315	281, 335
	64	3	1	3	265, 293	285, 336	287, 348
Group 23	61	3	2	3	264, 288	285, 337	287, 348
	91	3	2	3	259, 315	259, 323	279, 331
Group 24	94	3	2	*6	261, 276	332, 276	435, 298

Table 11. Classification with Toluene Extract EEM Spectra (continued)

Group 25	25	4	2	0	ND, ND	ND, ND	ND, ND
	93	4	2	1	261, 332	ND, ND	ND, ND
Group 26	M6	4	1	0	ND, ND	ND, ND	ND, ND

The classifications performed using the pentane and toluene extracts were combined to achieve maximum discrimination. Each sample was labeled using a two value code; the first number is the pentane group and the second is the toluene group. These two numbers are shown for each sample below in Table 12. The undistinguished pairs are shown in gray.

Table 12. Coded samples using EEM peak number and position.

Sample ID #	Pentane Group	Toluene Group
33	1	3
72	1	11
84	1	13
32	1	21
55	2	3
54	3	7
M19	3	7
63	3	9
53	3	17
52	3	20
81	3	20

Table 12. Coded samples using EEM peak number and position (continued).

93	3	24
M6	4	25
101	5	6
22	6	1
M46	6	1
21	6	3
65	6	8
102	6	8
71	6	11
82	6	12
92	6	14
M28	6	14
62	6	17
64	6	21
M36	7	1
74	8	8
104	9	6
34	9	16
91	9	22

Table 12. Coded samples using EEM peak number and position (continued).

105	10	1
M29	10	2
41	10	9
11	10	10
42	10	11
85	10	13
23	10	16
31	10	17
94	10	23
13	11	6
75	11	6
24	11	16
51	11	17
12	12	1
43	12	1
83	12	4
103	12	13
M12	12	15
M24	12	18
14	13	10
73	13	19

Table 12. Coded samples using EEM peak number and position (continued).

44	14	3
45	15	16
15	16	3
95	17	16
61	17	22
25	18	24
35	19	11
M10	20	5
M40	20	6

Five pairs, shaded gray in Table 12, were indistinguishable using this method. Two of these pairs contain a known sample with sample of unknown origin. When the origin key was consulted it is found that one pair (M46 and 22) are incorrectly grouped together. Unknown M46 is not from vehicle 2 (Ford Bronco XLT) A second pair M19 and 54 were correctly grouped. They share a common origin. Unknown M19 is from vehicle 5 (Honda Accord). None of the other samples of unknown origin were correctly

identified using this classification method. Nine of the ten samples of unknown origin were not grouped with the known sample that came from the same vehicle location.

Since much of the variation between samples occurs in the Group C region of the EEM spectra, a second grouping scheme was used that relies solely on that peak number and position information was performed. This scheme did not result in improved associations.

Table 13 shows the results from the pyridine extract sample group. These data were not used in the classification scheme since so many of the EEMs exhibited very weak intensities. This made the identification of peaks in the Group A region (200 nm – 225 nm) impossible to determine from 19 of the knowns and 5 of the unknowns.

Table 13. Classification with Pyridine Extract EEM Spectra.

Pyridine Extract Groups	Sample	No. of Peaks in Group A	No. of Peaks in Group B	No. of Peaks in Group C	Group C Peak 1 (Ex., Em.) nm	Group C Peak 2 (Ex., Em.) nm	Group C Peak 3 (Ex., Em.) nm
Group 1	13	0	1	1	285, 342	ND, ND	ND, ND
Group 2	M10	0	1	2	260, 320	280, 327	ND, ND
Group 3	15	0	2	2	304, 380	304, 415	ND, ND
Group 4	22	0	2	1	390, 450	ND, ND	ND, ND
Group 5	81	1	1	3	260, 326	280, 331	203, 317
Group 6	102	1	2	1	280, 340	ND, ND	ND, ND
	14	1	2	1	280, 451	ND, ND	ND, ND
Group 7	M40	1	2	2	270, 310	273, 313	ND, ND
Group 8	73	2	1	1	265, 328	ND, ND	ND, ND
	23	2	1	1	280, 408	ND, ND	ND, ND
	65	2	1	1	280, 330	ND, ND	ND, ND
	82	2	1	1	280, 306	ND, ND	ND, ND
	M36	2	1	1	280, 328	ND, ND	ND, ND
	54	2	1	1	290, 320	ND, ND	ND, ND
Group 9	21	2	1	2	286, 340	303, 458	ND, ND
	64	2	1	2	260, 323	282, 343	ND, ND
	M28	2	1	2	259, 228	280, 230	ND, ND
Group 10	11	2	2	0	ND, ND	ND, ND	ND, ND
Group 11	42	2	2	1	284, 312	ND, ND	ND, ND
	55	2	2	1	279, 327	ND, ND	ND, ND
	M12	2	2	1	259, 332	ND, ND	ND, ND
Group 12	53	2	3	1	262, 318	ND, ND	ND, ND
Group 13	95	3	1	1	256, 370	ND, ND	ND, ND
	52	3	1	1	280, 310	ND, ND	ND, ND
Group 14	24	3	2	2	280, 312	280, 328	ND, ND
Group 15	74	3	2	1	275, 328	ND, ND	ND, ND
	75	3	2	1	287, 342	ND, ND	ND, ND

Table 13. Classification with Pyridine Extract EEM Spectra. (continued)

Group 16	63	4	1	1	282, 339	ND, ND	ND, ND
Group 17	92	4	1	2	258, 320	283, 332	ND, ND
	62	4	1	2	270, 320	279, 330	ND, ND
Group 18	104	4	2	2	265, 318	294, 351	ND, ND
Group 19	12	4	3	2	269, 345	280, 450	ND, ND
Group 20	83	4	3	3	260, 315	260, 323	280, 324
Group 21	61	6	1	2	259, 329	279, 331	ND, ND
Group 22	M24	ND	1	0	ND, ND	ND, ND	ND, ND
Group 23	M29	ND	1	1	258, 320	ND, ND	ND, ND
	45	ND	1	1	274, 322	ND, ND	ND, ND
	31	ND	1	1	280, 310	ND, ND	ND, ND
	32	ND	1	1	280, 310	ND, ND	ND, ND
	35	ND	1	1	280, 310	ND, ND	ND, ND
	25	ND	1	1	283, 330	ND, ND	ND, ND
Group 24	44	ND	1	2	260, 325	282, 347	ND, ND
	M19	ND	1	2	262, 318	290, 311	ND, ND
Group 25	M6	ND	2	0	ND, ND	ND, ND	ND, ND
Group 26	101	ND	2	1	258, 320	ND, ND	ND, ND
	72	ND	2	1	260, 323	ND, ND	ND, ND
	33	ND	2	1	280, 310	ND, ND	ND, ND
	34	ND	2	1	280, 310	ND, ND	ND, ND
	51	ND	2	1	385, 360	ND, ND	ND, ND
Group 27	41	ND	2	2	259, 324	260, 310	ND, ND
	94	ND	2	2	259, 325	278, 312	ND, ND
	71	ND	2	2	260, 323	286, 314	ND, ND
Group 28	93	ND	3	3	260, 317	279, 317	283, 311
Group 29	103	ND	4	3	260, 321	273, 336	285, 402
Group 30	105	ND	ND	1	257, 320	ND, ND	ND, ND
	84	ND	ND	1	259, 323	ND, ND	ND, ND
	85	ND	ND	1	260, 317	ND, ND	ND, ND
	91	ND	ND	1	260, 323	ND, ND	ND, ND
	M46	ND	ND	1	260, 313	ND, ND	ND, ND

The spectral classification scheme based on peak number and position proved to be highly distinguishing but not reproducible in this case. Combination of data from pentane and toluene extracts uniquely identified all but 5 pairs of samples. One of these pairs shared a common origin. However, this classification scheme was not successful at correctly associating the knowns with the samples of unknown origin. This could be due to the fact that known and unknown sample concentrations were adjusted using residue weight rather than HPLC data. Differences in concentration of fluorescing components are known to cause wavelength shifting. Samples at low concentrations could have experienced loss of smaller secondary peaks. If the unknown and the known exhibit different concentrations of fluorescing compounds they would be incorrectly grouped using a system that relies on peak number as well as peak position to classify spectra. This could also be due to the sample origins having a high degree of heterogeneity at the sample source itself. Every care was taken to ensure that the multiple swabs from the same vehicle location were applied evenly to the same areas. If the areas touched by the swabs varied in their composition of fluorescing compounds in that area then two swabs from the same vehicle location may contain very different compounds. This could occur if the original motor vehicle undercarriage residues exist as a layer or heterogeneous mixture were the sample composition could vary by grease-layer depth. A variation in the spectral classification scheme which relied only on Group C peaks (i.e. those at excitation λs above 250) did not yield more accurate results.

3. Low Temperature Fluorescence

The discriminating power of the fluorescence spectra from the low temperature data collection were determined using spectral libraries constructed using Grams Spectra ID software. Three libraries were constructed from the data generated from the toluene extracts; one at excitation wavelength 220 nm , a second at excitation wavelength 235 nm and a third at synchronous scanning Δ 70 nm.[11]

All 10 unknowns at each excitation (or synchronous) setting were searched against the libraries. Using the library of spectra collected at excitation 220 nm, 2 of the 10 unknowns were identified to the correct motor vehicle (M19 associated to 51A and 54A, M10 associated to 84C) in the top three library search results. And 1 of those associations was to the correct motor vehicle location (M19 and known 54A). Using the library of spectra collected at excitation 235 nm, 3 of the 10 unknowns were associated to the correct motor vehicle (M29 associated to 41A, M06 associated to 42A, M24 associated to 42A) in the top three results and 1 of those associations was to the correct motor vehicle specific location (M29 and known 41A). Using the library of spectra collected at synchronous Δ70 nm, 3 of the 10 unknowns were associated with the correct motor vehicle (M46 associated to 81A, M19 associated to 55A, and M24 associated to 41A) in the top three library search results. One of those associations was to correct motor vehicle location (M29 and known 41A). No other unknown was associated with

[11] The spectra generated at low temperature from the pyridine extracts were not used due their weak fluorescence intensity and their similarity to the peaks seen on the spectra from the toluene extracts.

their correct source motor vehicle. These results, along with the H.Q.I. values are summarized in the table below. The closer the H.Q.I value. is to zero, the better the library match.

Figure 30. Summary of hits obtained using spectral libraries. (Yellow = library search result to correct vehicle, pink = library search result to correct vehicle and specific location).

	Ex. 220nm		Ex. 235 nm		Δ 70	
	MV Location	H. Q. I.	MV Location	H. Q. I.	MV Location	H. Q. I.
M19	51A	0.037595	33A	0.034737	105C	0.193519
	14C	0.04079	41A	0.039597	41A	0.193519
	54A	0.043603	43C	0.042814	55A	0.194749
M40	43C	0.010982	33A	0.015491	81A	0.211121
	42C	0.016132	41A	0.017078	33B	0.212594
	54C	0.016327	74C	0.02427	53A	0.213347
M29	103B	0.010294	33A	0.012905	41A	0.131694
	11B	0.010406	81A	0.018088	105C	0.132507
	14A	0.011237	41A	0.025181	55A	0.136528
M10	52C	0.077357	41C	0.357834	55A	0.585036
	84C	0.086463	32C	0.039889	91A	0.585536
	53B	0.093352	33B	0.040026	54A	0.588557
M06	53C	0.029646	52A	0.033286	81A	0.36348
	23C	0.02987	42A	0.036255	105C	0.3657
	82B	0.029872	33B	0.036751	94B	0.3676
M24	61B	0.010009	52A	0.037216	105C	0.386102
	64A	0.014316	34C	0.037803	94B	0.387406
	63A	0.015576	42A	0.03991	41A	0.387497

Interestingly, the one unknown that was correctly grouped with its exact motor vehicle source location with the comparison of EEM fluorescence spectra, M19, was also associated to the correct location (car 5 location 4) using the excitation = 220 nm spectral library. This indicates that the two methods are comparably ineffective at making correct associations between known and unknown. It should be noted that the top three library search results for each unknown as shown in the table above, rarely show matches to multiple samples from the same location. One would expect the triplicate swabs (i.e. the three swabs from the same vehicle and location) would be grouped together in the library search result list regardless of their overall position on that list. Since, this did not occur, it indicates that there is a fair amount of heterogeneity among the triplicate swabs taken from the same location. This could be due to actual compositional differences if the motor vehicle lubricants components vary with lubricants layer depth and are not a homogeneous mixture. Future studies should investigate alternative methods of residue collection designed to reduce this variability and collect more representative and homogeneous samples.

4. Characterization Using the HPLC Results

As previously stated, the chromatograms produced from extract solutions from triplicate swabs (i.e. three swabs from the same vehicle location) demonstrated excellent reproducibility and inter-vehicle-location variability in peak size, retention time and size and shape of the unresolved envelope. However, the technique was not used to determine concentration prior to fluorescence due to solvent incompatibility issues. The

chromatograms produced from the swabs of unknown origin were compared to these known sets on four criteria and the outcomes reported in the results section. Comparisons of the knowns to the samples of unknown origin were based on both numeric (peak retentions time) and spatial (unresolved envelope shape) characteristics. The table below shows each unknown and the predicted vehicle origins from the HPLC data and the actual origins as documented in the unknown key created by Ms. Grimly. The results show 7 of 10 correct associations made to vehicles with 6 of 10 to exact to the specific location on that vehicle. This data exhibits far better associative results than those achieved from the examination of peak number and position of EEM plots. This is especially remarkable considering that these data were collected in a solvent system designed for complete elution and maintenance of a stable baseline rather than optimum peak resolution and qualitative analysis.

Table 14. Determination of Unknown Residue Origin Using HPLC Data.

	Actual Origin		Predicted with HPLC data	
Unknown	Origin Motor Vehicle (MV)	Origin MV location	Predicted Motor Vehicle (MV)	Predicted MV location
M46	07 Ford Escort	071 Right Ball Joint	02 Ford Bronco II XLT	024 Engine Oil Pan
			09 Chevrolet Cavalier RS	091,092 R & L Ball Joints
M40	08 BMW 740 iL	083 Front Skid Guard	08 BMW 740 iL	083 Front Skid Guard
M36	06 Mercury Marquis	064 Engine Oil Pan	06 Mercury Marquis	064 Engine Oil Pan
				063 Undercarriage Position 1
M29	04 Ford Taurus	041 Right Ball Joint	04 Ford Taurus	041 Right Ball Joint
M12	01 GMC Denali	015 Undercarriage Position 2	01 GMC Denali	011 Left Ball Joint
				012 Right Ball Joint
				014 Undercarriage Position 1
				015 Undercarriage Position 2
M28	06 Mercury Marquis	061 Right Ball Joint	02 Ford Bronco II XLT	025 Under Radiator
M19	05 Honda Accord	054 Undercarriage Position 1	05 Honda Accord	055 Undercarriage Position 2
M10	08 BMW 740 iL	081 Right Ball Joint	08 BMW 740 iL	081 Right Ball Joint
M6	04 Ford Taurus	044 Under Radiator	05 Honda Accord	051 Right Ball Joint
M24	04 Ford Taurus	043 Engine Oil Pan	04 Ford Taurus	043 Engine Oil Pan

Number of correct vehicle associations = 7 of 10.

Number of correct vehicle location associations = 6 of 10.

Discussion

In this study, three analytical data sets were collected: room temperature EEM fluorescence, low temperature excitation and synchronous averaged scans at selected wavelengths, and chromatograms from the pentane extracts. Of those three, the chromatographic data exhibited the most agreement among triplicate swabs from the same motor vehicle location and more importantly, the best ability to associate motor vehicles of an unknown origin to the known collected from the same motor vehicle location.

Conclusion 1

Three-dimensional fluorescence spectroscopy, as performed in this experiment, and collected at room temperature, of motor vehicle undercarriage residues is highly distinguishing but unreliable for the successful association of residues of unknown origin to their source motor vehicles by the methods employed in this study.

Excitation-emission matrices are excellent representations of the overall fluorescence emission characteristics of a material. The ability to display data at multiple excitation wavelengths as a contour plot is a simple way to represent a large amount of spectral data. This type of data presentation is best suited to observe gross characteristics of fluorescence spectra (e.g. the number and position of multiple peaks at multiple wavelengths). It is not suitable for the representation of fine spectral detail. In this study, fluorescence EEMs were not a good tool to distinguish among motor vehicle residues with similar compositions from different sources.

Regarding the usefulness of this technique to distinguish among motor vehicle residues, an analogy can be made between the motor vehicle grease residues and the highly complex mixtures encountered during the analysis of ignitable liquid residues (ILRs) from fire debris. Ignitable liquid residues are multicomponent mixtures produced mostly from the refining of petroleum, that through use and exposure are subject to degradation and weathering. Gas chromatography – mass spectrometry (GC/MS) is the preferred analytical instrumentation for ILRs because it performs the separation of complex mixtures and supplies the mass spectral data necessary to identify compounds. If GC/MS is not available, the GC with a flame ionization detector will be able to identify many of the known ILRs through comparison of chromatographic patterns. Complex mixtures are not suitable for analysis by mass spectrometry alone. As chromatographic separation is more useful than the spectral data for the identification of ILRs of unknown origin, the same appears to be true of motor vehicle undercarriage residues.[12]

Effectiveness of the Extraction Method

The three-solvent extraction system was adopted in order to separate the motor vehicle residues into three distinct compound classes. In all extracts, the peaks in the Group A and B regions were the most intense and the variations peak λ maxima were not consistent among extracts from different solvents. This indicates that the three solvent extraction system did not result in three fractions with different groups of fluorophores.

[12] This analogy is not meant to equate mass and optical spectral data, just their usefulness in analyzing complex mixtures.

The Group C region of the EEM (excitations above 250nm) exhibited some spectral differences from in each extraction type. Ultimately, the fluorescence spectra data set from the successive three-solvent extraction system did not successfully associate the ten samples of unknown origin with the motor vehicles of origin.

Since the overall fluorescence intensity decreased with each successive extraction type (pentane → toluene → pyridine) along with the number of peaks observed, I advise that future research proceed with a single extraction procedure designed to maximize extractions of fluorescing compound types. Figure 31 shows how the fluorescence intensity of the most intense peak observed in the excitation emission matrix changed with each extraction.

Figure 31. Percentage of EEMs collected and the distribution of Fluorescent intensities. N=50

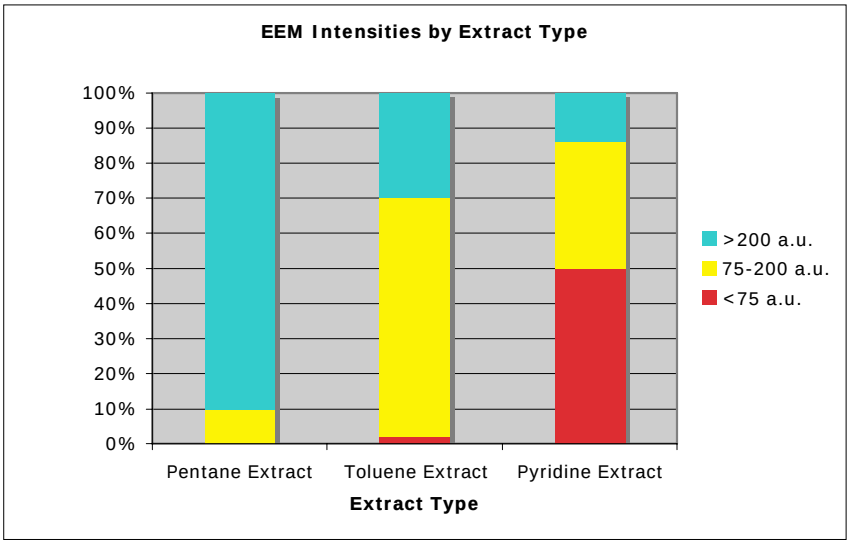

This decrease in intensity seen from the first extraction (pentane) to the third (pyridine) could be due to two factors. First, the three solvent extraction system successfully separated the motor vehicle residues in the oil, asphaltene and pre-asphaltene fractions and fluorescence component of the total extract residue decreased with each class of compounds. Or, second, the extraction system was not successful at the separation by compound class and the total fluorescing component of the motor vehicle undercarriage residue was unevenly distributed among the three fractions. Since no qualitative analysis of individual compounds in each fraction was performed it is not possible to opine on the actual components of the extractions. The fact that all three extract types exhibited their major peaks at the same excitation ranges (200 nm – 250 nm) that all three contained similar compound types, however, the less intense peaks present in the group C region (>250 nm) indicate compositional differences between the pyridine extracts and the other two solvent extracts.

Conclusion 2

In this study, adjusting concentration of extract residue solutions based on residue mass (e.g. w/w ppm) did not adjust all the fluorescing components of each triplicate swab to the same concentration.

Using total residue weights to bring motor vehicle undercarriage residues from the sample source location to a common concentration did not result in common fluorescent intensities among samples from the same source. It was thought that if the ratio of fluorescence compounds was the same in each swab from the same motor vehicle

location, then adjusting concentration based on to the total extract mass would also bring the fluorescing compounds to a common concentration. Since the fluorescent intensities of the major peaks in spectra from each triplicate sample were not the same, this was not the case.

Without adjusting the concentration of the fluorescencing compounds alone it is not possible to know if weak fluorescence emission observed in one sample, but not in another, is due to the compositional or concentration differences. This could lead to false exclusions in very dilute samples.

Conclusion 3

In the conditions used in this study, low temperature fluorescence emission scans, collected at 77K, of motor vehicle undercarriage residues exhibit increased resolution but are not reliable for the successful association of residues of unknown origin to their source motor vehicles.

The spectra collected at 77K exhibited increased resolution. This technique has some specific challenges. The sample compartment must be kept at extremely low humidity and dry nitrogen gas must flow at all times onto the tip of the Dewar in order to keep it frost free. The long sample tubes require an extensive cleaning procedure to ensure no sample carryover. After each cleaning, the tubes were scanned with the sample solvent to ensure that there was no carry-over from one sample to the next. The tubes

themselves are subject to breakage if the frozen solution is warmed too quickly. Clear freezes are only accomplished if the tube itself is lowered very slowly into the liquid nitrogen. Despite these disadvantages, the apparatus itself is very useful for generating spectra of increased resolution. However the observed increase in resolution did not result in an increased ability to distinguish among motor vehicle undercarriage residues, nor did it allow for a more successful association of the unknown residues with their respective source vehicles.

Conclusion 4

In this study, chromatography of motor vehicle undercarriage residues was better than room temperature or low temperature fluorescence spectroscopy at both discriminating among vehicle locations and making correct associations between samples of known origin and samples of unknown origin.

The successful associations made using the chromatographic data (7/10 unknown origin vehicles and 6/10 unknown vehicle locations) have important implications for future research. These data were produced primarily to determine concentration. They were not collected under conditions meant to optimize resolution and specific peak identification. The primary goal was to accomplish complete elution of all compounds injected to avoid carryover and then use total peak areas to represent overall concentration. Solvent incompatibility between the low temperature apparatus and the

HPLC system resulted in the a design shift to determine concentration by residue weights instead. The chromatographic data set exhibited poor peak resolution but excellent reproducibility among triplicate knowns and variation in chromatographic patterns between knowns. As a result the chromatographic data was more useful as a means to associate samples of unknown origin to their source vehicles rather than as a means to adjust concentration.

Conclusion 5

The low temperature apparatus, as designed, can be used to successfully generate fluorescence spectra that exhibit greater resolution than room temperature measurement.

The low temperature apparatus, after extensive modification and testing, can be used to produce fluorescence spectra with better resolution than room temperature data collection. Once frozen, the rigid matrix successfully inhibits band broadening due to non-radiative relaxation of excited fluorophores. This increase in resolution was accompanied by a decrease in fluorescence intensity.

The low temperature apparatus was successfully used to generate spectra with better resolution. This technique would be very useful to research projects that aim to better understand the specific electronic transitions that occur during fluorescence

emission. Future work with low temperature fluorescence for characterization of motor vehicle residues should proceed once a Dewar is obtained that can maintain a single freeze, without refilling the Dewar, for at least 30 minutes. This will provide enough time to obtain an excitation emission matrix data set for each sample. Low temperature work in this study was limited to the collection of scans at several excitation wavelengths. This did not provide the spectral detail necessary to successfully distinguish between motor vehicles nor did it provide enough information to make successful associations among all the samples of unknown origin and known samples using spectral library searching software. Additionally, future work should investigate alternative fluorescence instrumentation available to collect fluorescence spectra at low temperature.

Recommendation 1

I recommend that future research not use fluorescence excitation emission matrices, collected under the parameters used in this study, to distinguish among motor vehicles undercarriage residues until a suitable method is developed to establish the concentration of fluorescent materials in the sample. Basing sample concentration on the mass of all compounds extracted, as opposed to, relative amount of fluorescence compounds does not result in spectra of similar fluorescent intensity for samples from the same source motor vehicle.

Recommendation 2

Based on the results of these experiments, I do not recommend that low temperature fluorescence be used to distinguish among different sources of automotive undercarriage residue until a more reliable method of determining sample concentration is developed, most likely though a chromatographic process, and until an instrument design is identified that better suits the needs of the quartz-tipped Dewar.

This work confirms the recommendation made by Purcell about the concentration adjustments necessary to sample prior to collection of fluorescence spectral data. Residue weights are not ideal as they do not represent the overall concentration of the fluorescing compounds in the sample. Chromatographic methods that are more compatible with the solvent needs of low temperature analysis are necessary.

Recommendation 3

Future work should use HPLC with fluorescence detection to characterize motor vehicle undercarriage residues.

If successful associations can be made using a simple isocratic elution method with single wavelength UV absorbance detection methods, then it stands to reason that improvements in individualization will be obtained at conditions of higher chromatographic resolution and sensitivity. I recommend that future work be done using

HPLC with fluorescence detection. A fluorescence detection system would provide a better sensitivity than UV absorbance detection.

Impact on Criminal Justice and Forensic Science Policy and Practice

The contribution of this research to the field of forensic science is the advancement of knowledge about the analytical techniques applied to a long-observed transferable material, motor vehicle undercarriage residue, to attempt to create associations between automobiles and persons or objects. When the best analytical technique is identified, these associations can be used to help the trier of fact determine the likelihood that a specific automobile came into contact with a person or object. This project illustrates the inability of room temperature three dimensional fluorescence spectroscopy and low temperature two dimensional fluorescence spectroscopy to discriminate among transferred petroleum materials. This type of evidence can be found in "hit and run" type vehicular crimes.

Analysis of transfer evidence is one of the oldest and most challenging types of forensic analysis due to the limitless number of material types that may transfer between persons and/or objects during the commission of a criminal act. (Houck, 2001) The vast majority of the resources provided to forensic science laboratories and forensic science researchers through federal funding are put towards the forensic disciplines that are able to identify suspects through direct associations (i.e. DNA and fingerprints) (NAS, 2009).

While there is no doubt that both are very powerful investigative tools, the narrowing field-of-view by both funders and criminal justice researchers could have the unforeseen consequence of the underdevelopment of new and novel transfer evidence analysis techniques.

Transfer evidence is highly variable in composition and mode of transfer. The analyst must master a myriad of identification and quantification methods in order to proficiently analyze physical evidence. This research sought to add tools to the forensic chemist's arsenal in order to expand the impact of this forensic discipline. The conclusions of this project and the recommendations made for future research expand the body of knowledge about this form of transfer evidence and about the lessons one can apply from traditional oil and grease analysis.

This project is one of many that have investigated the discriminating power of an instrumental technique on a specific class of materials. Motor vehicle undercarriage residues have been observed as transferred materials in casework but are not routinely reported as a subset of forensic chemistry (Durose, 2008). The conclusions of this research project may be used to guide future research that continues to seek the optimal analytical tools needed to distinguish among motor vehicle undercarriage residues. Once future research identifies that method, more forensic laboratories may include oil and grease analysis in their forensic chemistry sections, thereby increasing the evidentiary

value of this physical evidence type as well as the impact of transfer evidence analysis on criminal investigations and prosecutions.

Summary

Overall, the fluorescence and chromatographic techniques used to differentiate transferred vehicle undercarriage residue from different vehicle locations and to associate samples of unknown origin with the correct source vehicle have been produced results of varying reliability. Chromatographic data proved to be more reliable than spectral data for this purpose. In this study and with the instrumentation used, the EEM contour plots collected at room temperature with overlapping excitation scans produced sufficient variation to differentiate most motor vehicle samples but did not successful associate most the unknown samples. The single scans taken at low temperature exhibited increased peak resolution than room temperature scans but the spectral detail in the five wavelengths collected (three excitation and two synchronous) were not sufficient to differentiate most samples through visual comparison alone. In this study, searching with spectral libraries produced increased differentiation but were also not more successful than visual examination of room temperature EEMs at the correct association of unknowns with known vehicle locations. It would be advantageous to combine the EEM data collection with the increased resolution of the low temperature environments. Any future work using fluorescence EEM to distinguish among motor vehicle undercarriage residues should utilize alternative fluorescence spectrometers that allow the user to have greater control over instrument parameters. Most surprising was the ability of

chromatographic data, collected under isocratic conditions, to correctly associate most of the unknown motor vehicle residues while exhibiting excellent reproducibility among the triplicate samples. Future work in this area should focus on the use of HPLC coupled with fluorescence detection to combine the best of each of these methods to differentiate among transferred vehicle petroleum products.

Appendices

A. Unknown Labeling Scheme

B. Cary Eclipse Specifications

C. Pentane Extract Chromatograms

D. Pentane Extract Contour Plots

E. Toluene Extract Contour Plots

F. Pyridine Extract Contour Plots

Original Set D	Unknown Code
11	M25
12	M37
13	M22
14	M32
15	M12
21	M01
22	M30
23	M17
24	M23
25	M39
31	M14
32	M38
33	M03
34	M08
35	M26
41	M29
42	M34
43	M24
44	M6
45	M41
51	M27
52	M45
53	M49
54	M19
55	M13
61	M28
62	M11
63	M20
64	M36
65	M50
71	M46
72	M35
73	M18
74	M44
75	M48
81	M10
82	M15
83	M40
84	M31
85	M42
91	M2
92	M43
93	M47
94	M04
95	M33
101	M21
102	M9
103	M7
104	M5
105	M16

Appendix B. Cary Eclipse Specifications

Cary Eclipse Specifications:

Monochromators

Excitation: Czerny-Turner, f3.6, 0.125 m focal length,

Emission: Czerny-Turner, f3.6, 0.125 m focal length,

Gratings

Excitation: 30 x 35 mm, 1200 l/mm, blaze at 370 nm,

Emission: 30 x 35 mm, 1200 l/mm, blaze at 440 nm

- All reflective optical system with quartz over-coated optics.
- Schwarzschild source optics for increased energy throughput and precise imaging and focusing.
- 80 data points per second maximum measurement rate in fluorescence mode.
- non- measurement phase stepping wavelength drive.
- room light immunity in fluorescence mode,
- Source Xenon pulse lamp with exceptionally long lifetime, pulsed at 80 Hz. Pulse width at half peak height ~ 2 µs, peak power equivalent to 75 kW.

Wavelength range (nm)

Mechanical

Excitation: 190 to 1100 nm. Zero order selectable.

Emission: 190 to 1100 nm. Zero order selectable.

Operational

Excitation: 200 to 900 nm with standard PM tube. Zero order selectable.

Emission: 200 to 900 nm with standard PM tube. Zero order selectable.

Wavelength accuracy (nm) ± 1.5 nm

Wavelength reproducibility (nm) ± 0.2 nm

Detectors

High performance R928 photomultiplier detector and separate R928 PMT

for reference signal.

Sensitivity (Raman Band of Water)

>500:1 RMS, 500 nm excitation, excitation and emission slits 10 nm, 1 sec Signal Averaging time. >750:1 RMS, 350 nm excitation, excitation and emission slits 10 nm, 1 sec Signal Averaging time.

* RUN # 24 JAN 1, 1901 08:43:19

START

101A

RUN# 24 JAN 1, 1901 08:43:19

AREAX

RT	AREA	TYPE	WIDTH	AREA%
.634	2228	PU	.073	16.00000
.752	4539	UU	.144	32.59605
.945	7158	UU	.192	51.40397

* RUN # 25 JAN 1, 1901 08:54:37

START

101B

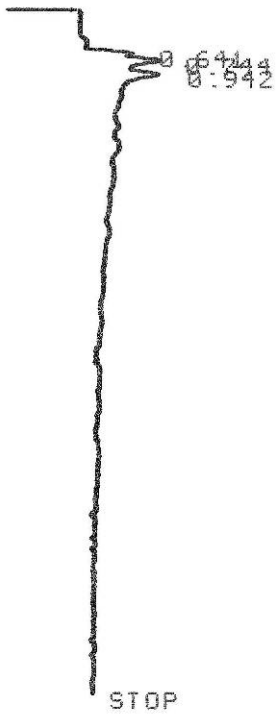

RUN# 25 JAN 1, 1901 08:54:37

AREA%

RT	AREA	TYPE	WIDTH	AREA%
.641	2489	PU	.067	13.61449
.744	7742	UU	.132	42.34766
.942	8051	UU	.156	44.03786

* RUN # 26 JAN 1, 1901 09:05:55

START

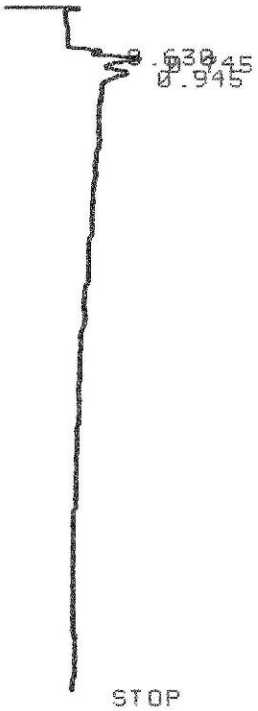

101C

RUN# 26 JAN 1, 1901 09:05:55

AREA%

RT	AREA	TYPE	WIDTH	AREA%
.630	1574	PU	.064	12.08167
.745	6089	UU	.117	46.73779
.945	5365	UU	.155	41.18053

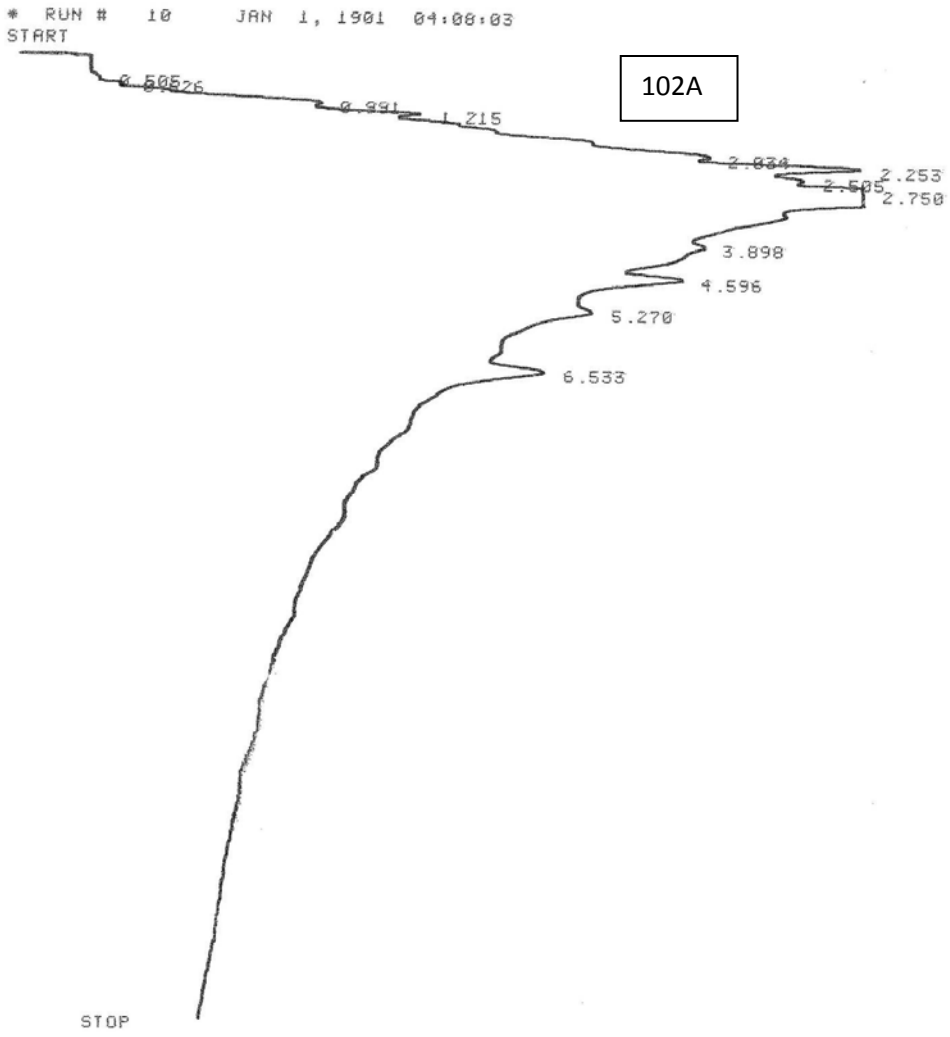

RUN# 10 JAN 1, 1901 04:08:03

AREA%

RT	AREA	TYPE	WIDTH	AREA%
.505	389	PP	.098	.01889
.626	1467	PU	.062	.07125
.991	54305	UU	.232	2.63745
1.215	60914	UU	.182	2.95843
*2.034	385839	UU	.625	18.73919
*2.253	199357	UU	.255	9.68225
*2.505	124023	UU	.179	6.02347
*2.750	657457	UU	.302	31.93097
3.898	260195	UU	.569	12.63699
4.596	168049	UU	.450	8.16170
5.270	131018	UU	.628	6.36320
*6.533	15982	BP	.190	.77620

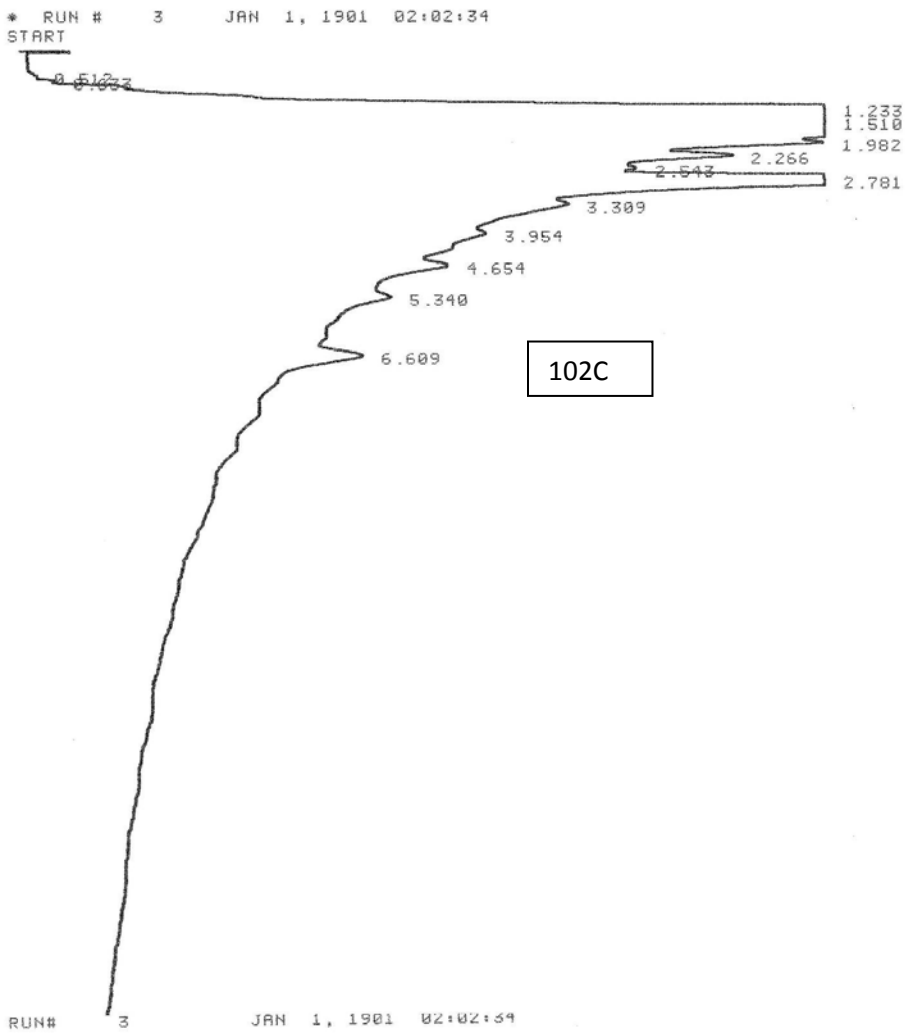

RUN# 3 JAN 1, 1901 02:02:34

AREA%

	RT	AREA	TYPE	WIDTH	AREA%
	.512	616	BV	.109	.01688
	.633	1687	VV	.065	.04623
	1.233	468292	VV	.226	12.83314
	1.510	828615	VV	.431	22.70750
a	1.982	216106	VV	.225	5.92220
b	2.266	233179	VV	.280	6.39008
c	2.543	108160	VV	.154	2.96403
d	2.781	580332	VV	.328	15.90351
	3.309	332261	VV	.561	9.10534
	3.954	281794	VV	.604	7.72233
	4.654	220710	VV	.558	6.04837
	5.340	217691	VV	.723	5.96564
e	6.609	159638	VV	.711	4.37475

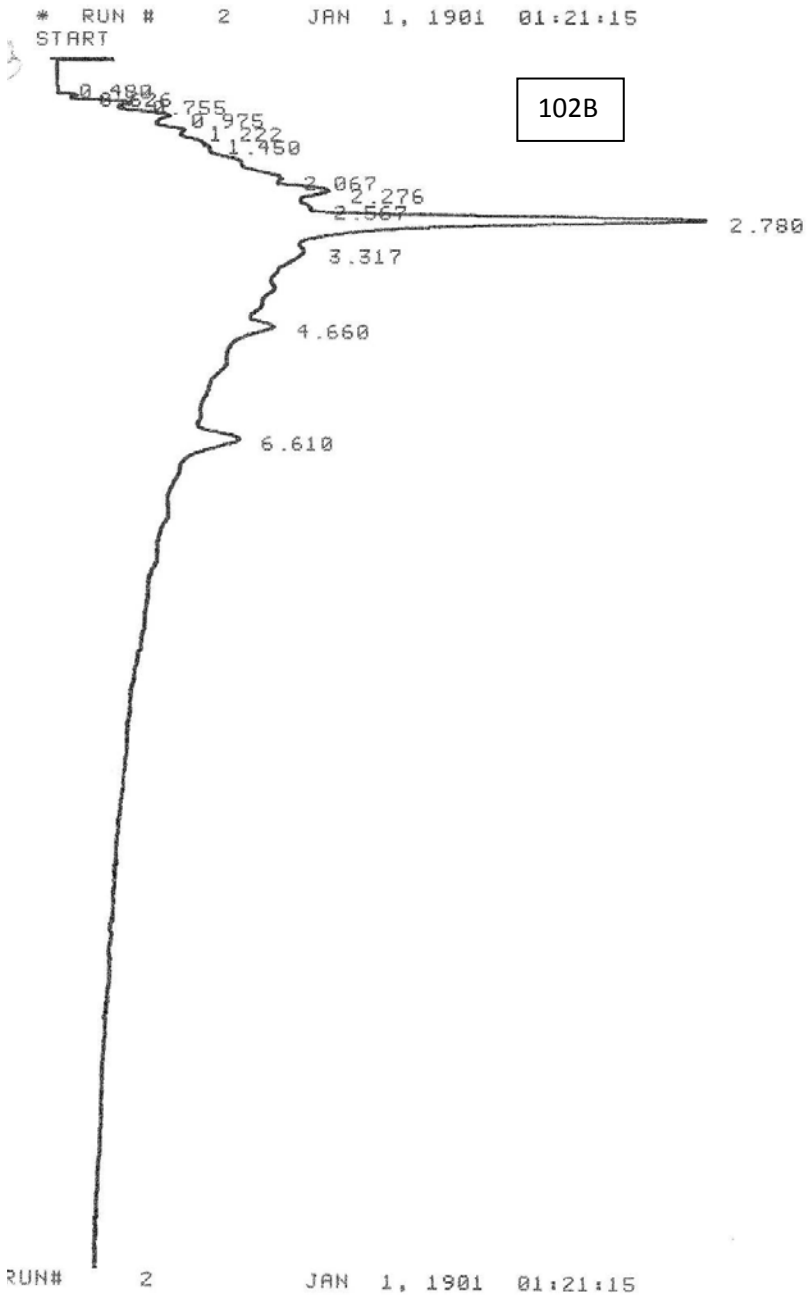

RUN# 2 JAN 1, 1901 01:21:15

AREA%

	RT	AREA	TYPE	WIDTH	AREA%
	.480	136	PB	.046	.02479
	.626	1239	BV	.060	.22585
	.755	8081	VV	.113	1.47304
	.975	22141	VV	.216	4.03595
	1.222	17764	VV	.162	3.23809
	1.450	22591	VV	.187	4.11797
*	2.067	84648	VV	.480	15.42996
*	2.276	57161	VV	.263	10.41952
*	2.567	32105	VV	.171	5.85222
*	2.780	179637	VV	.308	32.74491
	3.317	80915	VV	.523	14.74950
	4.660	26415	VV	.361	4.81503
*	6.610	15762	VP	.304	2.87316

* RUN # 29 JAN 1, 1901 09:39:49

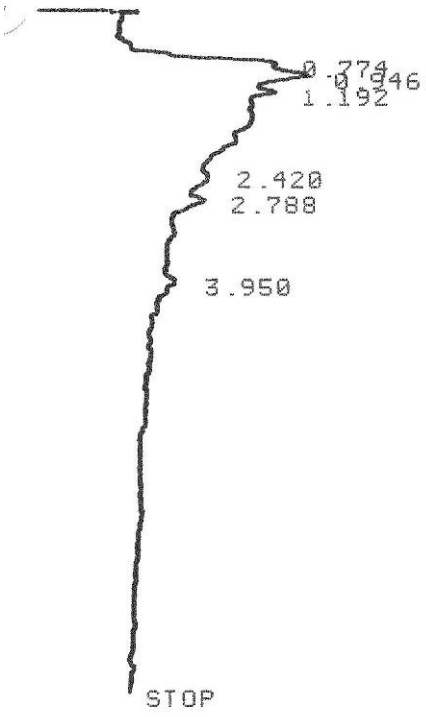

103C

RUN# 29 JAN 1, 1901 09:39:49

AREA%

RT	AREA	TYPE	WIDTH	AREA%
.774	19286	VV	.148	15.55234
.946	40770	VV	.260	32.87718
1.192	22249	VV	.175	17.94173
2.420	21047	VV	.328	16.97242
2.788	15679	VV	.276	12.64364
3.950	4976	VV	.188	4.01268

* RUN # 28 JAN 1, 1901 09:28:31

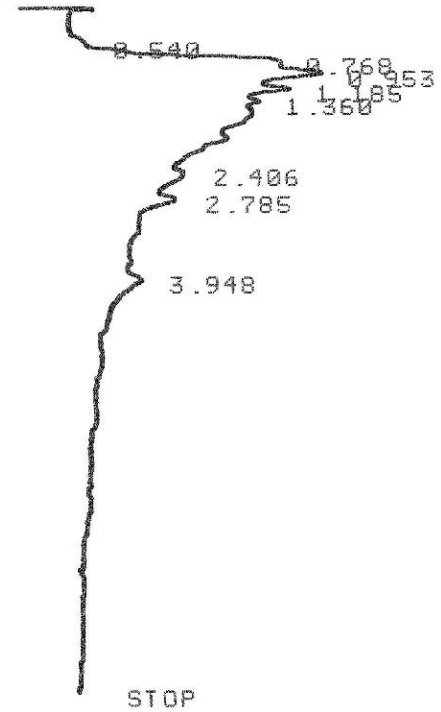

103B

RUN# 28 JAN 1, 1901 09:28:31

AREA%

RT	AREA	TYPE	WIDTH	AREA%
.540	1969	VV	.133	.97755
.768	21389	VV	.120	10.61900
* .953	59721	VV	.278	29.64969
* 1.185	29771	VV	.161	14.78041
1.360	22580	VV	.143	11.21029
* 2.406	27486	VV	.315	13.64597
* 2.785	23577	VV	.302	11.70528
* 3.948	14929	VV	.363	7.41180

* RUN # 27 JAN 1, 1901 09:17:14

START

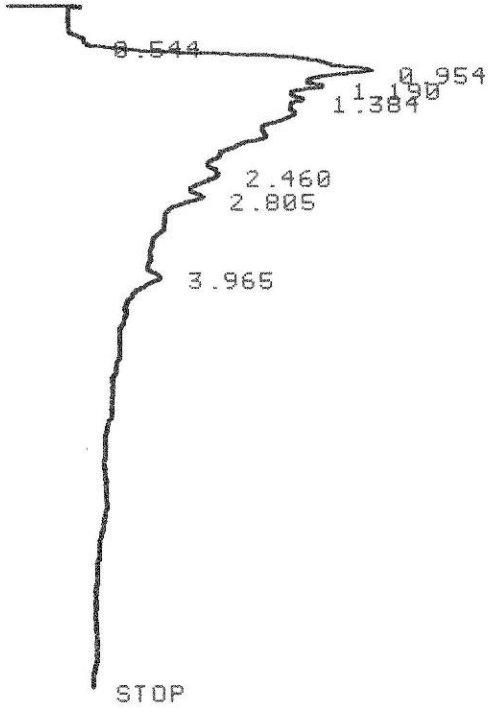

103A

RUN# 27 JAN 1, 1901 09:17:14

AREA%

RT	AREA	TYPE	WIDTH	AREA%
.544	1757	BV	.123	.72380
.954	95531	VV	.376	39.35430
1.190	34451	VV	.162	14.19220
1.384	30965	VV	.161	12.75614
2.460	36324	VV	.335	14.96379
2.805	27977	VV	.305	11.52522
3.965	15741	VV	.352	6.48456

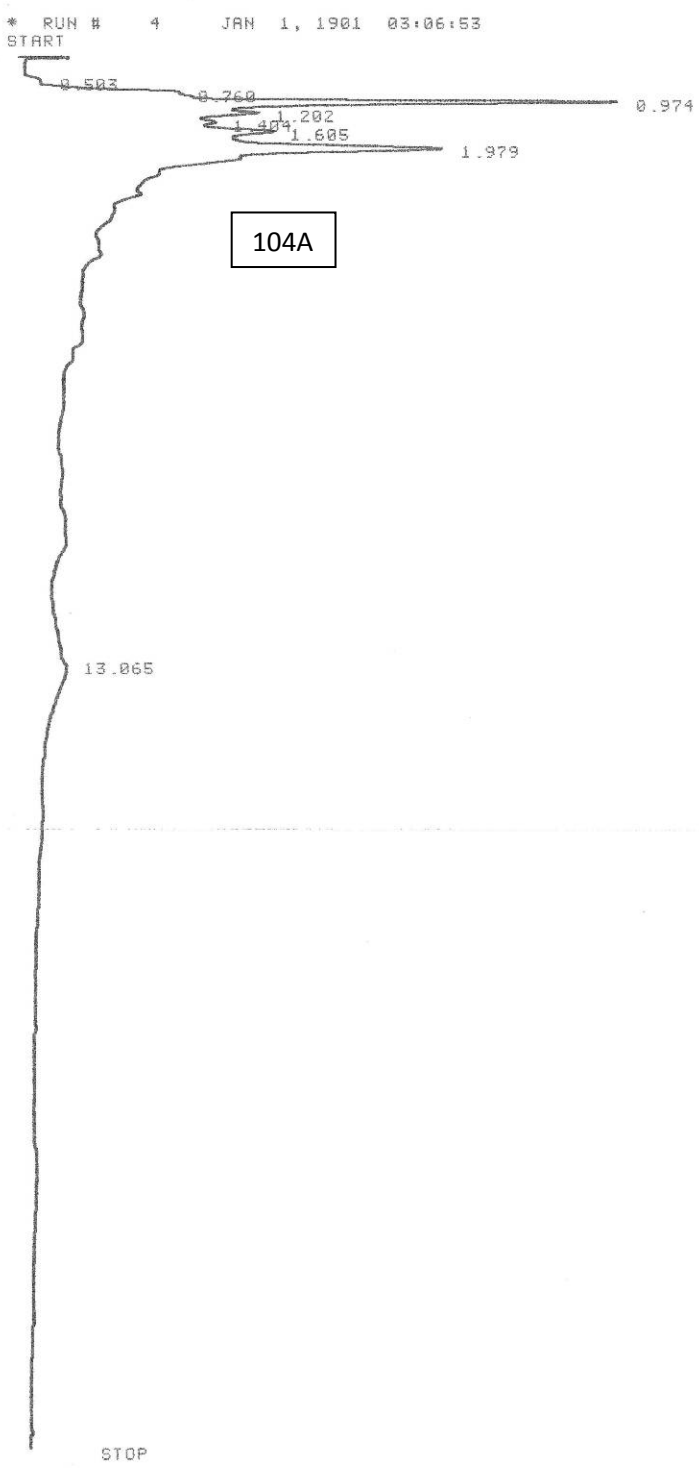

RUN# 4 JAN 1, 1901 03:06:53

AREA%

	RT	AREA	TYPE	WIDTH	AREA%
	.503	160	PB	.029	.04054
	.760	18389	PU	.105	4.65875
#	.974	121475	VV	.166	30.77498
	1.202	42470	VV	.163	10.75962
*	1.404	28735	VV	.144	7.27985
	1.605	57020	VV	.214	14.44569

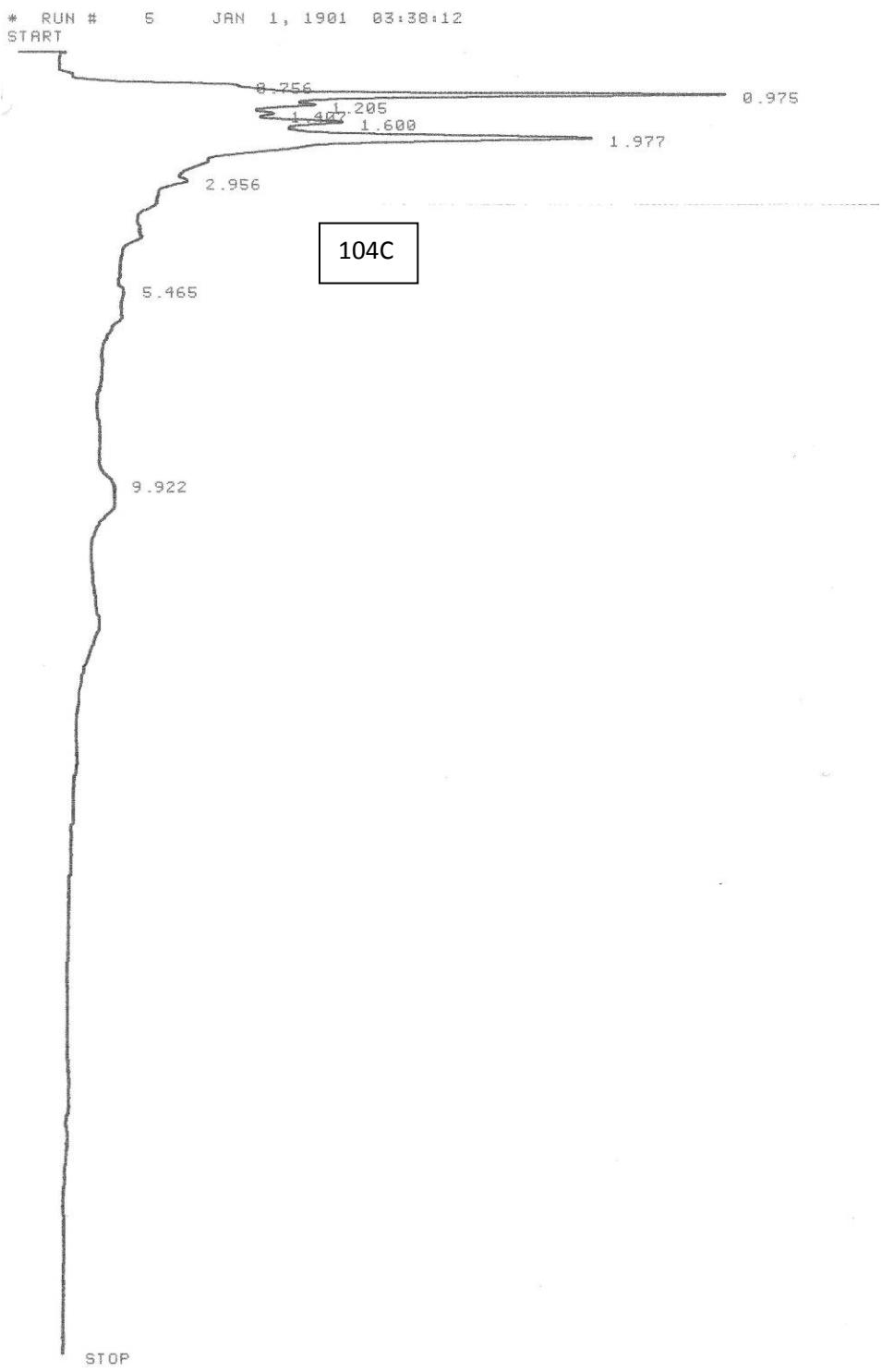

RUN# 5 JAN 1, 1901 03:38:12

AREA%

	RT	AREA	TYPE	WIDTH	AREA%
	.756	23377	PU	.103	4.04090
*	.975	157724	VV	.181	27.26384
	1.205	49990	VV	.162	8.64116
*	1.407	35541	VV	.145	6.14354
	1.600	70457	VV	.214	12.17905
*	1.977	223390	VV	.344	38.61472
	2.956	16147	VV	.247	2.79114
	5.465	71	PB	.028	.01227
	9.922	1813	VV	.232	.31339

```
*  RUN #    10      JAN  1, 1901  01:58:38
START
```

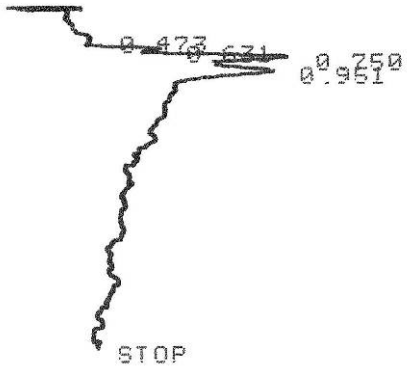

105A

```
RUN#     18           JAN  1, 1901  01:58:38

AREA%
        RT       AREA TYPE  WIDTH      AREA%
    *.473        1331   VV   .163    4.13444
     .631        2501   VV   .071    7.76877
    *.750       11050   VV   .125   34.32424
    *.951       17311   VV   .219   53.77256
```

* RUN # 5 JAN 1, 1901 00:36:35

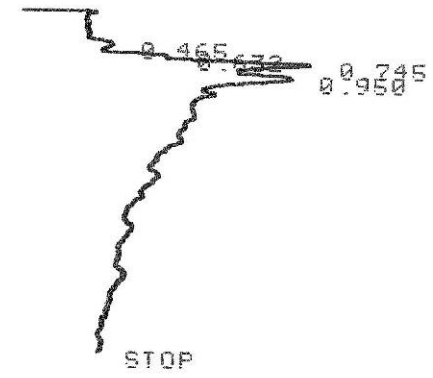

105B

RUN# 5 JAN 1, 1901 00:36:35

AREA%

RT	AREA	TYPE	WIDTH	AREA%
.465	1137	PU	.116	3.51849
.632	1731	UU	.057	5.35665
.745	13176	UU	.146	40.77363
.950	16271	UU	.205	50.35123

TOTAL AREA= 32315

* RUN # 19 JAN 1, 1901 02:04:56

START

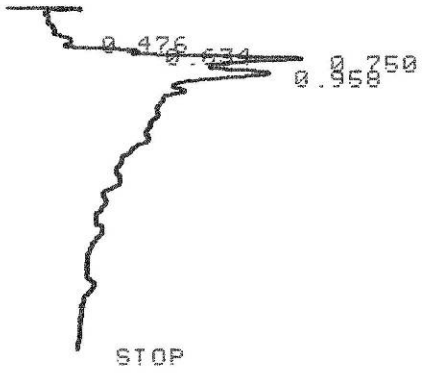

105C

RUN# 19 JAN 1, 1901 02:04:56

AREA%

	RT	AREA	TYPE	WIDTH	AREA%
v	.476	1207	VV	.130	3.17966
	.634	2332	VV	.065	6.14331
v	.750	14714	VV	.139	38.76186
v	.958	19707	VV	.219	51.91518

TOTAL AREA= 37960

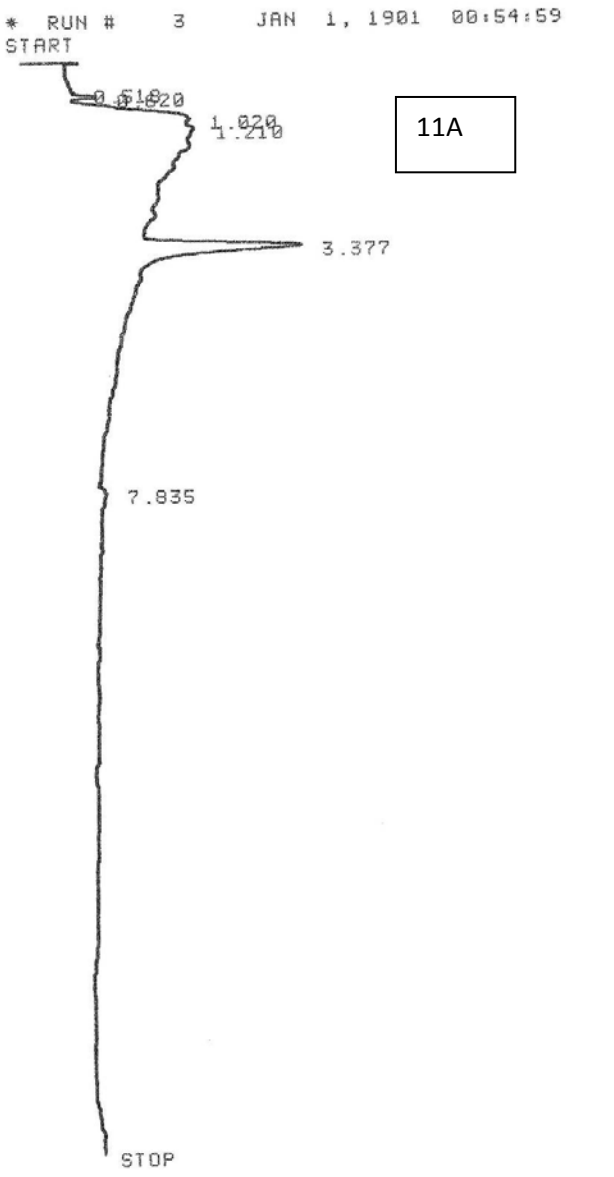

11A

RUN# 3 JAN 1, 1901 00:54:59

AREA%

RT	AREA	TYPE	WIDTH	AREA%
.518	985	PU	.219	.81147
.620	1859	UP	.064	1.53149
1.020	35151	PU	.283	28.95826
1.210	32075	UU	.253	26.42419
3.377	50754	UU	.251	41.81242
7.835	561	PB	.111	.46217

* RUN # 6 JAN 1, 1901 02:05:32
START

11B

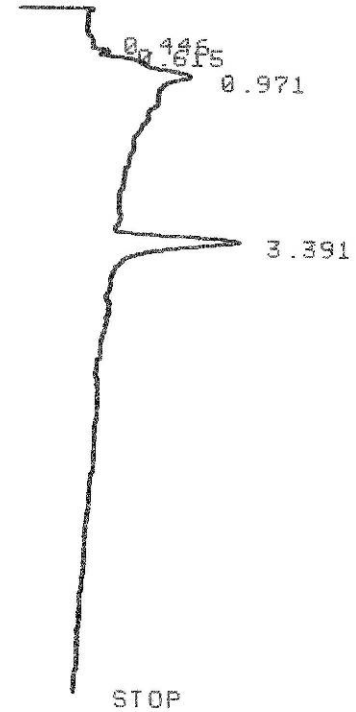

RUN# 6 JAN 1, 1901 02:05:32

AREA%

RT	AREA	TYPE	WIDTH	AREA%
.446	491	PU	.105	1.01965
.615	783	VV	.056	1.62603
* .971	24596	VV	.329	51.07779
*.3.391	22284	PP	.207	46.27653

```
* . RUN #   10      JAN  1, 1901  02:50:46
START
```

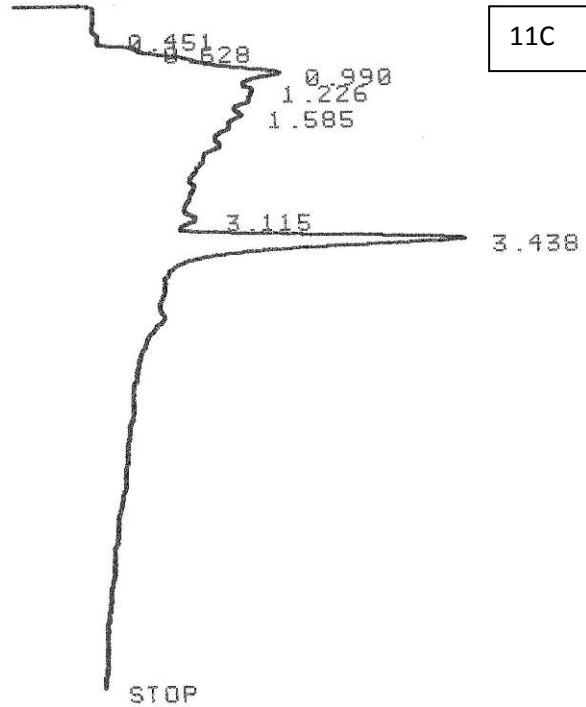

11C

```
RUN#    10           JAN  1, 1901  02:50:46

AREA%
       RT       AREA TYPE  WIDTH      AREA%
     .451        945   PU   .144      .45774
     .628       2459   VV   .065     1.19110
   * .990      52568   VV   .336    25.46307
   . 1.226     25279   VV   .191    12.24473
    1.585      23138   VV   .193    11.20766
   . 3.115     17882   VV   .255     8.66175
   * 3.438     84177   VV   .285    40.77394

TOTAL AREA= 206448
MUL FACTOR=1.0000E+00
```

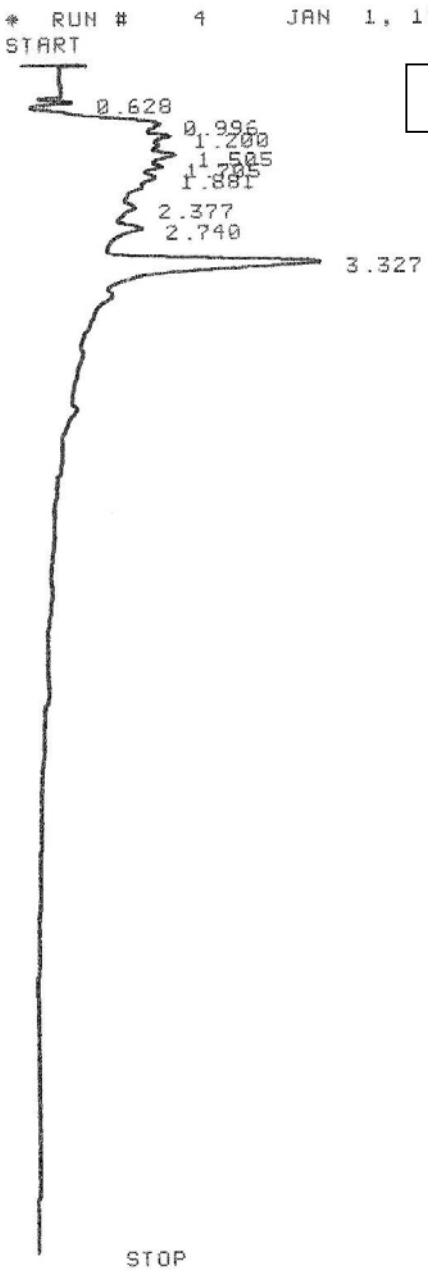

RUN# 4 JAN 1, 1901 01:16:17

AREA%

RT	AREA	TYPE	WIDTH	AREA%
.628	2377	VP	.062	.90440
* .996	31780	PU	.254	12.09170
.1.200	20332	VV	.152	7.73595
1.505	28266	VV	.208	10.75468
1.705	17959	VV	.148	6.83307
1.881	21357	VV	.187	8.12594
2.377	26719	VV	.299	10.16608
2.740	35817	VV	.385	13.62770
. *3.327	78218	VV	.295	29.76048

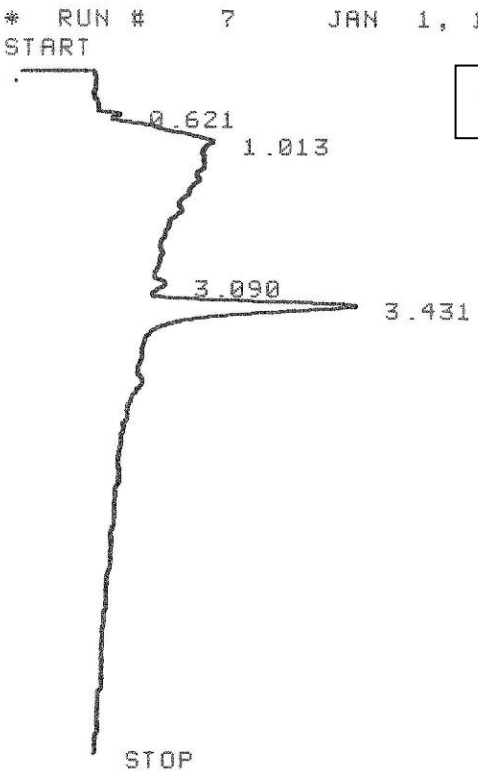

RUN# 7 JAN 1, 1901 02:16:51

AREA%

	RT	AREA	TYPE	WIDTH	AREA%
	.621	1238	PU	.065	1.72495
*	1.013	30666	VV	.344	42.72816
	3.090	1723	BV	.135	2.40072
*	3.431	38143	VV	.212	53.14614

* RUN # 11 JAN 1, 1901 03:02:05

START

12C

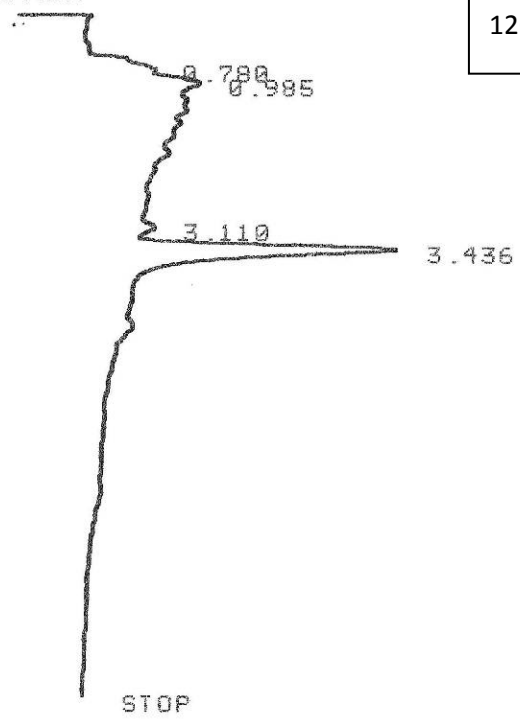

RUN# 11 JAN 1, 1901 03:02:05

AREA%

	RT	AREA	TYPE	WIDTH	AREA%
	.780	9039	PU	.181	11.01887
*	.985	22620	UU	.265	27.57460
	3.110	2115	BU	.147	2.57826
*	3.436	48258	UU	.214	58.82827

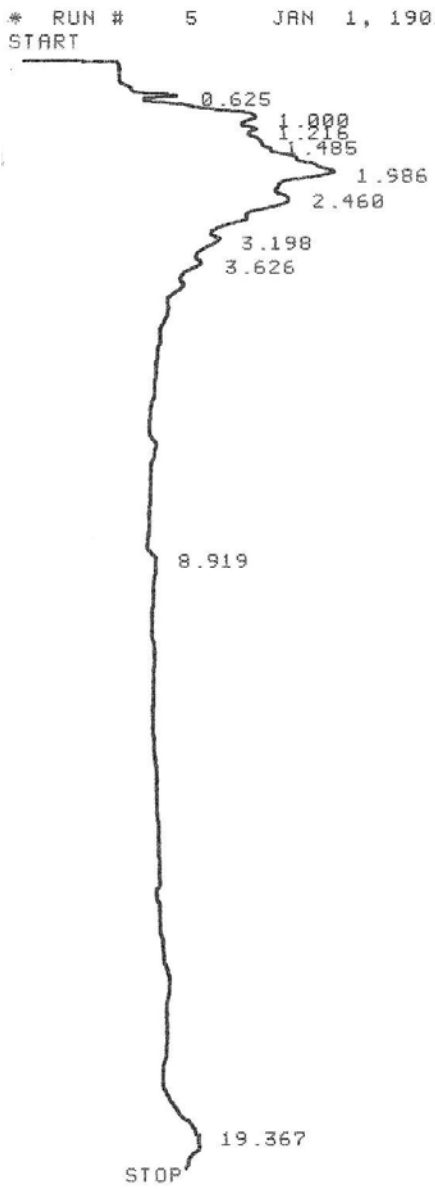

RUN# 5 JAN 1, 1901 01:37:36

AREA%

	RT	AREA	TYPE	WIDTH	AREA%
	.625	6339	PU	.109	2.01454
*	1.000	43277	VV	.315	13.75344
	1.216	21907	VV	.161	6.96205
	1.485	28941	VV	.204	9.19746
	1.986	127216	VV	.600	40.42930
	2.460	21265	VV	.132	6.75802
	3.198	28489	VV	.349	9.05381
	3.626	18188	VV	.306	5.78015
	8.919	873	PU	.122	.27744
	19.367	18168	VV	.472	5.77380

TOTAL AREA= 314663

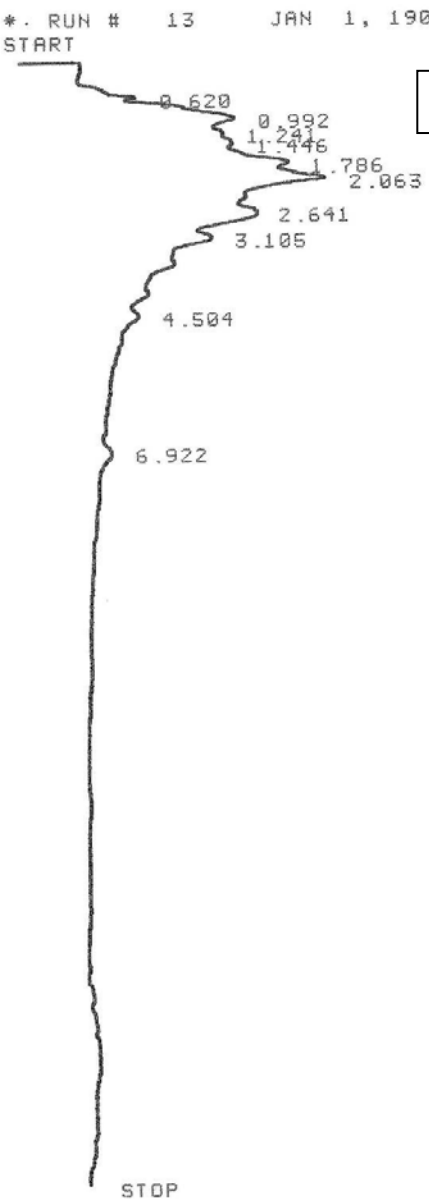

RUN# 13 JAN 1, 1901 03:33:19

AREA%

	RT	AREA	TYPE	WIDTH	AREA%
	.620	5020	PU	.129	3.28293
*	.992	39948	VU	.352	26.12483
.	1.241	9964	VU	.121	6.51617
	1.446	17949	VU	.231	11.73812
	1.786	32153	VU	.294	21.02713
.	2.063	36252	VU	.286	23.70776
	2.641	372	PB	.067	.24328
.	3.105	4754	BP	.195	3.10898
	4.504	2872	PP	.219	1.87820
.	6.922	3628	BU	.289	2.37261

*. RUN # 14 JAN 1, 1901 03:54:41

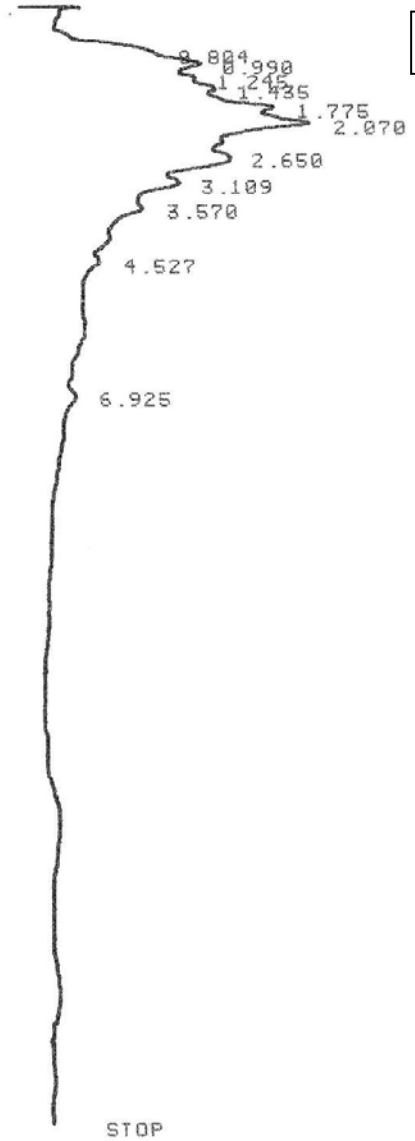

RUN# 14 JAN 1, 1901 03:54:41

AREA%

RT	AREA	TYPE	WIDTH	AREA%
.804	23068	BV	.222	5.88103
.990	40849	VV	.273	10.41418
1.245	19355	VV	.136	4.93443
1.435	35428	VV	.218	9.03213
1.775	68951	VV	.311	17.57860
2.070	94751	VV	.368	24.15614
2.650	27912	VV	.164	7.11598
3.109	43050	VV	.376	10.97531
3.570	28336	VV	.383	7.22408
4.527	7393	VV	.307	1.88480
6.925	3151	VP	.281	.80333

TOTAL AREA= 392244

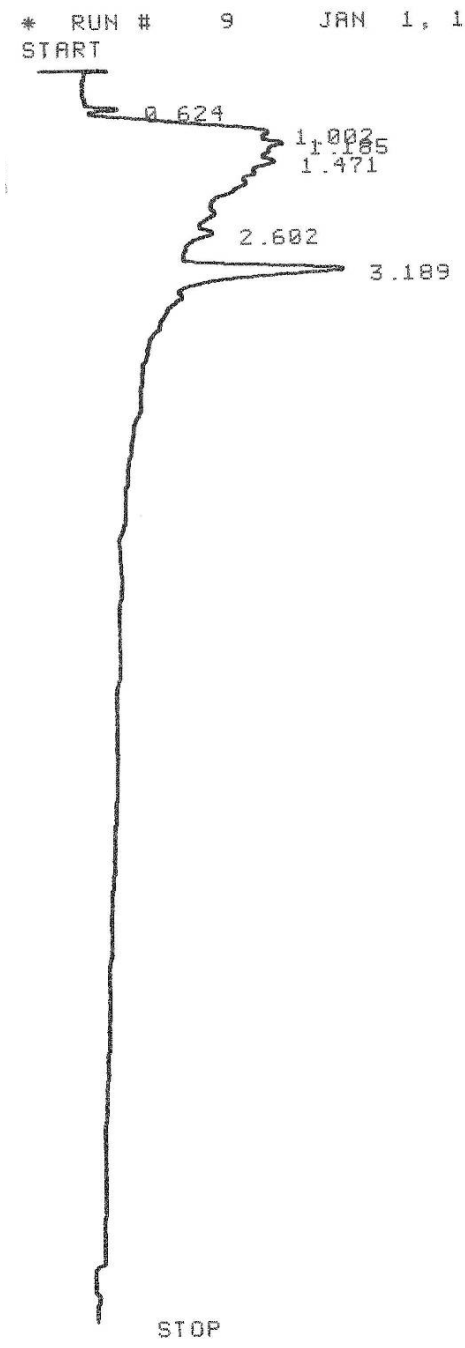

14A

RUN# 9 JAN 1, 1901 02:43:40

AREA%

RT	AREA	TYPE	WIDTH	AREA%
.624	1727	BV	.058	.85737
1.002	40595	VV	.245	20.15350
1.185	31023	VV	.175	15.40146
1.471	34143	VV	.205	16.95038
2.602	28474	VV	.295	14.13600
3.189	65467	VV	.307	32.50128

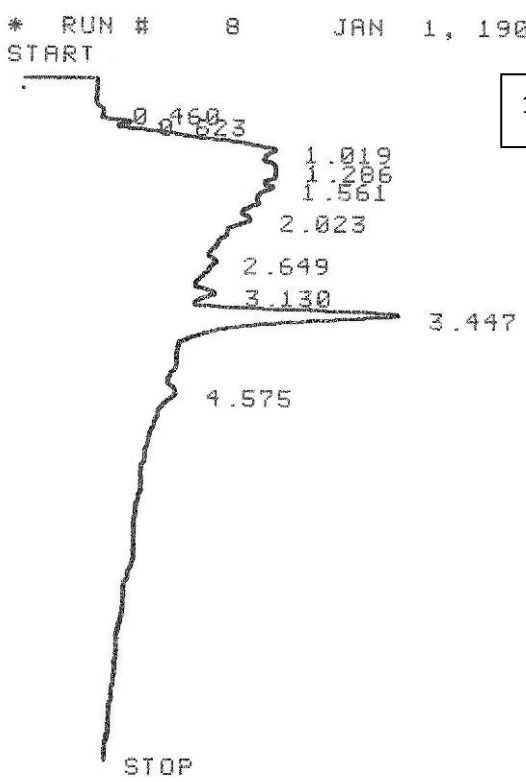

RUN# 8 JAN 1, 1901 02:28:09

AREA%

RT	AREA	TYPE	WIDTH	AREA%
.460	1007	BU	.127	.36712
.623	2374	VV	.084	.86549
1.019	49370	VV	.331	17.99887
1.286	27448	VV	.186	10.00674
1.561	29265	VV	.206	10.66917
2.023	29533	VV	.248	10.76688
2.649	32330	VV	.389	11.78658
3.130	19696	VV	.250	7.18059
3.447	70962	VV	.305	25.87068
4.575	12310	VV	.377	4.48787

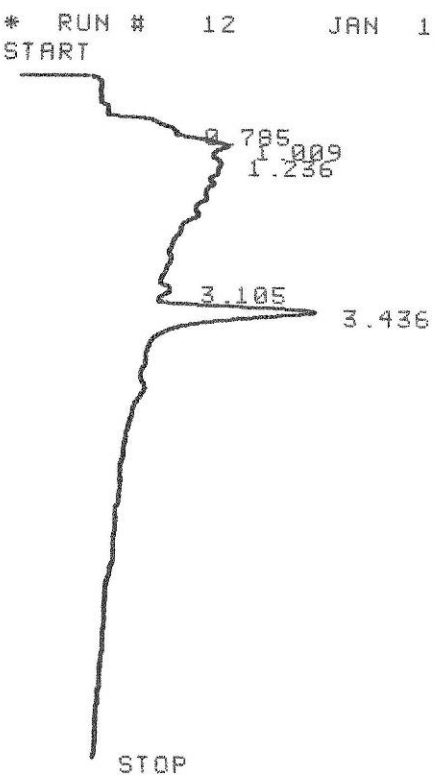

RUN# 12 JAN 1, 1901 03:13:23

AREA%

RT	AREA	TYPE	WIDTH	AREA%
.785	9865	PU	.193	12.55728
*1.009	22673	UU	.260	28.86075
*1.236	13919	UU	.192	17.71766
. 3.105	1881	PU	.148	2.39435
* 3.436	30222	UU	.216	38.46995

TOTAL AREA= 78560
MUL FACTOR=1.0000E+00

```
*  RUN #     9      JAN  1, 1901  02:39:28
START
```

15b

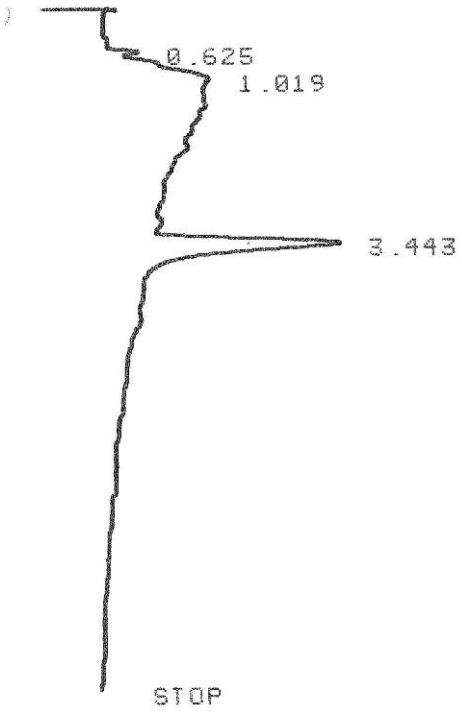


```
RUN#      9           JAN  1, 1901  02:39:28

AREA%
        RT       AREA TYPE  WIDTH      AREA%
      .625       2176   UU   .073    2.95905
    1.019       30559   UU   .352   41.55595
    3.443       40802   UU   .231   55.48499
```

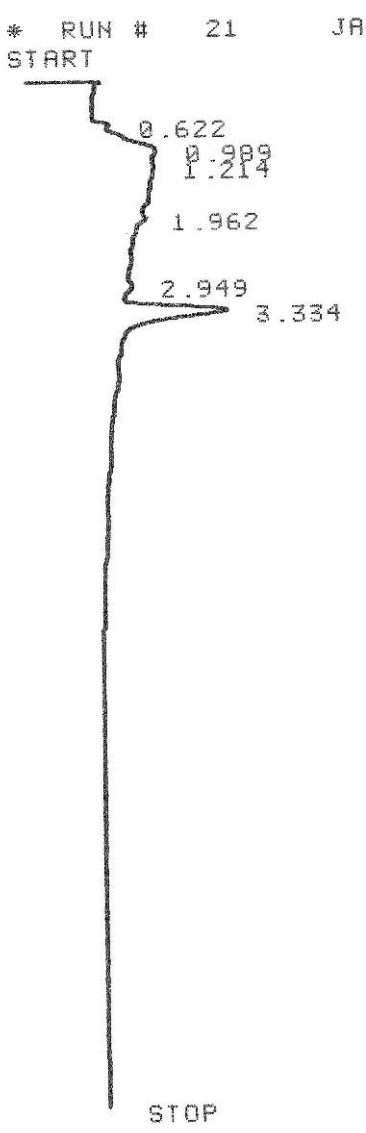

RUN# 21 JAN 1, 1901 07:19:39

AREA%

RT	AREA	TYPE	WIDTH	AREA%
.622	2158	PU	.071	1.68904
.989	33760	VV	.325	26.42350
1.214	18343	VV	.187	14.35683
1.962	23921	VV	.343	18.72266
2.949	9016	VV	.254	7.05670
3.334	40567	VV	.214	31.75126

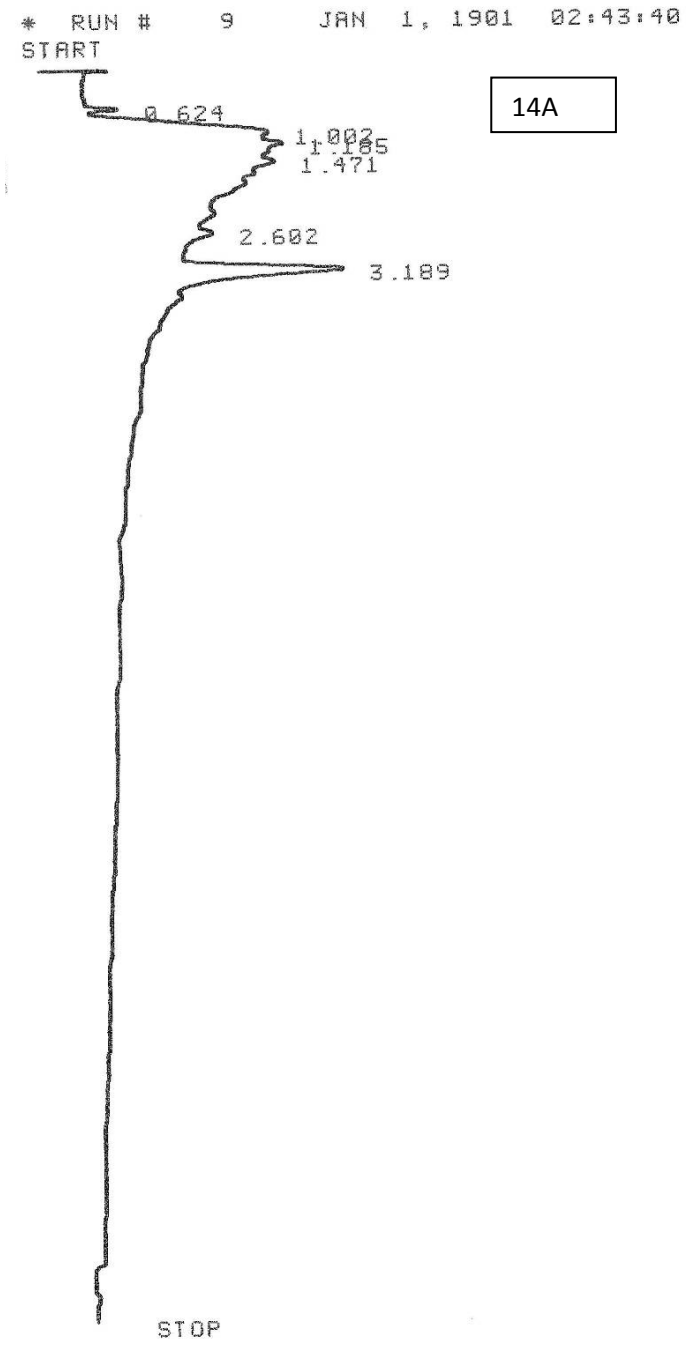

14A

RUN# 9 JAN 1, 1901 02:43:40

AREA%

RT	AREA	TYPE	WIDTH	AREA%
.624	1727	BV	.058	.85737
1.002	40595	VV	.245	20.15350
1.185	31023	VV	.175	15.40146
1.471	34143	VV	.205	16.95038
2.602	28474	VV	.295	14.13600
3.189	65467	VV	.307	32.50128

* RUN # 23 JAN 1, 1901 07:52:15

START

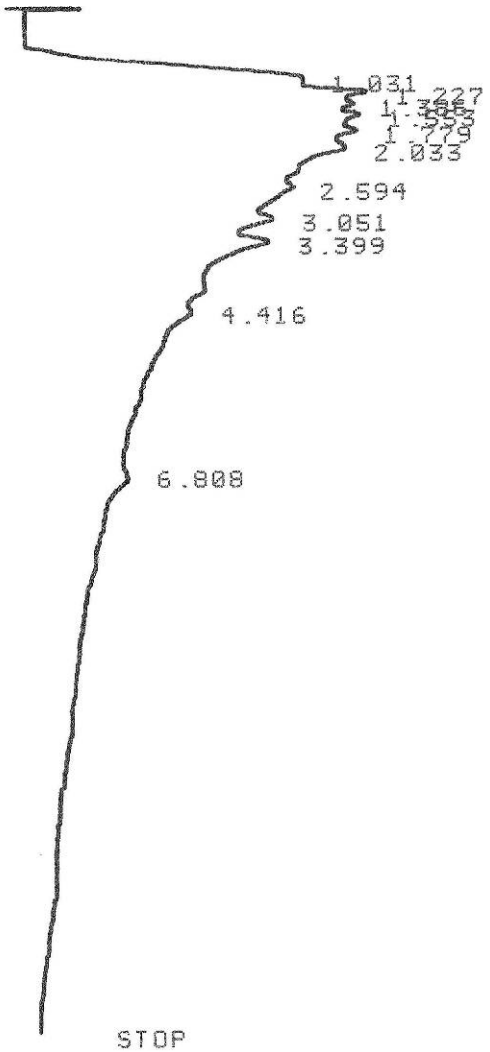

21C

RUN# 23 JAN 1, 1901 07:52:15

AREA%

	RT	AREA	TYPE	WIDTH	AREA%
*	1.031	126954	BV	.279	10.95871
*	1.227	115740	VV	.209	9.99071
*	1.386	80560	VV	.154	6.95396
*	1.553	102196	VV	.194	8.82159
*	1.779	106877	VV	.210	9.22566
*	2.033	184464	VV	.382	15.92299
	2.594	145713	VV	.396	12.57799
	3.051	91757	VV	.291	7.92049
*	3.399	142735	VV	.488	12.32093
	4.416	56027	VB	.482	4.83627
	6.808	5453	VB	.268	.47070

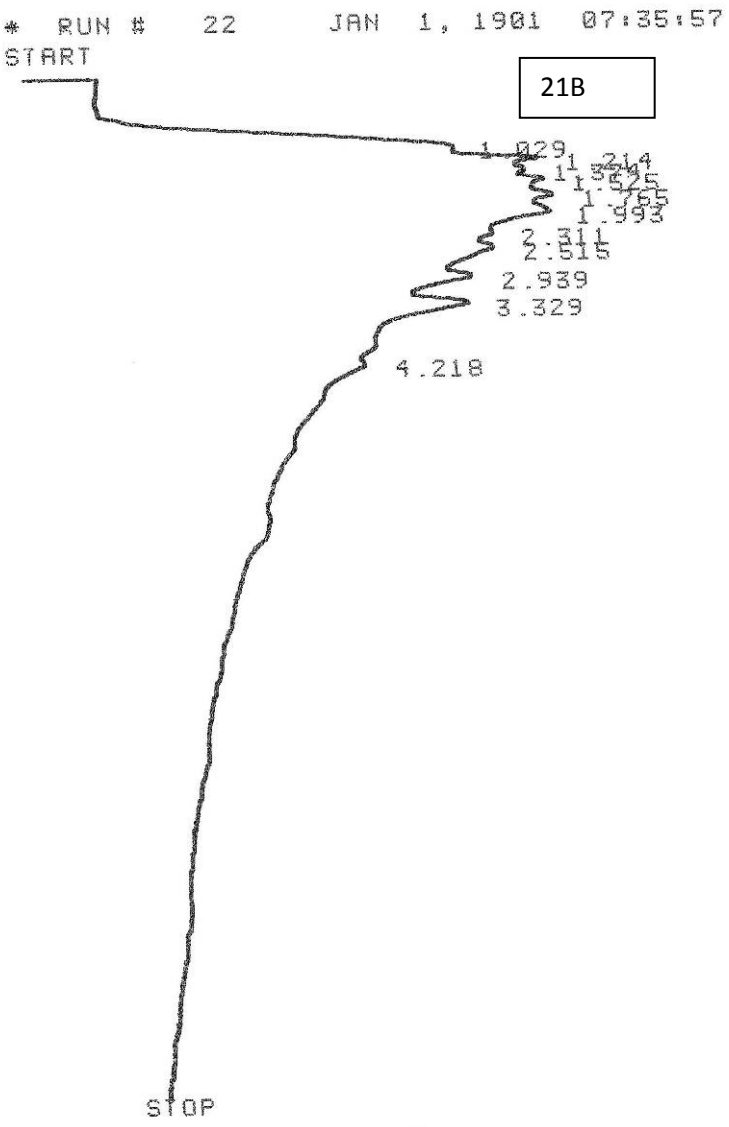

RUN# 22 JAN 1, 1901 07:35:57

AREA%

RT	AREA	TYPE	WIDTH	AREA%
1.029	134305	PU	.253	11.55763
1.214	127522	VU	.196	10.97392
1.374	93751	VU	.154	8.06775
1.525	113761	VU	.184	9.78972
1.765	126774	VU	.212	10.90955
1.993	193309	VU	.345	16.63523
2.311	73363	VU	.175	6.31326
2.515	136293	VU	.348	11.72871
2.939	86699	VU	.295	7.46089
3.329	70255	VU	.304	6.04580
4.218	6014	VP	.203	.51754

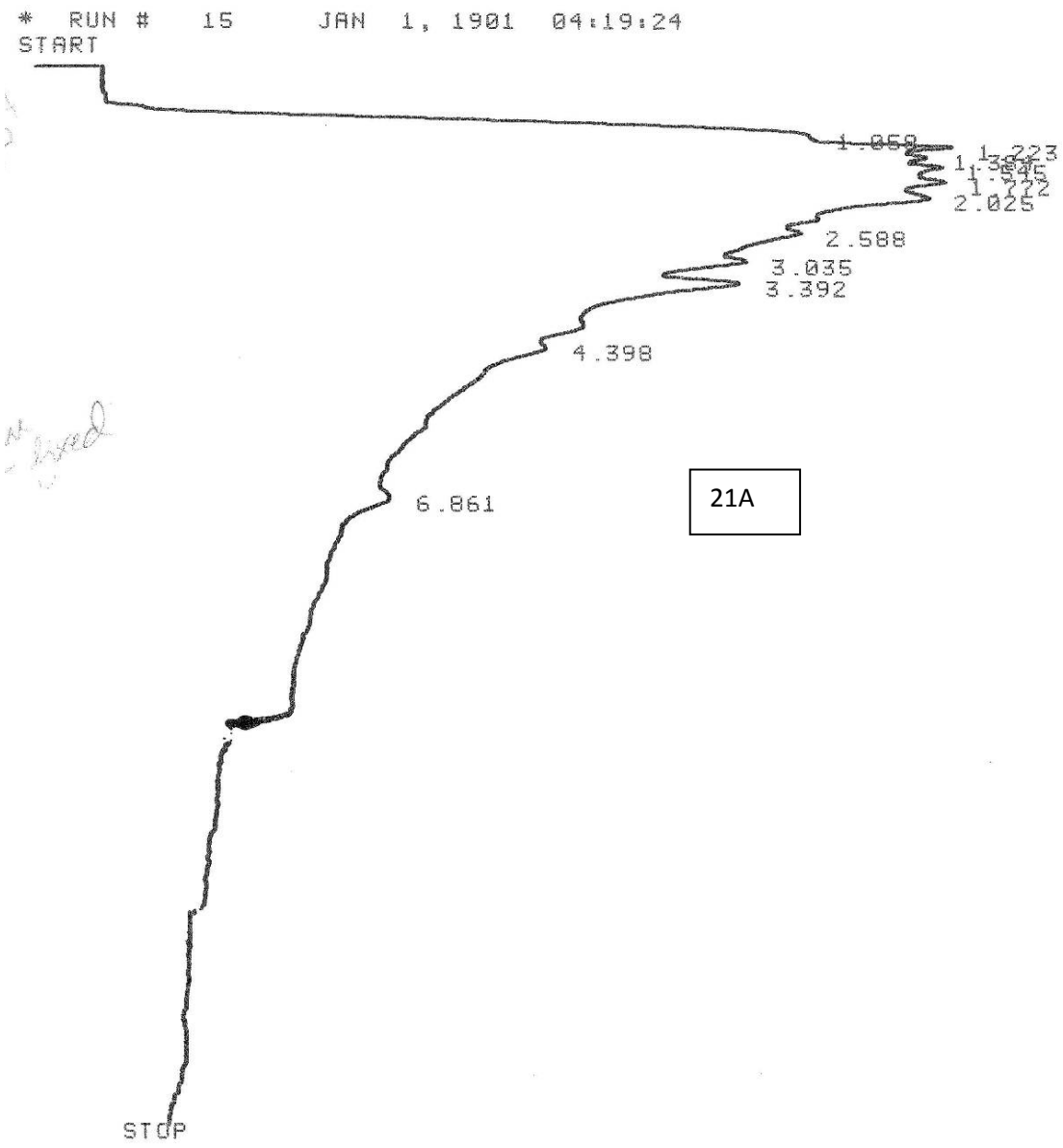

RUN# 15 JAN 1, 1901 04:19:24

AREA%

RT	AREA	TYPE	WIDTH	AREA%
1.058	160232	PU	.261	10.23710
1.223	161934	VV	.221	10.34583
1.384	110563	VV	.158	7.06378
1.545	133537	VV	.190	8.53157
1.772	151660	VV	.220	9.68943
2.025	240229	VV	.365	15.34804
2.588	211513	VV	.421	13.51340
3.035	120441	VV	.285	7.69488
3.392	199276	VV	.507	12.73158
4.398	70410	VB	.475	4.49844
6.861	5415	BP	.256	.34596

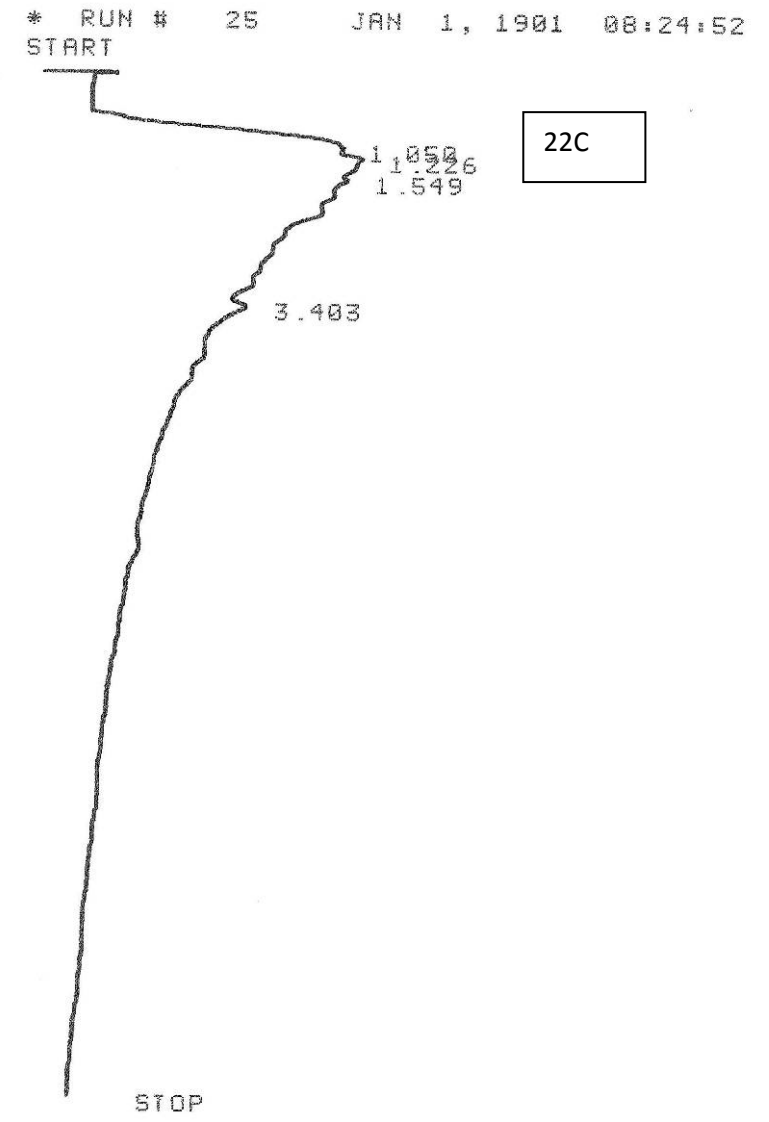

RUN# 25 JAN 1, 1901 08:24:52

AREA%

RT	AREA	TYPE	WIDTH	AREA%
1.050	144923	PU	.348	33.11466
1.226	88882	VU	.198	20.30938
1.549	92257	VU	.221	21.08057
3.403	111578	VU	.540	25.49539

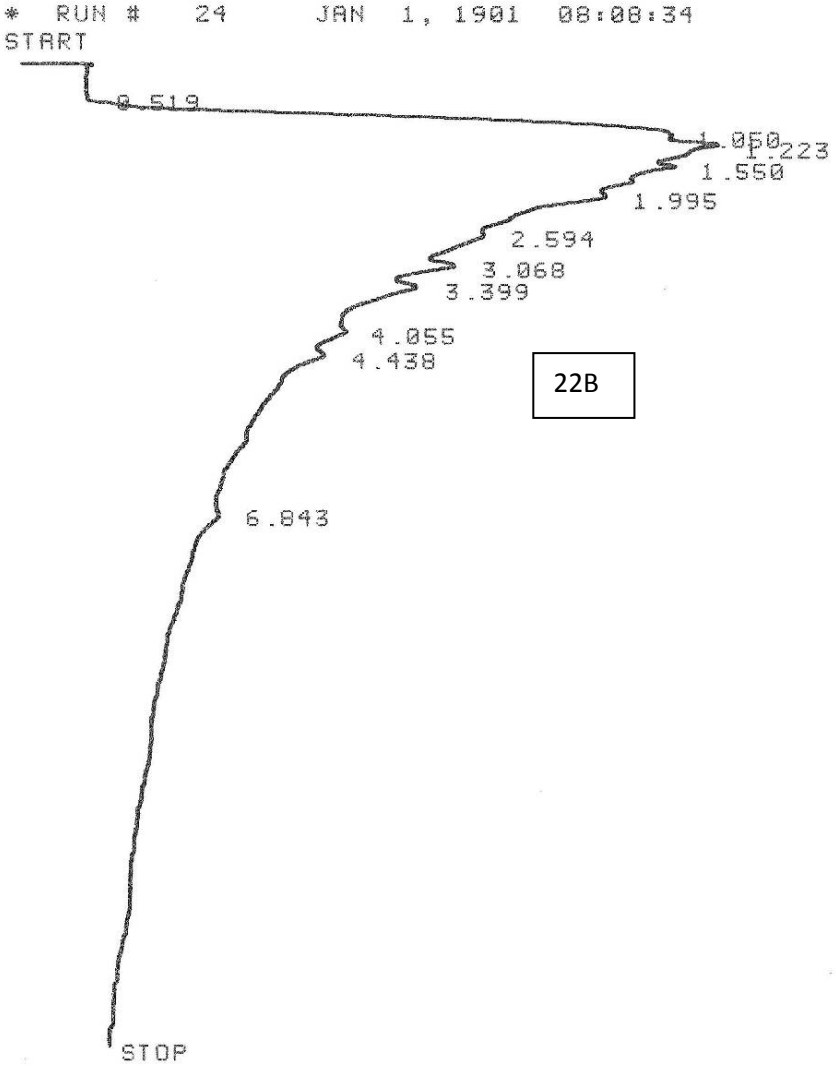

RUN# 24 JAN 1, 1901 08:08:34

AREA%

	RT	AREA	TYPE	WIDTH	AREA%
	.519	141	PP	.094	.00691
*	1.050	330862	PU	.330	16.20513
*	1.223	364063	UU	.338	17.83127
*	1.550	223593	UU	.229	10.95126
	1.995	423725	UU	.514	20.75342
	2.594	219352	UU	.386	10.74354
	3.068	139986	UU	.288	6.85631
*	3.399	191656	UU	.481	9.38703
	4.055	73766	UU	.324	3.61295
	4.438	71697	UB	.432	3.51161
	6.843	2870	BB	.159	.14057

TOTAL AREA=2041711
MUL FACTOR=1.0000E+00

*. ATT 2^ 2 @
*. RUN # 16 JAN 1, 1901 04:40:43

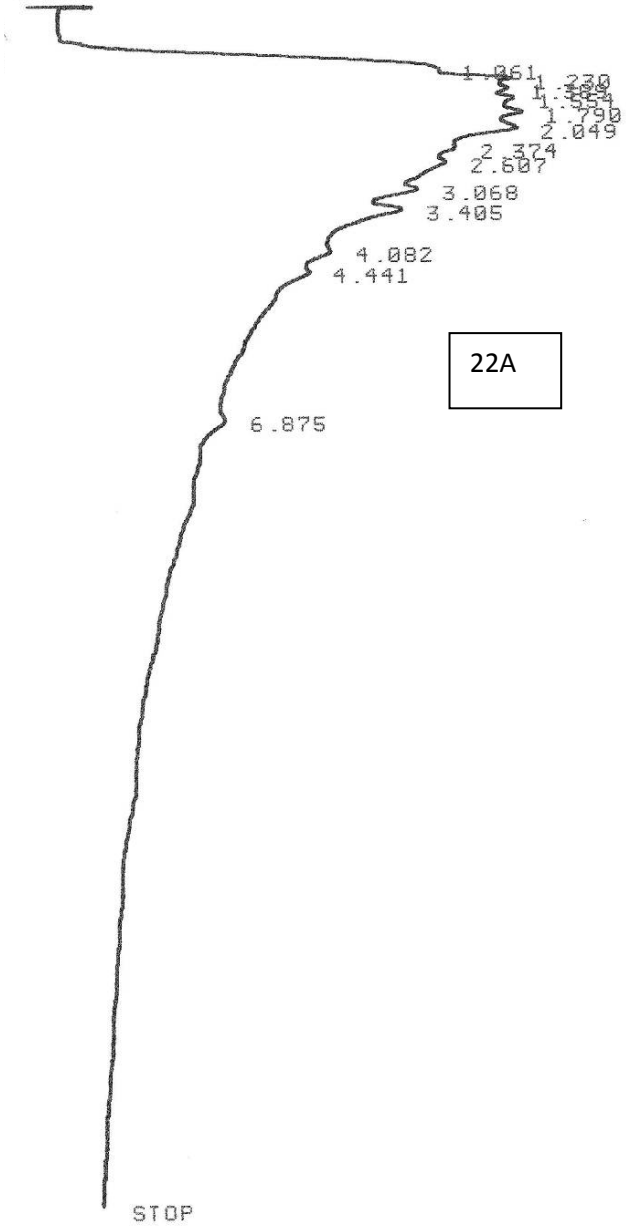

22A

RUN# 16 JAN 1, 1901 04:40:43

AREA%

	RT	AREA	TYPE	WIDTH	AREA%
*	1.061	178981	PU	.258	8.74037
*	1.230	160996	VV	.196	7.86209
	1.389	153309	VV	.191	7.48671
*	1.554	148213	VV	.184	7.23785
	1.790	177930	VV	.222	8.68905
	2.049	290497	VV	.375	14.18616
	2.374	132178	VV	.209	6.45479
	2.607	244888	VV	.411	11.95888
	3.068	145879	VV	.288	7.12387
*	3.405	241156	VV	.533	11.77664
	4.082	88515	VV	.333	4.32255
	4.441	78958	VV	.401	3.85584
	6.875	6250	BP	.256	.30521

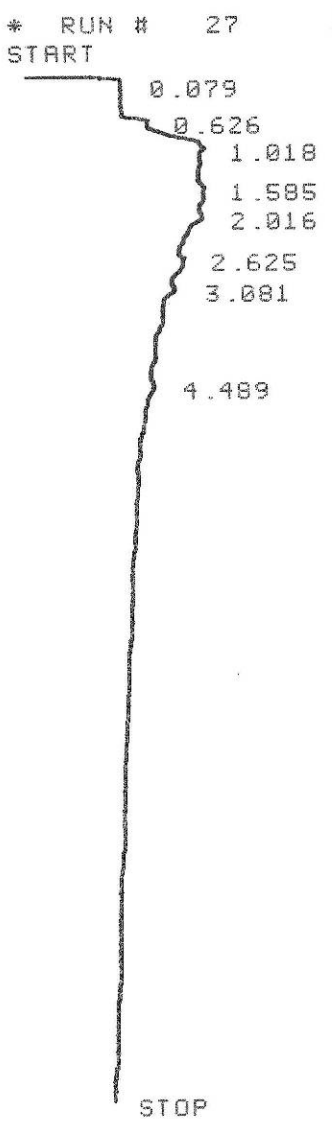

23C

RUN# 27 JAN 1, 1901 08:57:29

AREA%

RT	AREA	TYPE	WIDTH	AREA%
.079	4805	BU	.163	2.98648
.626	3169	PU	.072	1.96964
1.018	41177	UU	.303	25.59294
1.585	19134	UU	.145	11.89245
2.016	51933	UU	.408	32.27816
2.625	13046	UU	.149	8.10855
3.081	20724	UU	.290	12.88069
4.489	6904	UU	.291	4.29108

* RUN # 26 JAN 1, 1901 08:41:11

START

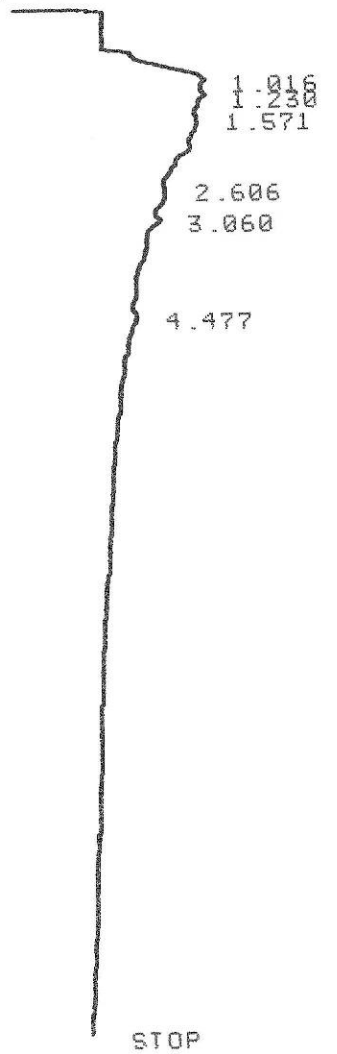

RUN# 26 JAN 1, 1901 08:41:11

AREA%

	RT	AREA	TYPE	WIDTH	AREA%
~	1.016	57208	PU	.343	30.99696
	1.230	57978	UU	.355	31.41417
*	1.571	21587	UU	.147	11.69647
	2.606	30009	UU	.400	16.25975
*	3.060	14868	UU	.261	8.05592
	4.477	2910	PU	.205	1.57672

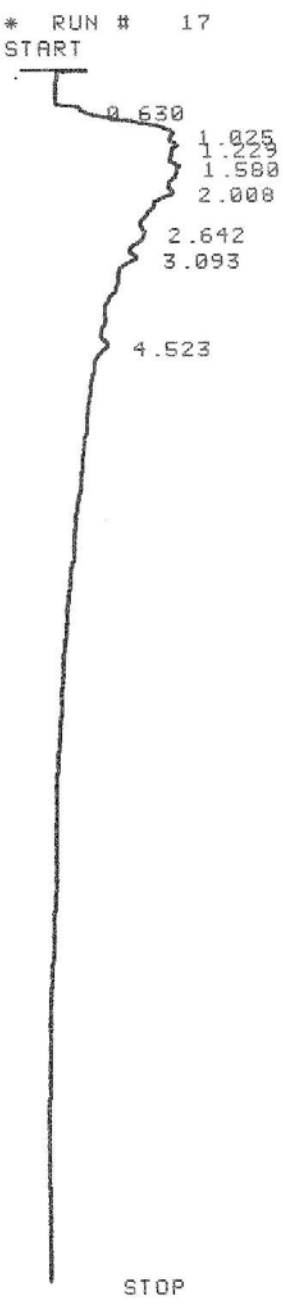

23A

RUN# 17 JAN 1, 1901 05:02:02

AREA%

	RT	AREA	TYPE	WIDTH	AREA%
	.630	3148	PU	.064	.79489
*	1.025	73907	UU	.334	18.66192
	1.229	46642	UU	.205	11.77736
*	1.580	34958	UU	.154	8.82708
	2.008	109850	UU	.514	27.73773
	2.642	60477	UU	.400	15.27078
*	3.093	41728	UU	.311	10.53655
	4.523	25321	UU	.380	6.39369

* RUN # 29 JAN 1, 1901 09:30:10

START

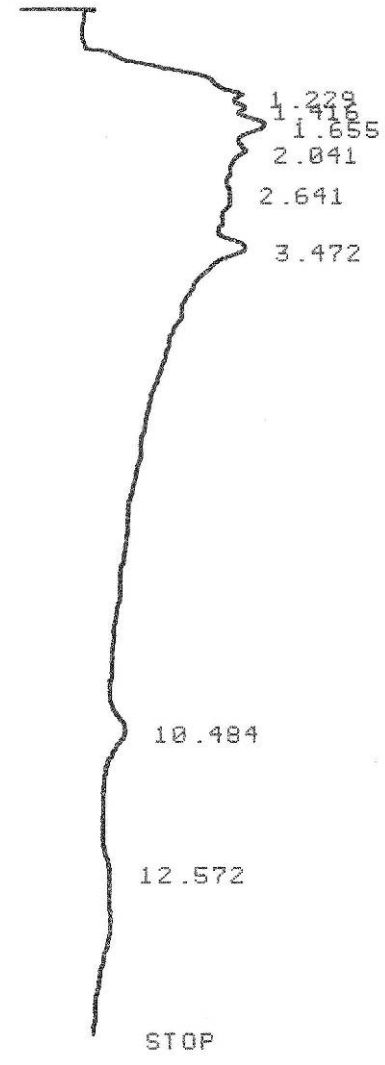

RUN# 29 JAN 1, 1901 09:30:10

AREA%

	RT	AREA	TYPE	WIDTH	AREA%
	1.229	118571	PU	.470	19.99160
	1.416	44302	VV	.174	7.46952
	1.655	103643	VV	.366	17.47468
	2.041	98046	VV	.410	16.53100
	2.641	50345	VV	.252	8.48840
	3.472	157719	VV	.759	26.59214
	10.484	17872	BV	.527	3.01330
	12.572	2606	BV	.359	.43938

```
*  RUN #    28      JAN  1, 1901   09:13:48
START
```

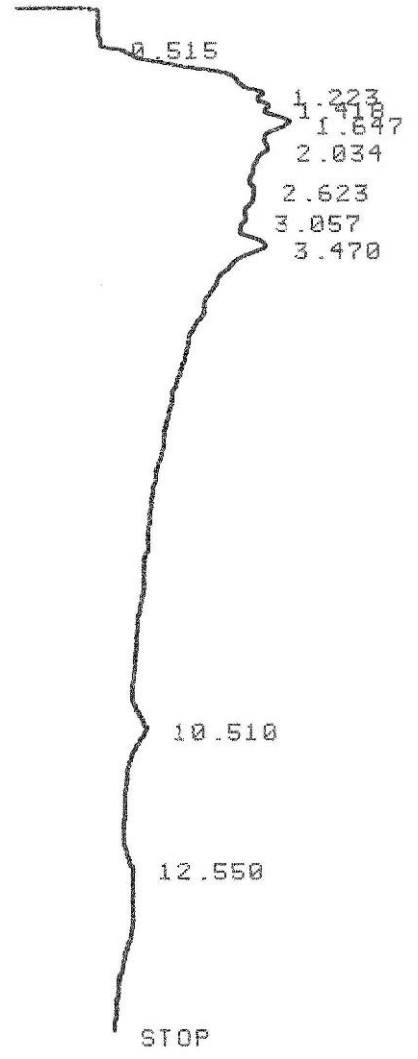

24B

```
RUN#     28           JAN  1, 1901   09:13:48

AREA%
       RT        AREA TYPE  WIDTH       AREA%
     .515         402   PV   .140       .05491
   * 1.223      122363   VV   .467    16.71498
   *1.418        45085   VV   .169     6.15868
   * 1.647      106456   VV   .361    14.54206
    2.034       138511   VV   .552    18.92082
    2.623        96383   VV   .457    13.16607
    3.057        45274   VV   .241     6.18450
   * 3.470      159111   VV   .753    21.73481
   10.510        16834   VP   .547     2.29955
   12.550         1637   PV   .284      .22362
```

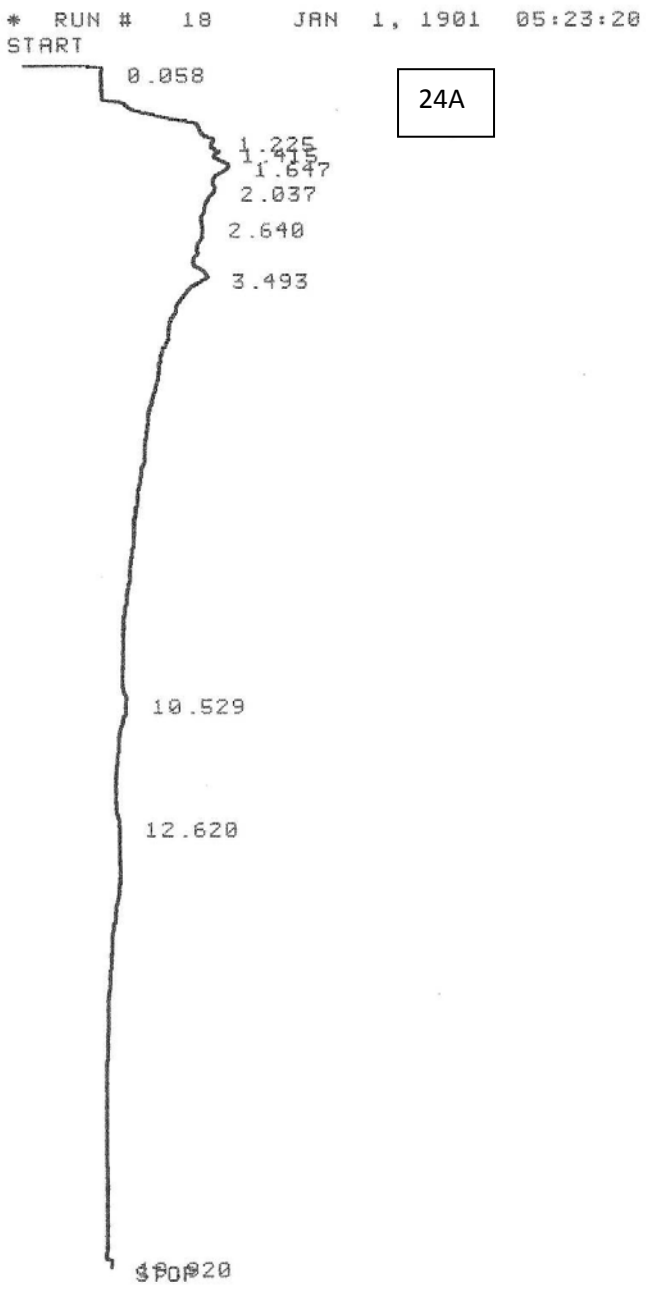

24A

RUN# 18 JAN 1, 1901 05:23:20

AREA%

RT	AREA	TYPE	WIDTH	AREA%
.058	1471	BB	.080	.38039
* 1.225	95671	PU	.493	24.74011
* 1.415	32049	UU	.165	8.28774
*1.647	79147	UU	.377	20.46708
2.037	92304	UU	.541	23.86942
2.640	19115	UU	.150	4.94306
* 3.493	60186	UU	.555	15.56304
10.529	5217	UU	.303	1.34909
12.620	1282	PU	.227	.33152
19.920	262	PB	.067	.06775

* RUN # 30 JAN 1, 1901 09:46:28

START

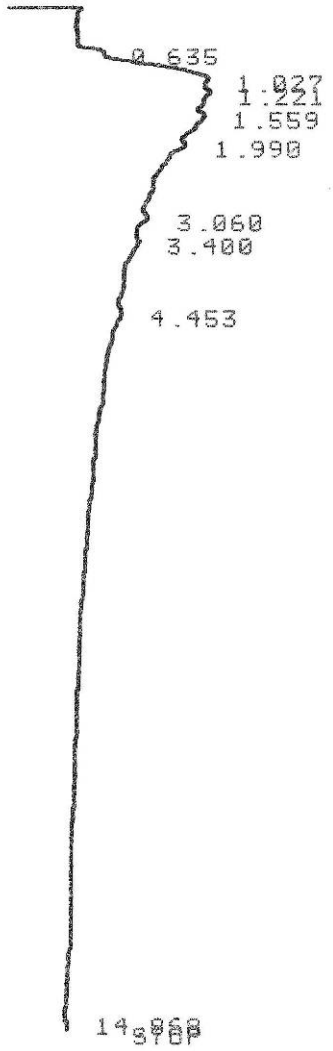

RUN# 30 JAN 1, 1901 09:46:28

AREA%

	RT	AREA	TYPE	WIDTH	AREA%
	.635	2671	PU	.065	.91866
*	1.027	70194	UU	.329	24.14230
	1.221	39846	UU	.187	13.70451
*	1.559	72487	UU	.371	24.93095
	1.990	70288	UU	.460	24.17464
*	3.060	16984	UU	.256	5.84142
	3.400	14954	UU	.350	5.14323
	4.453	3112	BU	.225	1.07033
	14.868	215	PU	.030	.07395

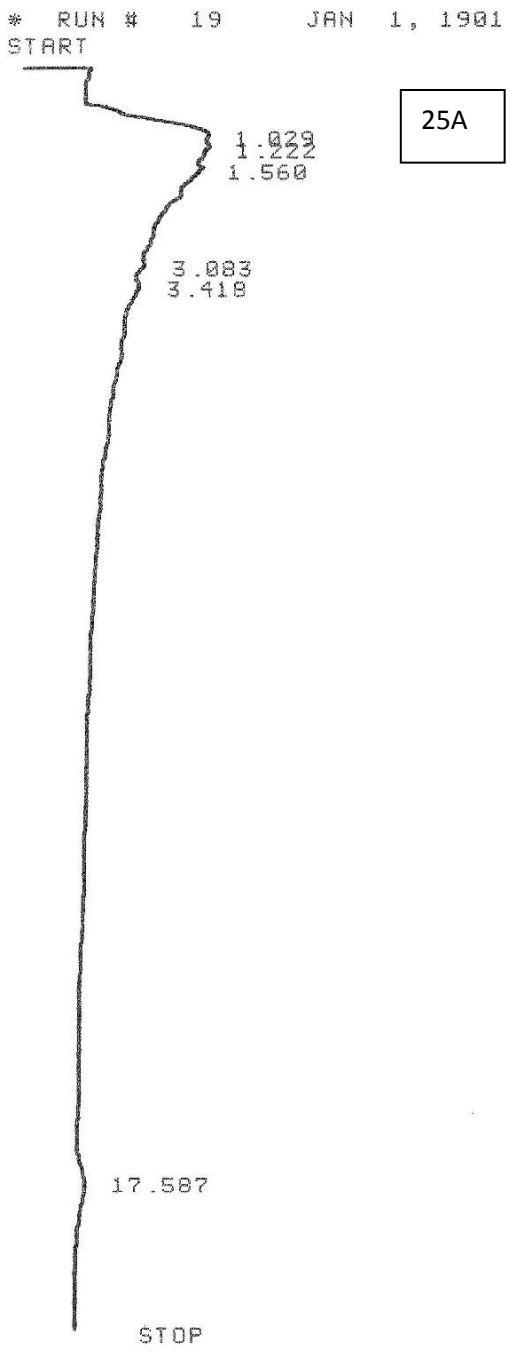

RUN# 19 JAN 1, 1901 05:44:39

AREA%

RT	AREA	TYPE	WIDTH	AREA%
*1.029	79222	PU	.359	33.75357
1.222	39757	VU	.182	16.93899
*1.560	75363	VU	.386	32.10939
*3.083	15833	VU	.260	6.74586
3.418	15330	VU	.354	6.53155
17.587	9202	BV	.579	3.92063

* RUN # 31 JAN 1, 1901 10:02:47
START

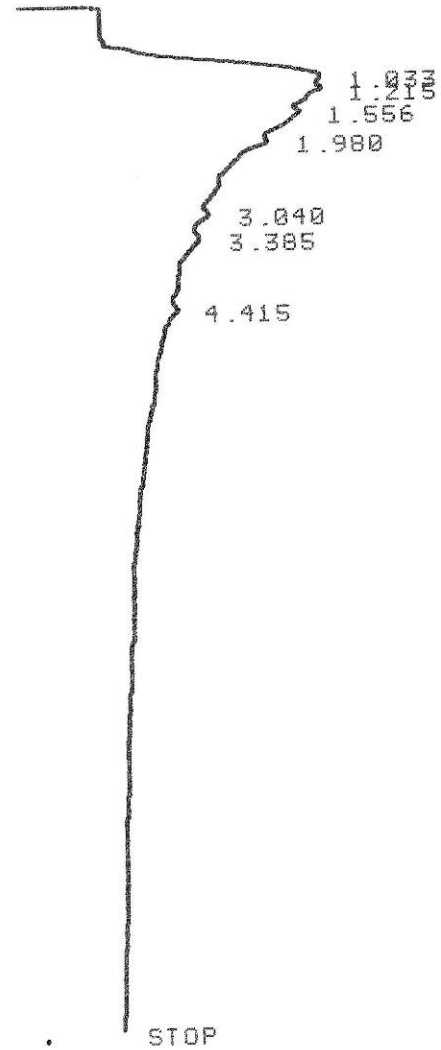

25C

. STOP

RUN# 31 JAN 1, 1901 10:02:47

AREA%

	RT	AREA	TYPE	WIDTH	AREA%
*	1.033	129238	PU	.354	20.83724
	1.215	115966	UU	.318	18.69738
*	1.556	125930	UU	.392	20.30389
	1.980	120459	UU	.468	19.42179
*	3.040	39071	UU	.282	6.29948
	3.385	61290	UU	.529	9.88188
	4.415	28272	UB	.497	4.55834

TOTAL AREA= 620226

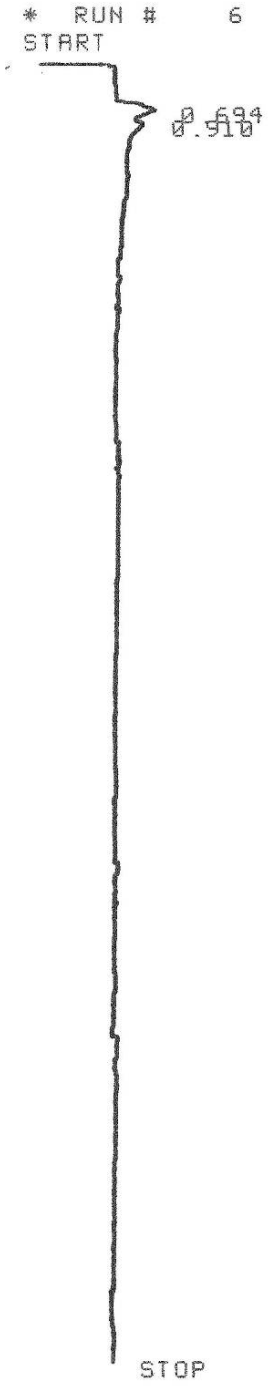

31A

RUN# 6 JAN 1, 1901 01:13:08

AREA%

RT	AREA	TYPE	WIDTH	AREA%
.694	5668	BV	.183	64.10314
.910	3174	VV	.165	35.89685

```
*  RUN #   19      JAN  1, 1901  06:51:17
START
```

31B

```
RUN#    19          JAN  1, 1901  06:51:17

AREA%
      RT       AREA TYPE  WIDTH      AREA%
    .625       2696   PU   .070   33.07570
    .978       5455   UU   .206   66.92429
```

* RUN # 20 JAN 1, 1901 07:02:35

START

31C

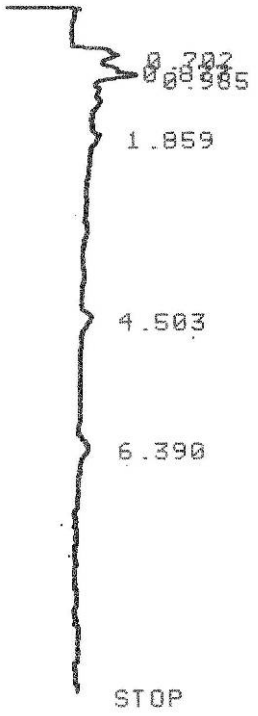

RUN# 20 JAN 1, 1901 07:02:35

AREA%

RT	AREA	TYPE	WIDTH	AREA%
.702	6061	PU	.168	33.59384
.877	2403	UU	.080	13.31892
.985	5820	UU	.129	32.25806
1.859	538	UU	.065	2.98193
4.503	2235	UP	.223	12.38776
6.390	985	BU	.126	5.45948

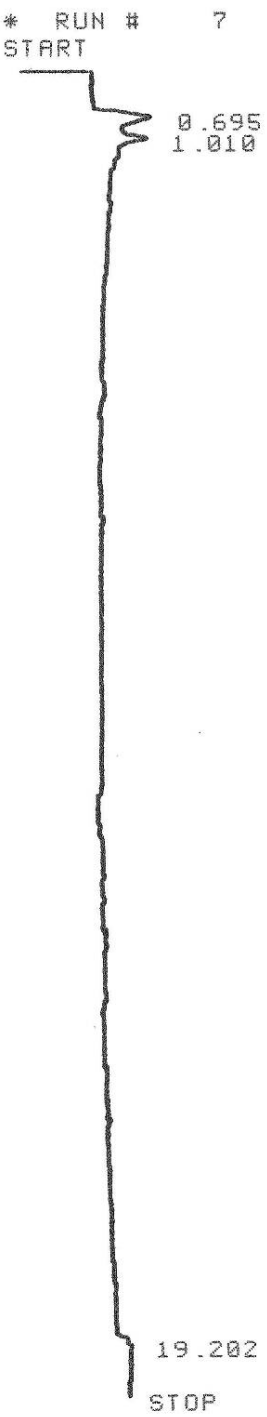

32A

RUN# 7 JAN 1, 1901 01:34:26

AREA%

RT	AREA	TYPE	WIDTH	AREA%
.695	8503	PU	.175	48.61357
1.010	7526	VU	.192	43.02784
19.202	1462	PU	.200	8.35859

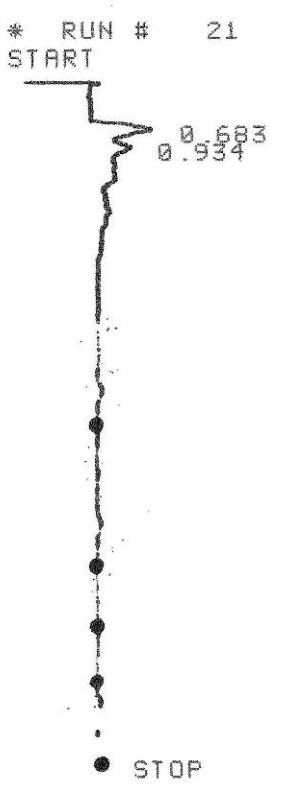

RUN# 21 JAN 1, 1901 07:13:54

AREA%

RT	AREA	TYPE	WIDTH	AREA%
.683	8949	PU	.169	57.55725
.934	6599	UU	.202	42.44277

```
*  RUN #    22      JAN  1, 1901  07:25:12
START
```

32C

```
RUN#     22           JAN  1, 1901  07:25:12

AREA%
       RT       AREA TYPE  WIDTH       AREA%
     .627       1863   BV   .063    32.92101
     .956       3796   VV   .183    67.07901
```

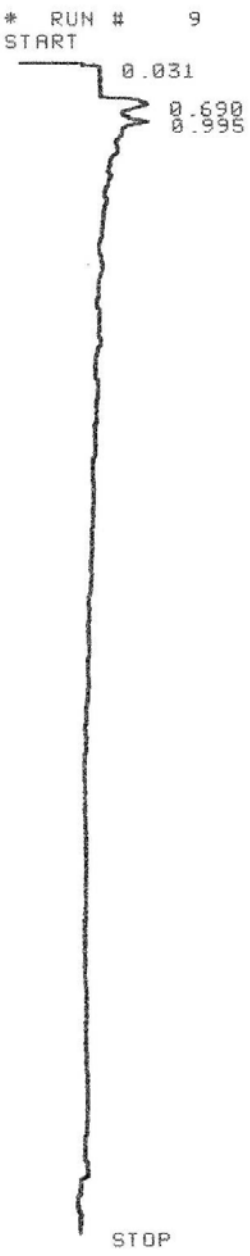

33A

RUN# 9 JAN 1, 1901 02:01:03

AREA%

RT	AREA	TYPE	WIDTH	AREA%
.031	462	BV	.031	2.47854
.690	9475	PV	.195	50.83154
.995	8703	VV	.194	46.68990

* RUN # 23 JAN 1, 1901 07:36:31

START

33B

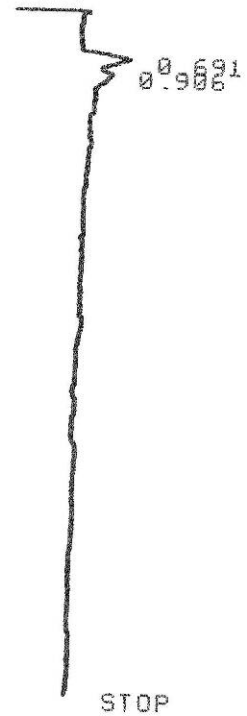

RUN# 23 JAN 1, 1901 07:36:31

AREA%

RT	AREA	TYPE	WIDTH	AREA%
.691	6625	PU	.167	56.02536
.906	5200	UU	.216	43.97462

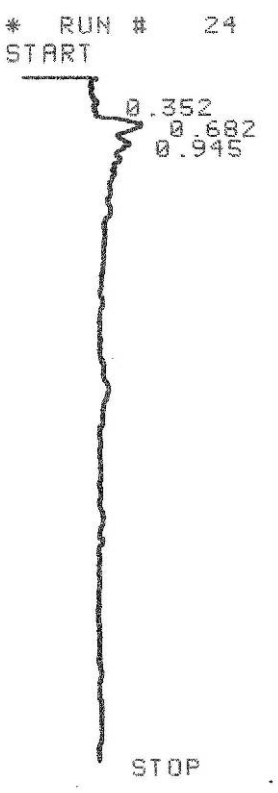

33C

RUN# 24 JAN 1, 1901 07:47:49

AREA%

RT	AREA	TYPE	WIDTH	AREA%
.352	454	PU	.097	3.31580
.682	7246	PU	.184	52.92142
.945	5992	UU	.219	43.76278

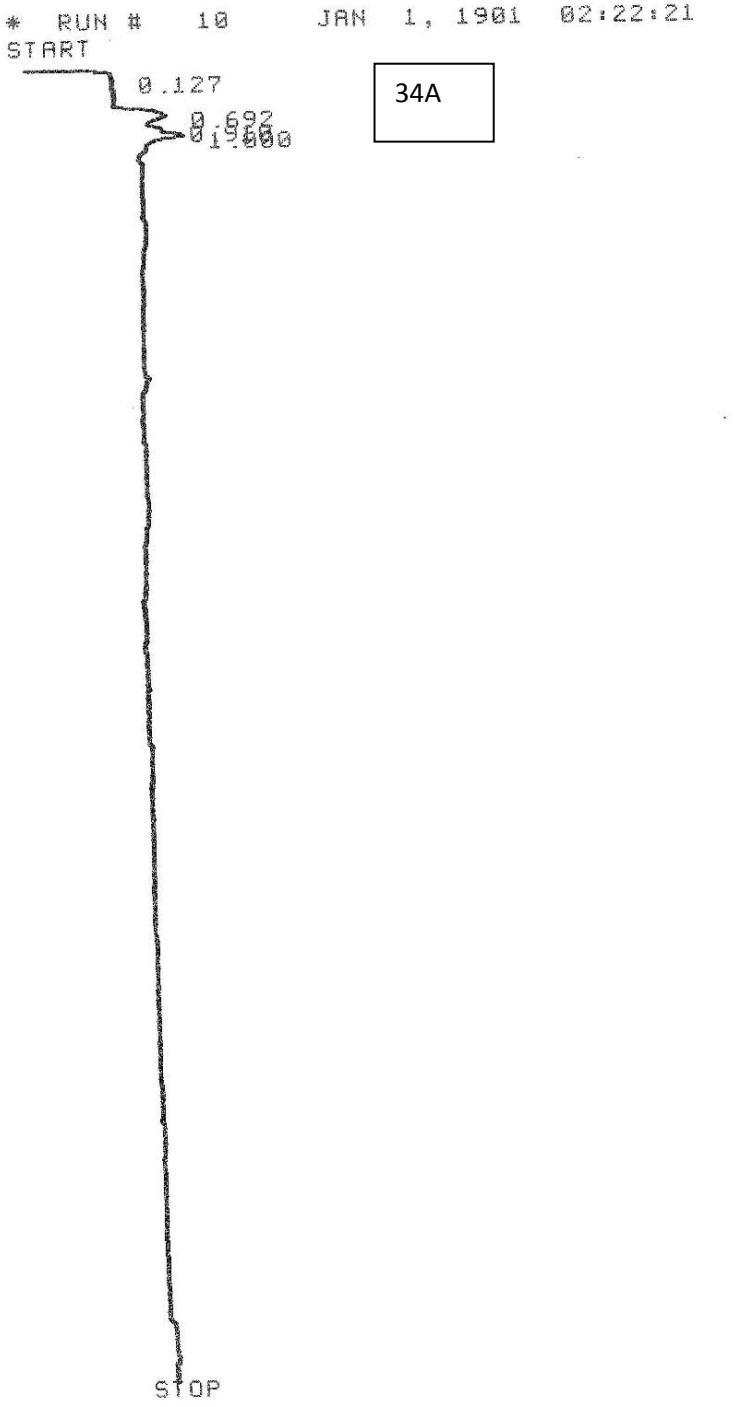

34A

RUN# 10 JAN 1, 1901 02:22:2

AREA%

RT	AREA	TYPE	WIDTH	AREA%
.127	1274	BV	.173	6.12412
.692	8518	PV	.193	40.94602
.910	3458	VV	.094	16.62261
1.000	7553	VV	.144	36.30726

* RUN # 25 JAN 1, 1901 07:59:08

START

34B

RUN# 25 JAN 1, 1901 07:59:08

AREA%

RT	AREA	TYPE	WIDTH	AREA%
.709	5765	PU	.194	39.18037
.905	2453	VU	.094	16.67119
1.000	5764	VU	.149	39.17357
4.518	732	PU	.094	4.97485

* RUN # 26 JAN 1, 1901 08:10:26

START

34C

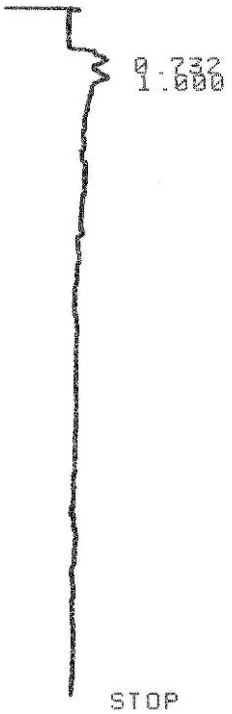

RUN# 26 JAN 1, 1901 08:10:26

AREA%

RT	AREA	TYPE	WIDTH	AREA%
.732	6236	PU	.206	50.92691
1.000	6009	UU	.204	49.07309

* RUN # 11 JAN 1, 1901 02:43:40

START

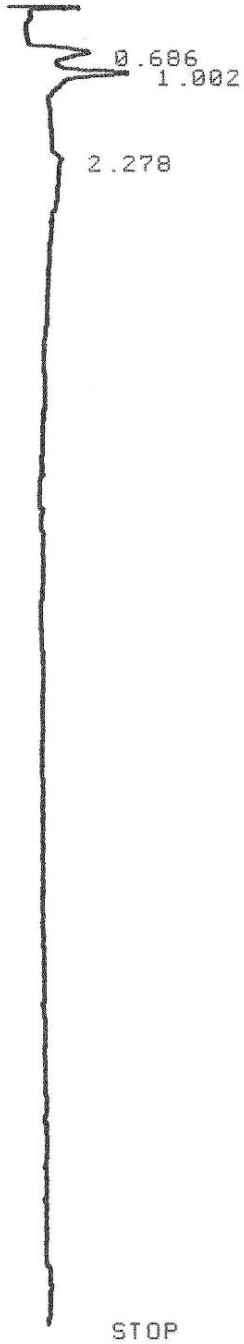

35A

RUN# 11 JAN 1, 1901 02:43:40

AREA%

RT	AREA	TYPE	WIDTH	AREA%
.686	8991	PU	.170	34.12274
1.002	16058	VV	.191	60.94349
2.278	1300	VV	.179	4.93377

```
*  RUN #    27      JAN  1, 1901  08:21:48
START
```

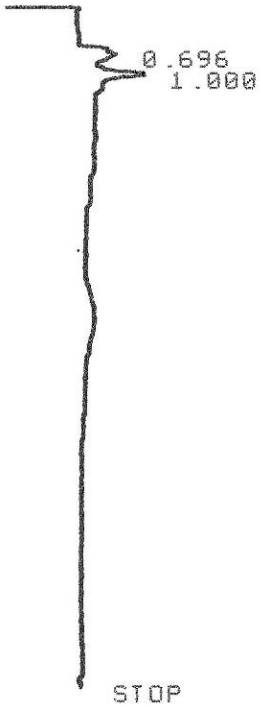

35B

```
RUN#     27           JAN  1, 1901  08:21:48

AREA%
       RT       AREA TYPE  WIDTH      AREA%
     .696       6146   PV    .201   42.48290
   1.000        8321   VV    .156   57.51712
```

* RUN # 28 JAN 1, 1901 08:33:07

START

35C

RUN# 28 JAN 1, 1901 08:33:07

AREA%

RT	AREA	TYPE	WIDTH	AREA%
.686	8055	VV	.169	58.75702
.994	5654	VV	.199	41.24298

```
*  RUN #   13      JAN  1, 1901  07:59:23
START
```

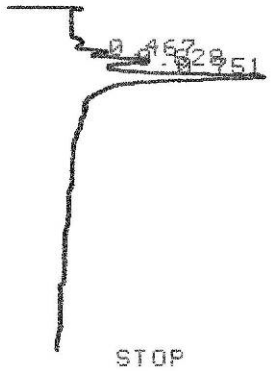

41A

```
RUN#    13           JAN  1, 1901  07:59:23

AREA%
       RT       AREA TYPE  WIDTH      AREA%
     .467       1297   VV    .120    3.24998
     .628       2364   VV    .072    5.92363
   * .751       8071   VV    .119   20.22402
   * .985      28176   VV    .169   70.60240

TOTAL AREA=  39908
MUL FACTOR=1.0000E+00
```

```
*  RUN #    14      JAN  1, 1901  08:05:42
START
```

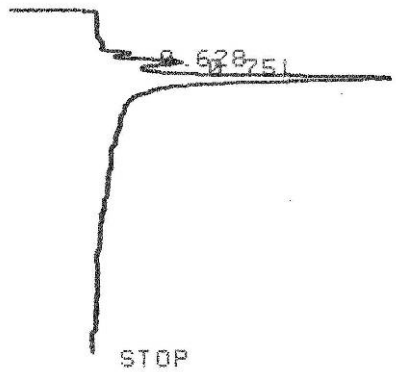

41B

```
RUN#     14           JAN  1, 1901  08:05:42

AREA%
       RT       AREA TYPE  WIDTH       AREA%
     .628       1519   PU   .061     3.35705
   * .751       7087   UU   .108    15.66250
   * .991      36642   UU   .151    80.98038

TOTAL AREA=   45248
MUL FACTOR=1.0000E+00
```

* RUN # 15 JAN 1, 1901 08:12:00
START

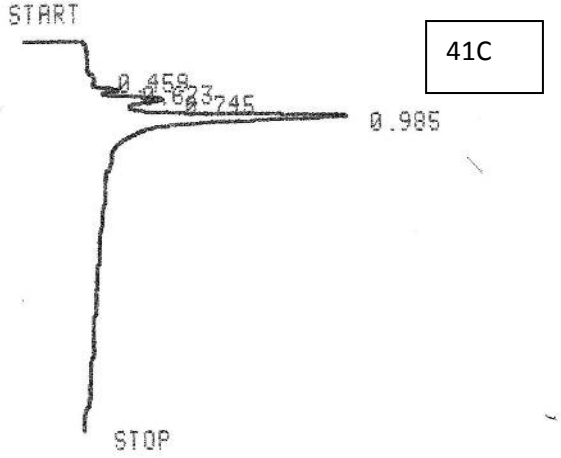

RUN# 15 JAN 1, 1901 08:12:00

AREA%

	RT	AREA	TYPE	WIDTH	AREA%
	.459	862	PV	.117	1.55120
	.623	1972	VV	.064	3.54868
*	.745	8077	VV	.108	14.53482
*	.985	44659	VV	.167	80.36528

TOTAL AREA= 55570
MUL FACTOR=1.0000E+00

```
*  RUN #    18      JAN  1, 1901   08:30:54
START
```

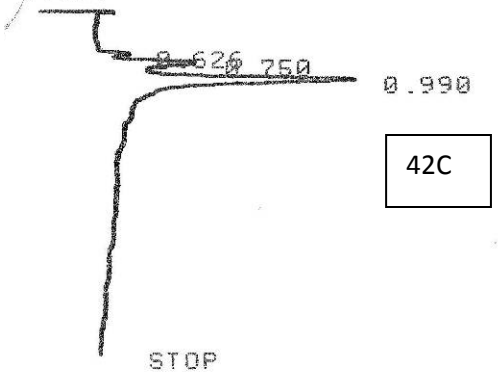


```
RUN#     18           JAN  1, 1901   08:30:54

AREA%
       RT       AREA TYPE  WIDTH       AREA%
     .626       1791   VV    .064     3.58609
    .750        9161   VV    .111    18.34291
    .990       38991   VV    .180    78.07098

TOTAL AREA=  49943
MUL FACTOR=1.0000E+00
```

```
*  RUN #    16      JAN  1, 1901  08:18:18
START
```

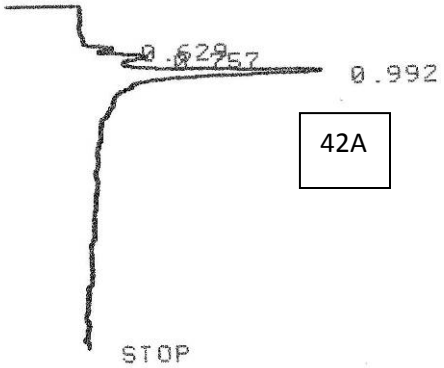


```
RUN#    16           JAN  1, 1901  08:18:18

AREA%
      RT       AREA TYPE  WIDTH      AREA%
    .629       1915   VV   .070    4.46762
    .757       6429   VV   .121   14.99860
    .992      34520   VV   .170   80.53379

TOTAL AREA=  42864
MUL FACTOR=1.0000E+00
```

```
*  RUN #    17      JAN  1, 1901   08:24:36
START
```

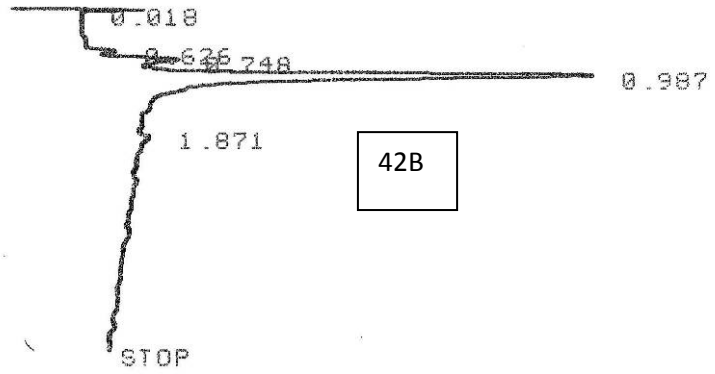


```
RUN#     17            JAN  1, 1901   08:24:36

AREA%
       RT        AREA TYPE  WIDTH       AREA%
     .018          83   BB   .002      .12786
     .626        1244   BU   .058     1.91641
    *.748        6836   UU   .102    10.53102
    \.987       55641   UB   .137    85.71629
    1.871        1109   PU   .106     1.70844

TOTAL AREA=  64913
MUL FACTOR=1.0000E+00
```

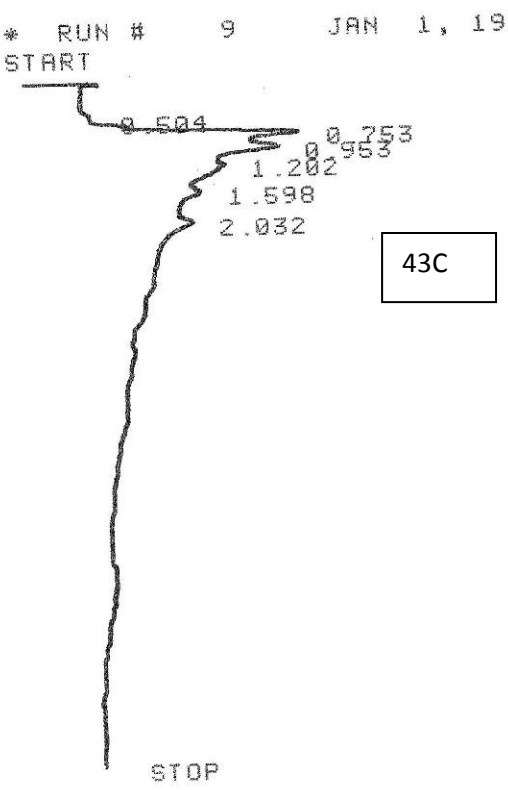

RUN# 9 JAN 1, 1901 07:12:10

AREA%

RT	AREA	TYPE	WIDTH	AREA%
.504	736	PU	.119	.58571
.753	25588	UU	.146	20.36305
* .953	34938	UU	.232	27.80382
* 1.202	29163	UU	.300	23.20805
* 1.598	20290	UU	.310	16.14687
* 2.032	14944	UU	.325	11.89250

TOTAL AREA= 125659
MUL FACTOR=1.0000E+00

* RUN # 7 JAN 1, 1901 06:49:32

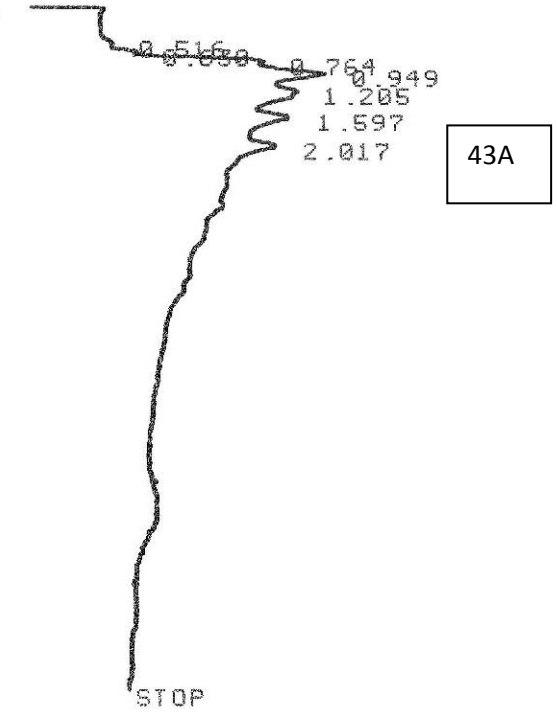

RUN# 7 JAN 1, 1901 06:49:32

AREA%

	RT	AREA	TYPE	WIDTH	AREA%
	.516	401	PU	.090	.25648
	.630	1269	VV	.059	.81165
	.764	13024	VV	.104	8.33008
*	.949	41567	VV	.241	26.58605
*	1.205	21678	VV	.153	13.86514
*	1.597	40188	VV	.325	25.70404
*	2.017	38222	VV	.384	24.44659

```
*  RUN #     8      JAN  1, 1901  07:00:51
START
```

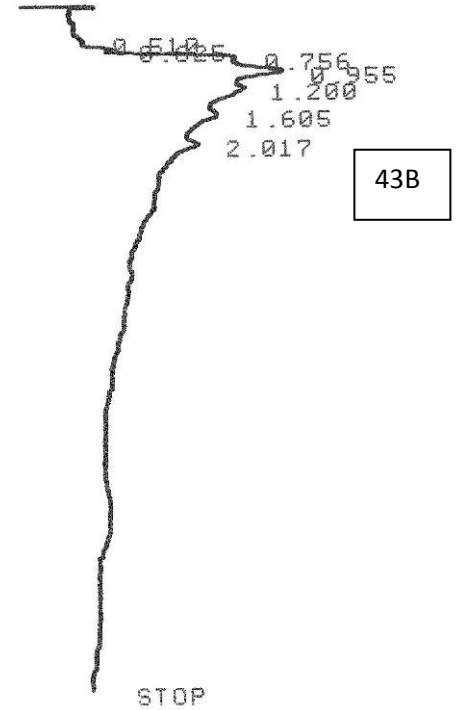

RUN# 8 JAN 1, 1901 07:00:51

AREA%

RT	AREA	TYPE	WIDTH	AREA%
.510	295	PU	.059	.20997
.625	1436	VU	.059	1.02207
.756	12864	VU	.101	9.15594
* .955	43763	VU	.272	31.14827
* 1.200	36846	VU	.308	26.22510
* 1.605	27840	VU	.329	19.81509
* 2.017	17455	VU	.320	12.42358

```
*  RUN #    19      JAN  1, 1901  08:52:45
START
```

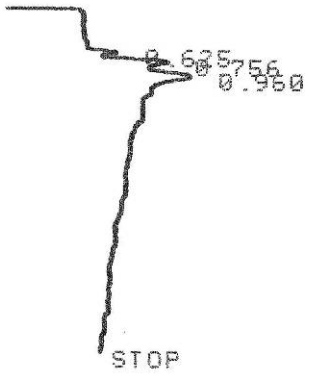

44A

```
RUN#     19           JAN  1, 1901  08:52:45

AREA%
       RT       AREA TYPE  WIDTH      AREA%
     .625        874   PU   .047    5.46421
   * .756       5236   UU   .103   32.73523
     .960       9885   UU   .181   61.80056

TOTAL AREA=   15995
MUL FACTOR=1.0000E+00
```

* RUN # 21 JAN 1, 1901 09:05:22

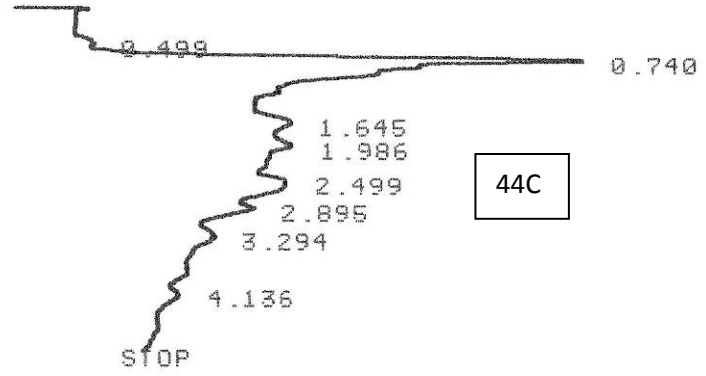

RUN# 21 JAN 1, 1901 09:05:22

AREA%

RT	AREA	TYPE	WIDTH	AREA%
.499	717	PP	.091	.74652
*.740	43276	PU	.110	45.05757
1.645	7235	BU	.212	7.53285
1.986	11735	VU	.260	12.21810
2.499	18961	VU	.339	19.74158
2.895	7194	VP	.181	7.49016
3.294	4459	PU	.250	4.64257
4.136	2469	PP	.210	2.57064

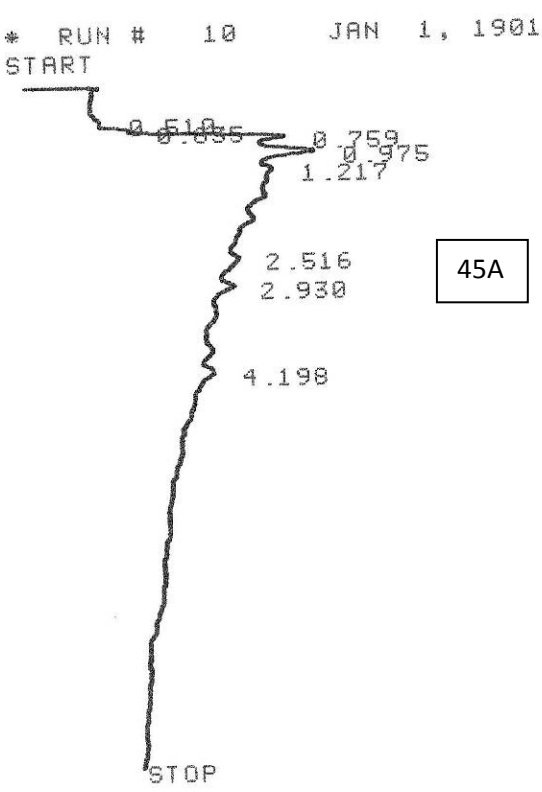

RUN# 10 JAN 1, 1901 07:23:28

AREA%

RT	AREA	TYPE	WIDTH	AREA%
.510	496	PU	.118	.38927
.635	1495	UU	.058	1.17331
* .759	18998	UU	.123	14.91010
.975	43344	UU	.249	34.01744
1.217	25675	UU	.196	20.15038
2.516	21771	UU	.349	17.08642
2.930	12145	UU	.260	9.53170
4.198	3493	UU	.227	2.74139

* RUN # 12 JAN 1, 1901 07:46:03

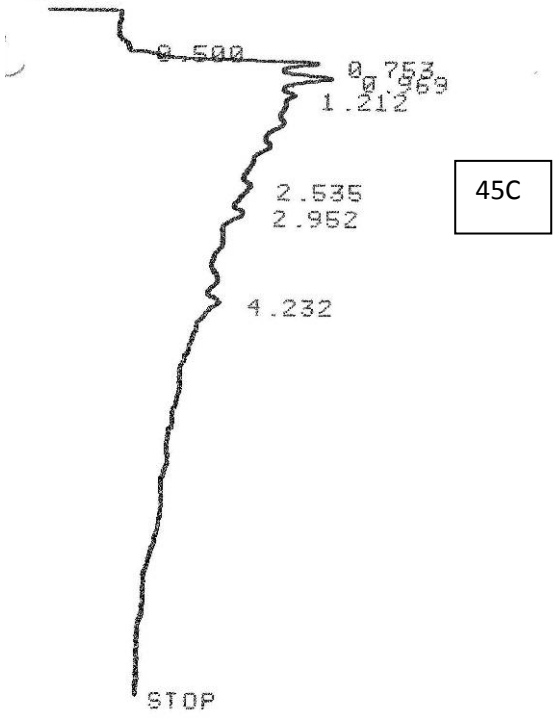

RUN# 12 JAN 1, 1901 07:46:03

AREA%

RT	AREA	TYPE	WIDTH	AREA%
.500	435	PP	.104	.81744
.753	16976	PV	.129	31.90078
.969	22203	VV	.206	41.72318
1.212	4497	VV	.131	8.45062
2.535	2300	PV	.218	4.32209
2.952	2240	VP	.156	4.20934
4.232	4564	VV	.270	8.57653

* RUN # 11 JAN 1, 1901 07:34:45

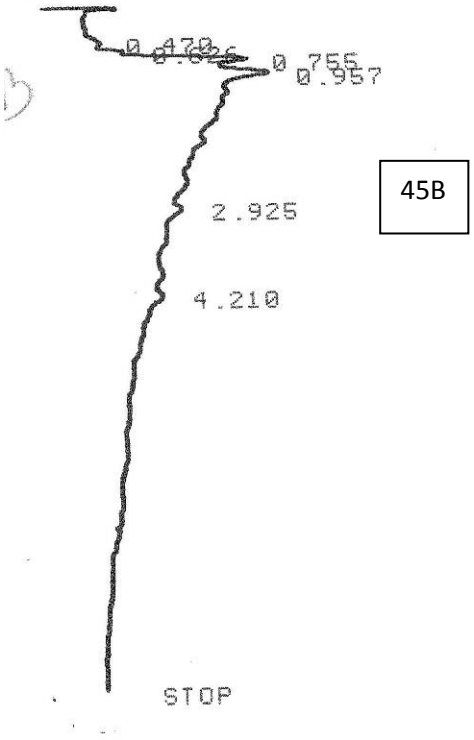

45B

RUN# 11 JAN 1, 1901 07:34:45

AREA%

RT	AREA	TYPE	WIDTH	AREA%
.470	1609	VV	.137	1.79546
.626	2113	VV	.066	2.35786
* .755	17217	VV	.127	19.21219
* .957	39755	VV	.260	44.36198
2.925	17833	VV	.287	19.89958
4.210	11088	VV	.315	12.37293

```
*  RUN #    22      JAN  1, 1901  09:13:52
START
```

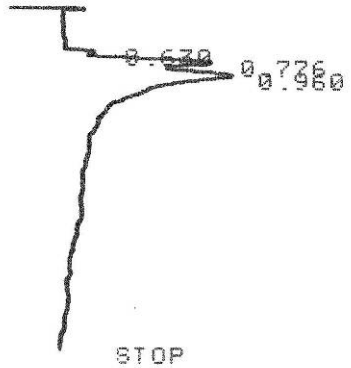

51A

```
STOP

RUN#     22           JAN  1, 1901  09:13:52

AREA%
       RT       AREA TYPE  WIDTH      AREA%
     .630       1370   PU   .056    2.35016
   ◊ .776      14709   VV   .122   25.23246
   ◊ .960      42215   VV   .315   72.41738

TOTAL AREA=  58294
MUL FACTOR=1.0000E+00
```

* RUN # 23 JAN 1, 1901 09:20:11

START

51B

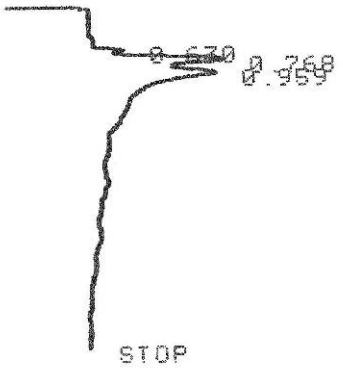

RUN# 23 JAN 1, 1901 09:20:11

AREA%

RT	AREA	TYPE	WIDTH	AREA%
.630	1604	VV	.063	3.62633
.768	13884	VV	.127	31.38904
.959	28744	VV	.283	64.98461

* RUN # 24 JAN 1, 1901 09:26:29

START

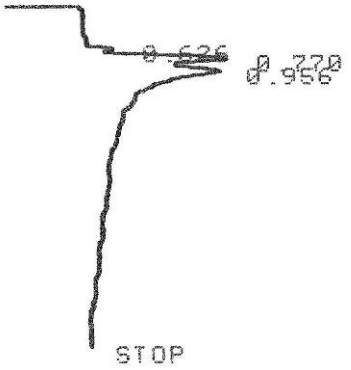

51C

RUN# 24 JAN 1, 1901 09:26:29

AREA%

RT	AREA	TYPE	WIDTH	AREA%
.626	1426	PU	.061	3.01251
.770	15050	VV	.127	31.79399
.956	30860	VV	.282	65.19350

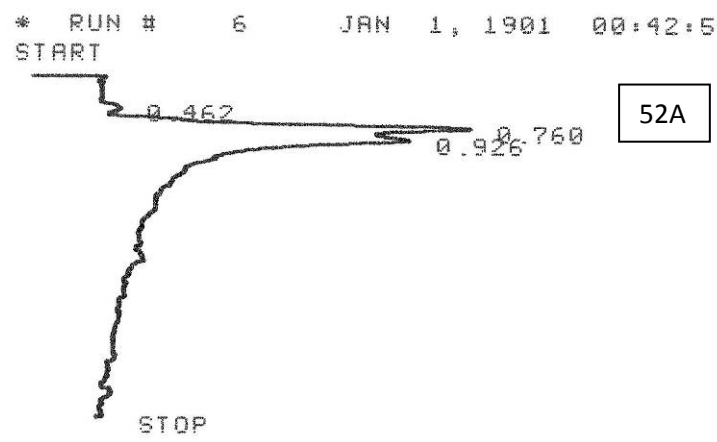

52A

RUN# 6 JAN 1, 1901 00:42:54

AREA%

	RT	AREA	TYPE	WIDTH	AREA%
	.462	860	BV	.117	1.57003
*	.760	21578	VV	.142	39.39315
*	.926	32338	VV	.260	59.03680

TOTAL AREA= 54776
MUL FACTOR=1.0000E+00

* RUN # 7 JAN 1, 1901 00:49:12
START

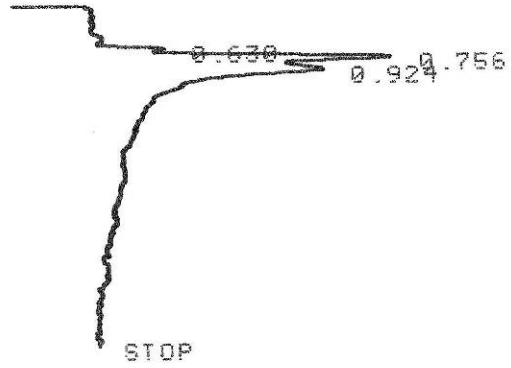

52B

RUN# 7 JAN 1, 1901 00:49:12

AREA%

RT	AREA	TYPE	WIDTH	AREA%
.630	1668	PU	.063	4.78211
* .756	13660	VU	.114	39.16285
*.924	19552	VU	.225	56.05506

TOTAL AREA= 34880
MUL FACTOR=1.0000E+00

* RUN # 8 JAN 1, 1901 00:55:31
START

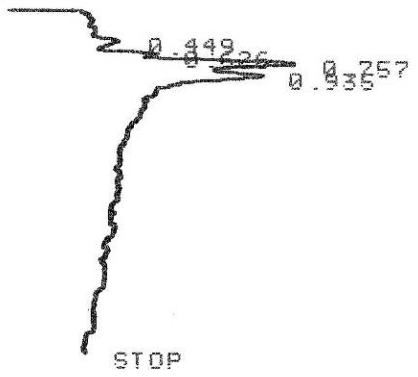

52C

RUN# 8 JAN 1, 1901 00:55:31

AREA%

RT	AREA	TYPE	WIDTH	AREA%
.449	1007	PP	.094	4.77116
.626	1390	PU	.061	6.58580
@ .757	9455	UU	.122	44.79768
▸.935	9254	UU	.164	43.84536

TOTAL AREA= 21106
MUL FACTOR=1.0000E+00

```
*  RUN #     9      JAN  1, 1901  01:01:49
START
```

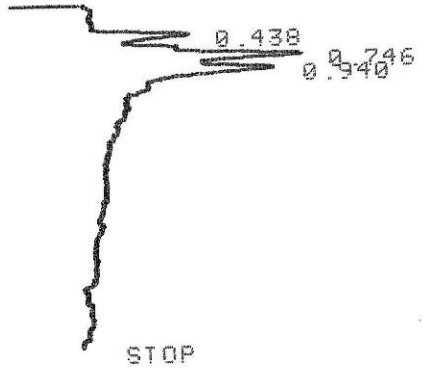

53A

```
RUN#      9           JAN  1, 1901  01:01:49

AREA%
       RT        AREA TYPE  WIDTH      AREA%
     .438        4503   PU   .112   15.21849
   *  .746       13200   UU   .157   44.61117
    *  .940      11886   UU   .170   40.17034

TOTAL AREA=  29589
MUL FACTOR=1.0000E+00
```

```
*  RUN #   10      JAN  1, 1901  01:08:08
START
```

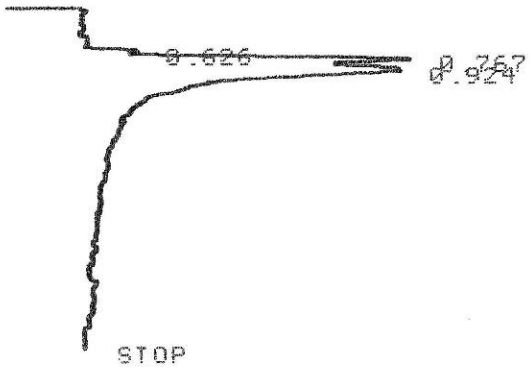

53B

```
RUN#    10           JAN  1, 1901  01:08:08

AREA%
      RT       AREA TYPE  WIDTH      AREA%
    .626       1339   PU   .060    2.58954
  * .767      14858   UU   .109   28.73444
  * .924      35511   UB   .273   68.67603

TOTAL AREA=  51708
MUL FACTOR=1.0000E+00
```

* RUN # 11 JAN 1, 1901 01:14:26
START

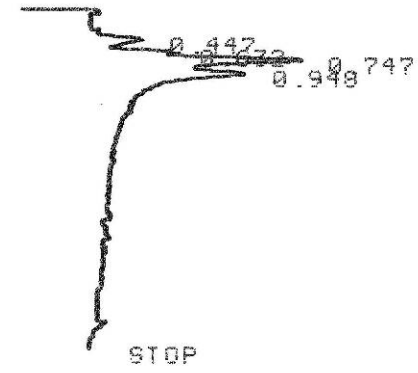

53C

RUN# 11 JAN 1, 1901 01:14:26

AREA%

RT	AREA	TYPE	WIDTH	AREA%
.447	2464	VV	.127	9.61336
.632	1985	VV	.066	7.74453
.747	10843	VV	.128	42.30424
.948	10339	VV	.181	40.33787

```
*  RUN #    15      JAN  1, 1901  01:39:43
START
```

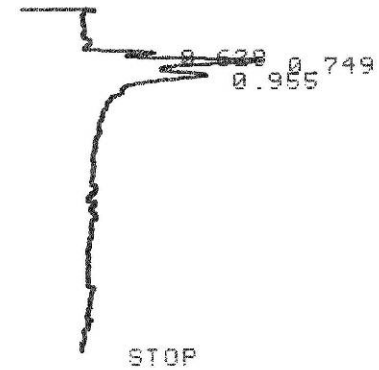

55A

```
RUN#     15           JAN  1, 1901  01:39:43

AREA%
       RT       AREA TYPE  WIDTH       AREA%
     .628       2063   PU    .068   10.44346
   ^ .749       8926   VV    .119   45.18579
   ^ .955       8765   VV    .174   44.37075

TOTAL AREA=  19754
MUL FACTOR=1.0000E+00
```

55B

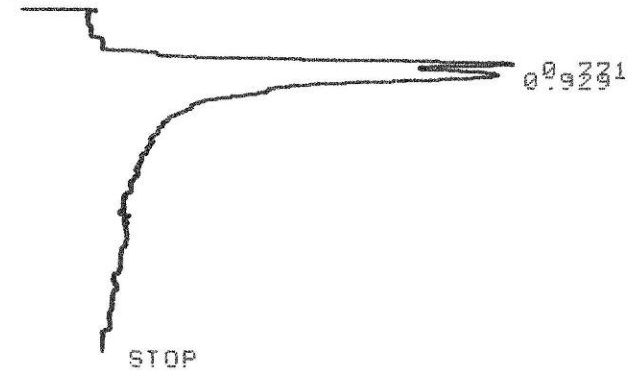

RUN# 16 JAN 1, 1901 01:46:02

AREA%

RT	AREA	TYPE	WIDTH	AREA%
.771	22652	VV	.127	29.17982
.929	54977	VV	.322	70.82019

TOTAL AREA= 77629
MUL FACTOR=1.0000E+00

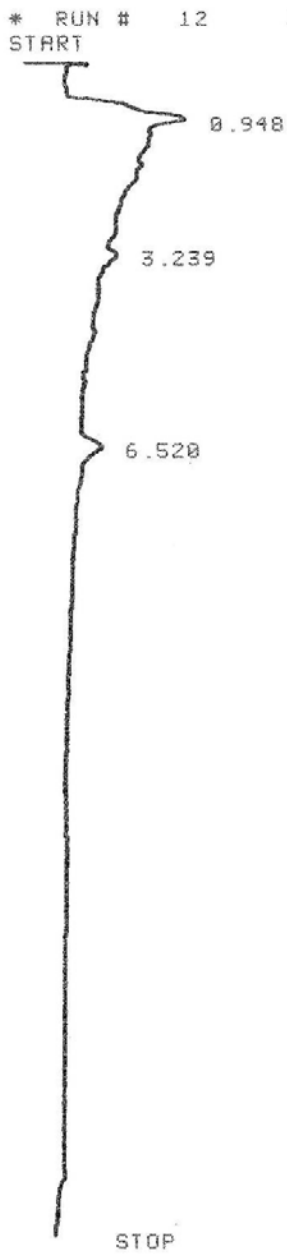

61A

RUN# 12 JAN 1, 1901 03:04:58

AREA%

RT	AREA	TYPE	WIDTH	AREA%
.948	38091	PU	.362	84.71632
3.239	2824	PU	.210	6.28072
6.520	4048	UU	.192	9.00296

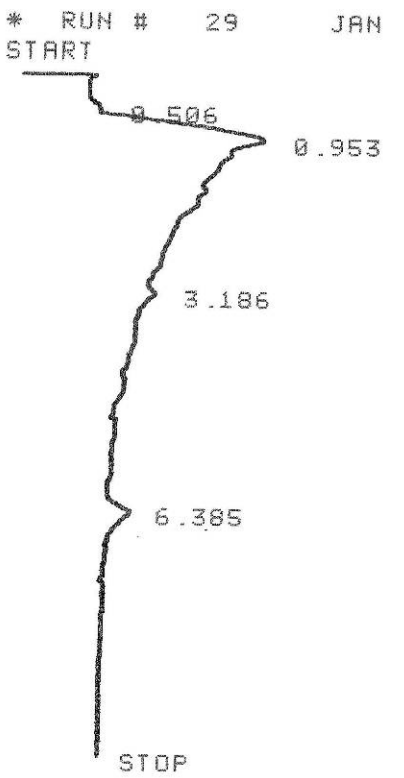

61B

RUN# 29 JAN 1, 1901 08:45:55

AREA%

	RT	AREA	TYPE	WIDTH	AREA%
	.506	555	PU	.117	1.00981
*	.953	49789	VV	.380	90.58970
	3.186	1908	BP	.186	3.47155
*	6.385	2709	VV	.136	4.92895

* RUN # 30 JAN 1, 1901 08:57:14
START

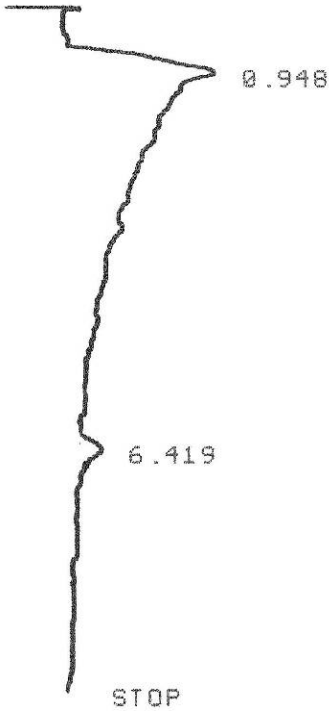

RUN# 30 JAN 1, 1901 08:57:14

AREA%

	RT	AREA	TYPE	WIDTH	AREA%
*	.948	48567	PU	.390	90.26317
*	6.419	5239	BV	.280	9.73683

62A

RUN# 13 JAN 1, 1901 03:26:17

AREA%

RT	AREA	TYPE	WIDTH	AREA%
.676	5012	PU	.120	44.72205
.958	4144	UU	.171	36.97690
3.335	2051	BP	.181	18.30106

* RUN # 31 JAN 1, 1901 09:08:32

START

62B

RUN# 31 JAN 1, 1901 09:08:32

AREA%

RT	AREA	TYPE	WIDTH	AREA%
.712	9010	PU	.192	47.38862
* .920	10003	UU	.244	52.61139

* RUN # 32 JAN 1, 1901 09:19:51

START

62C

RUN# 32 JAN 1, 1901 09:19:51

AREA%

RT	AREA	TYPE	WIDTH	AREA%
.723	7634	PU	.190	87.59610
6.389	1081	PU	.118	12.40390

63A

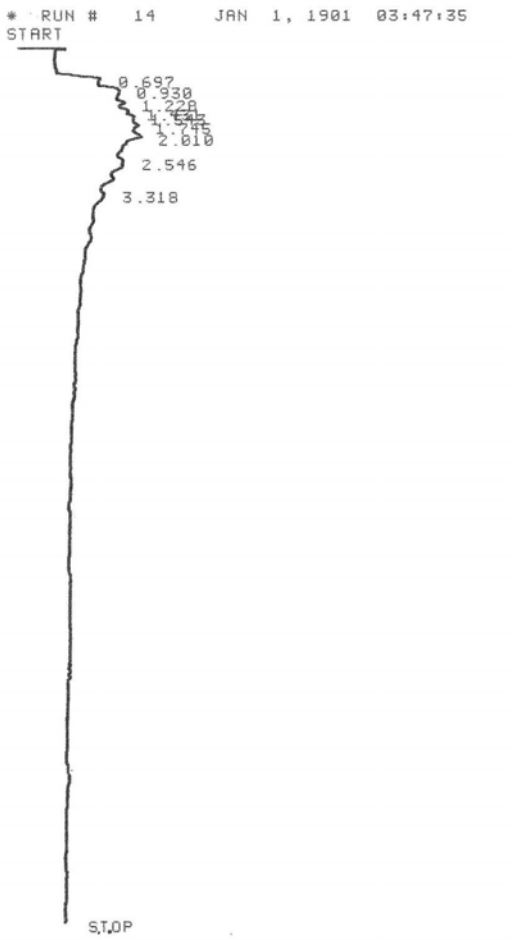

RUN# 14 JAN 1, 1901 03:47:35

AREA%

	RT	AREA	TYPE	WIDTH	AREA%
→	.697	6970	PU	.121	4.41584
→	.930	10984	UU	.138	6.95890
→	1.228	13570	UU	.161	8.59726
	1.431	13454	UU	.152	8.52377
	1.543	10818	UU	.115	6.85373
	1.745	26745	UU	.274	16.94426
	2.010	43853	UU	.439	27.78302
	2.546	15139	UU	.211	9.59130
	3.318	16308	UU	.419	10.33192

* RUN # 33 JAN 1, 1901 09:31:09

START

63B

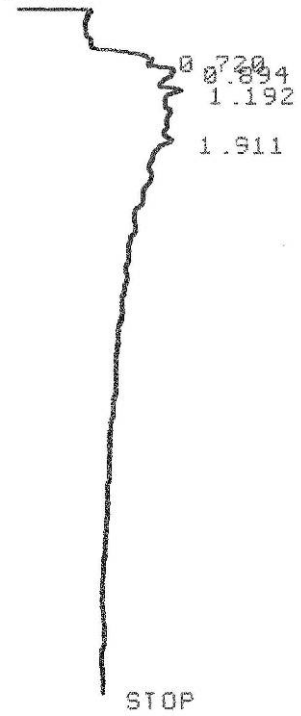

RUN# 33 JAN 1, 1901 09:31:09

AREA%

	RT	AREA	TYPE	WIDTH	AREA%
	.720	10323	VV	.190	16.24569
→	.894	19611	VV	.265	30.86257
→	1.192	14528	VV	.190	22.86326
	1.911	19081	VV	.298	30.02849

63C

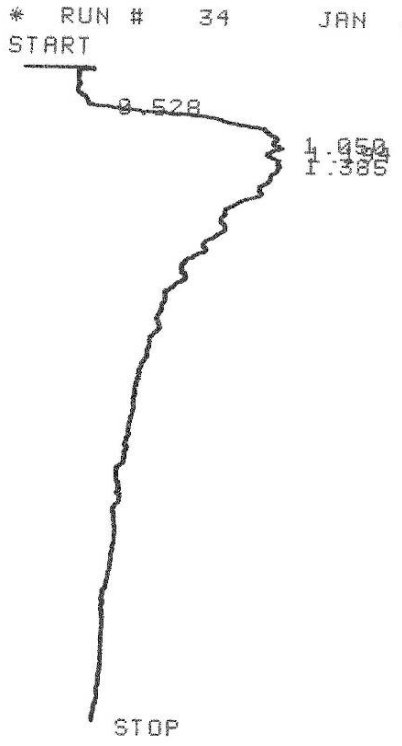

RUN# 34 JAN 1, 1901 09:42:27

AREA%

	RT	AREA	TYPE	WIDTH	AREA%
*	.528	1156	PV	.139	1.02850
→	1.050	65636	VV	.402	58.39658
→	1.194	26554	VV	.162	23.62518
	1.385	19051	VV	.122	16.94974

TOTAL AREA= 112397
MUL FACTOR=1.0000E+00

* RUN # 36 JAN 1, 1901 10:05:04

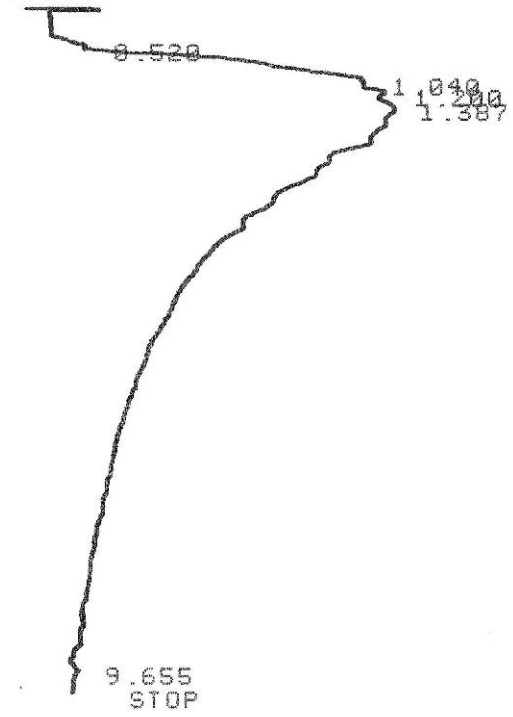

64C

RUN# 36 JAN 1, 1901 10:05:04

AREA%

RT	AREA	TYPE	WIDTH	AREA%
.520	804	PP	.100	1.43145
*1.040	40277	PU	.422	71.70938
*1.200	10657	UU	.165	18.97377
1.387	3484	UB	.257	6.20293
9.655	945	PU	.127	1.68248

TOTAL AREA= 56167

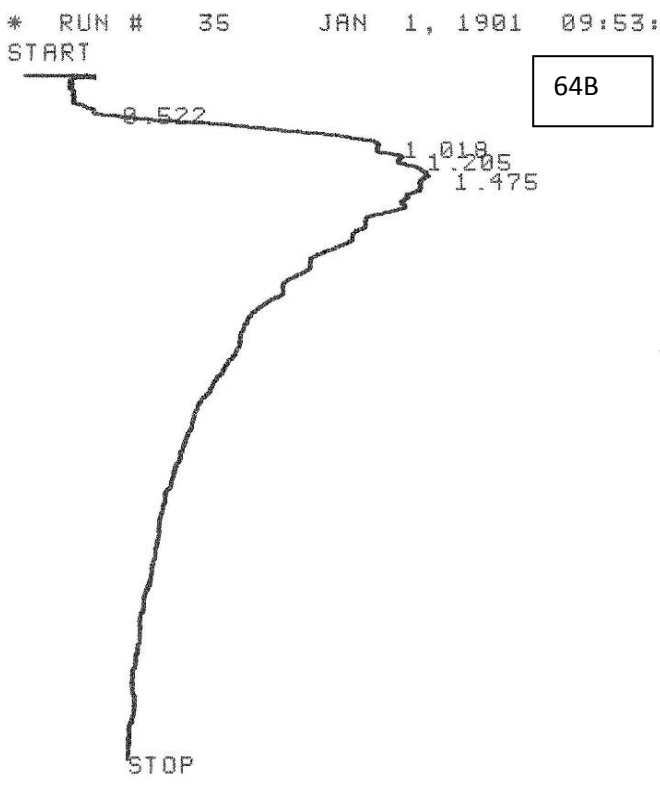

RUN# 35 JAN 1, 1901 09:53:45

AREA%

RT	AREA	TYPE	WIDTH	AREA%
.522	1326	PU	.089	.63236
*1.018	84447	UU	.346	40.27192
*1.205	43131	UU	.168	20.56874
1.475	80788	UU	.303	38.52698

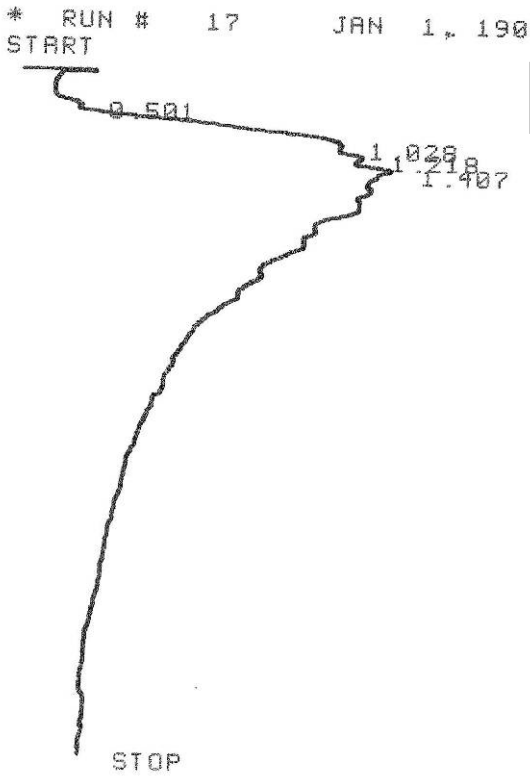

RUN# 17 JAN 1, 1901 05:58:36

AREA%

RT	AREA	TYPE	WIDTH	AREA%
.501	1619	PU	.092	.80422
1.028	76694	UU	.344	38.09669
1.218	46928	UU	.199	23.31086
1.407	76073	UU	.298	37.78822

```
*  RUN #    25      JAN  1, 1901  09:35:07
START
```

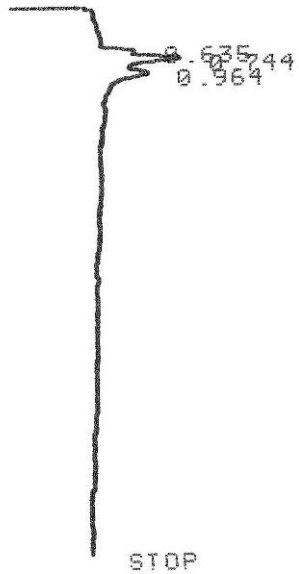

65A

```
RUN#     25           JAN  1, 1901  09:35:07

AREA%
       RT       AREA TYPE  WIDTH       AREA%
     .635       2238   UU   .070    12.25697
     .744       9125   UU   .130    49.97536
     .964       6896   UU   .166    37.76768

TOTAL AREA=  18259
MUL FACTOR=1.0000E+00
```

* RUN # 26 JAN 1, 1901 09:44:26
START

65B

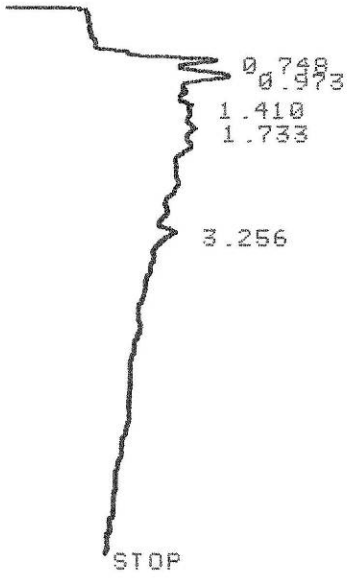

RUN# 26 JAN 1, 1901 09:44:26

AREA%

RT	AREA	TYPE	WIDTH	AREA%
.748	14213	PV	.145	24.13270
.973	23124	VV	.222	39.26309
1.410	7835	VV	.132	13.30334
1.733	11653	VV	.214	19.78606
3.256	2070	PV	.129	3.51473

* RUN # 27 JAN 1, 1901 09:53:44

START

65C

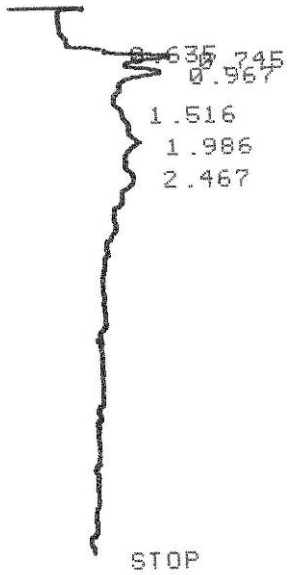

RUN# 27 JAN 1, 1901 09:53:44

AREA%

RT	AREA	TYPE	WIDTH	AREA%
.635	1834	VV	.055	3.05860
.745	12507	VV	.140	20.85821
.967	17406	VV	.219	29.02838
1.516	6460	VV	.167	10.77349
1.986	16452	VV	.348	27.43738
2.467	5303	VV	.144	8.84394

```
*  RUN #     5      JAN  1, 1901  00:24:15
START
```

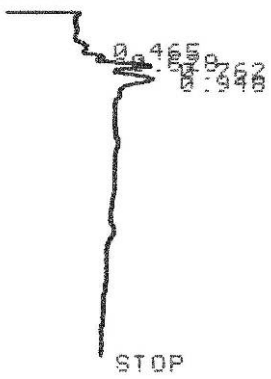

71A

```
RUN#      5           JAN  1, 1901  00:24:15

AREA%
       RT       AREA TYPE  WIDTH      AREA%
     .465        248   PB   .067    1.67432
     .628        908   PV   .058    6.13017
     .762       4977   VV   .095   33.60114
   * .948       8679   VV   .190   58.59430

TOTAL AREA=  14812
MUL FACTOR=1.0000E+00
```

* RUN # 6 JAN 1, 1901 00:36:13

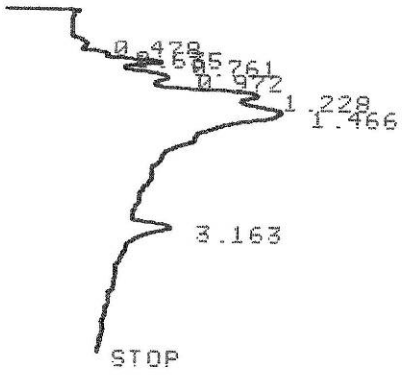

71B

RUN# 6 JAN 1, 1901 00:36:13

AREA%

RT	AREA	TYPE	WIDTH	AREA%
.478	1298	PU	.126	1.10037
.635	1516	UU	.063	1.28518
.761	7756	UU	.114	6.57511
.972	12505	UU	.182	10.60105
1.228	25723	UU	.185	21.80654
1.466	62263	UU	.401	52.78314
3.163	6899	BP	.191	5.84859

TOTAL AREA= 117960
MUL FACTOR=1.0000E+00

```
*  RUN #     7      JAN  1, 1901  00:42:31
START
```

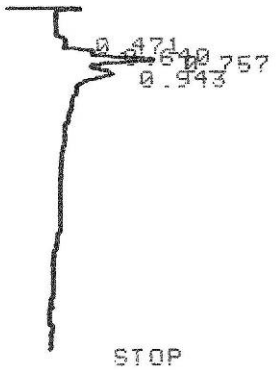

71C

```
STOP

RUN#      7           JAN  1, 1901  00:42:31

AREA%
       RT       AREA TYPE  WIDTH       AREA%
     .471       1042   PU   .119     5.07426
     .640       1935   UU   .063     9.42294
     .757       9094   UU   .112    44.28538
   @ .943       8464   UU   .201    41.21744

TOTAL AREA=  20535
MUL FACTOR=1.0000E+00
```

```
*  RUN #     4      JAN  1, 1901  01:45:18
START
```

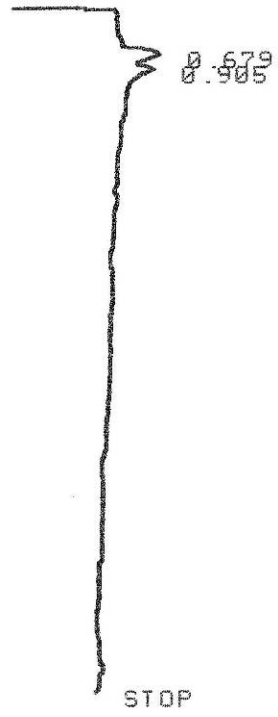

72A

```
RUN#      4           JAN  1, 1901  01:45:18

AREA%
       RT       AREA TYPE  WIDTH       AREA%
     .679       5175   BV   .165    54.13749
     .905       4384   VV   .172    45.86253

-----  -----     ----
```

```
*  RUN #    10      JAN  1, 1901  04:15:51
START
```

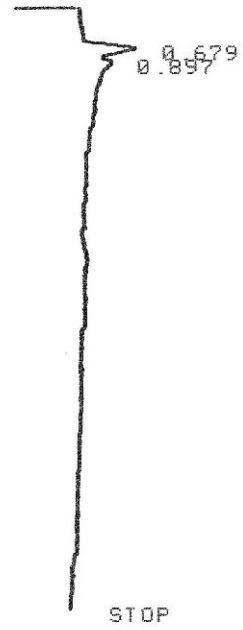

72B

```
RUN#     10           JAN  1, 1901  04:15:51

AREA%
      RT       AREA TYPE  WIDTH      AREA%
    .679       6829   PU    .146   68.63315
    .897       3121   VV    .163   31.36684
```

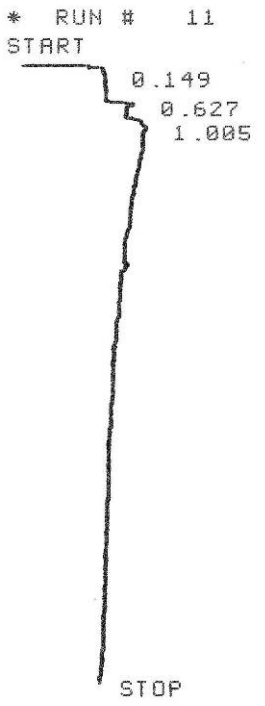

RUN# 11 JAN 1, 1901 04:27:09

AREA%

RT	AREA	TYPE	WIDTH	AREA%
.149	2960	BV	.249	33.34835
.627	1714	PV	.070	19.31050
1.005	4202	VV	.232	47.34114

```
*  RUN #    10      JAN  1, 1901   01:01:27
START
```

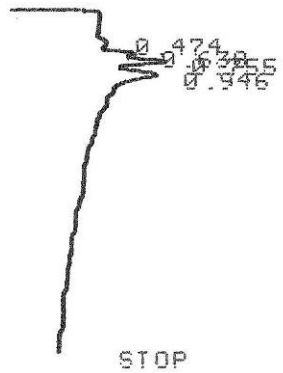

73A

```
STOP

RUN#     10           JAN  1, 1901   01:01:27

AREA%
       RT       AREA TYPE  WIDTH       AREA%
     .474       1268   PV    .123     6.06815
     .638       2520   UU    .073    12.05972
     .755       6549   UU    .109    31.34093
     .946      10559   UU    .196    50.53122

TOTAL AREA=  20896
MUL FACTOR=1.0000E+00
```

* RUN # 9 JAN 1, 1901 00:55:09

START

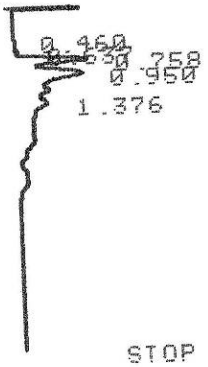

73B

STOP

RUN# 9 JAN 1, 1901 00:55:09

AREA%

RT	AREA	TYPE	WIDTH	AREA%
.460	4614	BU	.133	9.05665
.637	3542	UU	.077	6.95246
.758	12469	UU	.124	24.47494
.950	19996	UU	.222	39.24941
1.376	10325	UU	.212	20.26655

TOTAL AREA= 50946

MUL FACTOR=1.0000E+00

```
*  RUN #     8      JAN  1, 1901   00:48:50
START
```

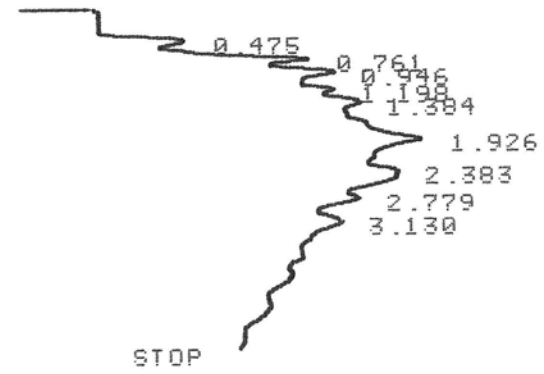

73C

```
RUN#     8           JAN  1, 1901   00:48:50

AREA%
       RT       AREA TYPE  WIDTH      AREA%
     .475       9653   PU    .141    2.49854
     .761      28136   VV    .169    7.28259
     .946      41145   VV    .224   10.64978
    1.198      27382   VV    .156    7.08743
    1.384      41153   VV    .212   10.65185
    1.926     110631   VV    .480   28.63522
    2.383      31192   VV    .158    8.07359
    2.779      38978   VV    .253   10.08888
    3.130      58076   VV    .447   15.03212

TOTAL AREA= 386346
MUL FACTOR=1.0000E+00
```

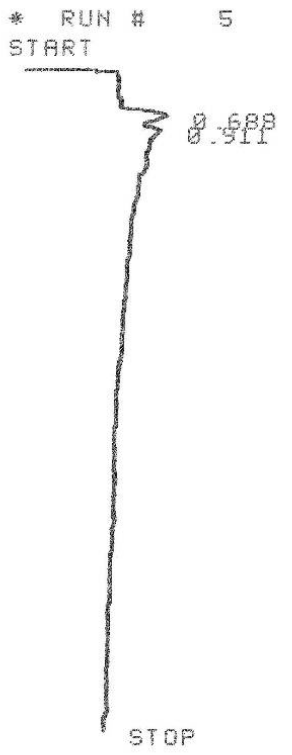

73A

RUN# 5 JAN 1, 1901 01:56:36

AREA%

RT	AREA	TYPE	WIDTH	AREA%
.688	5714	BV	.160	63.61611
.911	3268	VV	.160	36.38389

* RUN # 12 JAN 1, 1901 04:38:27

START

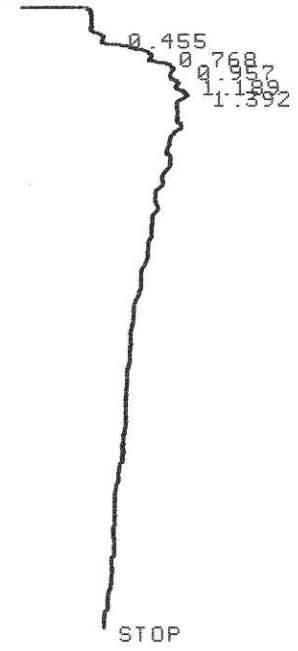

73B

RUN# 12 JAN 1, 1901 04:38:27

AREA%

RT	AREA	TYPE	WIDTH	AREA%
.455	336	PB	.073	1.26587
.768	6322	PV	.181	23.81795
.957	9181	VV	.225	34.58915
1.189	5487	VV	.177	20.67212
1.392	5217	VV	.197	19.65490

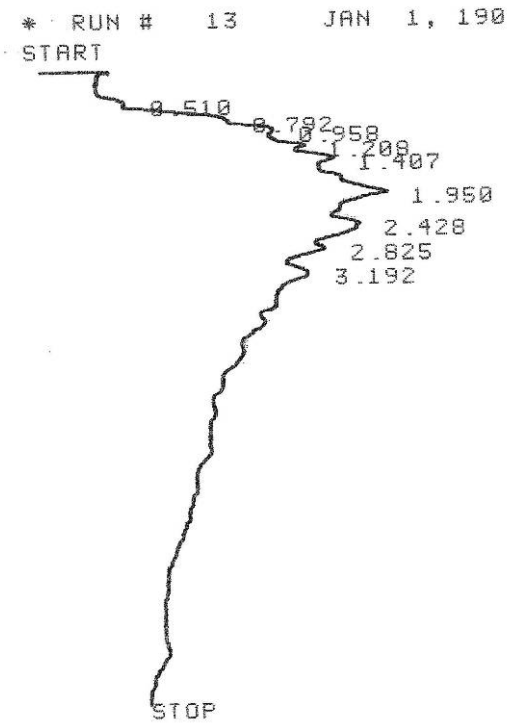

73C

RUN# 13 JAN 1, 1901 04:49:45

AREA%

RT	AREA	TYPE	WIDTH	AREA%
.510	1637	BV	.111	.62929
.792	15991	VV	.169	6.14722
.958	25172	VV	.194	9.67655
1.208	31787	VV	.219	12.21947
1.407	35896	VV	.222	13.79904
1.950	91292	VV	.496	35.09422
2.428	23257	VV	.173	8.94039
2.825	19524	VV	.231	7.50536
3.192	15578	VV	.305	5.98845

74A

```
*  RUN #    11      JAN  1, 1901  01:07:46
START
```

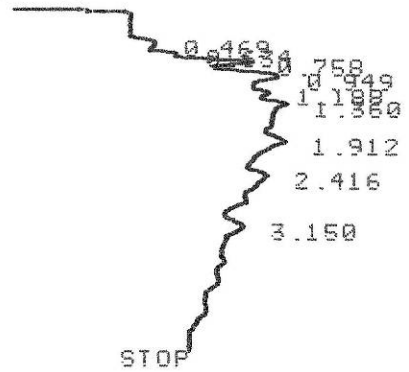


```
RUN#    11           JAN  1, 1901  01:07:46

AREA%
      RT       AREA TYPE  WIDTH      AREA%
    .469       1547   PP   .107    3.11280
    .634       1045   PU   .055    2.10270
    .758       7228   UU   .103   14.54385
    .949      13658   UU   .178   27.48199
   1.188       5627   UU   .121   11.32239
   1.360       6559   UU   .147   13.19772
   1.912       4507   BU   .197    9.06877
   2.416       5897   UU   .268   11.86567
   3.150       3630   PU   .187    7.30412

TOTAL AREA=  49698
MUL FACTOR=1.0000E+00
```

```
*  RUN #    12      JAN  1, 1901  01:14:04
START
```

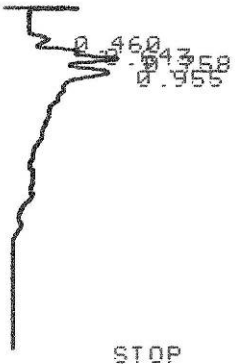

74B

```
STOP

RUN#     12           JAN  1, 1901  01:14:04

AREA%
       RT       AREA TYPE  WIDTH      AREA%
     .460       1217   PP    .093   11.76982
     .643        720   PB    .054    6.96325
     .758       3092   BP    .080   29.90329
     .955       5311   PU    .141   51.36365

TOTAL AREA=  10340
```

```
*  RUN #    13      JAN  1, 1901   01:20:26
START
```

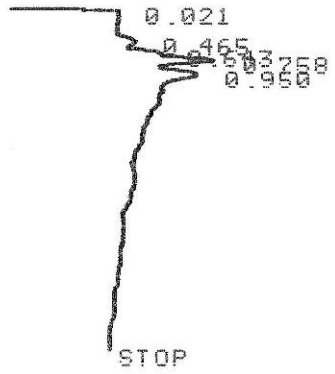

74C

```
RUN#     13           JAN  1, 1901   01:20:26

AREA%
       RT       AREA TYPE  WIDTH       AREA%
     .021        562   PB    .025     2.13234
     .465       1709   PV    .125     6.48429
     .643       2042   VV    .063     7.74776
     .758       9610   VV    .124    36.46229
   *.950      12433   VV    .206    47.17333

TOTAL AREA=  26356
MUL FACTOR=1.0000E+00
```

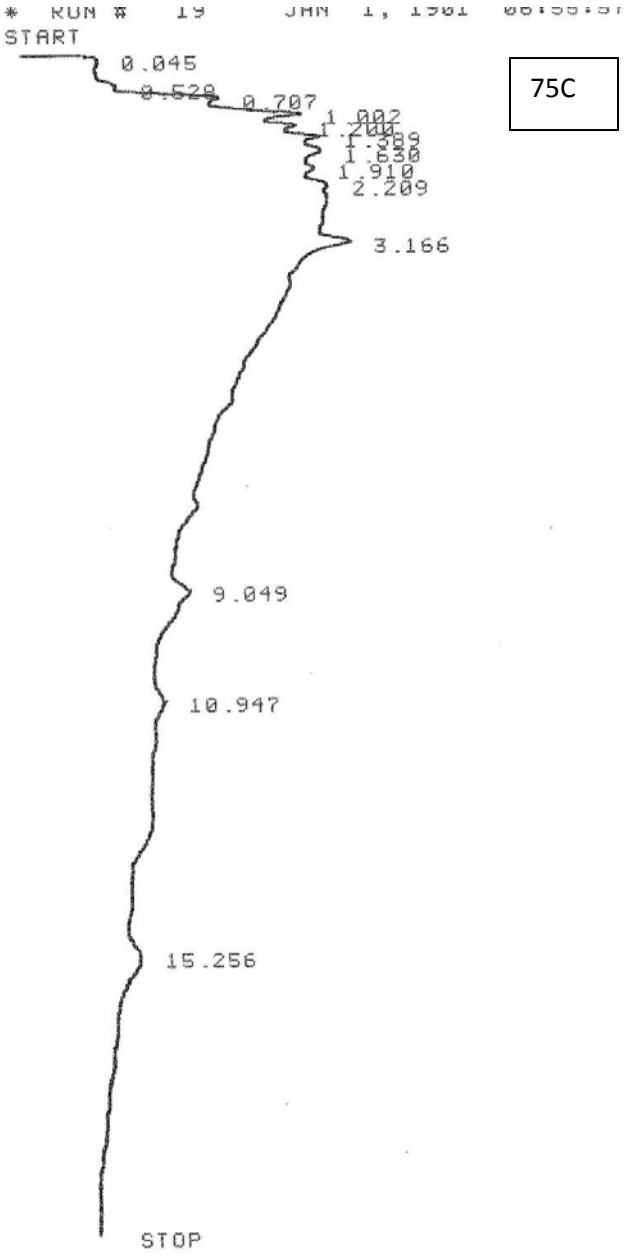

75C

RUN# 19 JAN 1, 1901 06:55:57

AREA%

RT	AREA	TYPE	WIDTH	AREA%
.045	336	BB	.054	.21494
.707	13165	PU	.150	8.42177
1.002	29205	UU	.211	18.68271
1.200	17200	UU	.155	11.00300
1.389	20866	UU	.180	13.34818
1.630	23060	UU	.252	14.75169
1.910	14436	UU	.261	9.23484
2.209	7818	UU	.215	5.00125
3.166	10211	UP	.236	6.53207
*9.049	12425	UP	.583	7.94839
10.947	3292	BU	.312	2.10592
15.256	4307	UU	.271	2.75523

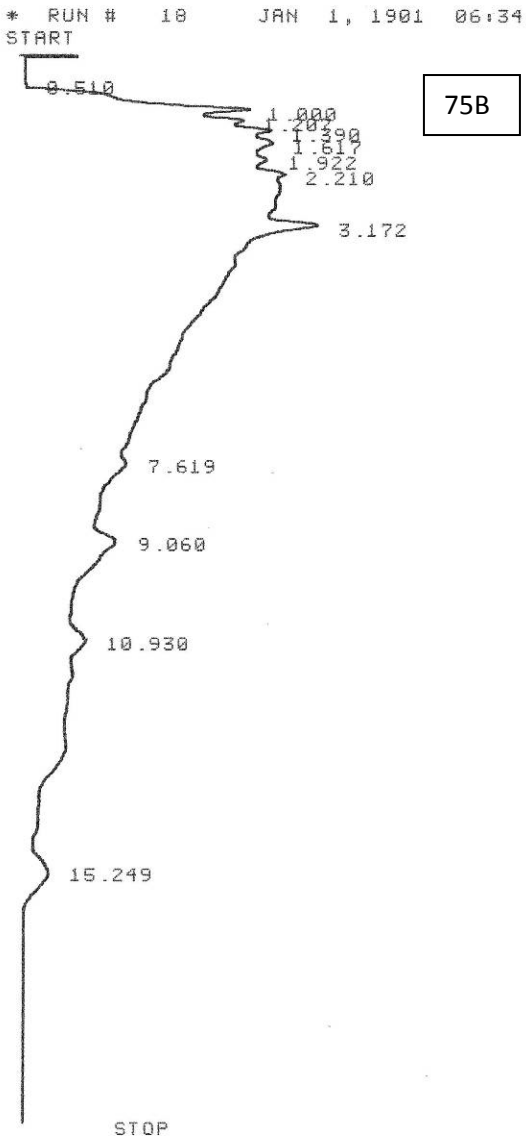

75B

RUN# 18 JAN 1, 1901 06:34:39

AREA%

RT	AREA	TYPE	WIDTH	AREA%
.510	238	PU	.035	.05477
1.000	66625	VV	.283	15.33181
1.207	35121	VV	.161	8.08208
1.390	45466	VV	.191	10.46268
1.617	65199	VV	.285	15.00366
1.922	56401	VV	.270	12.97906
2.210	45908	VV	.215	10.56440
3.172	85046	VV	.419	19.57087
7.619	4744	VP	.335	1.09169
* 9.060	11462	PU	.384	2.63765
10.930	5970	PP	.364	1.37382
15.249	12374 I	BB	.560	2.84752

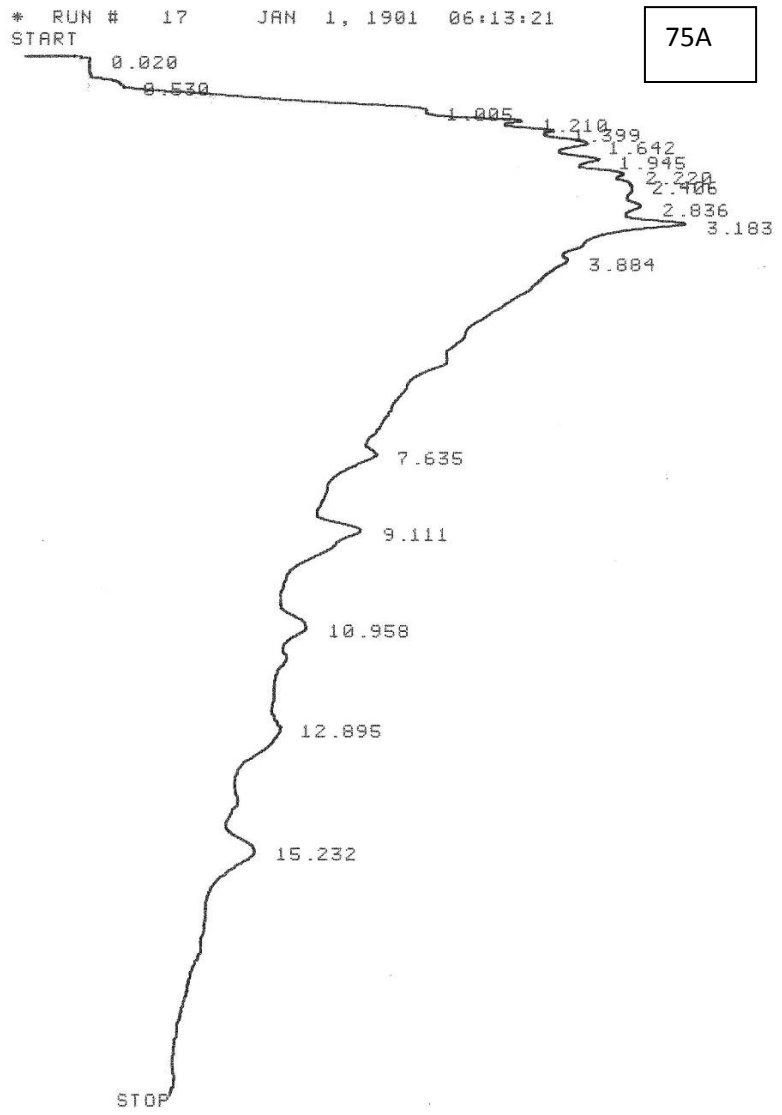

75A

RUN# 17 JAN 1, 1901 06:13:21

AREA%

RT	AREA	TYPE	WIDTH	AREA%
.020	648	BU	.061	.16733
.530	942	PP	.151	.24324
1.005	52447	PU	.245	13.54292
1.210	51074	UU	.196	13.18838
1.399	41128	UU	.170	10.62012
1.642	62168	UU	.299	16.05310
1.945	33653	UU	.256	8.68991
2.220	15788	UU	.198	4.07680
2.406	4723	UU	.148	1.21958
2.836	5715	BU	.208	1.47573
3.183	26548	UU	.265	6.85525
3.884	10518	UB	.600	2.71597
7.635	6291	BP	.268	1.62447
9.111	33818	PP	.545	8.73252
10.958	12027	PU	.407	3.10563
12.895	6255	UU	.254	1.61517
15.232	23522	BU	.588	6.07388

TOTAL AREA= 387265

```
*  RUN #     5      JAN  1, 1901  01:54:35
START
```

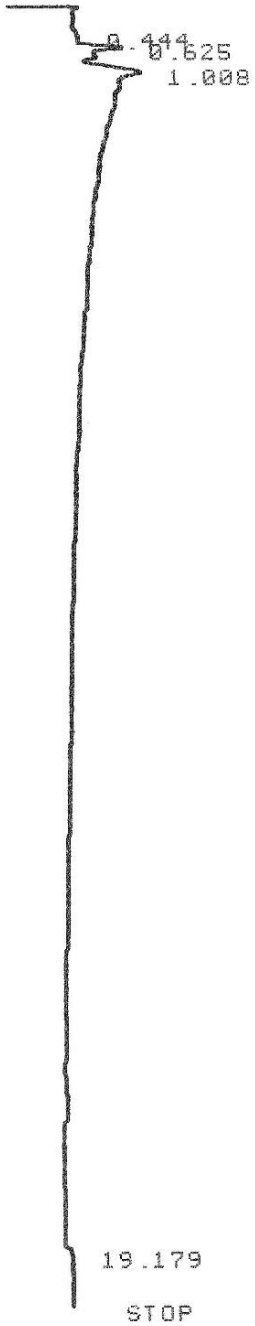

81A

```
RUN#      5           JAN  1, 1901  01:54:35

AREA%
       RT       AREA TYPE  WIDTH      AREA%
     .444        788   PU    .151    5.44876
     .625       3242   UU    .081   22.41737
   . 1.008      9274   PU    .192   64.12669
  . 19.179      1158   PU    .166    8.00719
```

```
*  RUN #    10      JAN  1, 1901   03:51:51
START
```

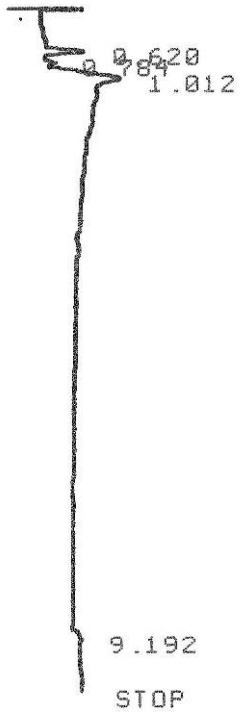

81B

```
RUN#     10           JAN  1, 1901   03:51:51

AREA%
       RT       AREA TYPE  WIDTH       AREA%
     .620       2629   VP   .071    19.02591
     .784        442   PP   .057     3.19873
    1.012       9843   PU   .189    71.23318
   .9.192        904   PU   .146     6.54219
```

*. RUN # 11 JAN 1, 1901 04:03:10
START

81C

STOP

RUN# 11 JAN 1, 1901 04:03:10

AREA%

RT	AREA	TYPE	WIDTH	AREA%
.625	3479	VV	.089	25.37194
1.007	10233	PV	.206	74.62810

*. RUN # 6 JAN 1, 1901 02:15:53

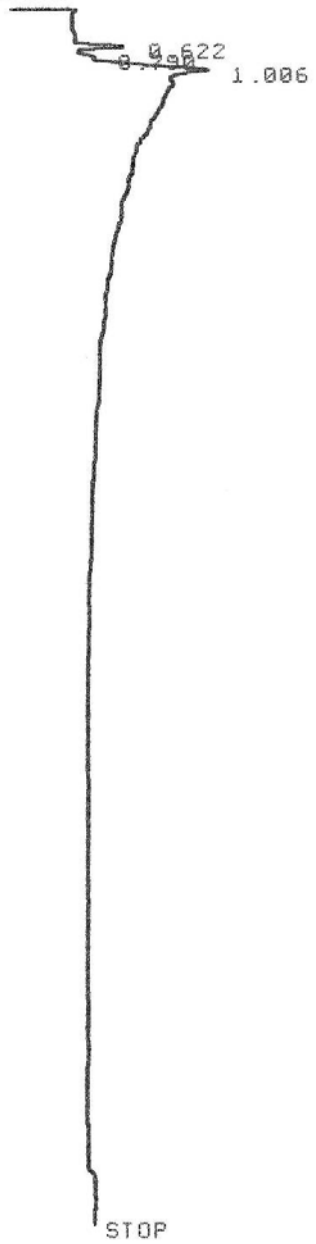

82A

RUN# 6 JAN 1, 1901 02:15:53

AREA%

RT	AREA	TYPE	WIDTH	AREA%
.622	3092	UP	.067	10.43537
.790	1046	PU	.068	3.53021
. 1.006	25492	UU	.215	86.03443

TOTAL AREA= 29630

*. RUN # 12 JAN 1, 1901 04:14:29

START

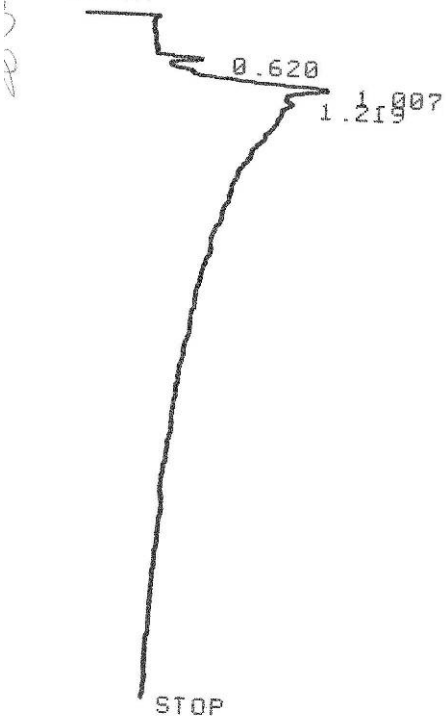

82B

RUN# 12 JAN 1, 1901 04:14:29

AREA%

RT	AREA	TYPE	WIDTH	AREA%
.620	2045	PU	.060	5.23339
1.007	24988	UU	.209	63.94717
1.219	12043	UU	.158	30.81942

TOTAL AREA=

```
*  RUN #    13      JAN  1, 1901   04:25:50
START
```

82C

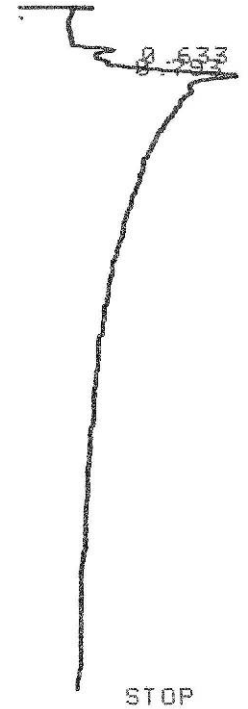


```
RUN#     13           JAN  1, 1901   04:25:50

AREA%
       RT       AREA TYPE  WIDTH       AREA%
     .633       1656   PU    .062     6.33730
     .793       1409   UU    .094     5.39206
    1.007      23066   UU    .197    88.27062
```

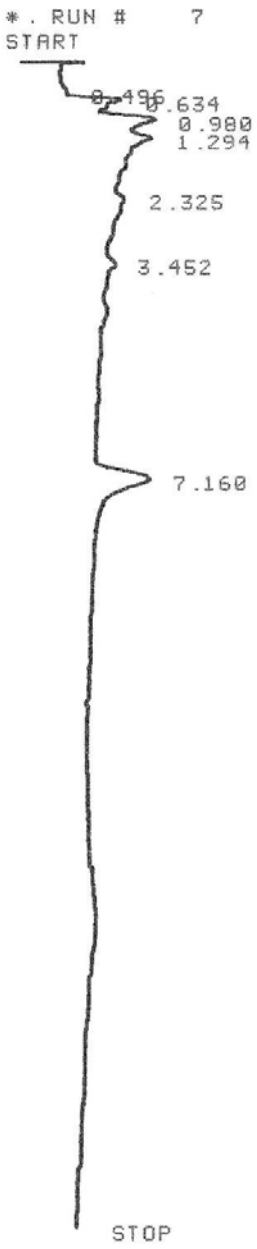

83A

RUN# 7 JAN 1, 1901 02:37:12

AREA%

RT	AREA	TYPE	WIDTH	AREA%
.496	692	PU	.154	.90680
.634	7626	VU	.136	9.99318
. .980	20108	VU	.246	26.34972
1.294	20533	VU	.280	26.90665
. 2.325	5778	VU	.226	7.57155
3.452	1058	VU	.122	1.38641
.7.160	20517	PU	.374	26.88568

*. RUN # 14 JAN 1, 1901 04:37:09

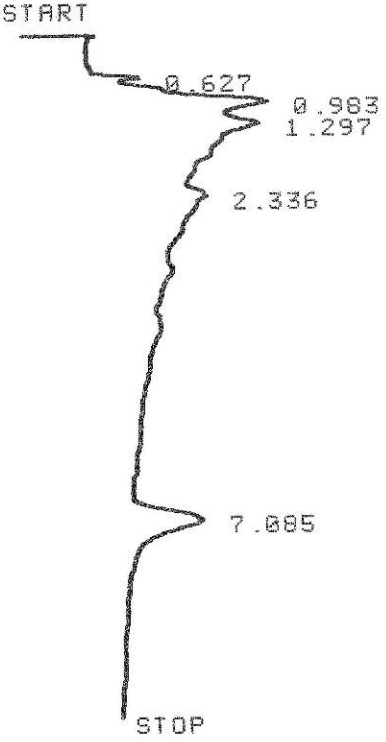

RUN# 14 JAN 1, 1901 04:37:09

AREA%

RT	AREA	TYPE	WIDTH	AREA%
.627	3790	PU	.088	2.50788
.983	43138	VV	.297	29.45538
1.297	40797	VV	.303	27.85690
2.336	37450	VV	.494	25.57152
7.085	21277	VV	.357	14.52831

*. RUN # 15 JAN 1, 1901 04:48:28

START

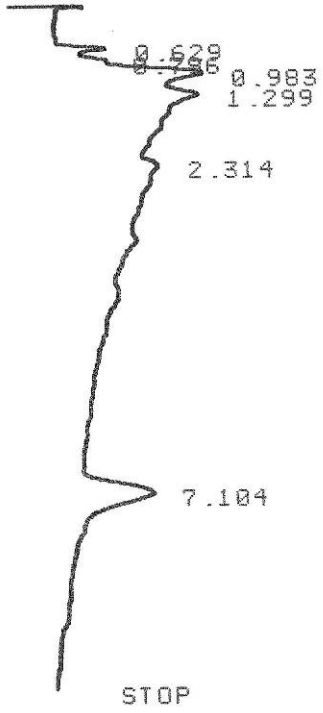

83C

RUN# 15 JAN 1, 1901 04:48:28

AREA%

RT	AREA	TYPE	WIDTH	AREA%
.629	2964	PU	.076	3.16045
.796	2930	VV	.083	3.12420
.983	26453	VV	.238	28.20631
. 1.299	28773	VV	.293	30.68007
2.314	8224	VV	.240	8.76909
7.104	24440	BV	.382	26.05989

*. RUN # 8 JAN 1, 1901 02:58:30

84A

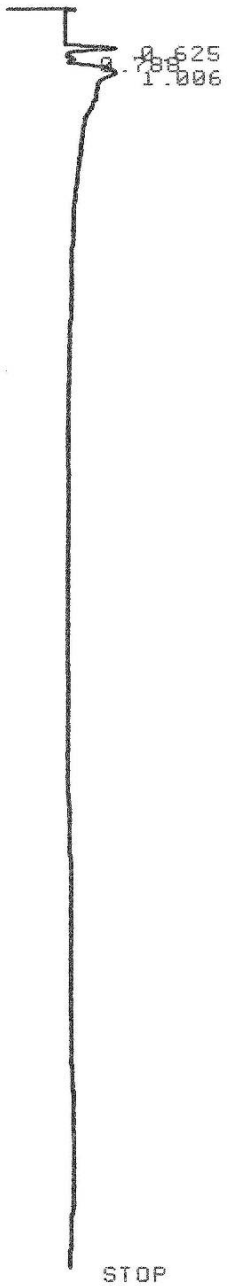

RUN# 8 JAN 1, 1901 02:58:30

AREA%

RT	AREA	TYPE	WIDTH	AREA%
.625	3388	UP	.071	23.15790
.788	470	PU	.057	3.21258
. 1.006	10772	UU	.237	73.62954

*. RUN # 16 JAN 1, 1901 04:59:46

START

84B

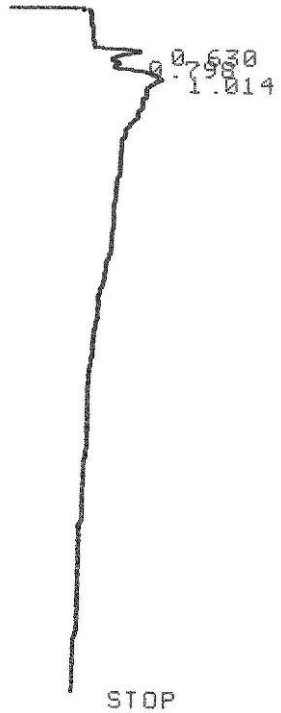

RUN# 16 JAN 1, 1901 04:59:46

AREA%

RT	AREA	TYPE	WIDTH	AREA%
.630	3809	PU	.098	21.44949
.798	1449	UU	.081	8.15970
1.014	12500	UU	.253	70.39082

```
*  RUN #    17       JAN  1, 1901   05:11:05
START
```

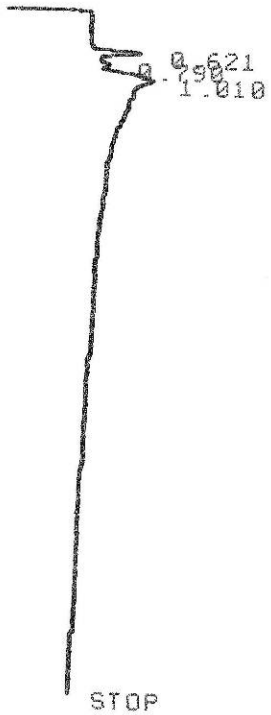

84C

```
UN#    17              JAN  1, 1901   05:11:05

REA%
      RT        AREA  TYPE   WIDTH       AREA%
    .621        2649    PU    .068    20.69531
    .790         878    UU    .082     6.85938
  1.010         9273    UU    .215    72.44531
.
DTAL AREA=   12800
JL FACTOR=1.0000E+00
```

```
*  RUN #    19      JAN  1, 1901  05:33:41
START
```

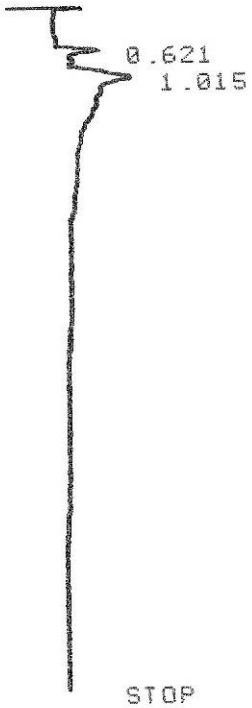

85C

```
RUN#     19           JAN  1, 1901  05:33:41

AREA%
        RT       AREA TYPE  WIDTH      AREA%
      .621       2809   PU   .079   22.40926
    1.015        9726   VU   .190   77.59075
```

*. RUN # 9 JAN 1, 1901 03:19:49

START

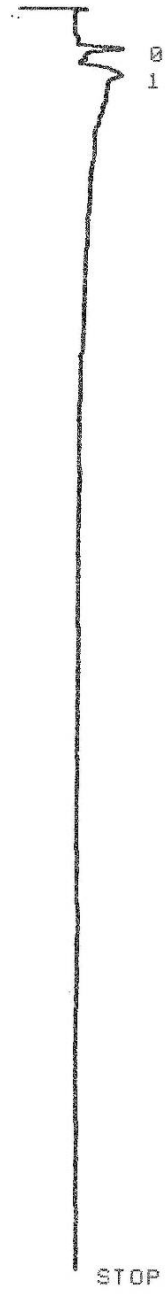

85A

RUN# 9 JAN 1, 1901 03:19:49

AREA%

RT	AREA	TYPE	WIDTH	AREA%
.625	3793	VV	.086	30.23515
1.025	8752	PV	.227	69.76483

* RUN # 18 JAN 1, 1901 05:22:23

START

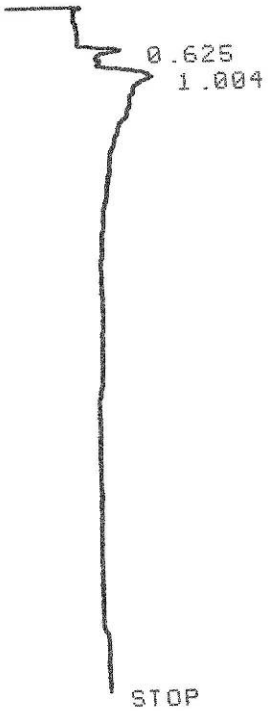

85B

RUN# 18 JAN 1, 1901 05:22:23

AREA%

RT	AREA	TYPE	WIDTH	AREA%
.625	3384	BU	.098	19.79990
1.004	13707	VV	.247	80.20010

```
*  RUN #    14      JAN  1, 1901  05:41:20
START
```

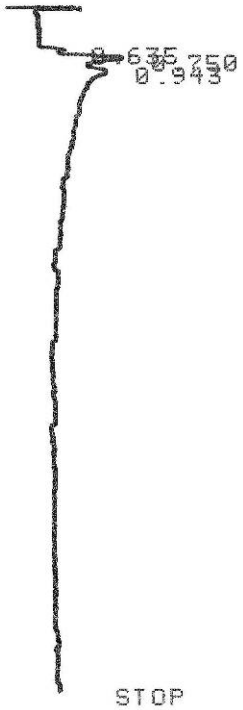

91B

```
RUN#     14          JAN  1, 1901  05:41:20

AREA%
       RT       AREA TYPE  WIDTH      AREA%
     .635       1430   PU   .068    5.28905
     .750       8145   UU   .118   30.12538
     .943      17462   UU   .339   64.58557
```

```
*  RUN #    15      JAN  1, 1901  05:52:39
START
```

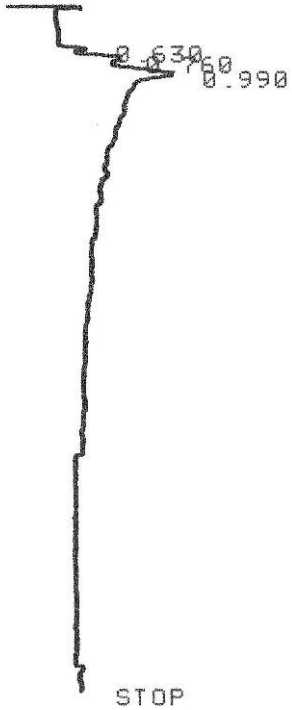

91C

```
RUN#     15           JAN  1, 1901  05:52:39

AREA%
       RT       AREA TYPE  WIDTH      AREA%
     .630       1299   PU   .060    5.43902
     .760       4550   VV   .109   19.05121
     .990      18034   VV   .255   75.50976
```

* RUN # 4 JAN 1, 1901 02:00:12

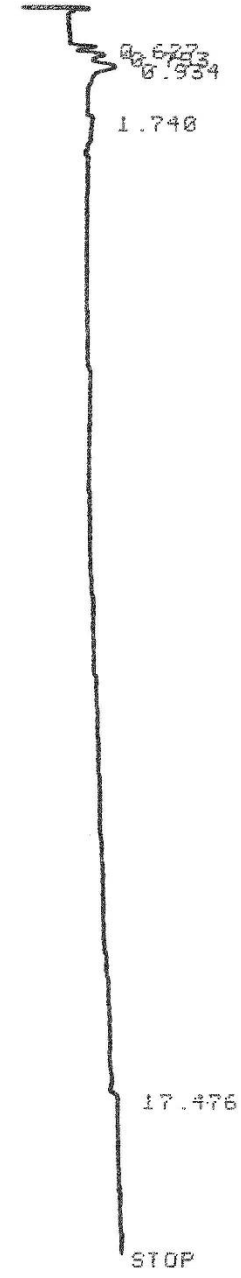

91A

RUN# 4 JAN 1, 1901 02:00:12

AREA%

RT	AREA	TYPE	WIDTH	AREA%
.627	1608	BU	.063	10.68154
.753	3615	UU	.109	24.01355
.934	7973	UU	.190	52.96267
1.740	1061	UU	.088	7.04796
17.476	797	PU	.125	5.29427

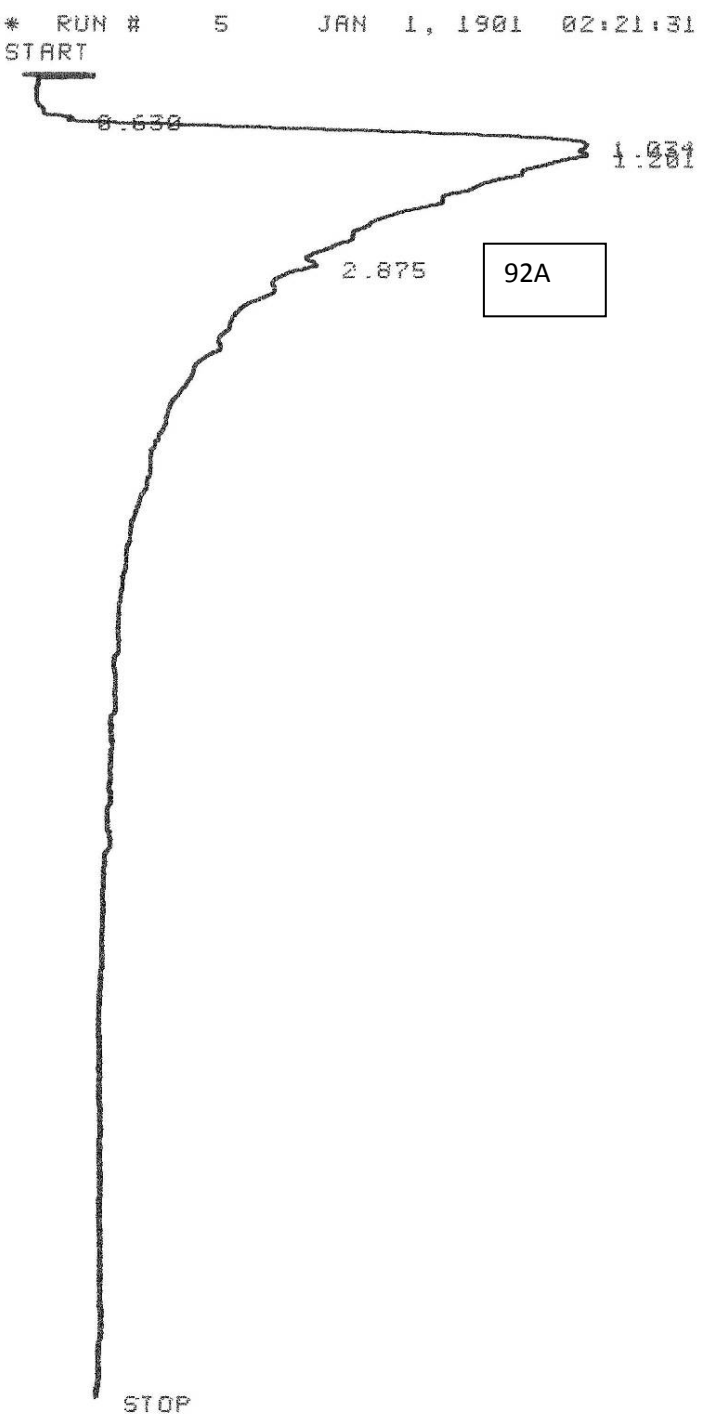

RUN# 5 JAN 1, 1901 02:21:31

AREA%

RT	AREA	TYPE	WIDTH	AREA%
.630	1331	PU	.058	.38160
1.034	149635	UU	.321	42.90043
1.201	138641	UU	.299	39.74845
2.875	59189	UU	.326	16.96952

* RUN #   16   JAN 1, 1901 06:03:57

START

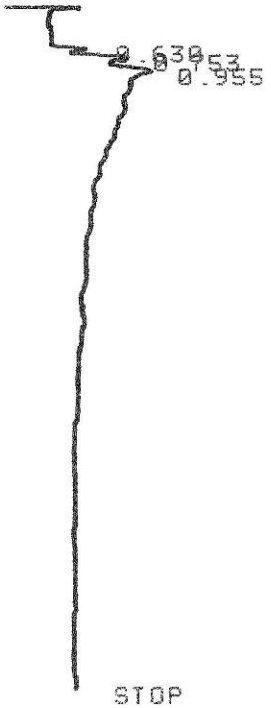

92B

RUN#   16   JAN 1, 1901 06:03:57

AREA%

RT	AREA	TYPE	WIDTH	AREA%
.630	1382	PU	.056	7.62946
.753	4952	UU	.101	27.33797
.955	11780	UU	.212	65.03261

* RUN # 17 JAN 1, 1901 06:15:15

START

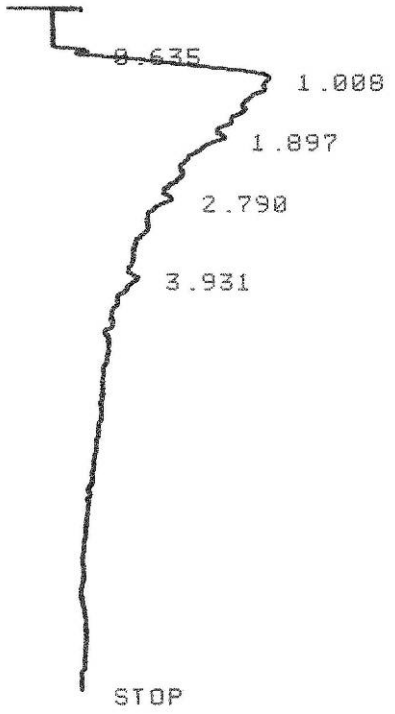

92C

RUN# 17 JAN 1, 1901 06:15:15

AREA%

RT	AREA	TYPE	WIDTH	AREA%
.635	1563	PV	.061	1.82538
1.008	52777	VV	.321	61.63666
1.897	27409	VV	.327	32.01013
2.790	2124	BP	.145	2.48056
3.931	1753	BV	.164	2.04728

TOTAL AREA= 85626

MUL FACTOR=1.0000E+00

* RUN # 6 JAN 1, 1901 02:42:49

START

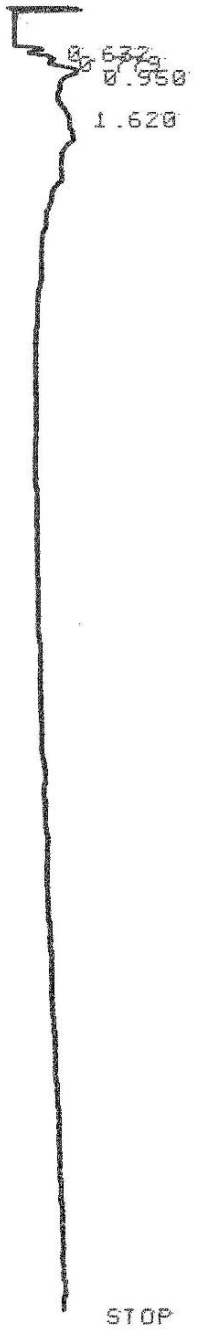

93A

RUN# 6 JAN 1, 1901 02:42:49

AREA%

RT	AREA	TYPE	WIDTH	AREA%
.632	1739	PU	.066	6.90792
.779	3922	UU	.121	15.57957
.950	12354	UU	.245	49.07445
1.620	7159	UU	.265	28.43808

* RUN # 18 JAN 1, 1901 06:26:33

START

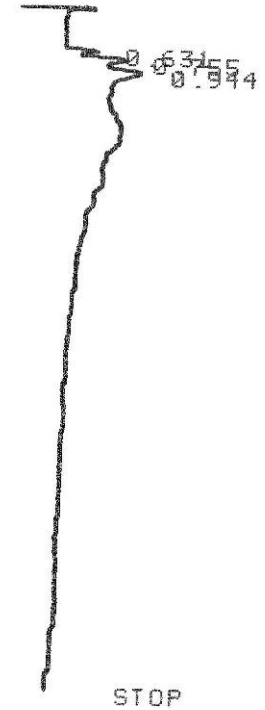

RUN# 18 JAN 1, 1901 06:26:33

AREA%

RT	AREA	TYPE	WIDTH	AREA%
.631	1535	PU	.061	8.90423
.755	4963	UU	.110	28.78938
.944	10741	UU	.202	62.30640

* RUN # 19 JAN 1, 1901 06:37:51

START

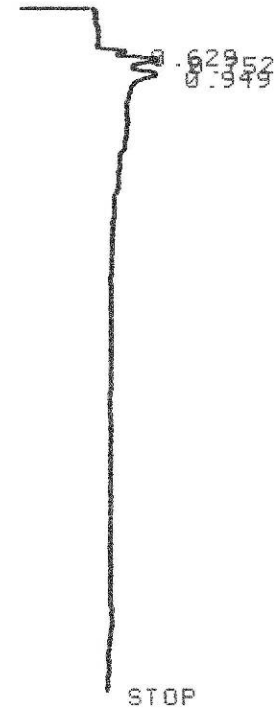

RUN# 19 JAN 1, 1901 06:37:51

AREA%

RT	AREA	TYPE	WIDTH	AREA%
.629	1488	BV	.067	10.33549
.752	5473	VV	.115	38.01486
.949	7436	VV	.190	51.64966

```
*  RUN #     7      JAN  1, 1901  03:04:08
START
```

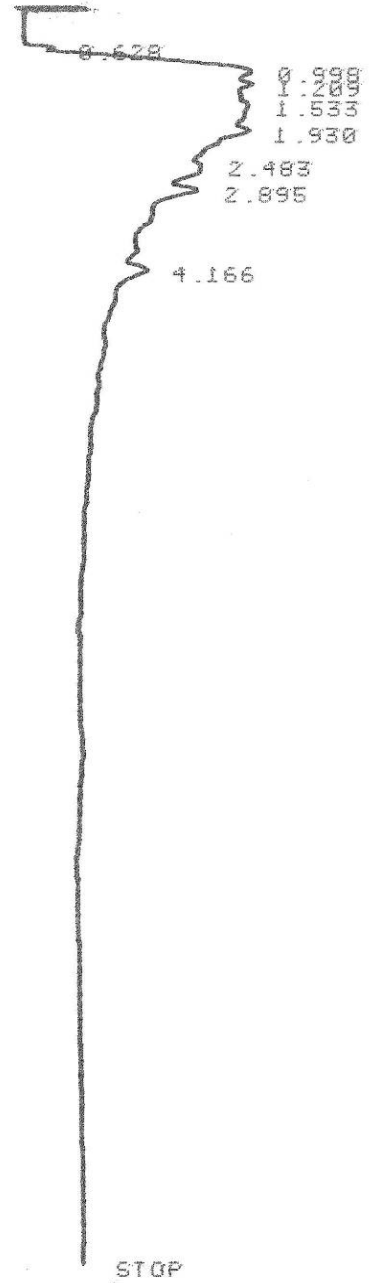

94A

```
RUN#      7           JAN  1, 1901  03:04:08

AREA%
       RT        AREA TYPE  WIDTH       AREA%
     .628        1302   PU    .059      .63439
   * .998       58463   UU    .320    28.48561
   *1.209       32940   UU    .189    16.04974
    1.533       35791   UU    .226    17.43886
   *1.930       37261   UU    .263    18.15511
   * 2.483      22799   UU    .299    11.10862
   * 2.895      12094   UU    .218     5.89270
    4.166        4587   UP    .202     2.23498

TOTAL AREA= 205237
MUL FACTOR=1.0000E+00
```

* RUN # 21 JAN 1, 1901 07:00:27

START

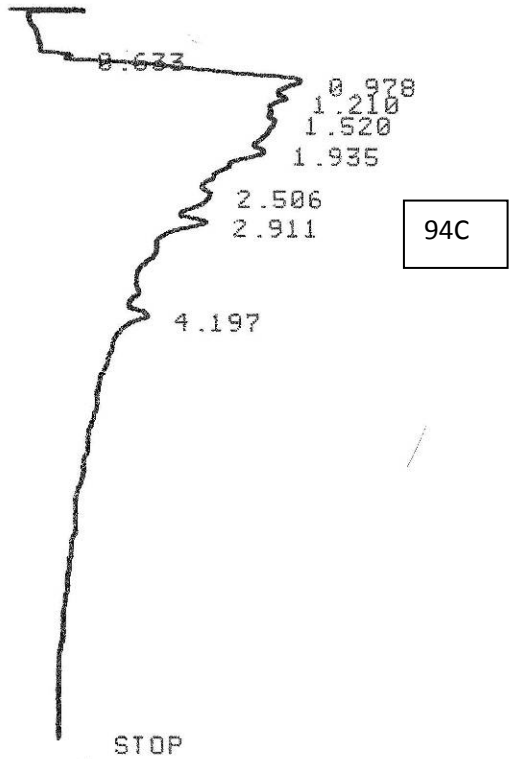

RUN# 21 JAN 1, 1901 07:00:27

AREA%

	RT	AREA	TYPE	WIDTH	AREA%
	.633	2014	VV	.067	.55717
*	.978	73994	VV	.331	20.47047
*	1.210	40053	VV	.193	11.08068
	1.520	74525	VV	.381	20.61737
*	1.935	64629	VV	.355	17.87964
*	2.506	46961	VV	.367	12.99178
*	2.911	38915	VV	.325	10.76585
	4.197	20376	VV	.360	5.63703

TOTAL AREA= 361467

MUL FACTOR=1.0000E+00

* RUN # 20 JAN 1, 1901 06:49:09

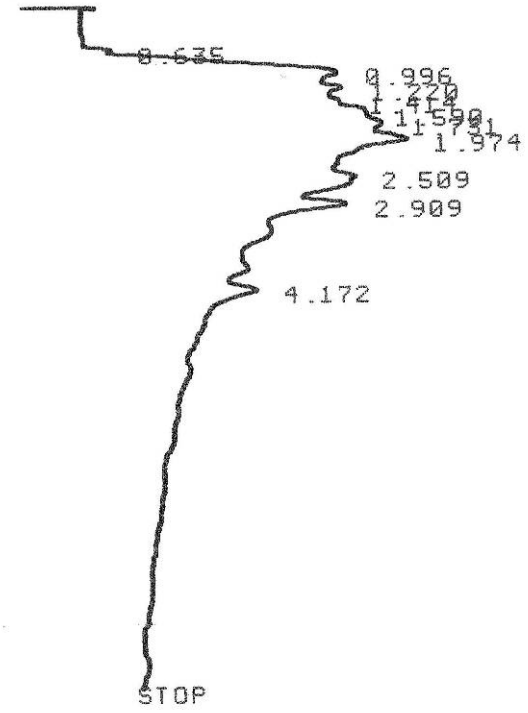

94B

RUN# 20 JAN 1, 1901 06:49:09

AREA%

RT	AREA	TYPE	WIDTH	AREA%
.635	1395	PU	.059	.30878
.996	69447	UU	.327	15.37186
1.220	38572	UU	.181	8.53779
1.414	26445	UU	.127	5.85351
1.590	35579	UU	.155	7.87529
1.731	53929	UU	.224	11.93700
1.974	93547	UU	.363	20.70631
2.509	35908	UU	.174	7.94812
2.909	56414	UU	.291	12.48705
4.172	40544	UU	.409	8.97428

TOTAL AREA= 451780
MUL FACTOR=1.0000E+00

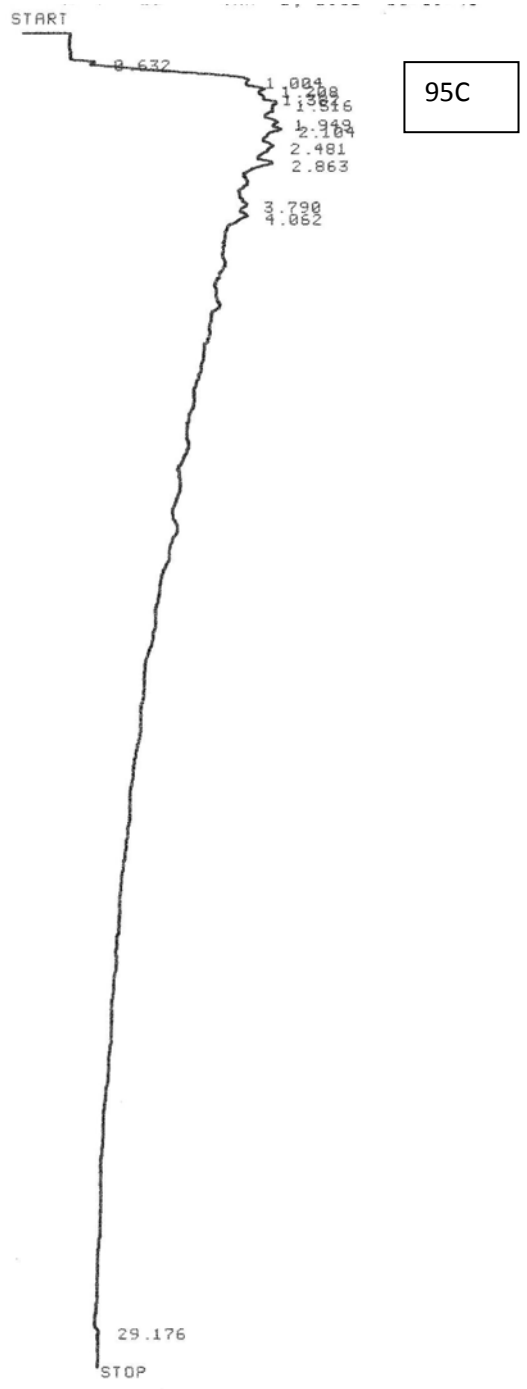

95C

RUN# 23 JAN 1, 1901 08:09:48

AREAX

RT	AREA	TYPE	WIDTH	AREAX
.632	1376	PU	.058	.50078
*1.004	51772	UU	.268	18.84194
*1.208	38807	UU	.198	14.12345
*1.382	25646	UU	.141	9.33363
*1.516	32428	UU	.174	11.80187
1.949	31282	UU	.209	11.38480
2.104	37671	UU	.267	13.71002
2.481	33952	UU	.344	12.35652
2.863	15166	UU	.229	5.51953
3.790	1321	PU	.098	.48077
4.062	4495	UP	.211	1.63591
29.176	854	PU	.115	.31081

95B

RUN# 22 JAN 1, 1901 07:38:30

AREAX

	RT	AREA	TYPE	WIDTH	AREAX
*	.986	98965	UU	.284	12.28132
*	1.217	61815	UU	.183	7.67110
*	1.410	45216	UU	.140	5.61120
*	1.535	49300	UU	.148	6.11802
	1.735	73506	UU	.228	9.12192
	1.991	78255	UU	.241	9.71126
	2.165	89706	UU	.282	11.13230
	2.515	110274	UU	.385	13.68474
	2.939	77313	UU	.314	9.59436
	3.347	33907	UU	.208	4.20778
	3.896	50301	UU	.438	6.24224
	4.202	23494	UU	.291	2.91555
	5.388	3312	UP	.211	.41101
	6.164	2318	BU	.164	.28766
	7.036	2550	PU	.276	.31645
	11.799	5585	UU	.355	.69309

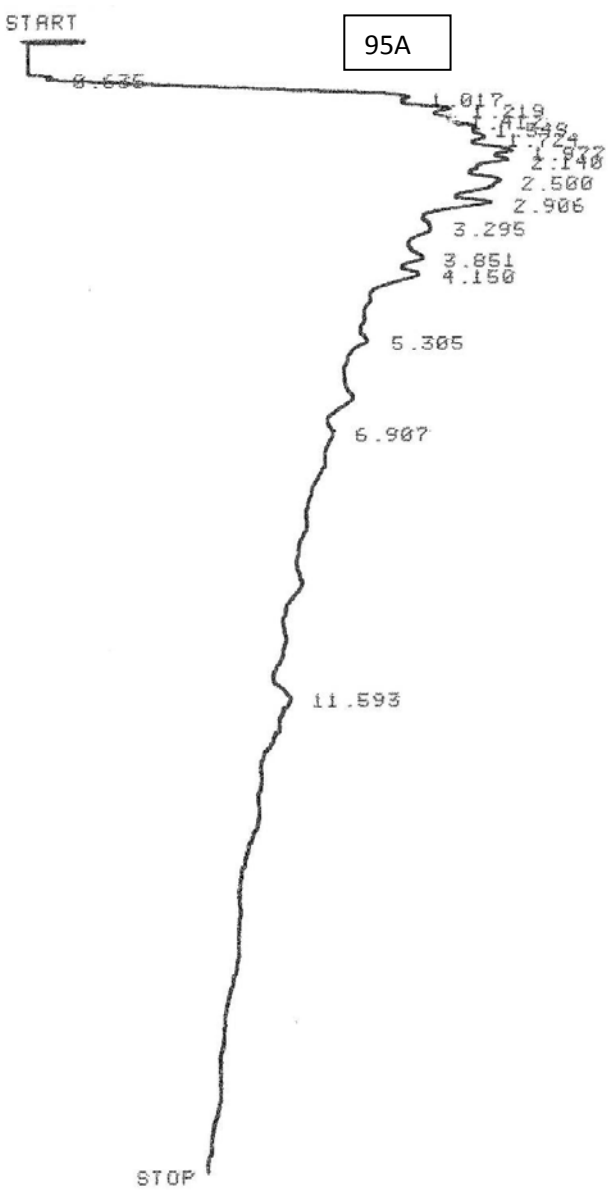

RUN# 8 JAN 1, 1901 03:25:26

AREA%

RT	AREA	TYPE	WIDTH	AREA%
.635	1115	PU	.055	.12468
* 1.017	90476	UU	.256	10.11672
* 1.219	80793	UU	.214	9.03399
* 1.412	49872	UU	.139	5.57652
* 1.549	51867	UU	.138	5.79959
1.724	70189	UU	.190	7.84829
1.977	87812	UU	.235	9.81884
2.140	97895	UU	.274	10.94628
2.500	125366	UU	.396	14.01799
2.906	79023	UU	.290	8.83608
3.295	75921	UU	.433	8.48922
3.851	46349	UU	.389	5.18259
4.150	25742	UU	.290	2.87838
5.305	3569	UP	.238	.39907
6.907	3773	PU	.386	.42188
11.593	4560	BU	.250	.50988

```
*  RUN #     3      JAN  1, 1901  00:21:20
START
```

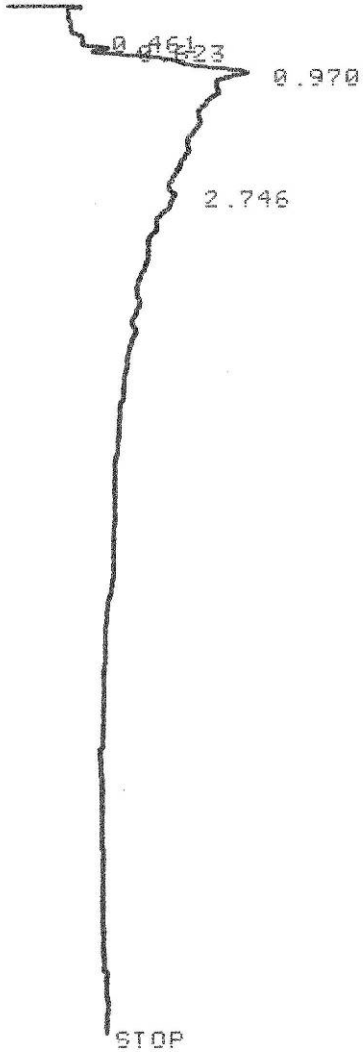


```
RUN#      3           JAN  1, 1901  00:21:20

AREA%
       RT       AREA TYPE  WIDTH      AREA%
     .461       1279   PU   .134    2.18349
     .623       1801   VV   .065    3.07464
     .970      41595   VV   .301   71.01030
    2.746      13901   VV   .347   23.73156
```

```
*  RUN #     4      JAN  1, 1901   00:37:38
START
```

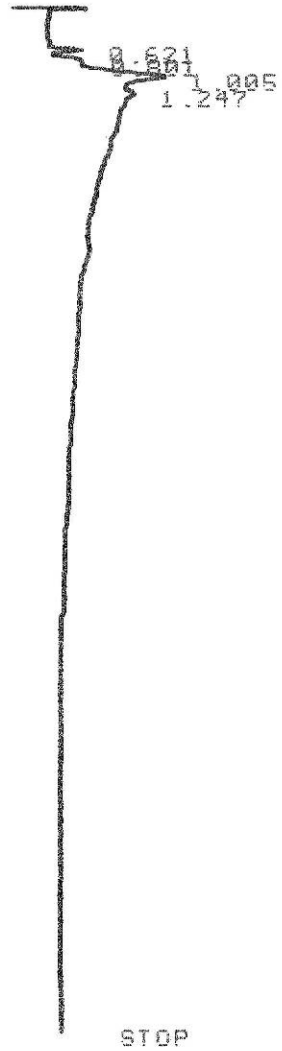

M10

```
RUN#      4           JAN  1, 1901   00:37:38

AREA%
       RT       AREA TYPE  WIDTH       AREA%
     .621       1460   PP   .054     4.21576
     .801       2628   PV   .109     7.58836
   1.005      18794   VV   .210    54.26773
   1.247      11750   VV   .209    33.92816

TOTAL AREA=   34632
```

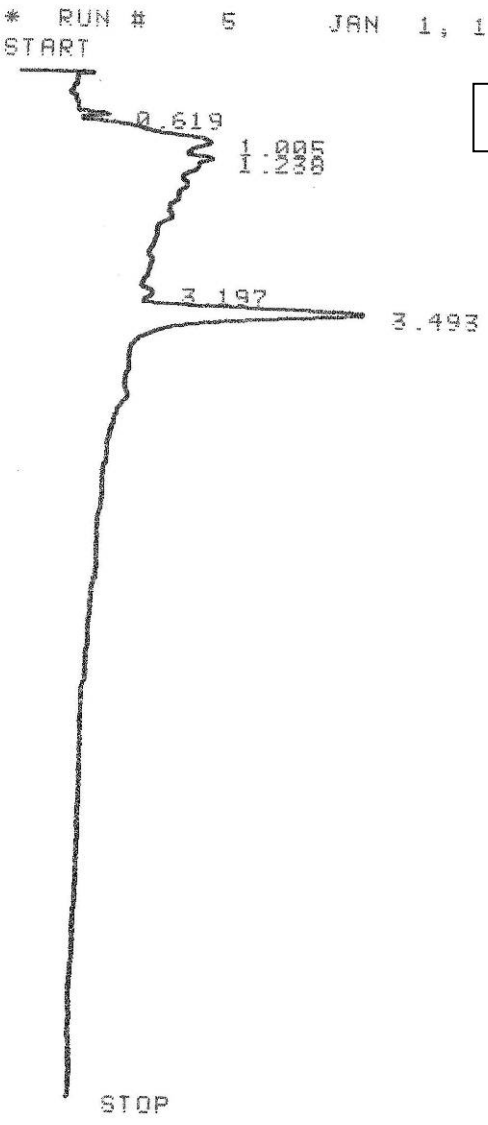

M12

UN# 5 JAN 1, 1901 00:53:57

REA%

RT	AREA	TYPE	WIDTH	AREA%
.619	1401	PP	.056	1.48542
1.005	31136	PU	.313	33.01208
1.238	19298	UU	.212	20.46078
3.197	1519	BU	.136	1.61053
3.493	40963	UP	.210	43.43120

```
*  RUN #     6      JAN  1, 1901   01:10:15
START
```

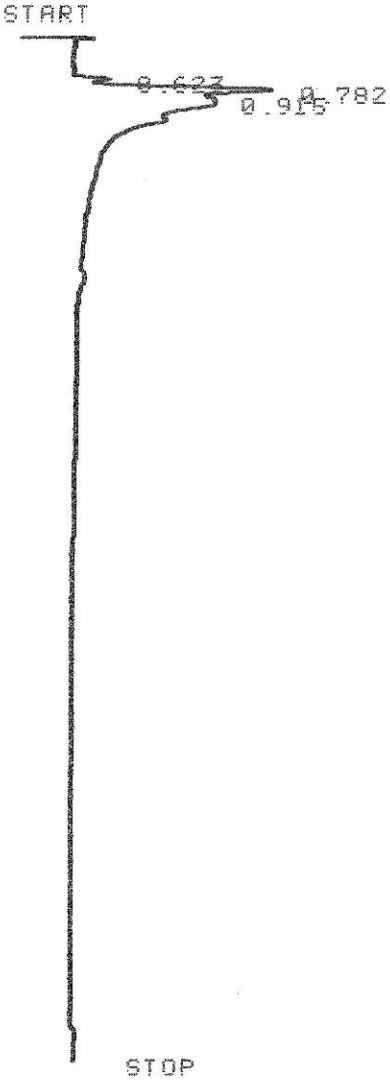


```
RUN#      6           JAN  1, 1901   01:10:15

AREAX
       RT       AREA TYPE  WIDTH       AREAX
     .623        912   PP   .046     6.64965
     .782      10885   PU   .095    79.36566
     .915       1918   UB   .092    13.98469
```

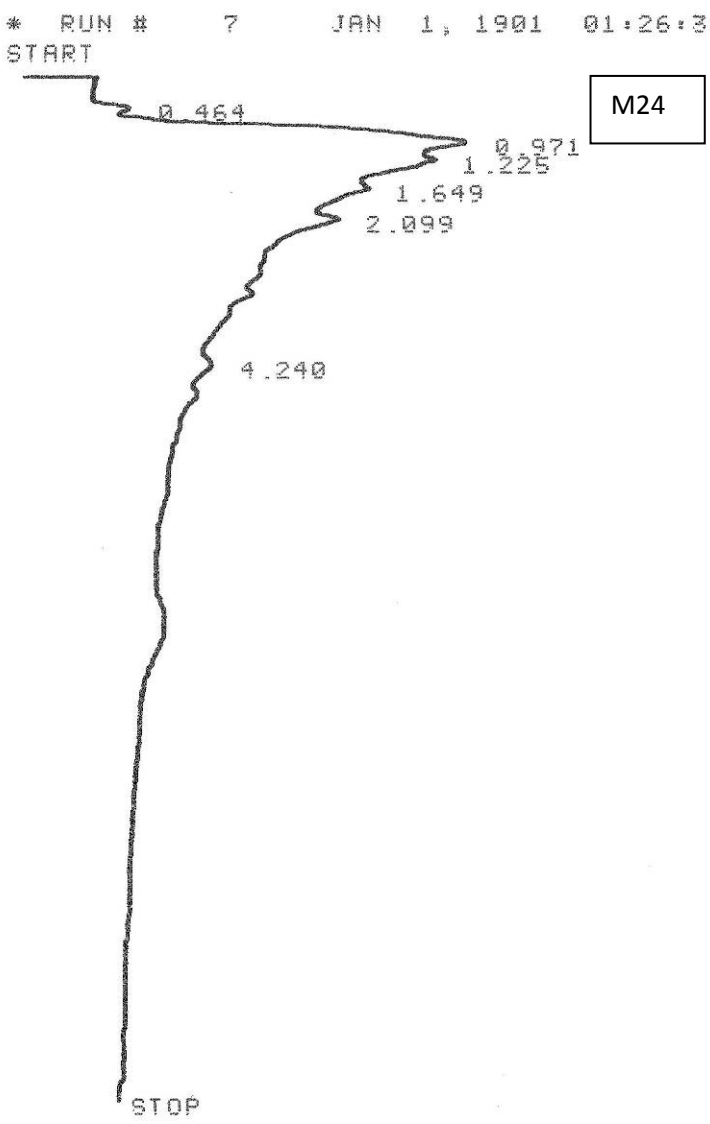

RUN# 7 JAN 1, 1901 01:26:34

AREA%

RT	AREA	TYPE	WIDTH	AREA%
.464	2716	PU	.111	.90998
.971	105911	UU	.375	35.48501
1.225	84371	UU	.348	28.26811
1.649	60388	UU	.373	20.23272
2.099	42017	UU	.377	14.07761
4.240	3064	PU	.235	1.02658

```
*  RUN #     8      JAN  1, 1901   01:42:52
START
```

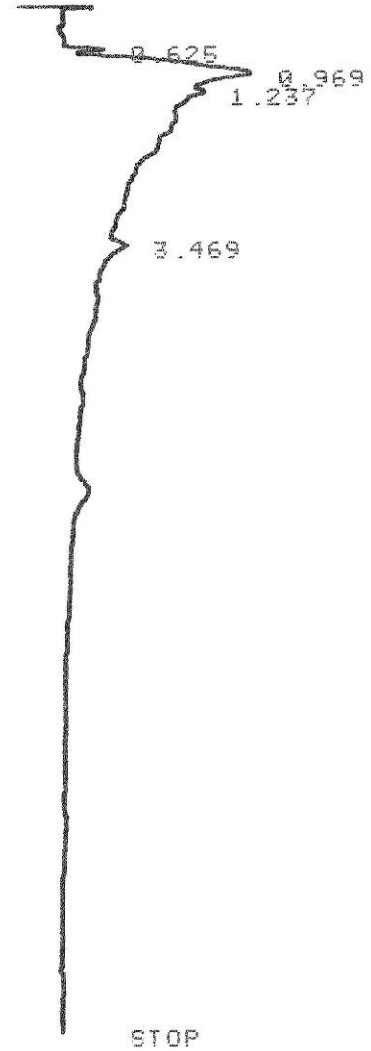

M28

```
RUN#      8           JAN  1, 1901   01:42:52

AREAX
        RT       AREA TYPE  WIDTH      AREA%
      .625       2134   VV    .061    2.01338
      .969      55726   VV    .351   52.57618
     1.237      34433   VV    .294   32.48672
     3.469      13698   VV    .382   12.92374
```

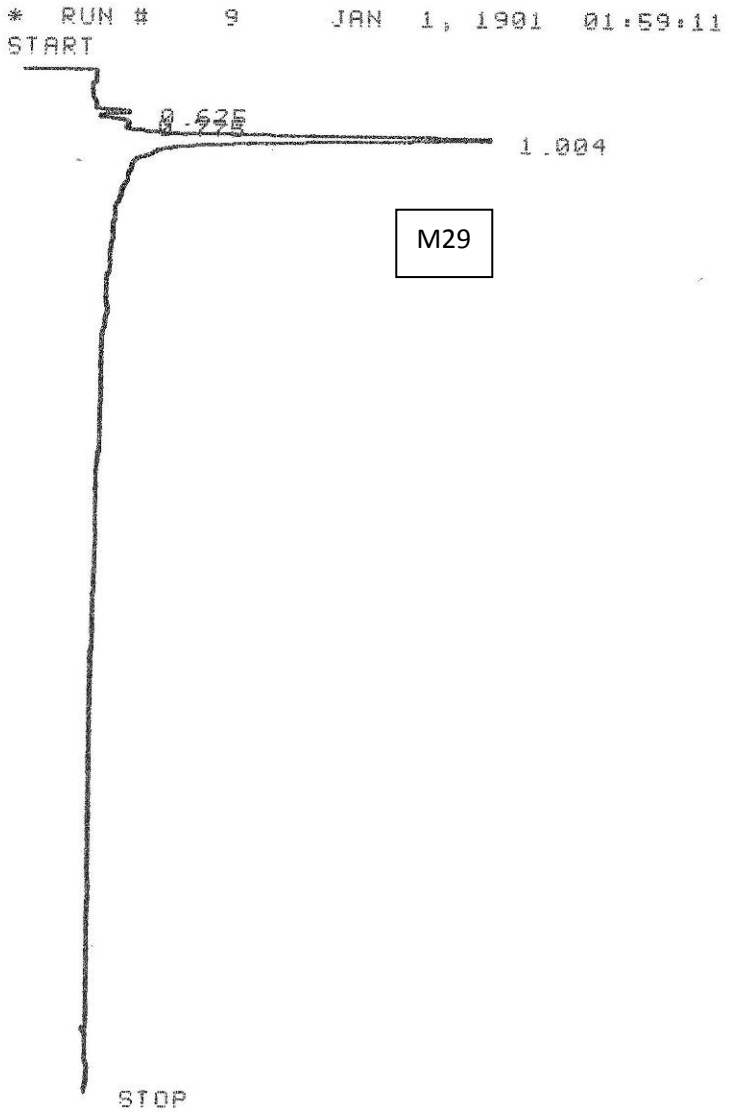

RUN# 9 JAN 1, 1901 01:59:11

AREA%

RT	AREA	TYPE	WIDTH	AREA%
.625	1647	PP	.056	3.48380
.775	2579	PU	.112	5.45520
1.004	43050	UB	.133	91.06099

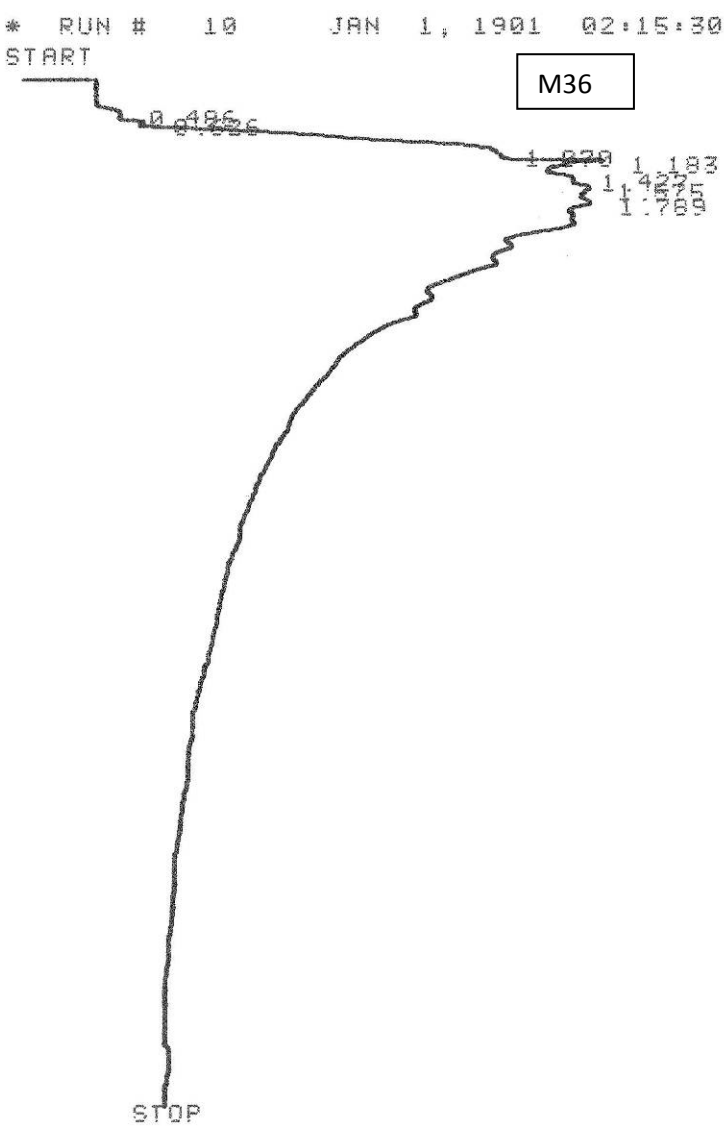

RUN# 10 JAN 1, 1901 02:15:30

AREA%

RT	AREA	TYPE	WIDTH	AREA%
.486	1939	PV	.127	.53046
.626	1987	VV	.069	.54359
1.070	85965	VV	.275	23.51765
1.183	85004	VV	.214	23.25474
1.427	42033	VV	.116	11.49906
1.575	69639	VV	.189	19.05130
1.789	78967	VV	.218	21.60318

TOTAL AREA= 365534

```
*  RUN #   11      JAN  1, 1901  02:31:51
START
```

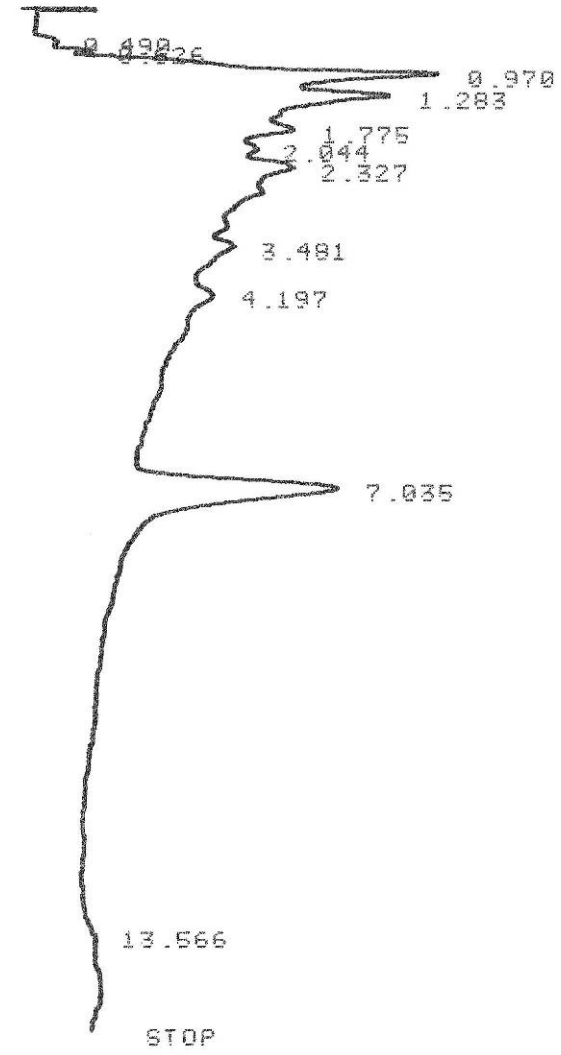


```
RUN#    11           JAN  1, 1901  02:31:51

AREA%
       RT       AREA TYPE  WIDTH      AREA%
     .490       2356   BV    .133      .43952
     .626       3317   VV    .074      .61879
     .970      97445   VV    .290    18.17854
    1.283      88092   VV    .303    16.43373
    1.775      55699   VV    .277    10.39075
    2.044      37226   VV    .226     6.94458
    2.327      72377   VV    .378    13.50207
    3.481      59477   VV    .482    11.09554
    4.197      52236   VV    .550     9.74472
    7.035      67407   BV    .384    12.57490
   13.566        412   PV    .202      .07686
```

```
*  RUN #   12      JAN  1, 1901  02:48:10
START
```

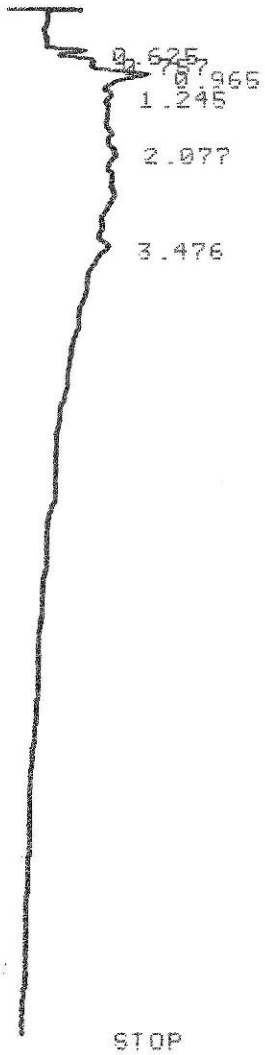

M46

```
STOP
```

```
RUN#    12          JAN  1, 1901  02:48:10

AREA%
      RT       AREA TYPE  WIDTH      AREA%
    .625       1737   PU   .059    5.53572
    .757       2927   UU   .095    9.32819
    .965      13514   UU   .207   43.06838
   1.245       3632   UU   .153   11.57499
   2.077       3894   UU   .291   12.40997
   3.476       5674   UU   .300   18.08274
```

```
*  LIST: ATT 2^ =   0

*  ATT 2^ 1   @
*  RUN #     2      JAN  1, 1901   00:05:01
START
```

Blank

```
RUN#      2           JAN  1, 1901   00:05:01

AREA%
       RT        AREA TYPE  WIDTH       AREA%
     .620        2004   VP    .066    73.51430
     .778         722   PV    .096    26.48569

TOTAL AREA=    2726
```

```
*  RUN #     3      JAN  1, 1901  01:51:57
START
```

BLANK

```
        STOP

RUN#      3           JAN  1, 1901  01:51:57

AREA%
       RT       AREA TYPE  WIDTH      AREA%
     .731       5322   VV    .191  100.00000
```

Pentane Contour Plots and Excitation Scan Overlays
11CP

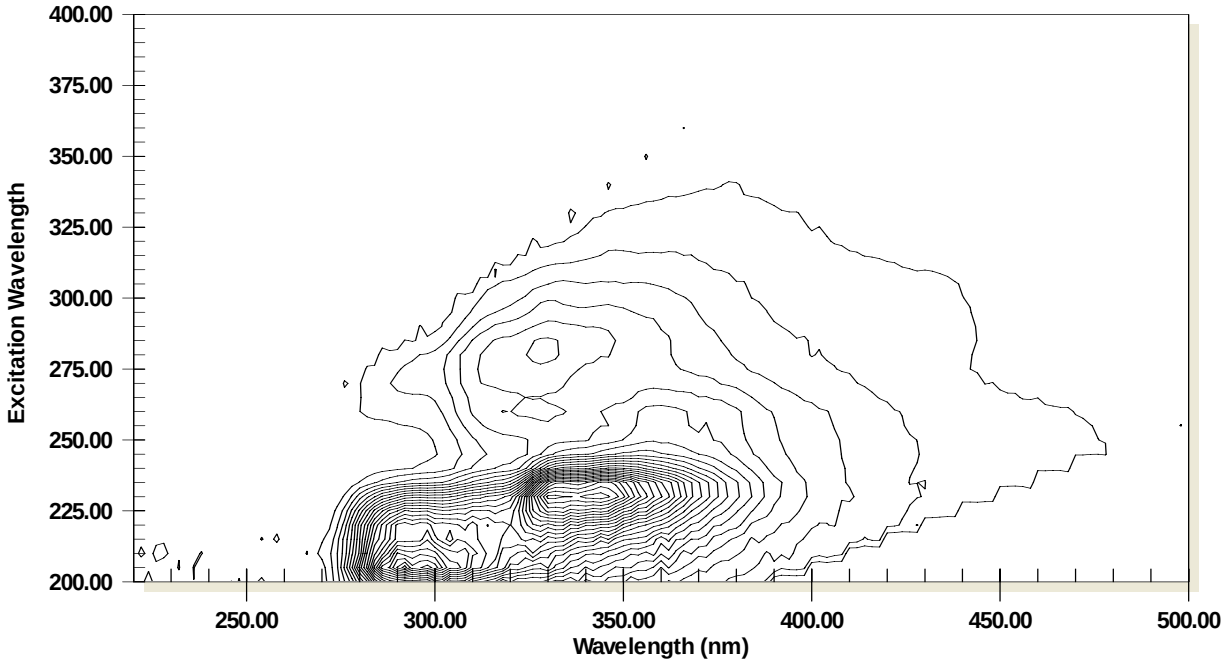

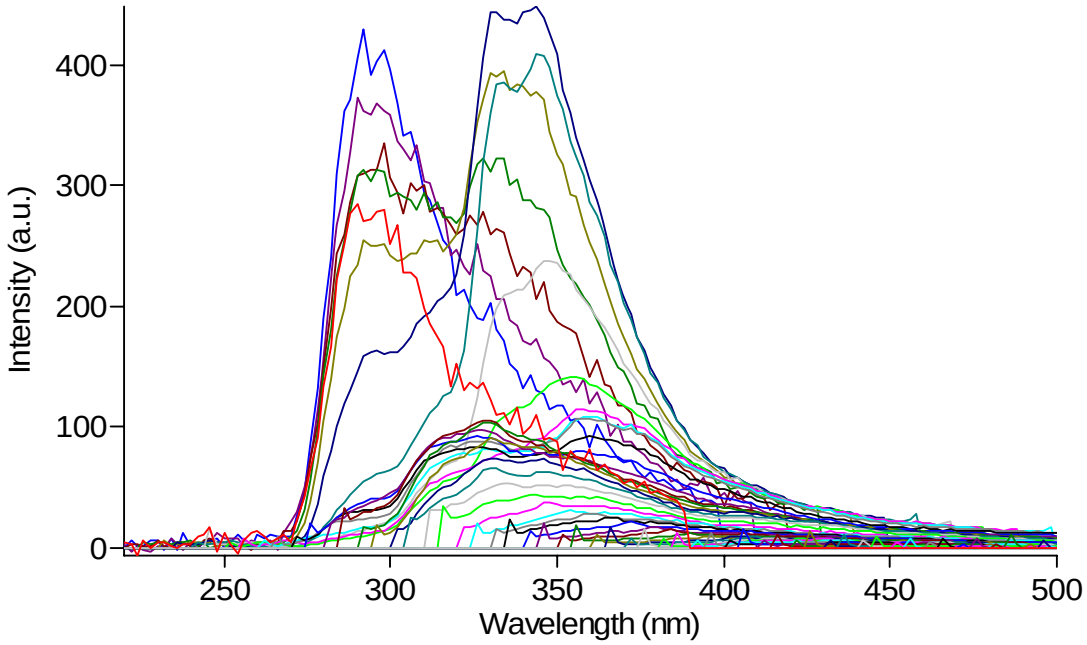

12CP

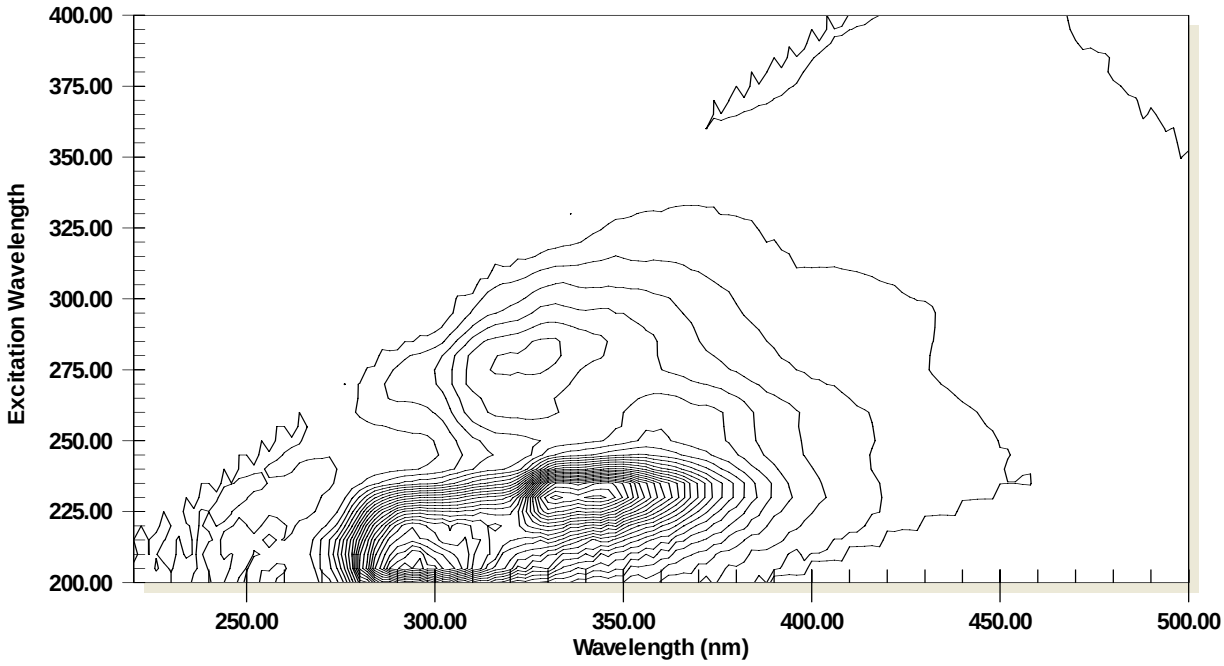
Excitation Wavelength
400.00
375.00
350.00
325.00
300.00
275.00
250.00
225.00
200.00
250.00
300.00
350.00
400.00
450.00
500.00
Wavelength (nm)

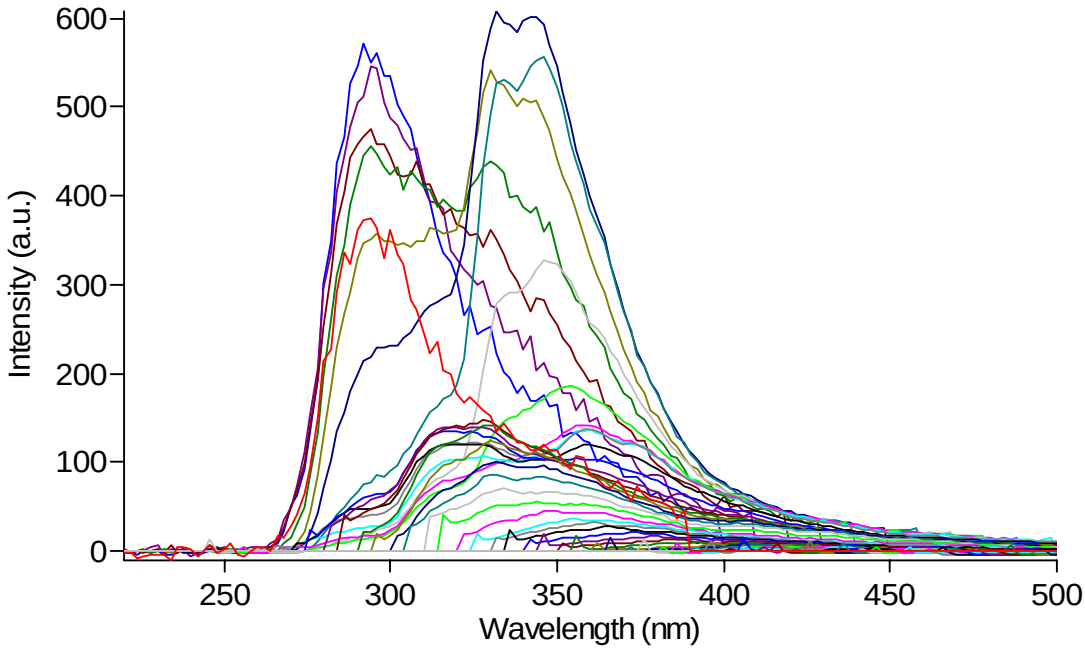
Intensity (a.u.)
600
500
400
300
200
100
0
250
300
350
400
450
500
Wavelength (nm)

13BP

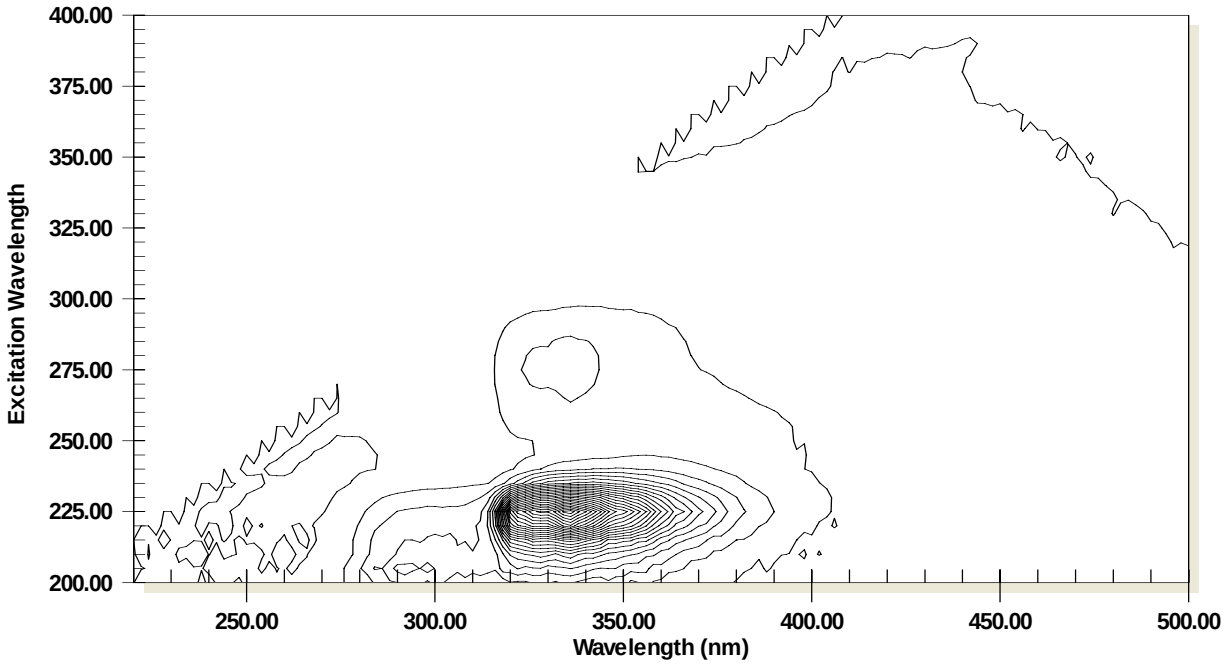
400.00
375.00
350.00
325.00
300.00
275.00
250.00
225.00
200.00
Excitation Wavelength
250.00
300.00
350.00
400.00
450.00
500.00
Wavelength (nm)

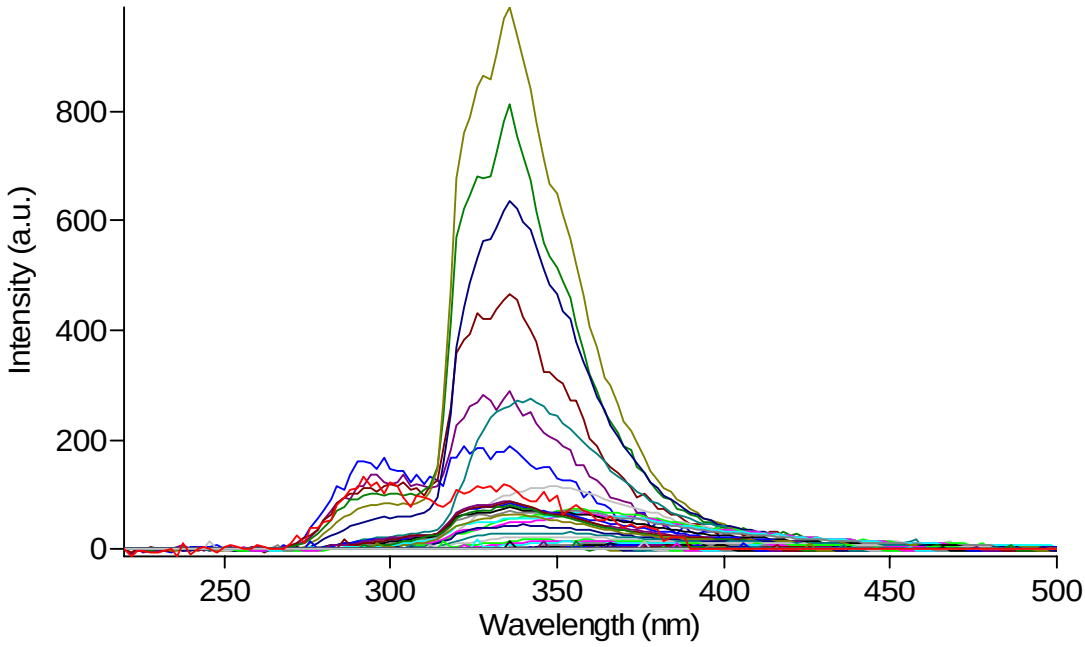
800
600
400
200
0
Intensity (a.u.)
250
300
350
400
450
500
Wavelength (nm)

14BP

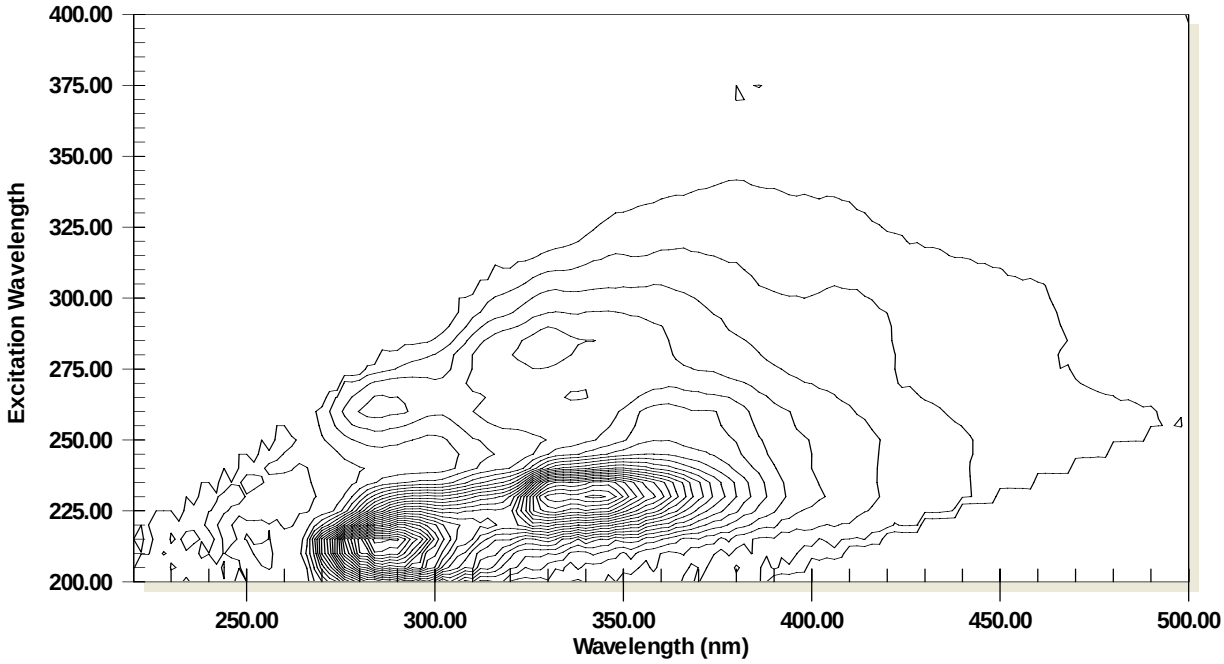
400.00
375.00
350.00
325.00
300.00
275.00
250.00
225.00
200.00
Excitation Wavelength
250.00
300.00
350.00
400.00
450.00
500.00
Wavelength (nm)

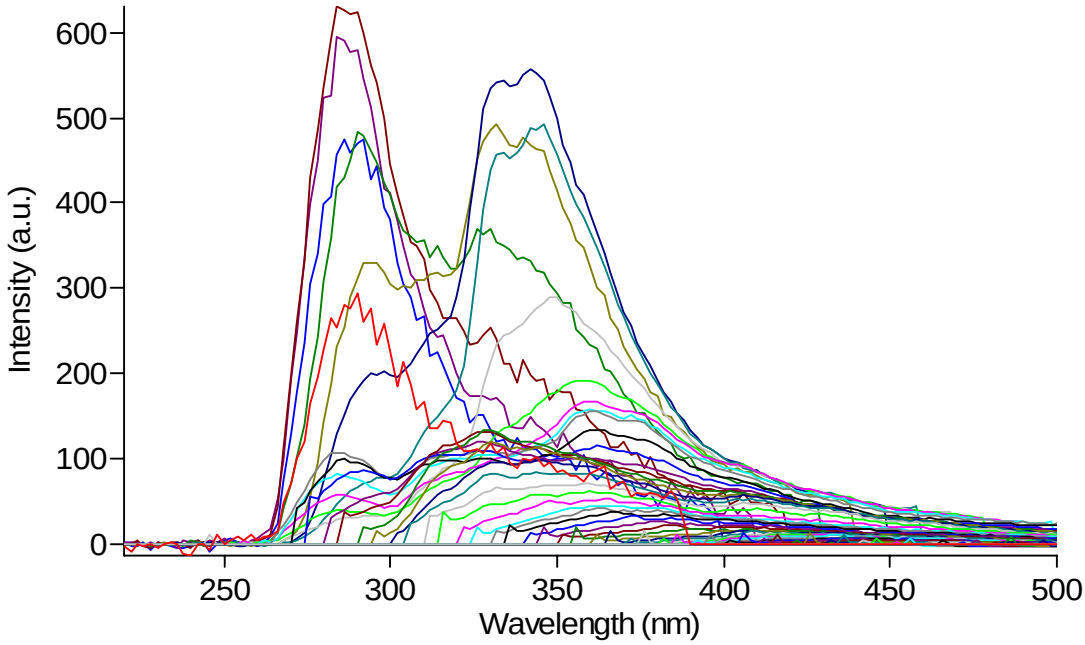
600
500
400
300
200
100
0
Intensity (a.u.)
250
300
350
400
450
500
Wavelength (nm)

15BP

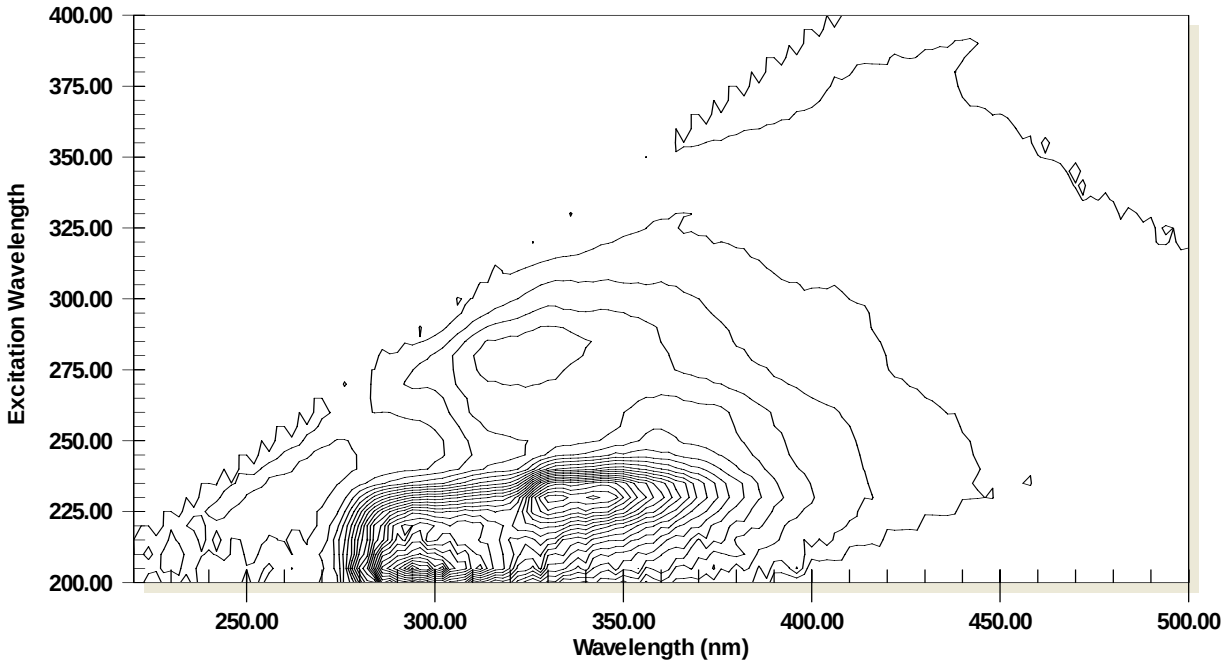
400.00
375.00
350.00
325.00
300.00
275.00
250.00
225.00
200.00
Excitation Wavelength
250.00
300.00
350.00
400.00
450.00
500.00
Wavelength (nm)

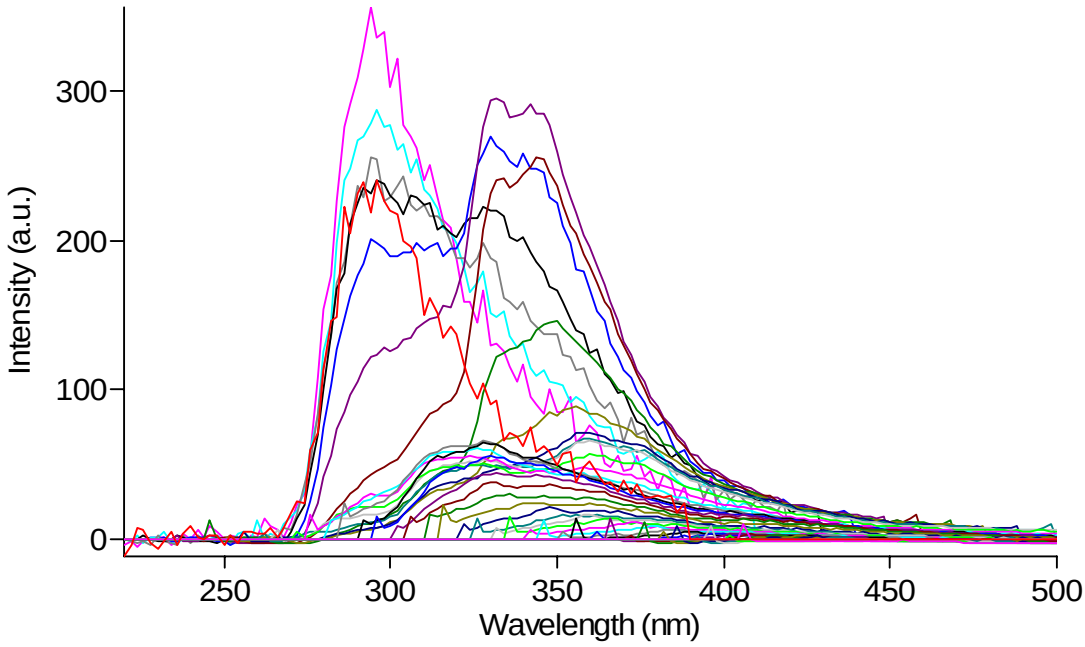
300
200
100
0
Intensity (a.u.)
250
300
350
400
450
500
Wavelength (nm)

21BP

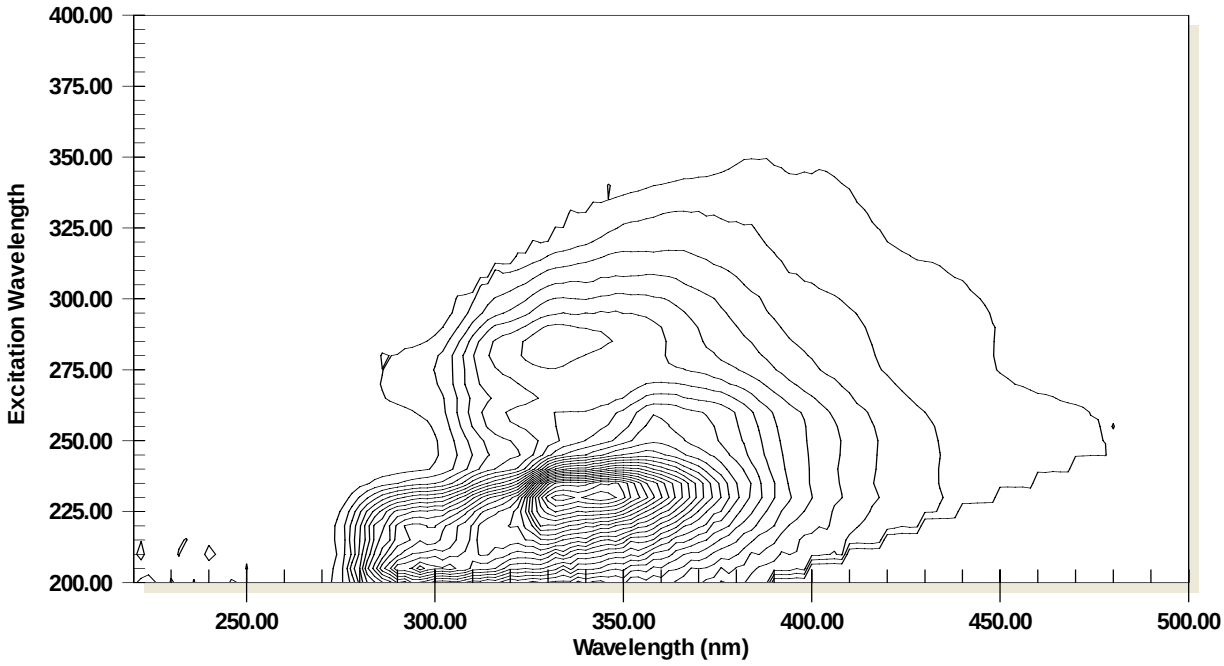
400.00
375.00
350.00
325.00
300.00
275.00
250.00
225.00
200.00
Excitation Wavelength
250.00
300.00
350.00
400.00
450.00
500.00
Wavelength (nm)

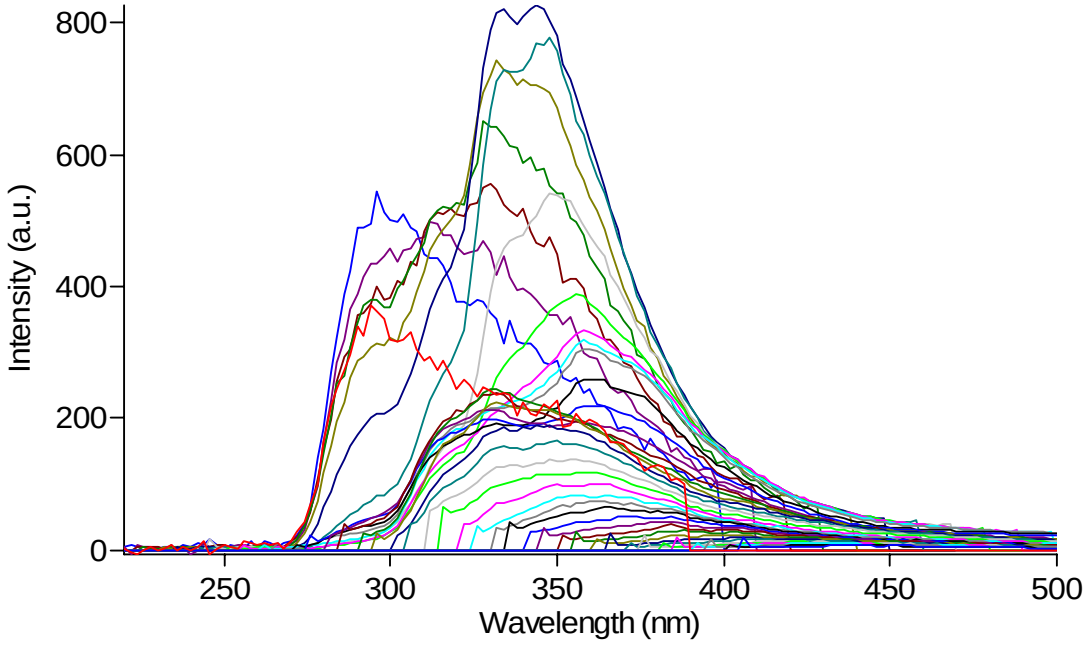
800
600
400
200
0
Intensity (a.u.)
250
300
350
400
450
500
Wavelength (nm)

22AP

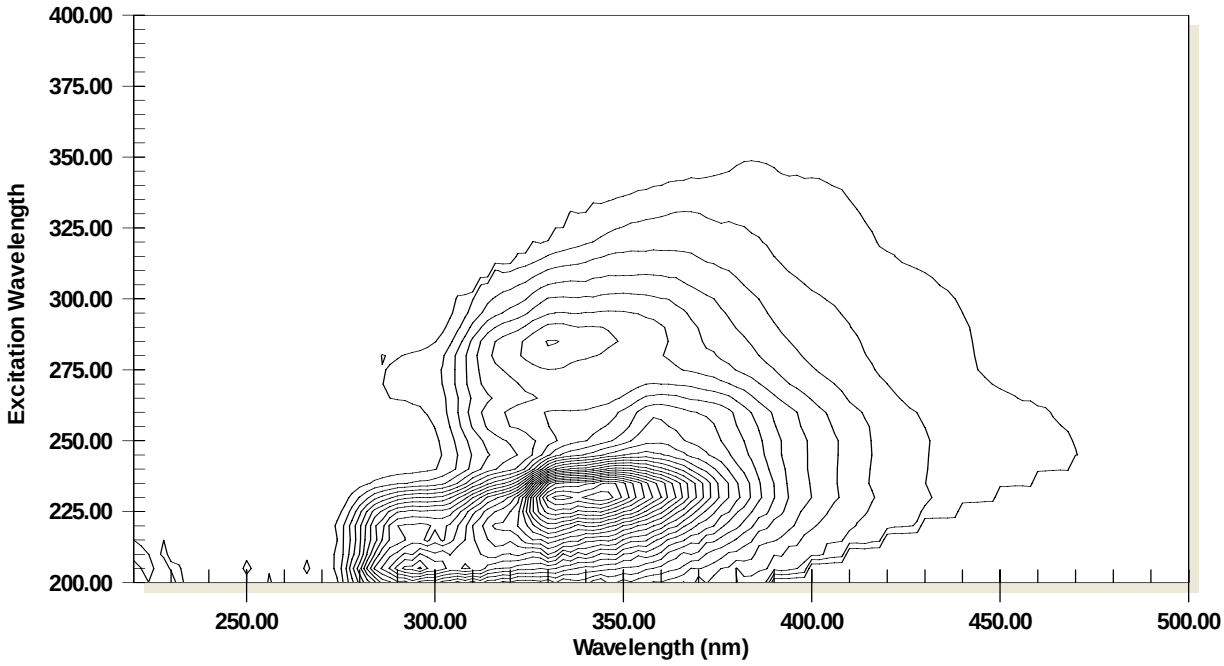
400.00
375.00
350.00
325.00
300.00
275.00
250.00
225.00
200.00
Excitation Wavelength
250.00
300.00
350.00
400.00
450.00
500.00
Wavelength (nm)

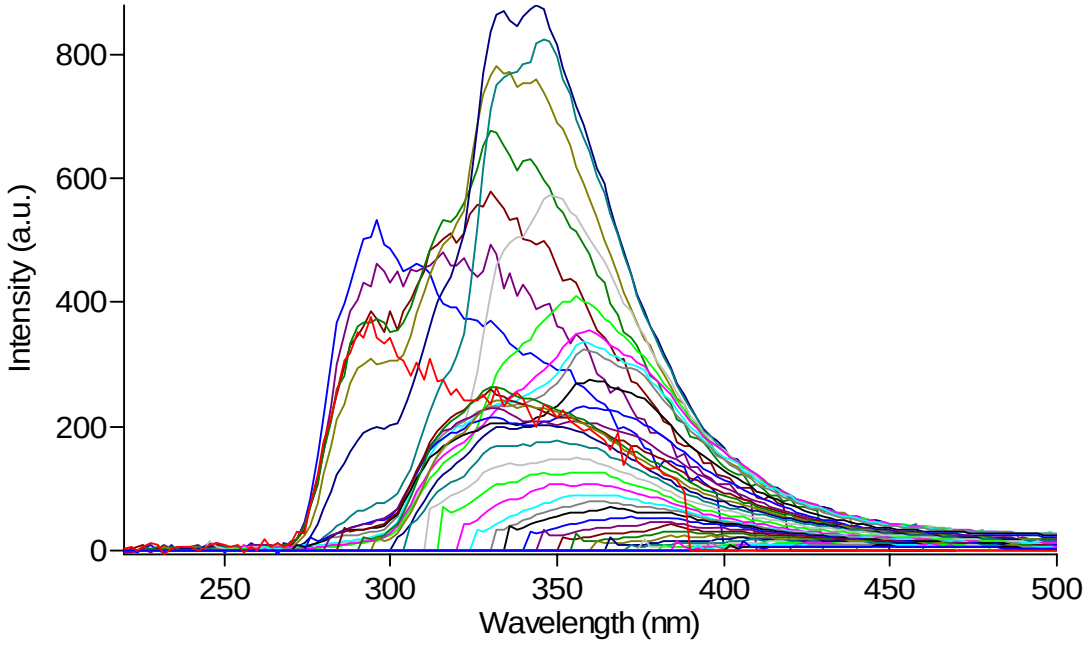
800
600
400
200
0
Intensity (a.u.)
250
300
350
400
450
500
Wavelength (nm)

23AP

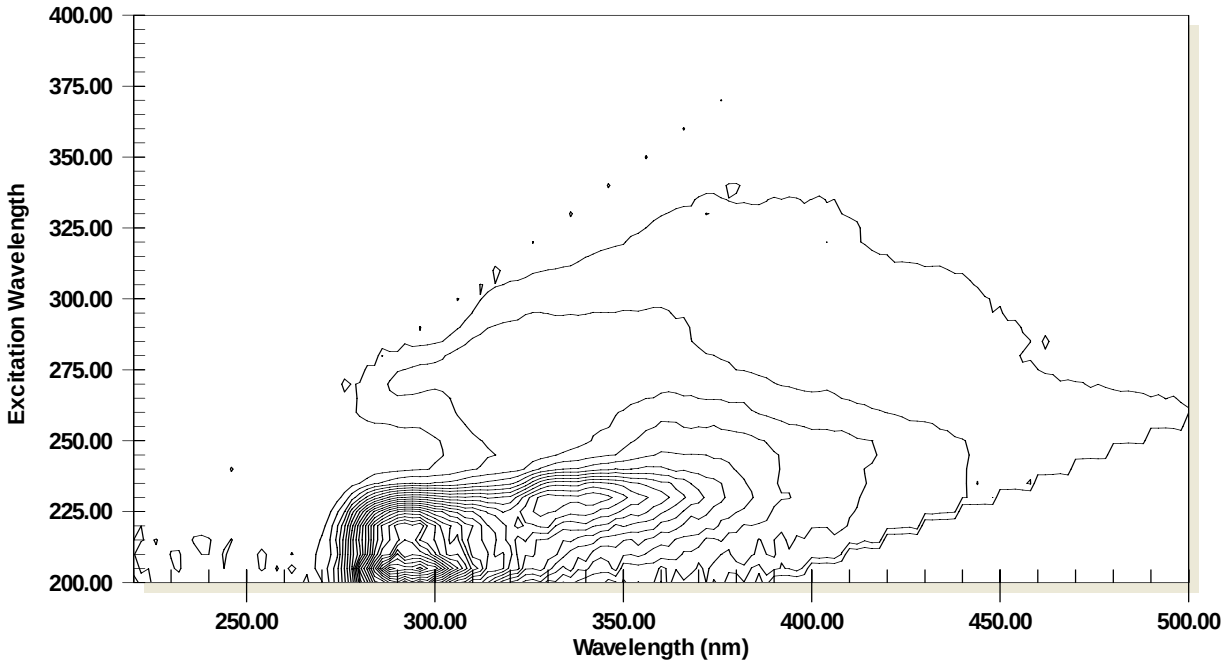
400.00
375.00
350.00
325.00
300.00
275.00
250.00
225.00
200.00
Excitation Wavelength
250.00
300.00
350.00
400.00
450.00
500.00
Wavelength (nm)

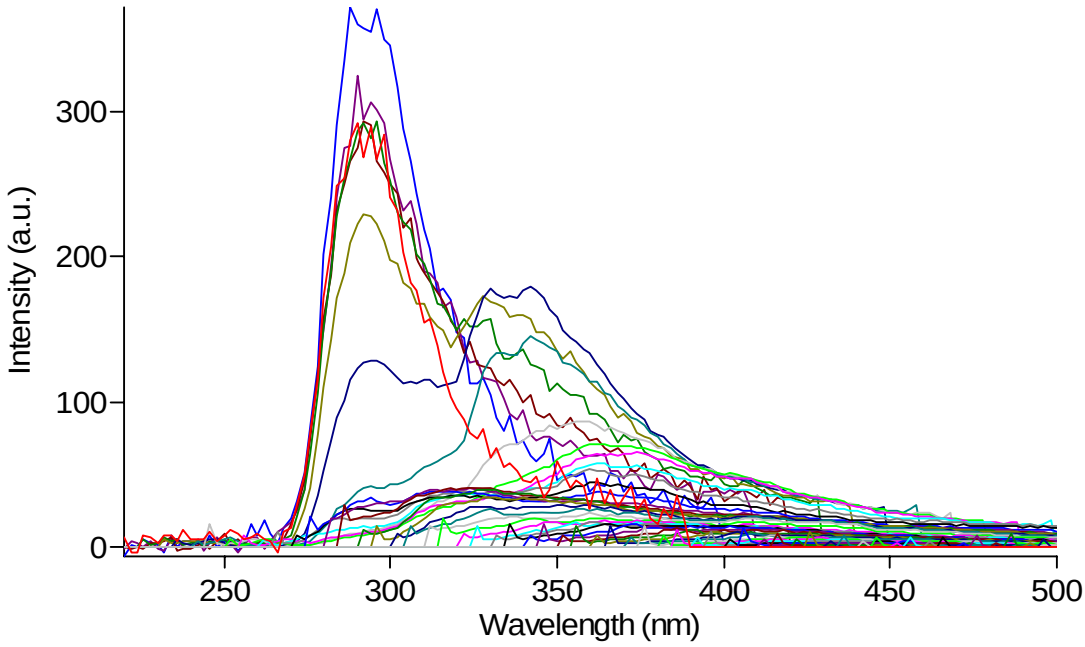
300
200
100
0
Intensity (a.u.)
250
300
350
400
450
500
Wavelength (nm)

24CP

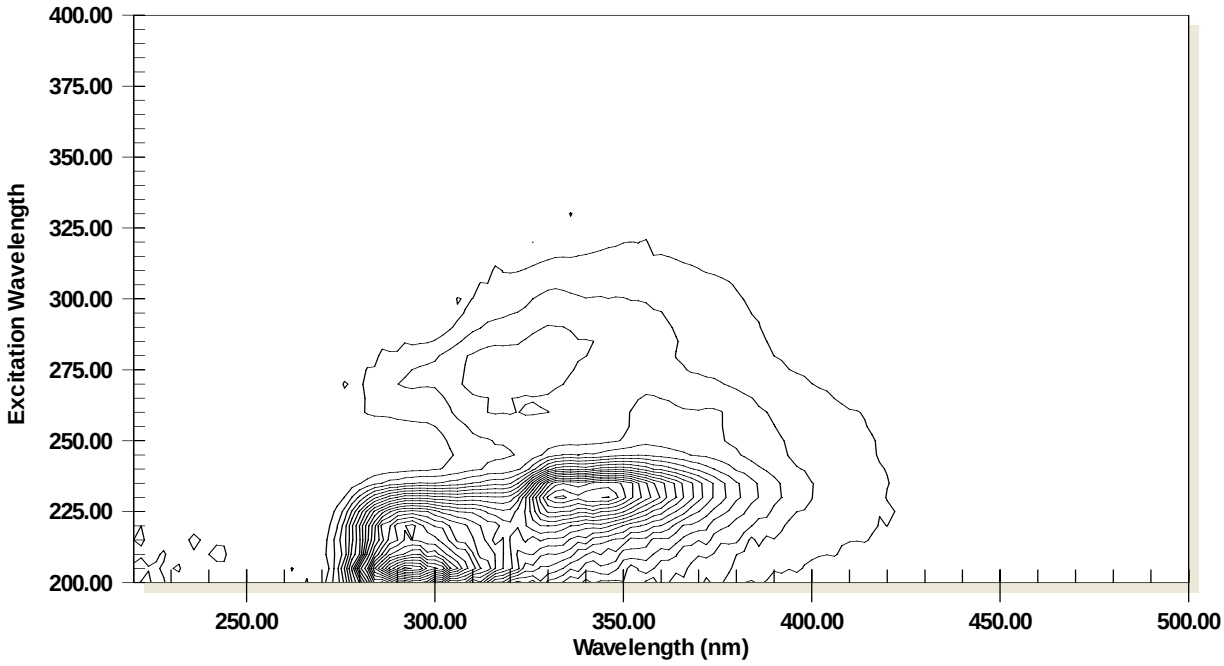
400.00
375.00
350.00
325.00
300.00
275.00
250.00
225.00
200.00
Excitation Wavelength
250.00
300.00
350.00
400.00
450.00
500.00
Wavelength (nm)

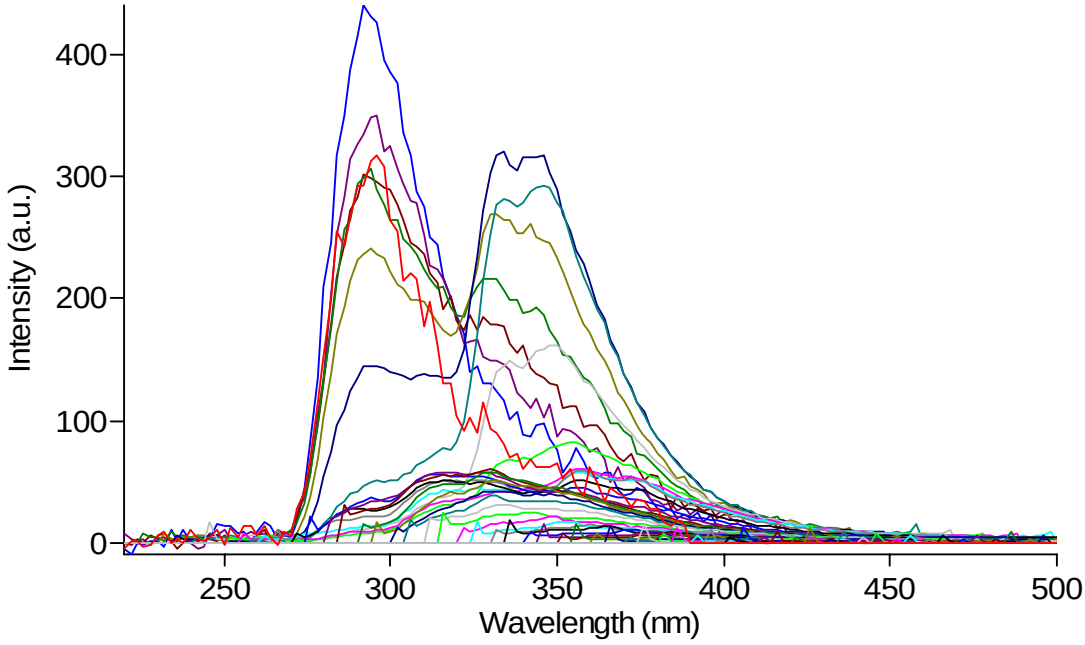
400
300
200
100
0
Intensity (a.u.)
250
300
350
400
450
500
Wavelength (nm)

25CP

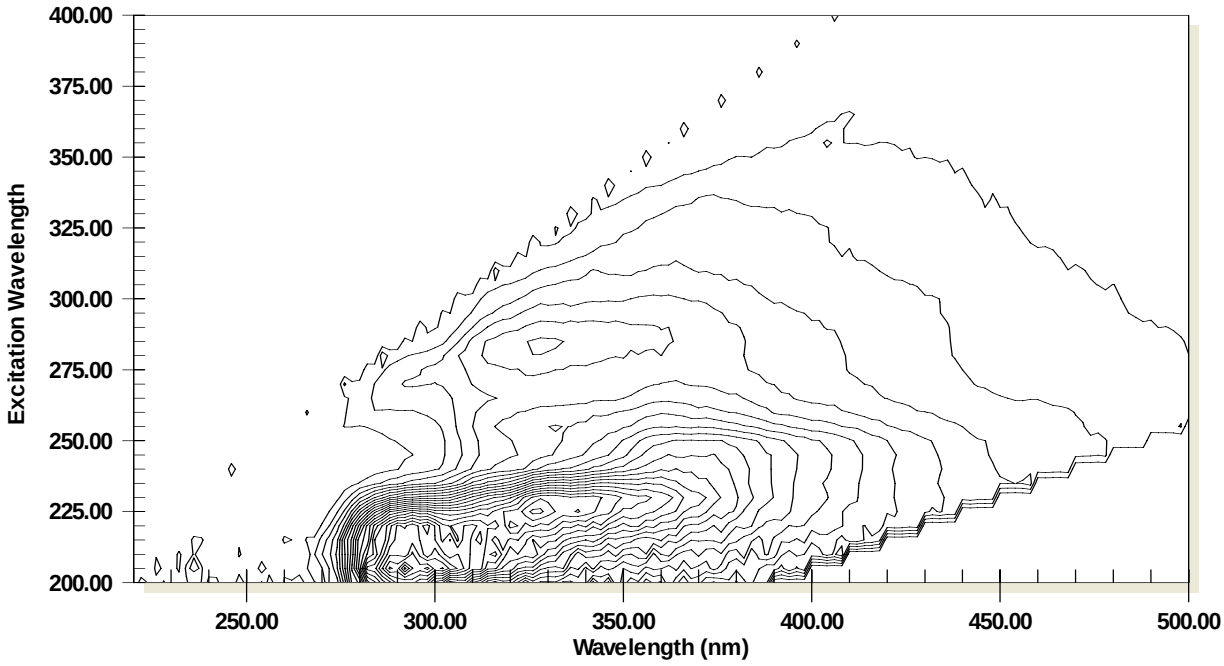
400.00
375.00
350.00
325.00
300.00
275.00
250.00
225.00
200.00
Excitation Wavelength
250.00
300.00
350.00
400.00
450.00
500.00
Wavelength (nm)

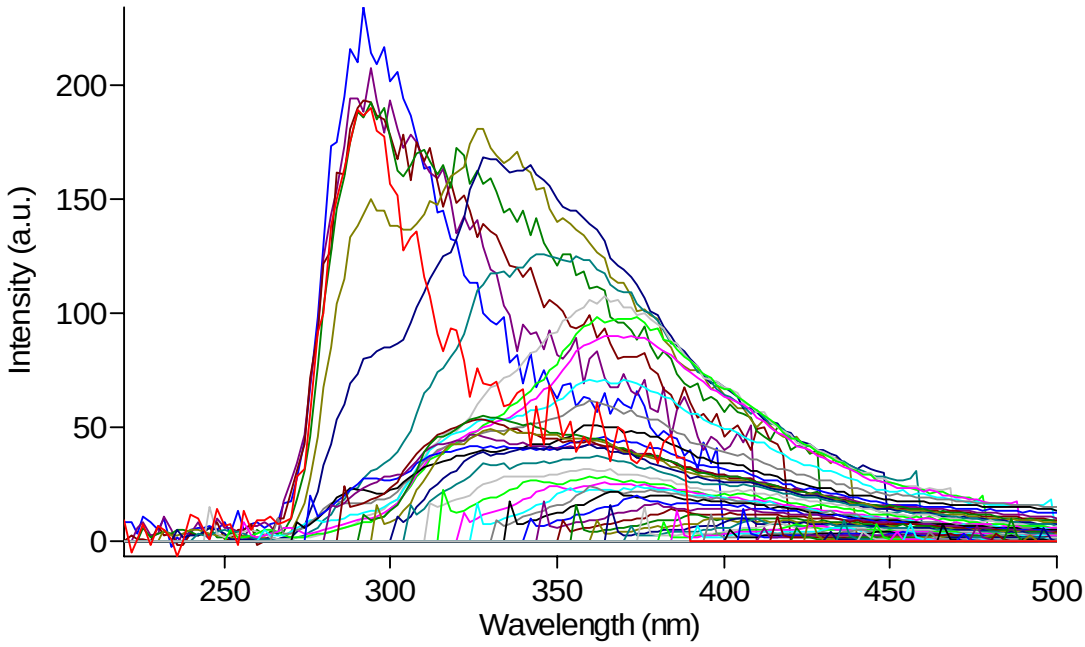
200
150
100
50
0
Intensity (a.u.)
250
300
350
400
450
500
Wavelength (nm)

31CP

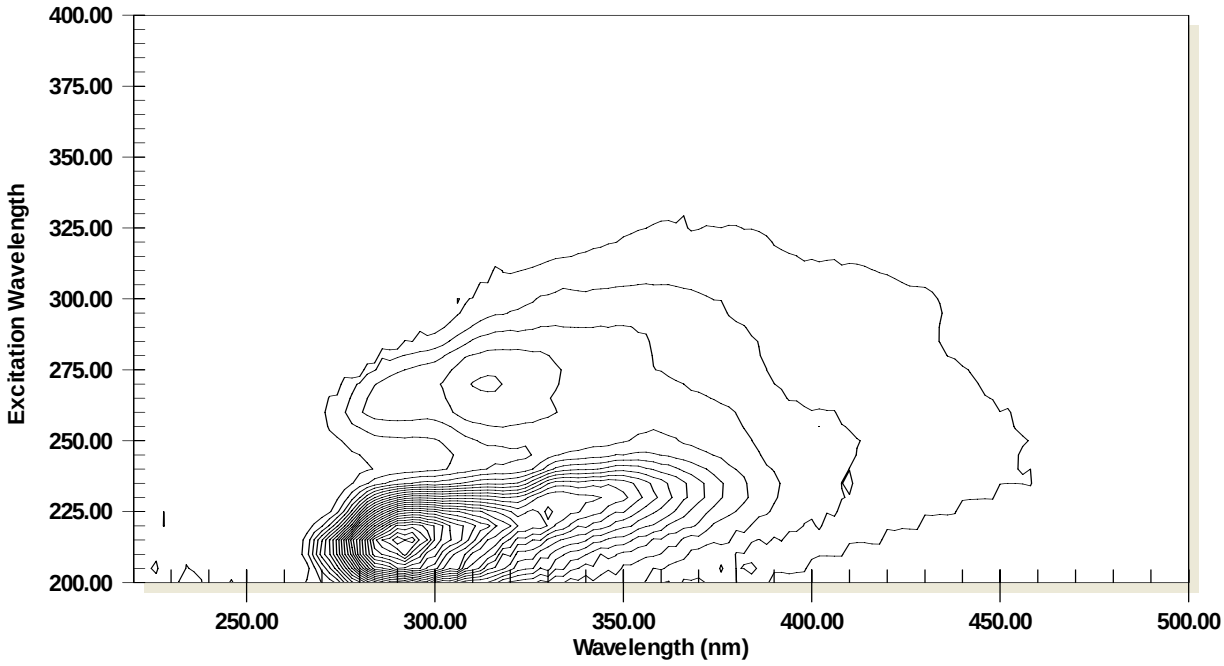
400.00
375.00
350.00
325.00
300.00
275.00
250.00
225.00
200.00
Excitation Wavelength
250.00
300.00
350.00
400.00
450.00
500.00
Wavelength (nm)

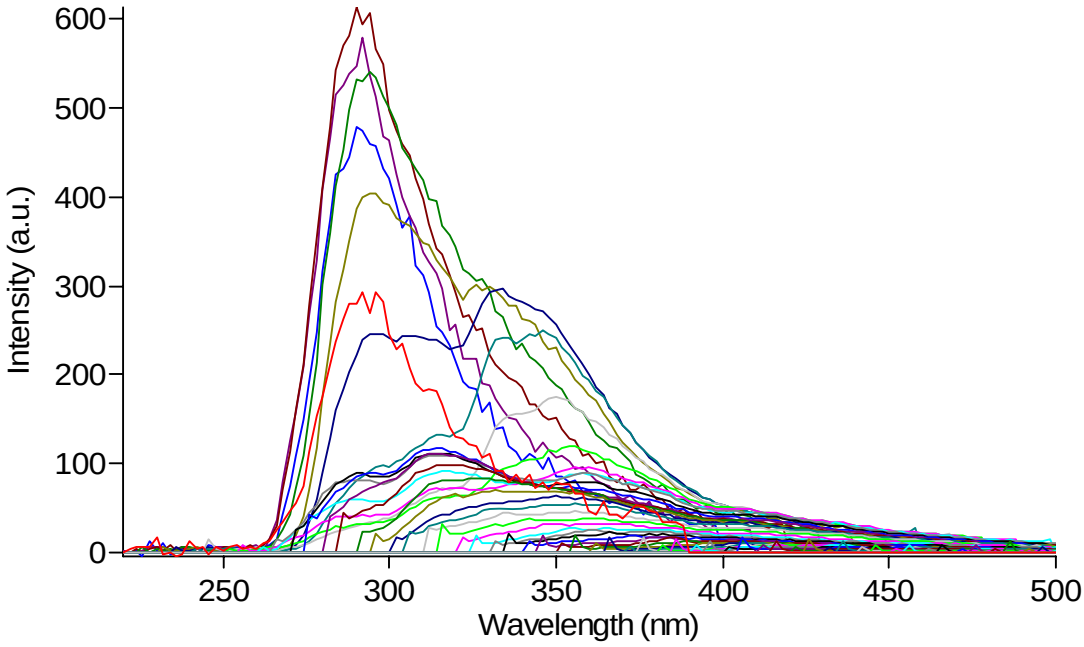
600
500
400
300
200
100
0
Intensity (a.u.)
250
300
350
400
450
500
Wavelength (nm)

32CP

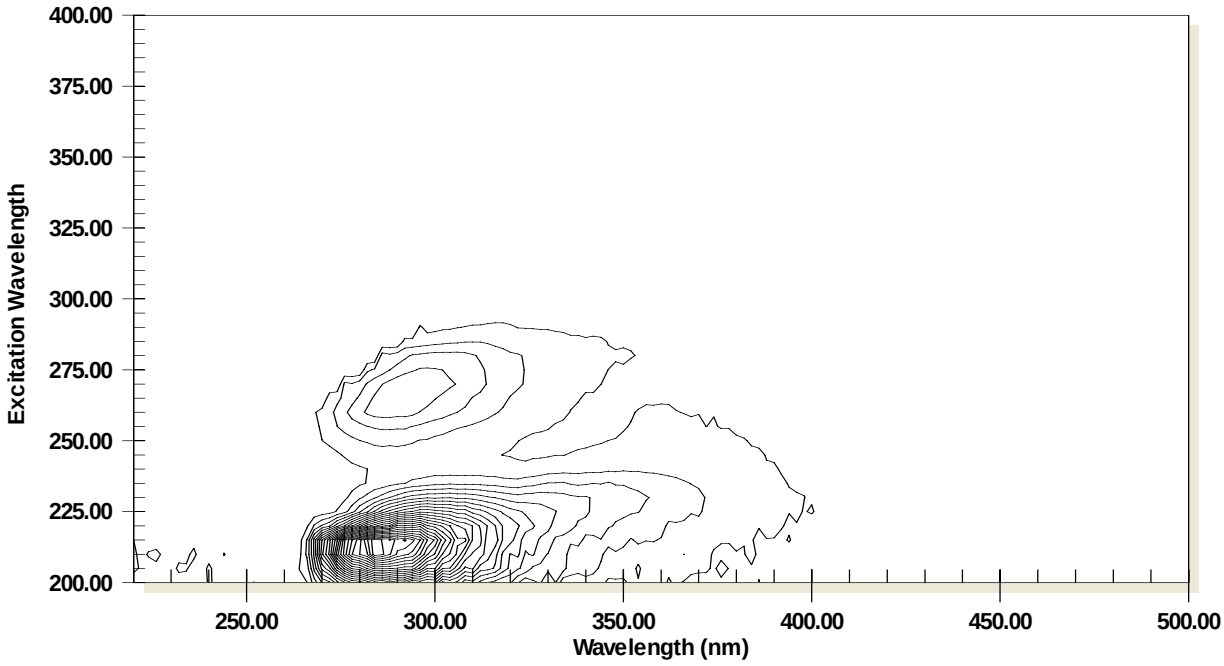
400.00
375.00
350.00
325.00
300.00
275.00
250.00
225.00
200.00
Excitation Wavelength
250.00
300.00
350.00
400.00
450.00
500.00
Wavelength (nm)

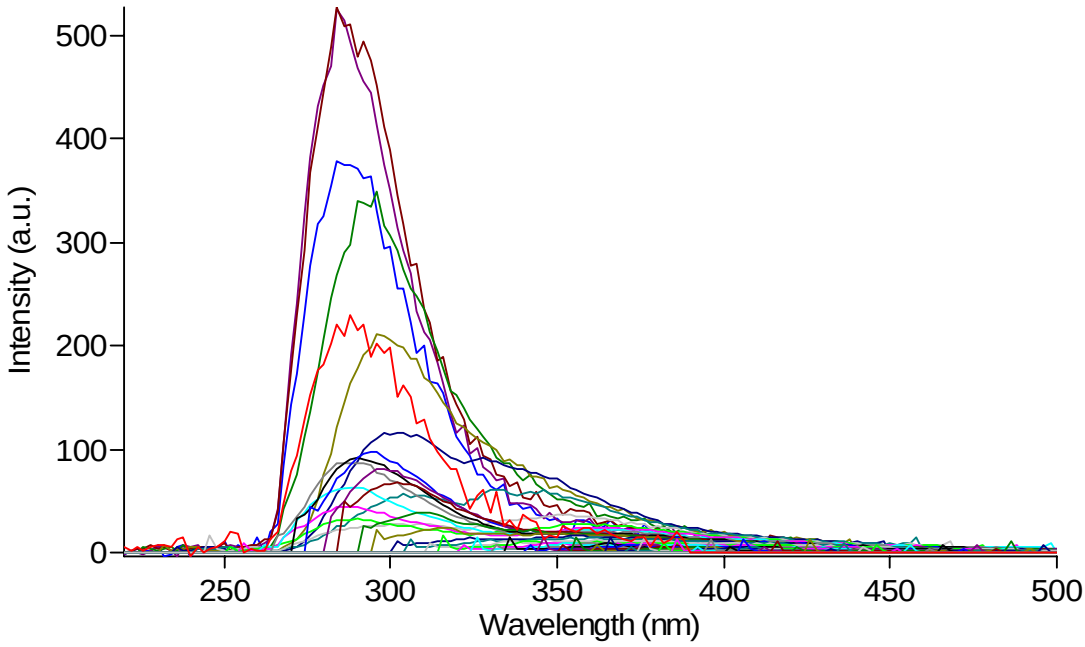
500
400
300
200
100
0
Intensity (a.u.)
250
300
350
400
450
500
Wavelength (nm)

33AP

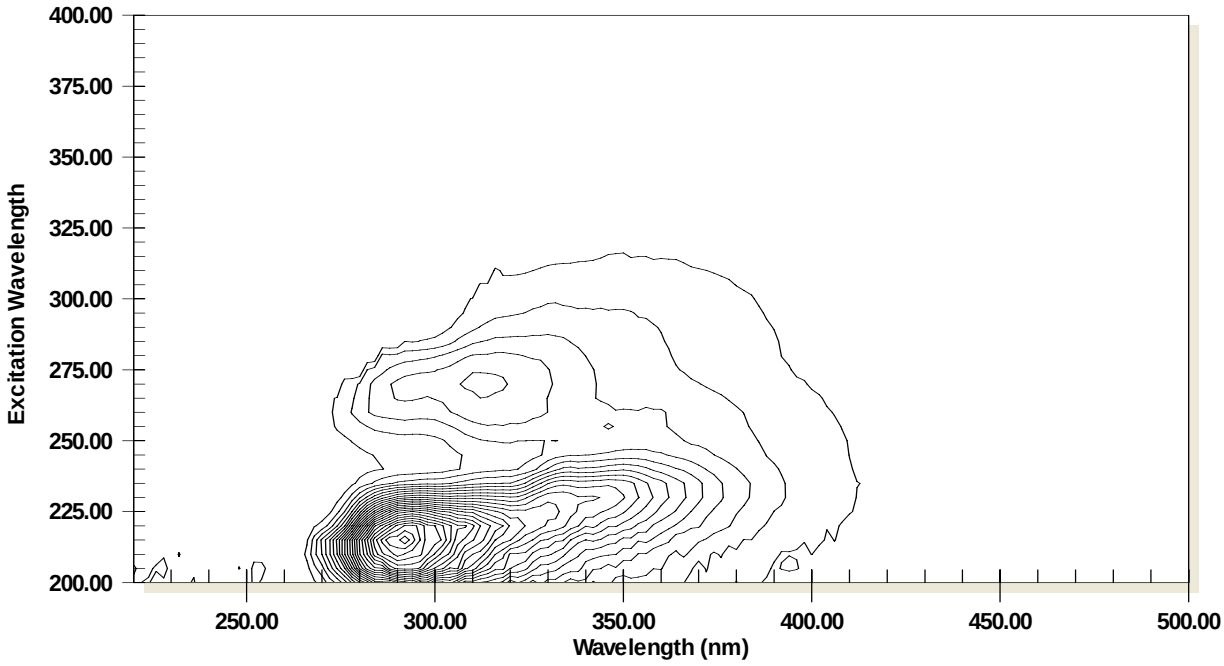
400.00
375.00
350.00
325.00
300.00
275.00
250.00
225.00
200.00
Excitation Wavelength
250.00
300.00
350.00
400.00
450.00
500.00
Wavelength (nm)

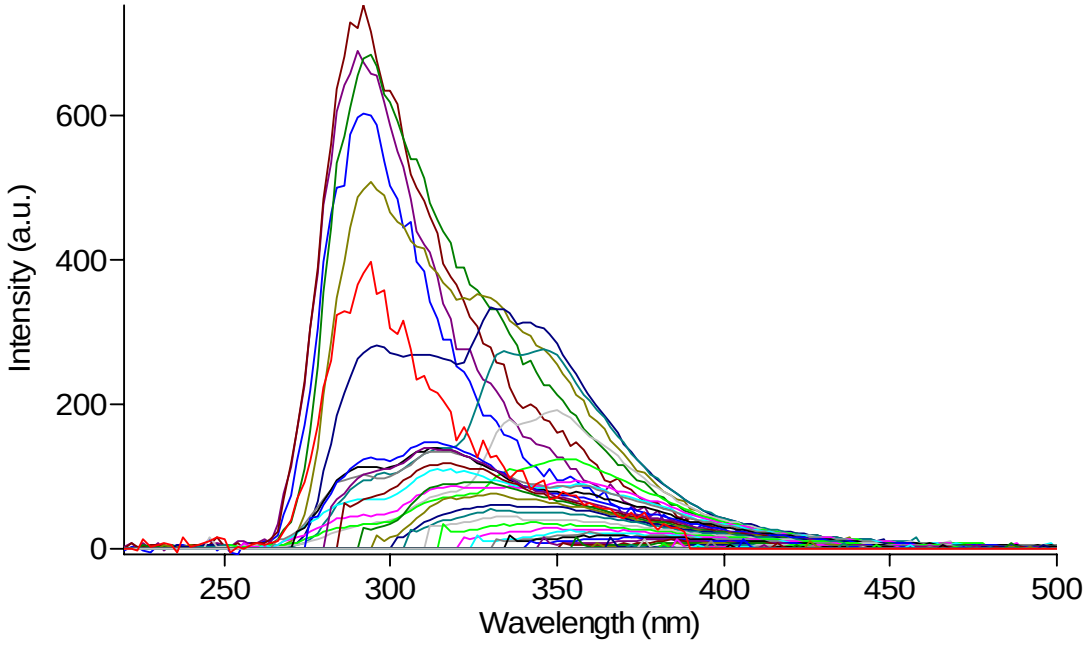
600
400
200
0
Intensity (a.u.)
250
300
350
400
450
500
Wavelength (nm)

34BP

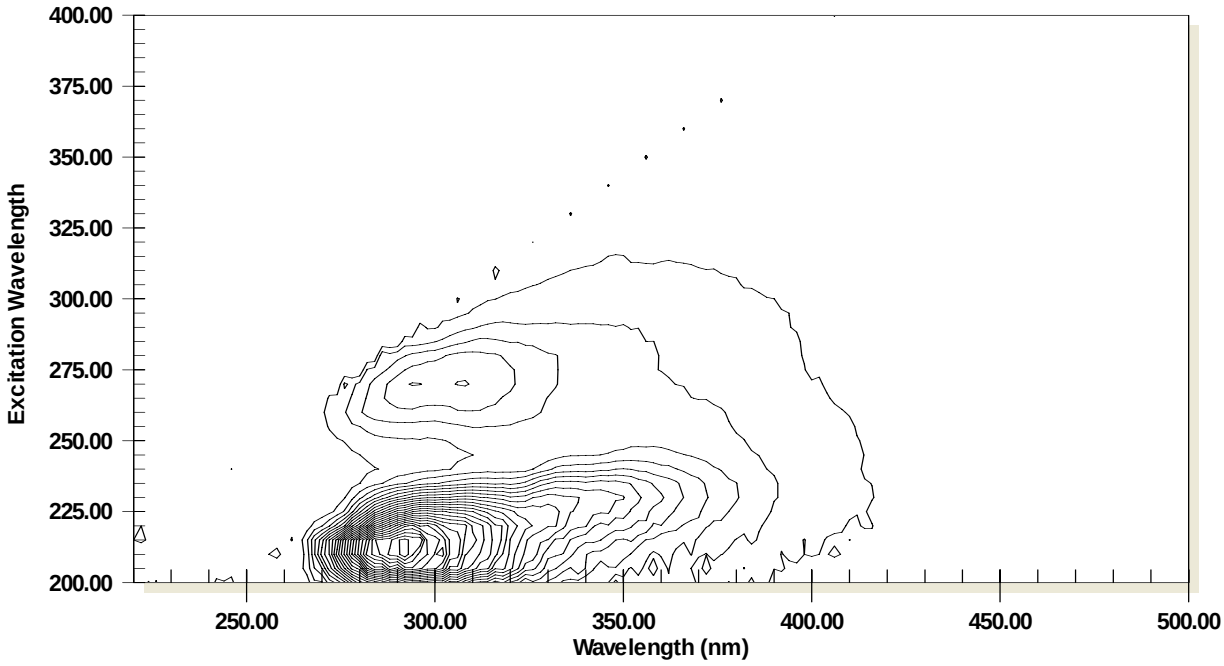
400.00
375.00
350.00
325.00
300.00
275.00
250.00
225.00
200.00
Excitation Wavelength
250.00
300.00
350.00
400.00
450.00
500.00
Wavelength (nm)

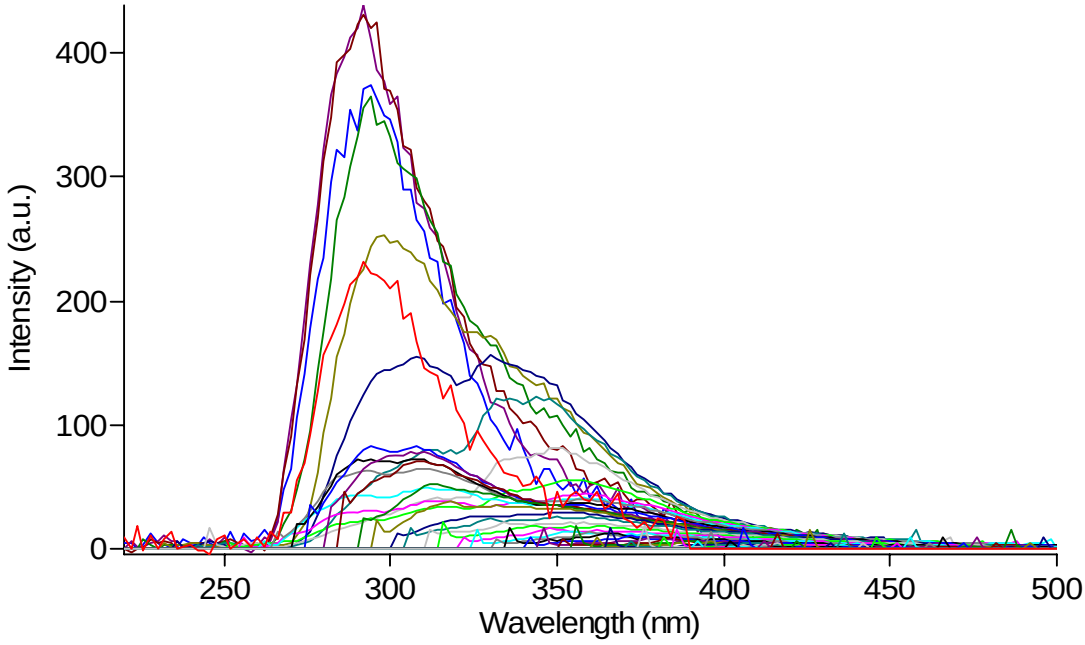
400
300
200
100
0
Intensity (a.u.)
250
300
350
400
450
500
Wavelength (nm)

35CP

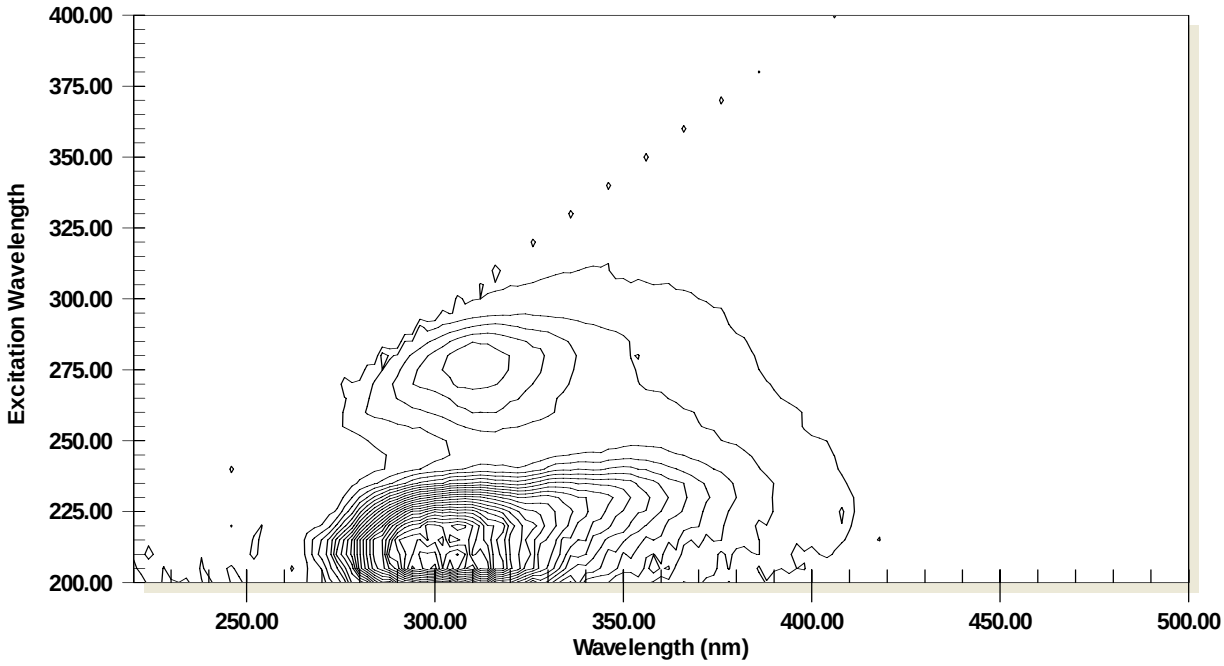
Excitation Wavelength
400.00
375.00
350.00
325.00
300.00
275.00
250.00
225.00
200.00
250.00
300.00
350.00
400.00
450.00
500.00
Wavelength (nm)

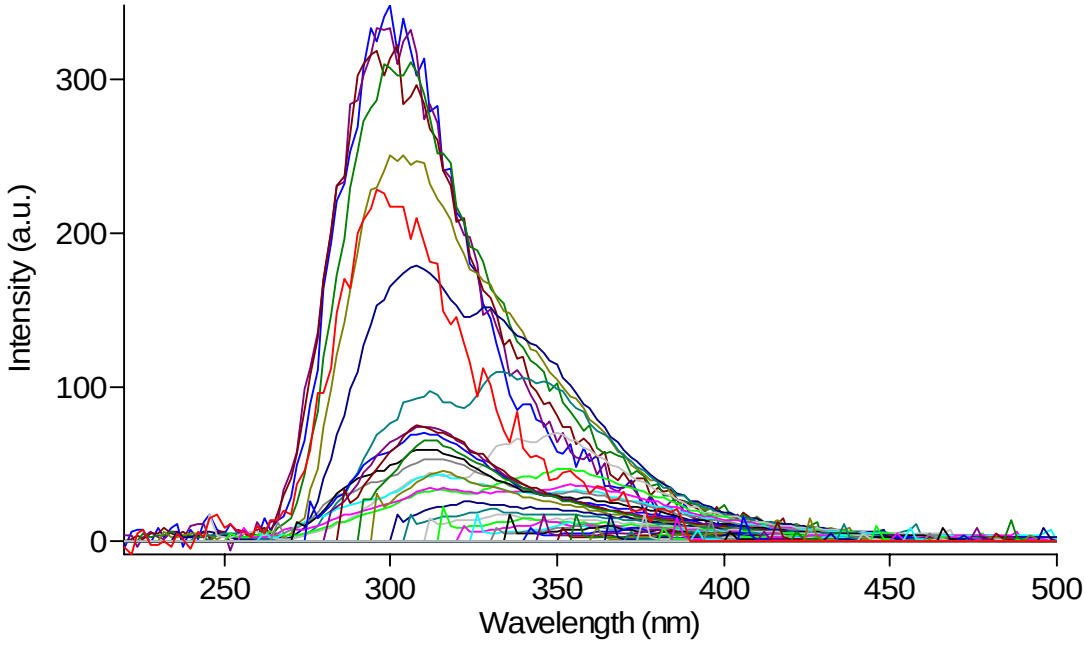
Intensity (a.u.)
300
200
100
0
250
300
350
400
450
500
Wavelength (nm)

41CP

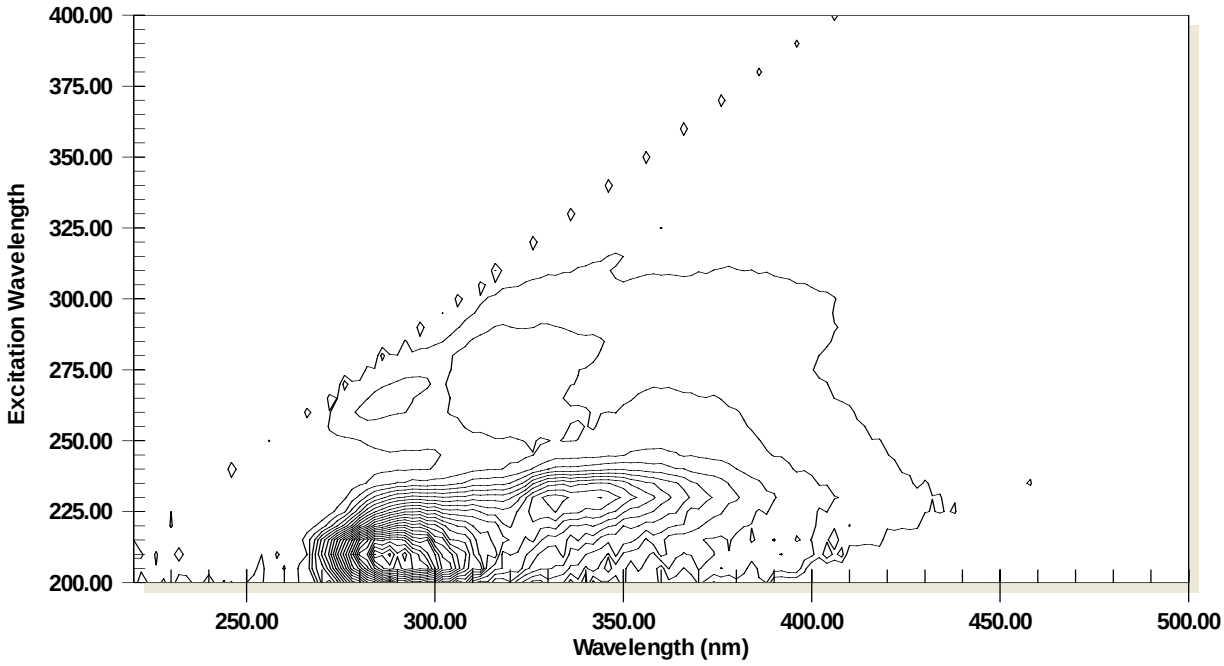
400.00
375.00
350.00
325.00
300.00
275.00
250.00
225.00
200.00
Excitation Wavelength
250.00
300.00
350.00
400.00
450.00
500.00
Wavelength (nm)

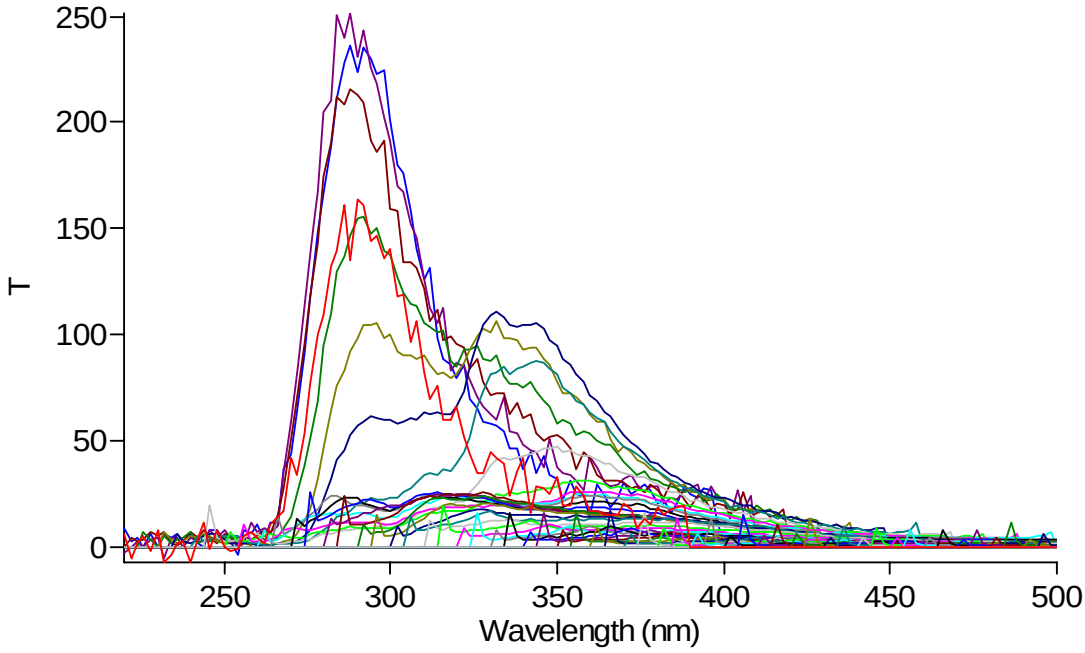
250
200
150
100
50
0
T
250
300
350
400
450
500
Wavelength (nm)

42BP

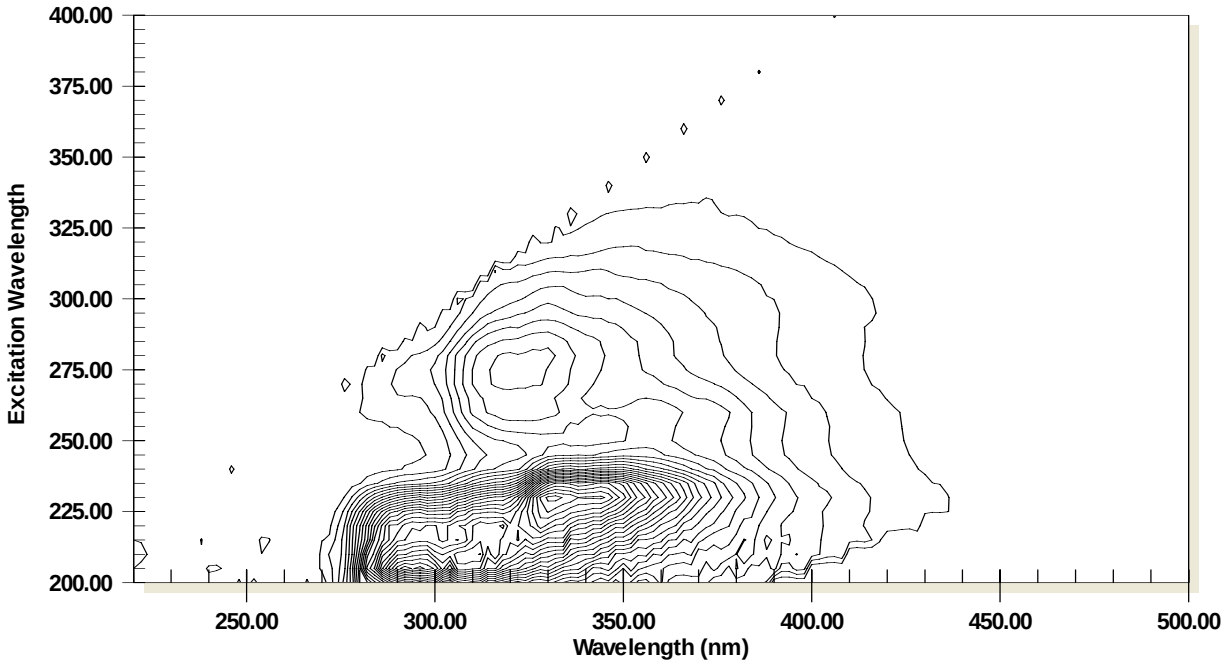
400.00
375.00
350.00
325.00
300.00
275.00
250.00
225.00
200.00
Excitation Wavelength
250.00
300.00
350.00
400.00
450.00
500.00
Wavelength (nm)

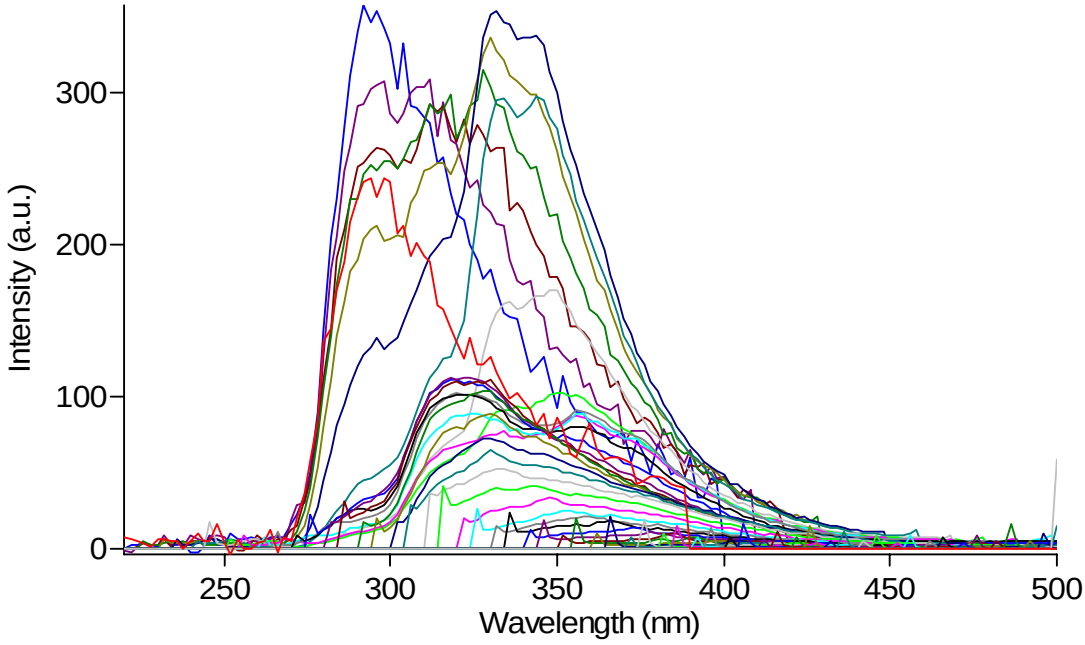
300
200
100
0
Intensity (a.u.)
250
300
350
400
450
500
Wavelength (nm)

43AP

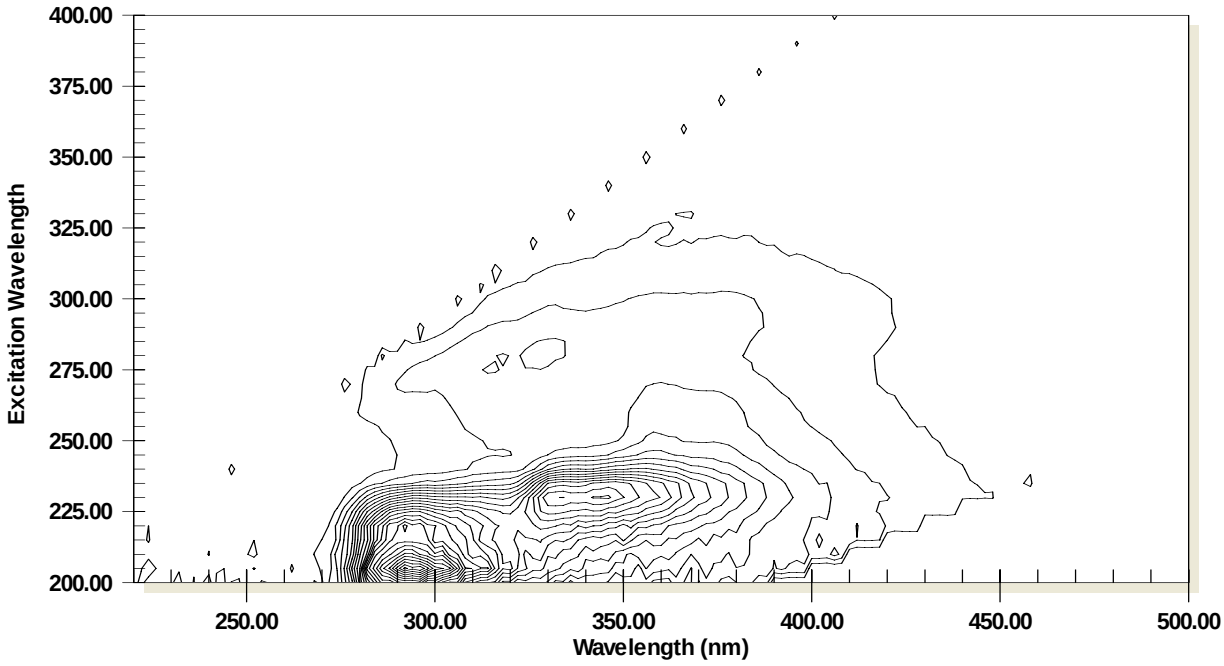
400.00
375.00
350.00
325.00
300.00
275.00
250.00
225.00
200.00
Excitation Wavelength
250.00
300.00
350.00
400.00
450.00
500.00
Wavelength (nm)

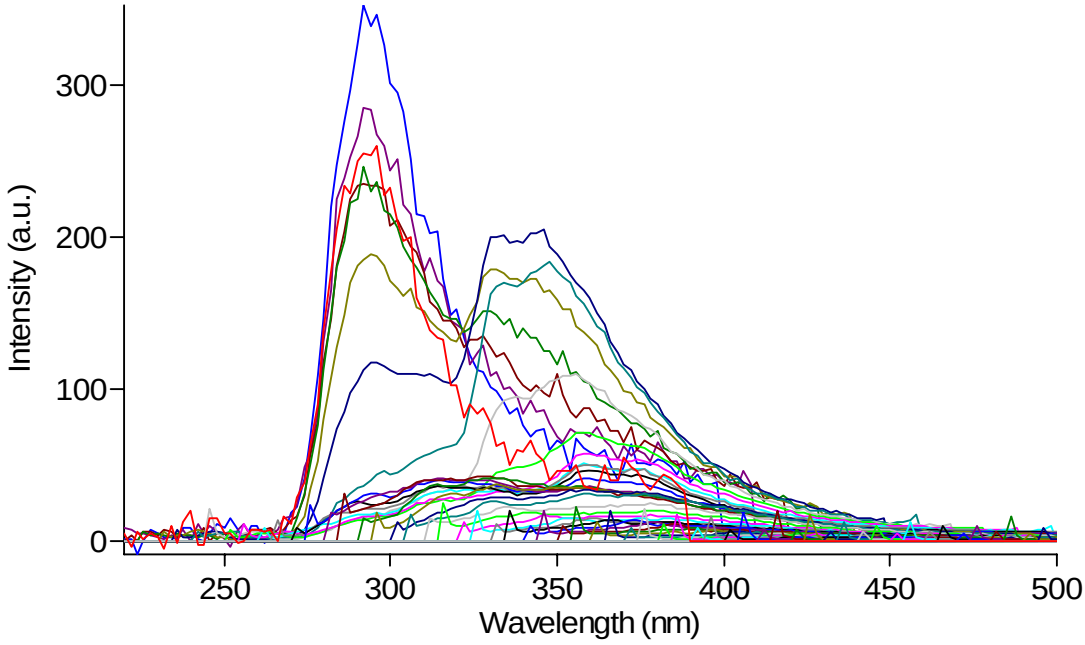
300
200
100
0
Intensity (a.u.)
250
300
350
400
450
500
Wavelength (nm)

44AP

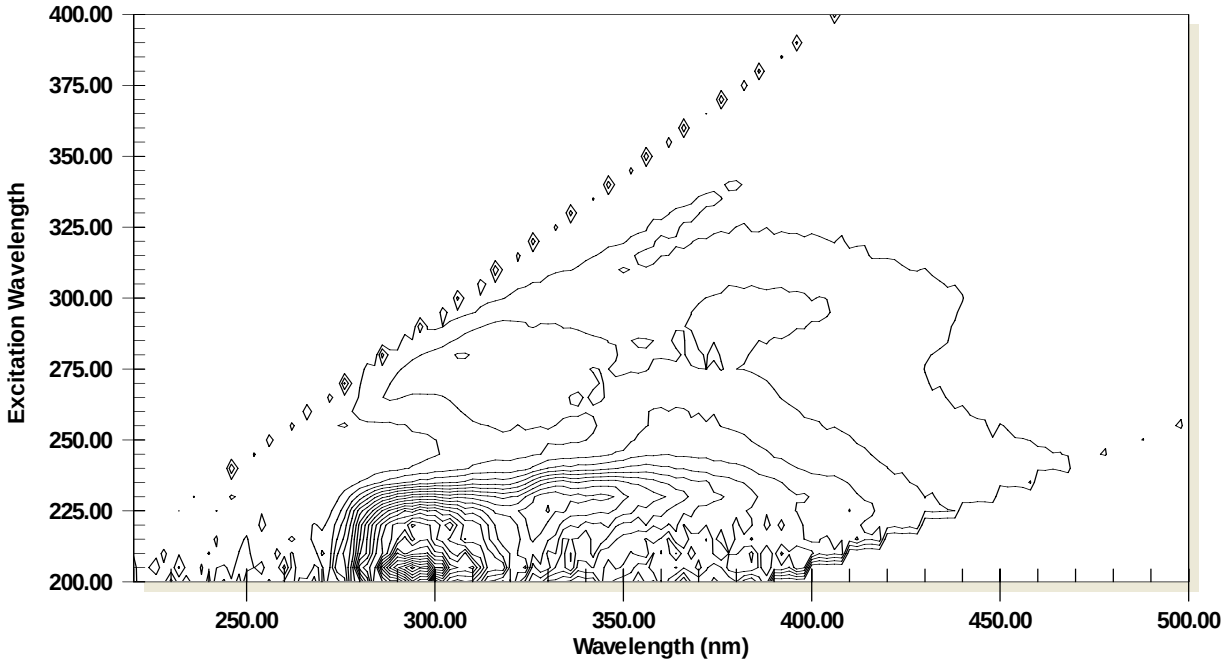
400.00
375.00
350.00
325.00
300.00
275.00
250.00
225.00
200.00
Excitation Wavelength
250.00
300.00
350.00
400.00
450.00
500.00
Wavelength (nm)

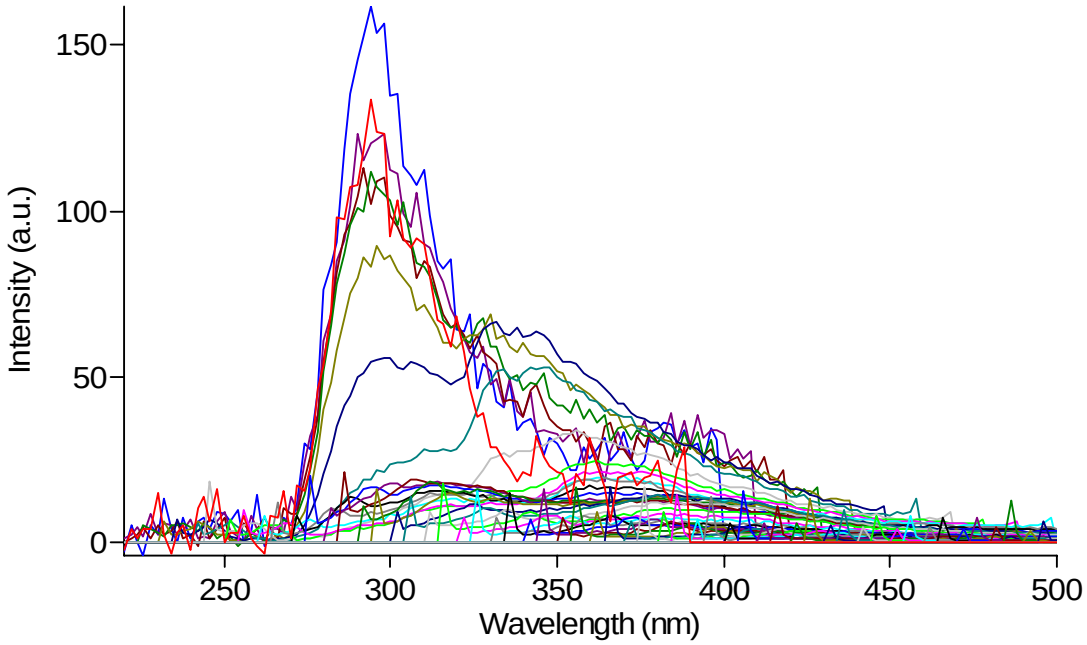
150
100
50
0
Intensity (a.u.)
250
300
350
400
450
500
Wavelength (nm)

45CP

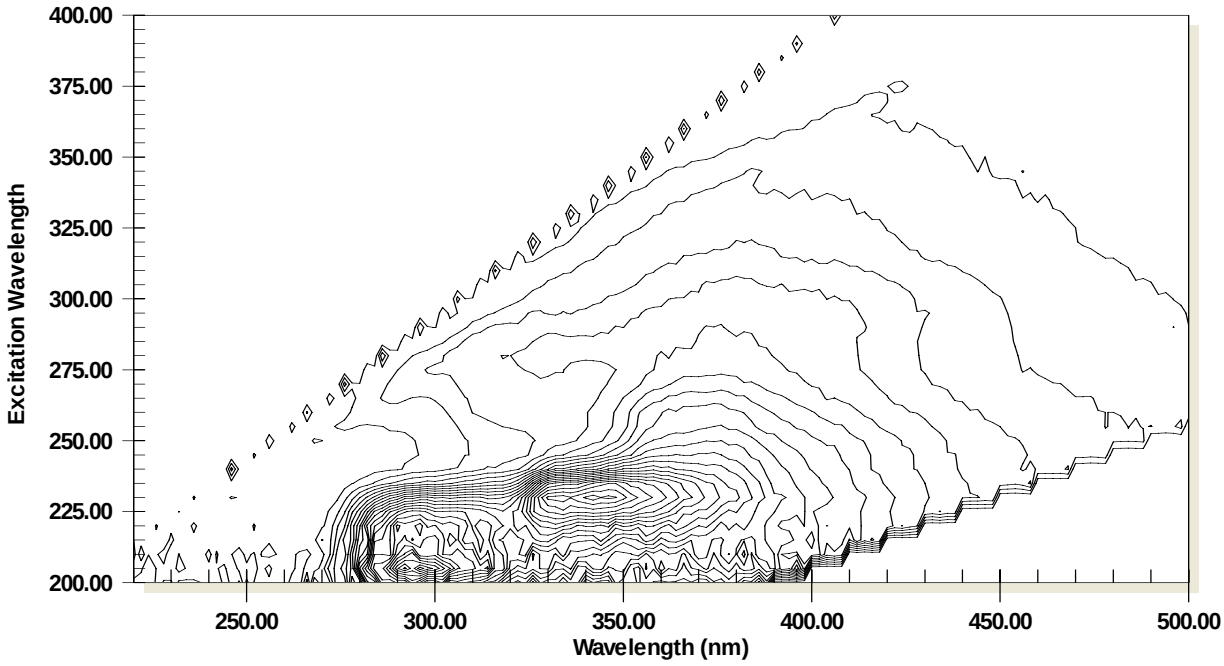
400.00
375.00
350.00
325.00
300.00
275.00
250.00
225.00
200.00
Excitation Wavelength
250.00
300.00
350.00
400.00
450.00
500.00
Wavelength (nm)

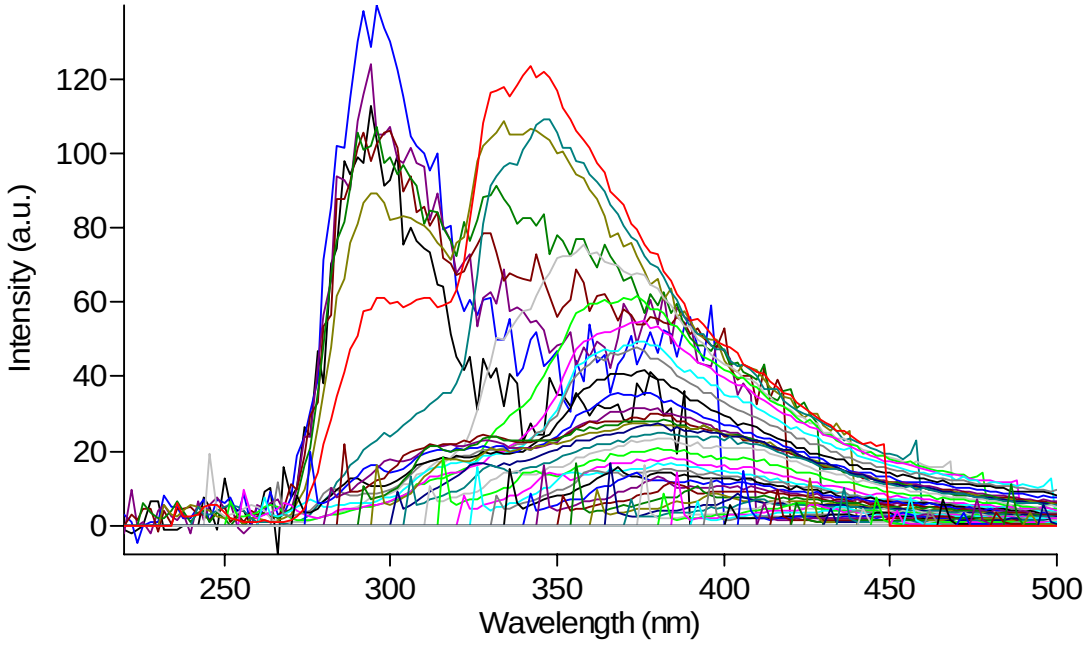
120
100
80
60
40
20
0
Intensity (a.u.)
250
300
350
400
450
500
Wavelength (nm)

51CP

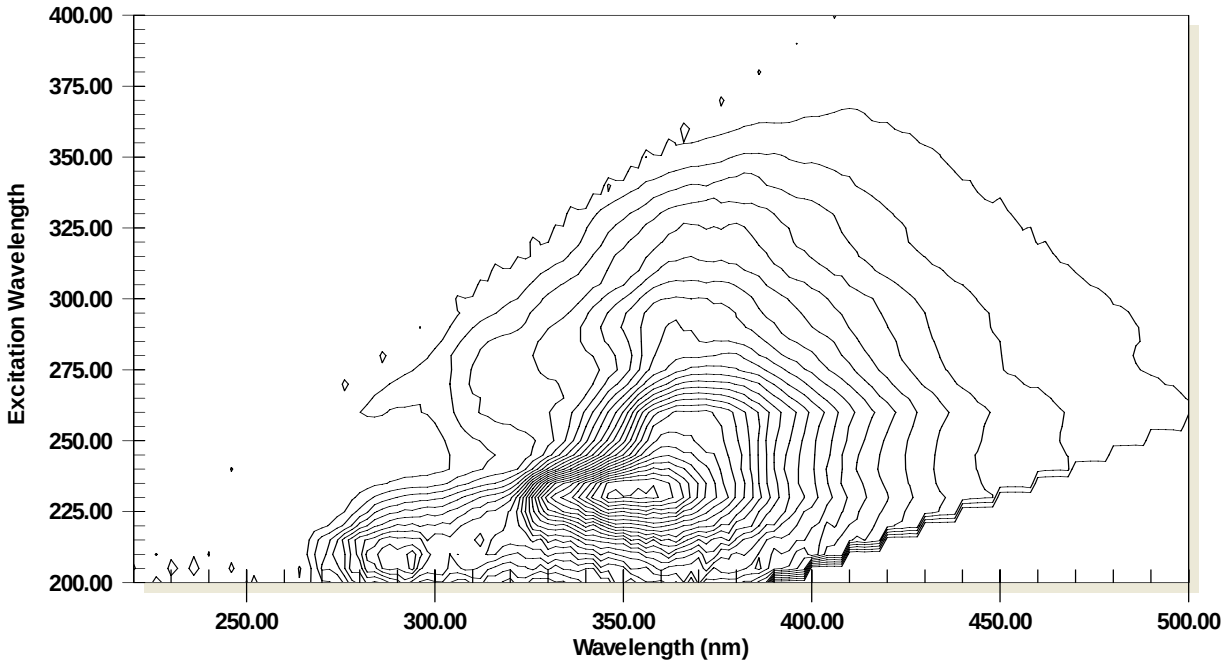
Excitation Wavelength
400.00
375.00
350.00
325.00
300.00
275.00
250.00
225.00
200.00
250.00
300.00
350.00
400.00
450.00
500.00
Wavelength (nm)

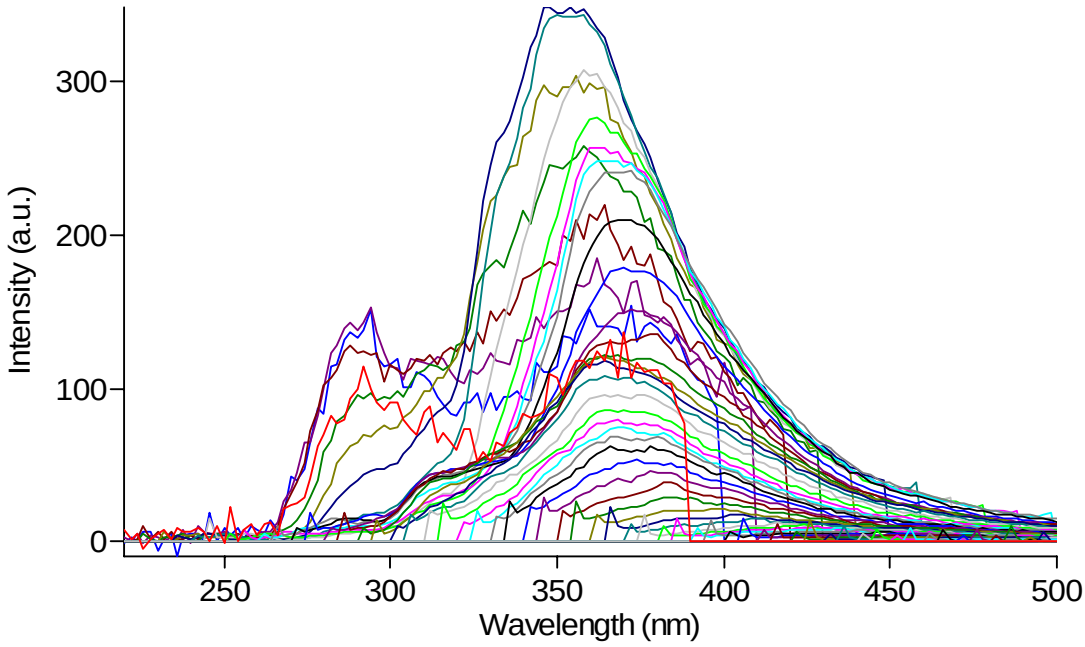
Intensity (a.u.)
300
200
100
0
250
300
350
400
450
500
Wavelength (nm)

52BP

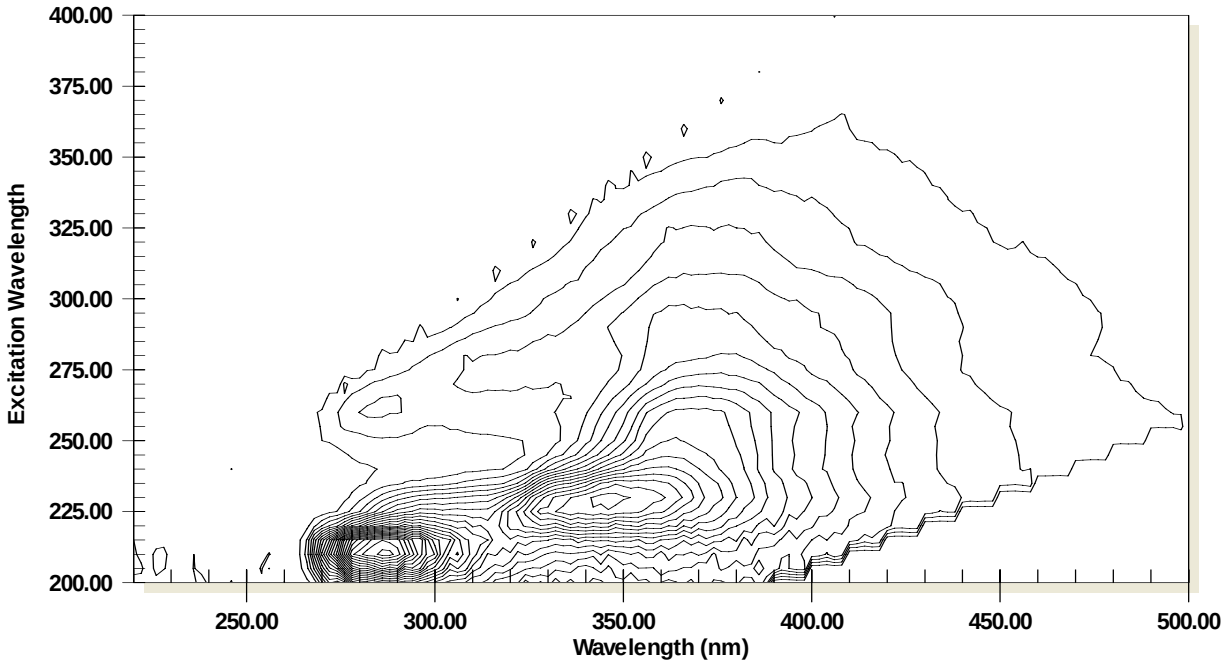
400.00
375.00
350.00
325.00
300.00
275.00
250.00
225.00
200.00
Excitation Wavelength
250.00
300.00
350.00
400.00
450.00
500.00
Wavelength (nm)

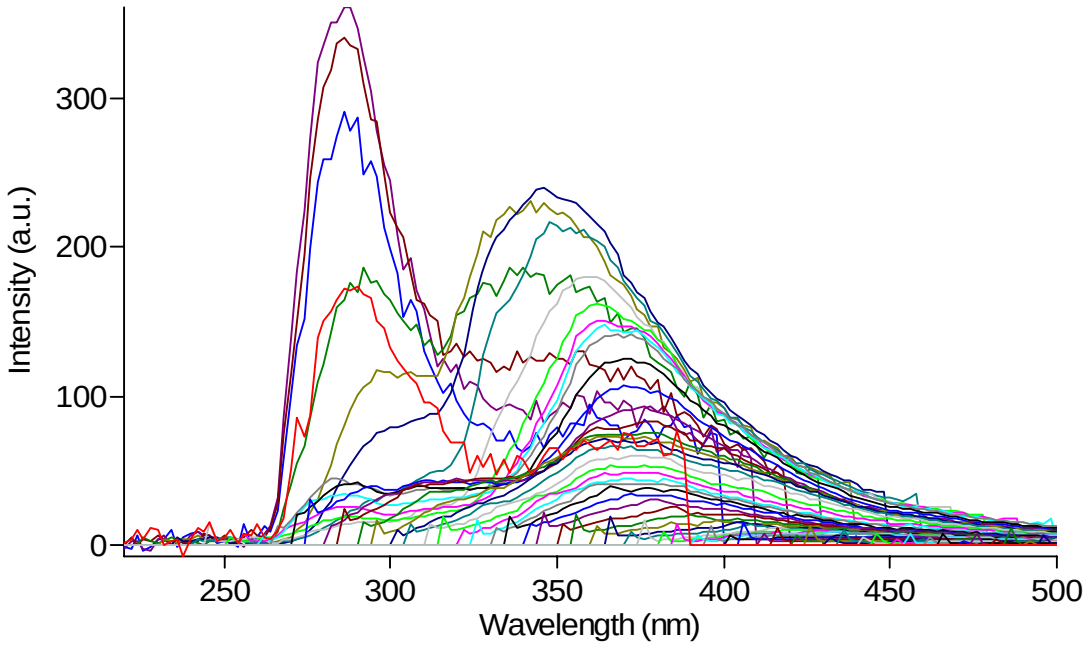
300
200
100
0
Intensity (a.u.)
250
300
350
400
450
500
Wavelength (nm)

53AP

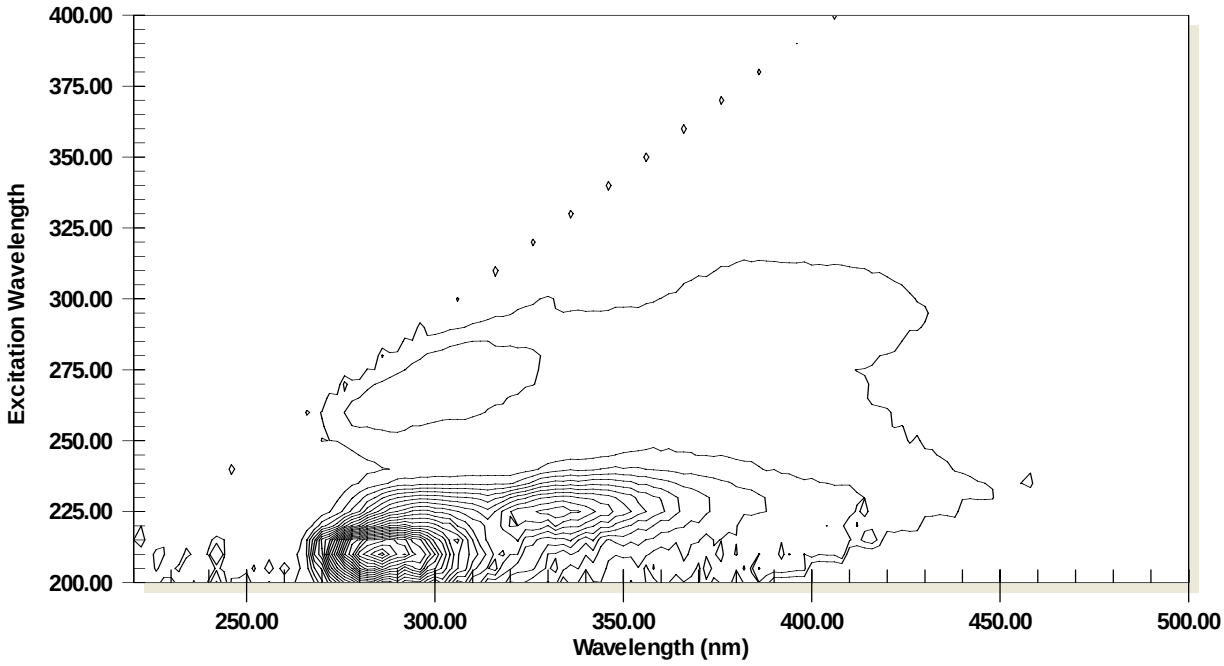
400.00
375.00
350.00
325.00
300.00
275.00
250.00
225.00
200.00
Excitation Wavelength
250.00
300.00
350.00
400.00
450.00
500.00
Wavelength (nm)

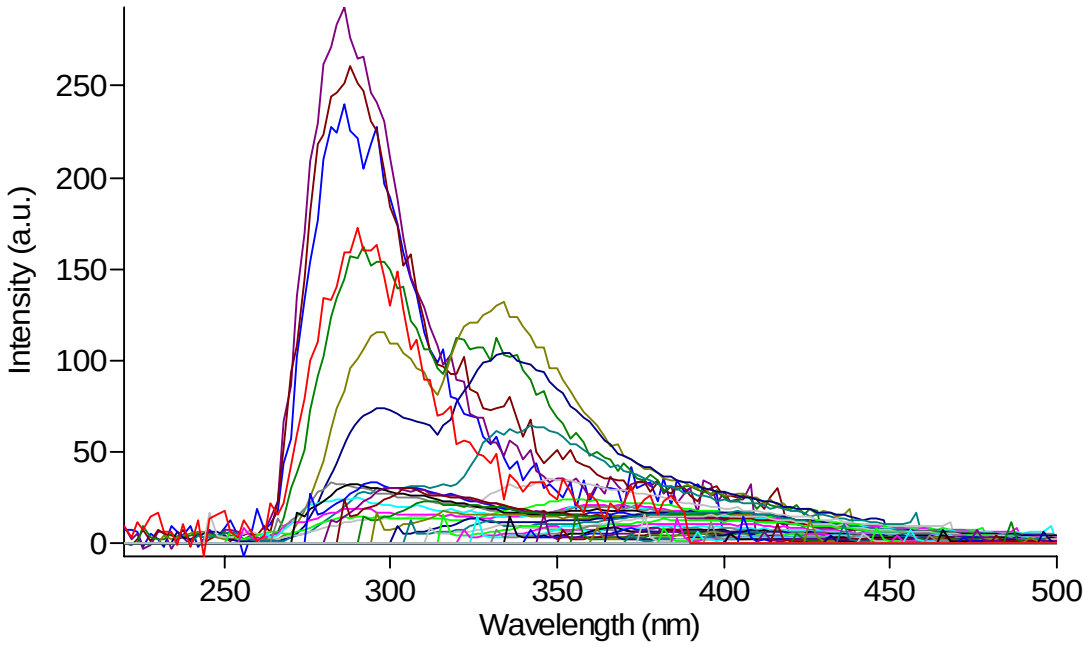
250
200
150
100
50
0
Intensity (a.u.)
250
300
350
400
450
500
Wavelength (nm)

54BP

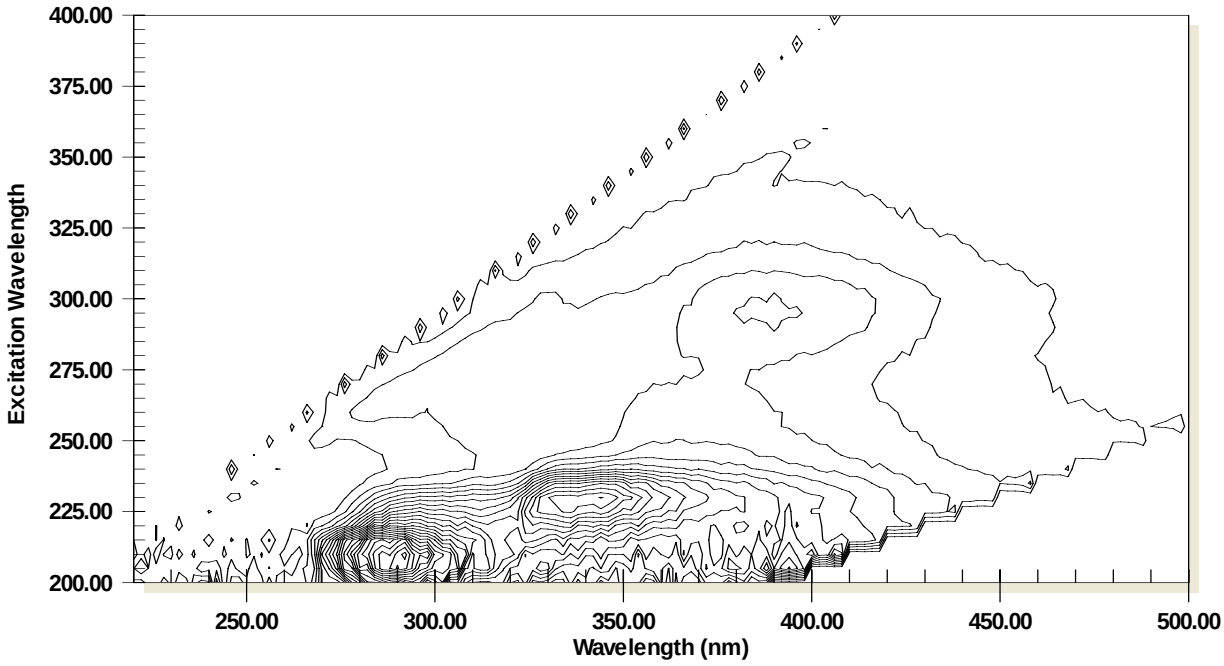
400.00
375.00
350.00
325.00
300.00
275.00
250.00
225.00
200.00
Excitation Wavelength
250.00
300.00
350.00
400.00
450.00
500.00
Wavelength (nm)

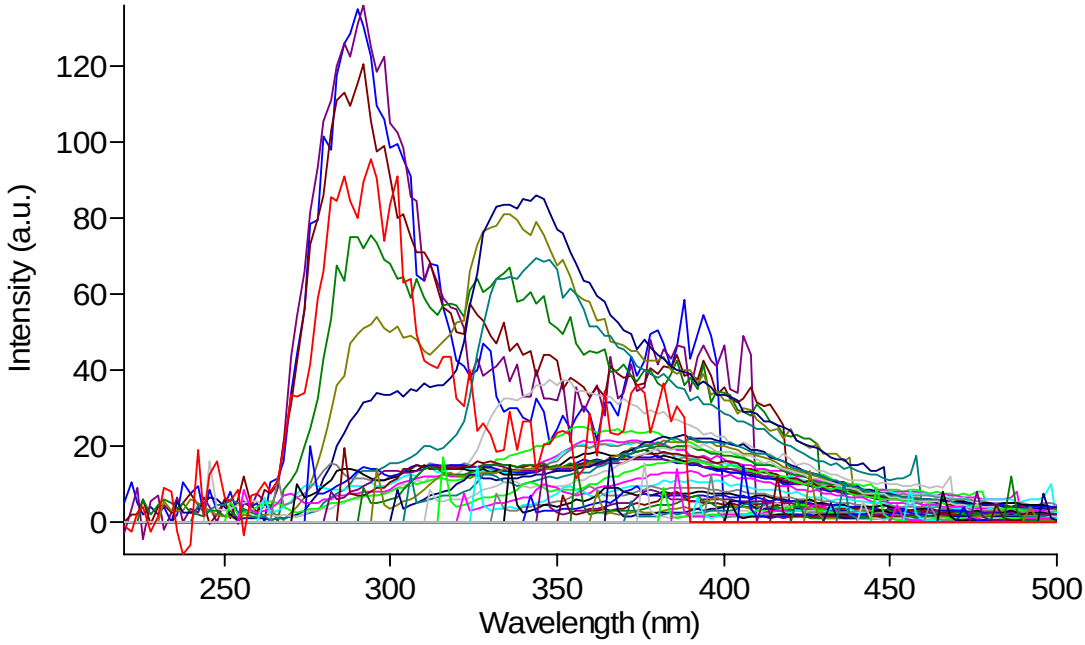
120
100
80
60
40
20
0
Intensity (a.u.)
250
300
350
400
450
500
Wavelength (nm)

55CP

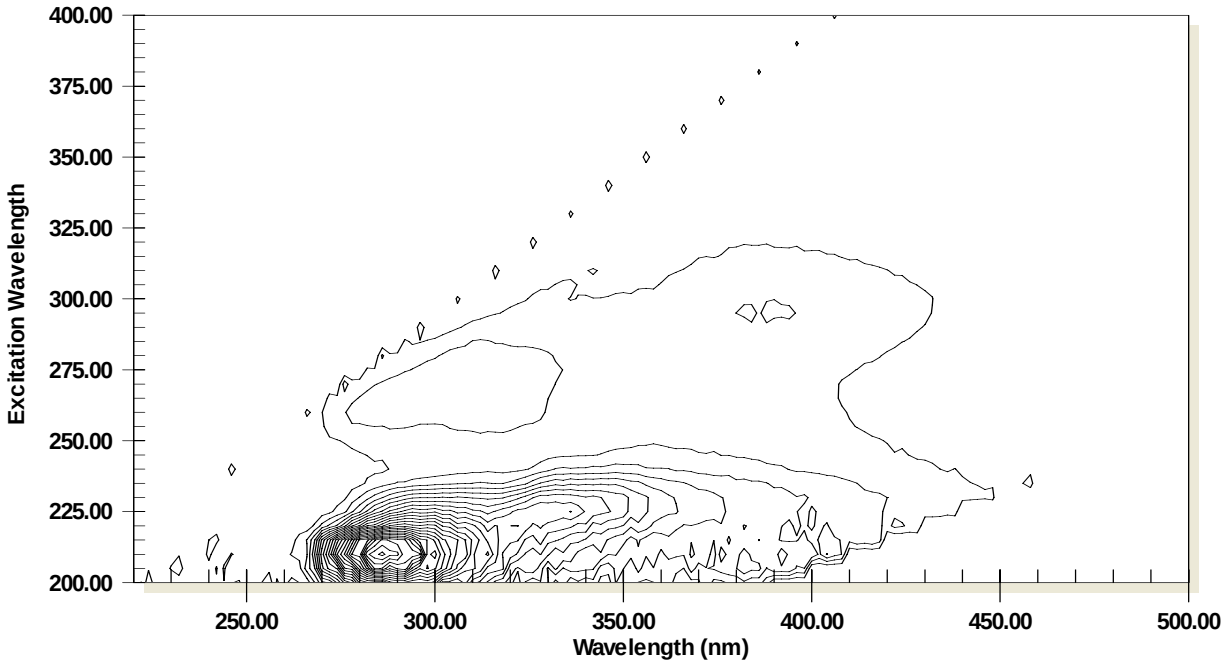
400.00
375.00
350.00
325.00
300.00
275.00
250.00
225.00
200.00
Excitation Wavelength
250.00
300.00
350.00
400.00
450.00
500.00
Wavelength (nm)

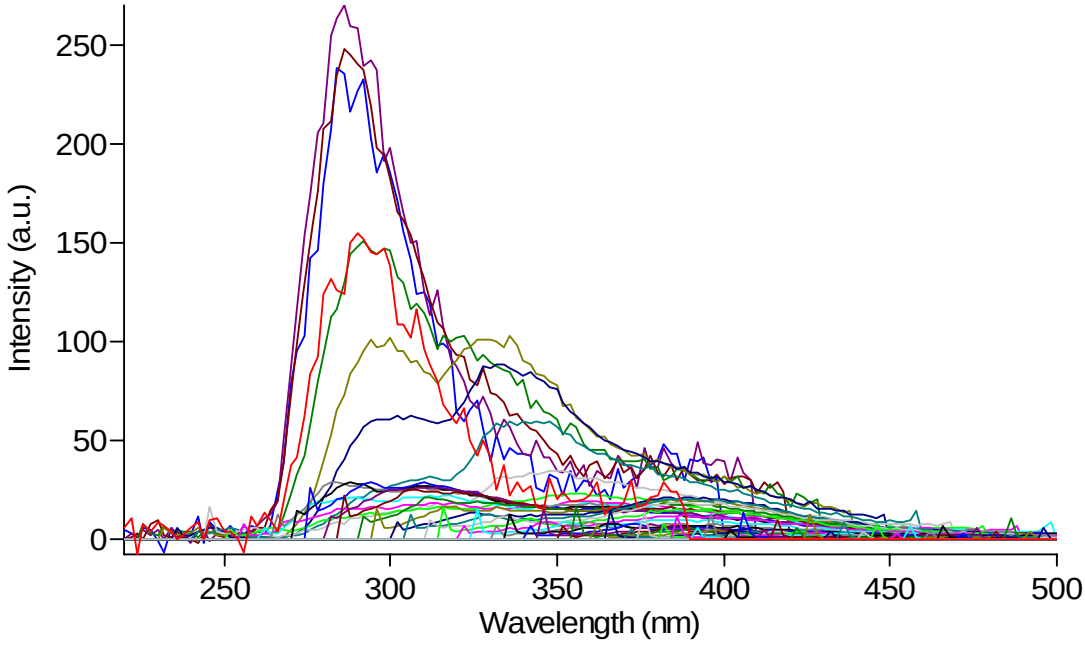
250
200
150
100
50
0
Intensity (a.u.)
250
300
350
400
450
500
Wavelength (nm)

61AP

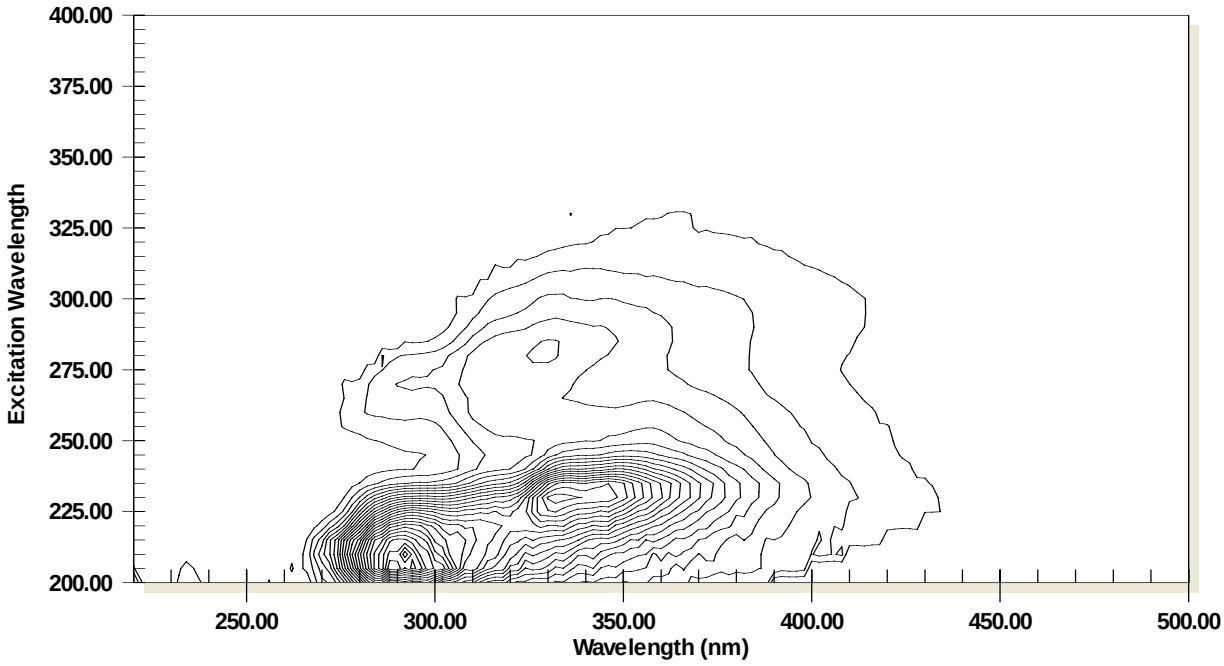
400.00
375.00
350.00
325.00
300.00
275.00
250.00
225.00
200.00
Excitation Wavelength
250.00
300.00
350.00
400.00
450.00
500.00
Wavelength (nm)

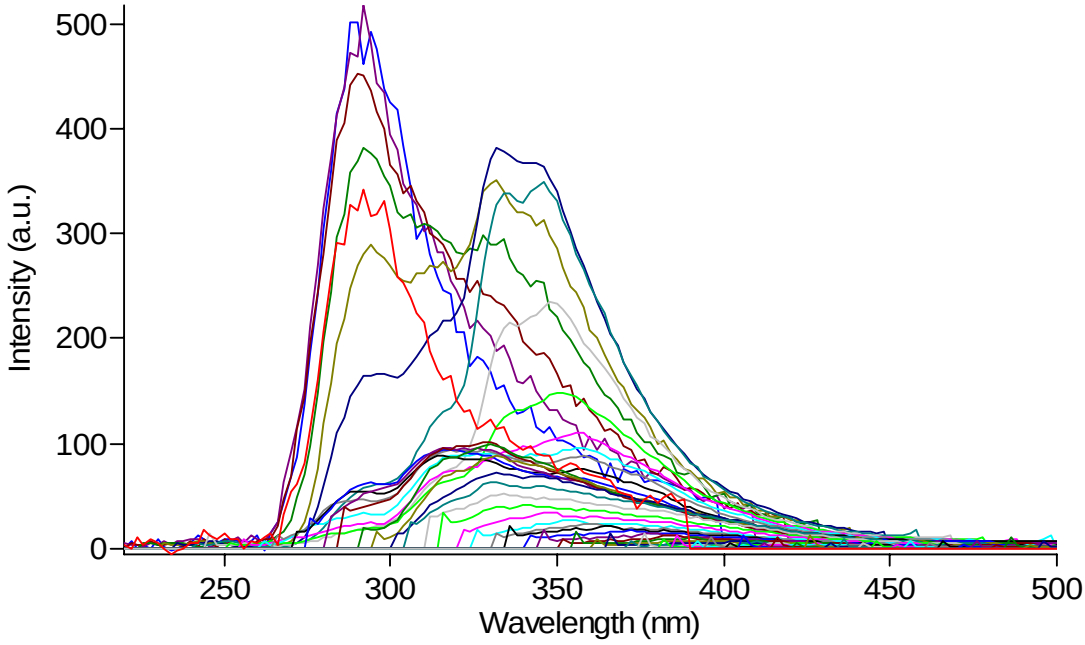
500
400
300
200
100
0
Intensity (a.u.)
250
300
350
400
450
500
Wavelength (nm)

62CP

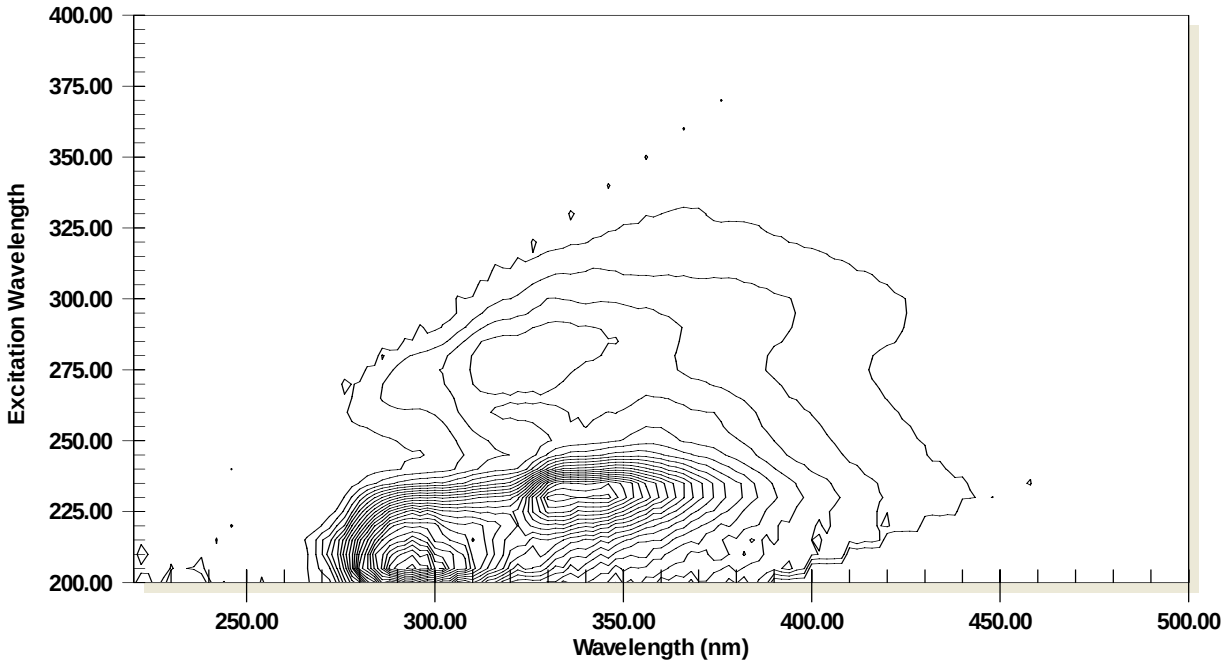
Excitation Wavelength
400.00
375.00
350.00
325.00
300.00
275.00
250.00
225.00
200.00
250.00
300.00
350.00
400.00
450.00
500.00
Wavelength (nm)

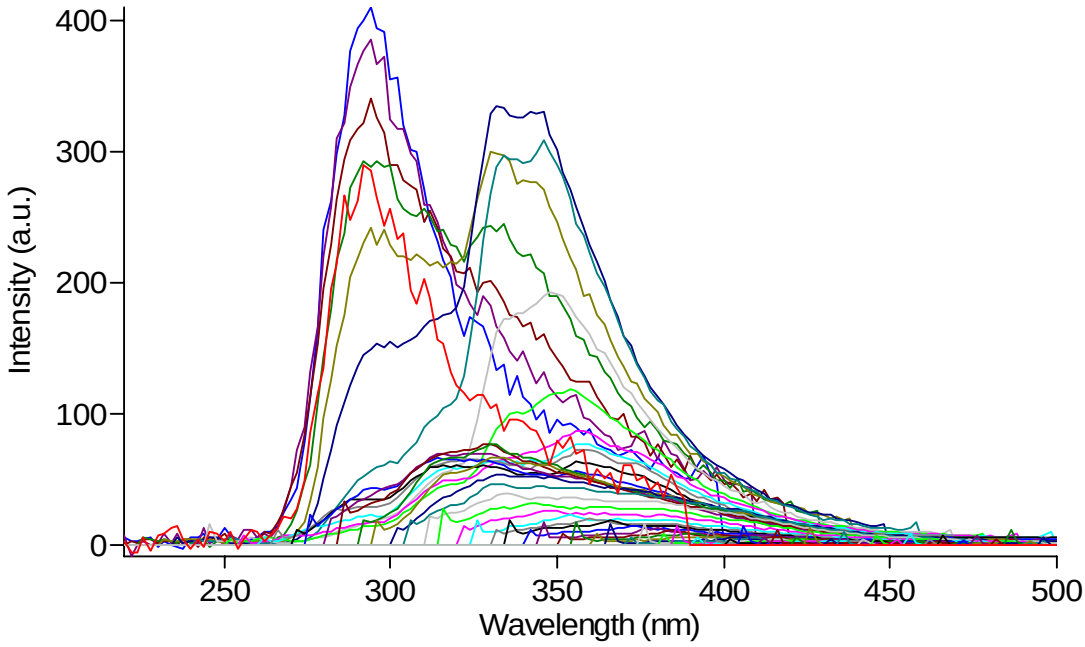
Intensity (a.u.)
400
300
200
100
0
250
300
350
400
450
500
Wavelength (nm)

63BP

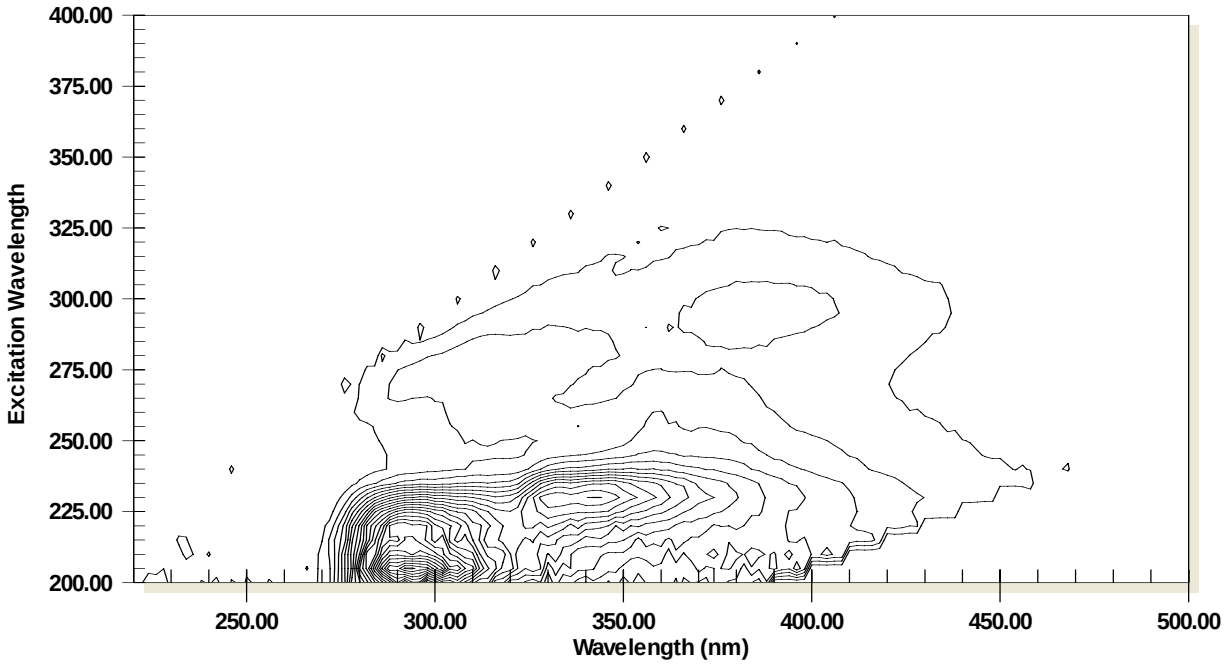
Excitation Wavelength
400.00
375.00
350.00
325.00
300.00
275.00
250.00
225.00
200.00
250.00
300.00
350.00
400.00
450.00
500.00
Wavelength (nm)

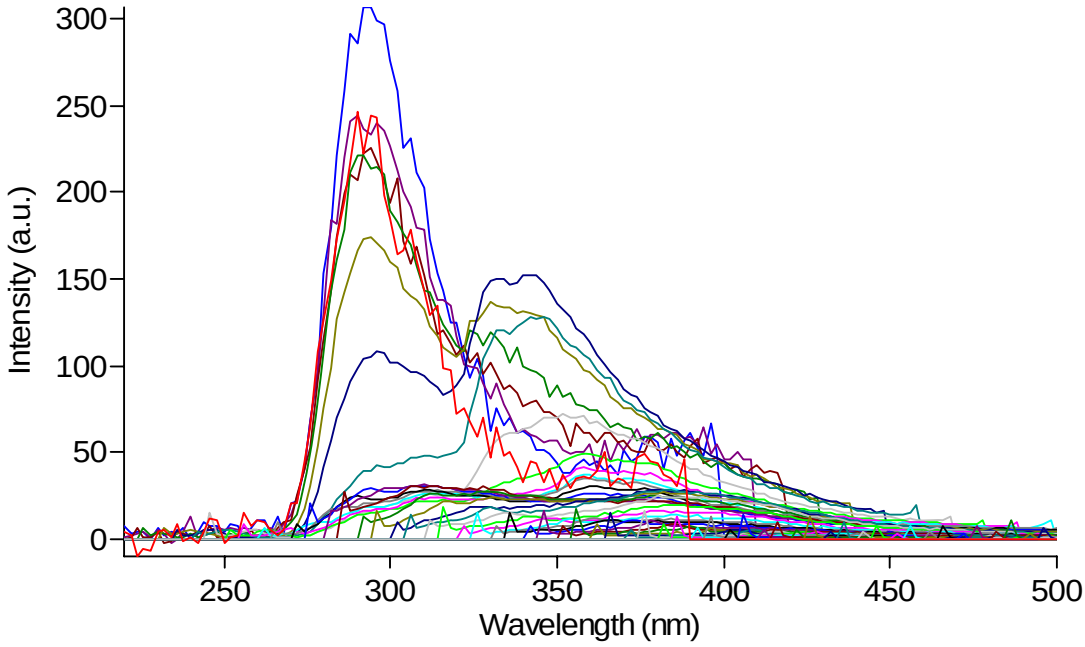
Intensity (a.u.)
300
250
200
150
100
50
0
250
300
350
400
450
500
Wavelength (nm)

64AP

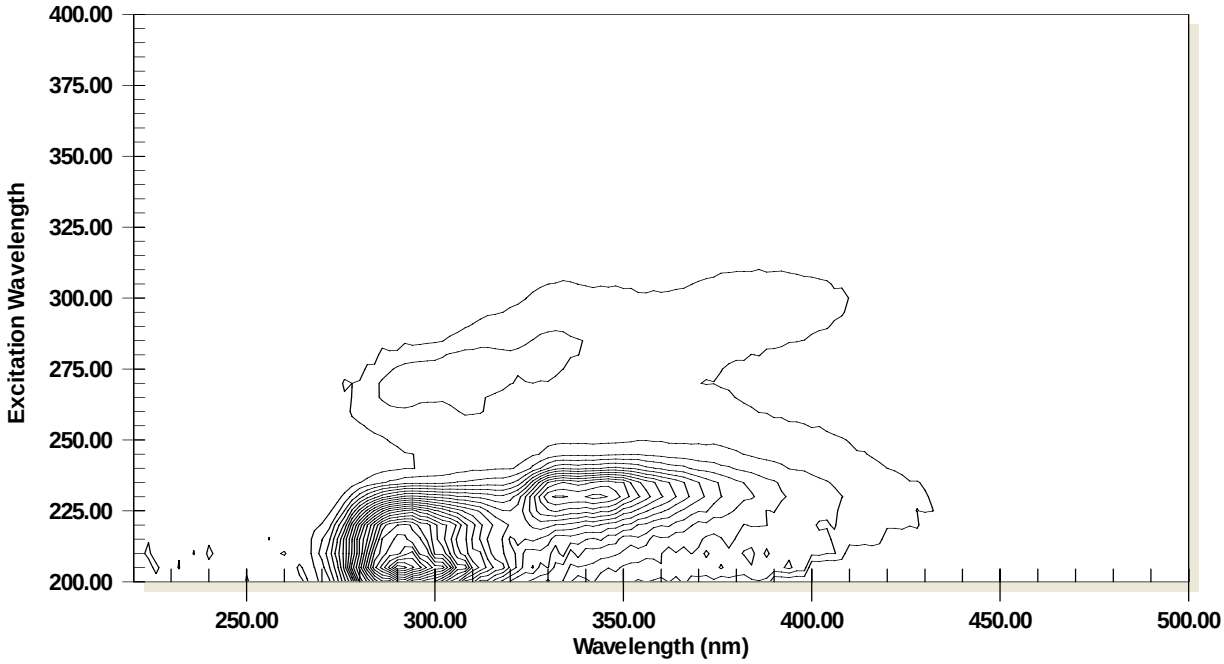
Excitation Wavelength
400.00
375.00
350.00
325.00
300.00
275.00
250.00
225.00
200.00
250.00
300.00
350.00
400.00
450.00
500.00
Wavelength (nm)

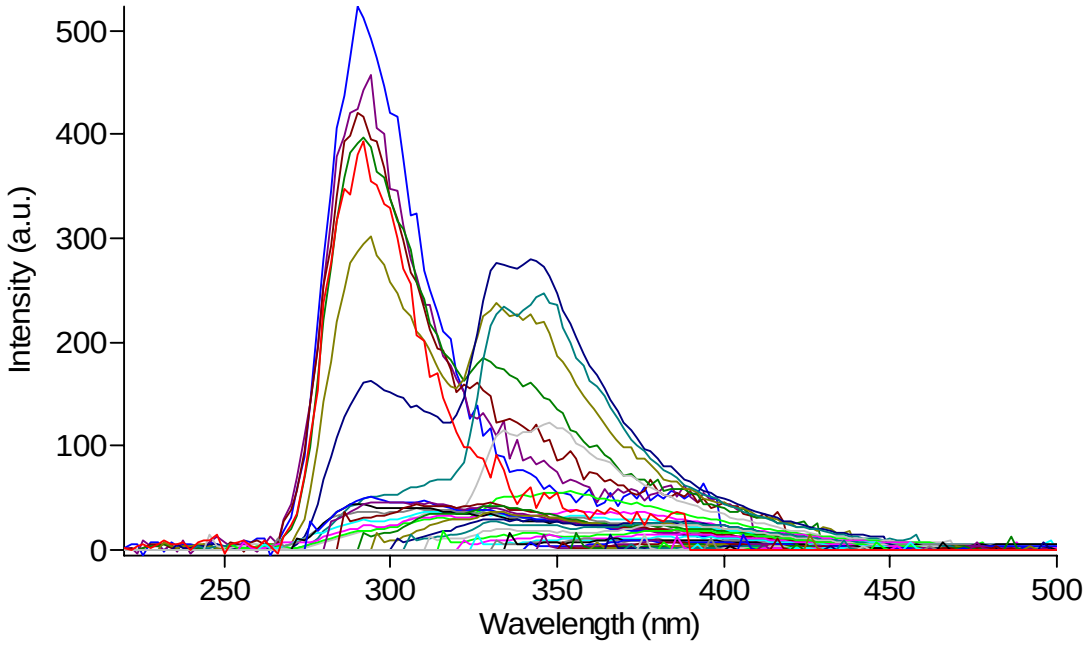
Intensity (a.u.)
500
400
300
200
100
0
250
300
350
400
450
500
Wavelength (nm)

65BP

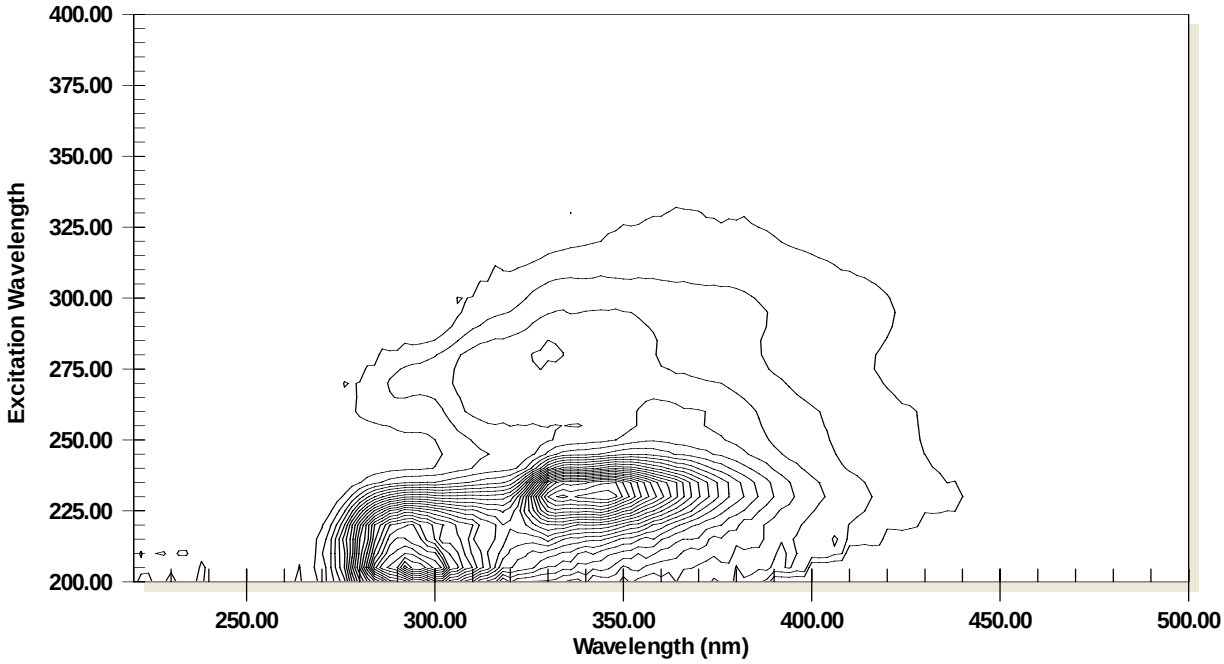
Excitation Wavelength
400.00
375.00
350.00
325.00
300.00
275.00
250.00
225.00
200.00
250.00
300.00
350.00
400.00
450.00
500.00
Wavelength (nm)

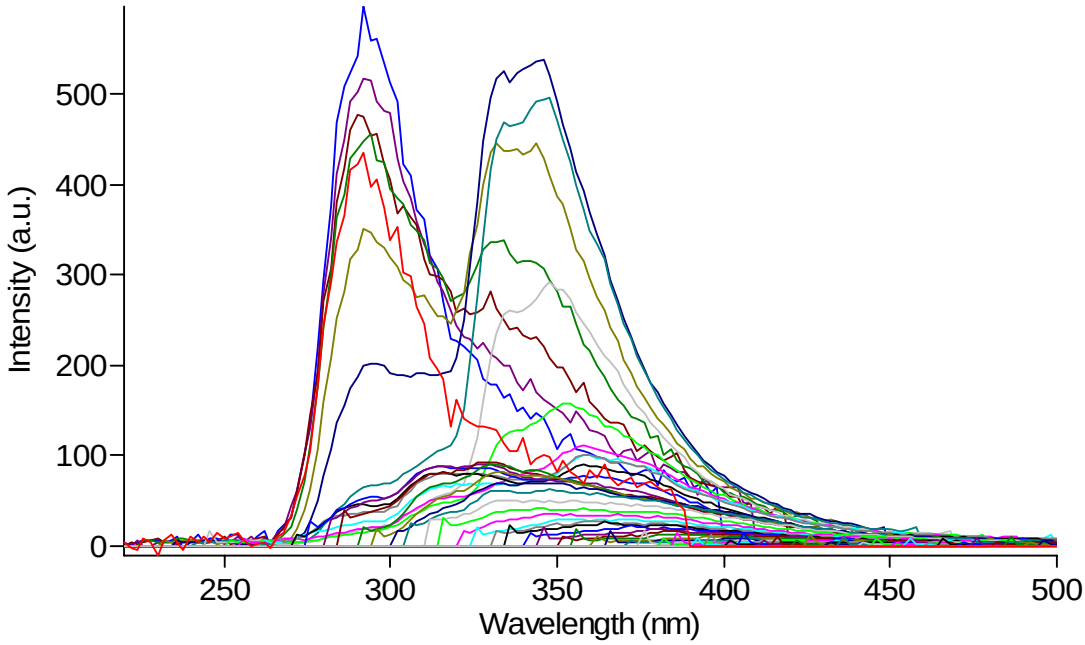
Intensity (a.u.)
500
400
300
200
100
0
250
300
350
400
450
500
Wavelength (nm)

71BP

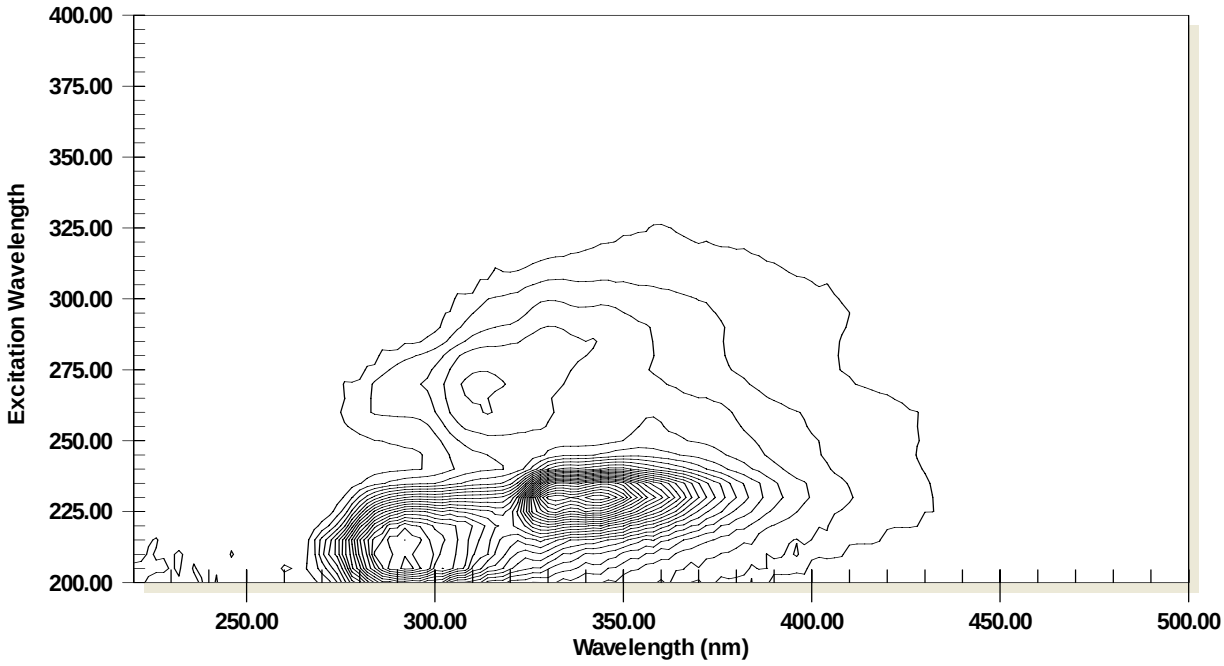
400.00
375.00
350.00
325.00
300.00
275.00
250.00
225.00
200.00
Excitation Wavelength
250.00
300.00
350.00
400.00
450.00
500.00
Wavelength (nm)

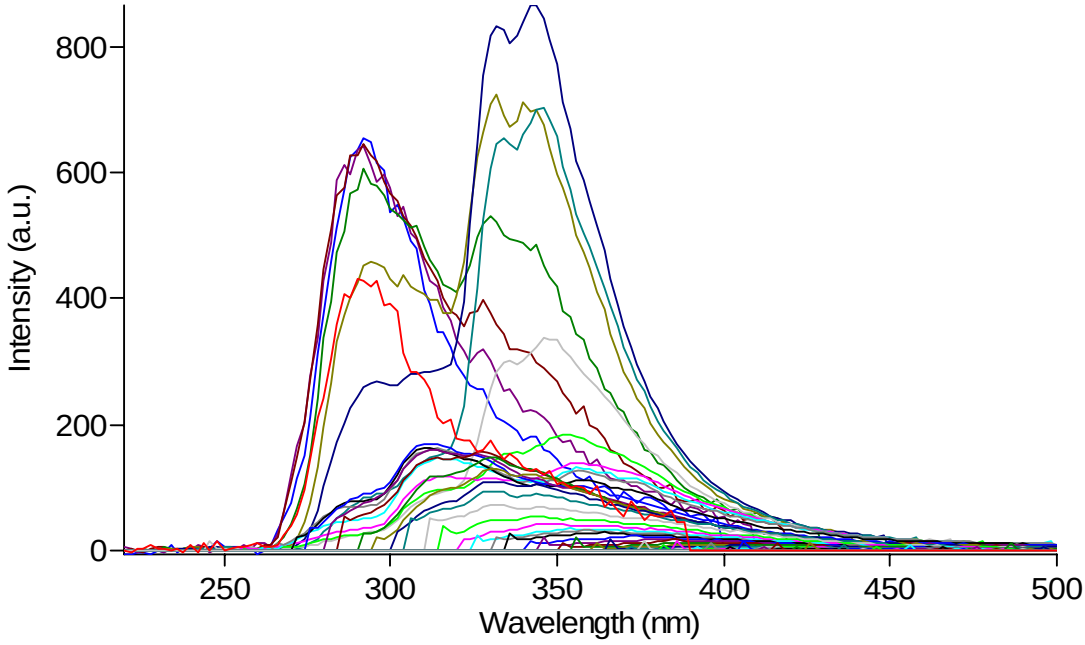
800
600
400
200
0
Intensity (a.u.)
250
300
350
400
450
500
Wavelength (nm)

72AP

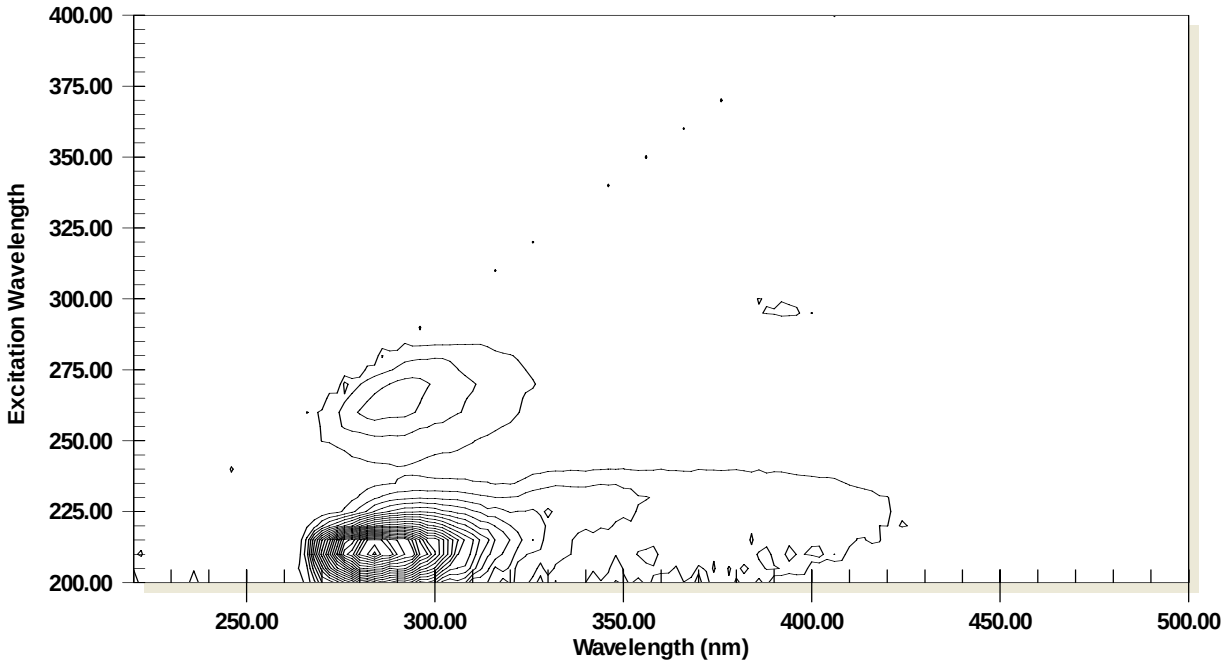
400.00
375.00
350.00
325.00
300.00
275.00
250.00
225.00
200.00
Excitation Wavelength
250.00
300.00
350.00
400.00
450.00
500.00
Wavelength (nm)

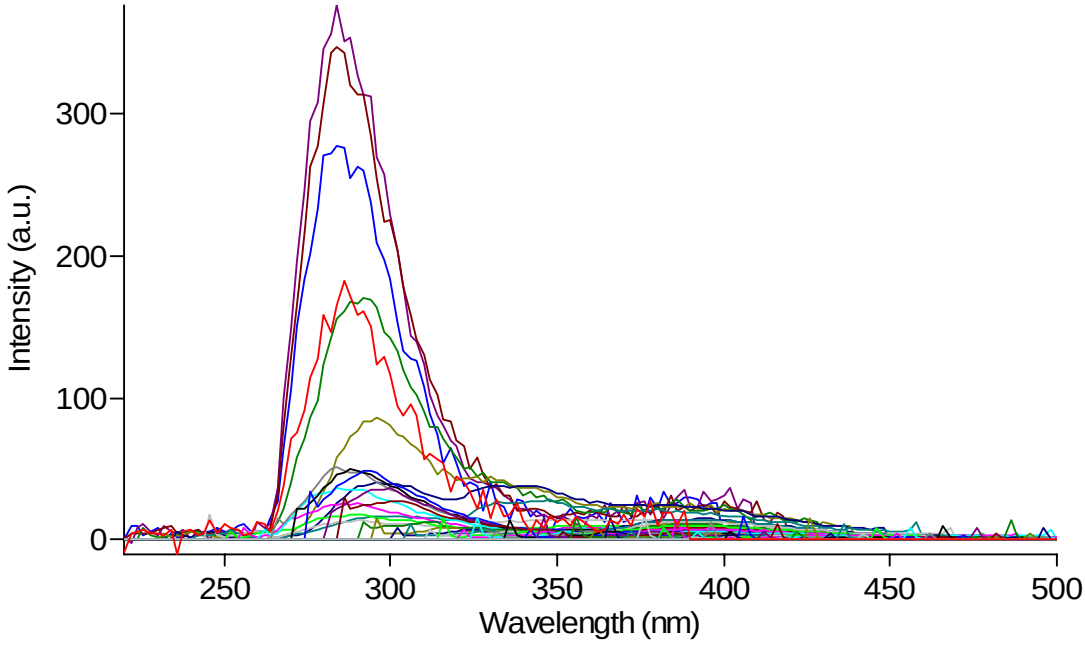
300
200
100
0
Intensity (a.u.)
250
300
350
400
450
500
Wavelength (nm)

73CP

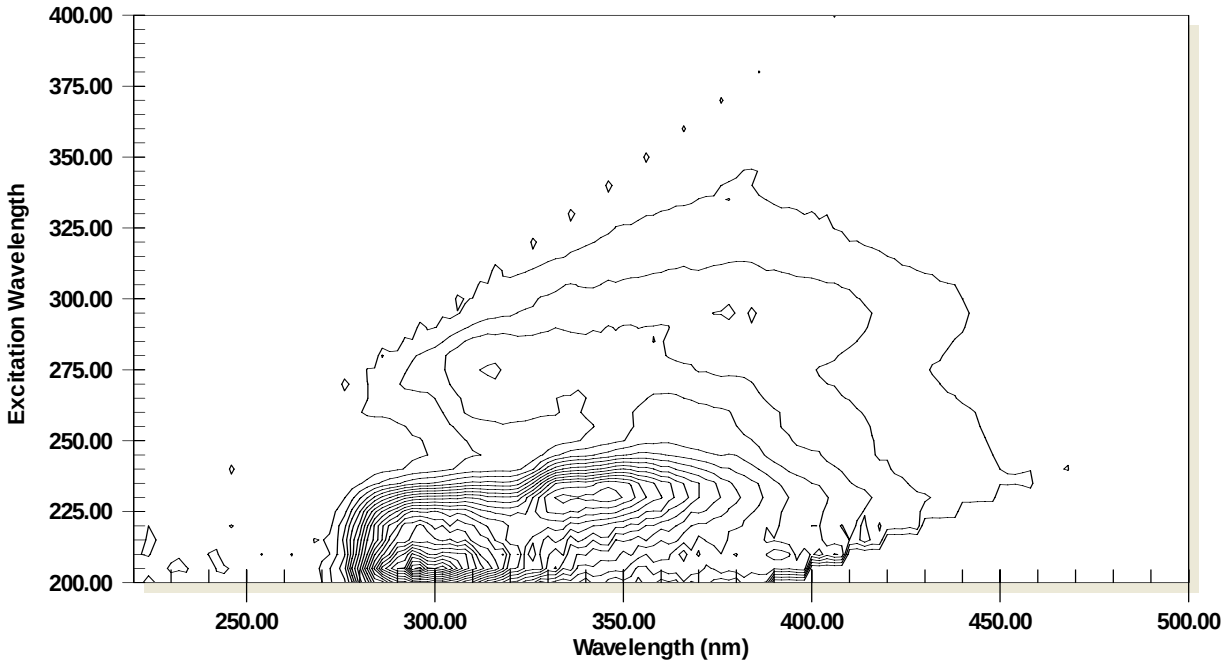
400.00
375.00
350.00
325.00
300.00
275.00
250.00
225.00
200.00
Excitation Wavelength
250.00
300.00
350.00
400.00
450.00
500.00
Wavelength (nm)

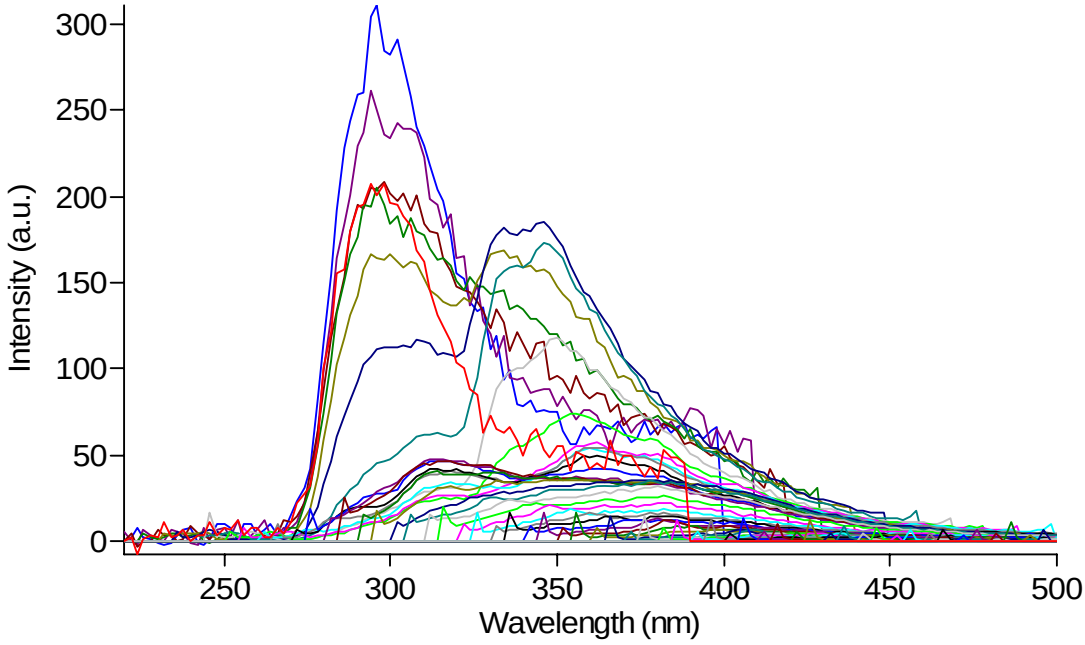
300
250
200
150
100
50
0
Intensity (a.u.)
250
300
350
400
450
500
Wavelength (nm)

74AP

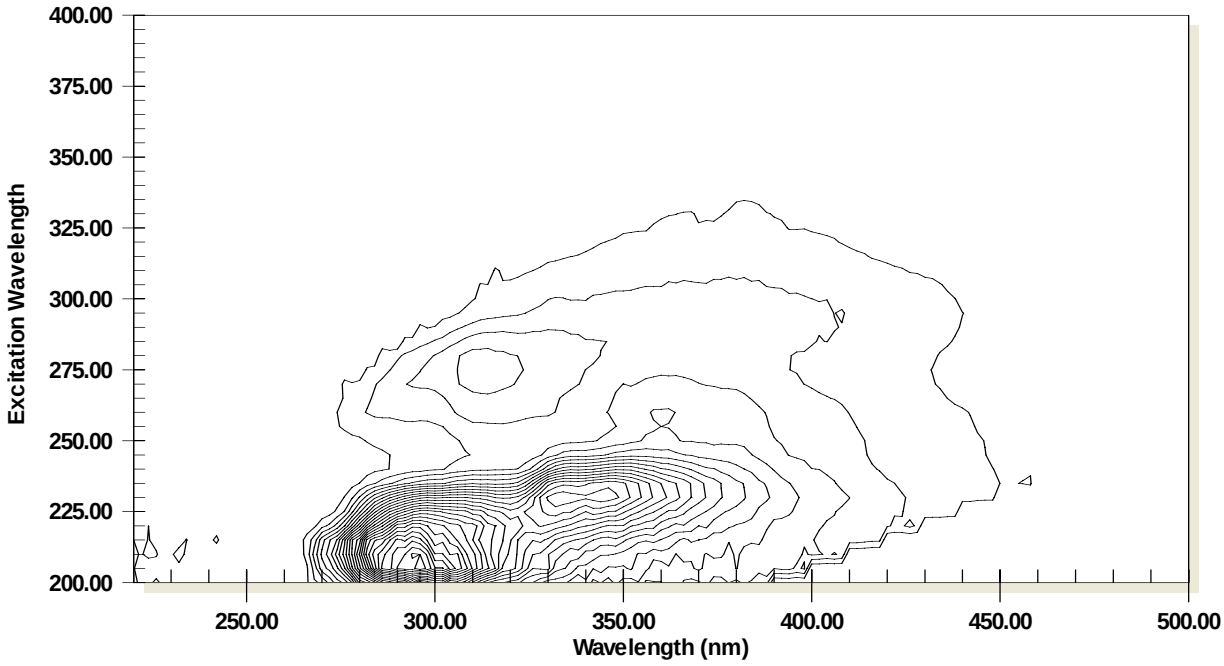
400.00
375.00
350.00
325.00
300.00
275.00
250.00
225.00
200.00
Excitation Wavelength
250.00
300.00
350.00
400.00
450.00
500.00
Wavelength (nm)

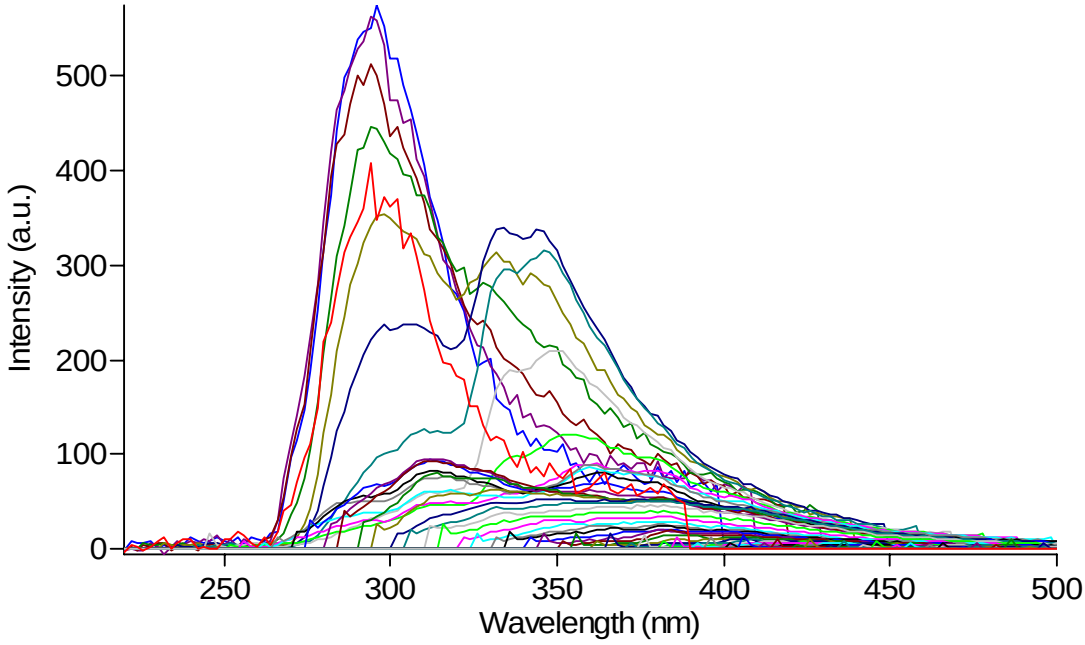
500
400
300
200
100
0
Intensity (a.u.)
250
300
350
400
450
500
Wavelength (nm)

300

75AP

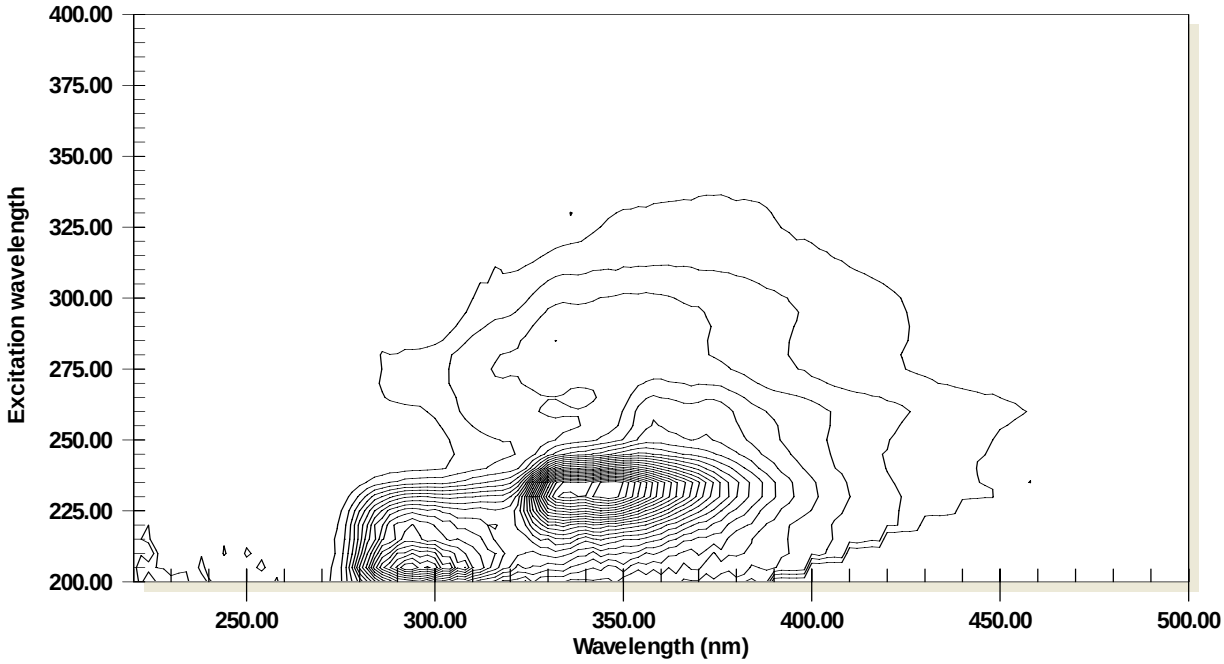
Excitation wavelength
400.00
375.00
350.00
325.00
300.00
275.00
250.00
225.00
200.00
250.00
300.00
350.00
400.00
450.00
500.00
Wavelength (nm)

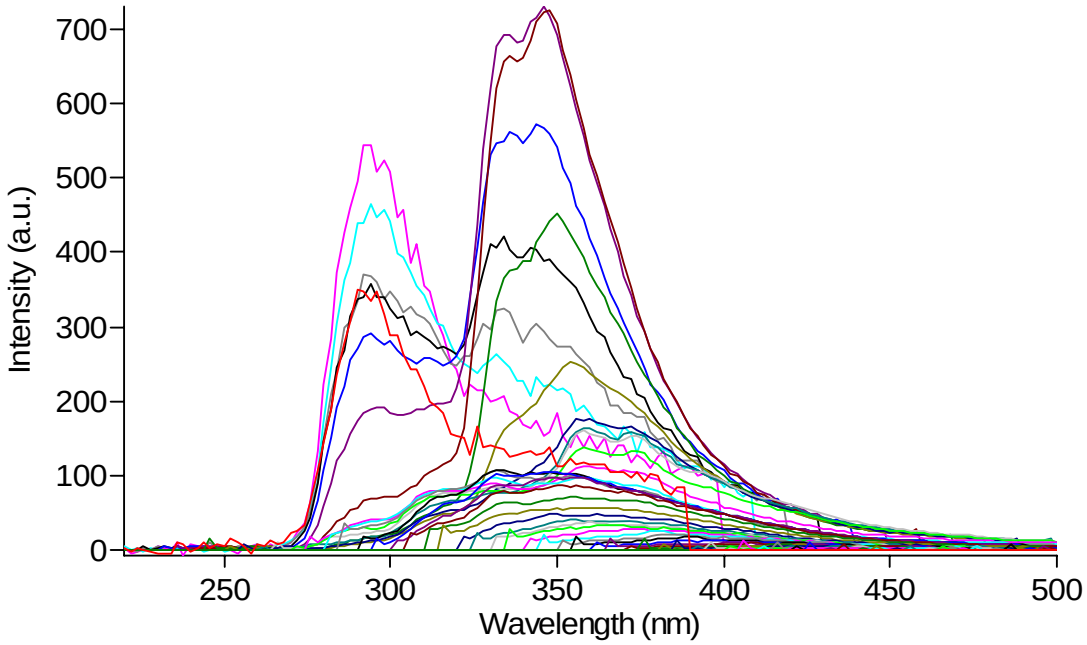
Intensity (a.u.)
700
600
500
400
300
200
100
0
250
300
350
400
450
500
Wavelength (nm)

81AP

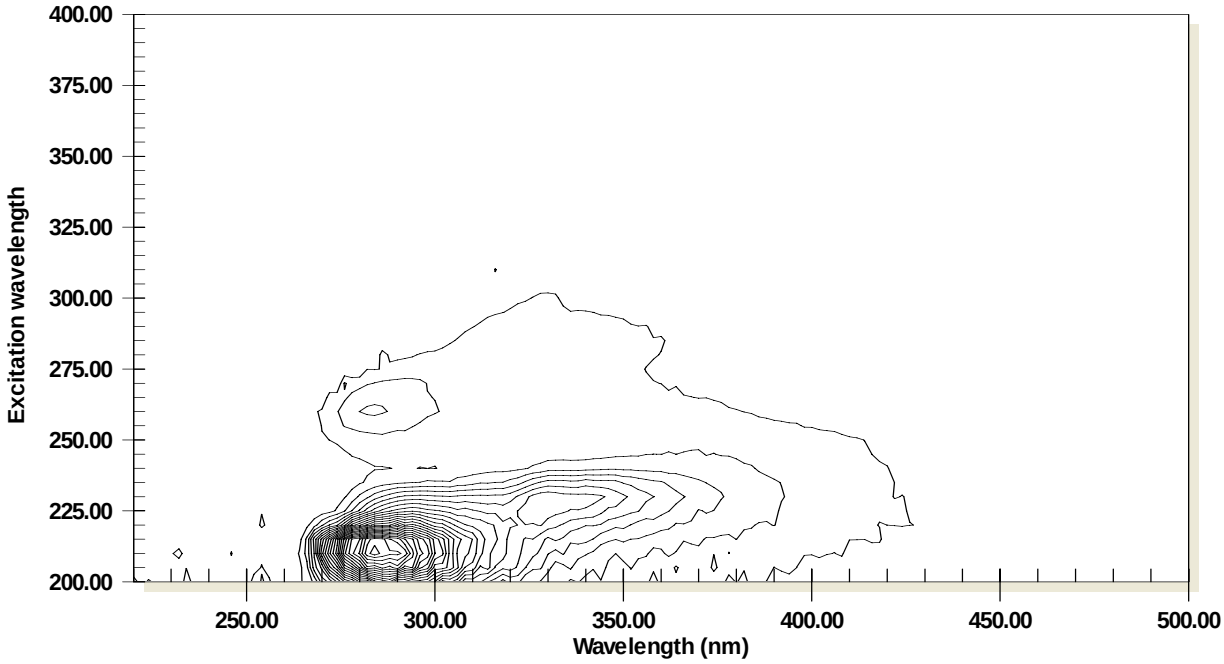
Excitation wavelength
400.00
375.00
350.00
325.00
300.00
275.00
250.00
225.00
200.00
250.00
300.00
350.00
400.00
450.00
500.00
Wavelength (nm)

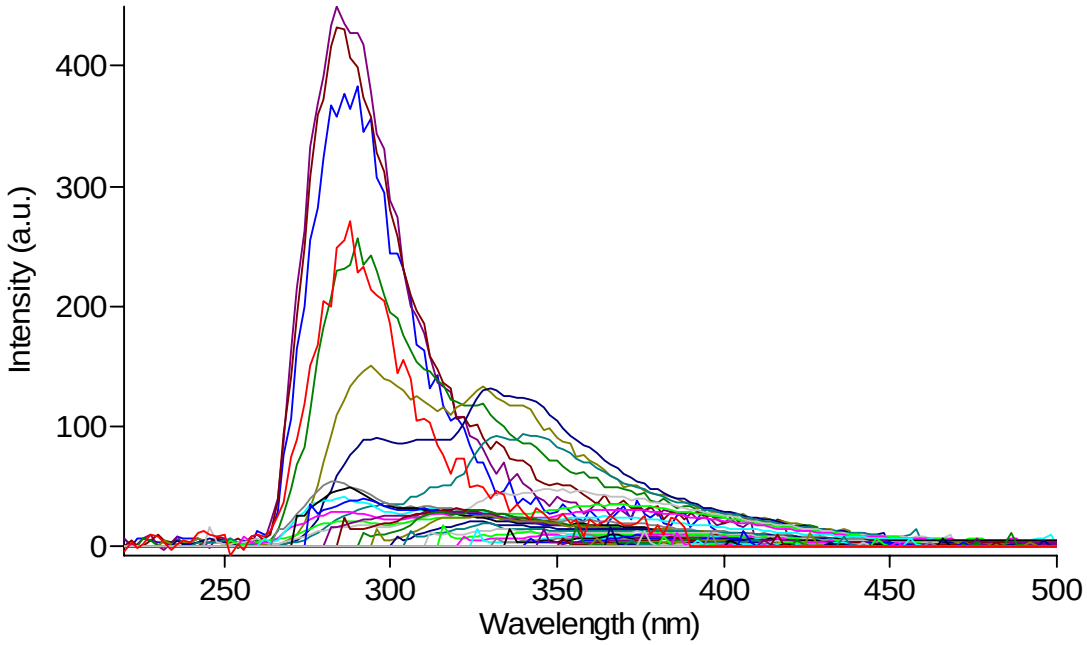
Intensity (a.u.)
400
300
200
100
0
250
300
350
400
450
500
Wavelength (nm)

82BP

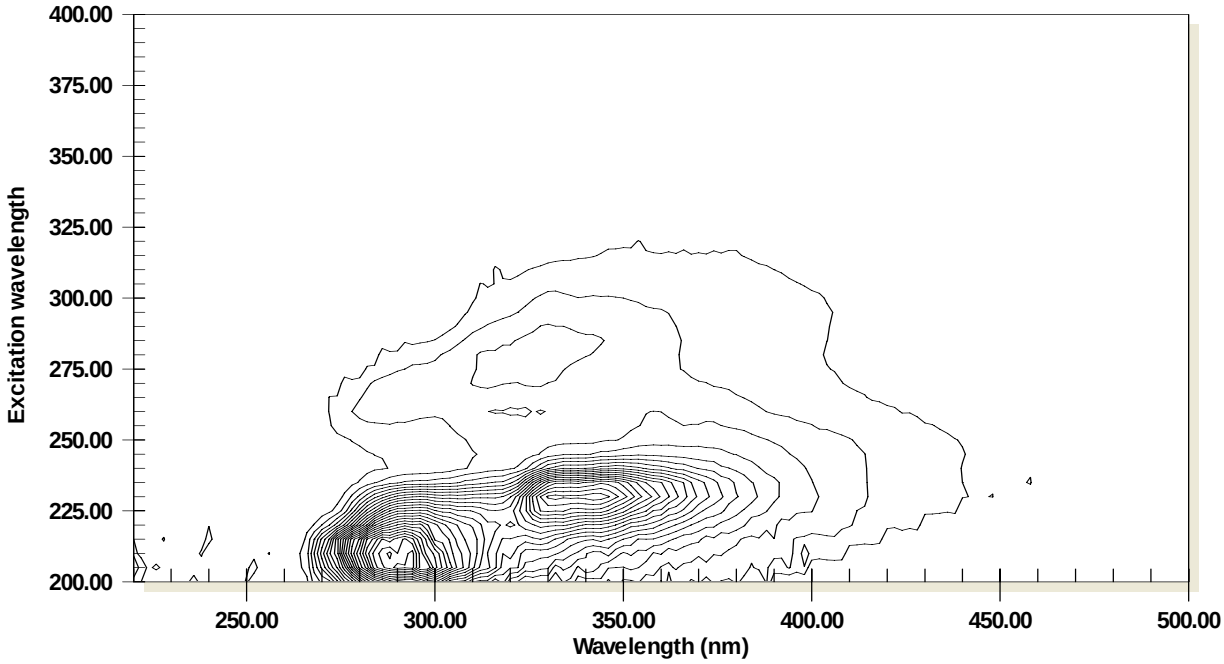
400.00
375.00
350.00
325.00
300.00
275.00
250.00
225.00
200.00
Excitation wavelength
250.00
300.00
350.00
400.00
450.00
500.00
Wavelength (nm)

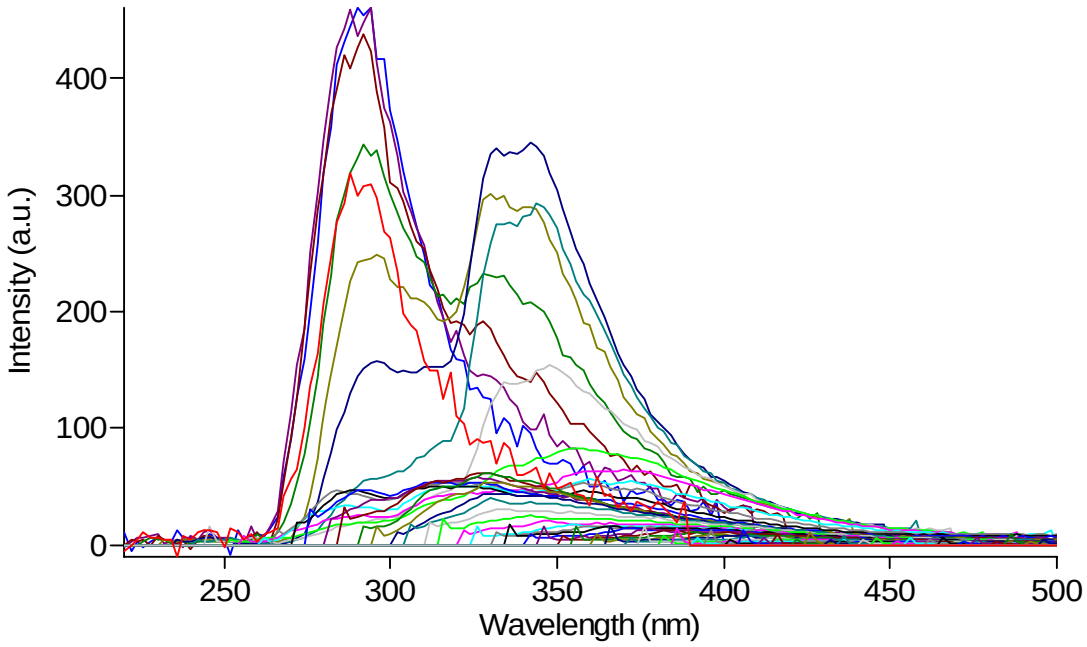
400
300
200
100
0
Intensity (a.u.)
250
300
350
400
450
500
Wavelength (nm)

83BP

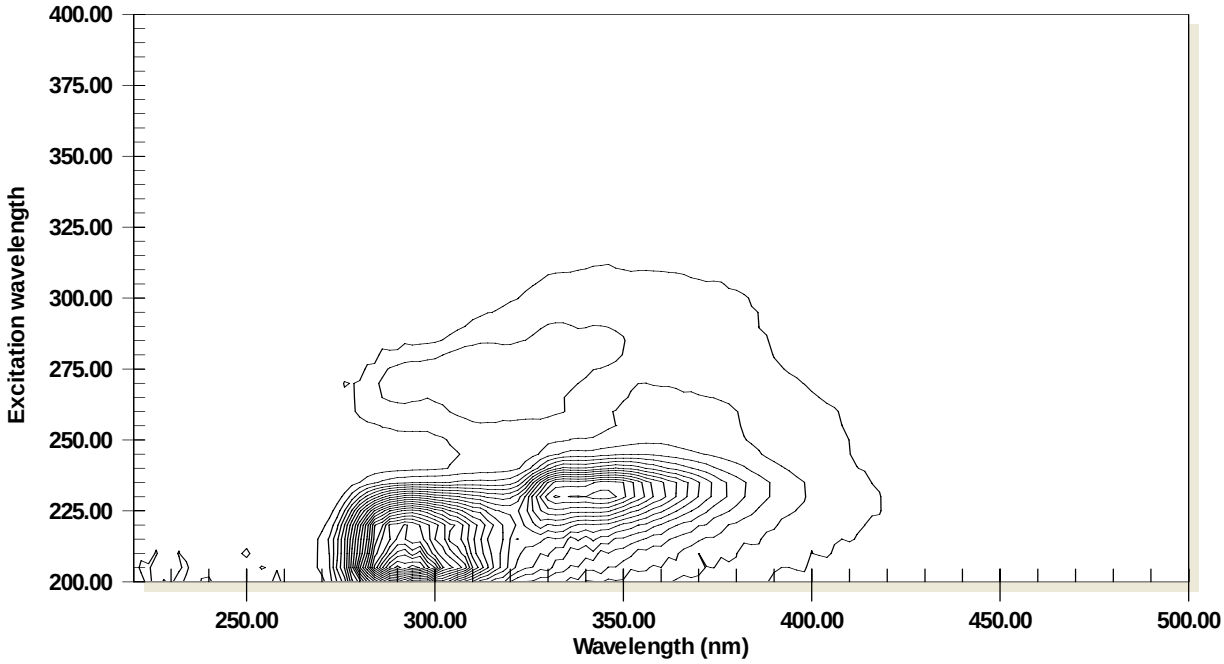
400.00
375.00
350.00
325.00
300.00
275.00
250.00
225.00
200.00
Excitation wavelength
250.00
300.00
350.00
400.00
450.00
500.00
Wavelength (nm)

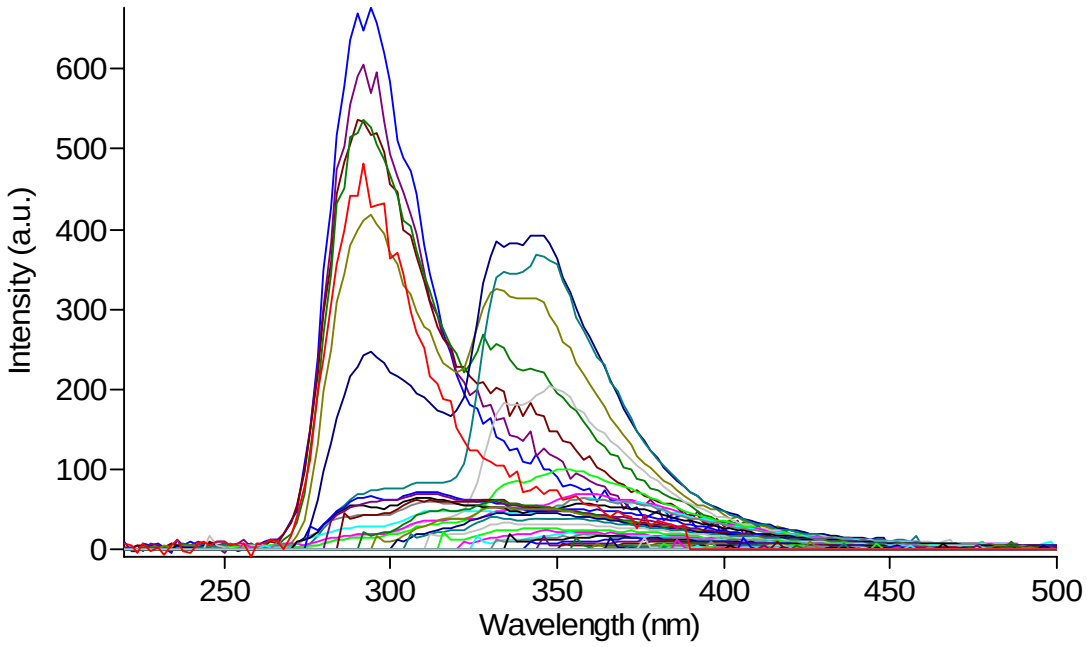
600
500
400
300
200
100
0
Intensity (a.u.)
250
300
350
400
450
500
Wavelength (nm)

84BP

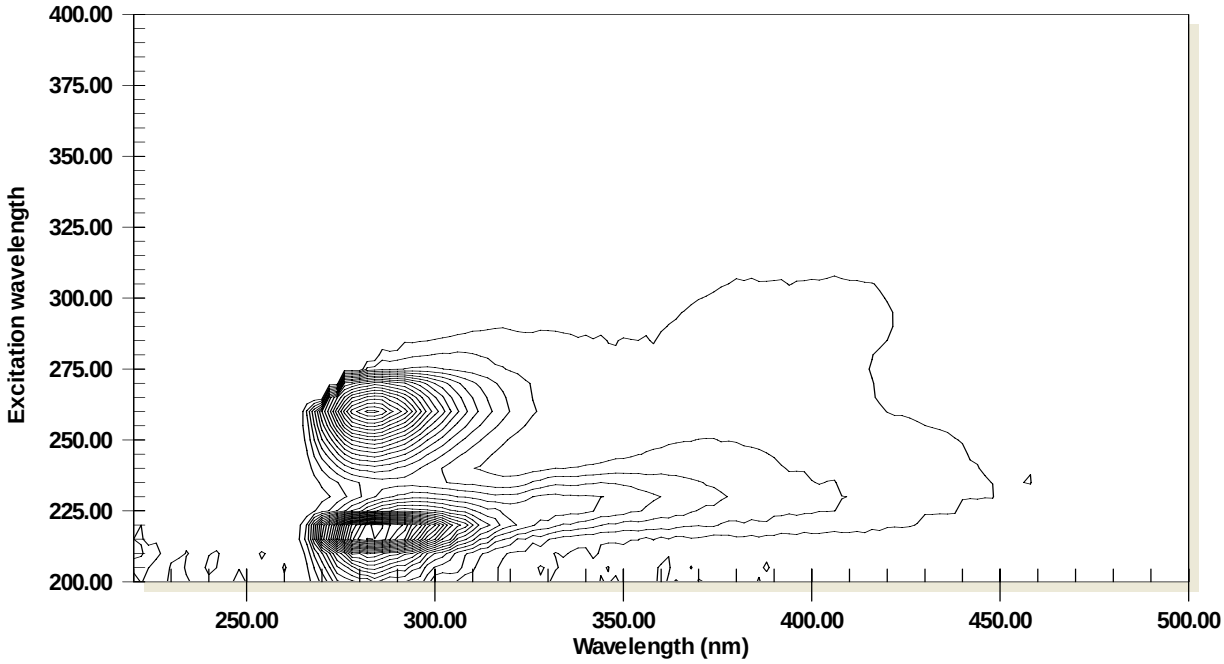
400.00
375.00
350.00
325.00
300.00
275.00
250.00
225.00
200.00
Excitation wavelength
250.00
300.00
350.00
400.00
450.00
500.00
Wavelength (nm)

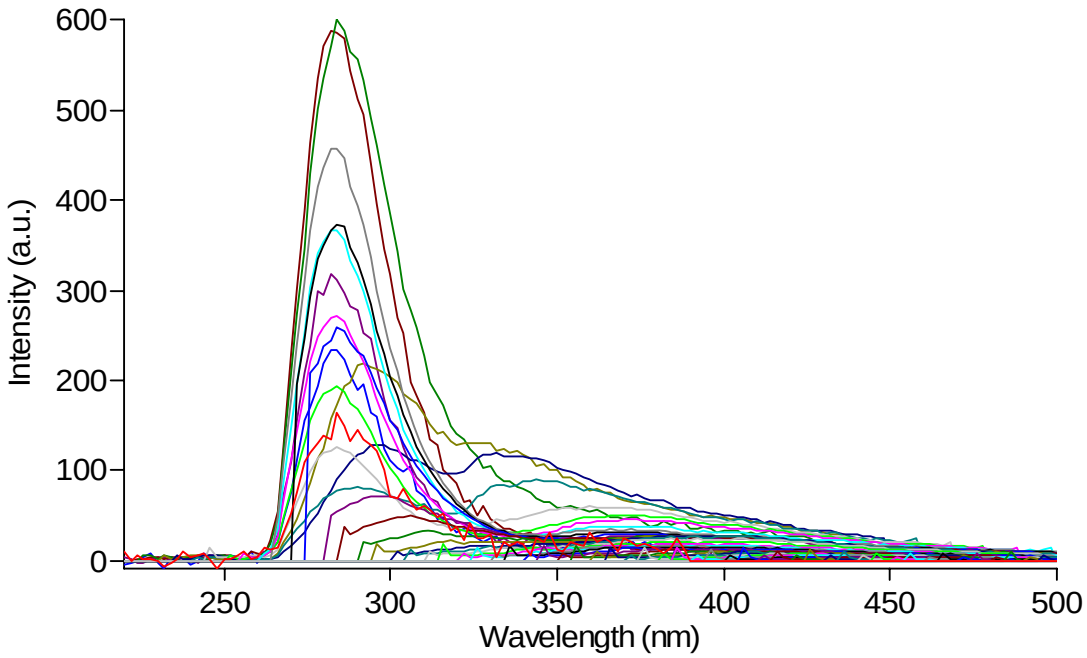
600
500
400
300
200
100
0
Intensity (a.u.)
250
300
350
400
450
500
Wavelength (nm)

85AP

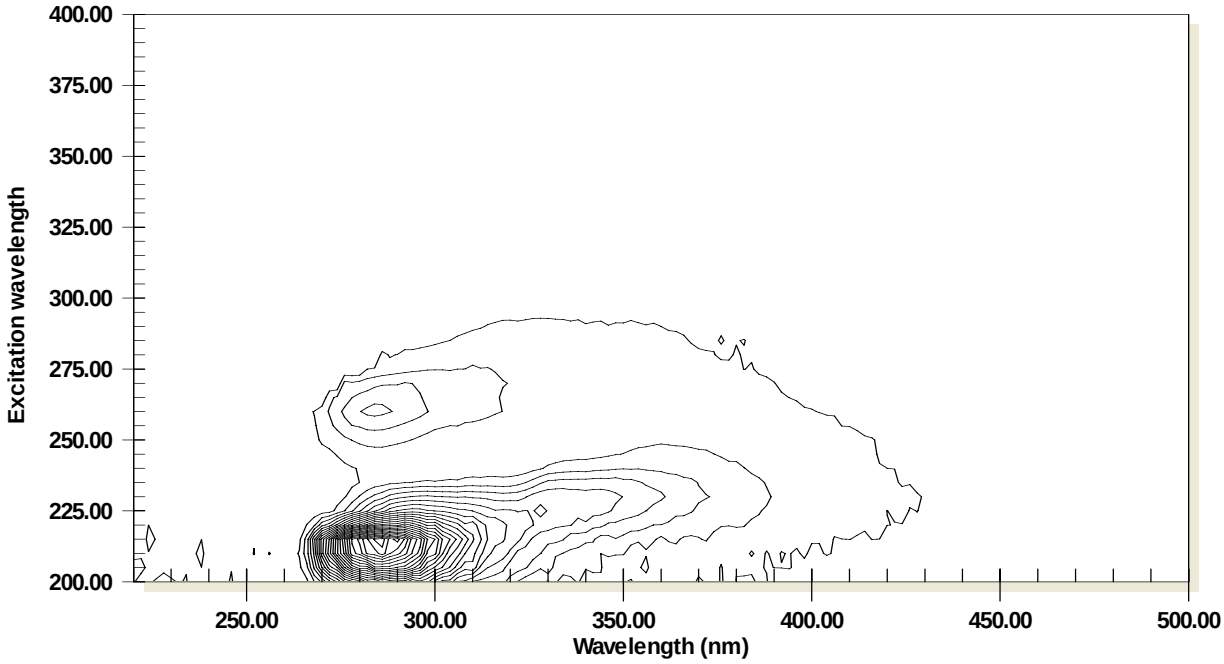
400.00
375.00
350.00
325.00
300.00
275.00
250.00
225.00
200.00
Excitation wavelength
250.00
300.00
350.00
400.00
450.00
500.00
Wavelength (nm)

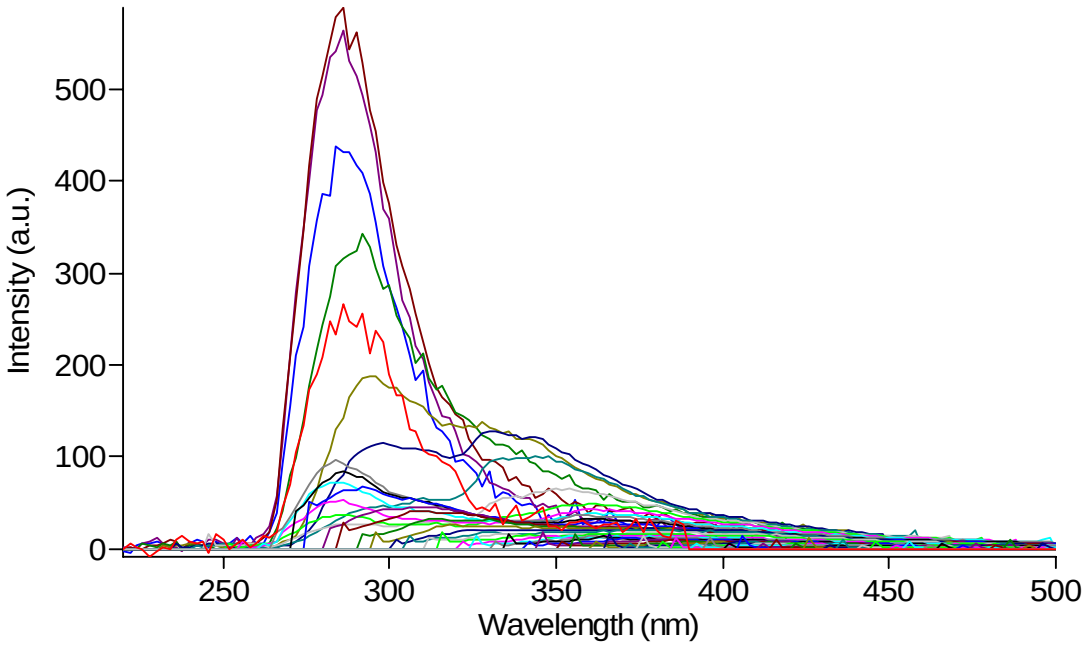
500
400
300
200
100
0
Intensity (a.u.)
250
300
350
400
450
500
Wavelength (nm)

91AP

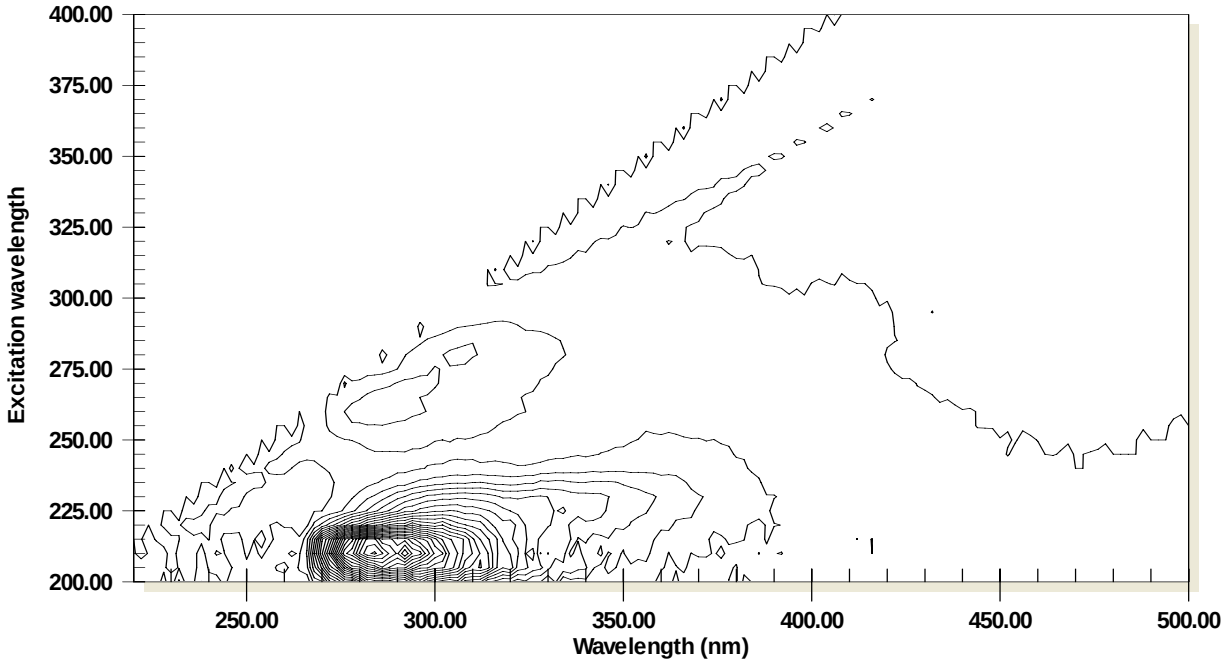
Excitation wavelength
400.00
375.00
350.00
325.00
300.00
275.00
250.00
225.00
200.00
250.00
300.00
350.00
400.00
450.00
500.00
Wavelength (nm)

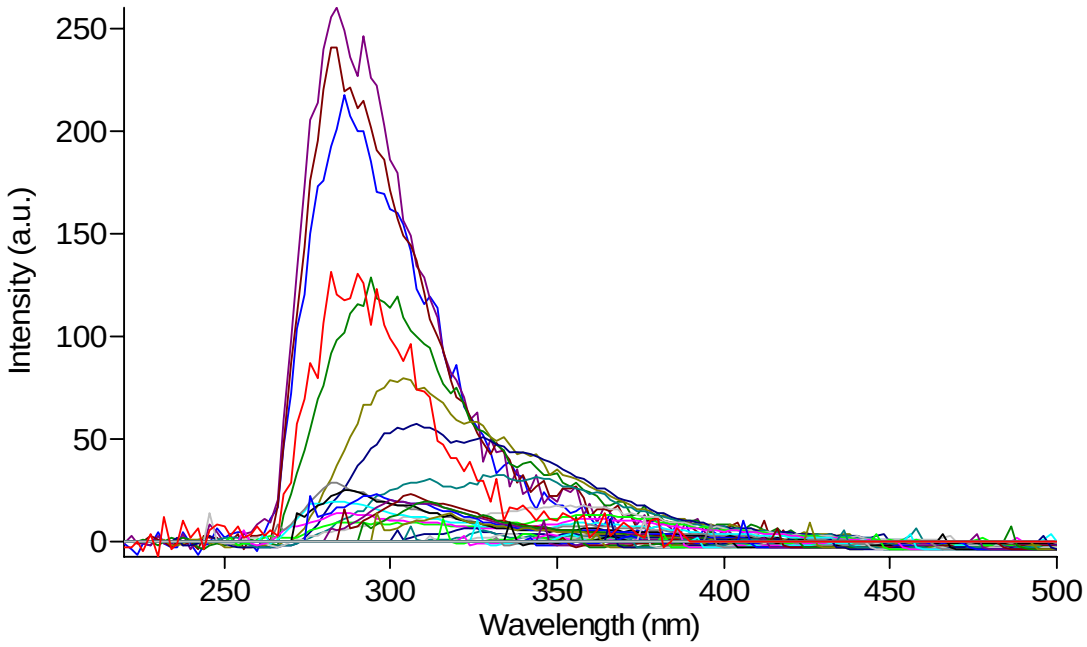
Intensity (a.u.)
250
200
150
100
50
0
250
300
350
400
450
500
Wavelength (nm)

92AP

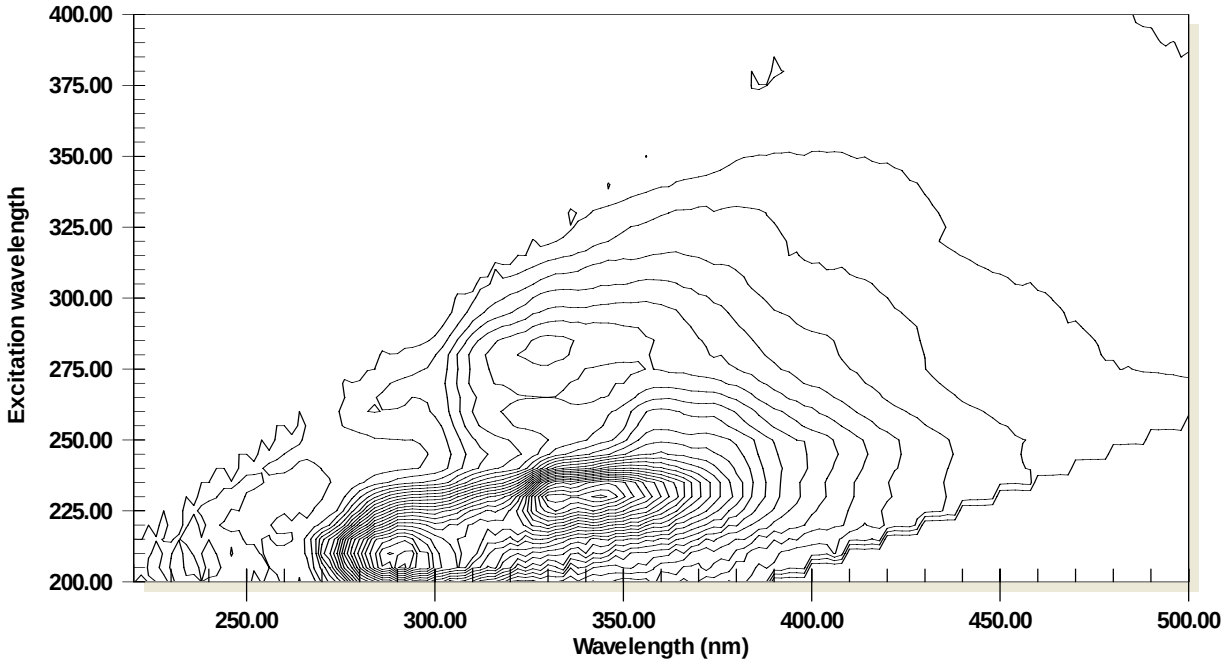
400.00
375.00
350.00
325.00
300.00
275.00
250.00
225.00
200.00
Excitation wavelength
250.00
300.00
350.00
400.00
450.00
500.00
Wavelength (nm)

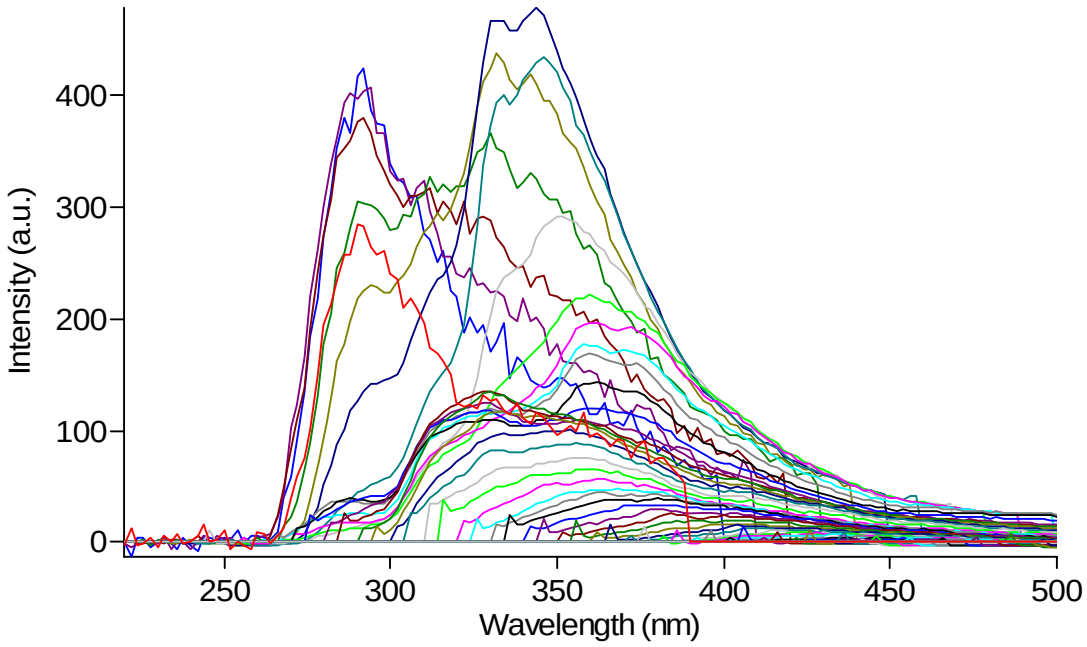
400
300
200
100
0
Intensity (a.u.)
250
300
350
400
450
500
Wavelength (nm)

93AP

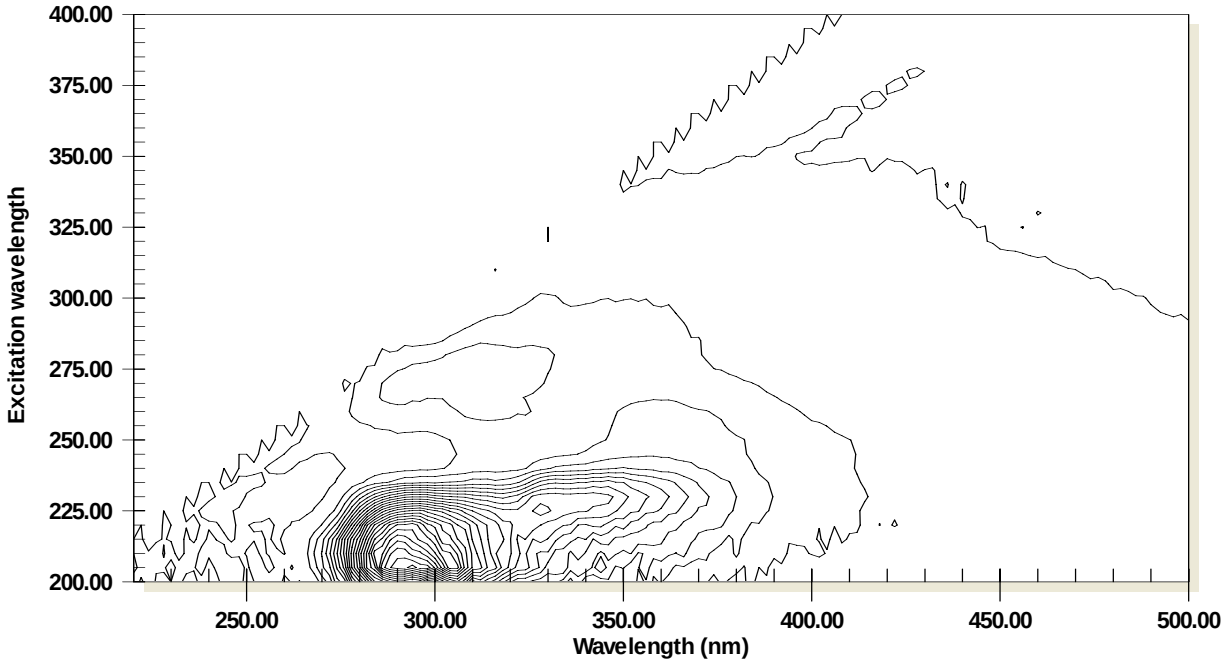
Excitation wavelength
400.00
375.00
350.00
325.00
300.00
275.00
250.00
225.00
200.00
250.00
300.00
350.00
400.00
450.00
500.00
Wavelength (nm)

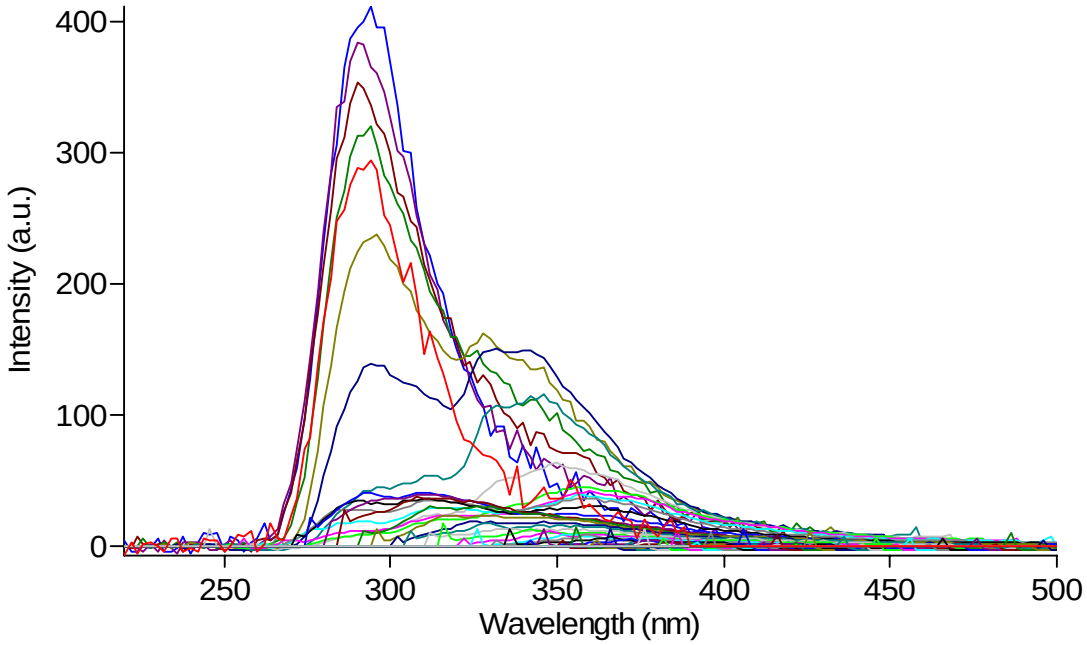
Intensity (a.u.)
400
300
200
100
0
250
300
350
400
450
500
Wavelength (nm)

94BP

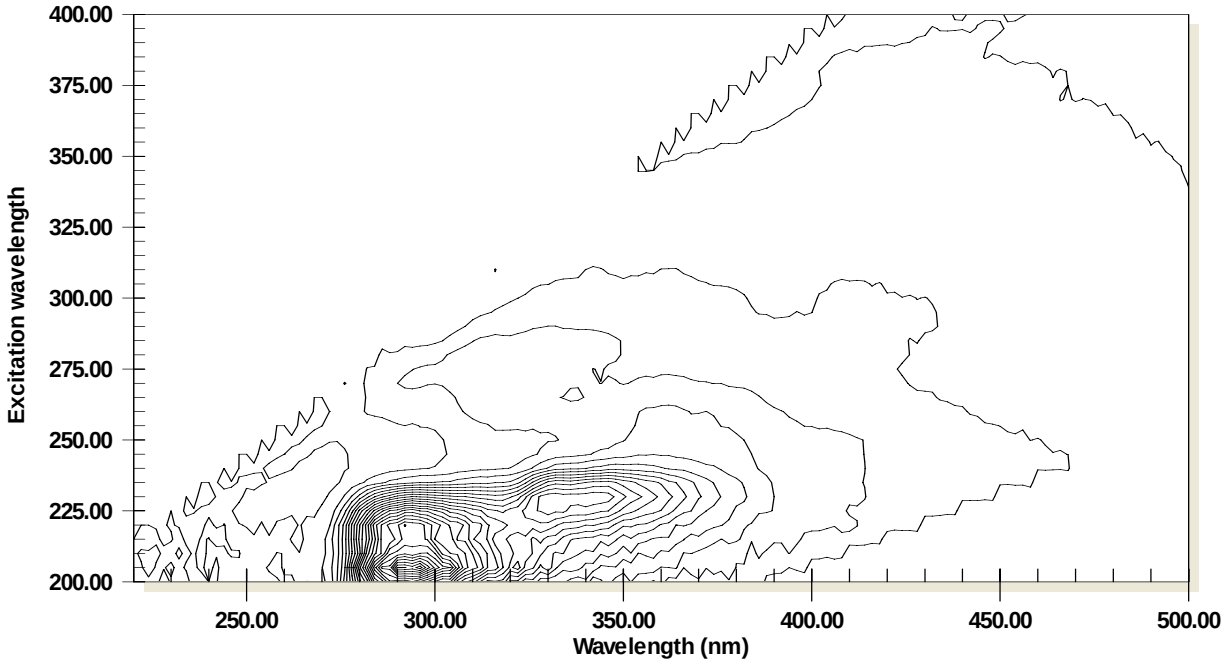
400.00
375.00
350.00
325.00
300.00
275.00
250.00
225.00
200.00
Excitation wavelength
250.00
300.00
350.00
400.00
450.00
500.00
Wavelength (nm)

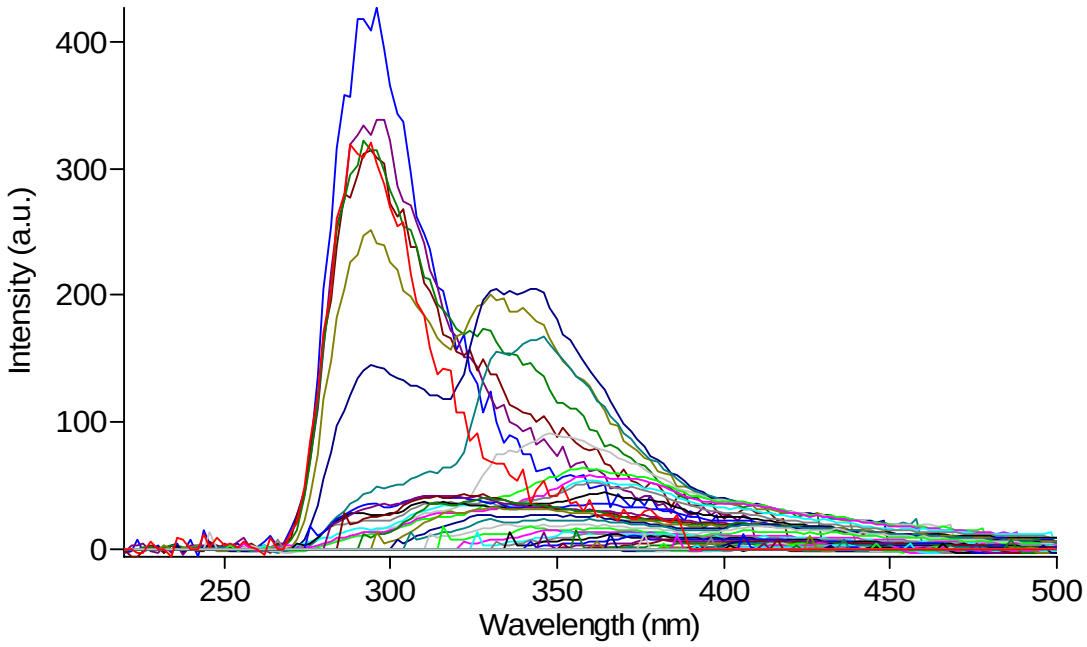
400
300
200
100
0
Intensity (a.u.)
250
300
350
400
450
500
Wavelength (nm)

95BP

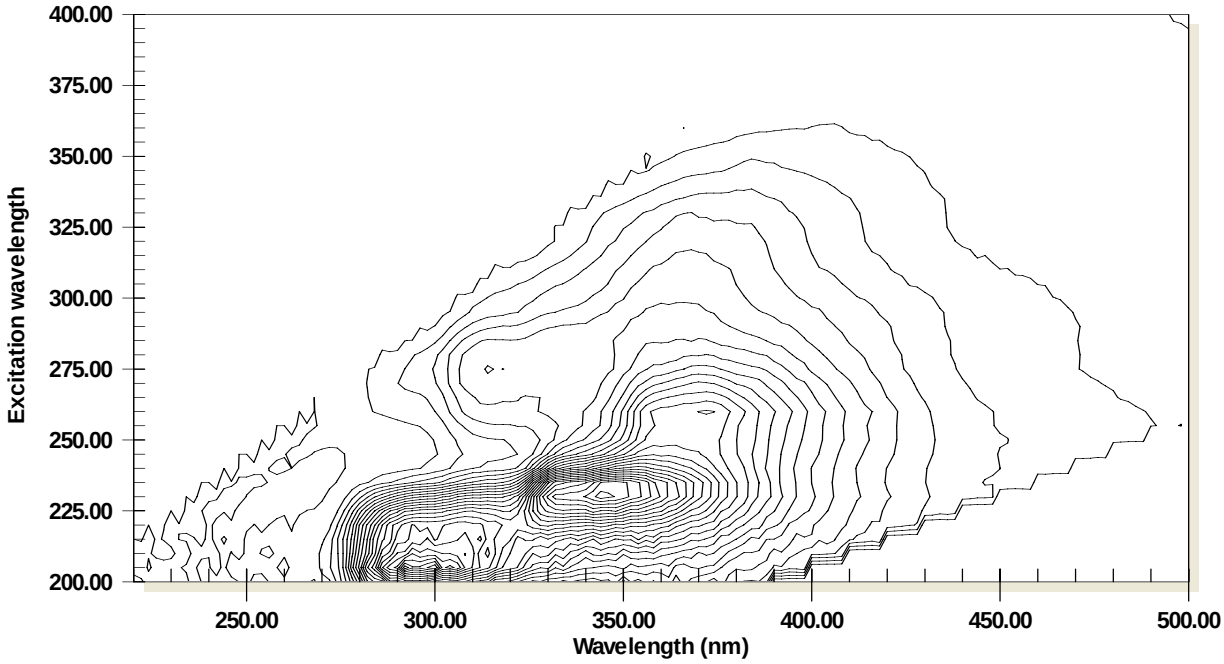
400.00
375.00
350.00
325.00
300.00
275.00
250.00
225.00
200.00
Excitation wavelength
250.00
300.00
350.00
400.00
450.00
500.00
Wavelength (nm)

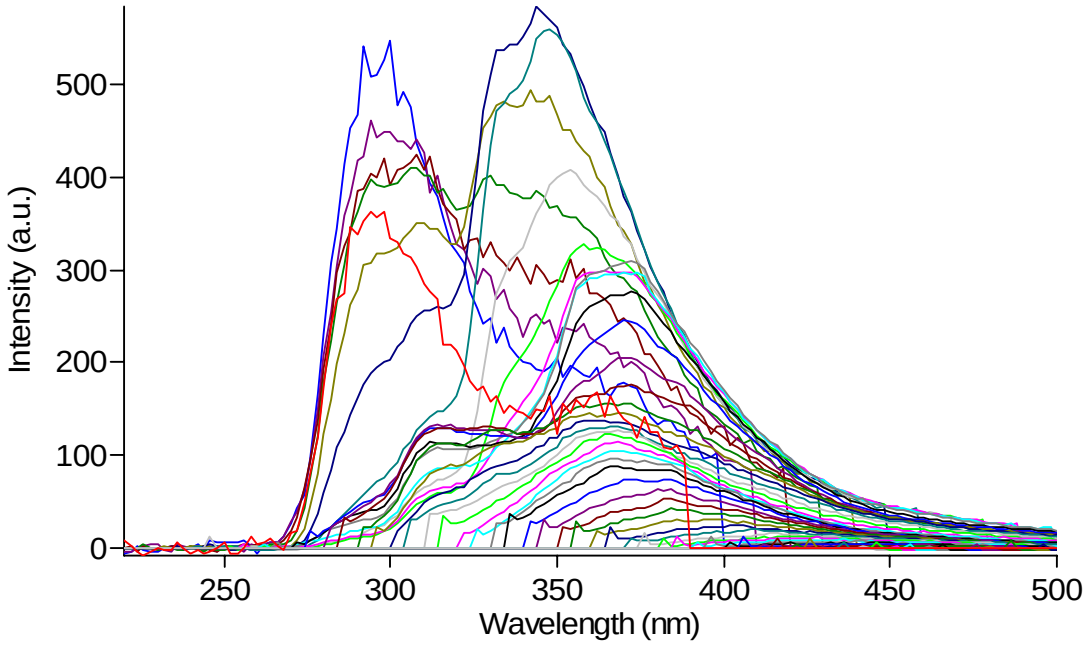
500
400
300
200
100
0
Intensity (a.u.)
250
300
350
400
450
500
Wavelength (nm)

101AP

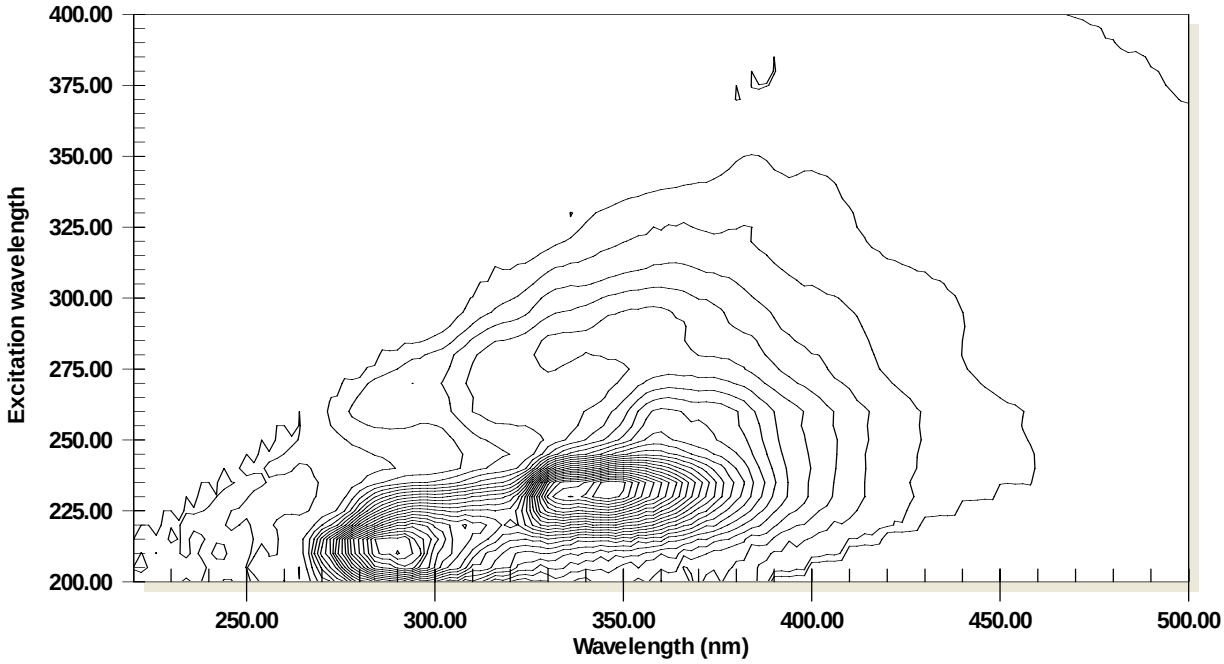
400.00
375.00
350.00
325.00
300.00
275.00
250.00
225.00
200.00
Excitation wavelength
250.00
300.00
350.00
400.00
450.00
500.00
Wavelength (nm)

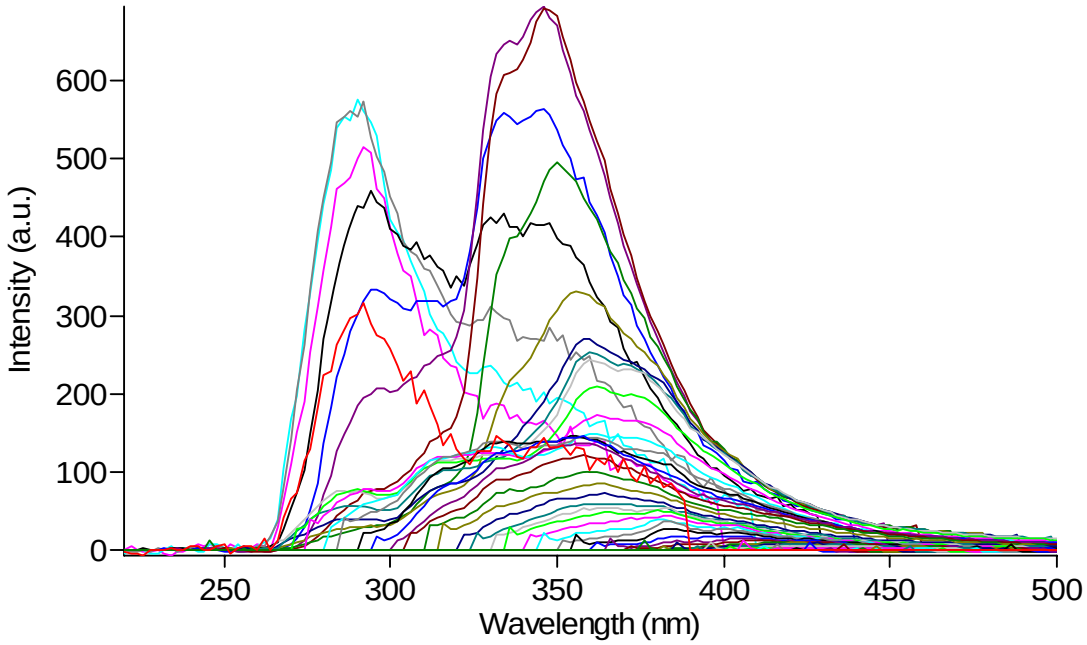
600
500
400
300
200
100
0
Intensity (a.u.)
250
300
350
400
450
500
Wavelength (nm)

102AP

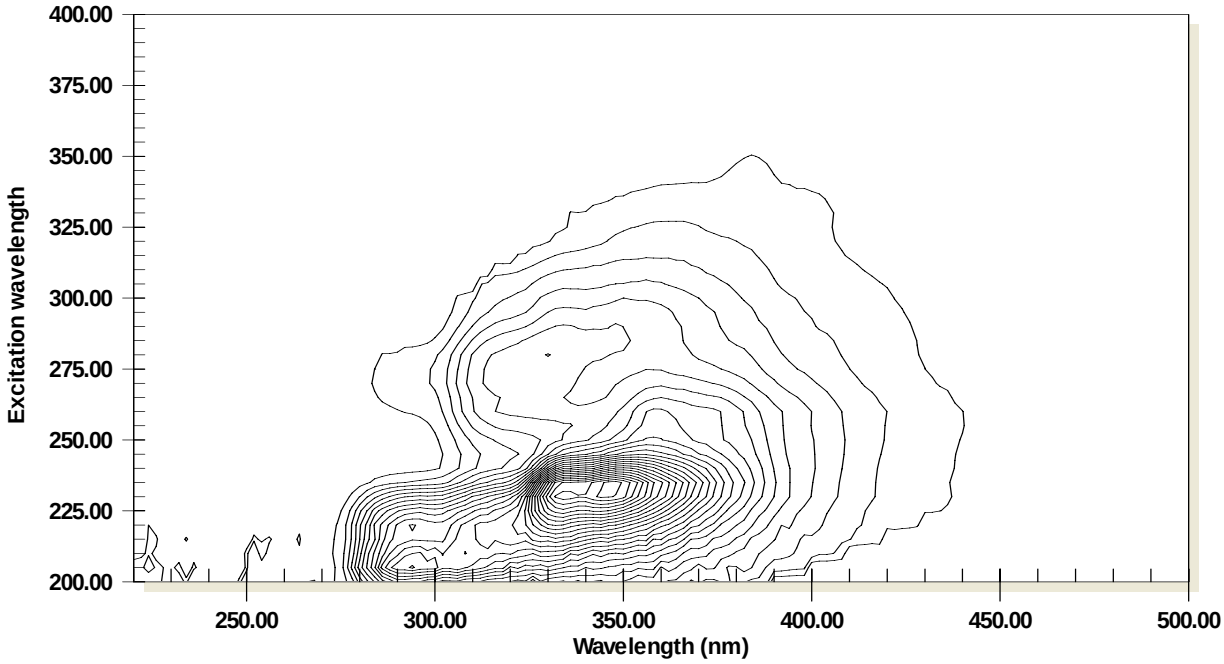
400.00
375.00
350.00
325.00
300.00
275.00
250.00
225.00
200.00
Excitation wavelength
250.00
300.00
350.00
400.00
450.00
500.00
Wavelength (nm)

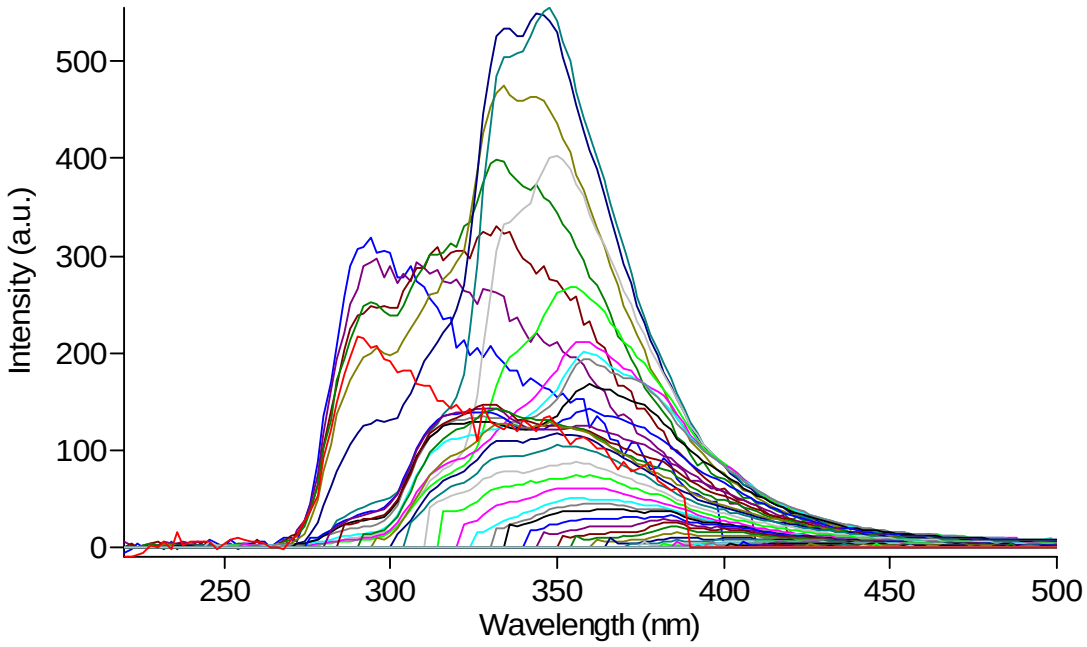
500
400
300
200
100
0
Intensity (a.u.)
250
300
350
400
450
500
Wavelength (nm)

103BP

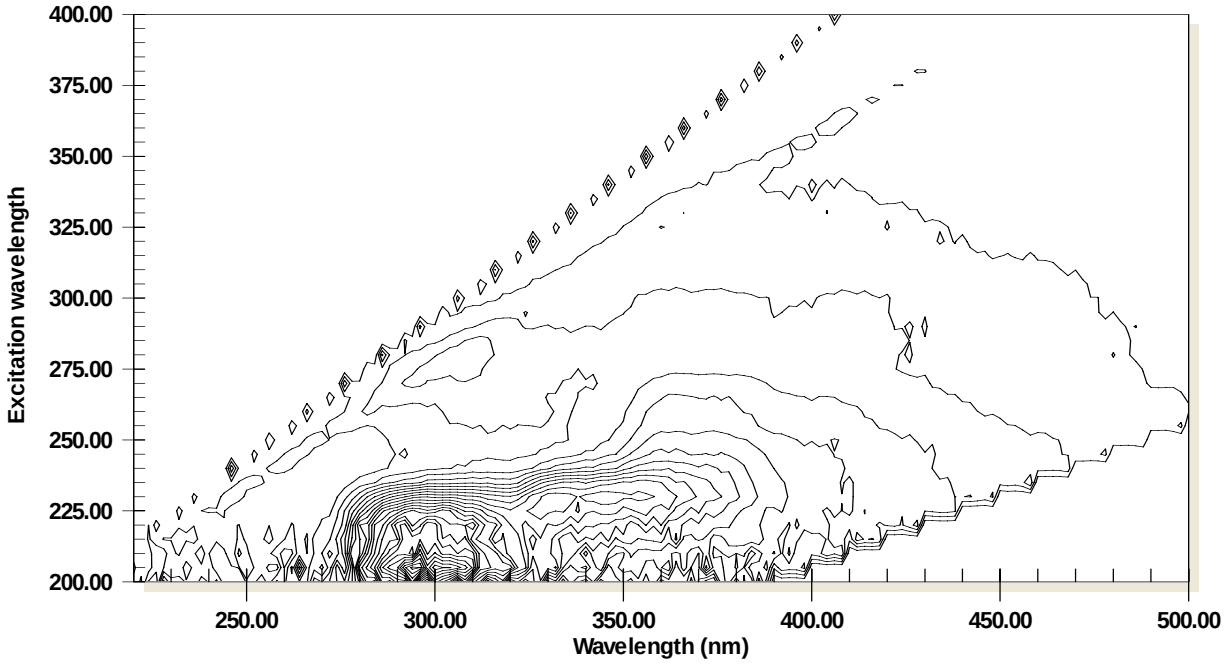
400.00
375.00
350.00
325.00
300.00
275.00
250.00
225.00
200.00
Excitation wavelength
250.00
300.00
350.00
400.00
450.00
500.00
Wavelength (nm)

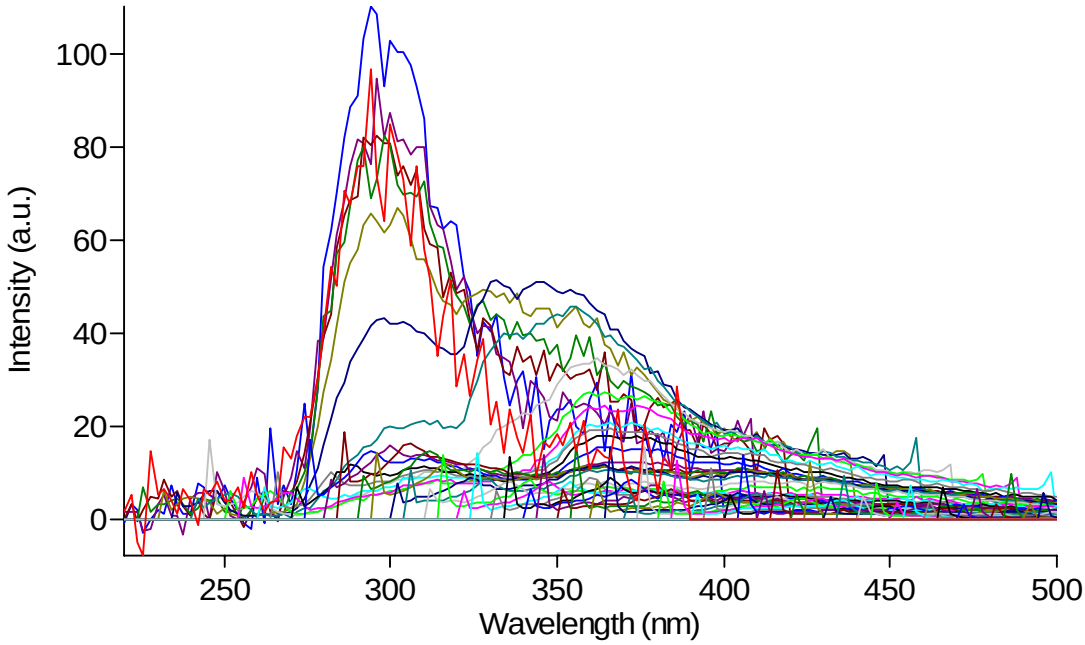
100
80
60
40
20
0
Intensity (a.u.)
250
300
350
400
450
500
Wavelength (nm)

104CP

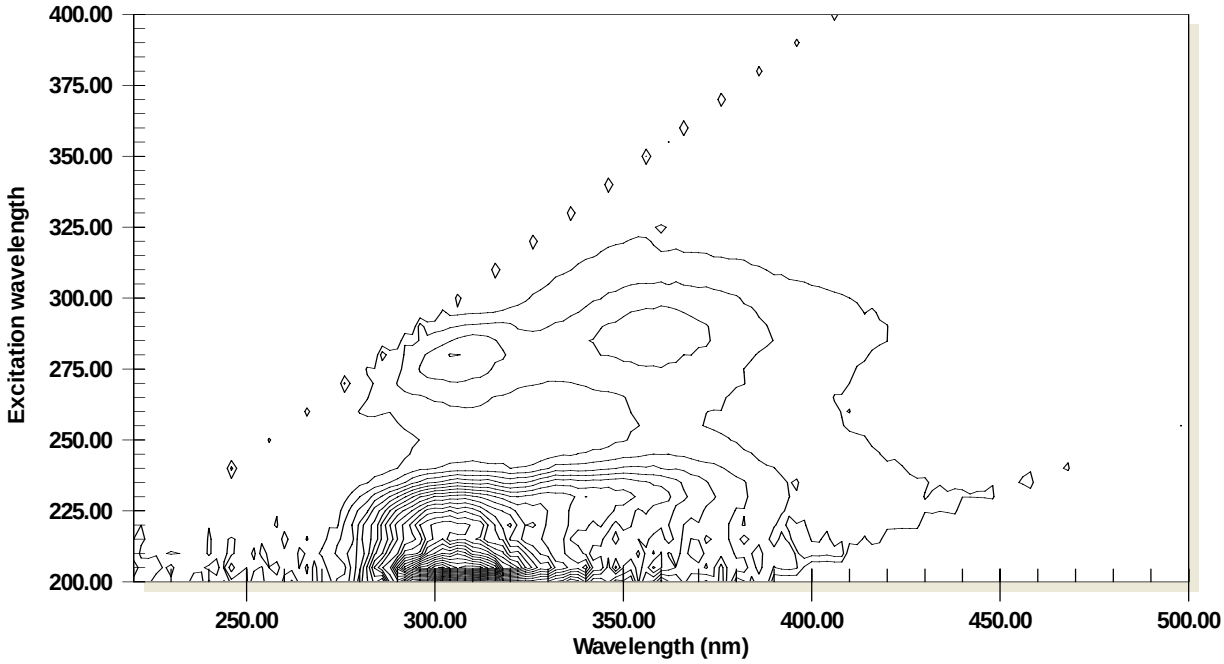
400.00
375.00
350.00
325.00
300.00
275.00
250.00
225.00
200.00
Excitation wavelength
250.00
300.00
350.00
400.00
450.00
500.00
Wavelength (nm)

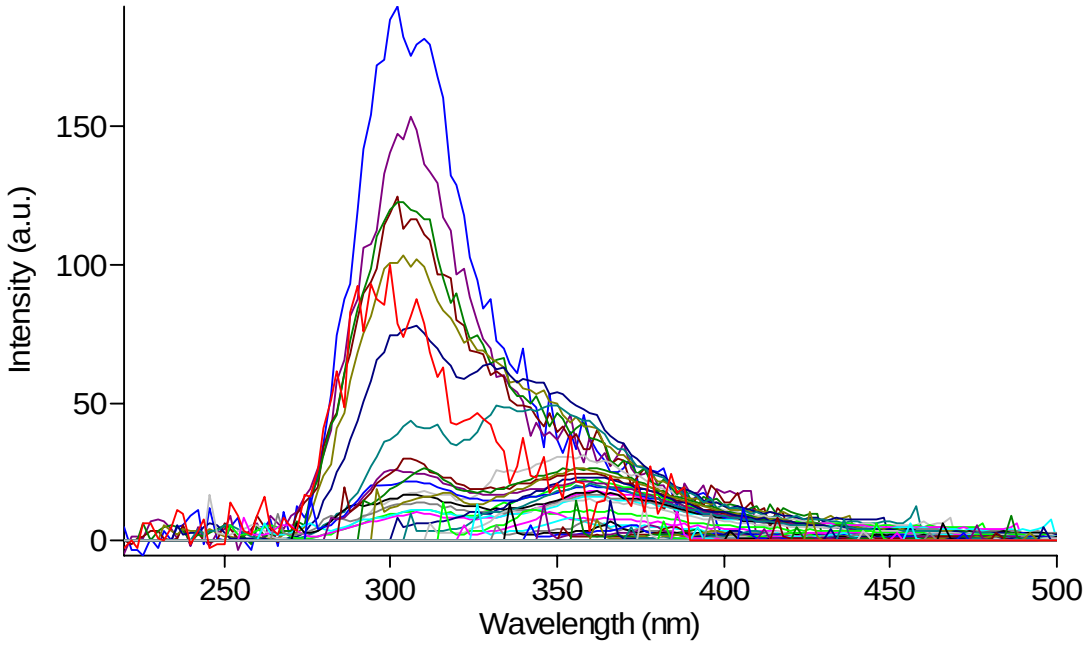
150
100
50
0
Intensity (a.u.)
250
300
350
400
450
500
Wavelength (nm)

105CP

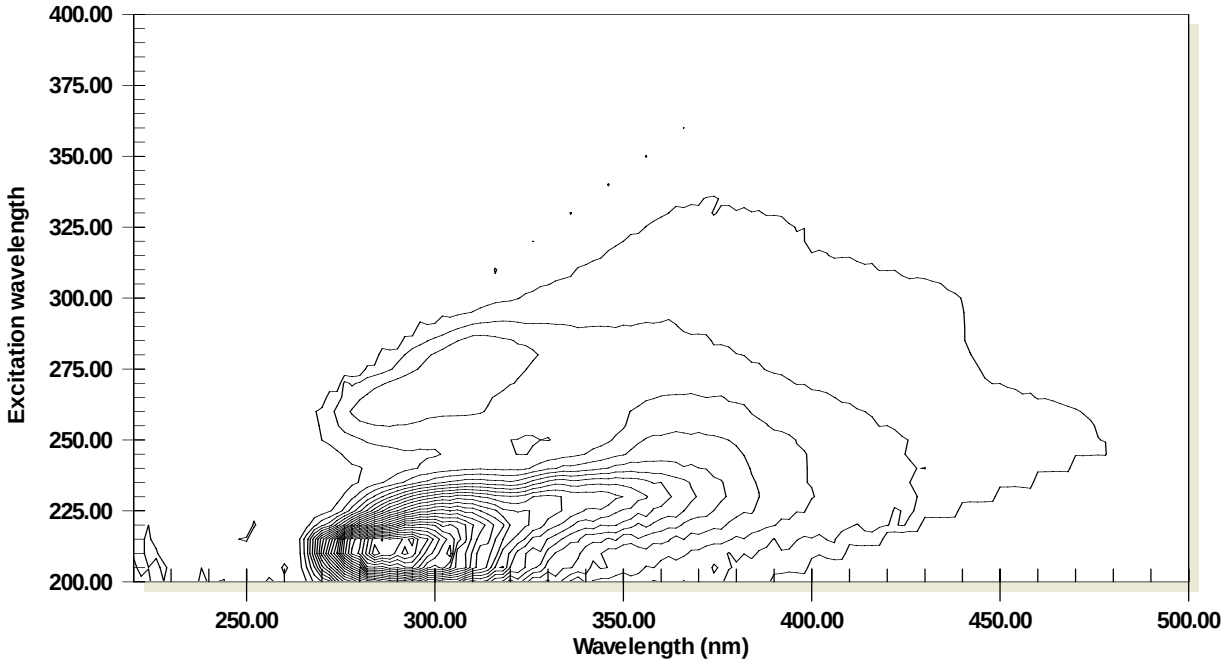
400.00
375.00
350.00
325.00
300.00
275.00
250.00
225.00
200.00
Excitation wavelength
250.00
300.00
350.00
400.00
450.00
500.00
Wavelength (nm)

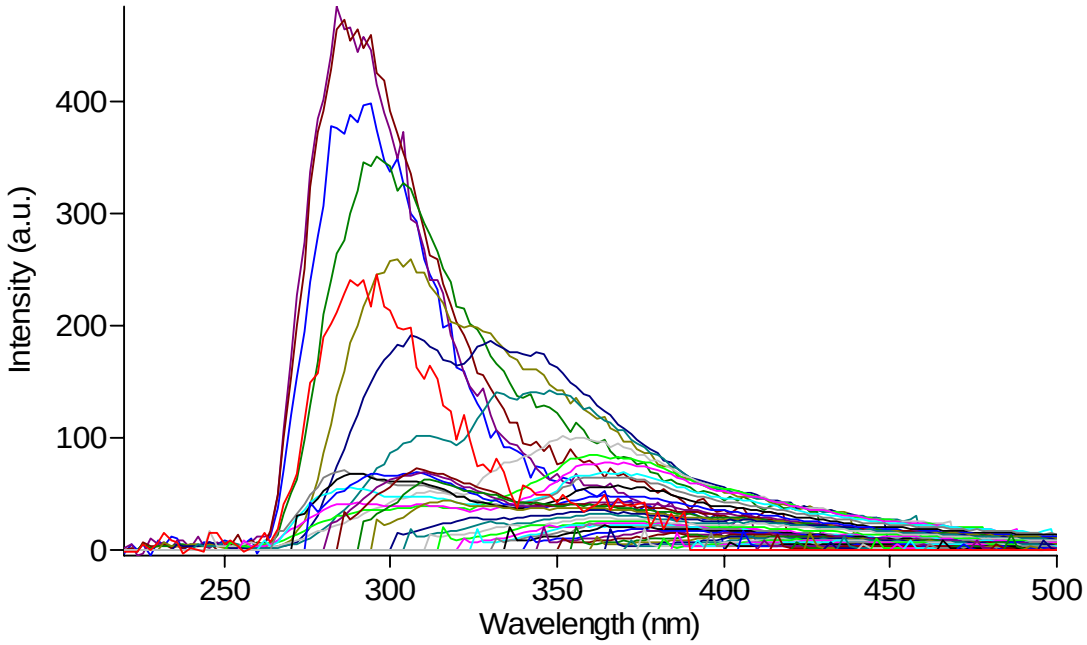
400
300
200
100
0
Intensity (a.u.)
250
300
350
400
450
500
Wavelength (nm)

M06

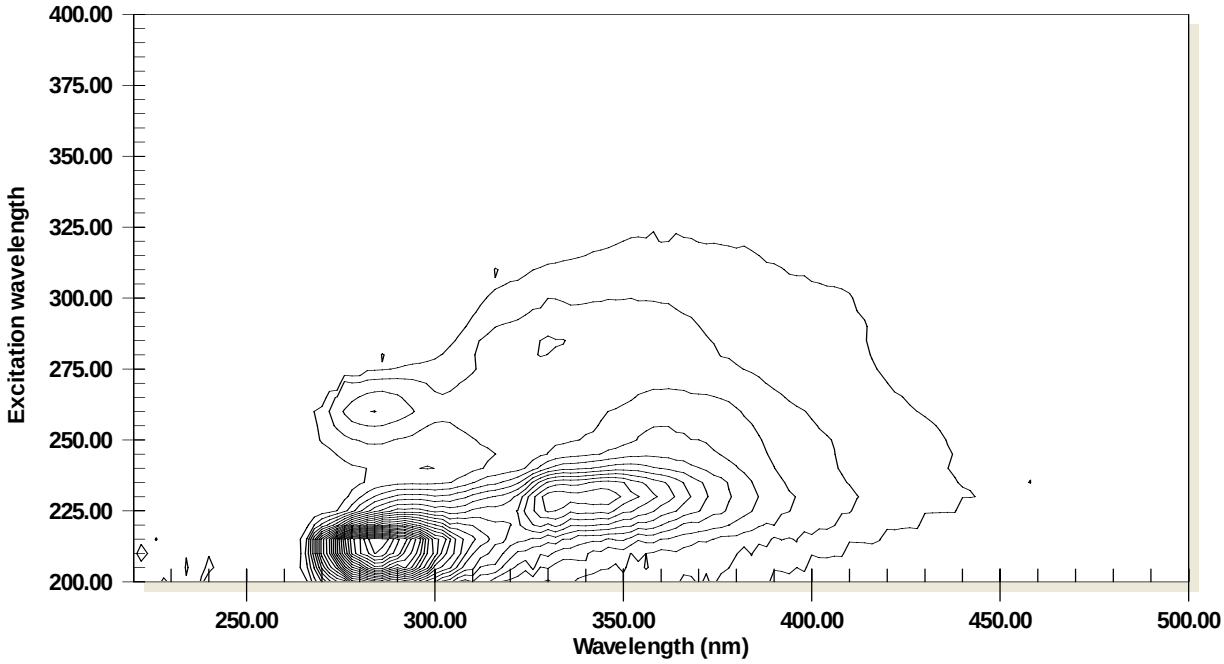
Excitation wavelength
400.00
375.00
350.00
325.00
300.00
275.00
250.00
225.00
200.00
250.00
300.00
350.00
400.00
450.00
500.00
Wavelength (nm)

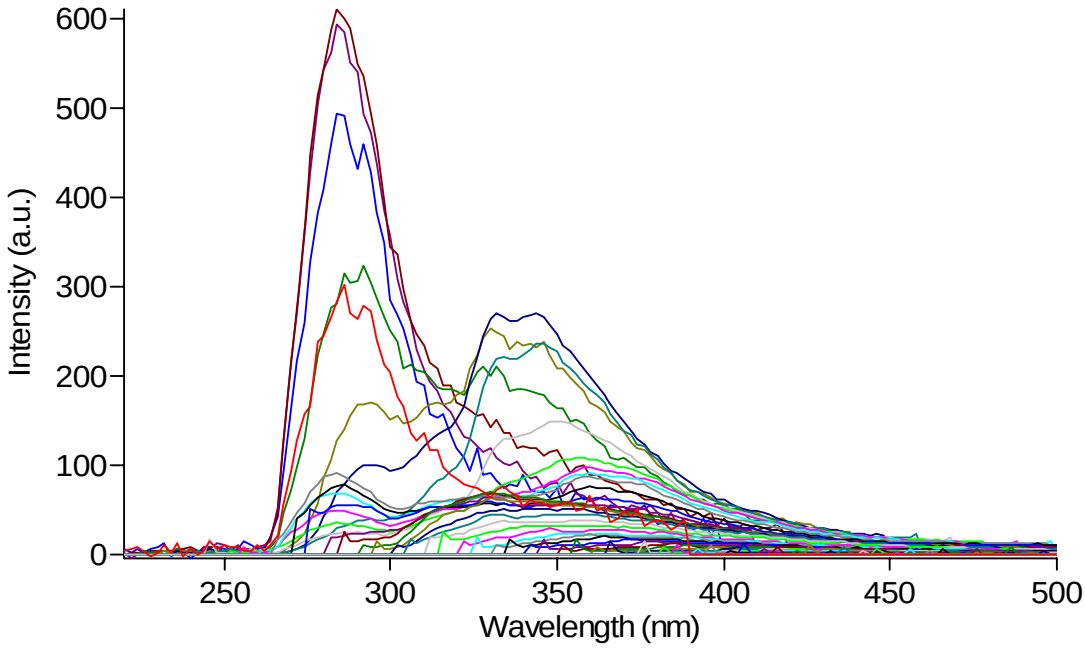
Intensity (a.u.)
600
500
400
300
200
100
0
250
300
350
400
450
500
Wavelength (nm)

M10

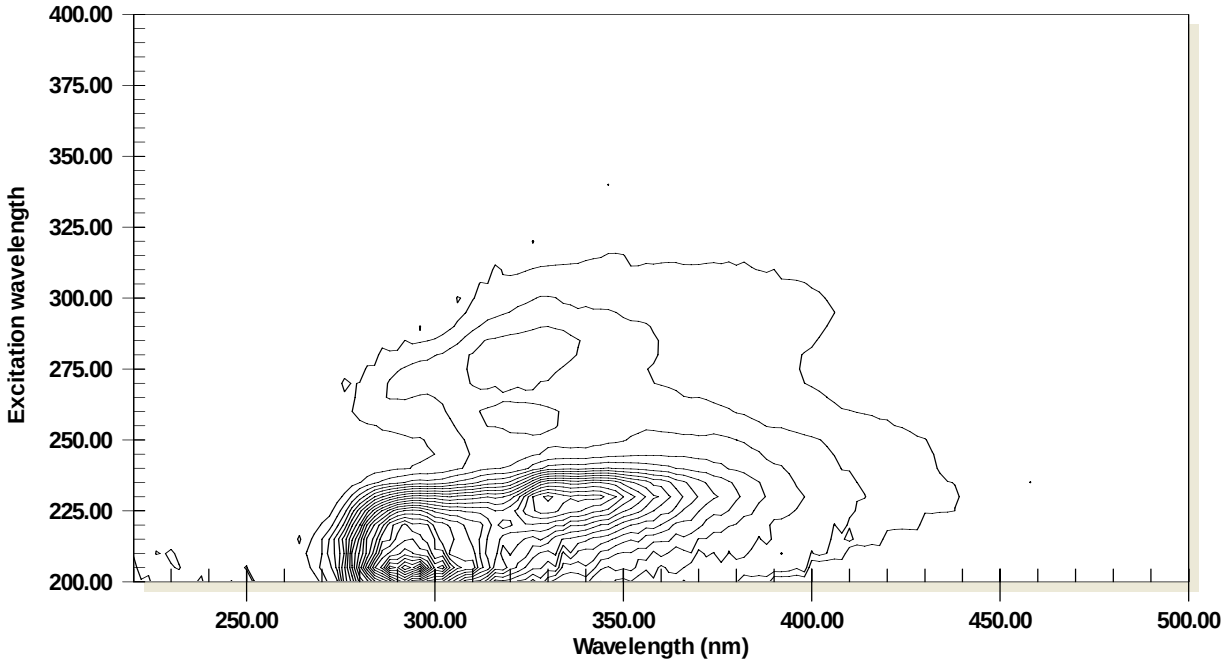
400.00
375.00
350.00
325.00
300.00
275.00
250.00
225.00
200.00
Excitation wavelength
250.00
300.00
350.00
400.00
450.00
500.00
Wavelength (nm)

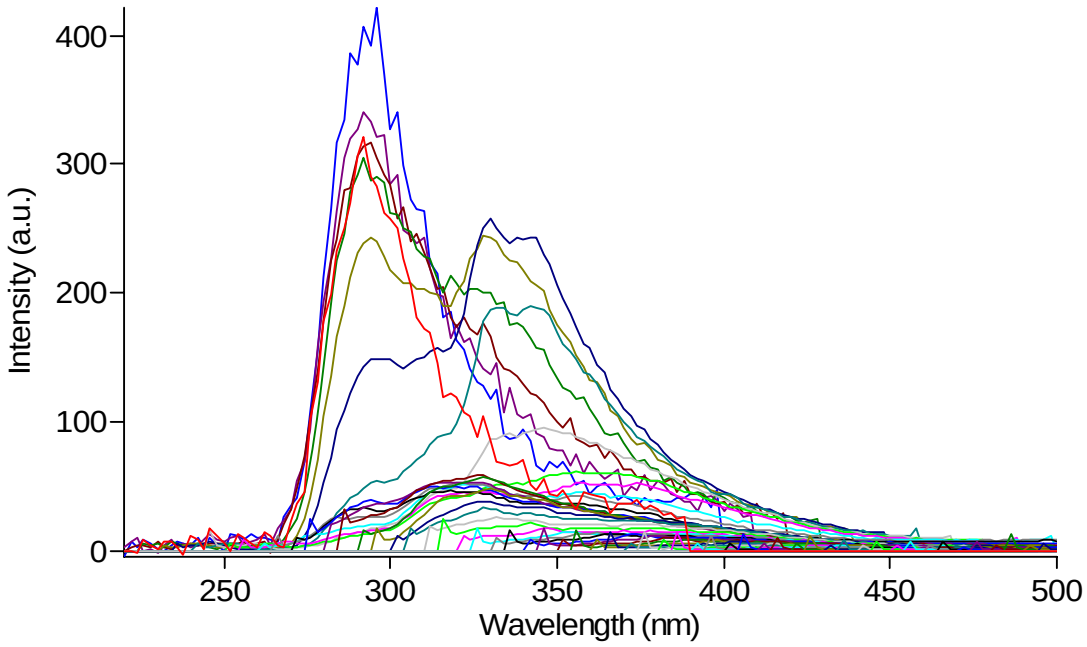
400
300
200
100
0
Intensity (a.u.)
250
300
350
400
450
500
Wavelength (nm)

M12

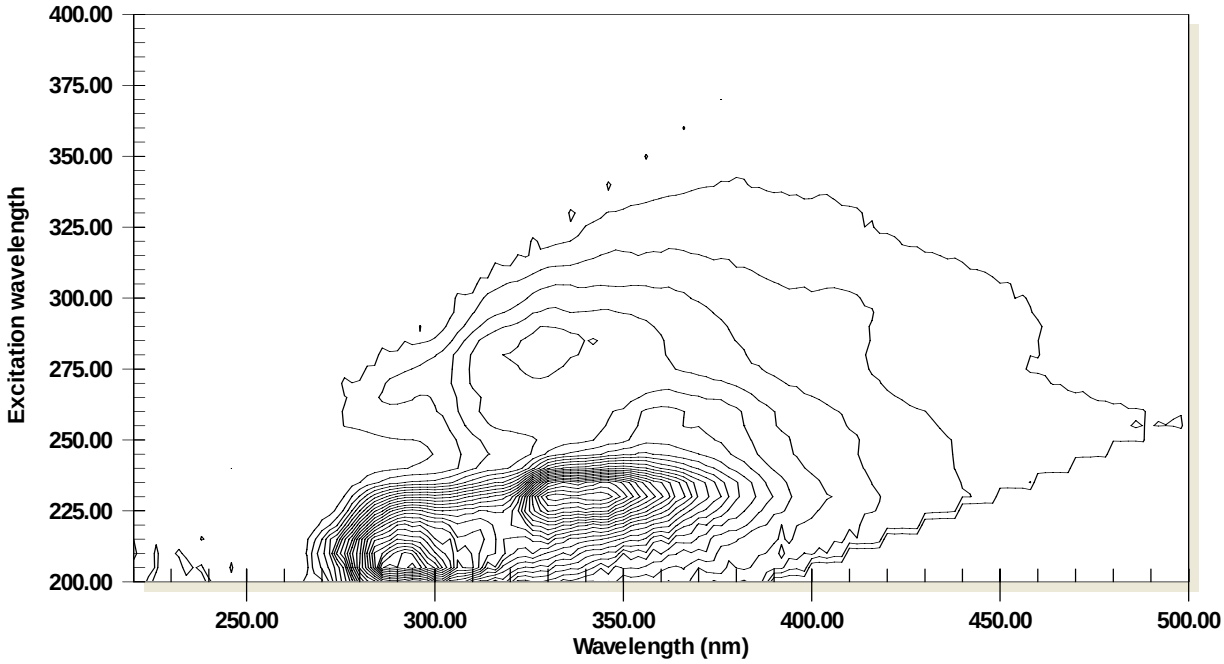
400.00
375.00
350.00
325.00
300.00
275.00
250.00
225.00
200.00
Excitation wavelength
250.00
300.00
350.00
400.00
450.00
500.00
Wavelength (nm)

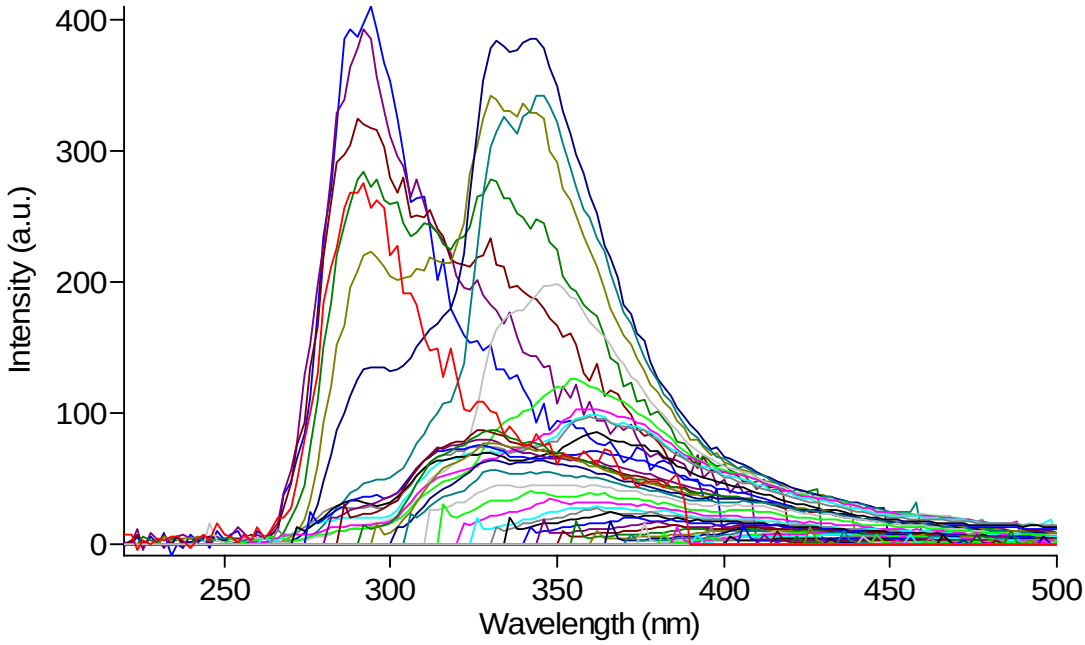
400
300
200
100
0
Intensity (a.u.)
250
300
350
400
450
500
Wavelength (nm)

M19

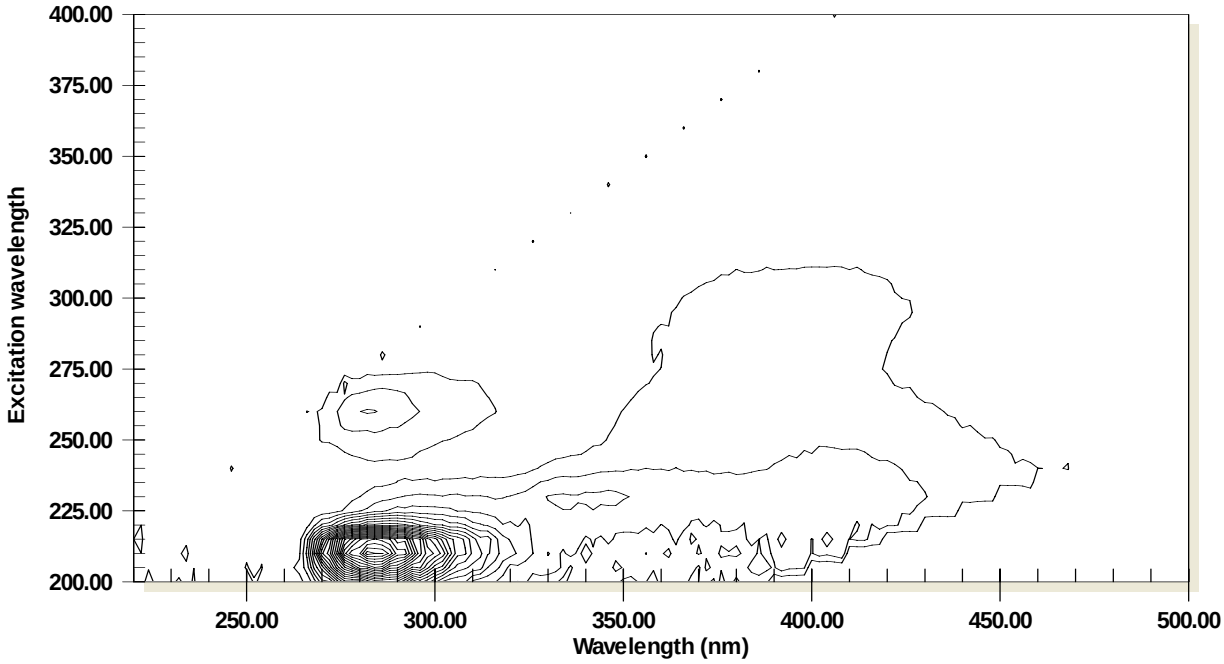
400.00
375.00
350.00
325.00
300.00
275.00
250.00
225.00
200.00
Excitation wavelength
250.00
300.00
350.00
400.00
450.00
500.00
Wavelength (nm)

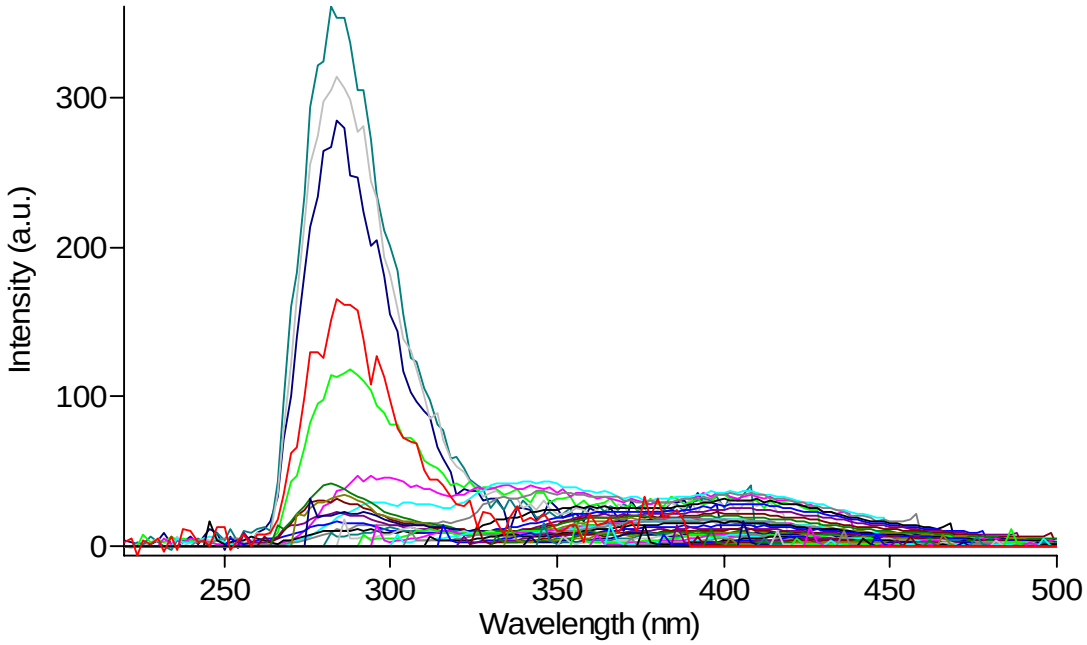
300
200
100
0
Intensity (a.u.)
250
300
350
400
450
500
Wavelength (nm)

M24

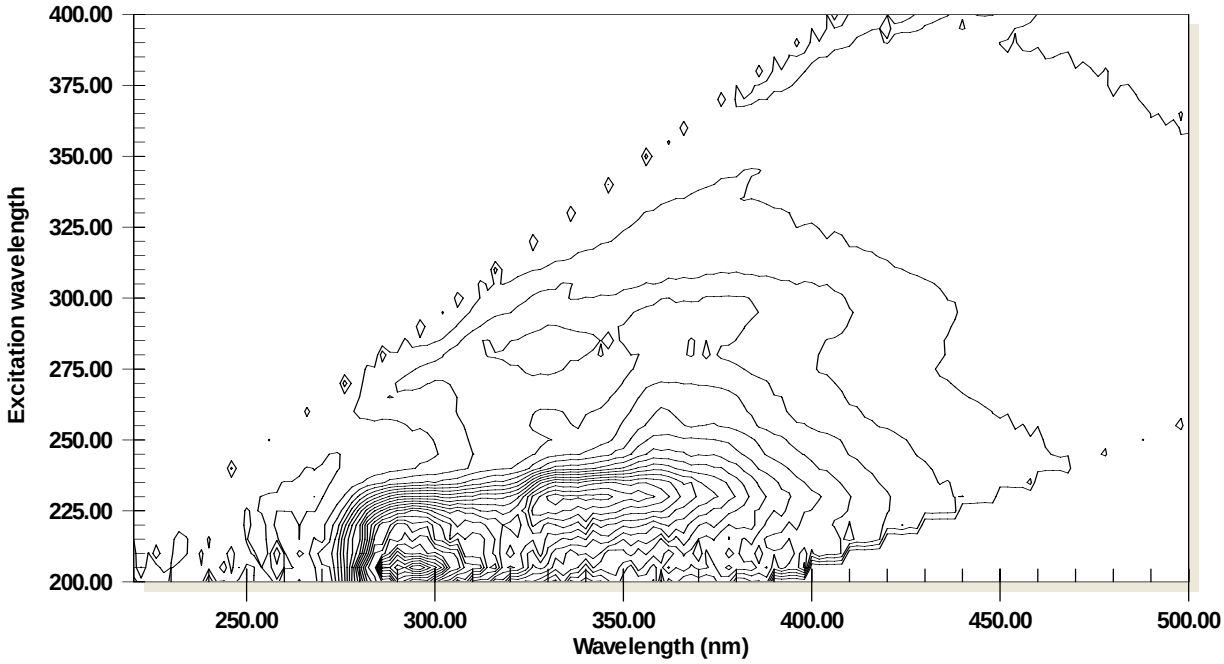
400.00
375.00
350.00
325.00
300.00
275.00
250.00
225.00
200.00
Excitation wavelength
250.00
300.00
350.00
400.00
450.00
500.00
Wavelength (nm)

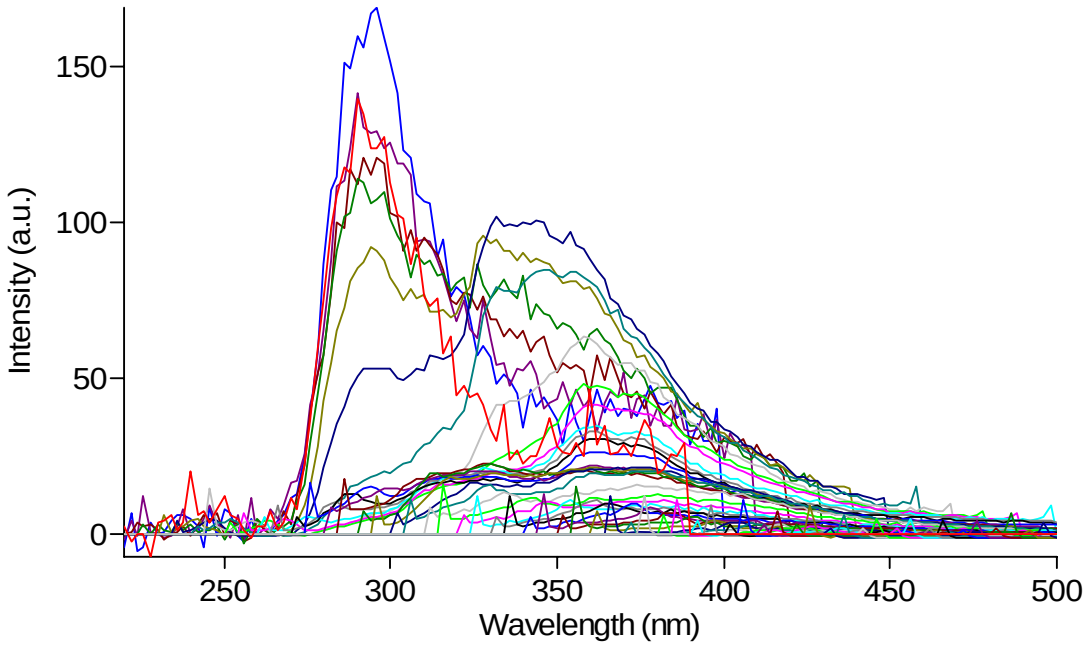
150
100
50
0
Intensity (a.u.)
250
300
350
400
450
500
Wavelength (nm)

M28

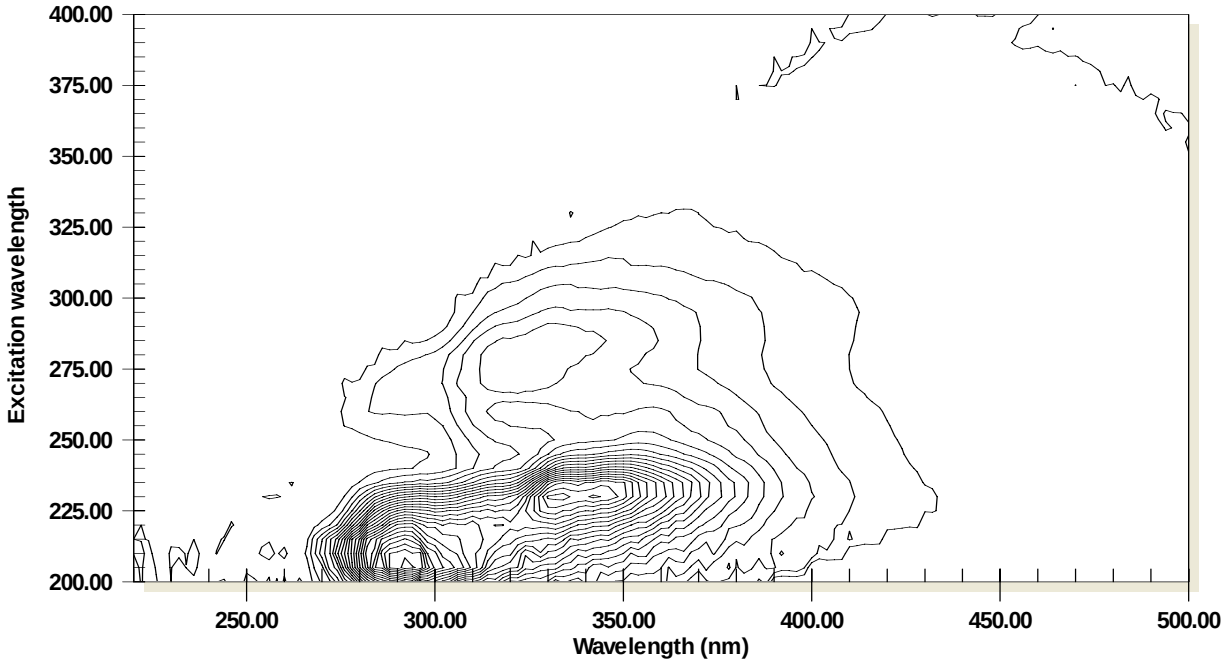
Excitation wavelength
400.00
375.00
350.00
325.00
300.00
275.00
250.00
225.00
200.00
250.00
300.00
350.00
400.00
450.00
500.00
Wavelength (nm)

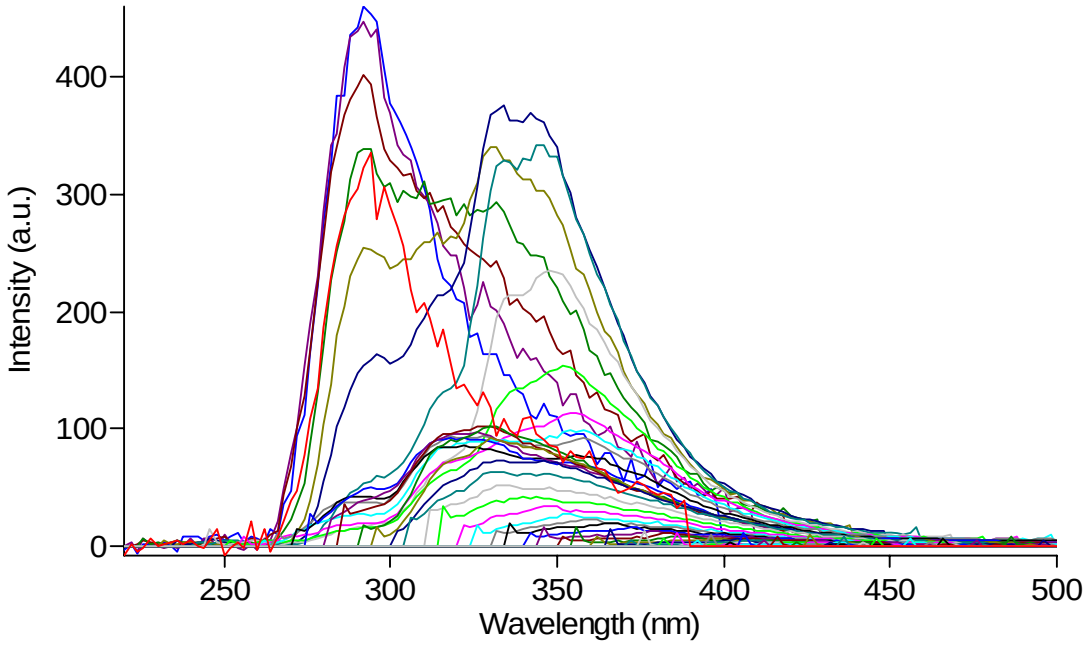
Intensity (a.u.)
400
300
200
100
0
250
300
350
400
450
500
Wavelength (nm)

M29

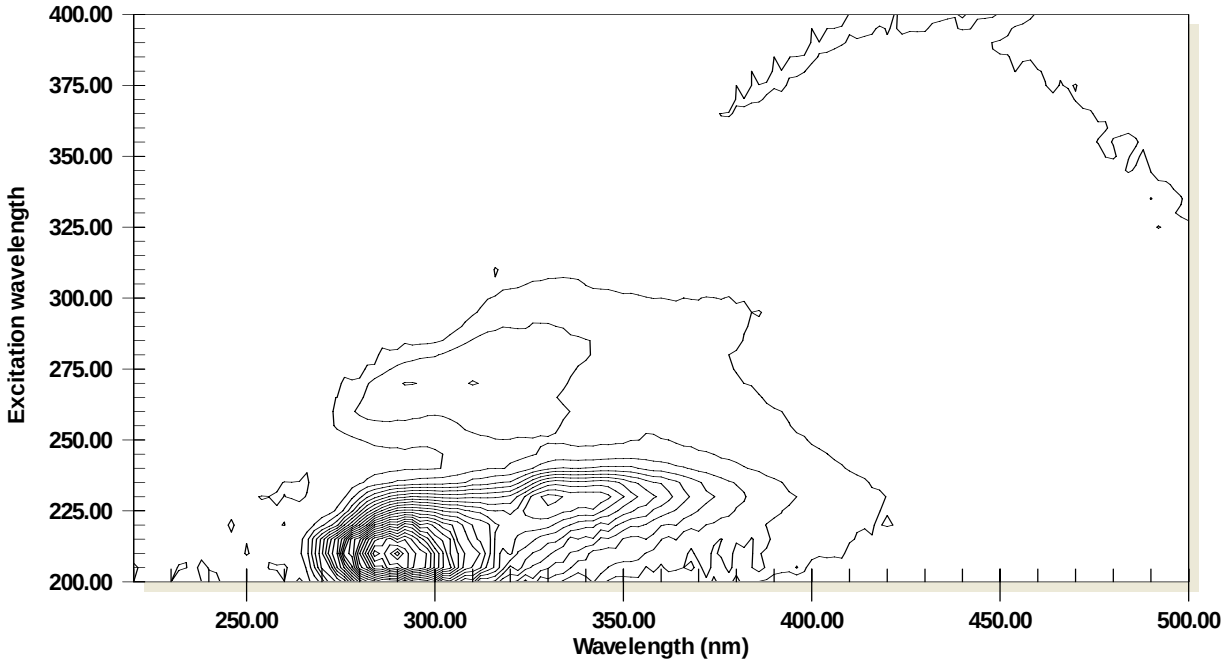
Excitation wavelength
400.00
375.00
350.00
325.00
300.00
275.00
250.00
225.00
200.00
250.00
300.00
350.00
400.00
450.00
500.00
Wavelength (nm)

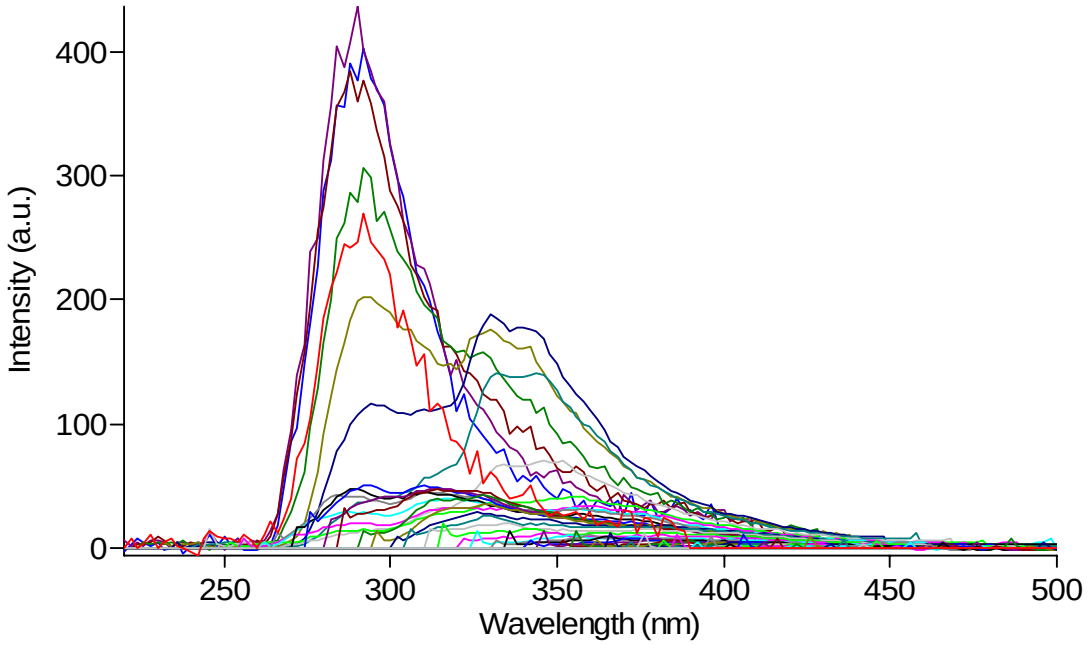
Intensity (a.u.)
400
300
200
100
0
250
300
350
400
450
500
Wavelength (nm)

M36

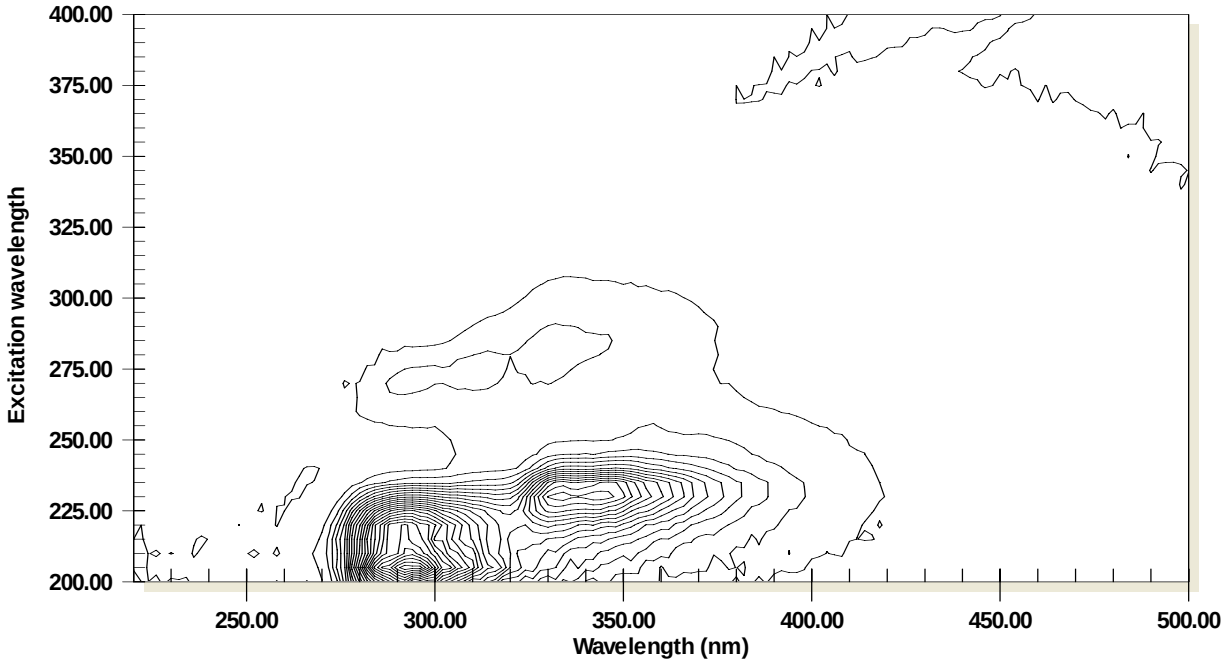
400.00
375.00
350.00
325.00
300.00
275.00
250.00
225.00
200.00
Excitation wavelength
250.00
300.00
350.00
400.00
450.00
500.00
Wavelength (nm)

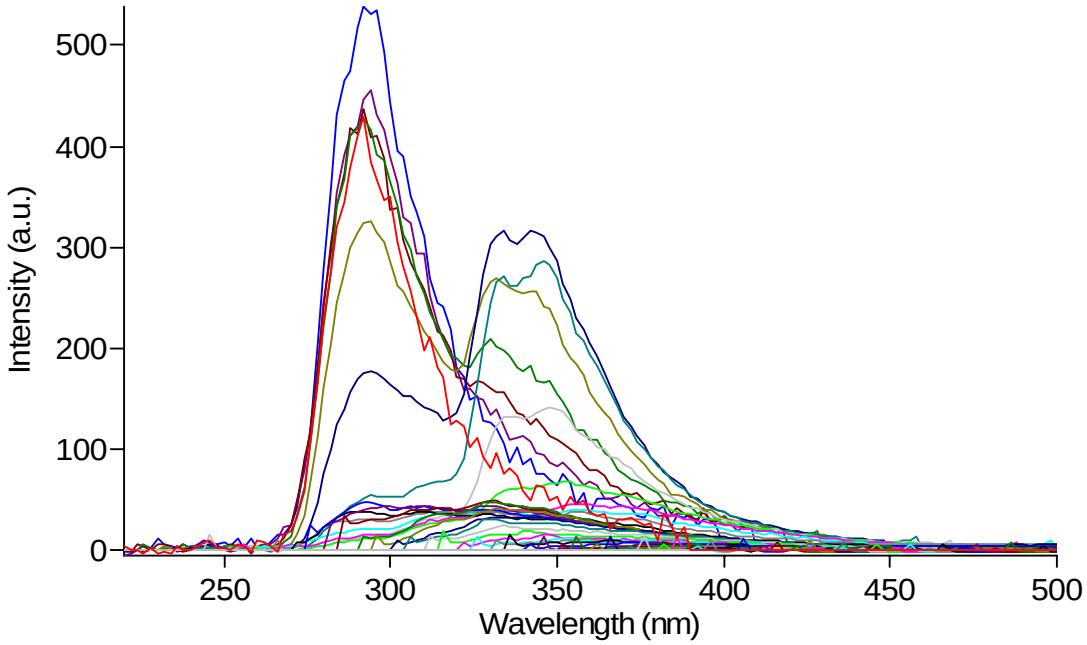
500
400
300
200
100
0
Intensity (a.u.)
250
300
350
400
450
500
Wavelength (nm)

M40

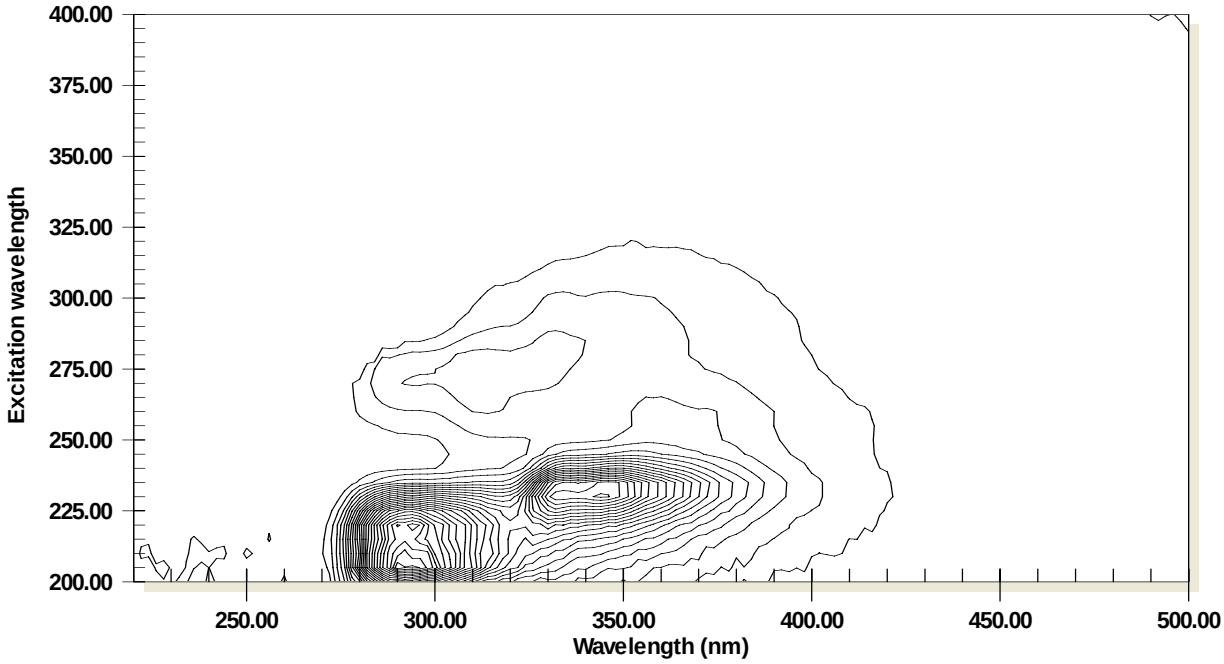
400.00
375.00
350.00
325.00
300.00
275.00
250.00
225.00
200.00
Excitation wavelength
250.00
300.00
350.00
400.00
450.00
500.00
Wavelength (nm)

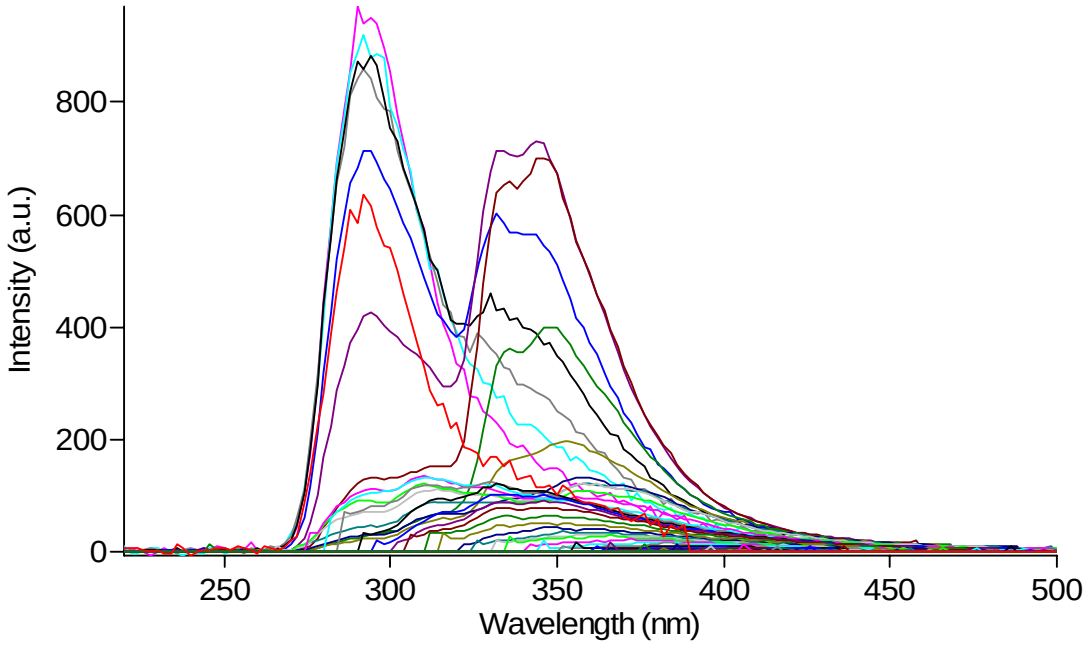
800
600
400
200
0
Intensity (a.u.)
250
300
350
400
450
500
Wavelength (nm)

M46

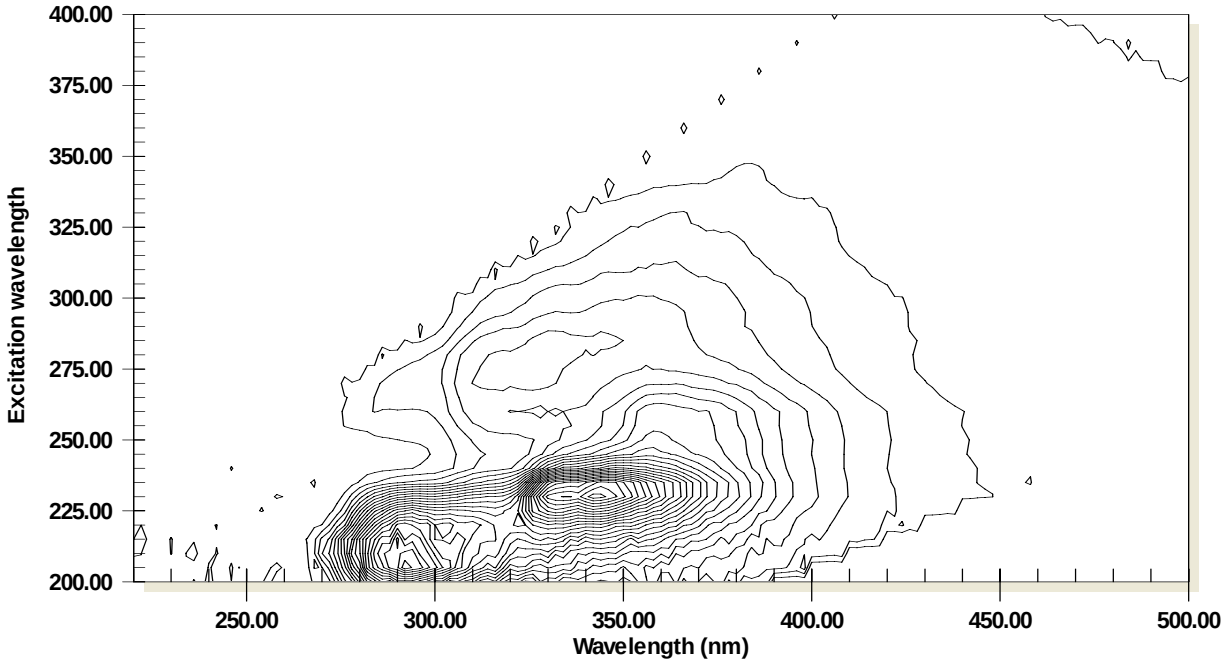
400.00
375.00
350.00
325.00
300.00
275.00
250.00
225.00
200.00
Excitation wavelength
250.00
300.00
350.00
400.00
450.00
500.00
Wavelength (nm)

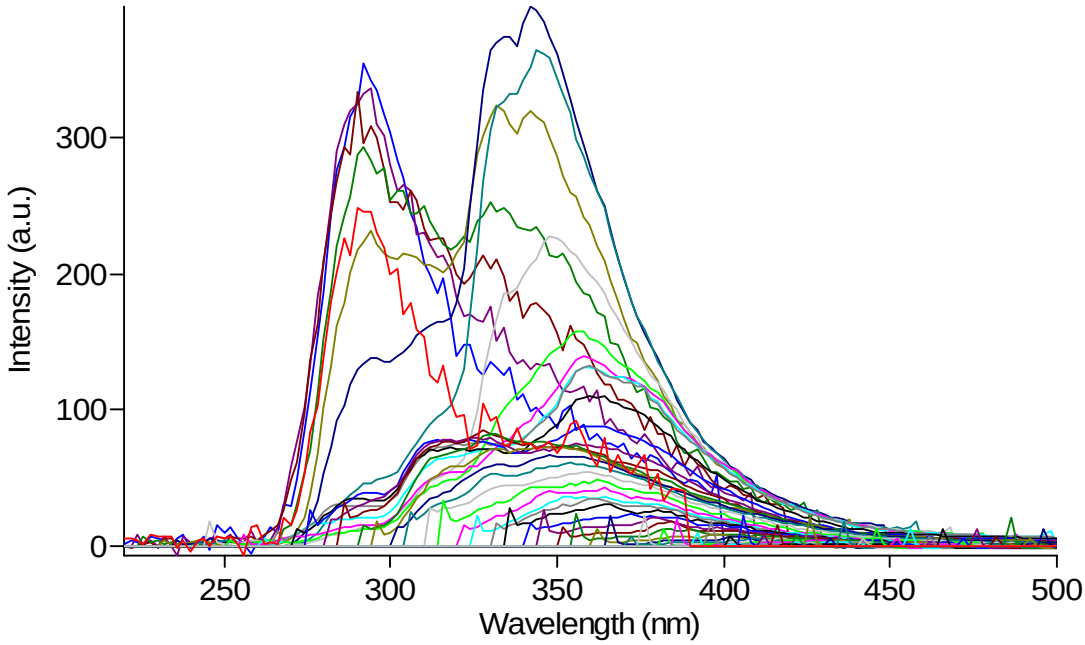
300
200
100
0
Intensity (a.u.)
250
300
350
400
450
500
Wavelength (nm)

Toluene Contour Plots and Excitation Scan Overlays
11CT

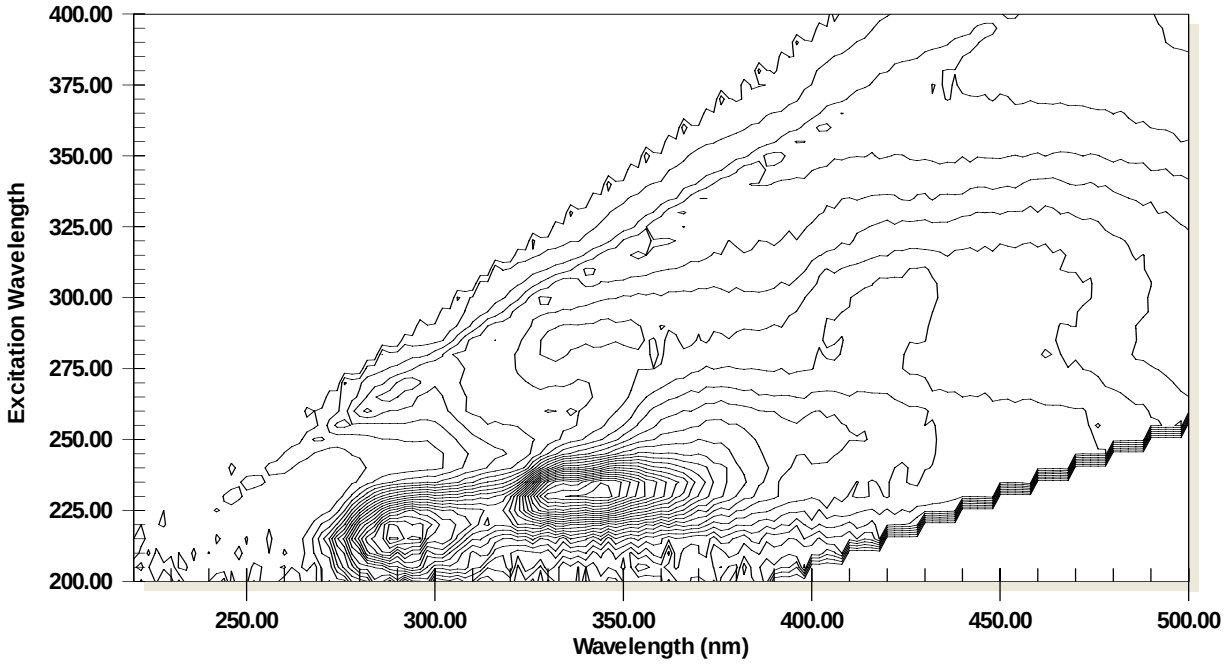

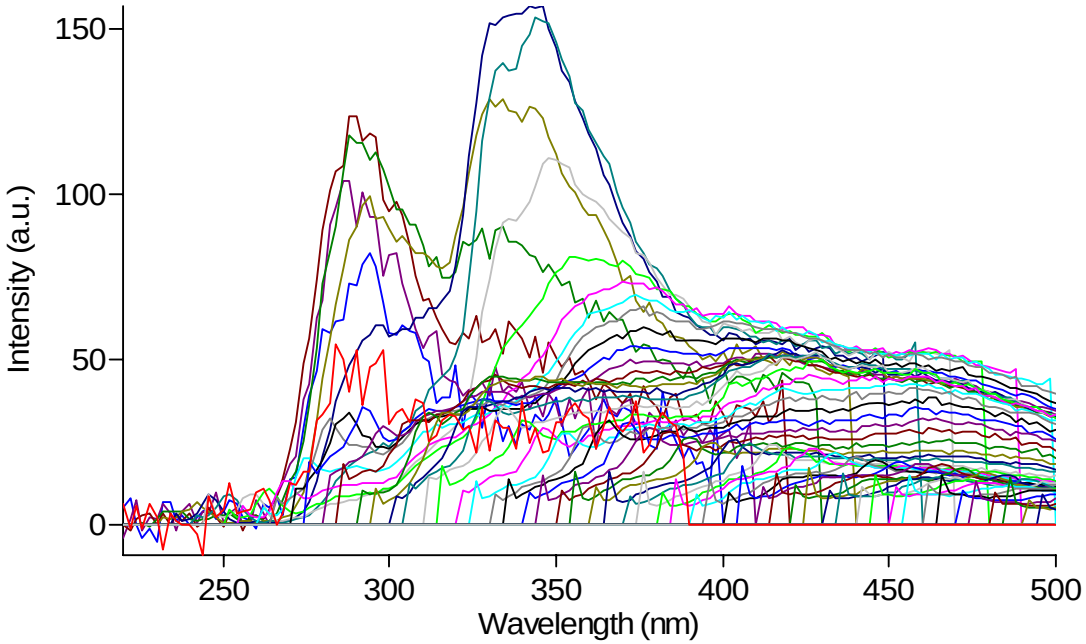

13BT

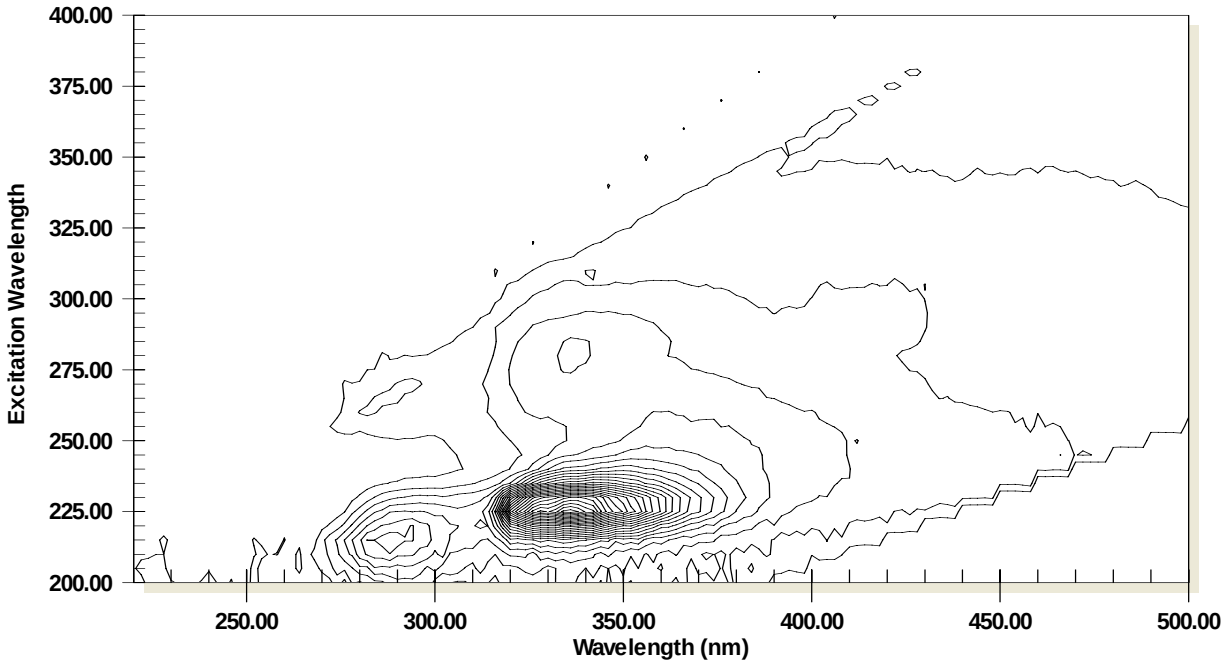
400.00
375.00
350.00
325.00
300.00
275.00
250.00
225.00
200.00
Excitation Wavelength
250.00
300.00
350.00
400.00
450.00
500.00
Wavelength (nm)

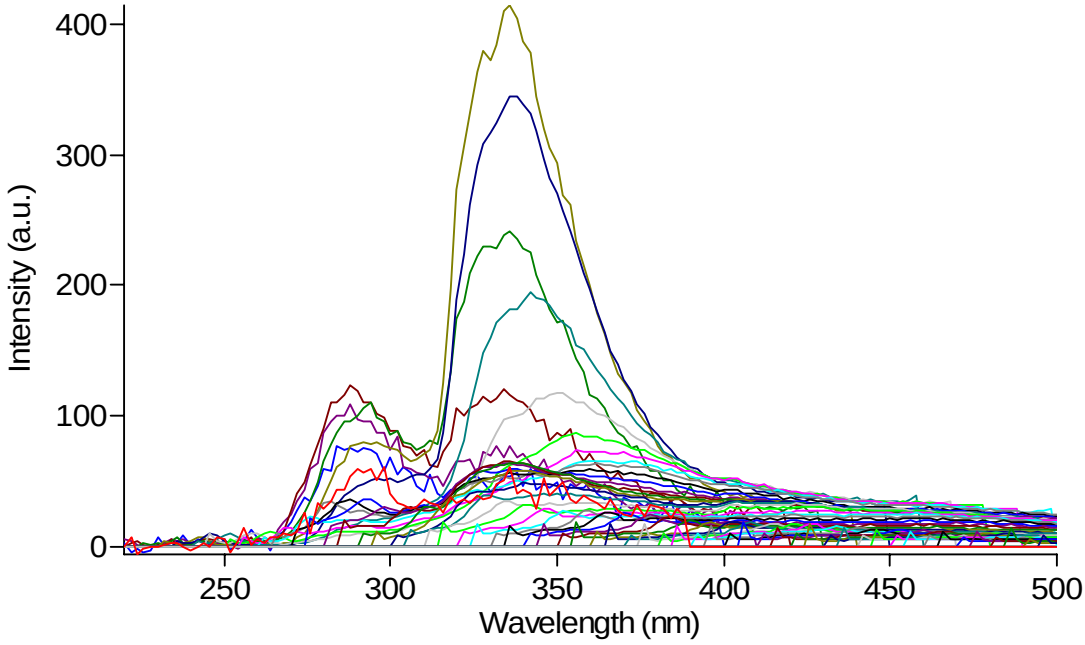
400
300
200
100
0
Intensity (a.u.)
250
300
350
400
450
500
Wavelength (nm)

14BT

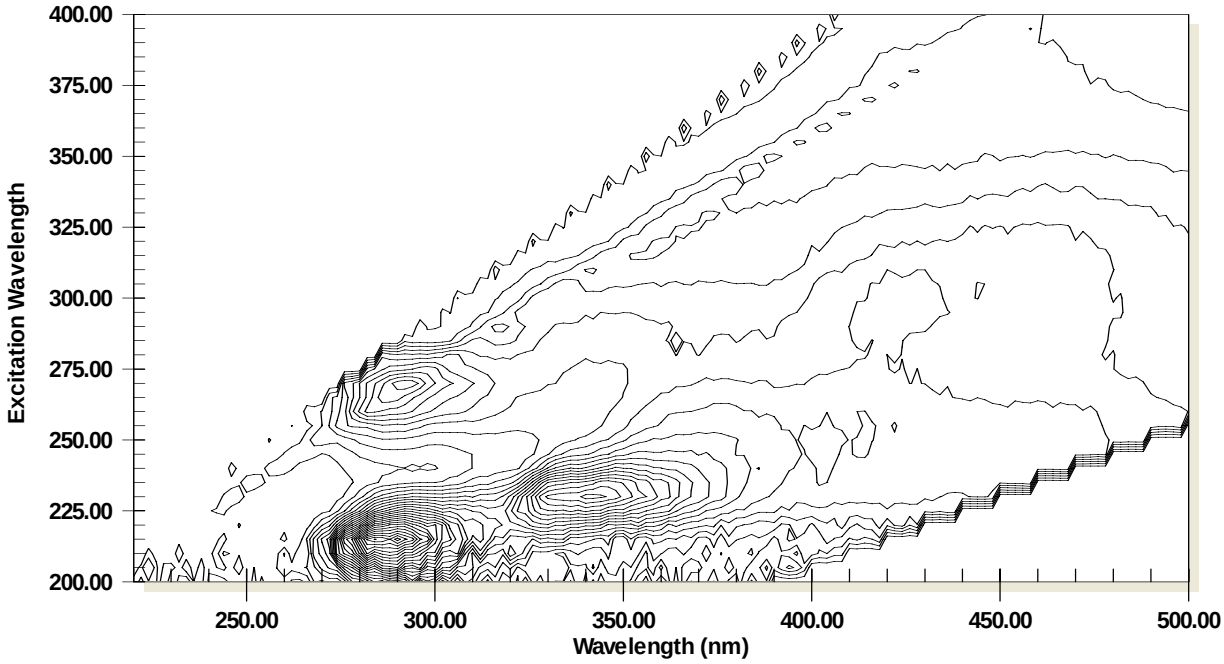
Excitation Wavelength
400.00
375.00
350.00
325.00
300.00
275.00
250.00
225.00
200.00
250.00
300.00
350.00
400.00
450.00
500.00
Wavelength (nm)

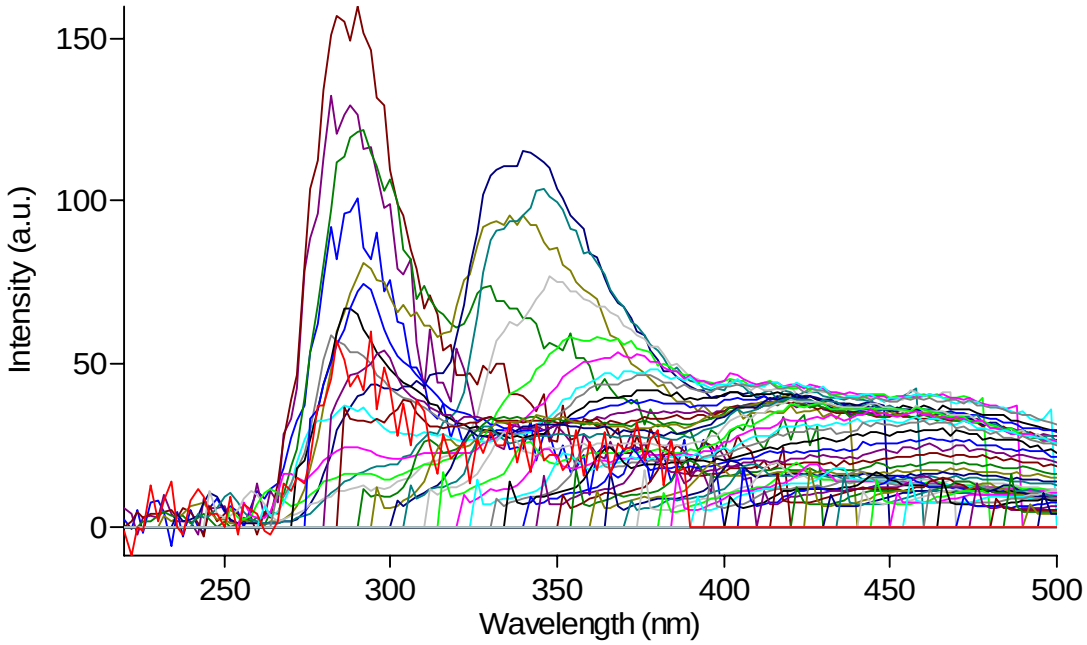
Intensity (a.u.)
150
100
50
0
250
300
350
400
450
500
Wavelength (nm)

15BT

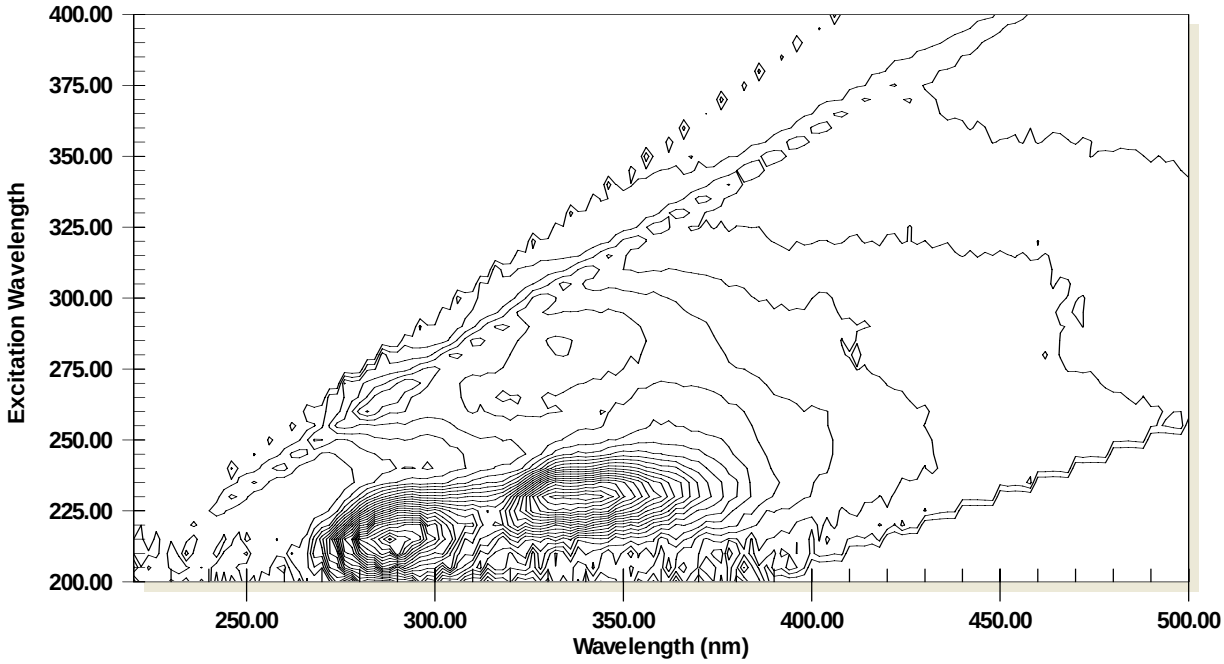
Excitation Wavelength
400.00
375.00
350.00
325.00
300.00
275.00
250.00
225.00
200.00
250.00
300.00
350.00
400.00
450.00
500.00
Wavelength (nm)

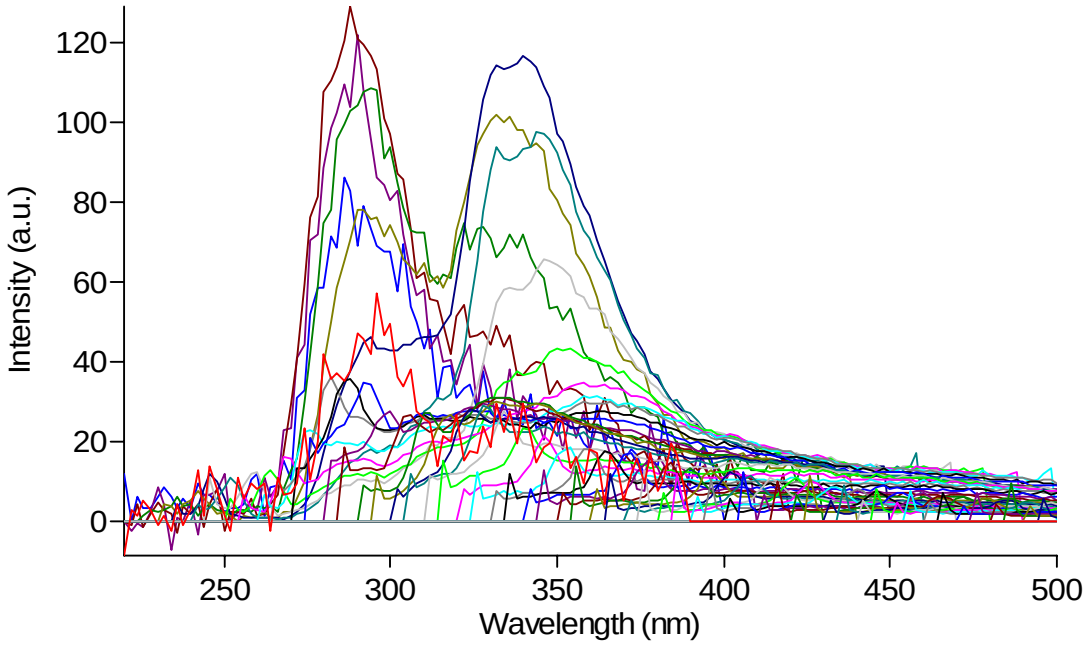
Intensity (a.u.)
120
100
80
60
40
20
0
250
300
350
400
450
500
Wavelength (nm)

21BT

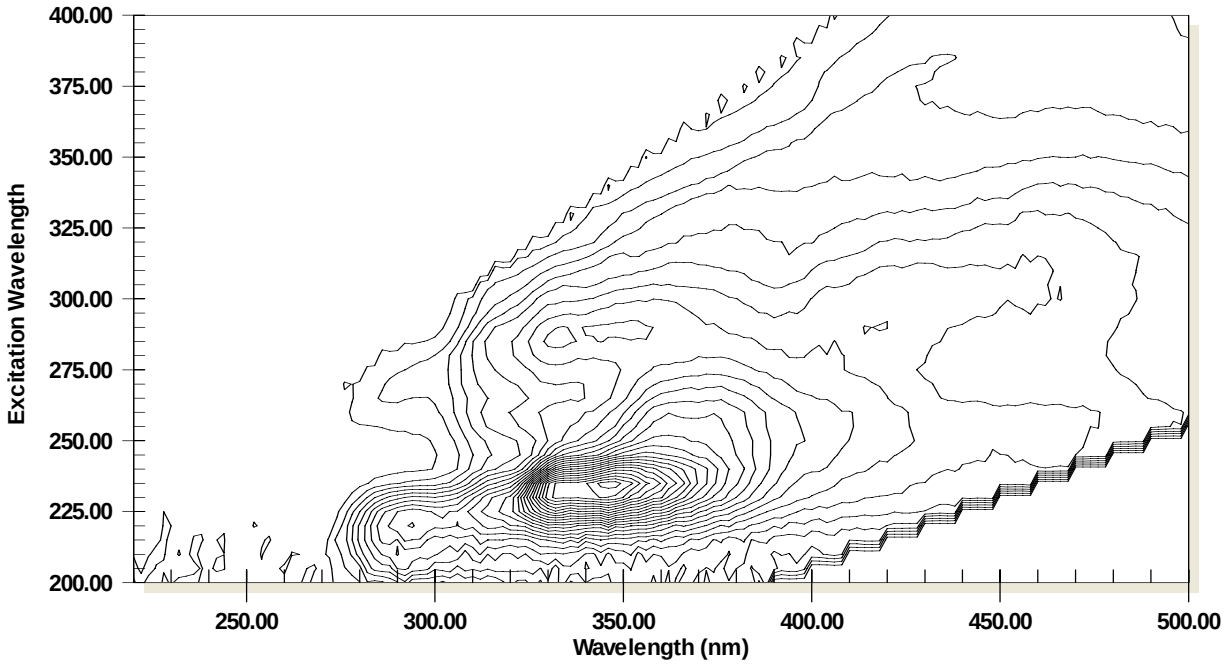
Excitation Wavelength
400.00
375.00
350.00
325.00
300.00
275.00
250.00
225.00
200.00
250.00
300.00
350.00
400.00
450.00
500.00
Wavelength (nm)

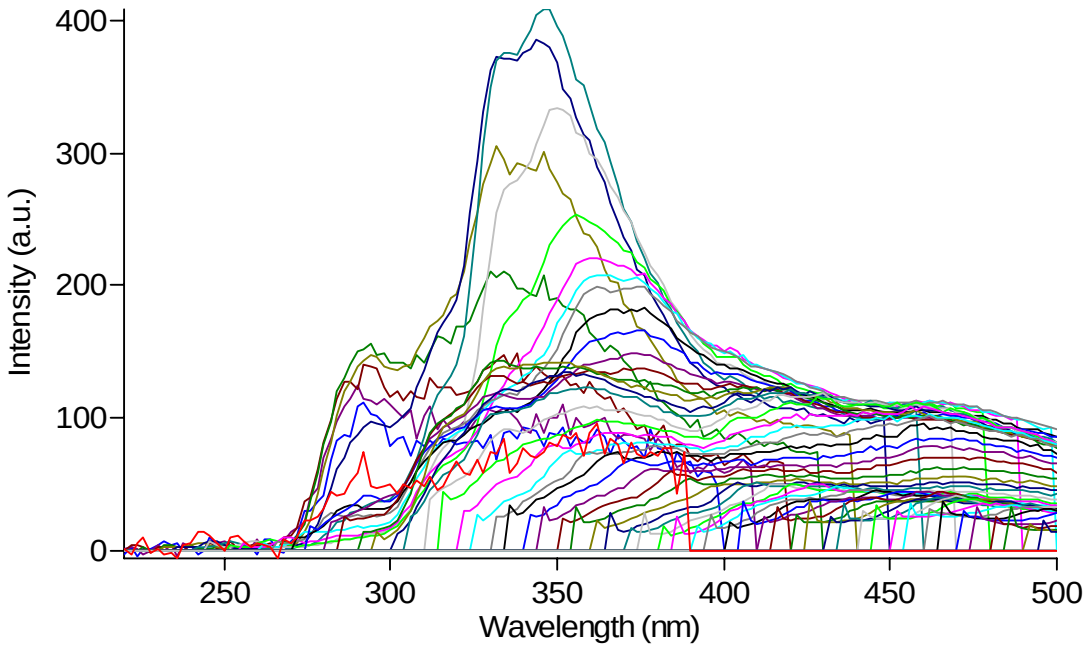
Intensity (a.u.)
400
300
200
100
0
250
300
350
400
450
500
Wavelength (nm)

22AT

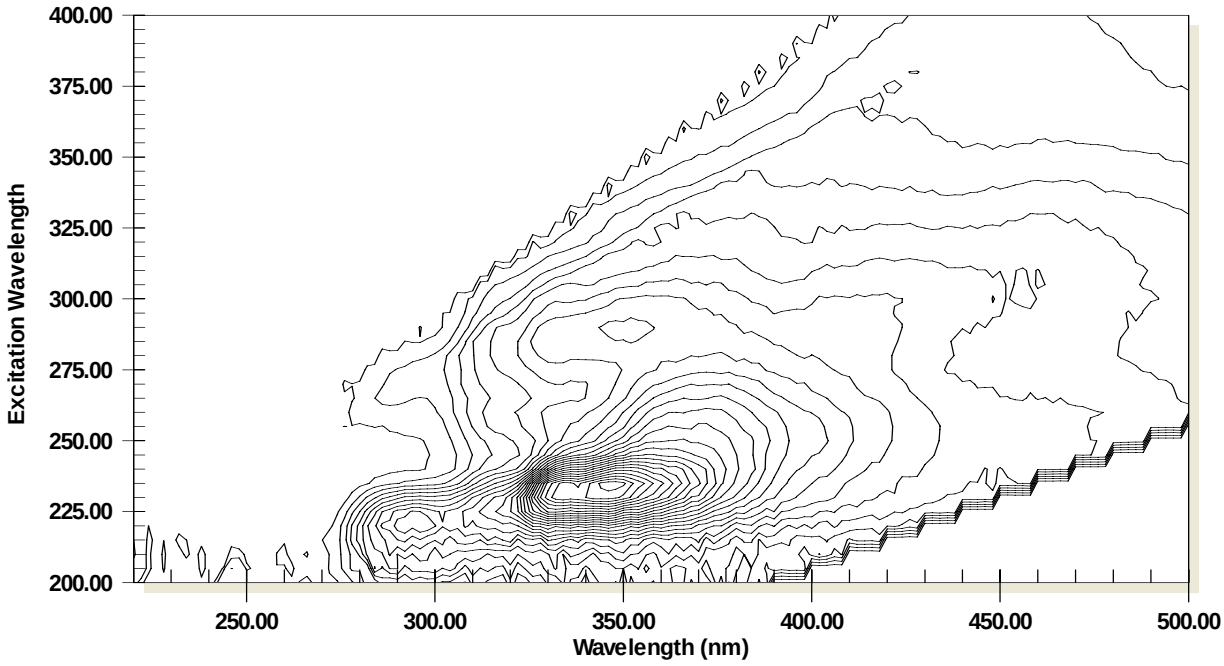
400.00
375.00
350.00
325.00
300.00
275.00
250.00
225.00
200.00
Excitation Wavelength
250.00
300.00
350.00
400.00
450.00
500.00
Wavelength (nm)

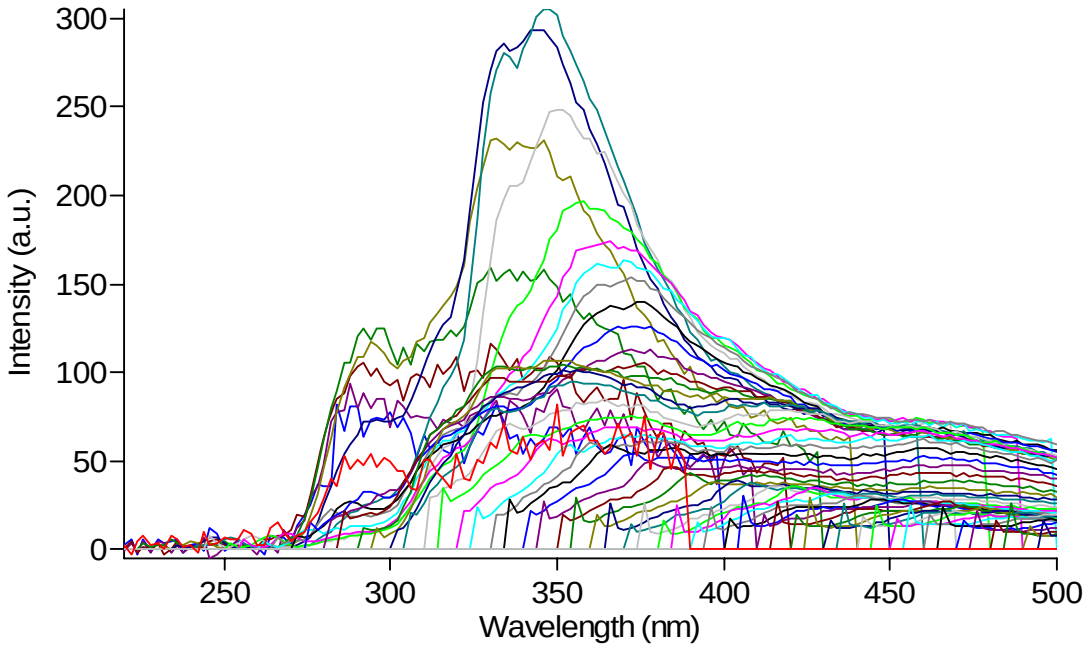
300
250
200
150
100
50
0
Intensity (a.u.)
250
300
350
400
450
500
Wavelength (nm)

23AT

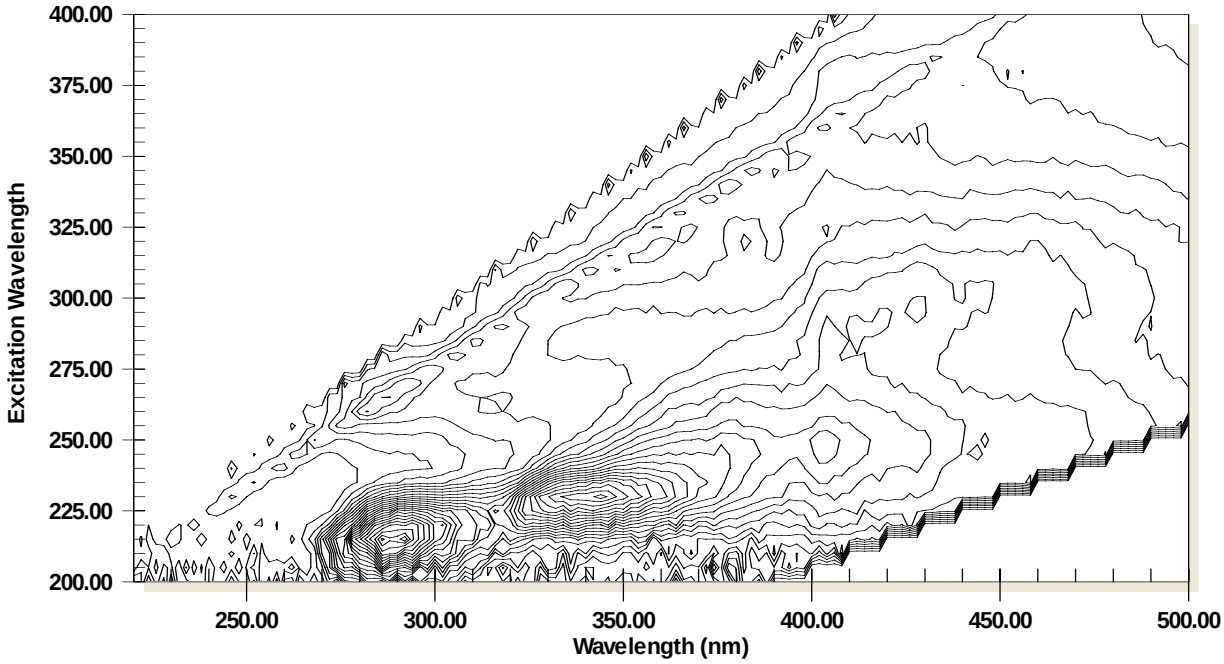
400.00
375.00
350.00
325.00
300.00
275.00
250.00
225.00
200.00
Excitation Wavelength
250.00
300.00
350.00
400.00
450.00
500.00
Wavelength (nm)

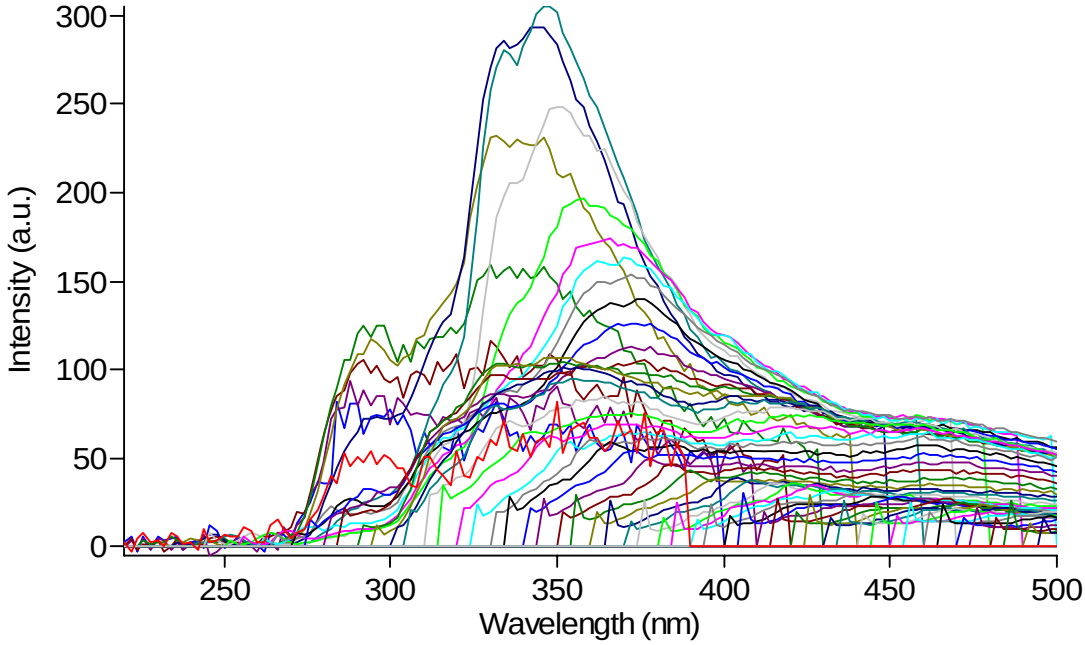
300
250
200
150
100
50
0
Intensity (a.u.)
250
300
350
400
450
500
Wavelength (nm)

24CT

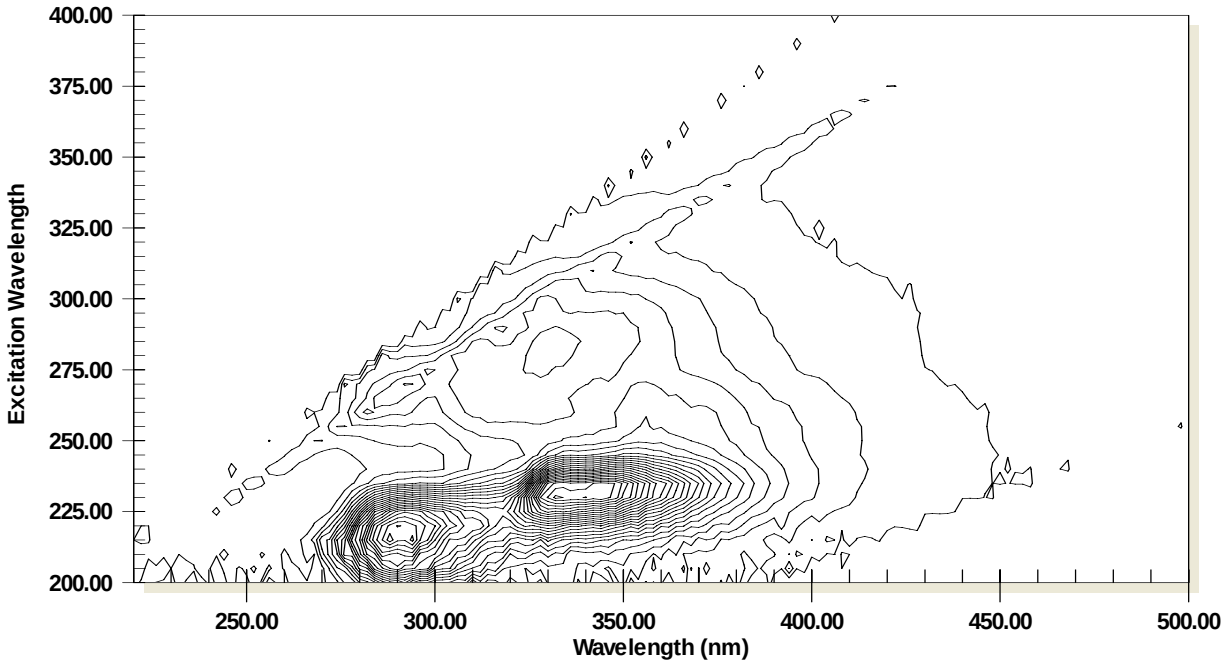
Excitation Wavelength
400.00
375.00
350.00
325.00
300.00
275.00
250.00
225.00
200.00
250.00
300.00
350.00
400.00
450.00
500.00
Wavelength (nm)

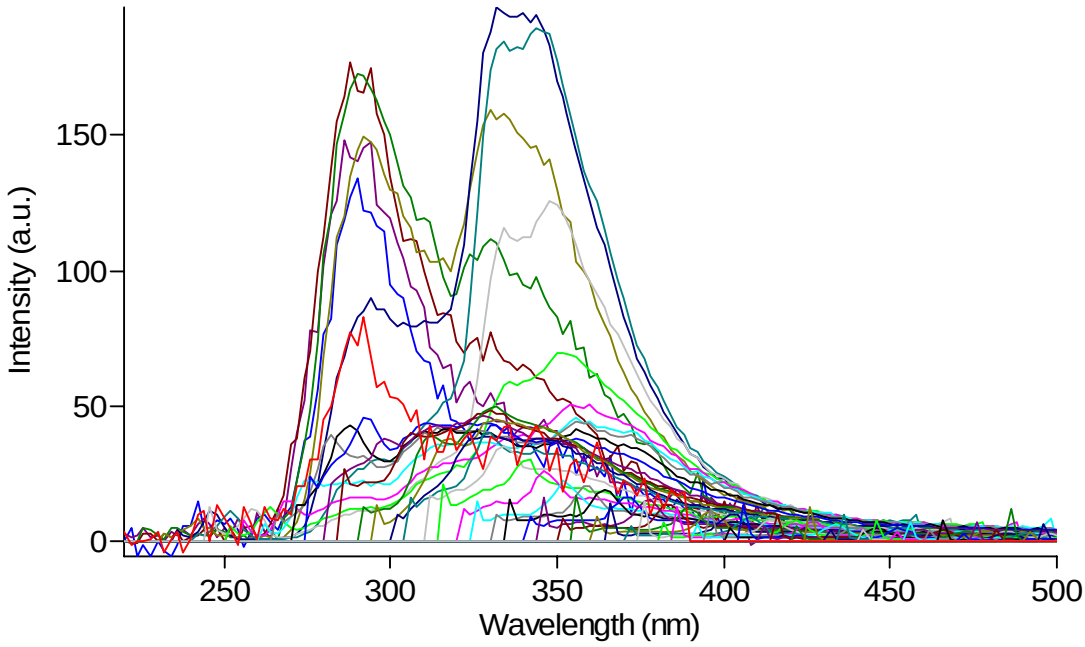
Intensity (a.u.)
150
100
50
0
250
300
350
400
450
500
Wavelength (nm)

25CT

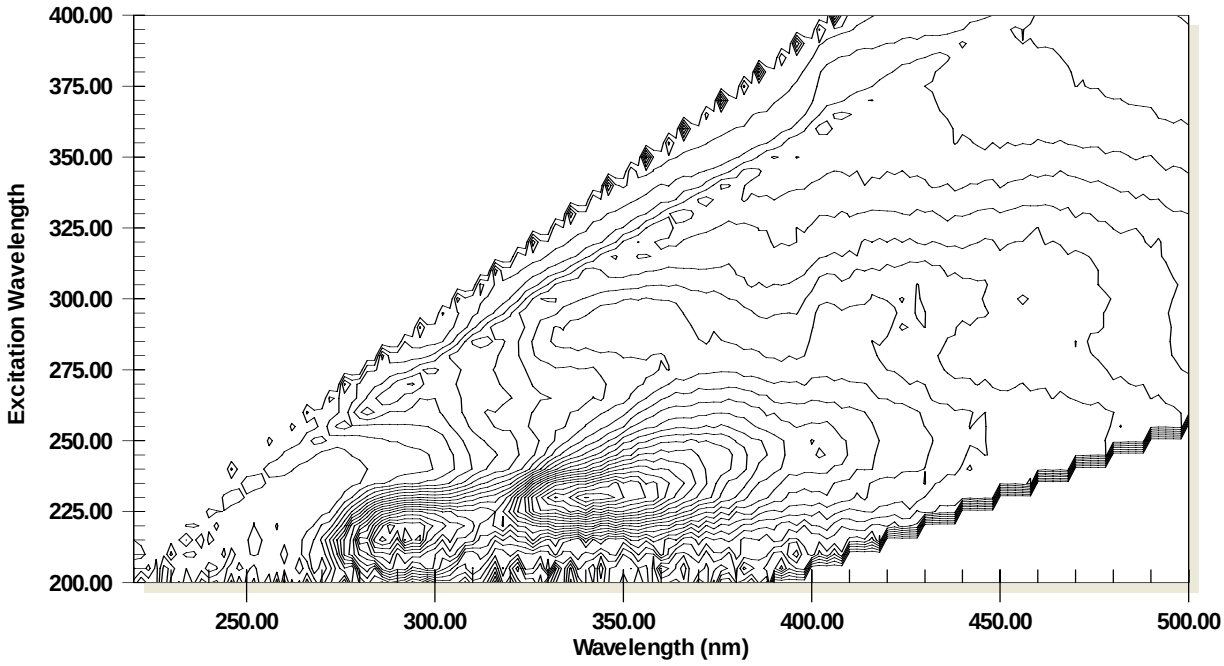
400.00
375.00
350.00
325.00
300.00
275.00
250.00
225.00
200.00
Excitation Wavelength
250.00
300.00
350.00
400.00
450.00
500.00
Wavelength (nm)

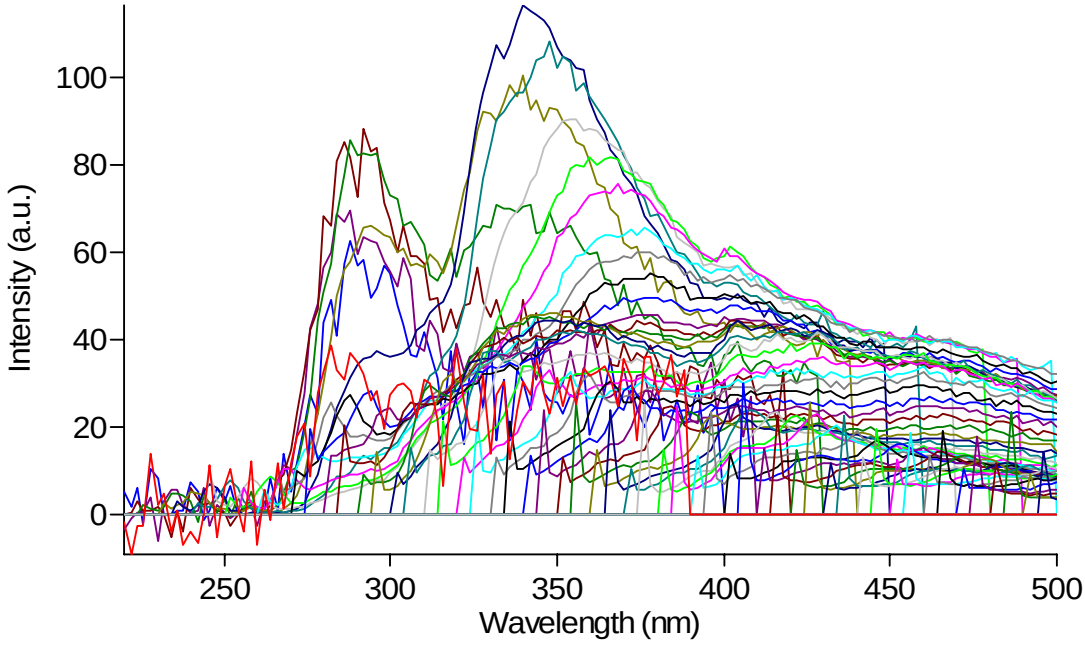
100
80
60
40
20
0
Intensity (a.u.)
250
300
350
400
450
500
Wavelength (nm)

31CT

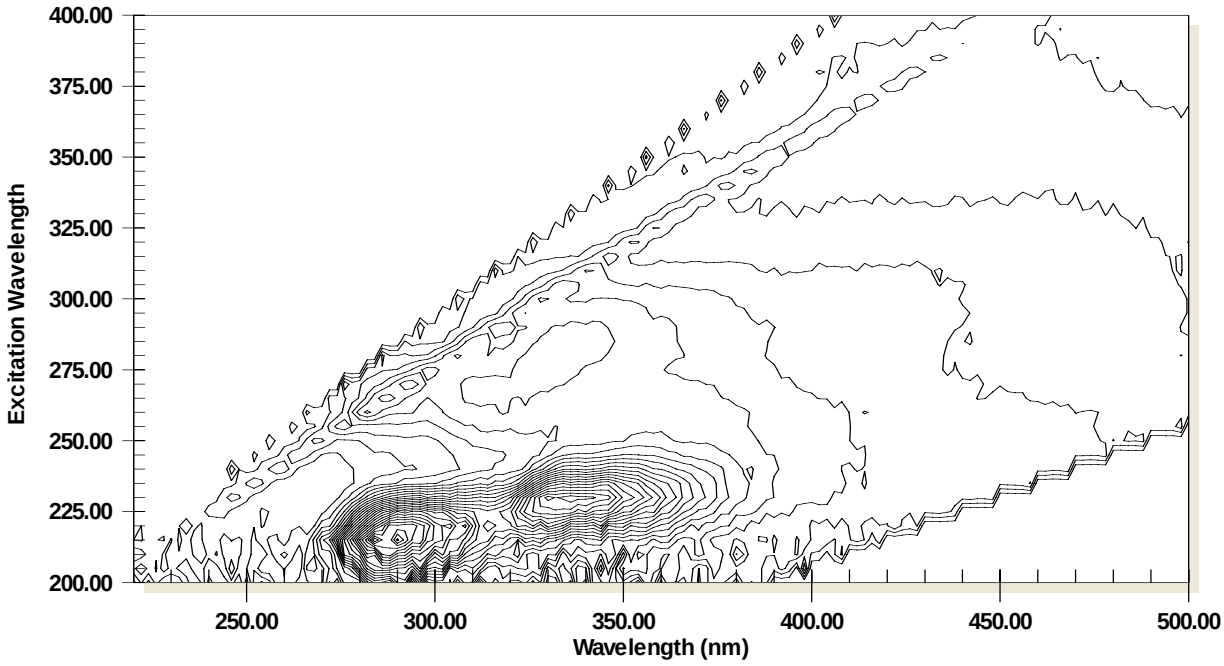
Excitation Wavelength
400.00
375.00
350.00
325.00
300.00
275.00
250.00
225.00
200.00
250.00
300.00
350.00
400.00
450.00
500.00
Wavelength (nm)

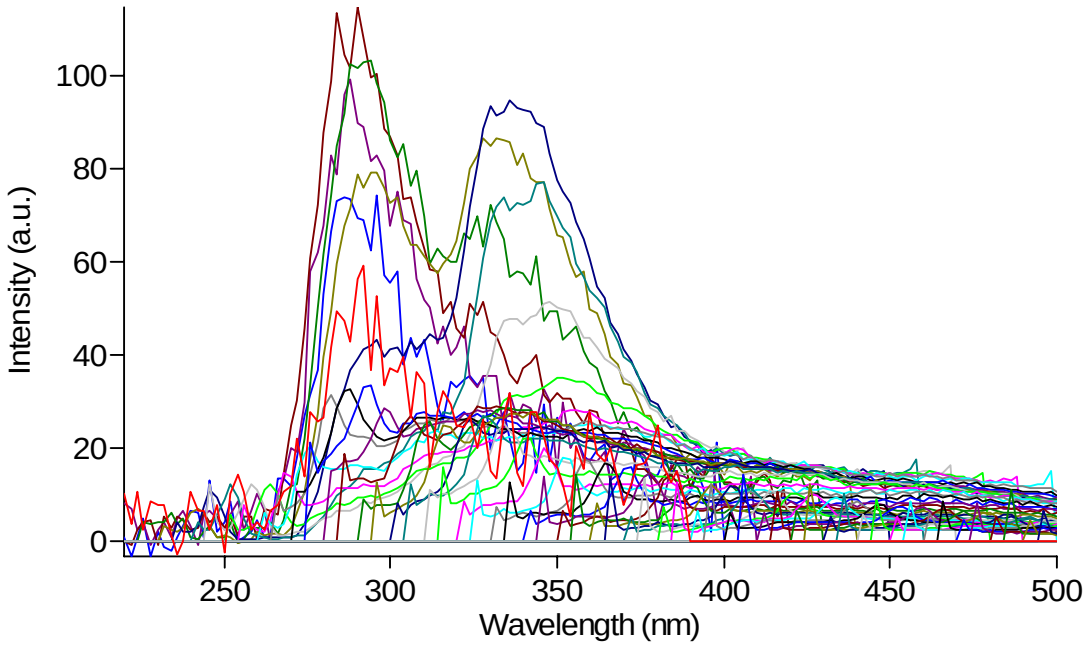
Intensity (a.u.)
100
80
60
40
20
0
250
300
350
400
450
500
Wavelength (nm)

32CT

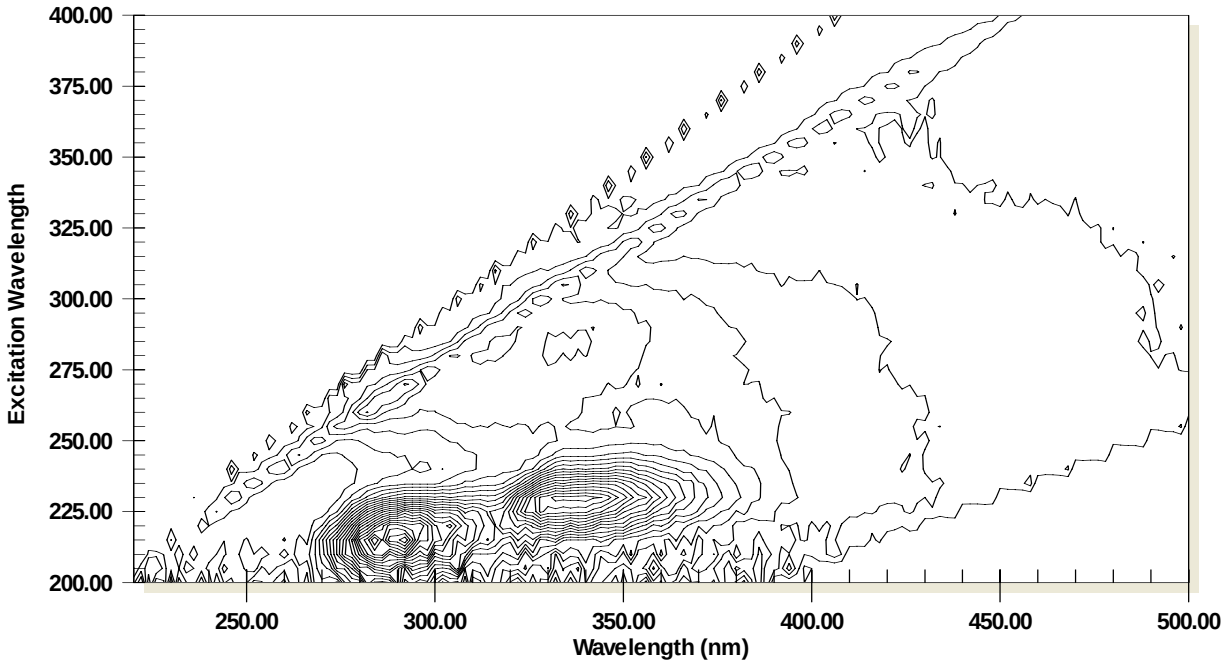
400.00
375.00
350.00
325.00
300.00
275.00
250.00
225.00
200.00
Excitation Wavelength
250.00
300.00
350.00
400.00
450.00
500.00
Wavelength (nm)

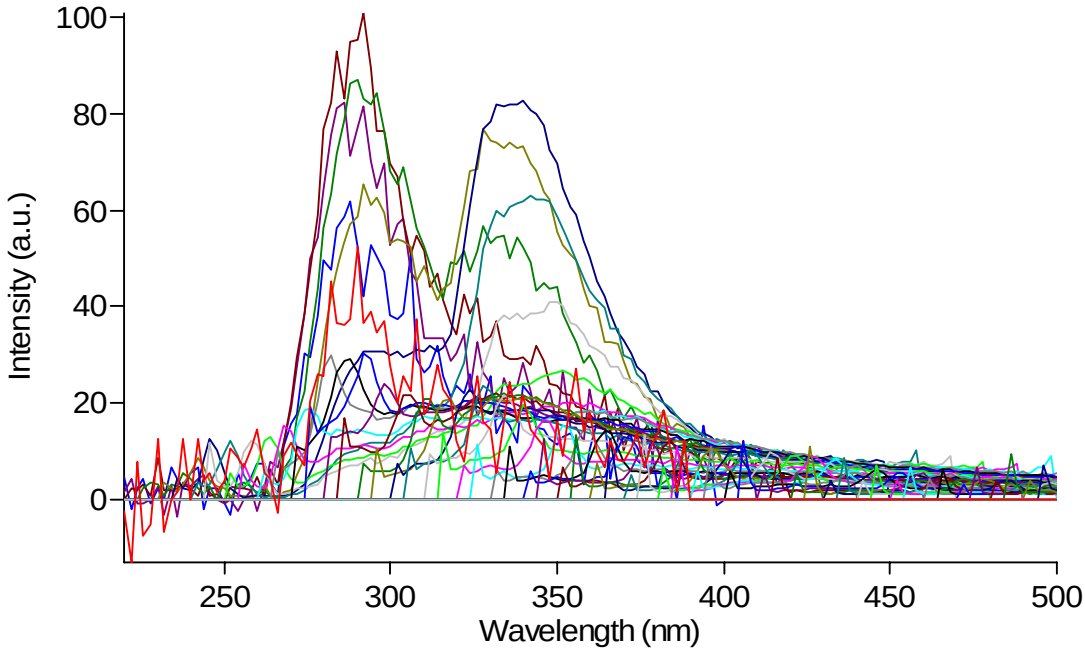
100
80
60
40
20
0
Intensity (a.u.)
250
300
350
400
450
500
Wavelength (nm)

33AT

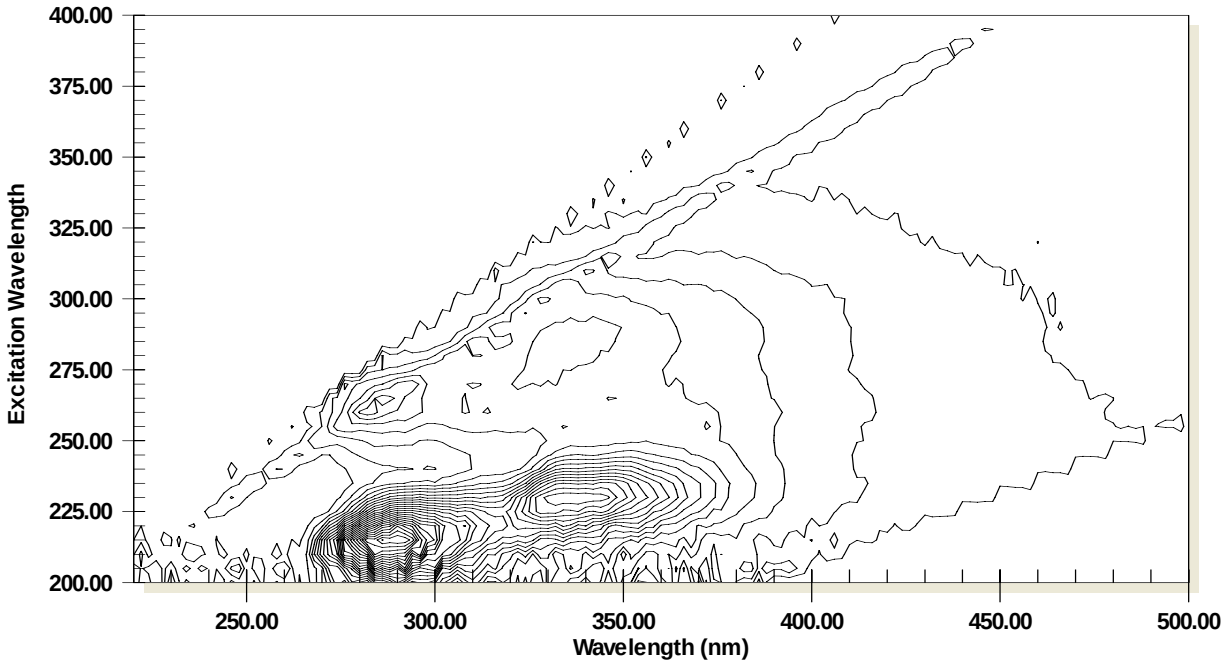
400.00
375.00
350.00
325.00
300.00
275.00
250.00
225.00
200.00
Excitation Wavelength
250.00
300.00
350.00
400.00
450.00
500.00
Wavelength (nm)

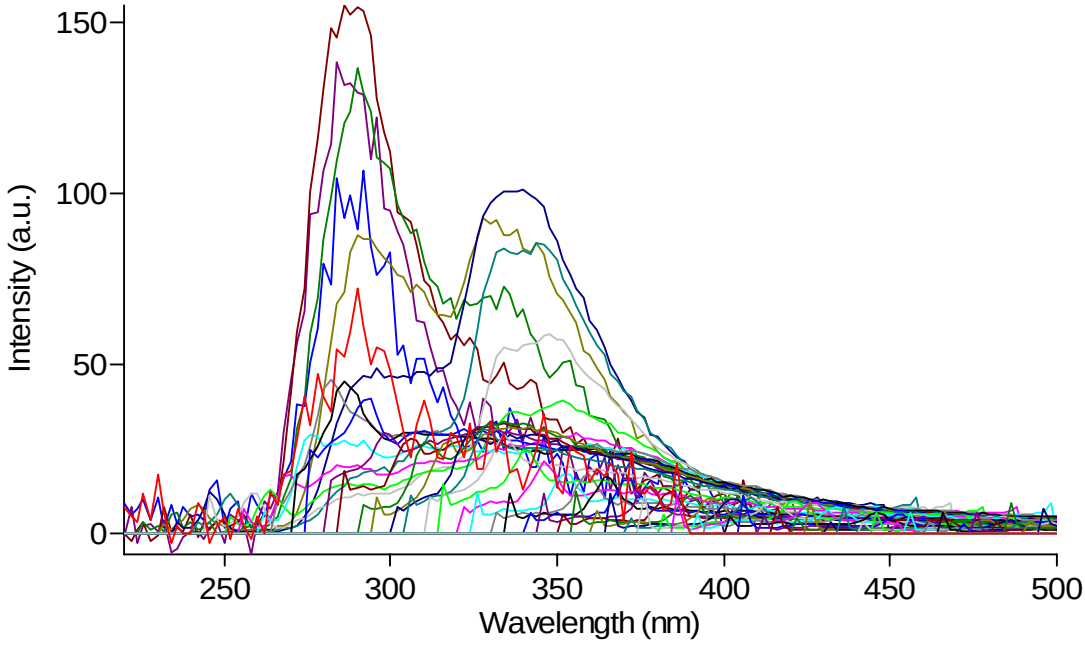
150
100
50
0
Intensity (a.u.)
250
300
350
400
450
500
Wavelength (nm)

34BT

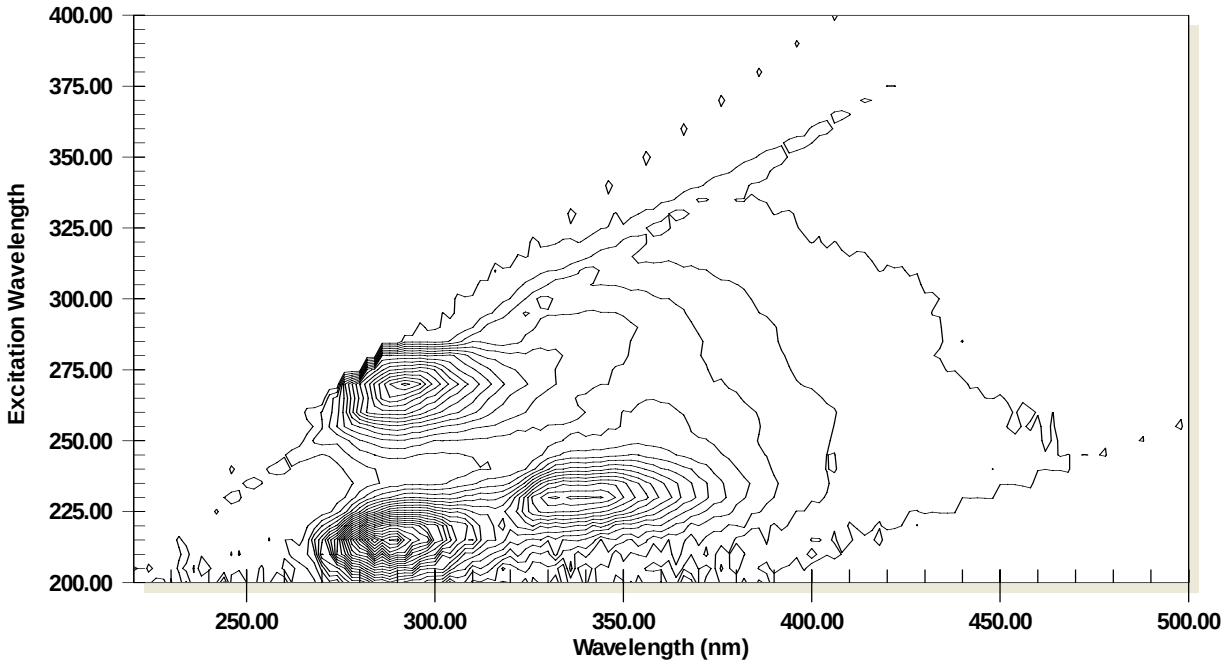
Excitation Wavelength
400.00
375.00
350.00
325.00
300.00
275.00
250.00
225.00
200.00
250.00
300.00
350.00
400.00
450.00
500.00
Wavelength (nm)

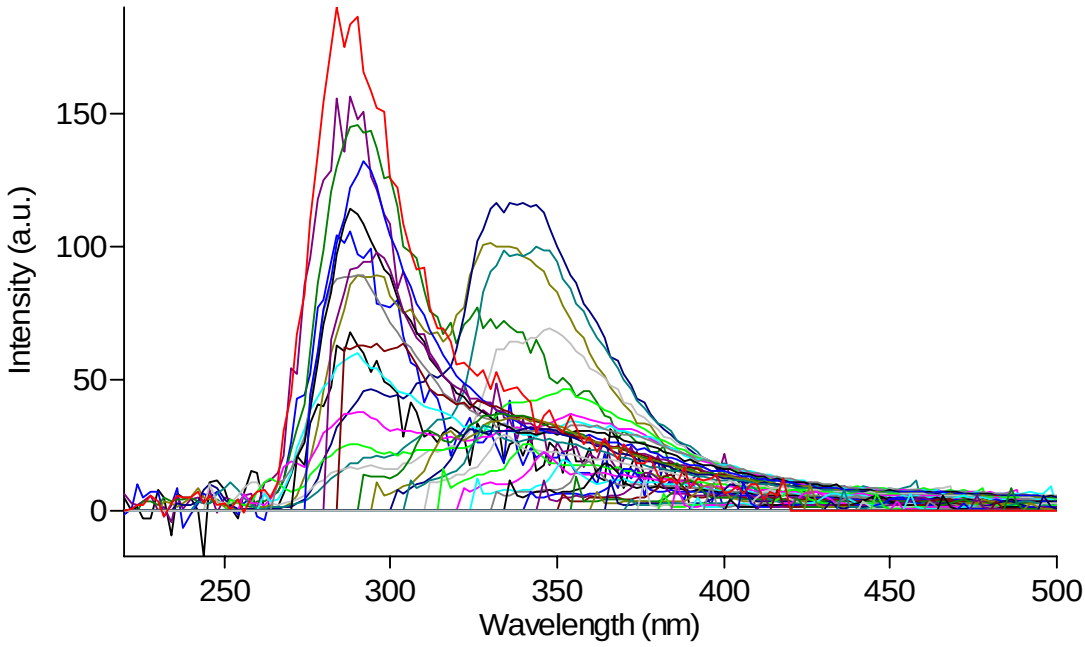
Intensity (a.u.)
150
100
50
0
250
300
350
400
450
500
Wavelength (nm)

35CT

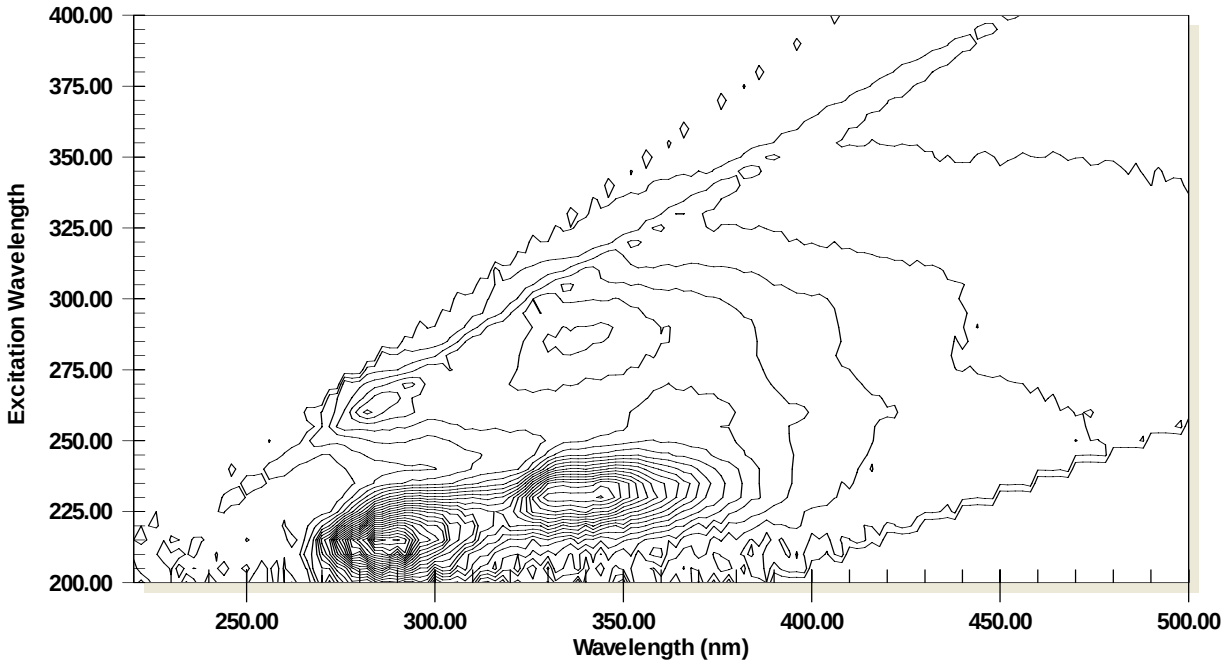
400.00
375.00
350.00
325.00
300.00
275.00
250.00
225.00
200.00
Excitation Wavelength
250.00
300.00
350.00
400.00
450.00
500.00
Wavelength (nm)

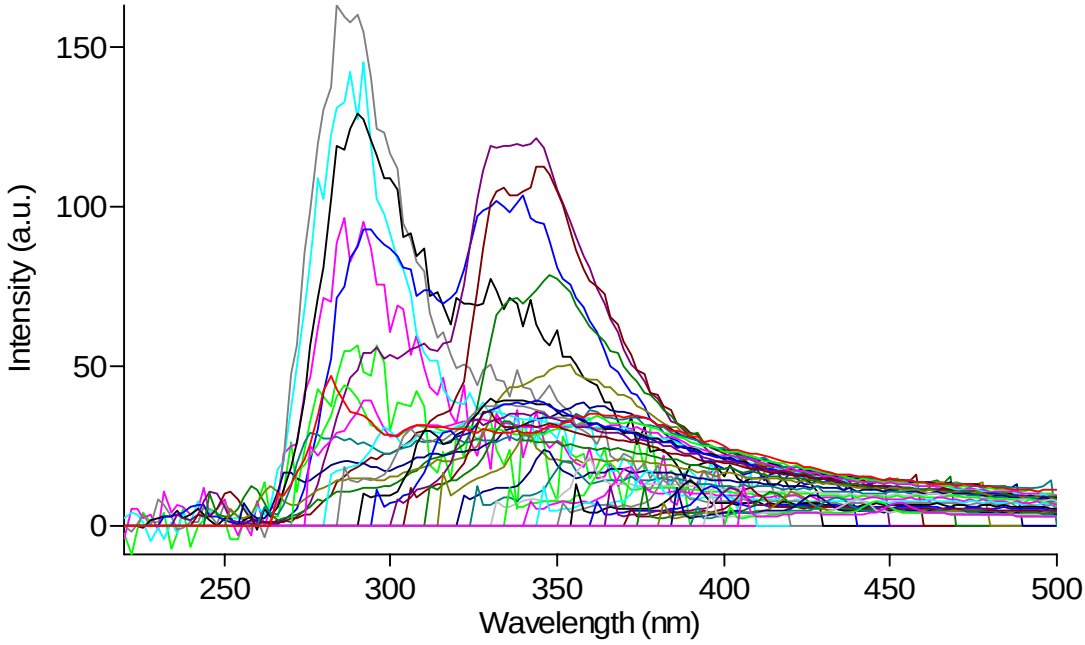
150
100
50
0
Intensity (a.u.)
250
300
350
400
450
500
Wavelength (nm)

41CT

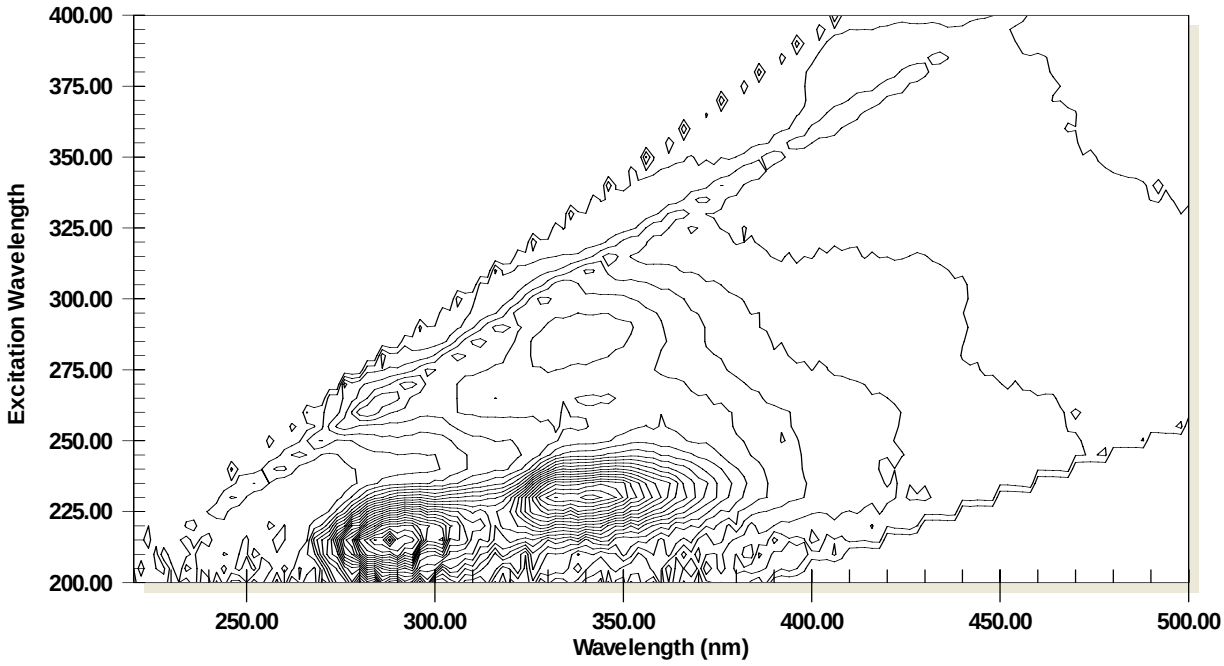
Excitation Wavelength
400.00
375.00
350.00
325.00
300.00
275.00
250.00
225.00
200.00
250.00
300.00
350.00
400.00
450.00
500.00
Wavelength (nm)

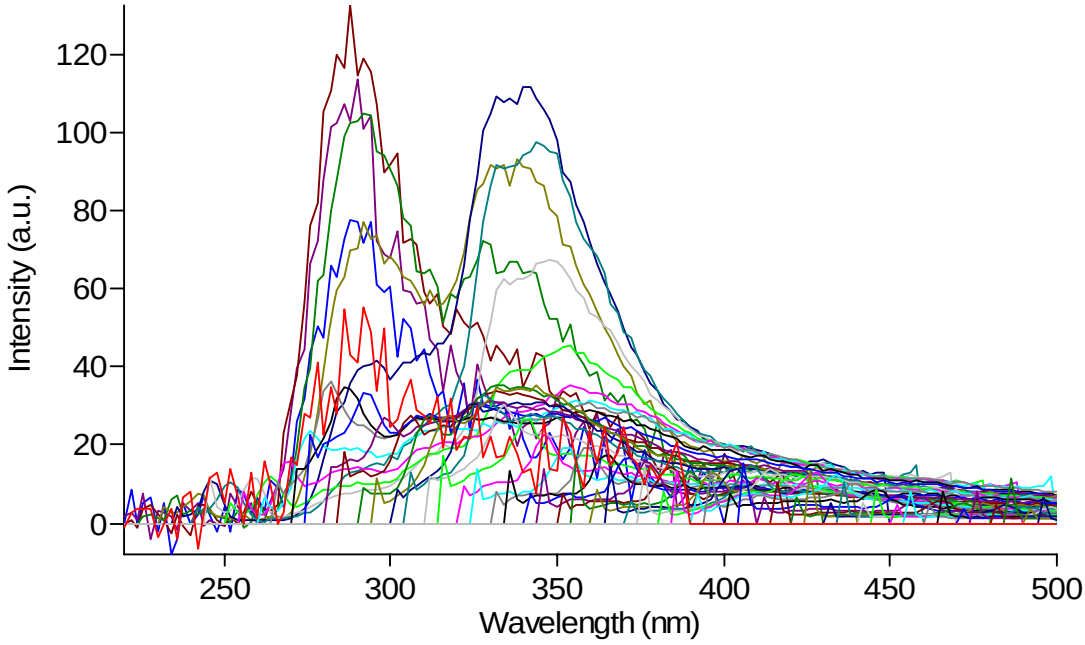
Intensity (a.u.)
120
100
80
60
40
20
0
250
300
350
400
450
500
Wavelength (nm)

42BT

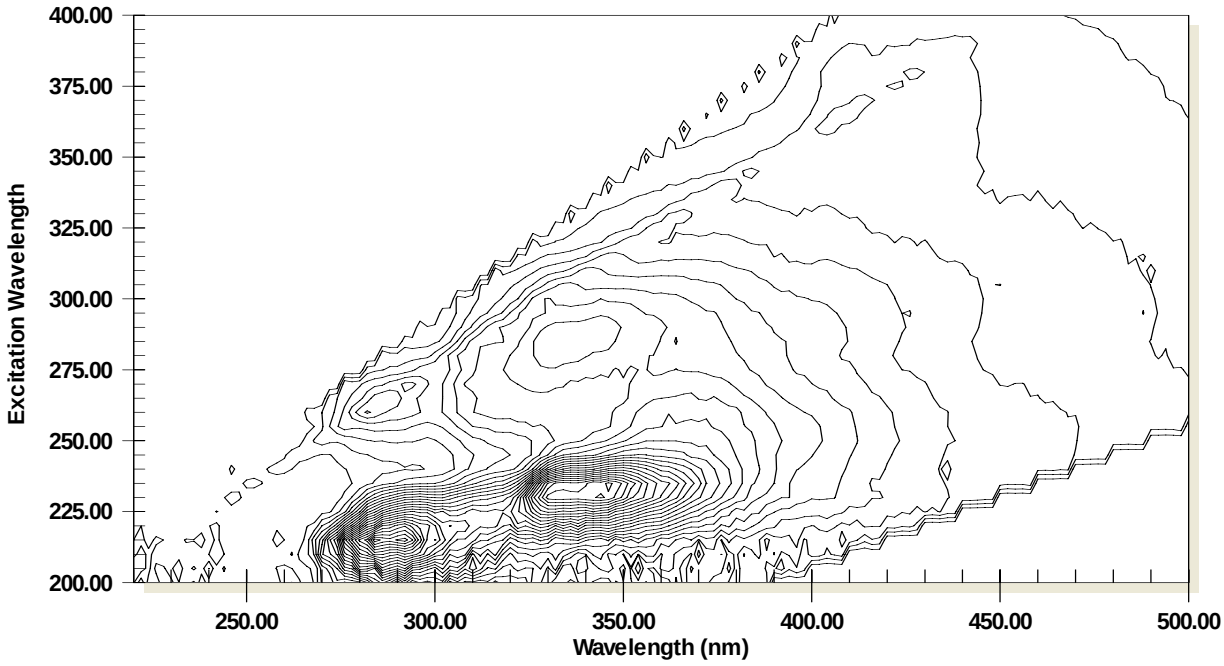
400.00
375.00
350.00
325.00
300.00
275.00
250.00
225.00
200.00
Excitation Wavelength
250.00
300.00
350.00
400.00
450.00
500.00
Wavelength (nm)

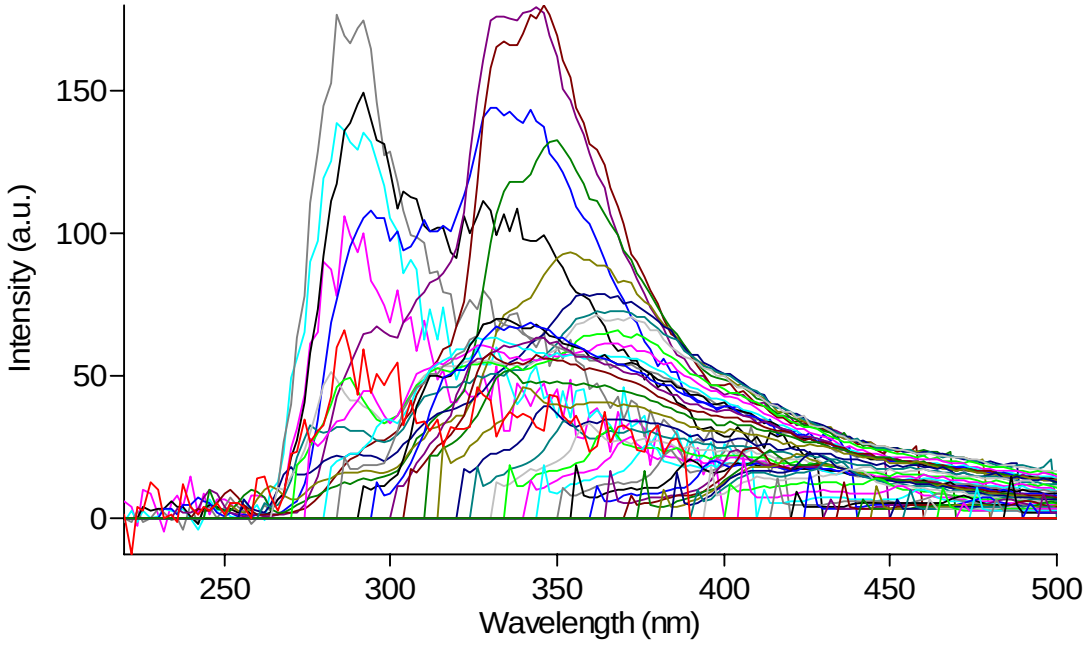
150
100
50
0
Intensity (a.u.)
250
300
350
400
450
500
Wavelength (nm)

43AT

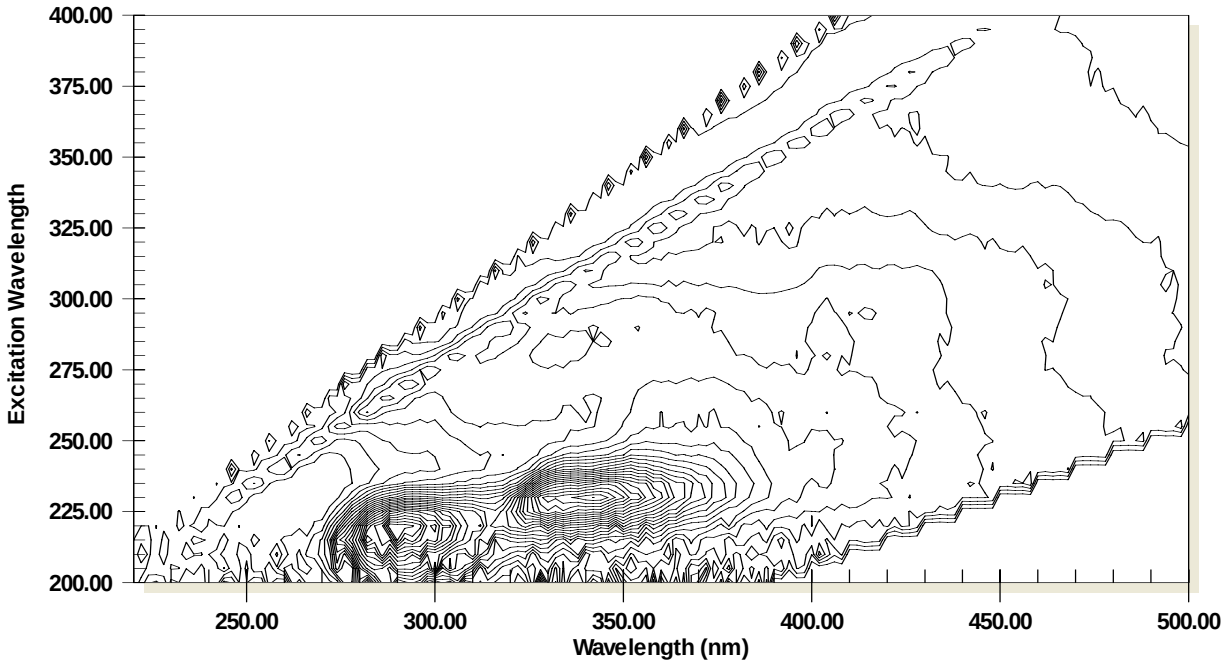
Excitation Wavelength
400.00
375.00
350.00
325.00
300.00
275.00
250.00
225.00
200.00
250.00
300.00
350.00
400.00
450.00
500.00
Wavelength (nm)

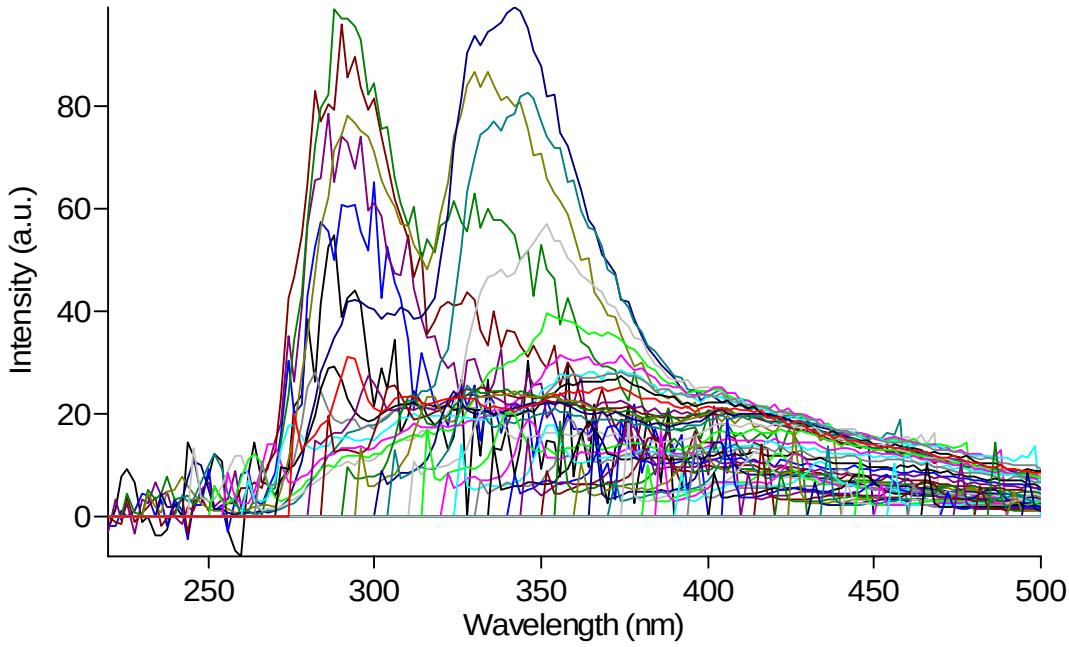
Intensity (a.u.)
80
60
40
20
0
250
300
350
400
450
500
Wavelength (nm)

44AT

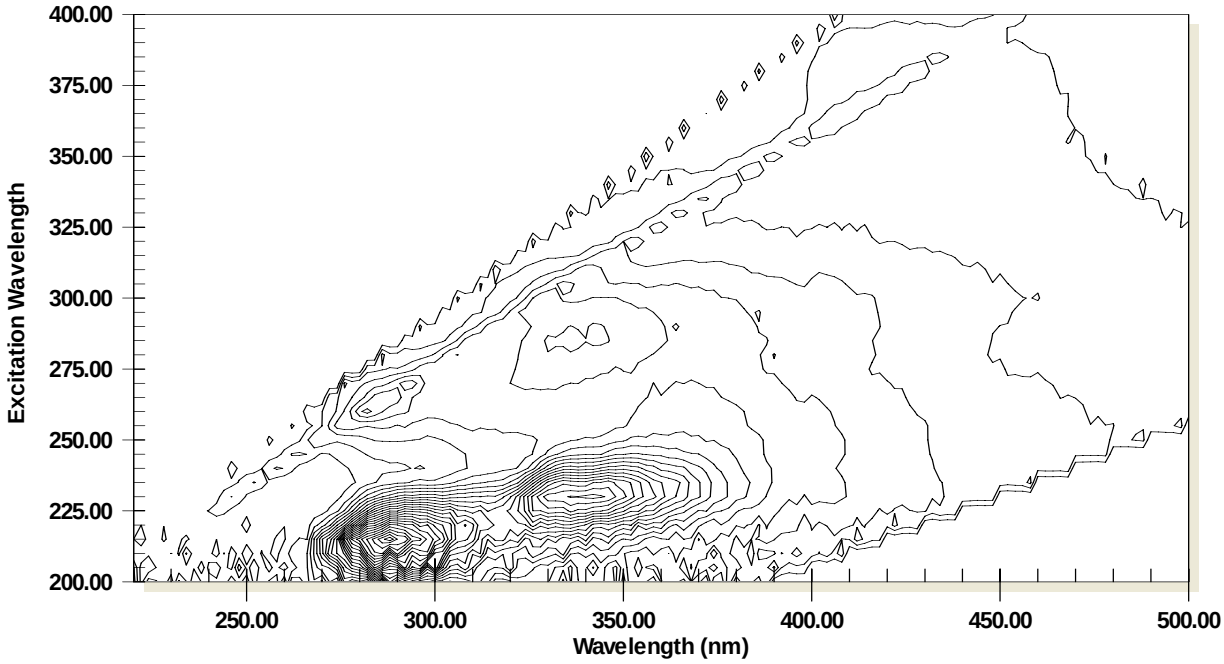
400.00
375.00
350.00
325.00
300.00
275.00
250.00
225.00
200.00
Excitation Wavelength
250.00
300.00
350.00
400.00
450.00
500.00
Wavelength (nm)

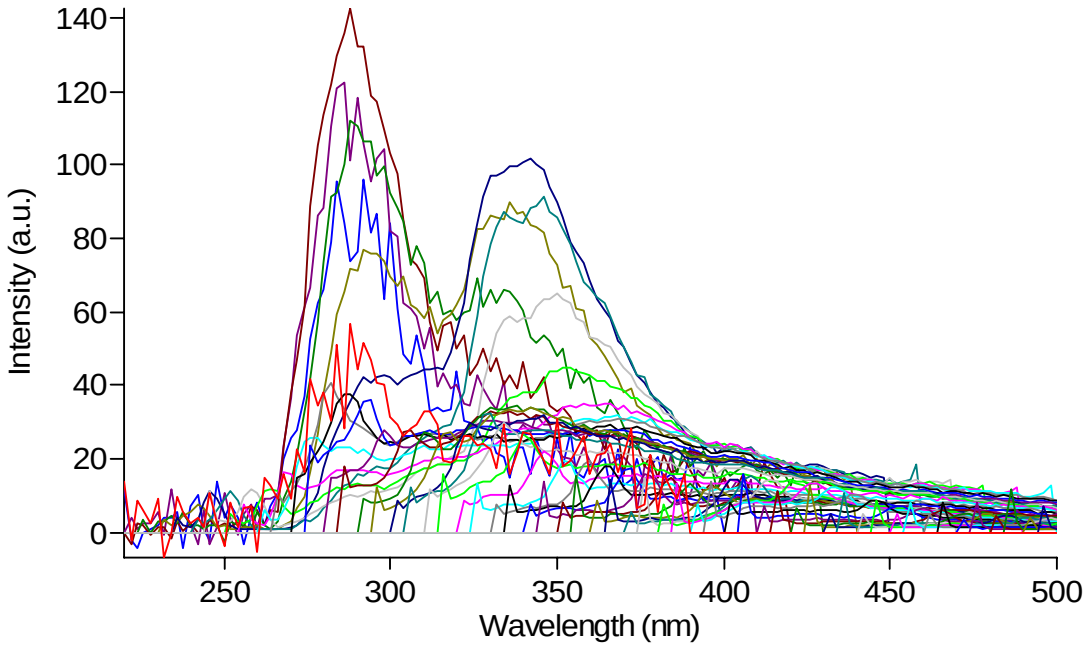
140
120
100
80
60
40
20
0
Intensity (a.u.)
250
300
350
400
450
500
Wavelength (nm)

45CT

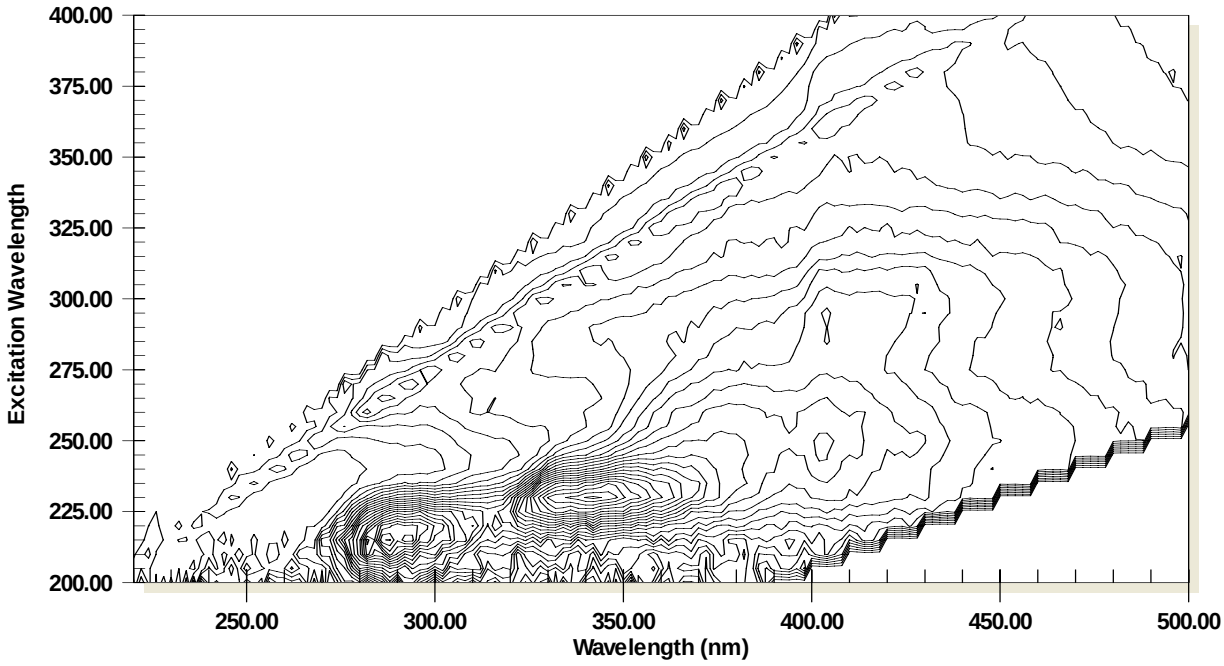
400.00
375.00
350.00
325.00
300.00
275.00
250.00
225.00
200.00
Excitation Wavelength
250.00
300.00
350.00
400.00
450.00
500.00
Wavelength (nm)

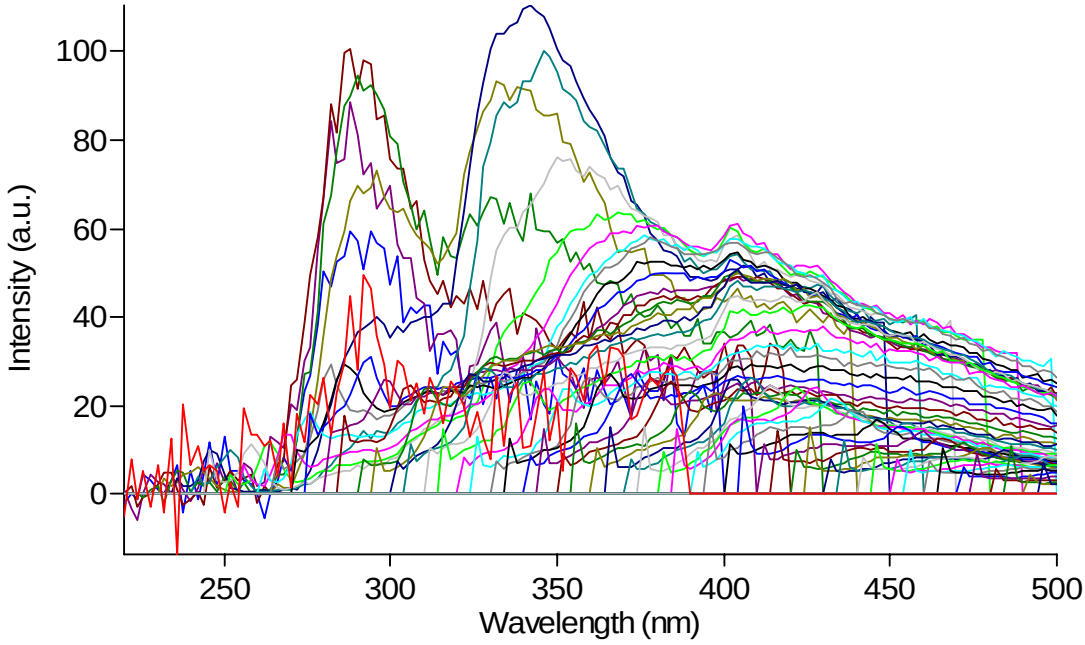
100
80
60
40
20
0
Intensity (a.u.)
250
300
350
400
450
500
Wavelength (nm)

51CT

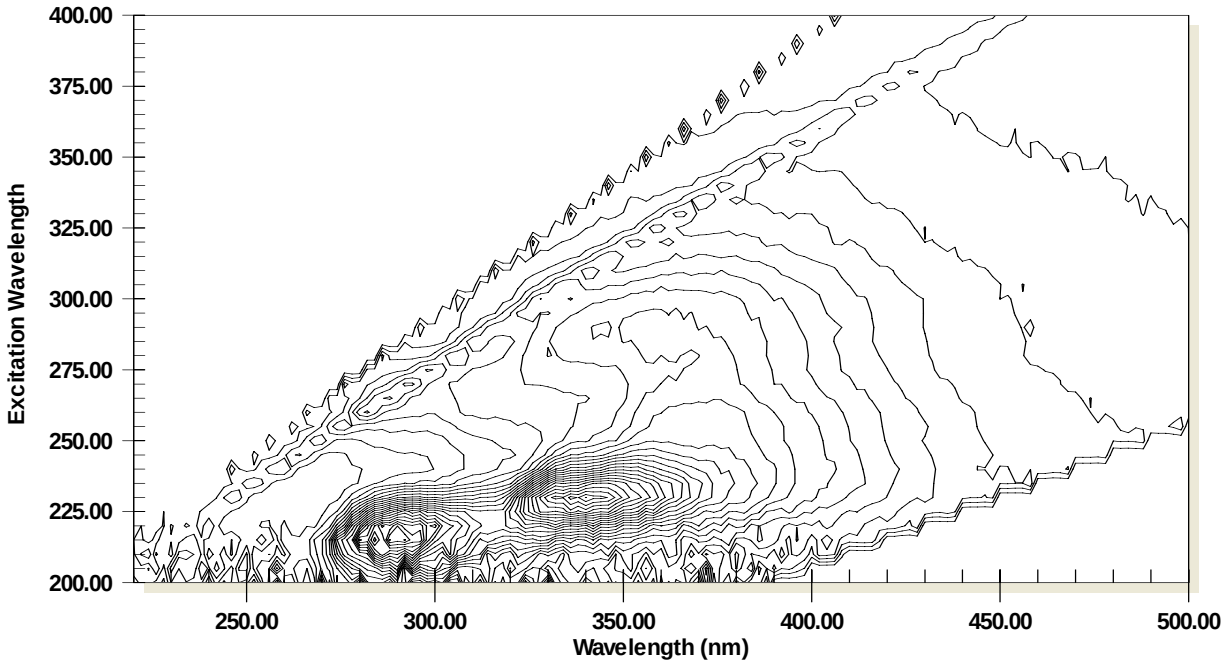
Excitation Wavelength
400.00
375.00
350.00
325.00
300.00
275.00
250.00
225.00
200.00
250.00
300.00
350.00
400.00
450.00
500.00
Wavelength (nm)

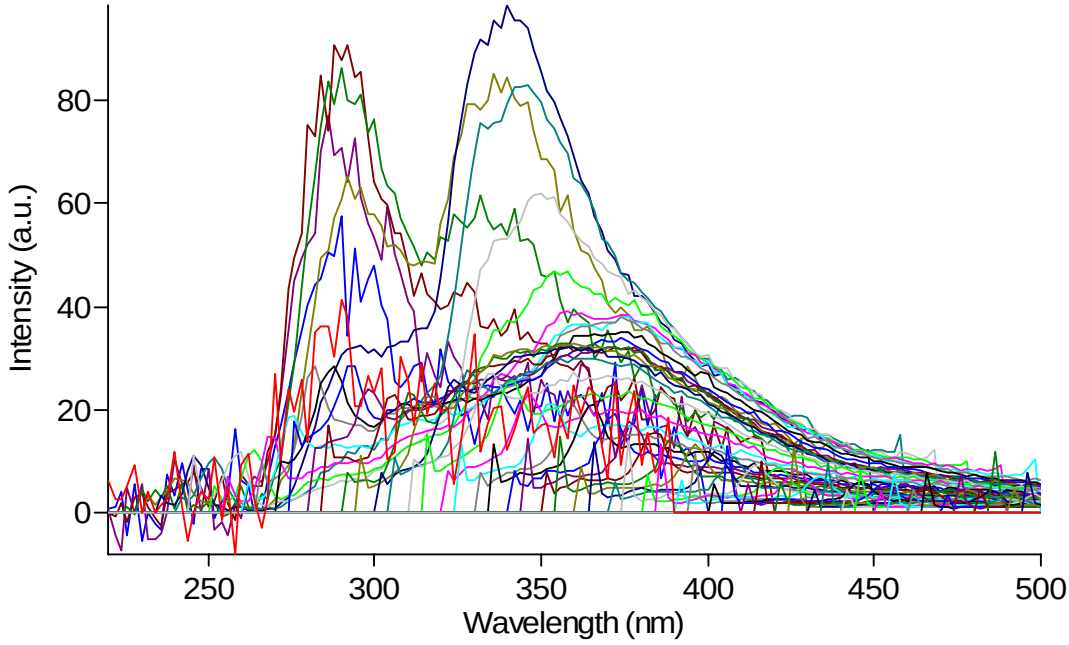
Intensity (a.u.)
80
60
40
20
0
250
300
350
400
450
500
Wavelength (nm)

52BT

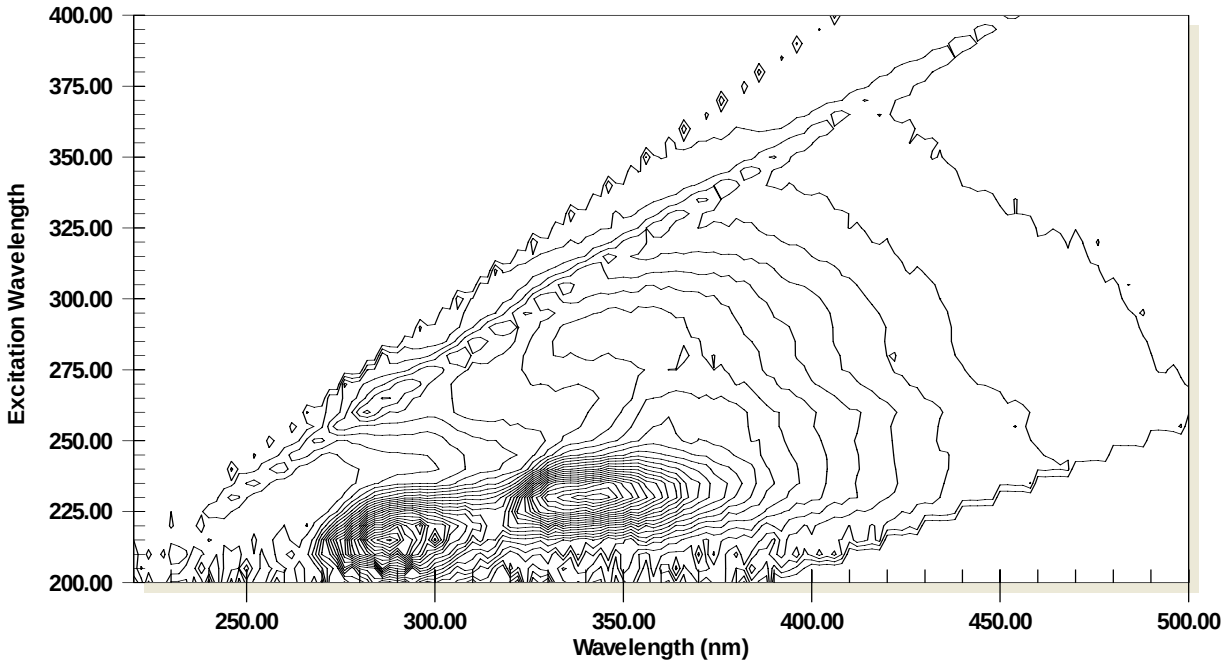
400.00
375.00
350.00
325.00
300.00
275.00
250.00
225.00
200.00
Excitation Wavelength
250.00
300.00
350.00
400.00
450.00
500.00
Wavelength (nm)

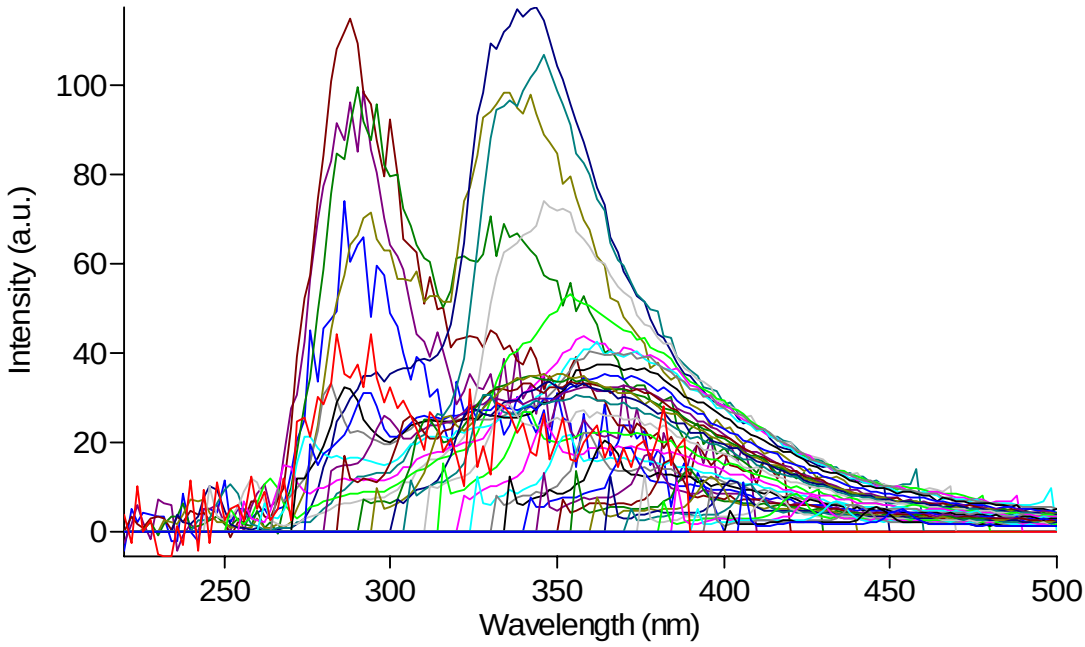
100
80
60
40
20
0
Intensity (a.u.)
250
300
350
400
450
500
Wavelength (nm)

53AT

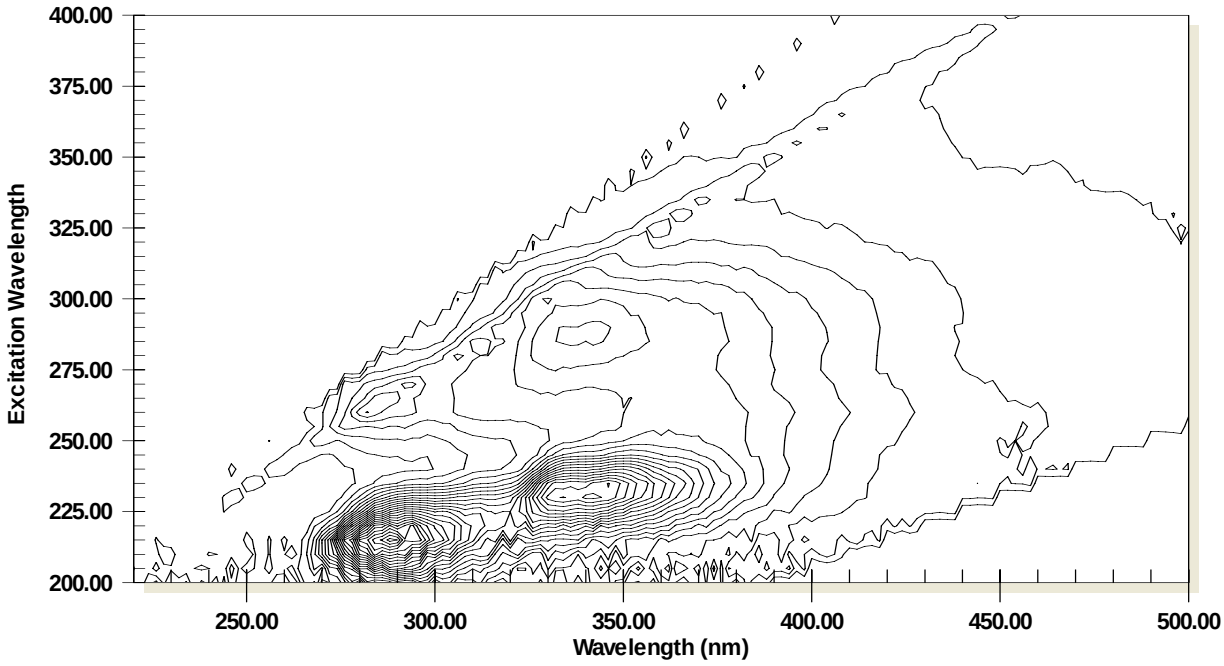
400.00
375.00
350.00
325.00
300.00
275.00
250.00
225.00
200.00
Excitation Wavelength
250.00
300.00
350.00
400.00
450.00
500.00
Wavelength (nm)

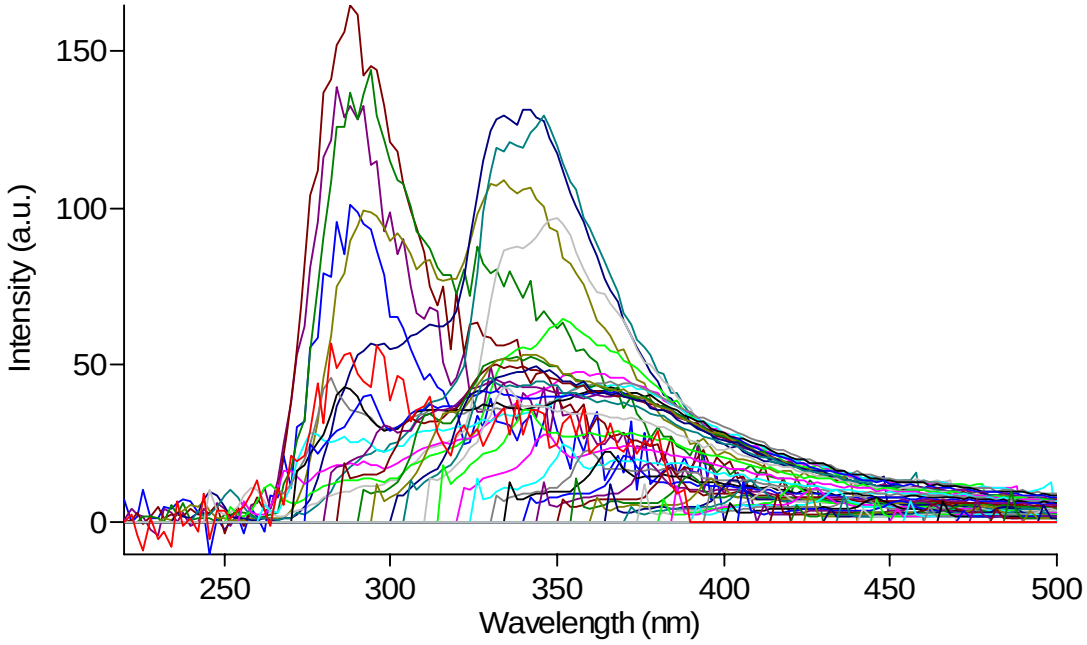
150
100
50
0
Intensity (a.u.)
250
300
350
400
450
500
Wavelength (nm)

54BT

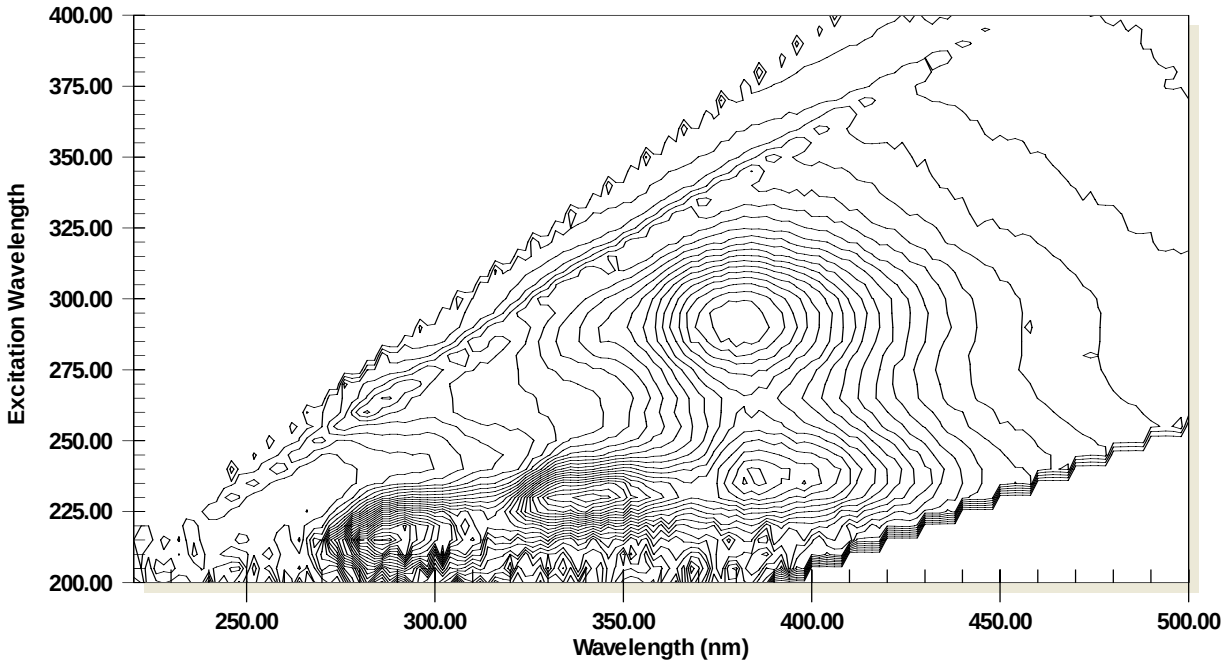
400.00
375.00
350.00
325.00
300.00
275.00
250.00
225.00
200.00
Excitation Wavelength
250.00
300.00
350.00
400.00
450.00
500.00
Wavelength (nm)

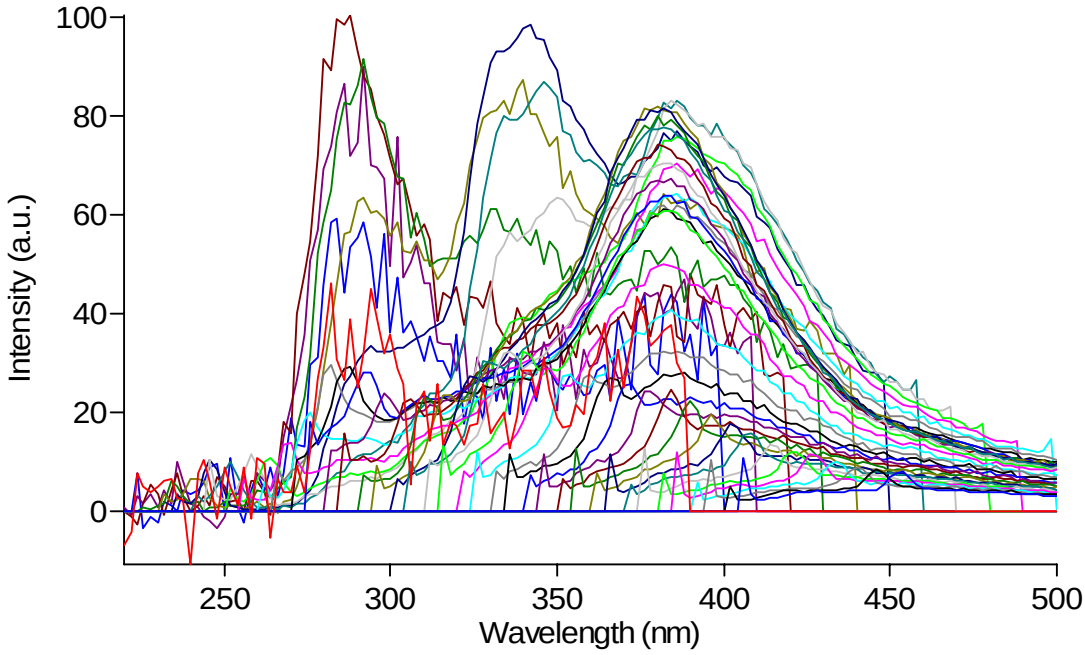
100
80
60
40
20
0
Intensity (a.u.)
250
300
350
400
450
500
Wavelength (nm)

55CT

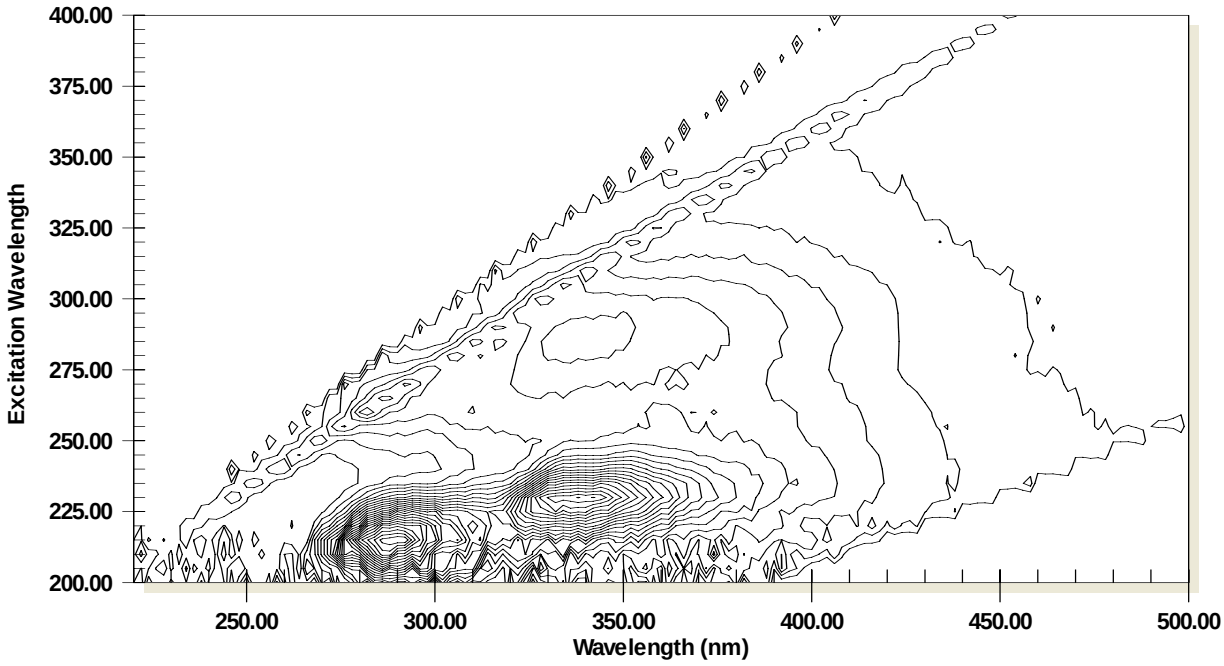
400.00
375.00
350.00
325.00
300.00
275.00
250.00
225.00
200.00
Excitation Wavelength
250.00
300.00
350.00
400.00
450.00
500.00
Wavelength (nm)

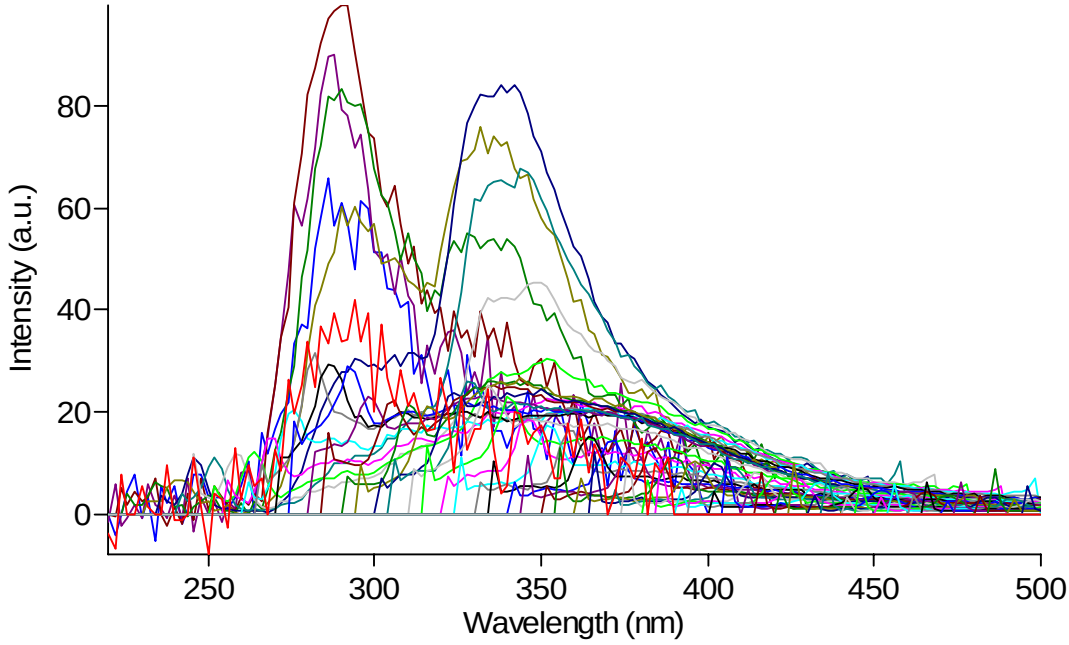
80
60
40
20
0
Intensity (a.u.)
250
300
350
400
450
500
Wavelength (nm)

350

61AT

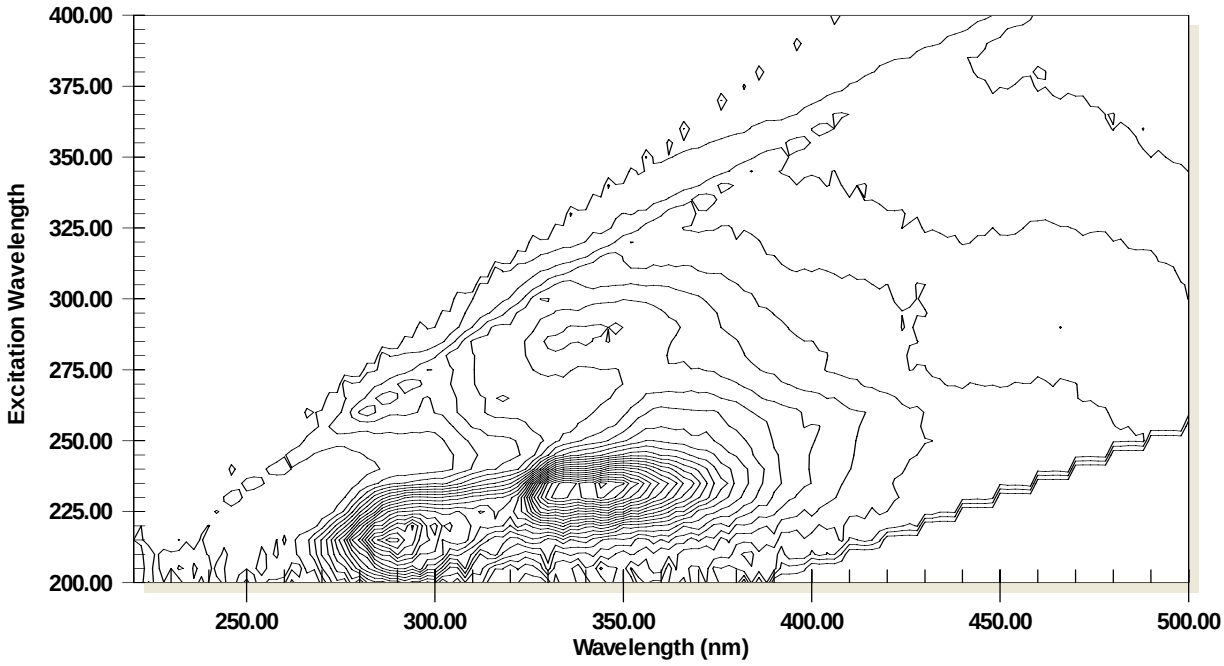
400.00
375.00
350.00
325.00
300.00
275.00
250.00
225.00
200.00
Excitation Wavelength
250.00
300.00
350.00
400.00
450.00
500.00
Wavelength (nm)

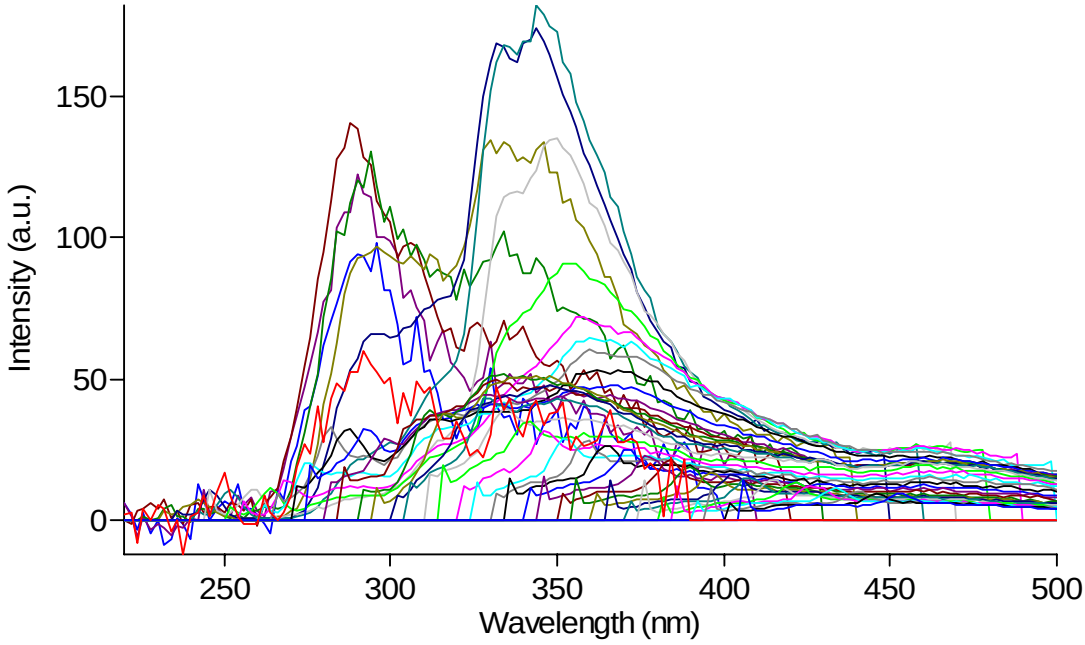
150
100
50
0
Intensity (a.u.)
250
300
350
400
450
500
Wavelength (nm)

62CT

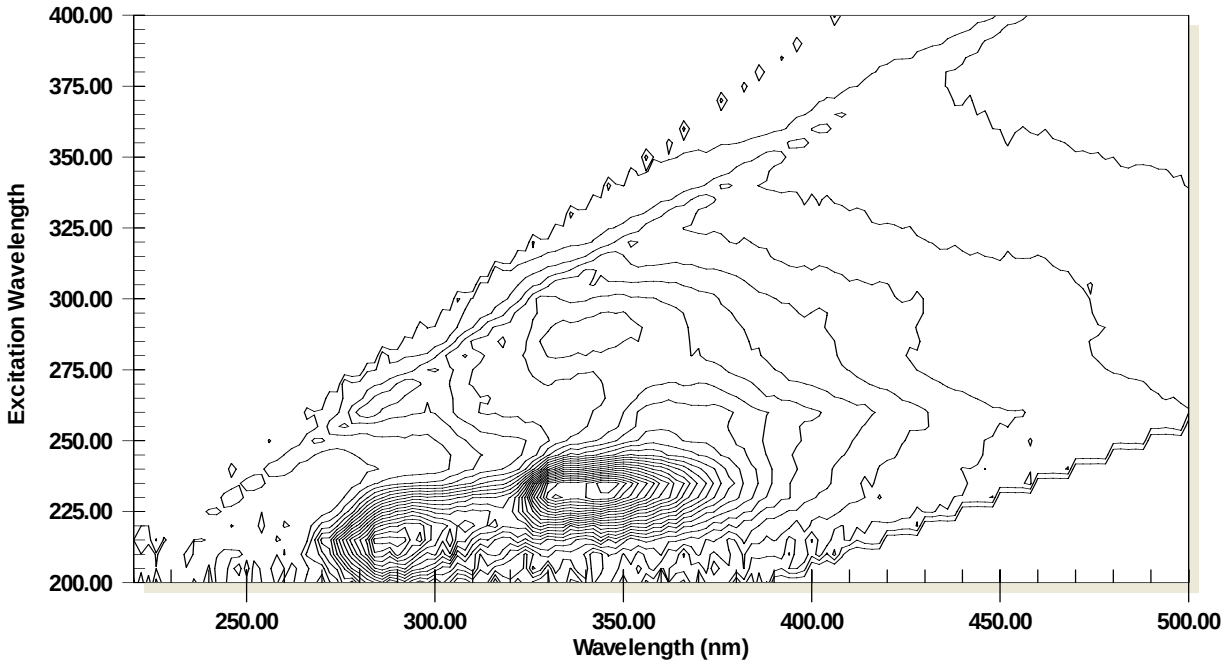
Excitation Wavelength
400.00
375.00
350.00
325.00
300.00
275.00
250.00
225.00
200.00
250.00
300.00
350.00
400.00
450.00
500.00
Wavelength (nm)

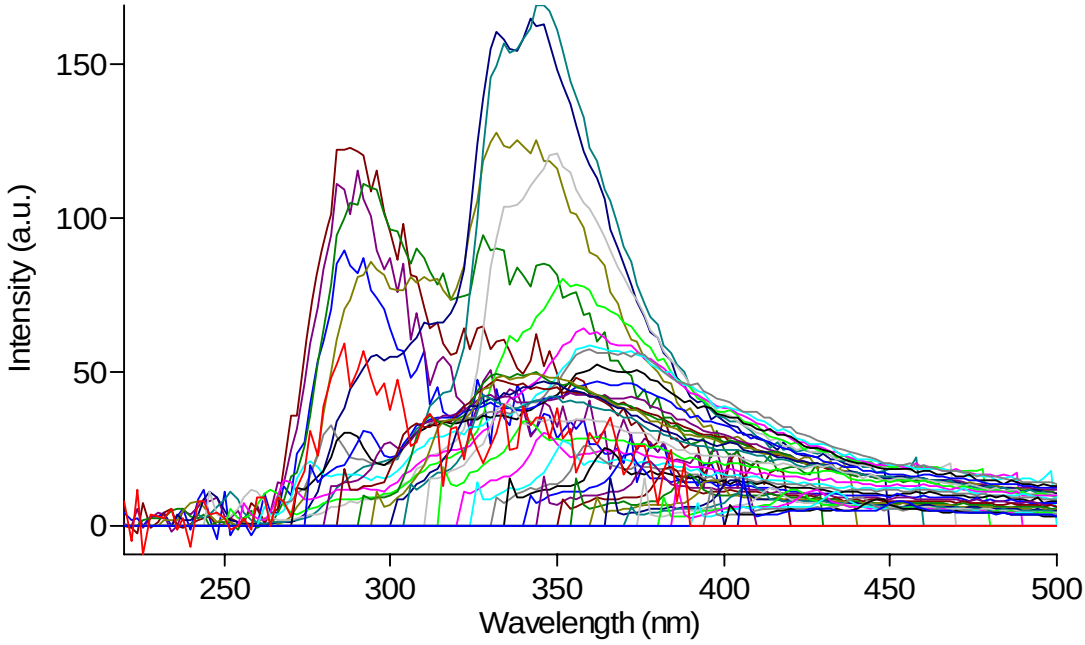
Intensity (a.u.)
150
100
50
0
250
300
350
400
450
500
Wavelength (nm)

63BT

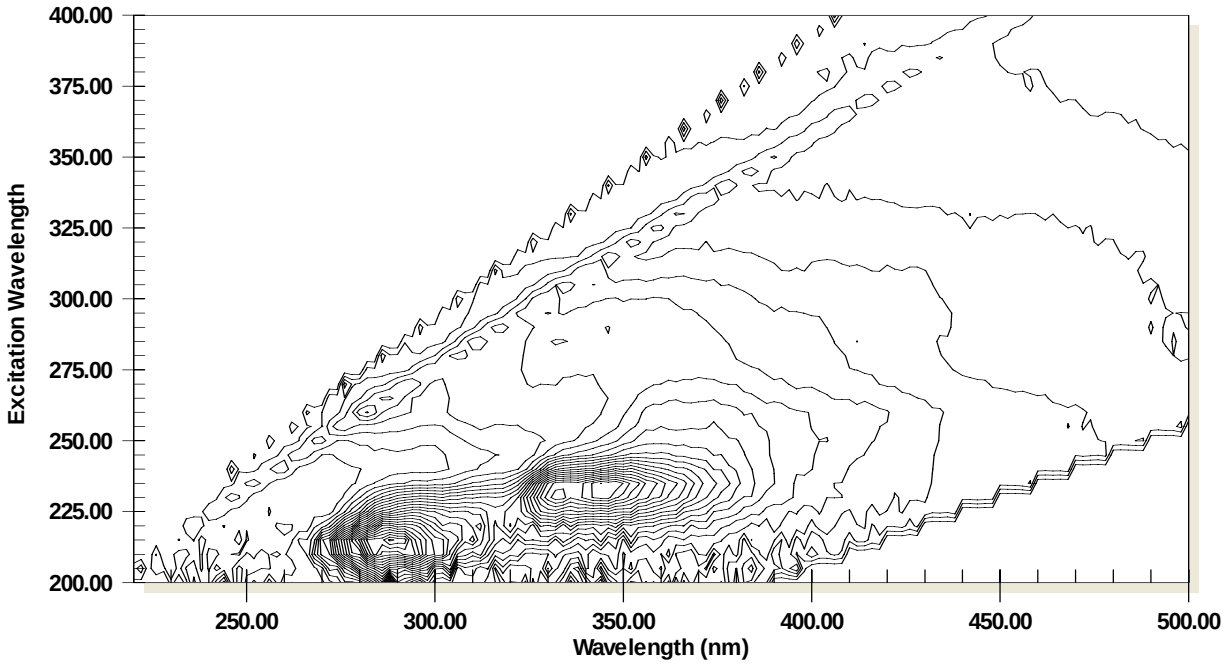
400.00
375.00
350.00
325.00
300.00
275.00
250.00
225.00
200.00
Excitation Wavelength
250.00
300.00
350.00
400.00
450.00
500.00
Wavelength (nm)

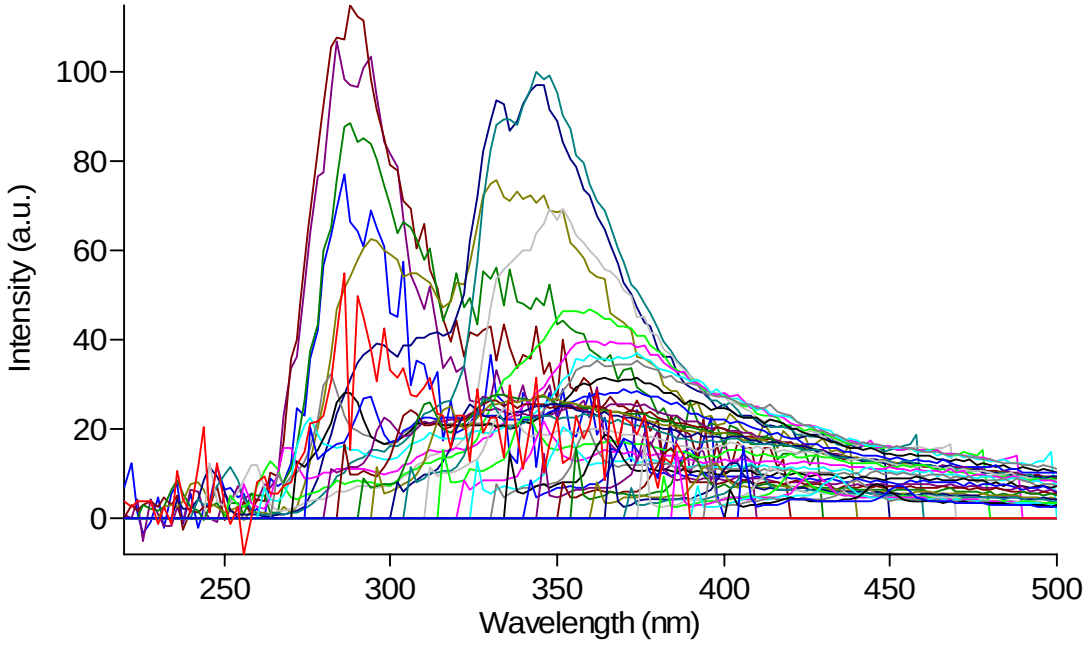
100
80
60
40
20
0
Intensity (a.u.)
250
300
350
400
450
500
Wavelength (nm)

64AT

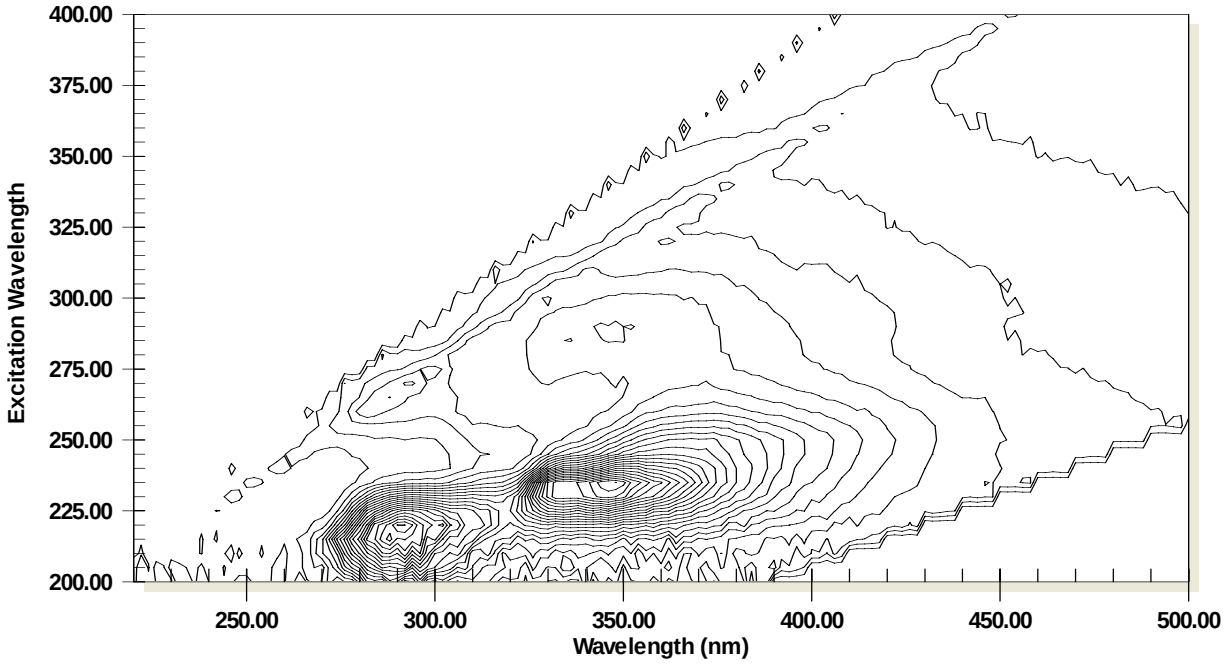
Excitation Wavelength
400.00
375.00
350.00
325.00
300.00
275.00
250.00
225.00
200.00
250.00
300.00
350.00
400.00
450.00
500.00
Wavelength (nm)

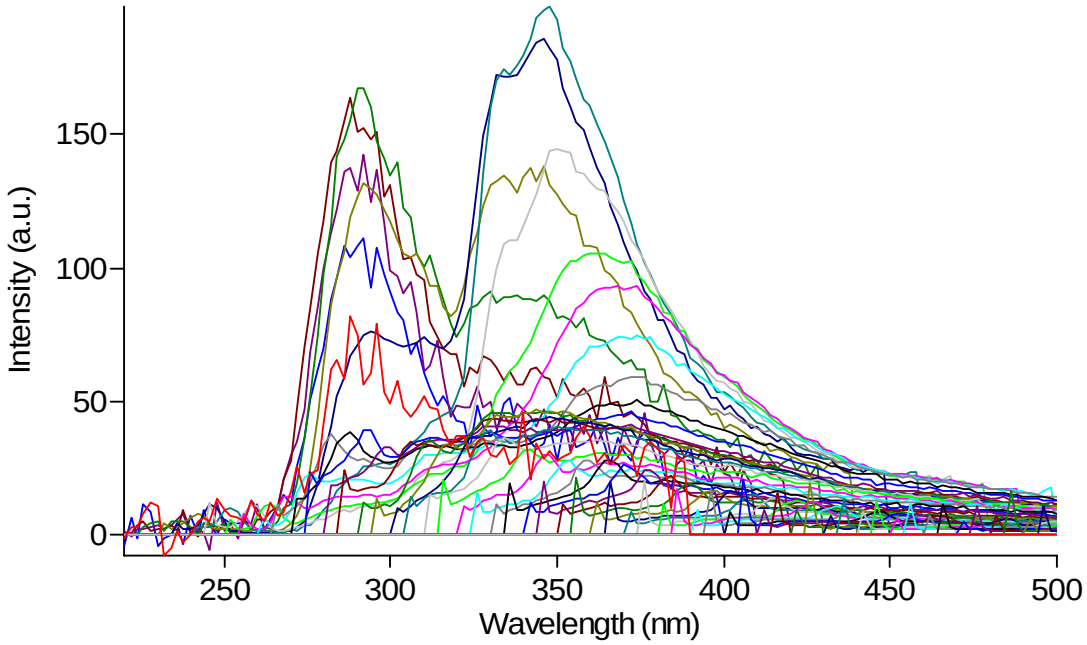
Intensity (a.u.)
150
100
50
0
250
300
350
400
450
500
Wavelength (nm)

65BT

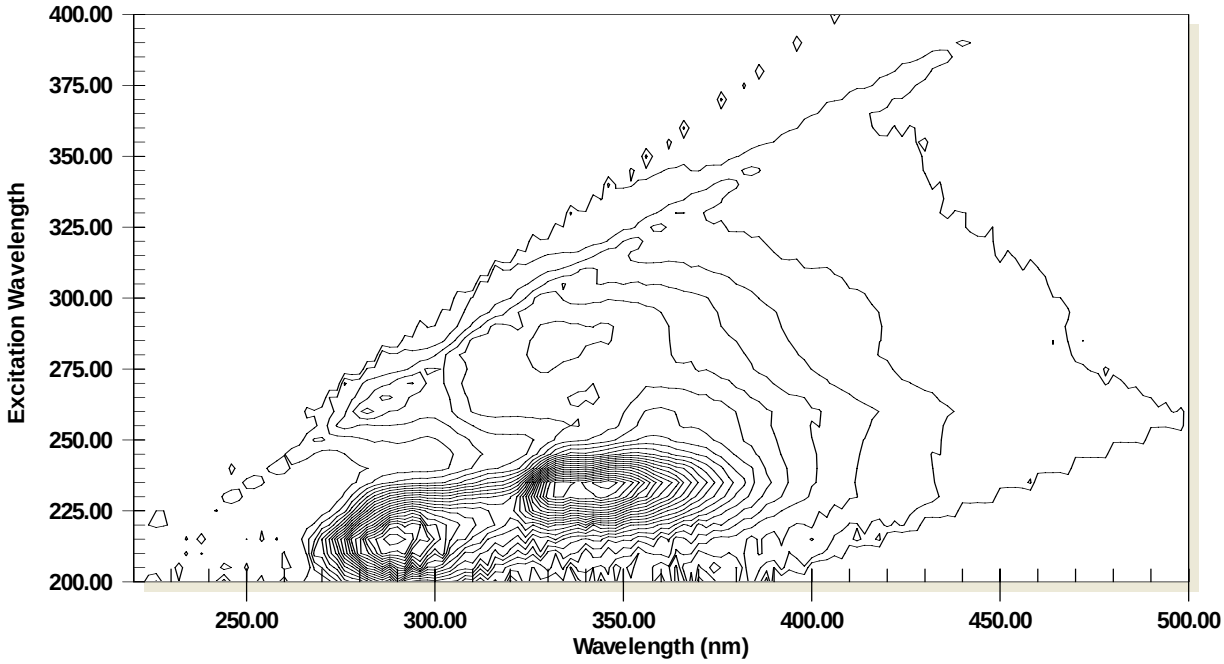
Excitation Wavelength
400.00
375.00
350.00
325.00
300.00
275.00
250.00
225.00
200.00
250.00
300.00
350.00
400.00
450.00
500.00
Wavelength (nm)

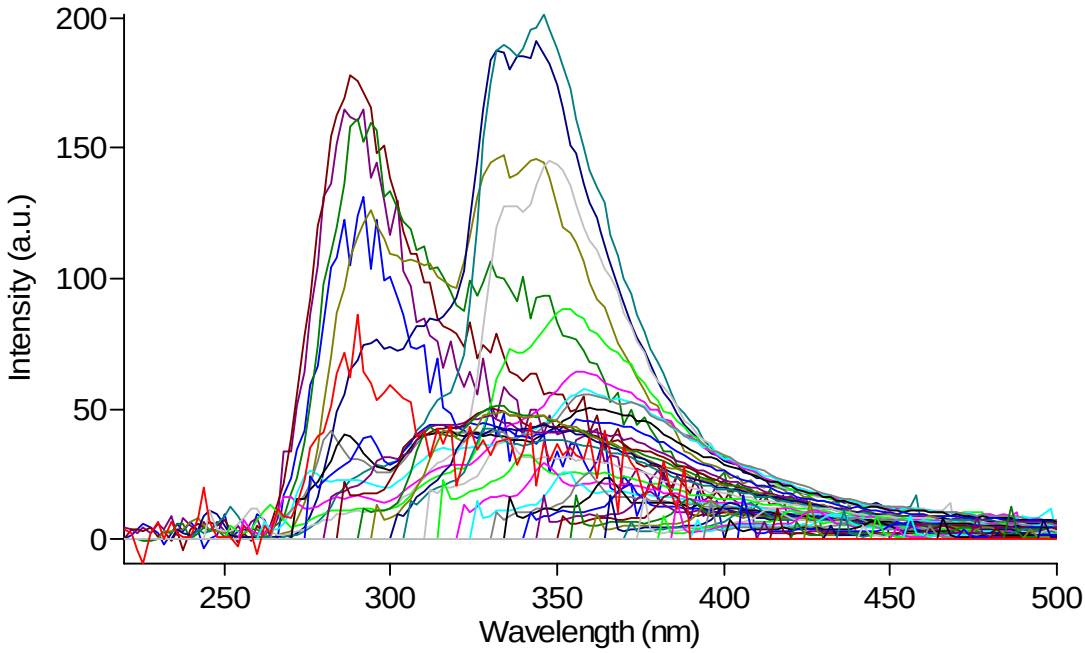
Intensity (a.u.)
200
150
100
50
0
250
300
350
400
450
500
Wavelength (nm)

71BT

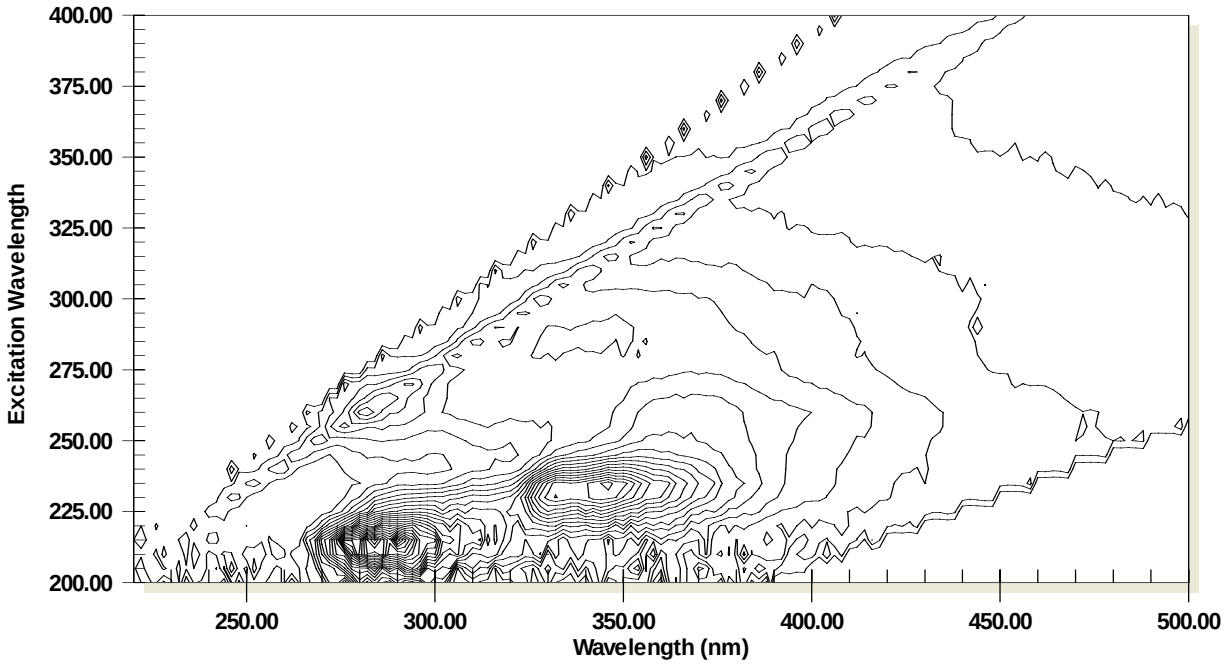
400.00
375.00
350.00
325.00
300.00
275.00
250.00
225.00
200.00
Excitation Wavelength
250.00
300.00
350.00
400.00
450.00
500.00
Wavelength (nm)

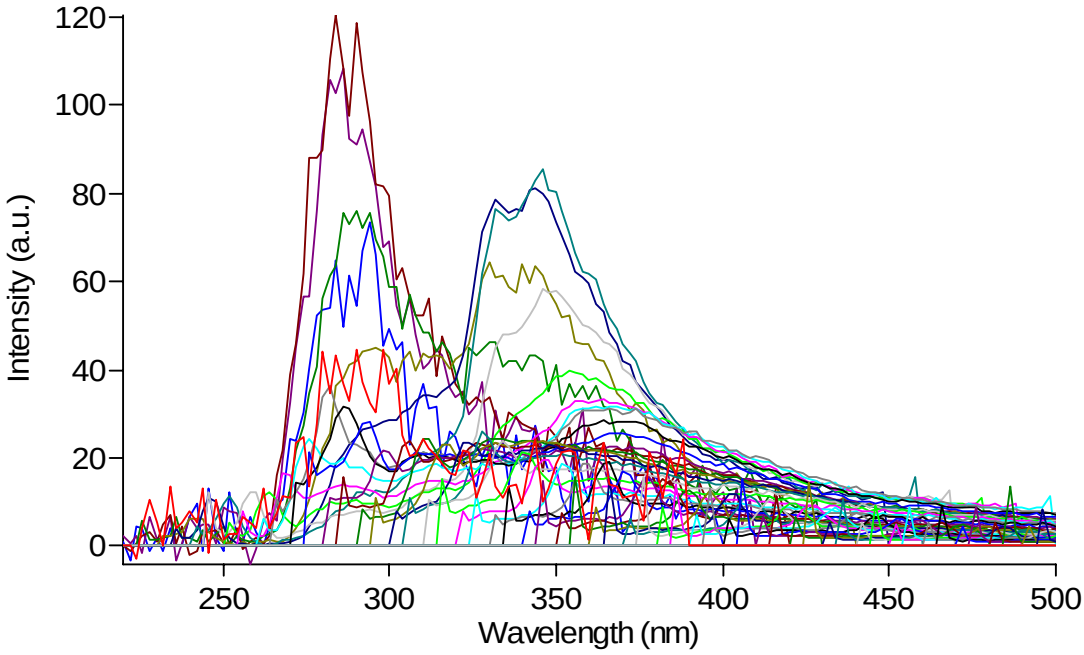
120
100
80
60
40
20
0
Intensity (a.u.)
250
300
350
400
450
500
Wavelength (nm)

72AT

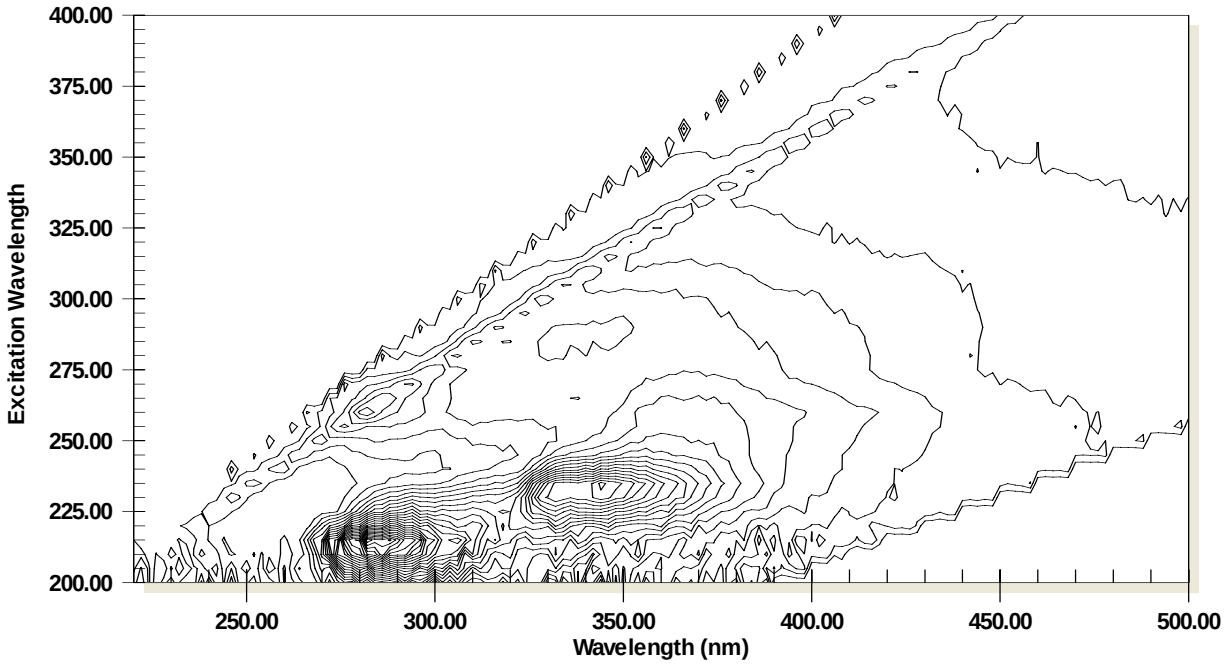
400.00
375.00
350.00
325.00
300.00
275.00
250.00
225.00
200.00
Excitation Wavelength
250.00
300.00
350.00
400.00
450.00
500.00
Wavelength (nm)

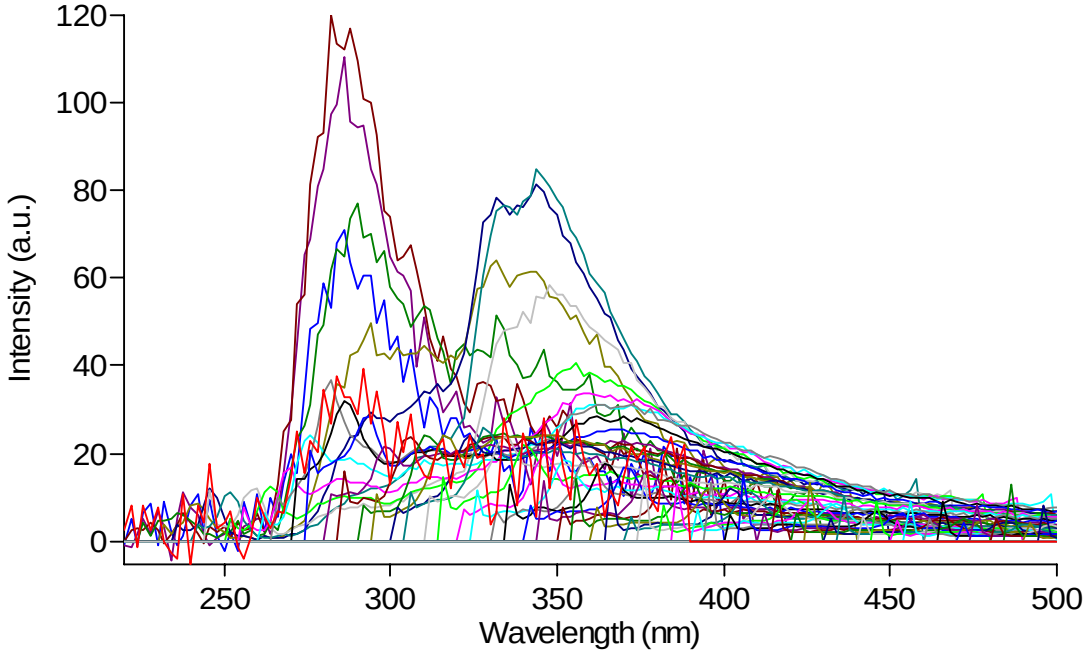
120
100
80
60
40
20
0
Intensity (a.u.)
250
300
350
400
450
500
Wavelength (nm)

73CT

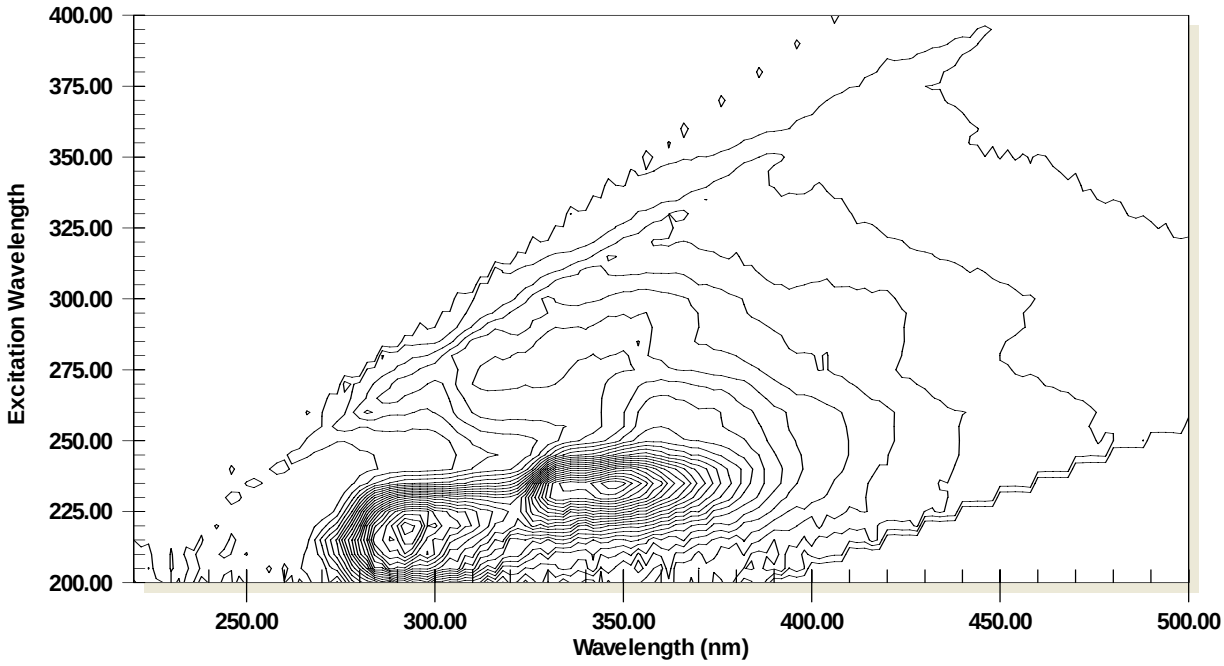
400.00
375.00
350.00
325.00
300.00
275.00
250.00
225.00
200.00
Excitation Wavelength
250.00
300.00
350.00
400.00
450.00
500.00
Wavelength (nm)

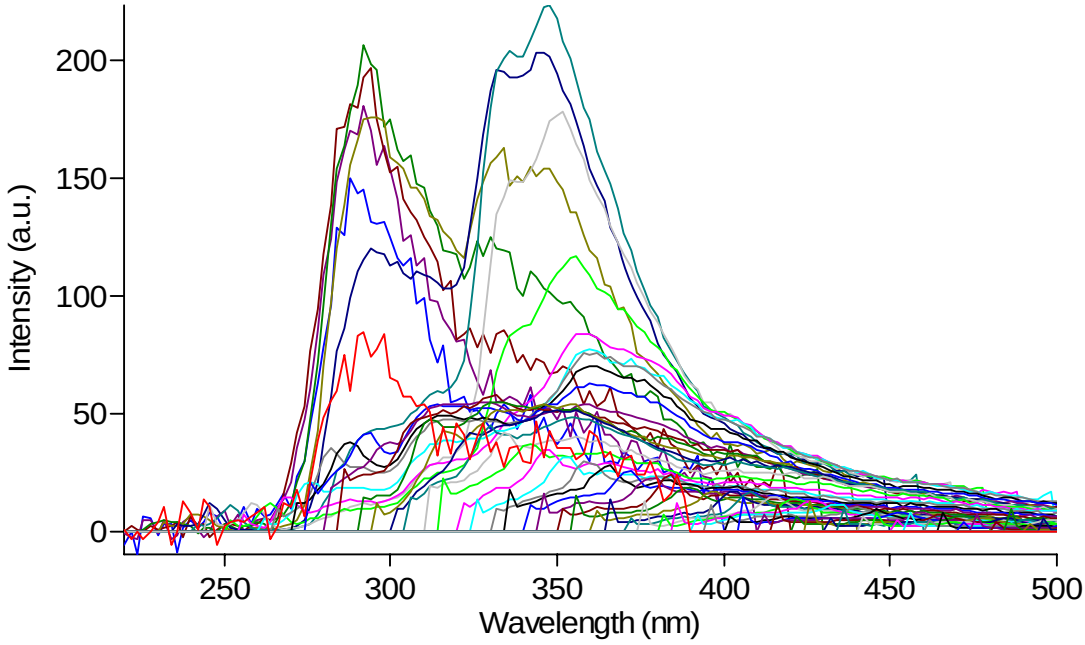
200
150
100
50
0
Intensity (a.u.)
250
300
350
400
450
500
Wavelength (nm)

74AT

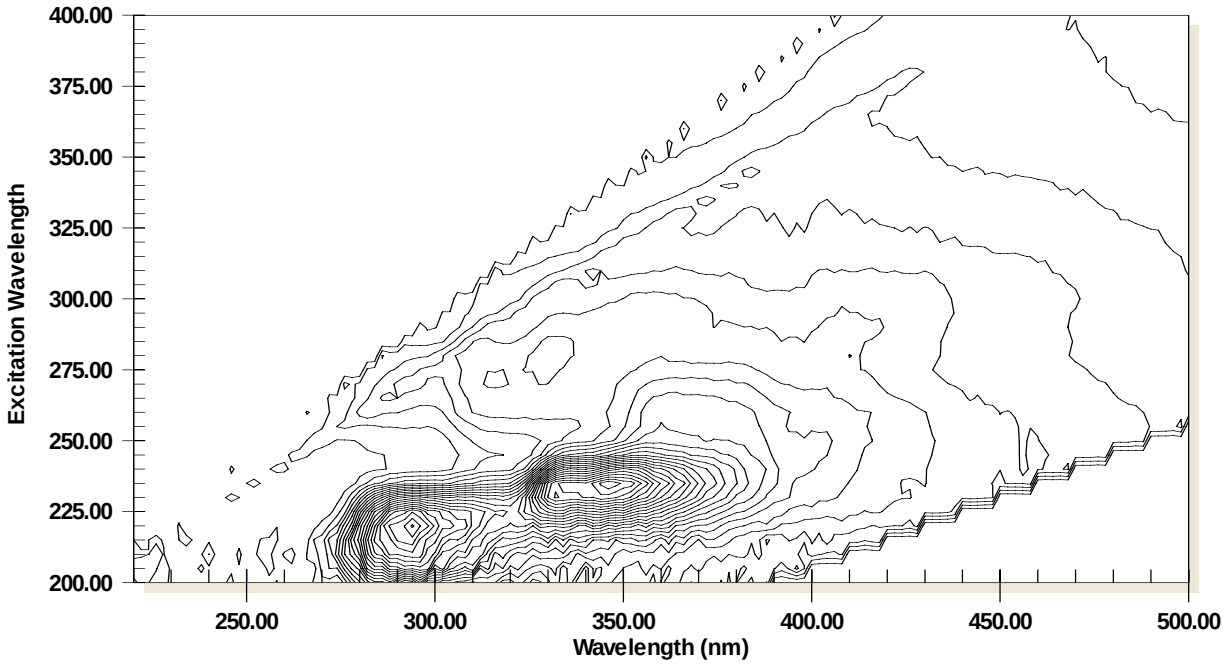
400.00
375.00
350.00
325.00
300.00
275.00
250.00
225.00
200.00
Excitation Wavelength
250.00
300.00
350.00
400.00
450.00
500.00
Wavelength (nm)

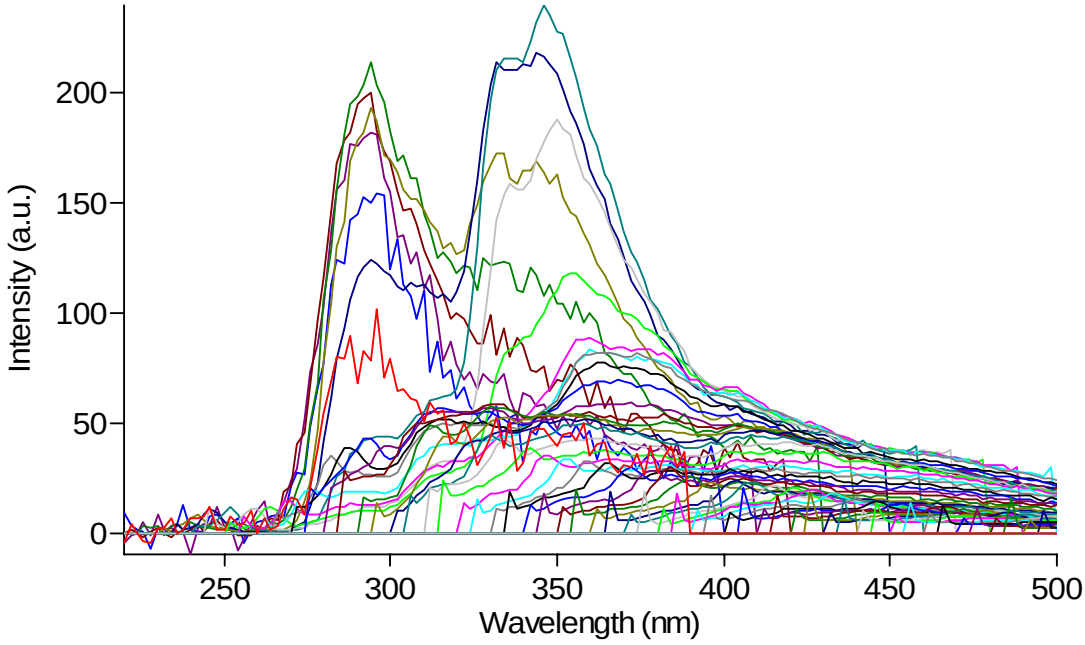
200
150
100
50
0
Intensity (a.u.)
250
300
350
400
450
500
Wavelength (nm)

75AT

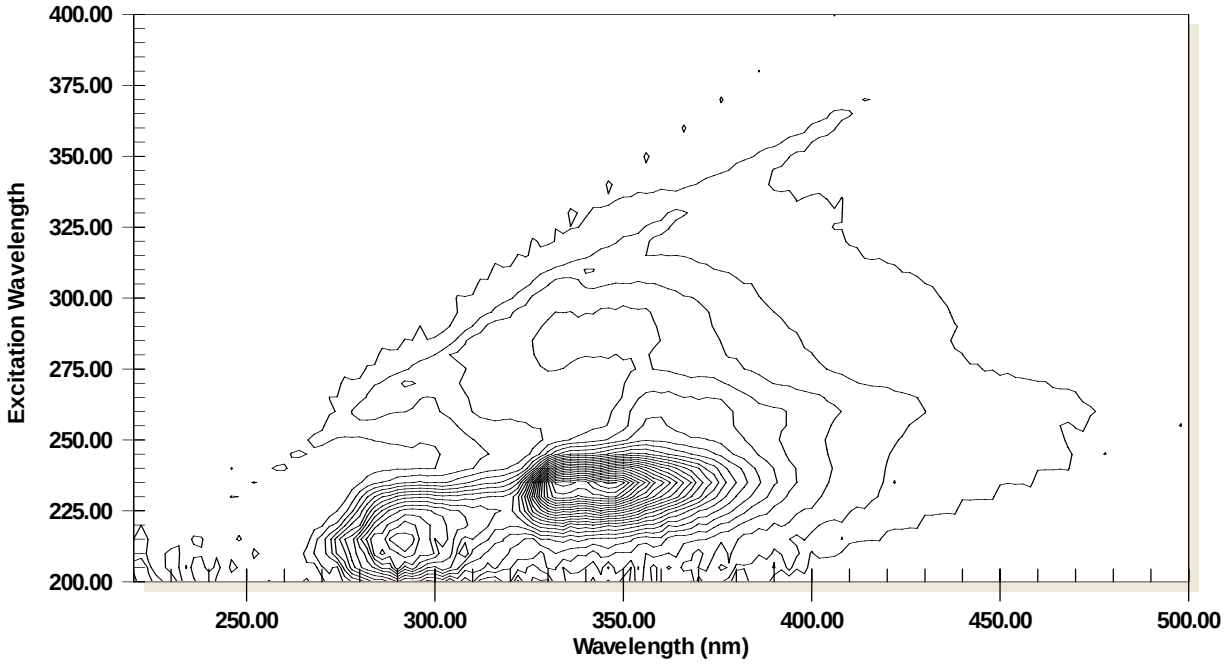
400.00
375.00
350.00
325.00
300.00
275.00
250.00
225.00
200.00
Excitation Wavelength
250.00
300.00
350.00
400.00
450.00
500.00
Wavelength (nm)

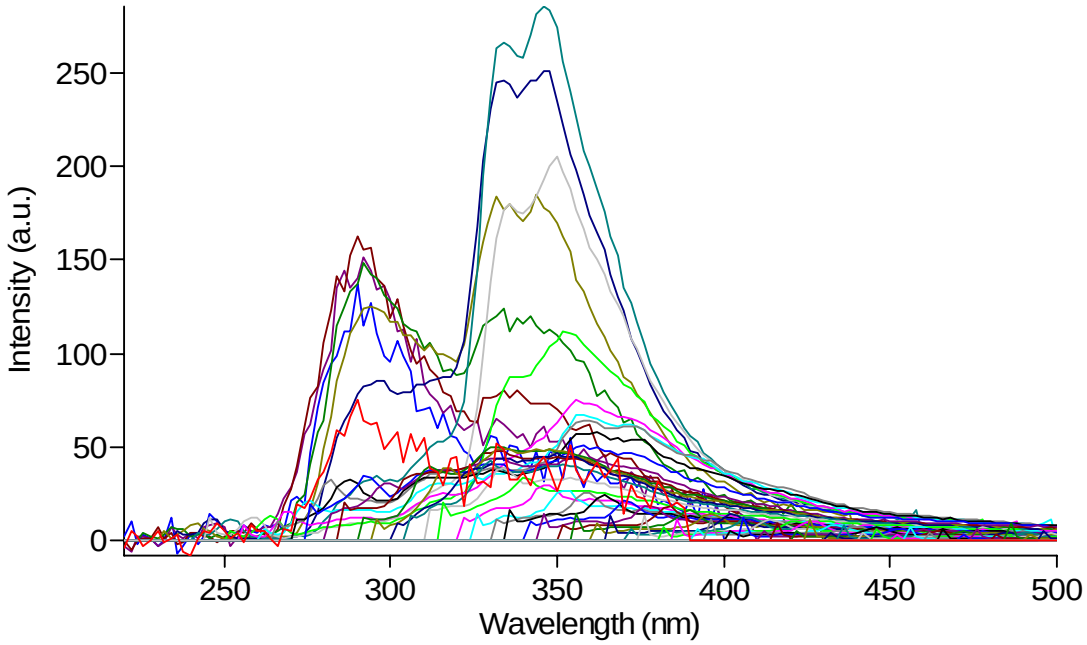
250
200
150
100
50
0
Intensity (a.u.)
250
300
350
400
450
500
Wavelength (nm)

81AT

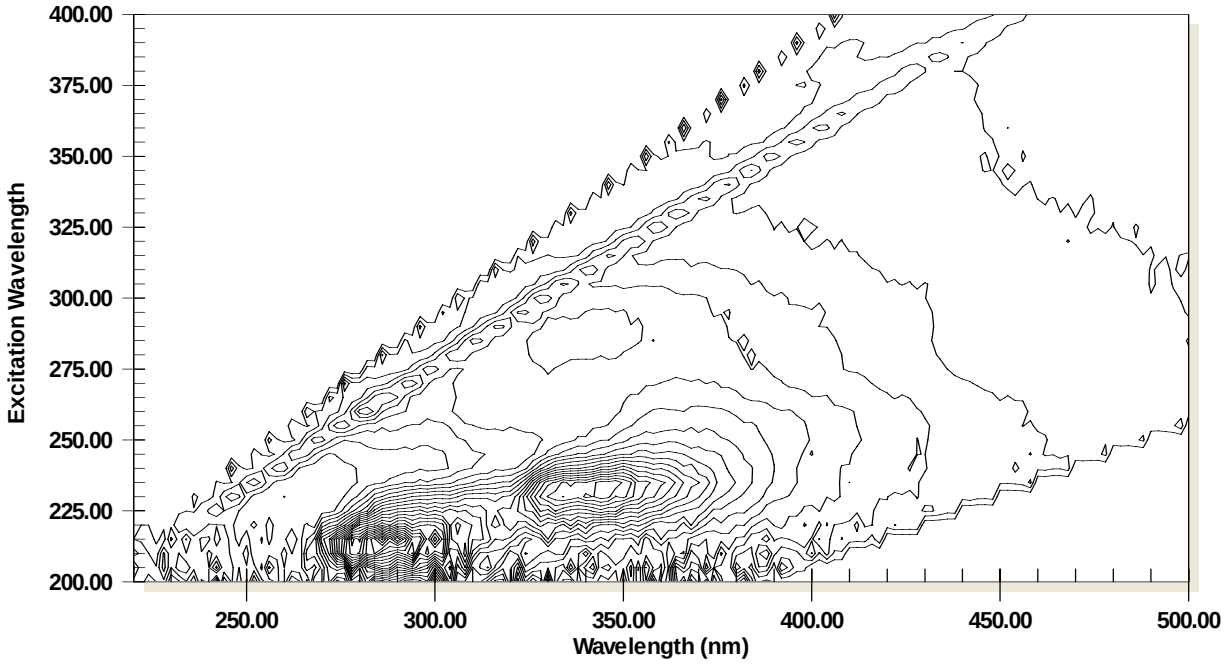
Excitation Wavelength
400.00
375.00
350.00
325.00
300.00
275.00
250.00
225.00
200.00
250.00
300.00
350.00
400.00
450.00
500.00
Wavelength (nm)

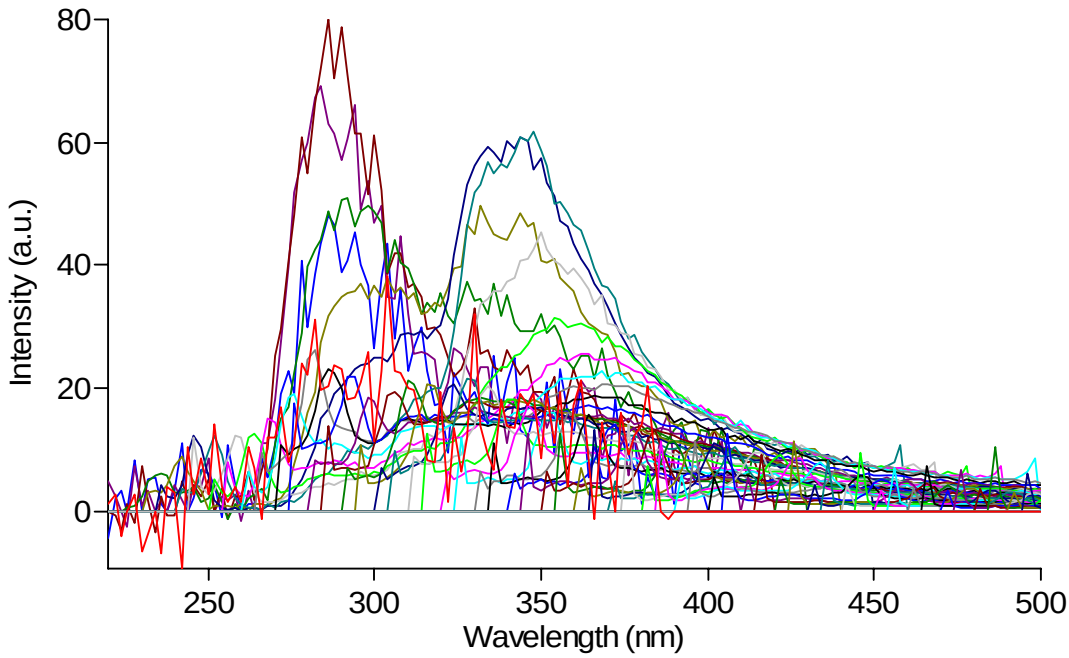
Intensity (a.u.)
80
60
40
20
0
250
300
350
400
450
500
Wavelength (nm)

82BT

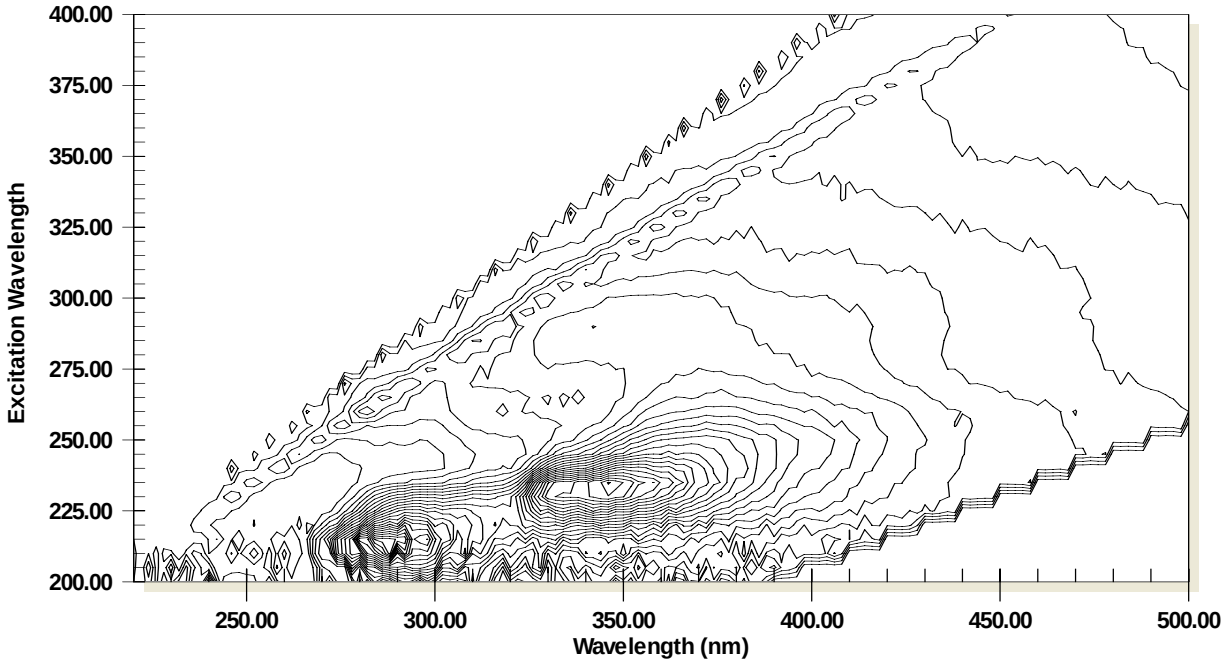
Excitation Wavelength
400.00
375.00
350.00
325.00
300.00
275.00
250.00
225.00
200.00
250.00
300.00
350.00
400.00
450.00
500.00
Wavelength (nm)

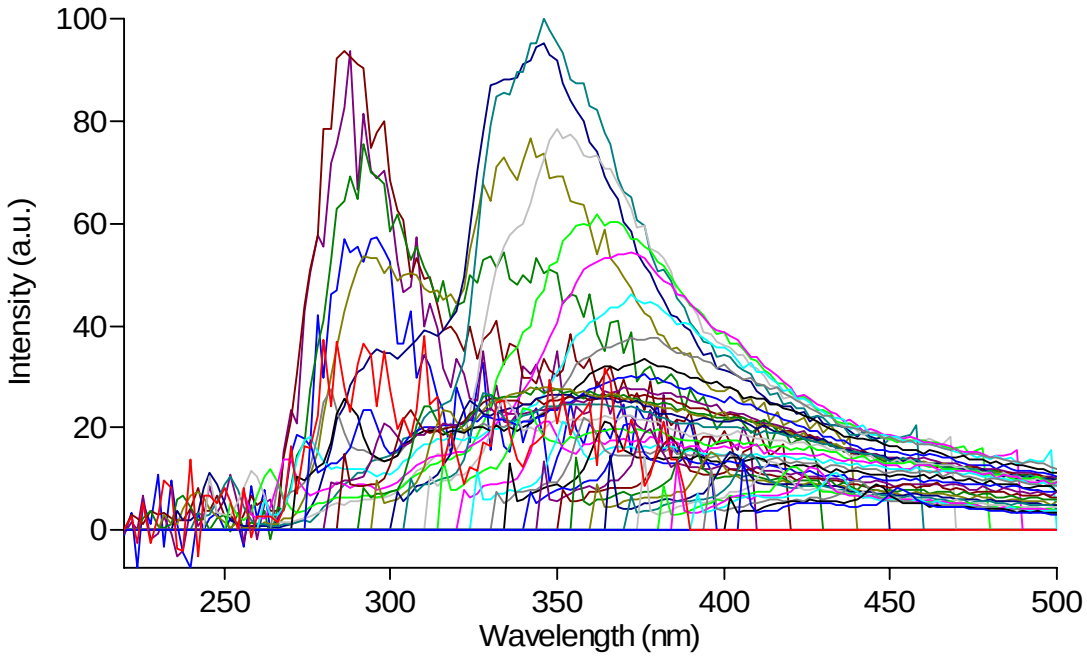
Intensity (a.u.)
100
80
60
40
20
0
250
300
350
400
450
500
Wavelength (nm)

83BT

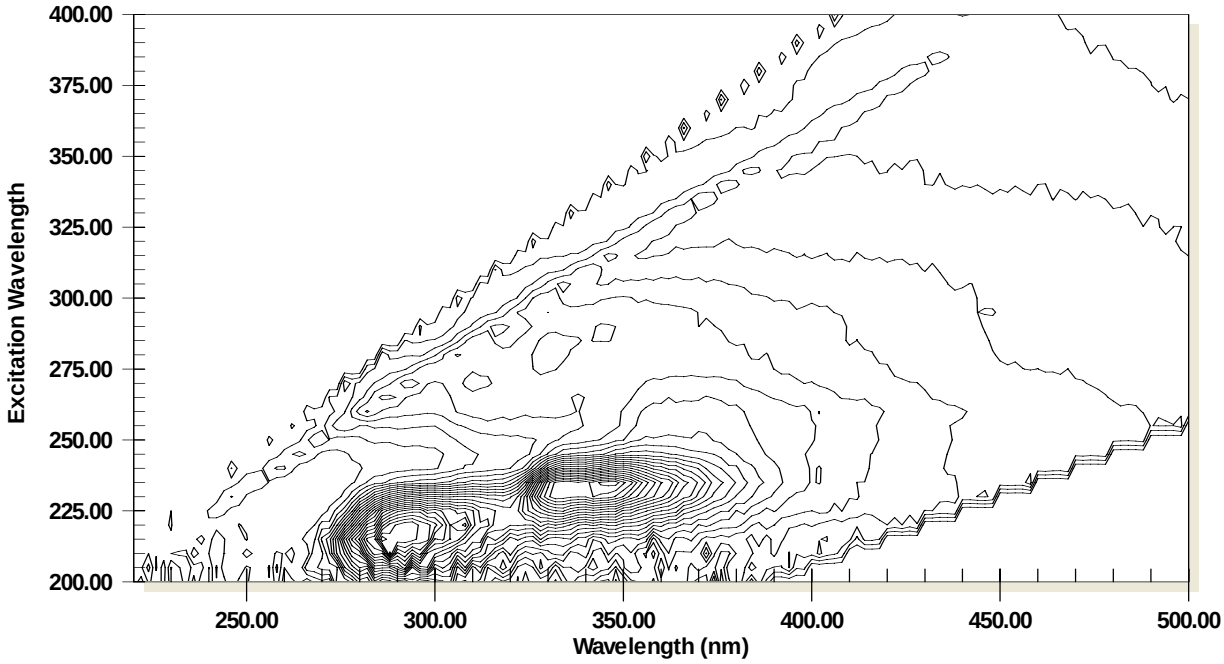
Excitation Wavelength
400.00
375.00
350.00
325.00
300.00
275.00
250.00
225.00
200.00
250.00
300.00
350.00
400.00
450.00
500.00
Wavelength (nm)

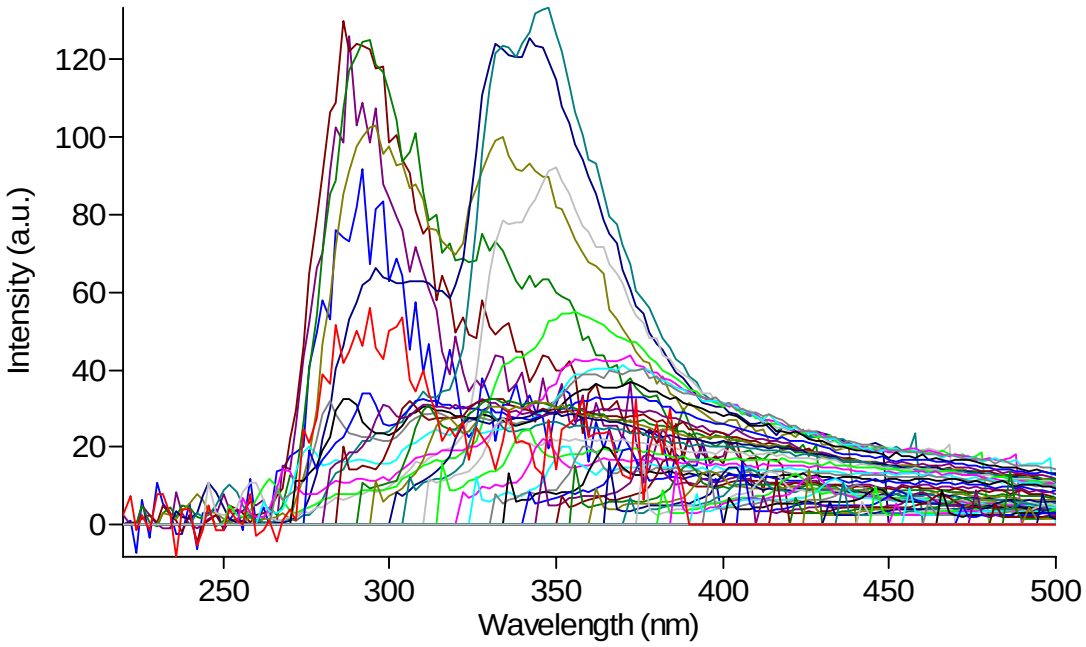
Intensity (a.u.)
120
100
80
60
40
20
0
250
300
350
400
450
500
Wavelength (nm)

84BT

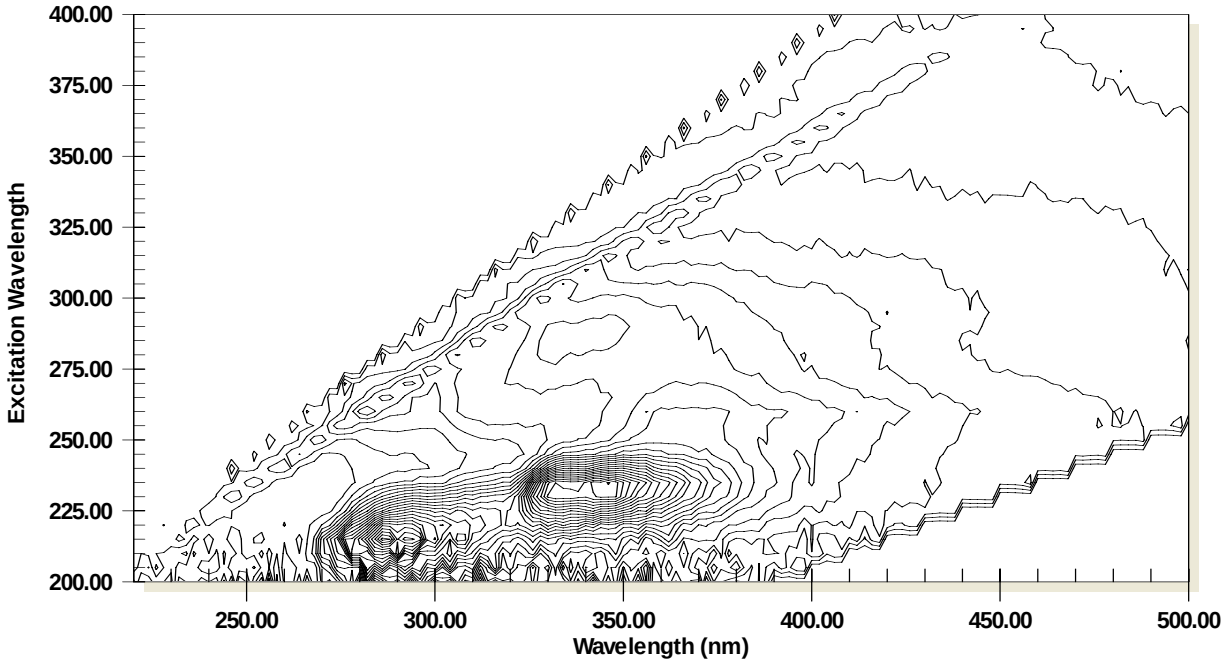
Excitation Wavelength
400.00
375.00
350.00
325.00
300.00
275.00
250.00
225.00
200.00
250.00
300.00
350.00
400.00
450.00
500.00
Wavelength (nm)

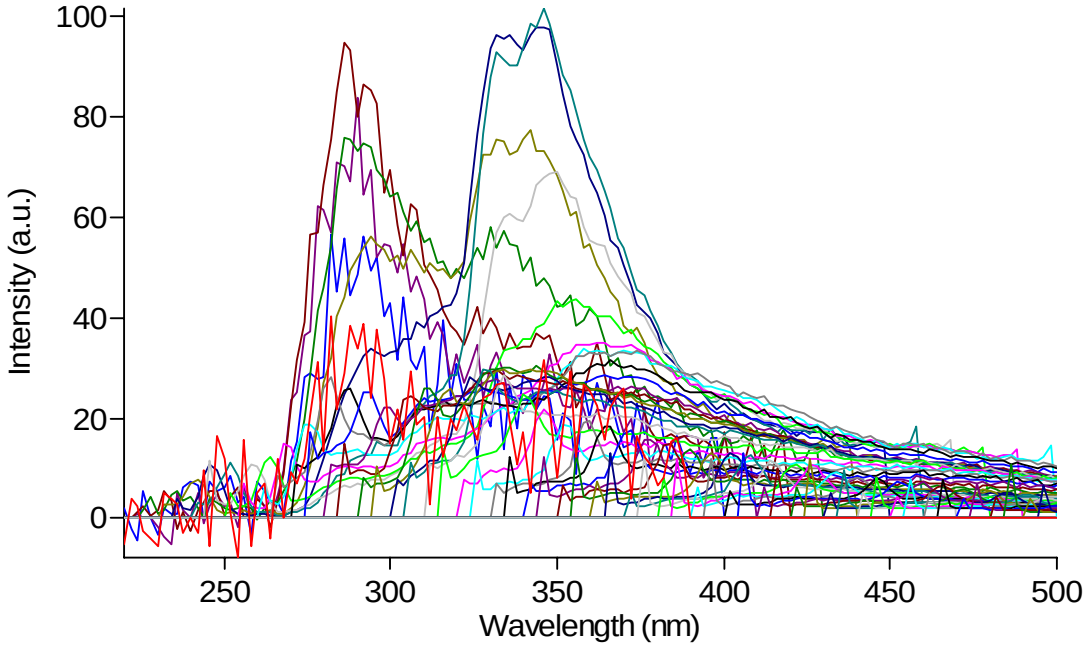
Intensity (a.u.)
100
80
60
40
20
0
250
300
350
400
450
500
Wavelength (nm)

85AT

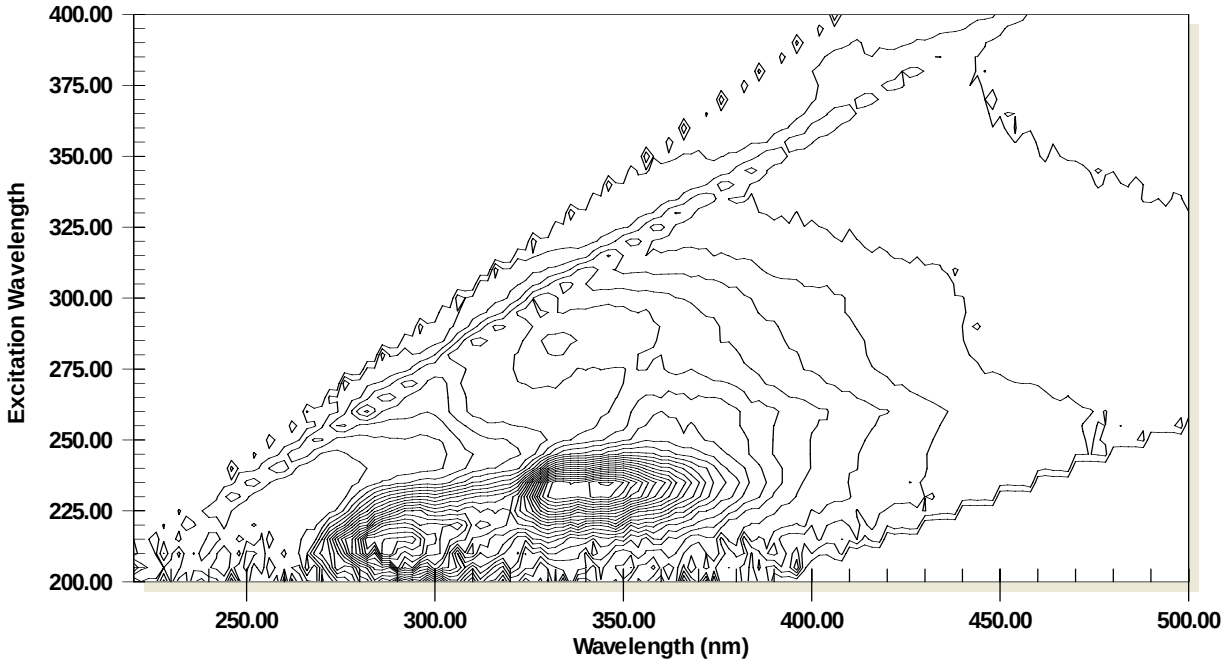
Excitation Wavelength
400.00
375.00
350.00
325.00
300.00
275.00
250.00
225.00
200.00
250.00
300.00
350.00
400.00
450.00
500.00
Wavelength (nm)

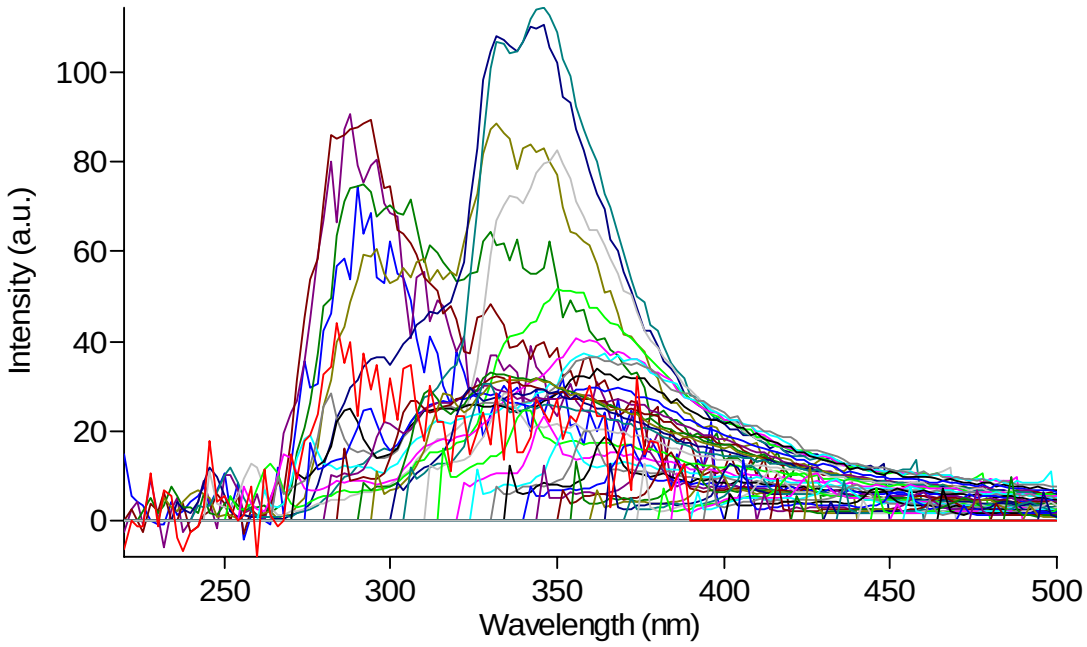
Intensity (a.u.)
100
80
60
40
20
0
250
300
350
400
450
500
Wavelength (nm)

91AT

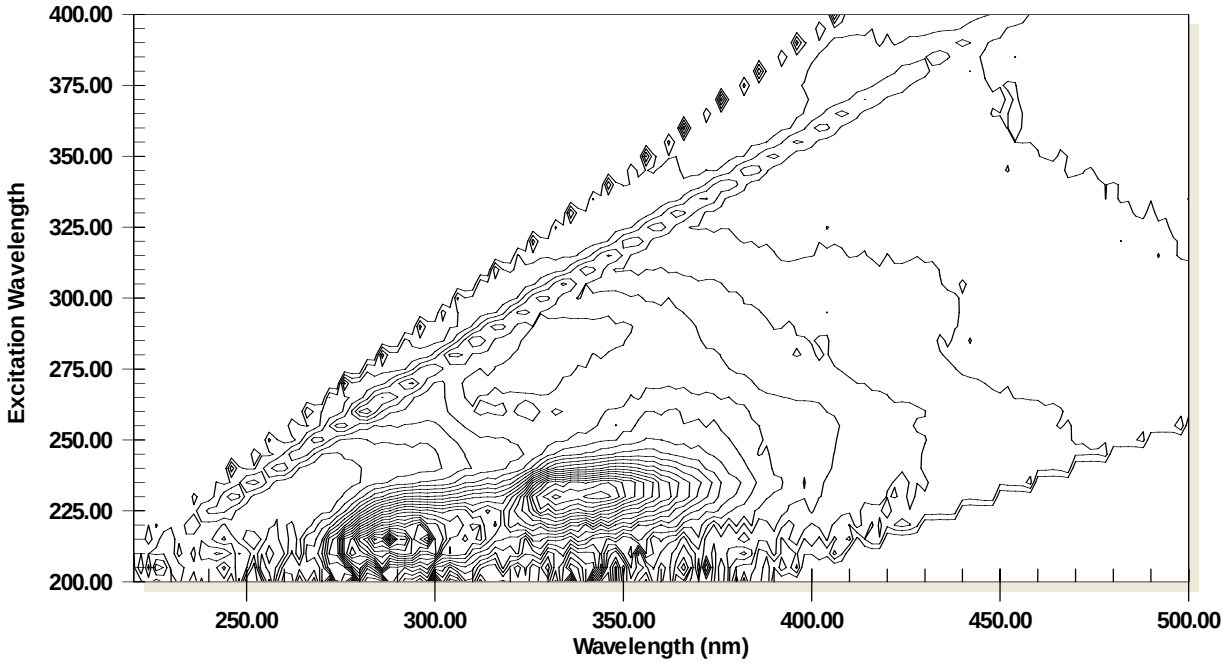
400.00
375.00
350.00
325.00
300.00
275.00
250.00
225.00
200.00
Excitation Wavelength
250.00
300.00
350.00
400.00
450.00
500.00
Wavelength (nm)

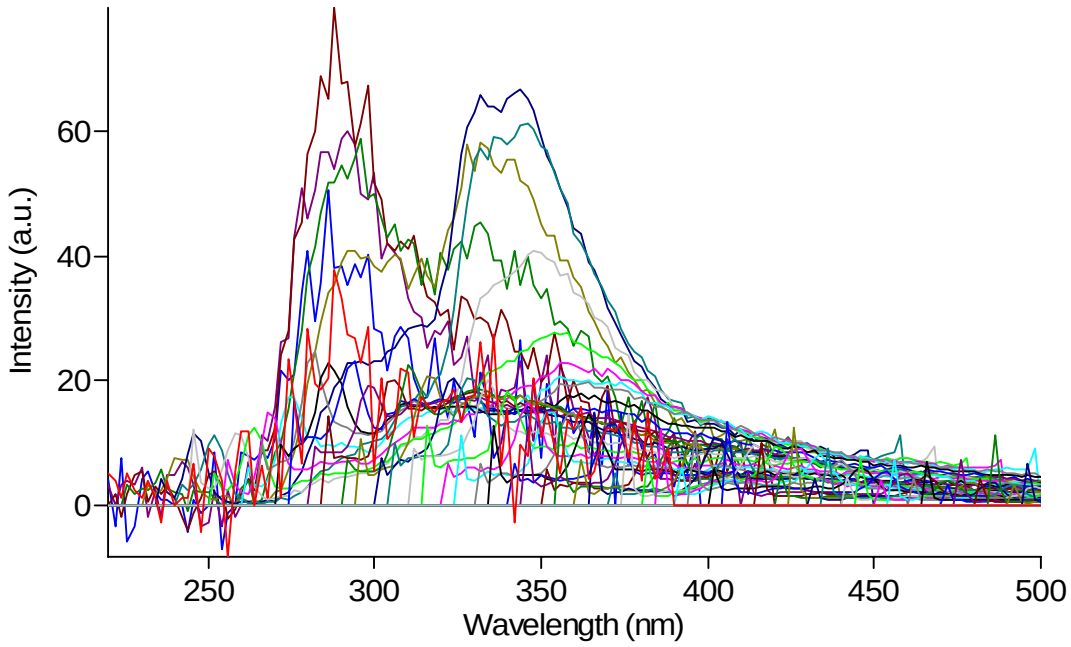
60
40
20
0
Intensity (a.u.)
250
300
350
400
450
500
Wavelength (nm)

92AT

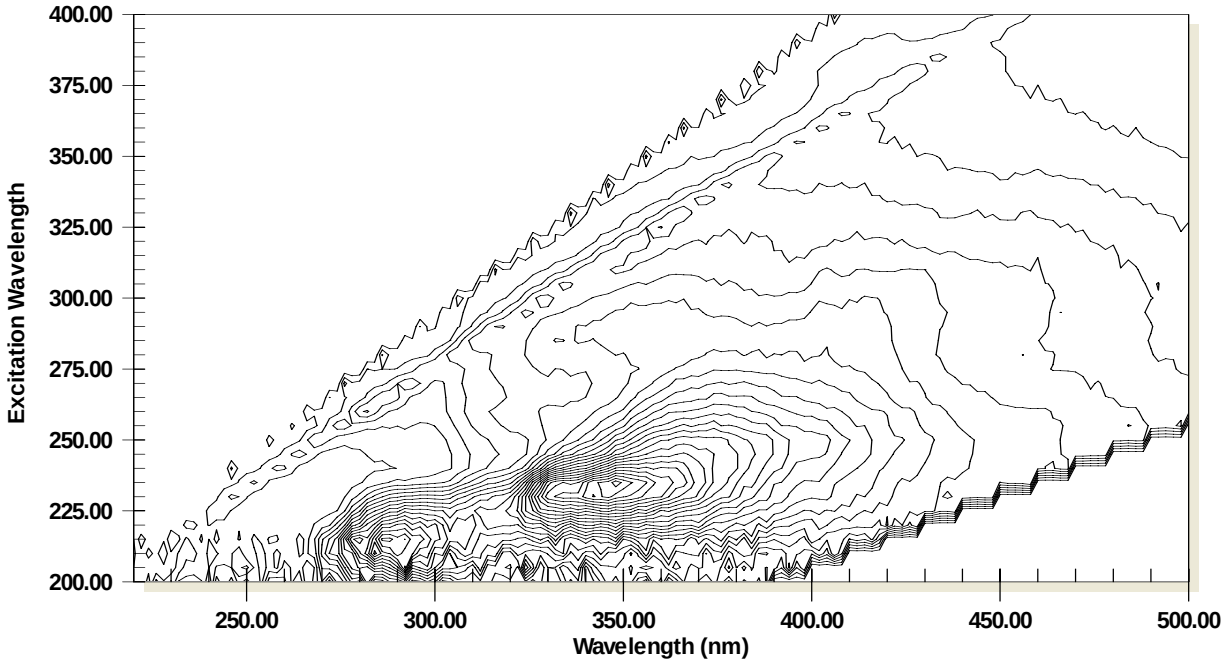
Excitation Wavelength
400.00
375.00
350.00
325.00
300.00
275.00
250.00
225.00
200.00
250.00
300.00
350.00
400.00
450.00
500.00
Wavelength (nm)

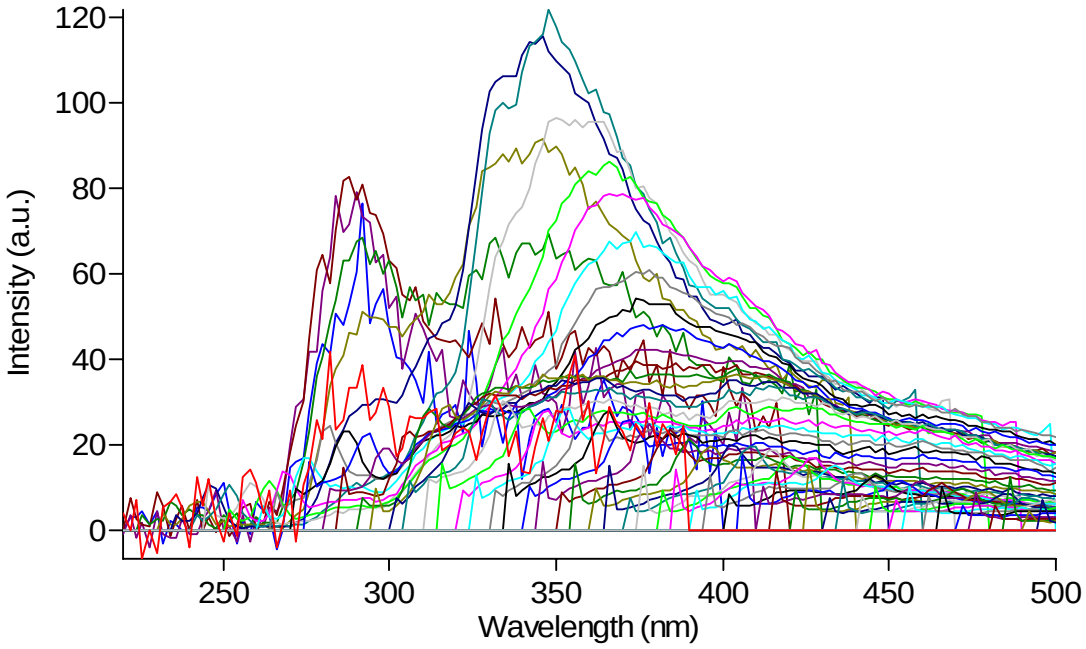
Intensity (a.u.)
120
100
80
60
40
20
0
250
300
350
400
450
500
Wavelength (nm)

93AT

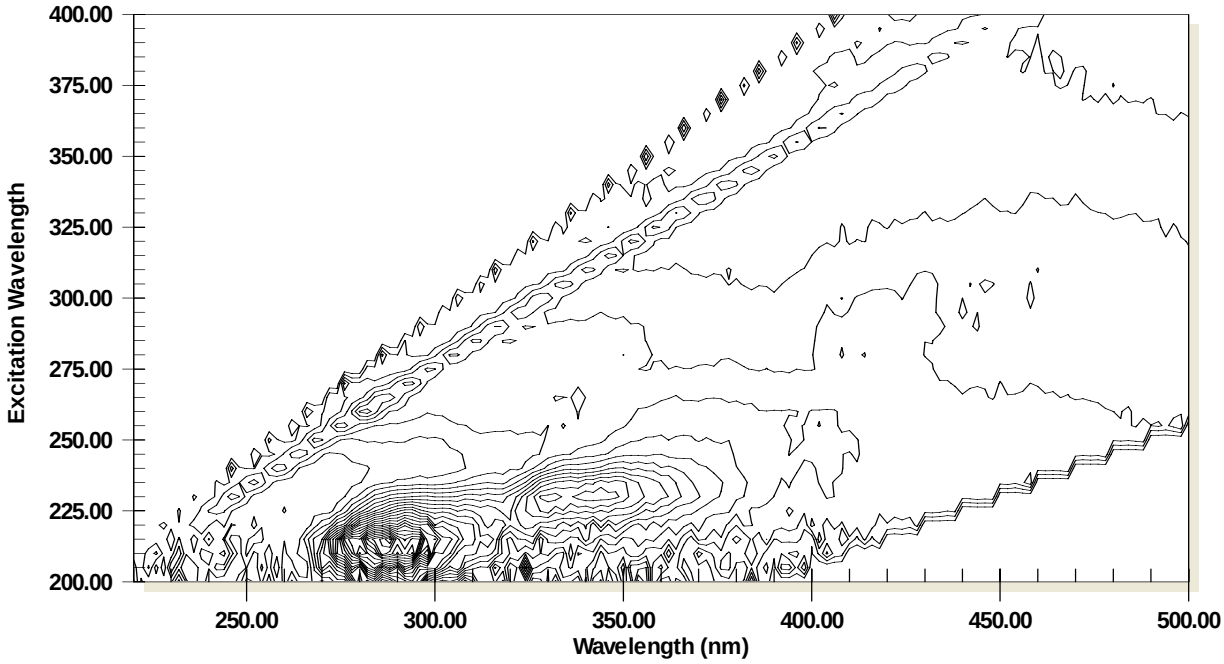
400.00
375.00
350.00
325.00
300.00
275.00
250.00
225.00
200.00
Excitation Wavelength
250.00
300.00
350.00
400.00
450.00
500.00
Wavelength (nm)

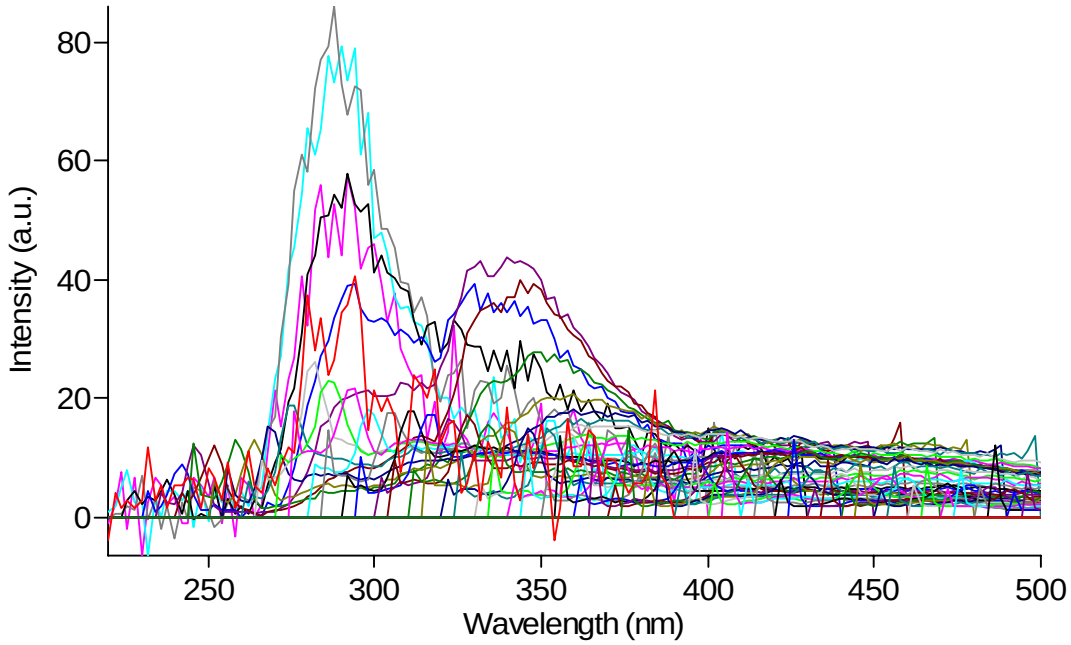
80
60
40
20
0
Intensity (a.u.)
250
300
350
400
450
500
Wavelength (nm)

94BT

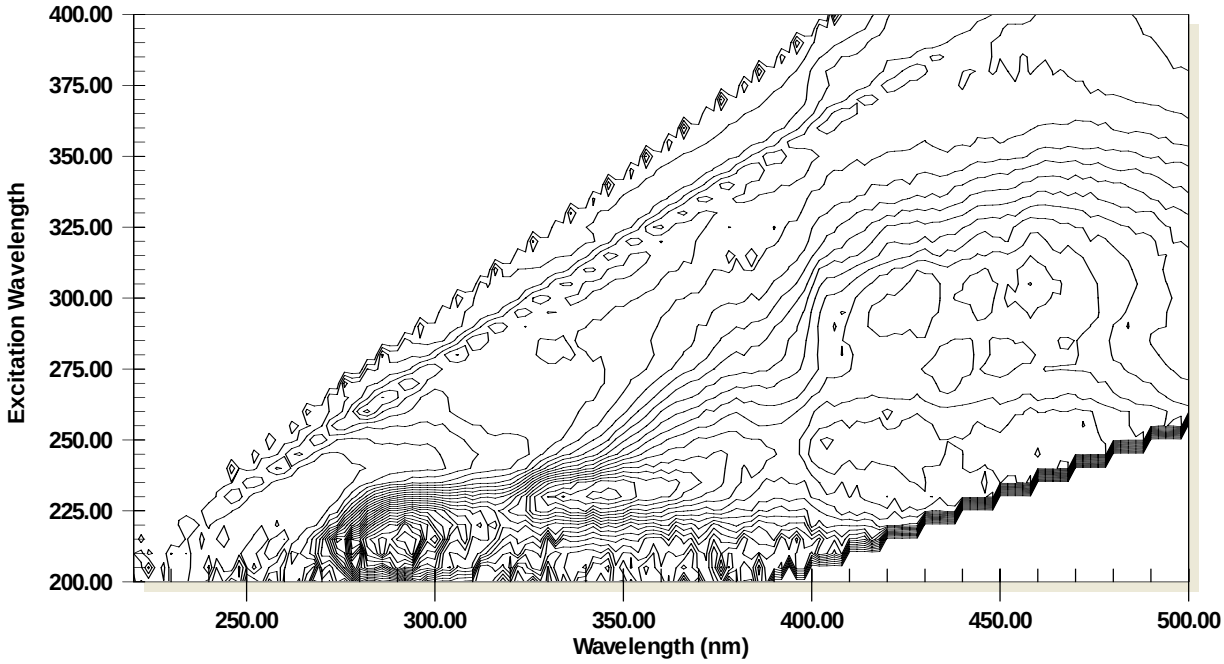
400.00
375.00
350.00
325.00
300.00
275.00
250.00
225.00
200.00
Excitation Wavelength
250.00
300.00
350.00
400.00
450.00
500.00
Wavelength (nm)

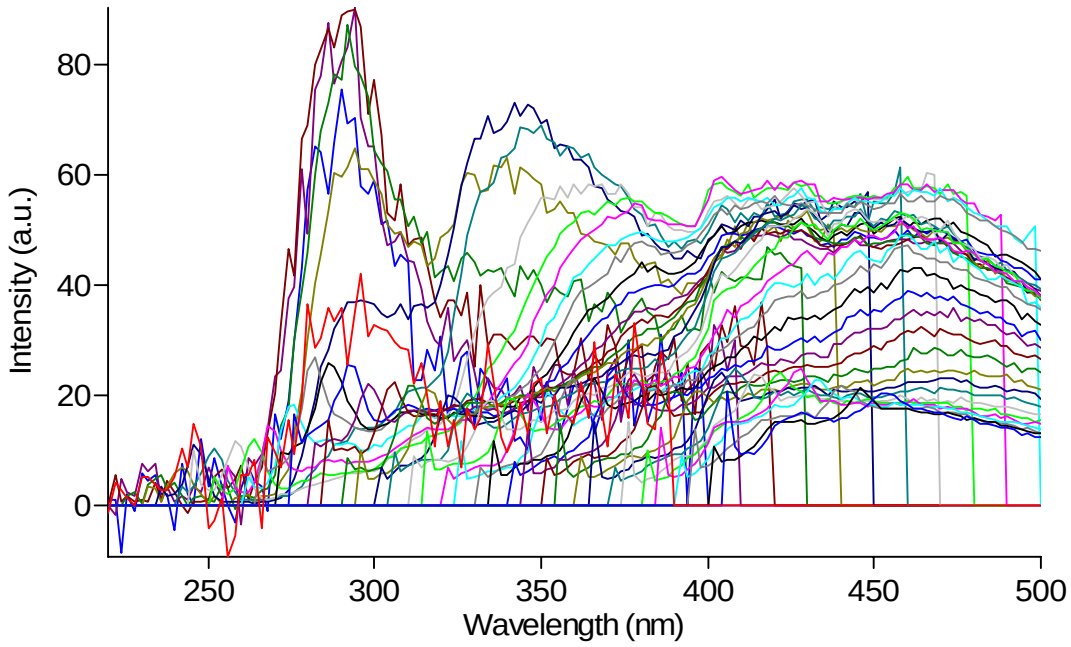
80
60
40
20
0
Intensity (a.u.)
250
300
350
400
450
500
Wavelength (nm)

95BT

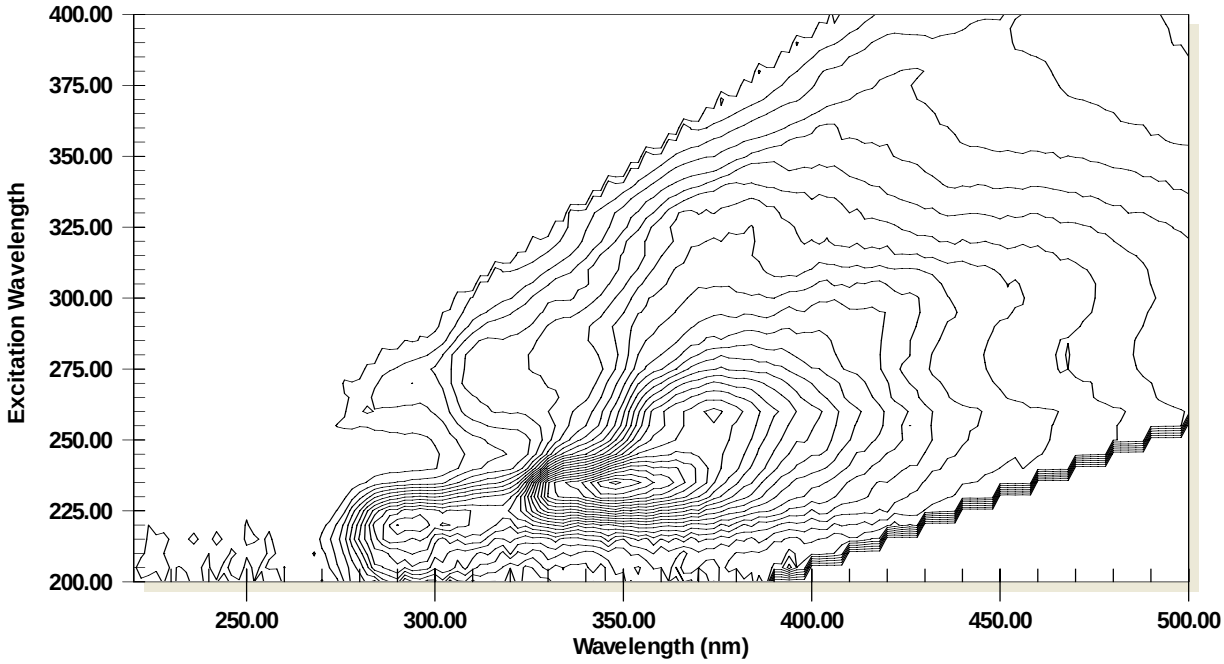
Excitation Wavelength
400.00
375.00
350.00
325.00
300.00
275.00
250.00
225.00
200.00
250.00
300.00
350.00
400.00
450.00
500.00
Wavelength (nm)

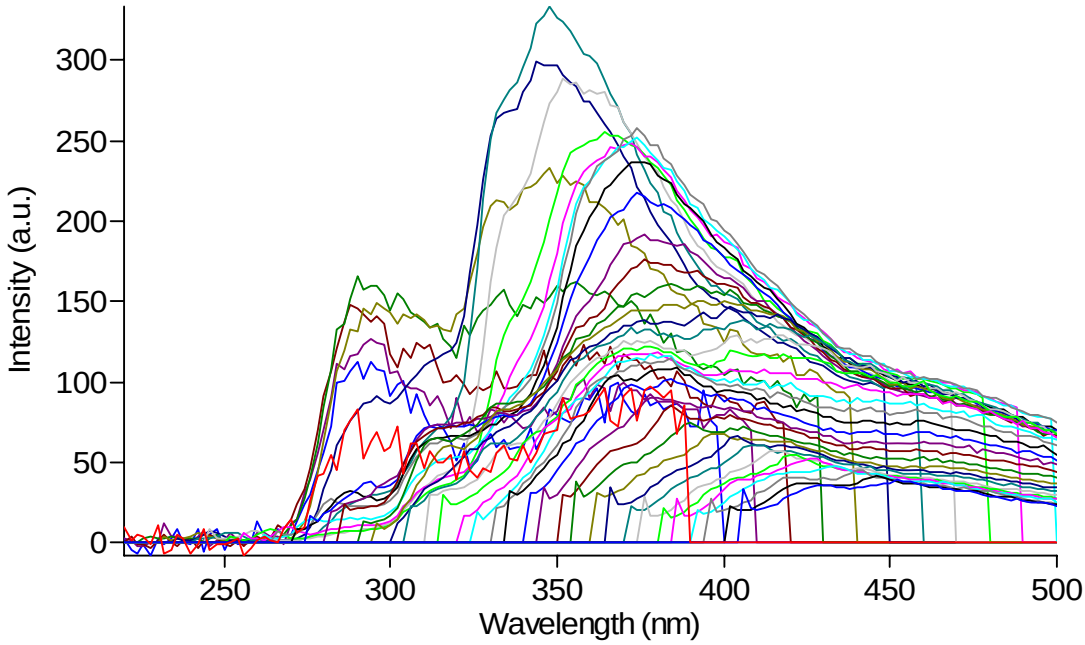
Intensity (a.u.)
300
250
200
150
100
50
0
250
300
350
400
450
500
Wavelength (nm)

101AT

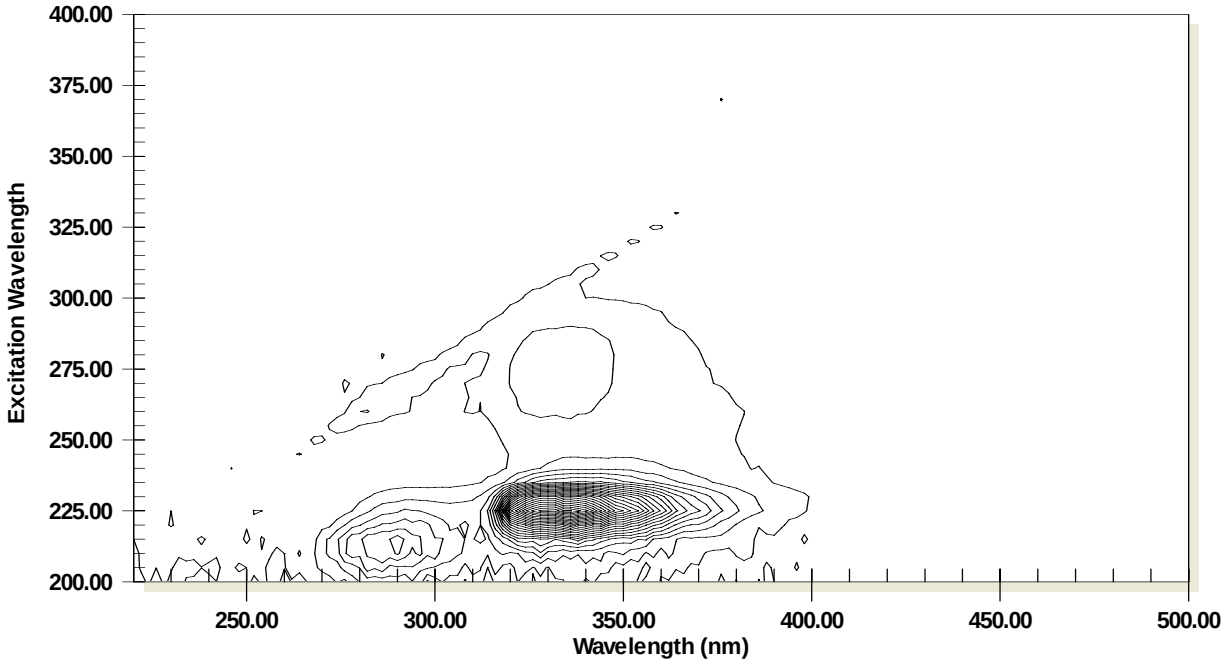
400.00
375.00
350.00
325.00
300.00
275.00
250.00
225.00
200.00
Excitation Wavelength
250.00
300.00
350.00
400.00
450.00
500.00
Wavelength (nm)

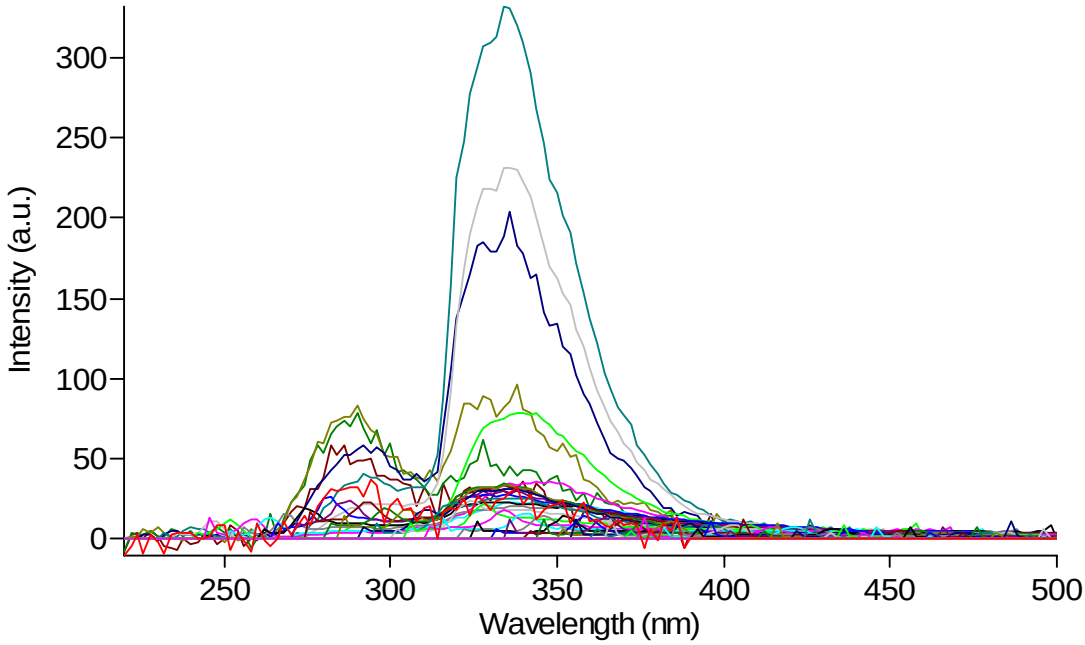
300
250
200
150
100
50
0
Intensity (a.u.)
250
300
350
400
450
500
Wavelength (nm)

102AT

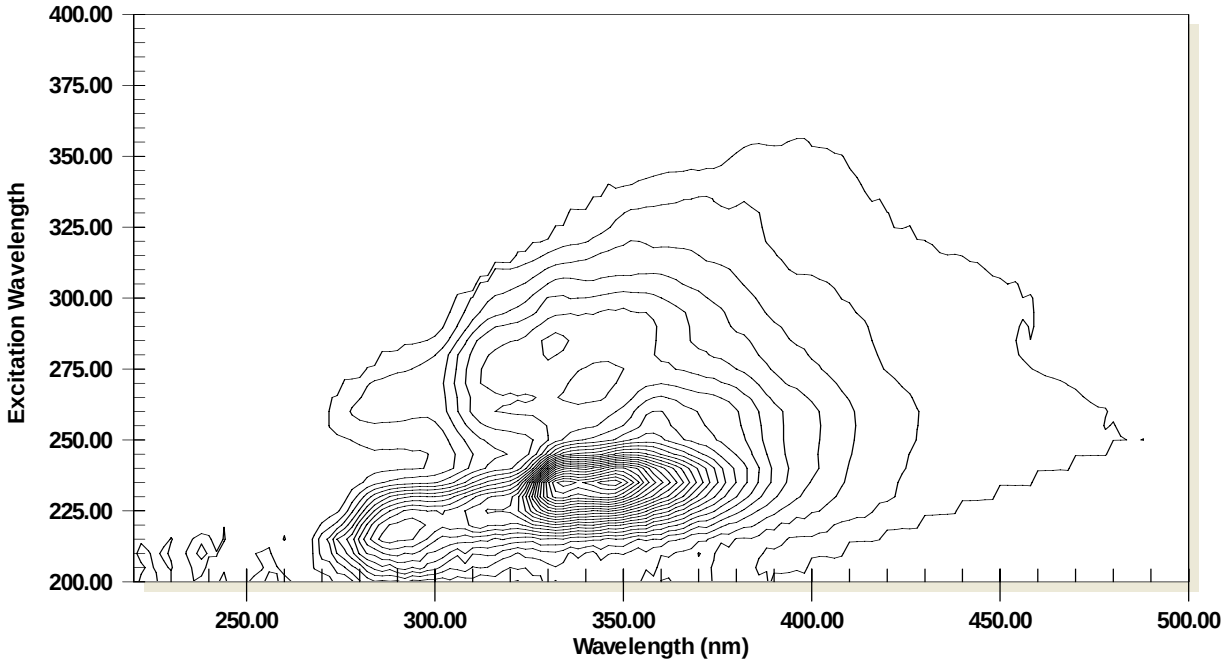
400.00
375.00
350.00
325.00
300.00
275.00
250.00
225.00
200.00
Excitation Wavelength
250.00
300.00
350.00
400.00
450.00
500.00
Wavelength (nm)

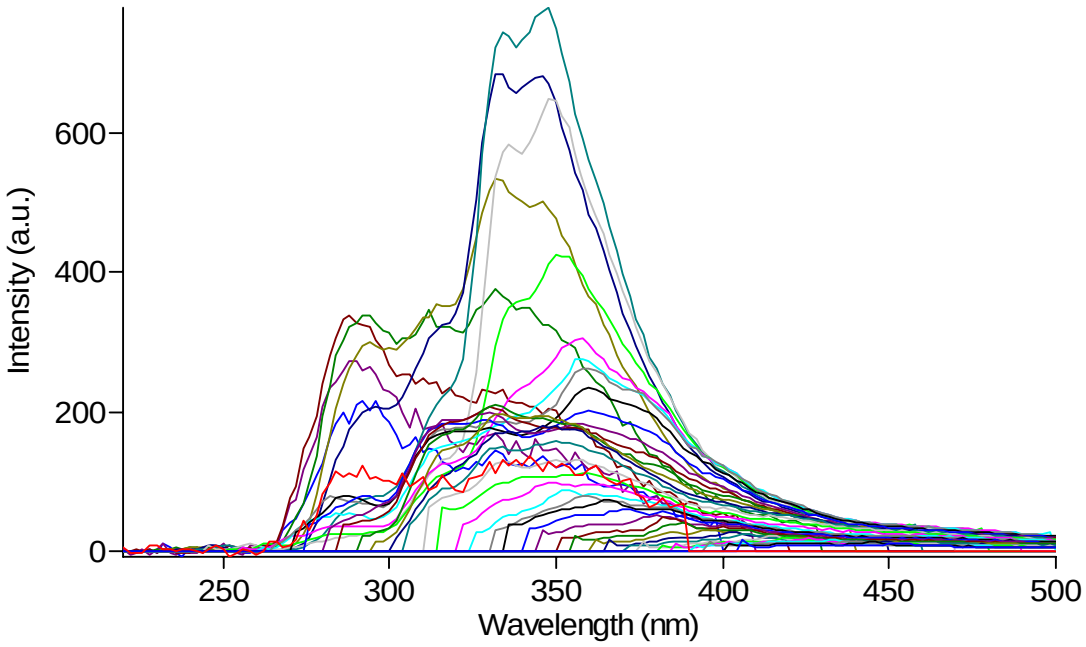
600
400
200
0
Intensity (a.u.)
250
300
350
400
450
500
Wavelength (nm)

103BT

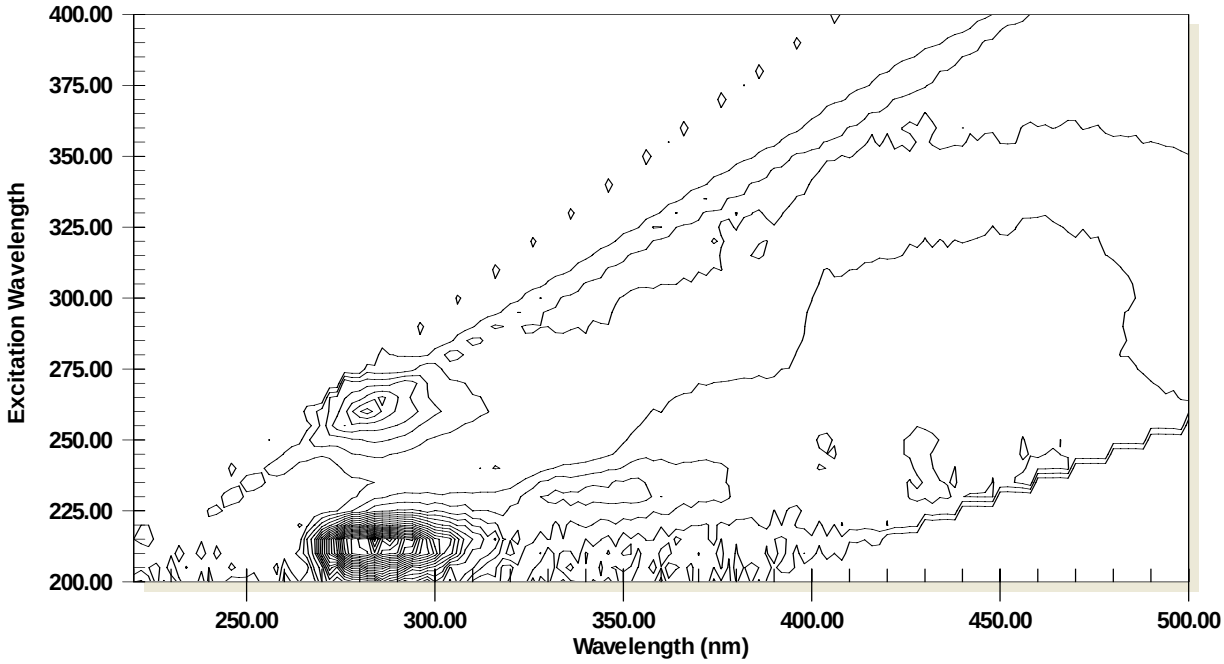
Excitation Wavelength
400.00
375.00
350.00
325.00
300.00
275.00
250.00
225.00
200.00
250.00
300.00
350.00
400.00
450.00
500.00
Wavelength (nm)

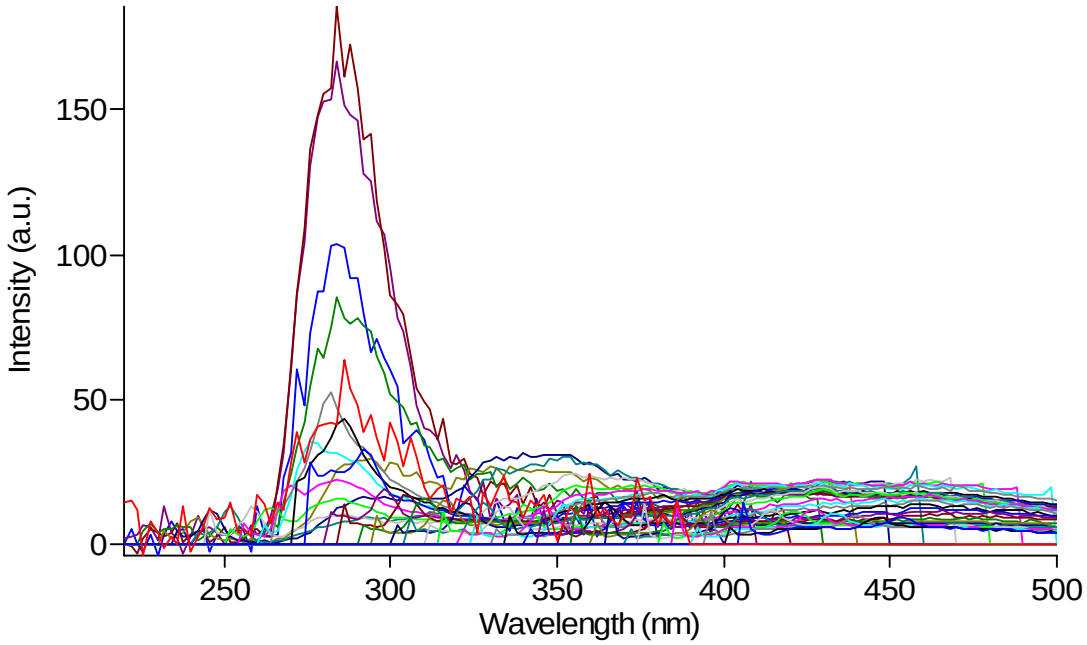
Intensity (a.u.)
150
100
50
0
250
300
350
400
450
500
Wavelength (nm)

104CT

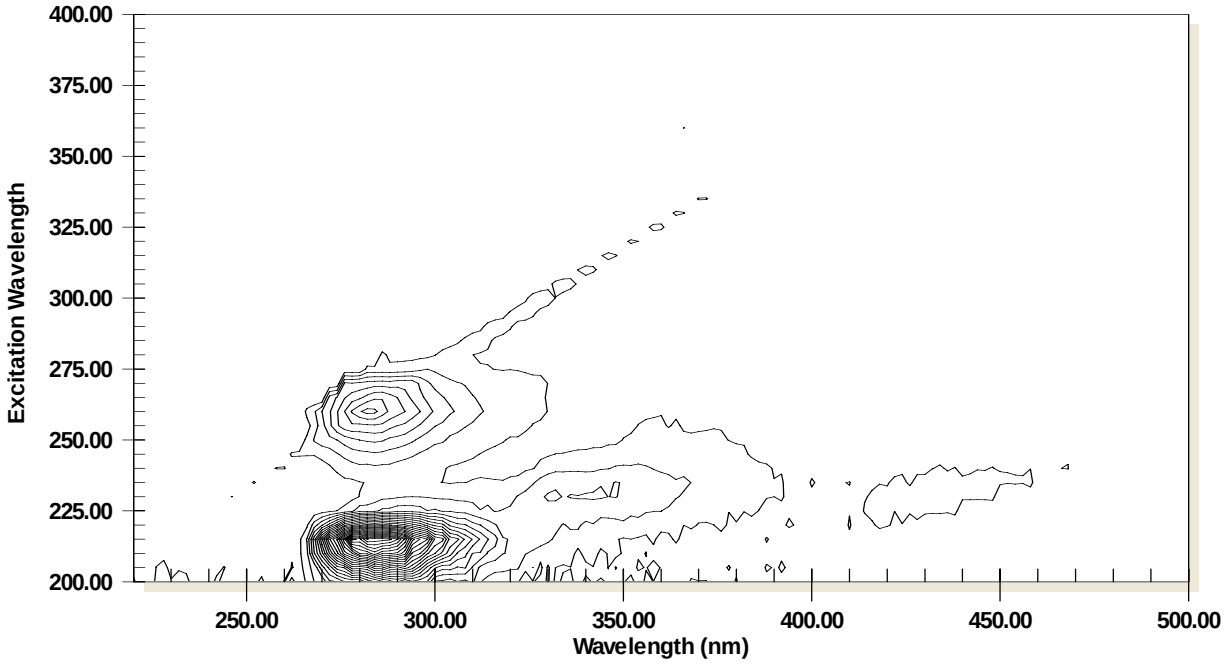
Excitation Wavelength
400.00
375.00
350.00
325.00
300.00
275.00
250.00
225.00
200.00
250.00
300.00
350.00
400.00
450.00
500.00
Wavelength (nm)

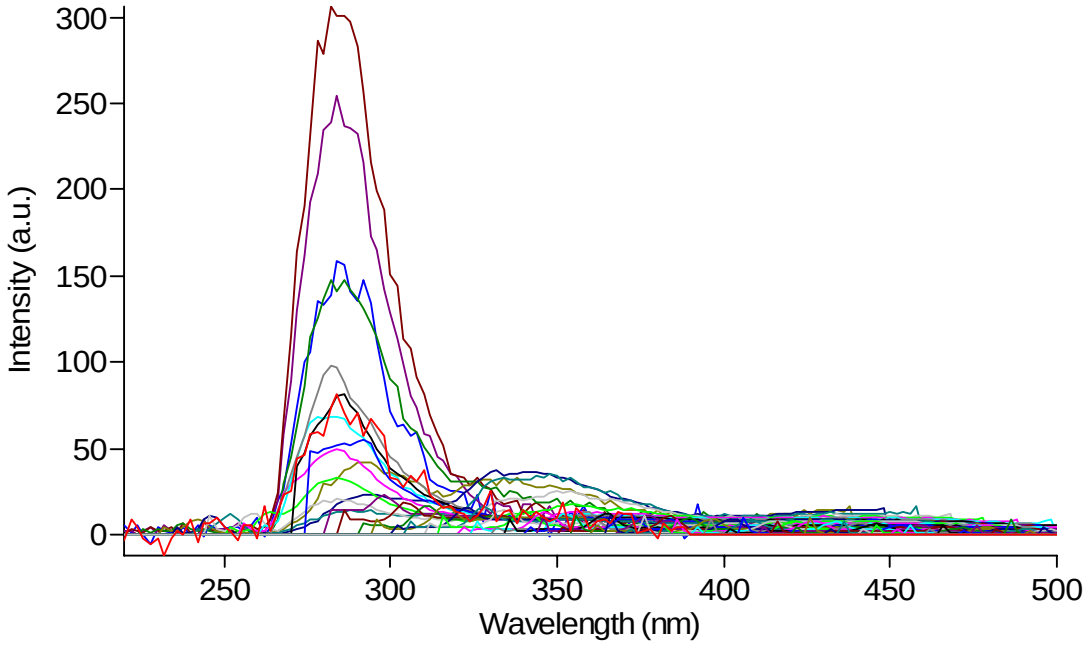
Intensity (a.u.)
300
250
200
150
100
50
0
250
300
350
400
450
500
Wavelength (nm)

105CT

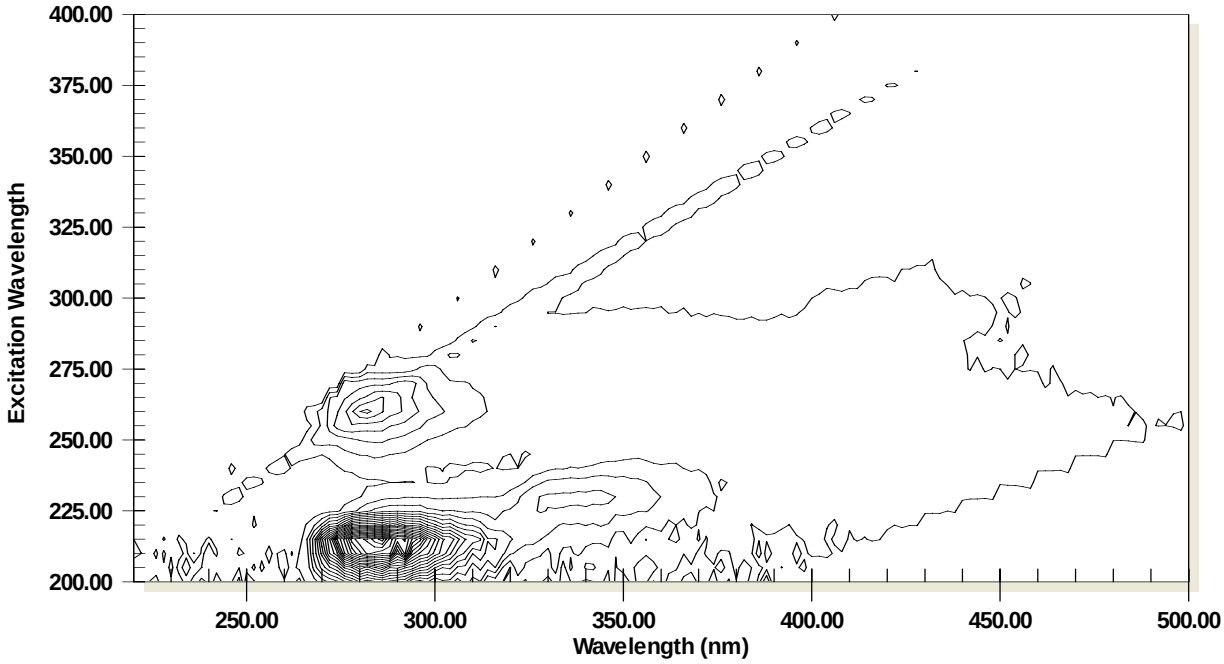
Excitation Wavelength
400.00
375.00
350.00
325.00
300.00
275.00
250.00
225.00
200.00
250.00
300.00
350.00
400.00
450.00
500.00
Wavelength (nm)

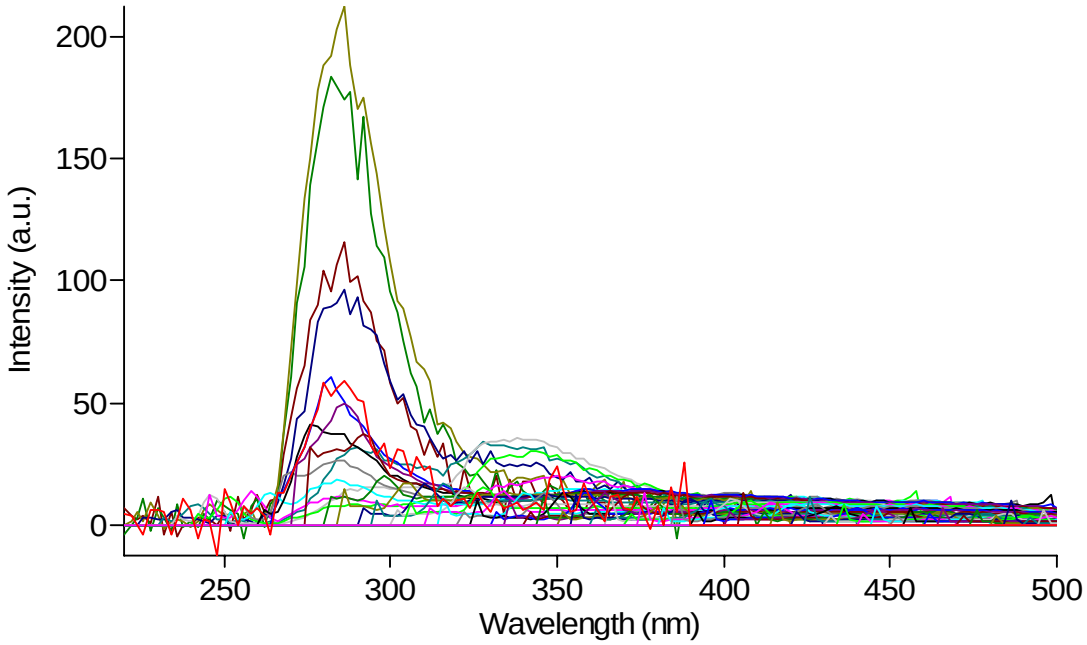
Intensity (a.u.)
200
150
100
50
0
250
300
350
400
450
500
Wavelength (nm)

M06T

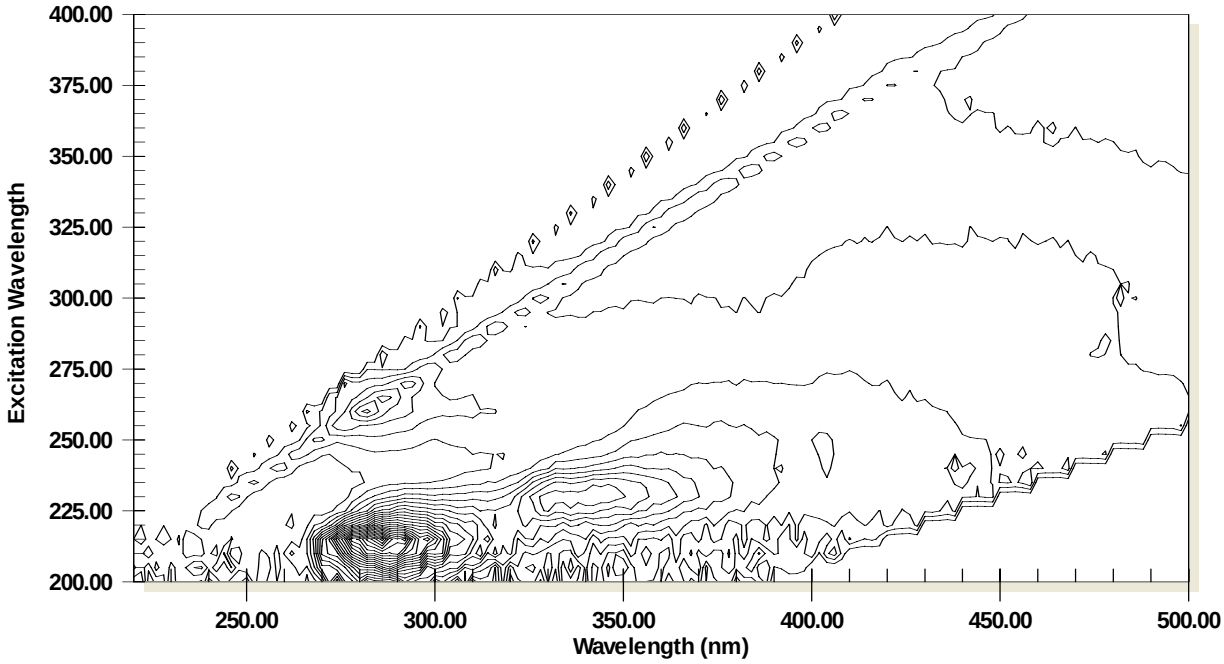
Excitation Wavelength
400.00
375.00
350.00
325.00
300.00
275.00
250.00
225.00
200.00
250.00
300.00
350.00
400.00
450.00
500.00
Wavelength (nm)

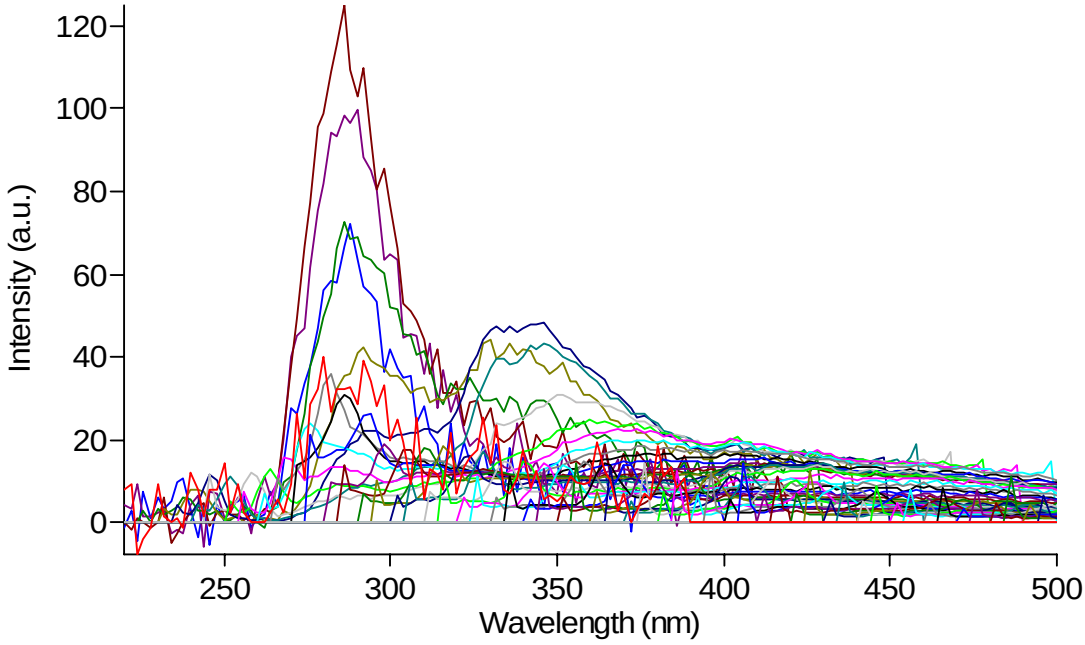
Intensity (a.u.)
120
100
80
60
40
20
0
250
300
350
400
450
500
Wavelength (nm)

M10T

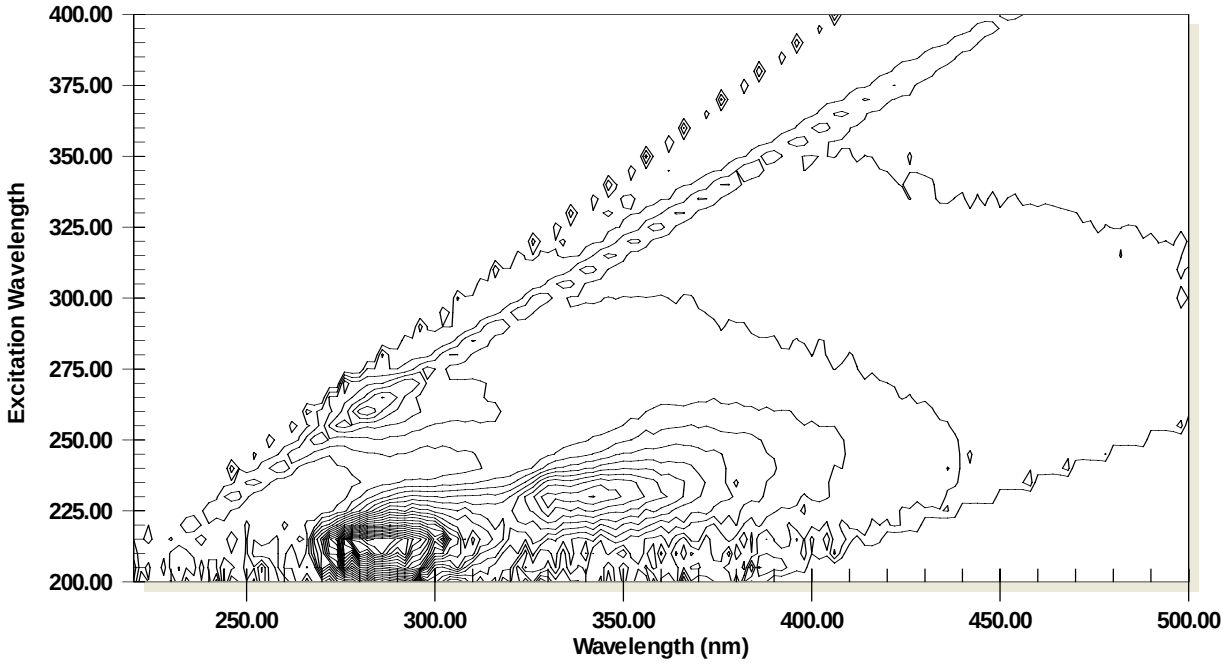
Excitation Wavelength
400.00
375.00
350.00
325.00
300.00
275.00
250.00
225.00
200.00
250.00
300.00
350.00
400.00
450.00
500.00
Wavelength (nm)

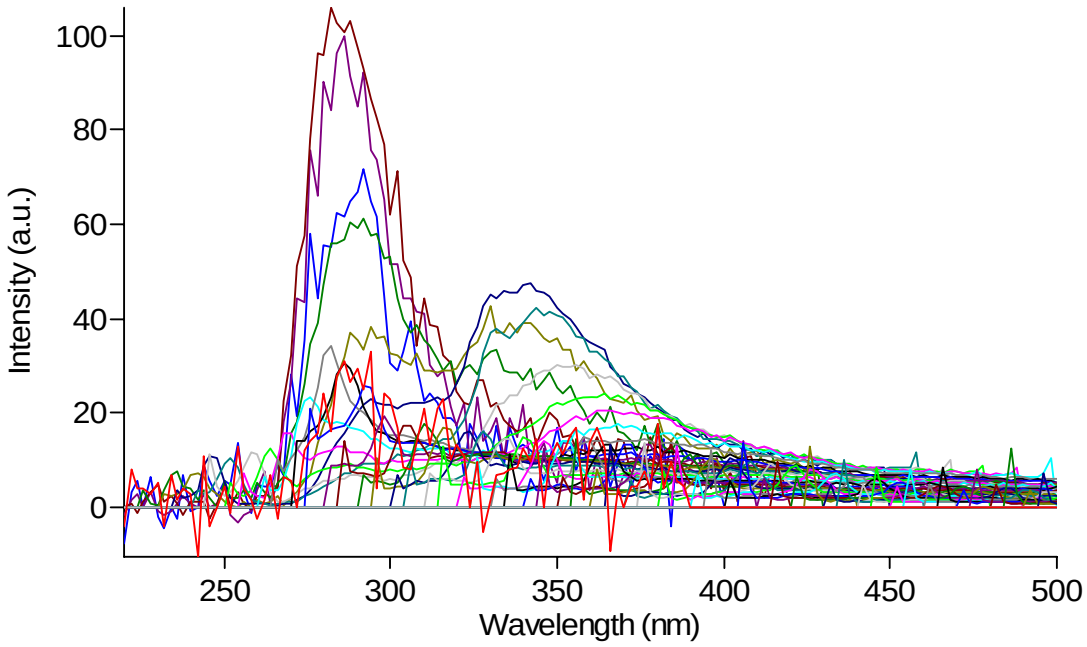
Intensity (a.u.)
100
80
60
40
20
0
250
300
350
400
450
500
Wavelength (nm)

M12T

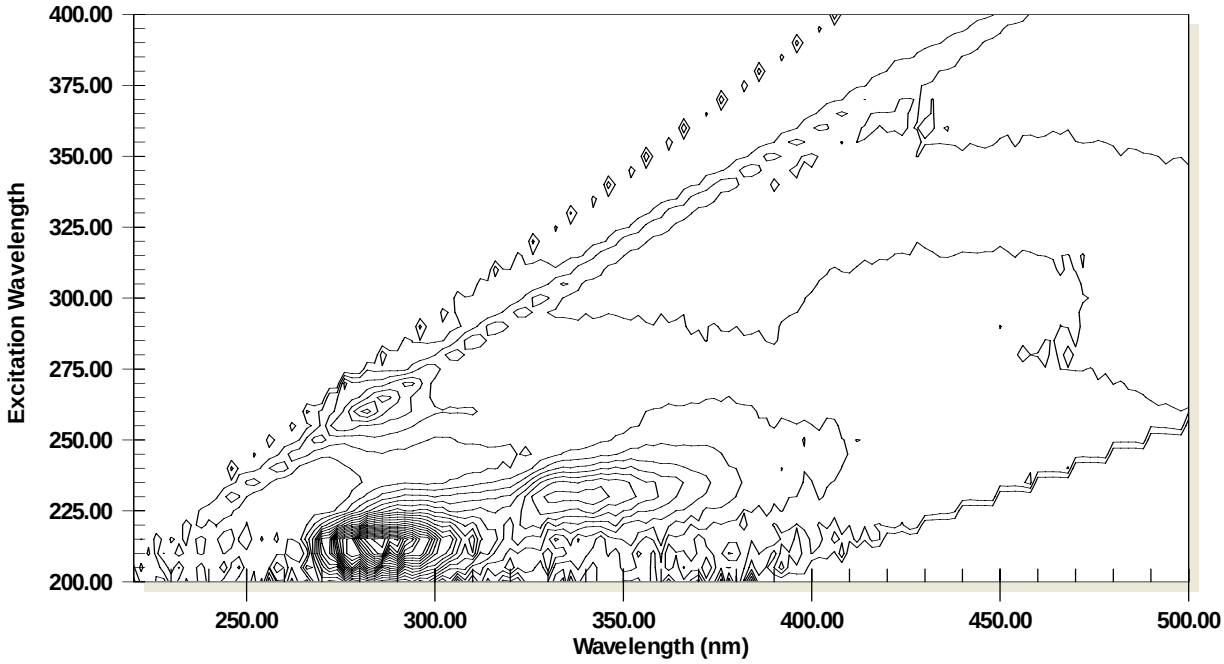
Excitation Wavelength
400.00
375.00
350.00
325.00
300.00
275.00
250.00
225.00
200.00
250.00
300.00
350.00
400.00
450.00
500.00
Wavelength (nm)

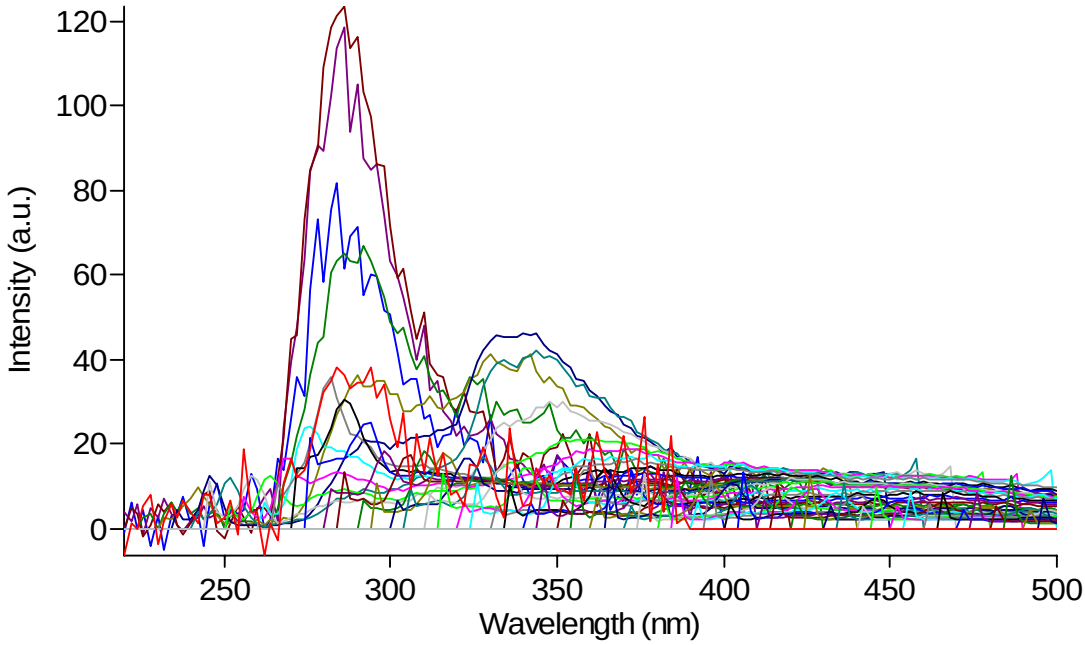
Intensity (a.u.)
120
100
80
60
40
20
0
250
300
350
400
450
500
Wavelength (nm)

M19T

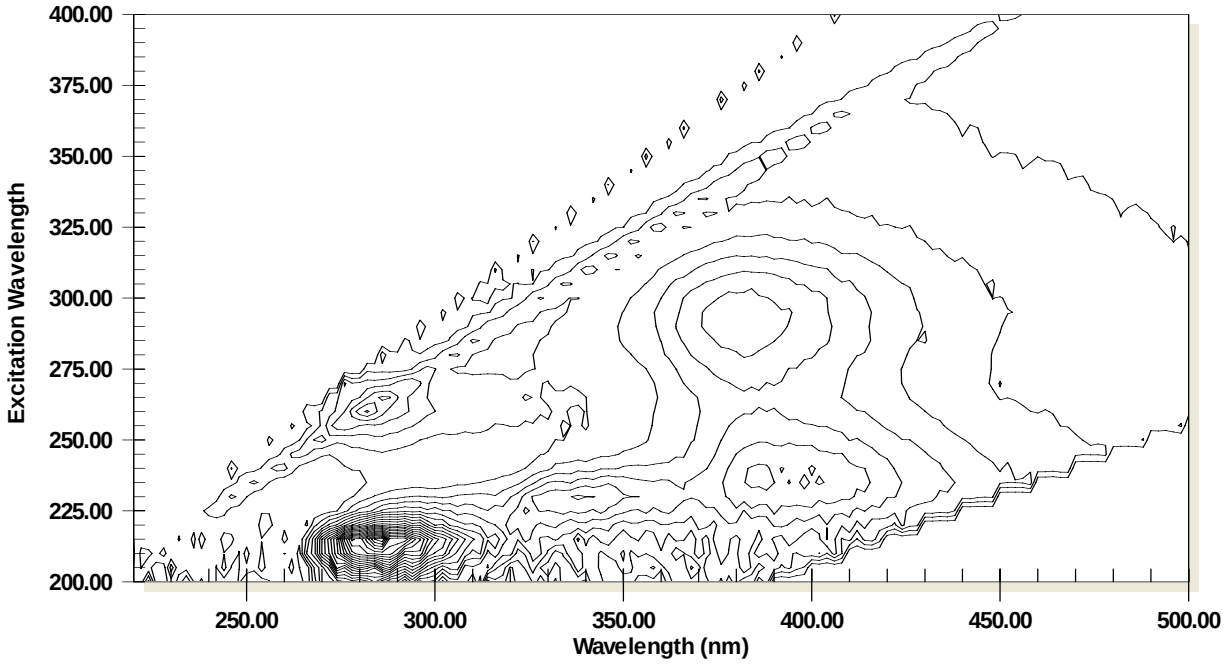
Excitation Wavelength
400.00
375.00
350.00
325.00
300.00
275.00
250.00
225.00
200.00
250.00
300.00
350.00
400.00
450.00
500.00
Wavelength (nm)

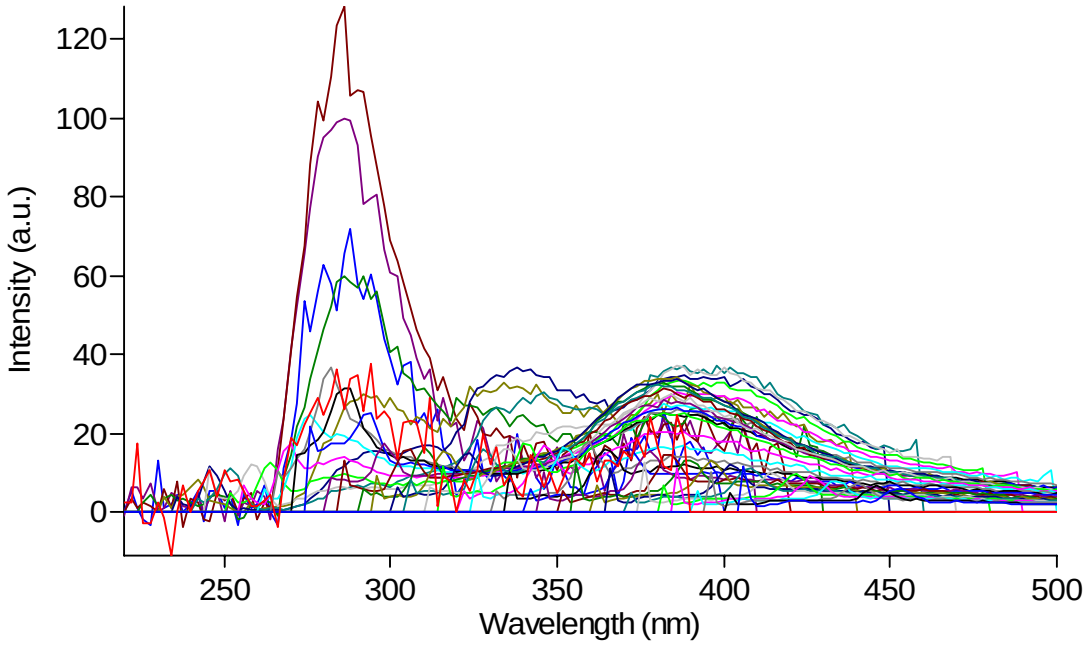
Intensity (a.u.)
120
100
80
60
40
20
0
250
300
350
400
450
500
Wavelength (nm)

M24T

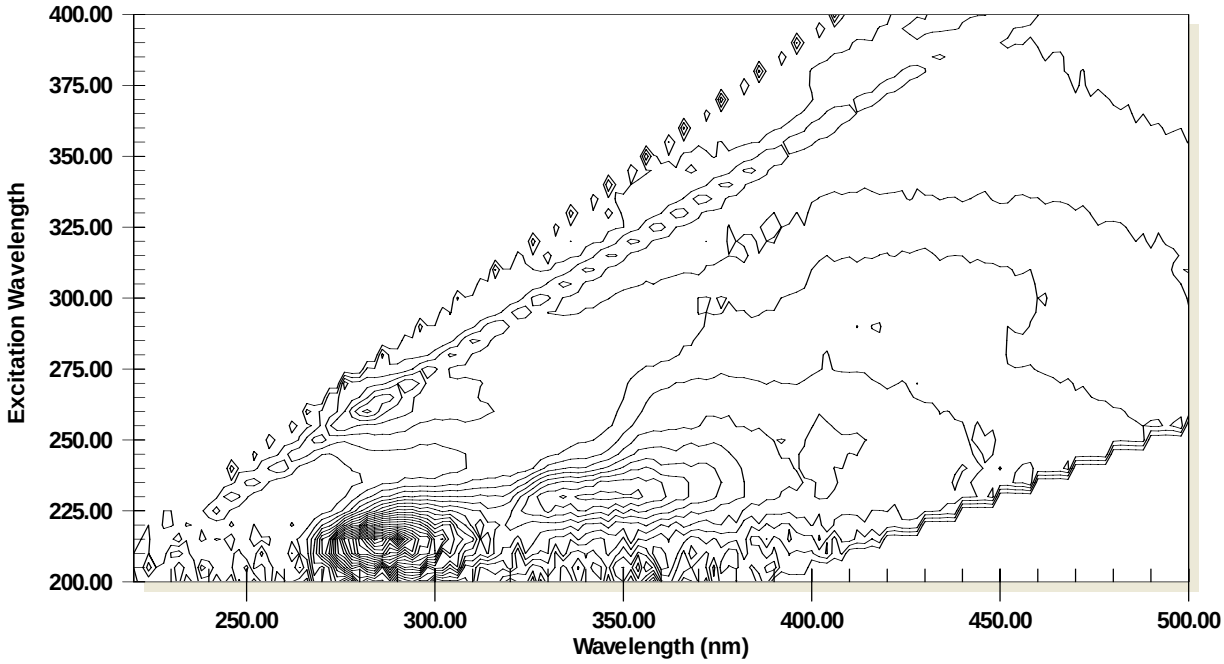
400.00
375.00
350.00
325.00
300.00
275.00
250.00
225.00
200.00
Excitation Wavelength
250.00
300.00
350.00
400.00
450.00
500.00
Wavelength (nm)

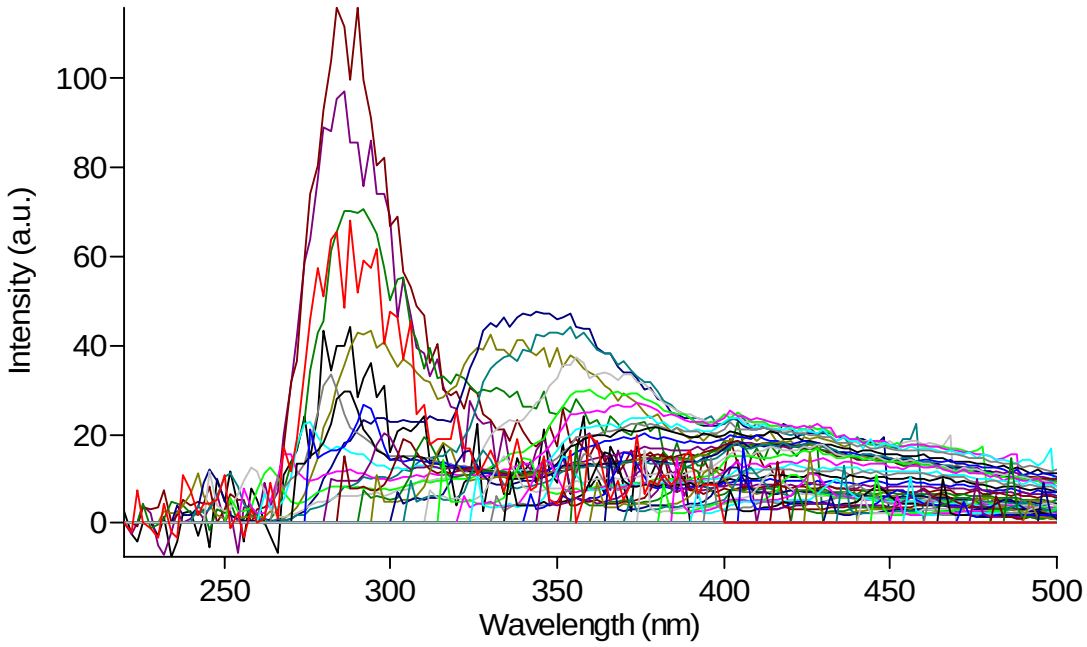
100
80
60
40
20
0
Intensity (a.u.)
250
300
350
400
450
500
Wavelength (nm)

M28T

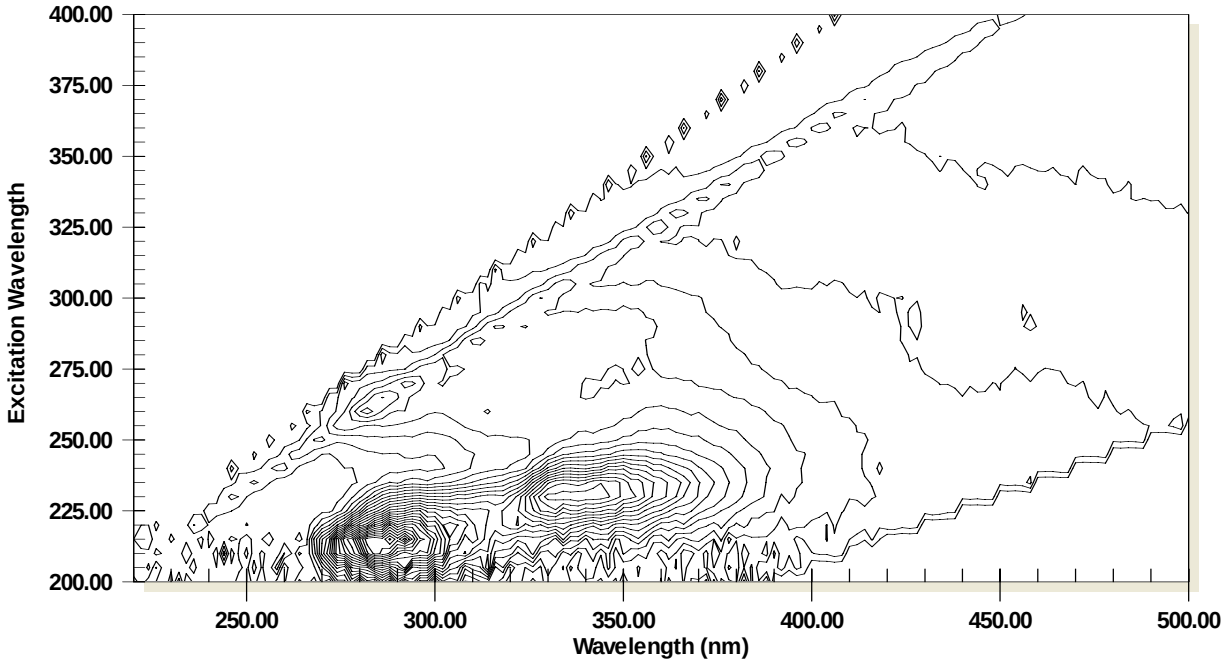
Excitation Wavelength
400.00
375.00
350.00
325.00
300.00
275.00
250.00
225.00
200.00
250.00
300.00
350.00
400.00
450.00
500.00
Wavelength (nm)

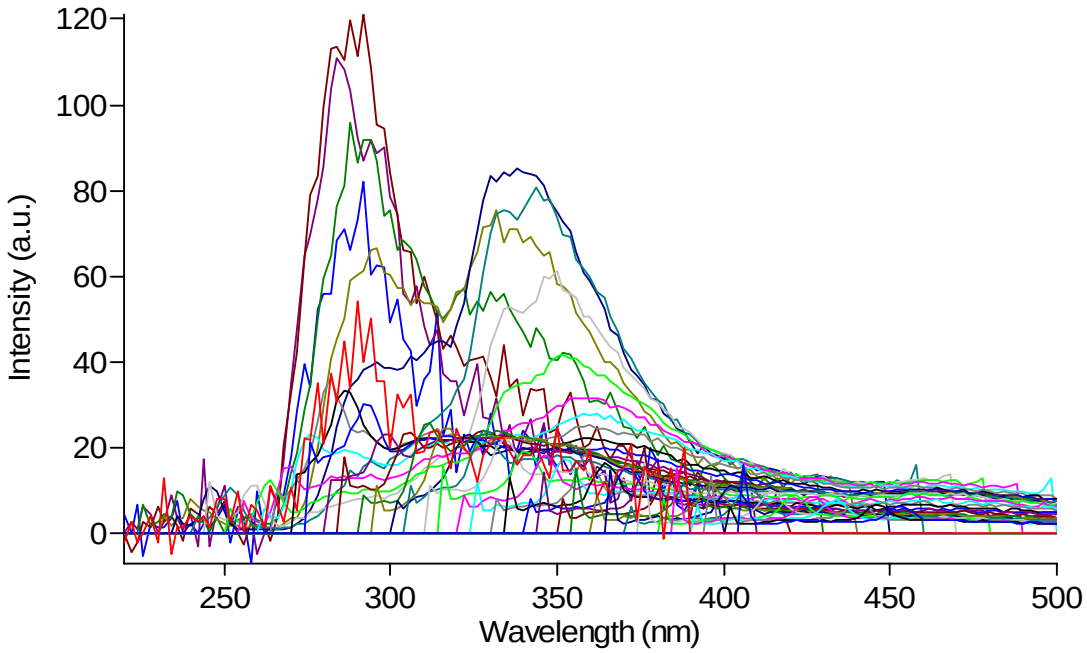
Intensity (a.u.)
120
100
80
60
40
20
0
250
300
350
400
450
500
Wavelength (nm)

M29T

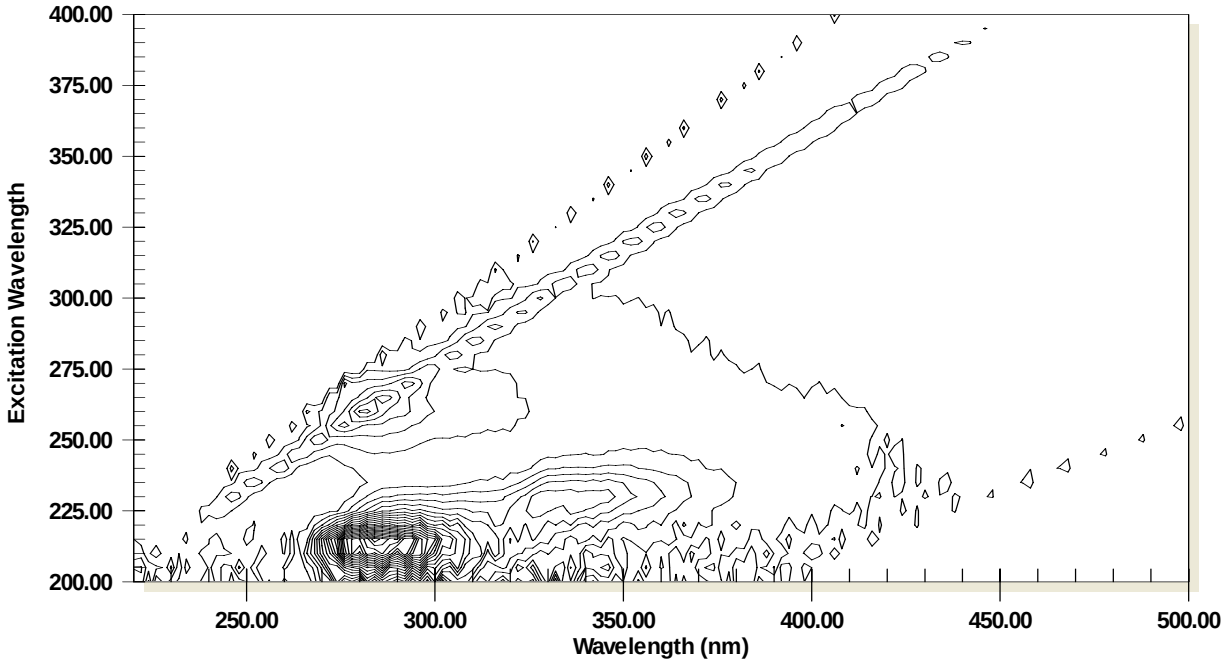
Excitation Wavelength
400.00
375.00
350.00
325.00
300.00
275.00
250.00
225.00
200.00
250.00
300.00
350.00
400.00
450.00
500.00
Wavelength (nm)

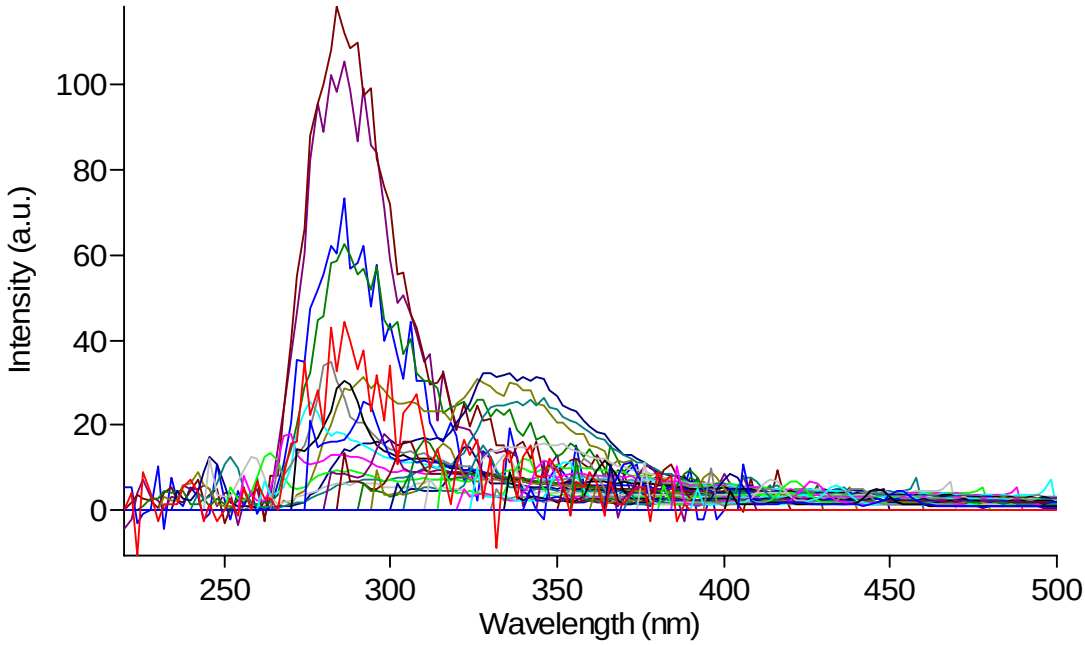
Intensity (a.u.)
100
80
60
40
20
0
250
300
350
400
450
500
Wavelength (nm)

M36T

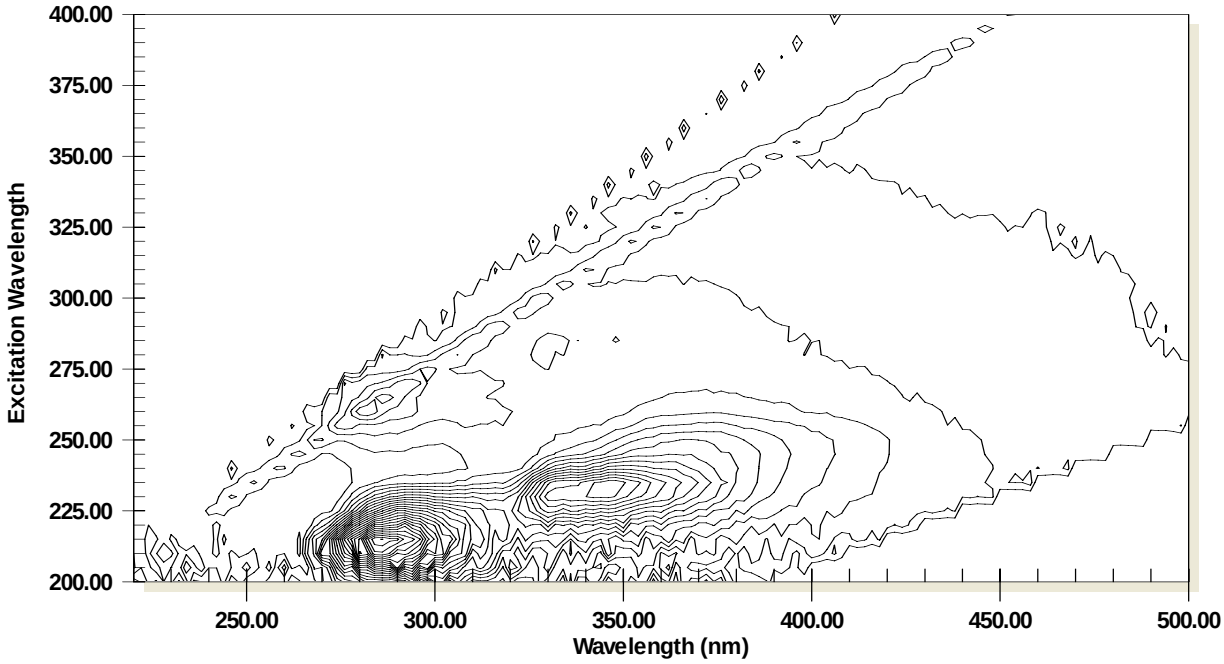
Excitation Wavelength
400.00
375.00
350.00
325.00
300.00
275.00
250.00
225.00
200.00
250.00
300.00
350.00
400.00
450.00
500.00
Wavelength (nm)

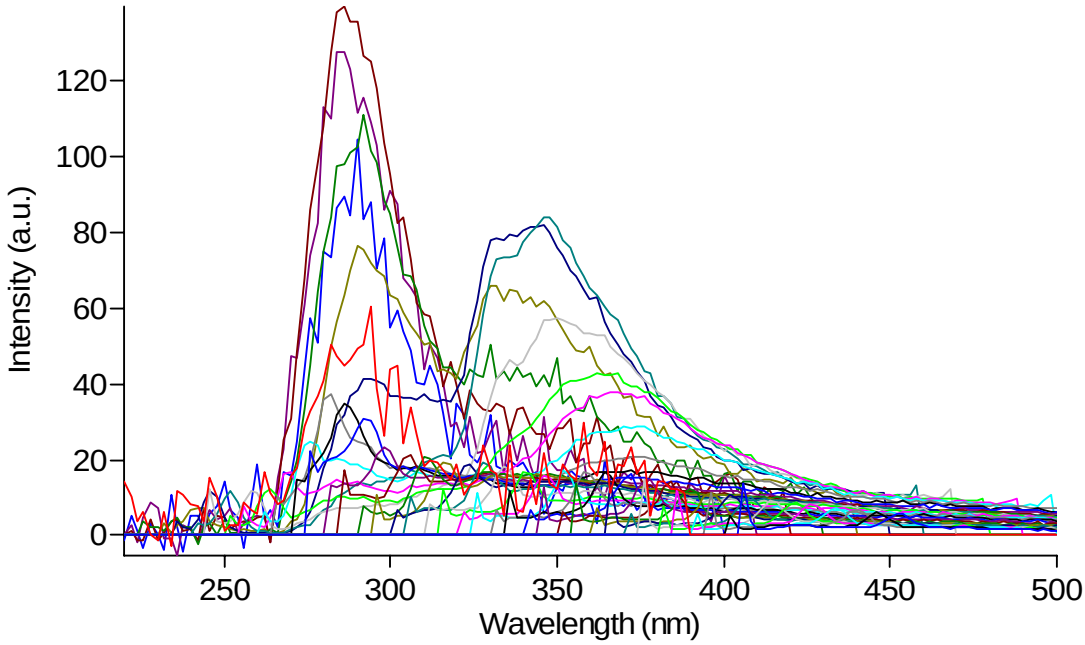
Intensity (a.u.)
120
100
80
60
40
20
0
250
300
350
400
450
500
Wavelength (nm)

M40T

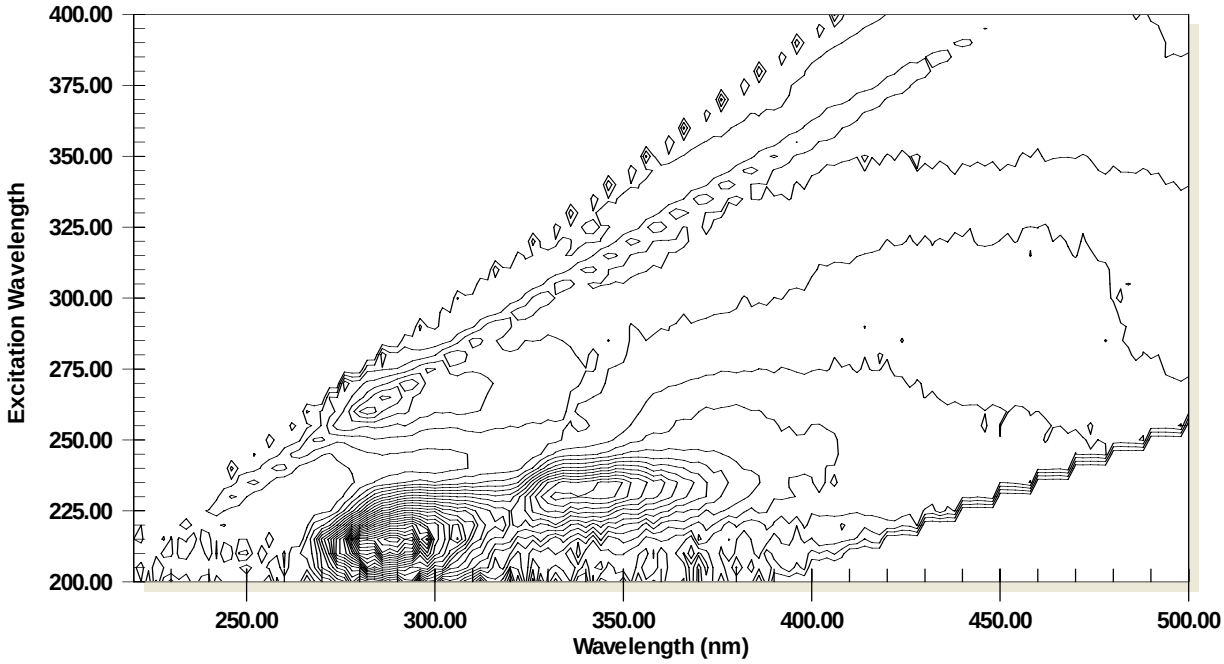
Excitation Wavelength
400.00
375.00
350.00
325.00
300.00
275.00
250.00
225.00
200.00
250.00
300.00
350.00
400.00
450.00
500.00
Wavelength (nm)

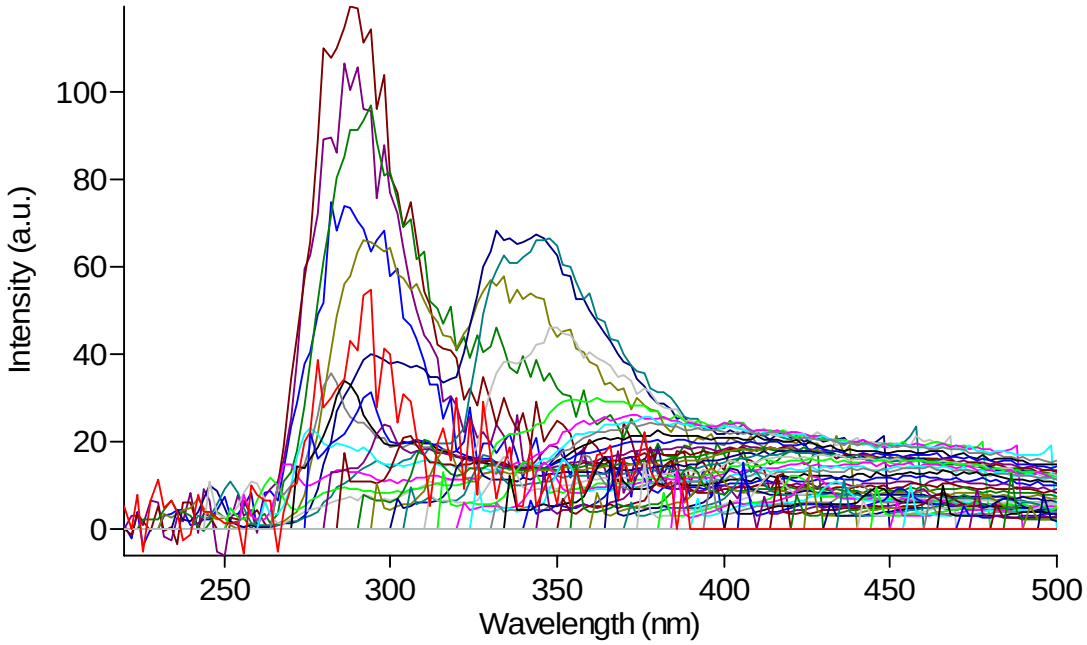
Intensity (a.u.)
100
80
60
40
20
0
250
300
350
400
450
500
Wavelength (nm)

M46T

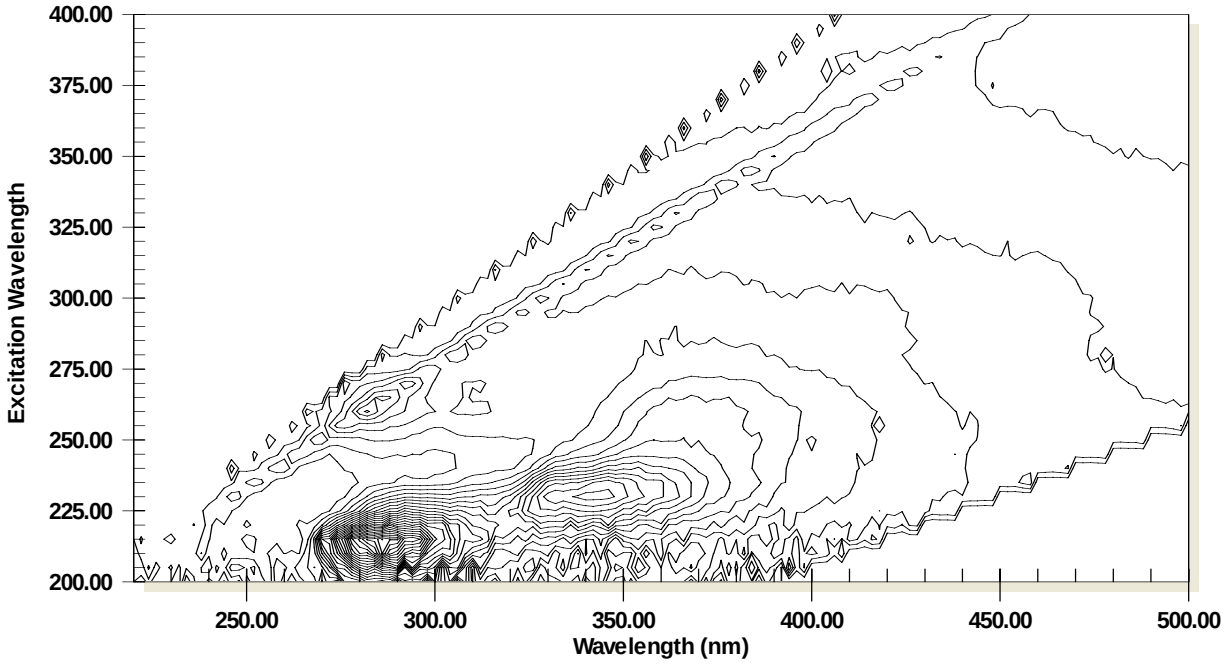
400.00
375.00
350.00
325.00
300.00
275.00
250.00
225.00
200.00
Excitation Wavelength
250.00
300.00
350.00
400.00
450.00
500.00
Wavelength (nm)

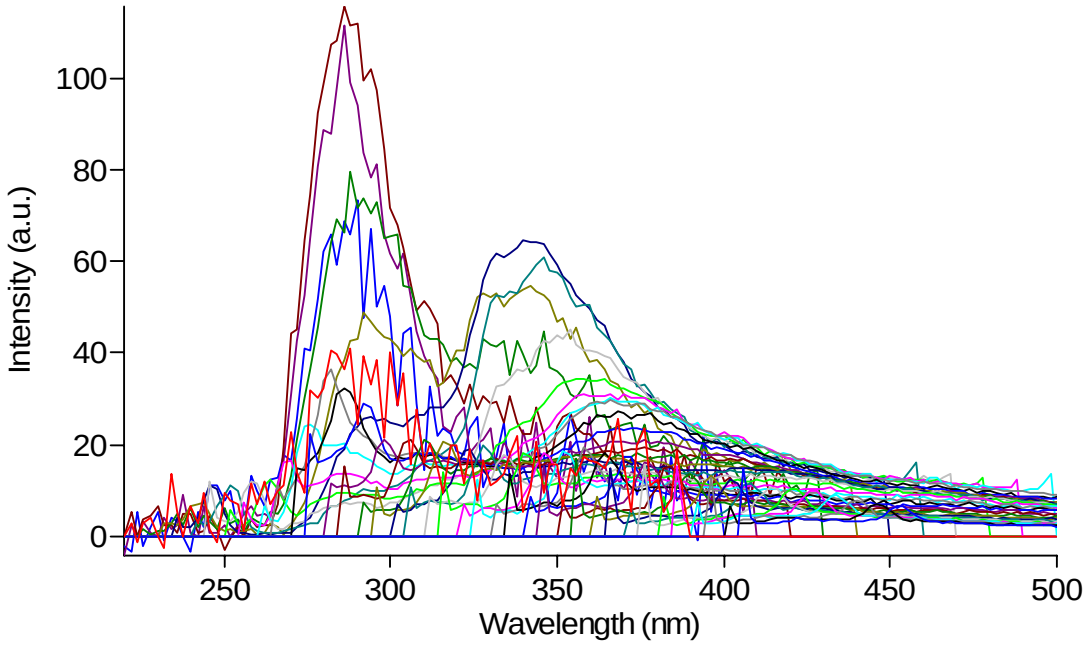
100
80
60
40
20
0
Intensity (a.u.)
250
300
350
400
450
500
Wavelength (nm)

Pyridine Contour Plots and Excitation Scan Overlays
11Cy

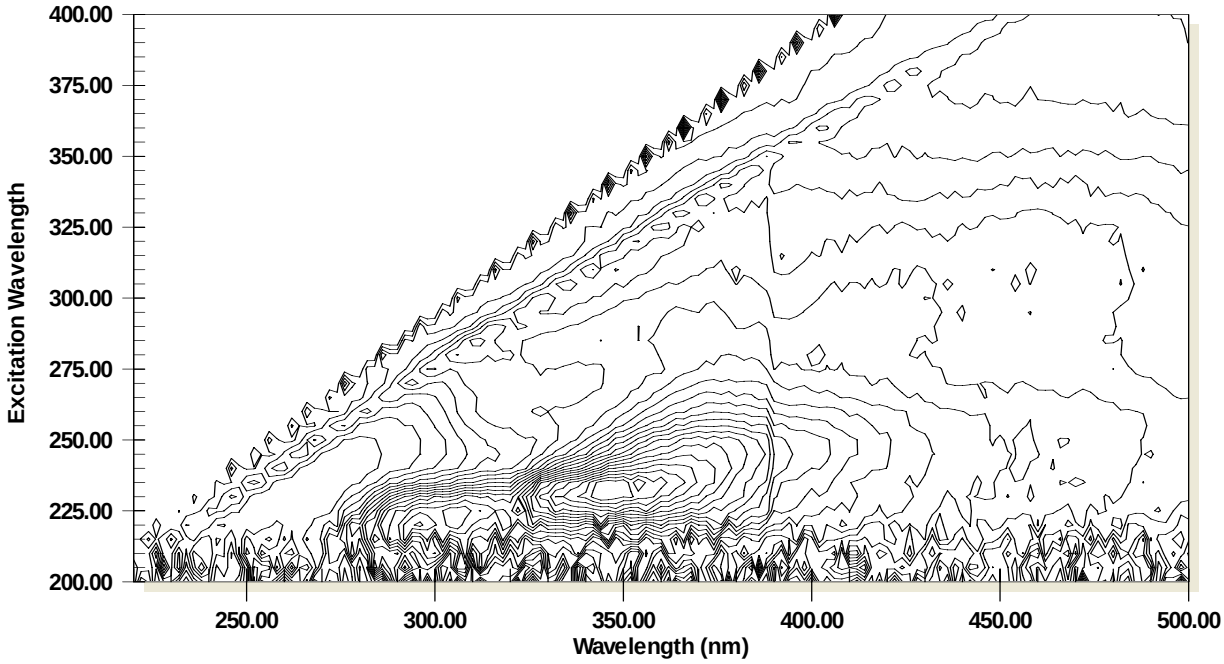

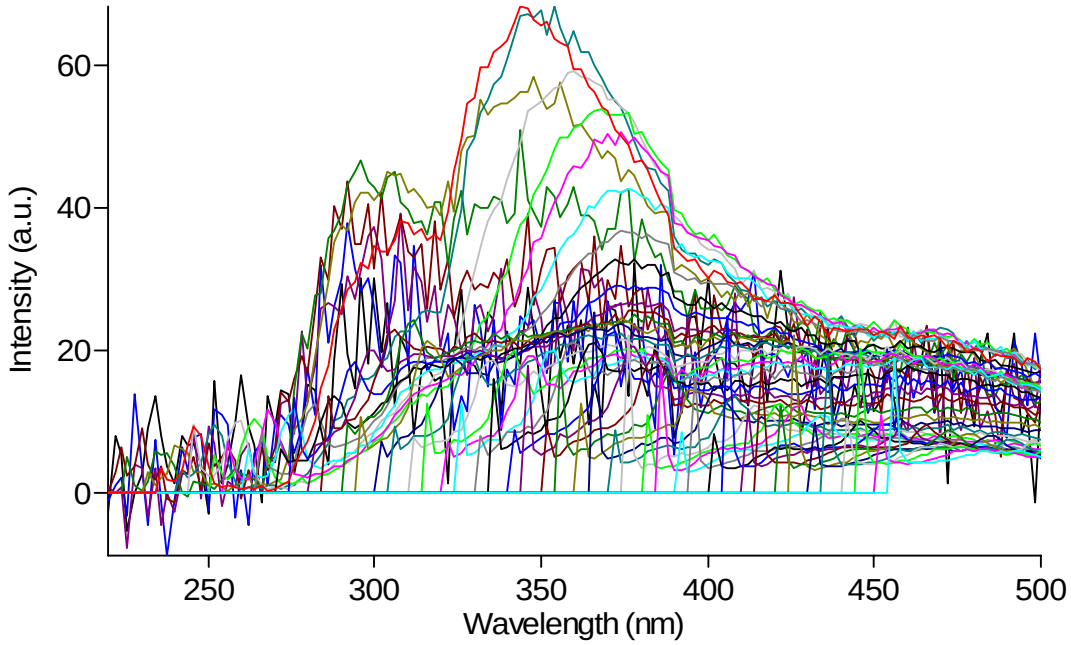

12Cy

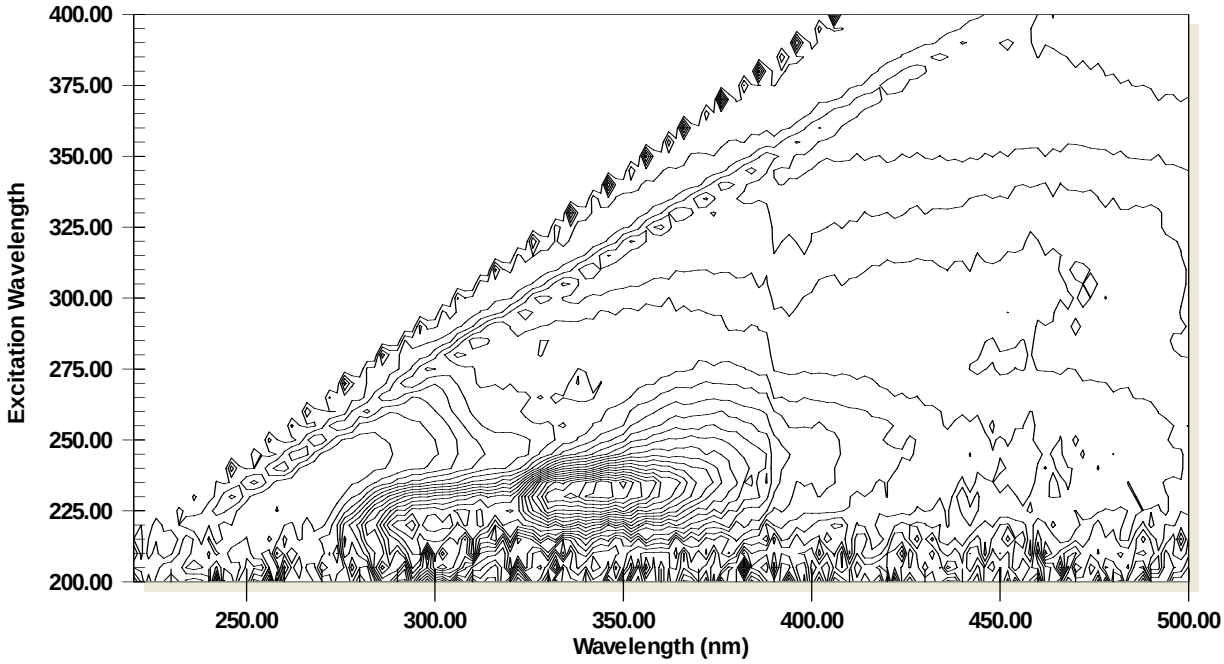
Excitation Wavelength
400.00
375.00
350.00
325.00
300.00
275.00
250.00
225.00
200.00
250.00
300.00
350.00
400.00
450.00
500.00
Wavelength (nm)

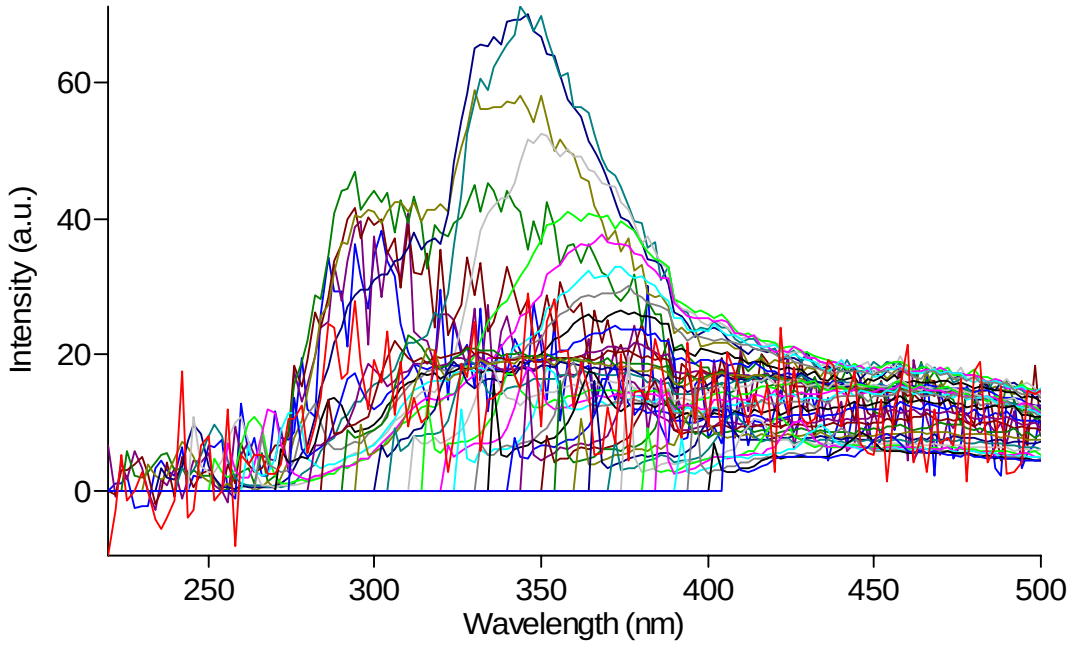
Intensity (a.u.)
60
40
20
0
250
300
350
400
450
500
Wavelength (nm)

13By

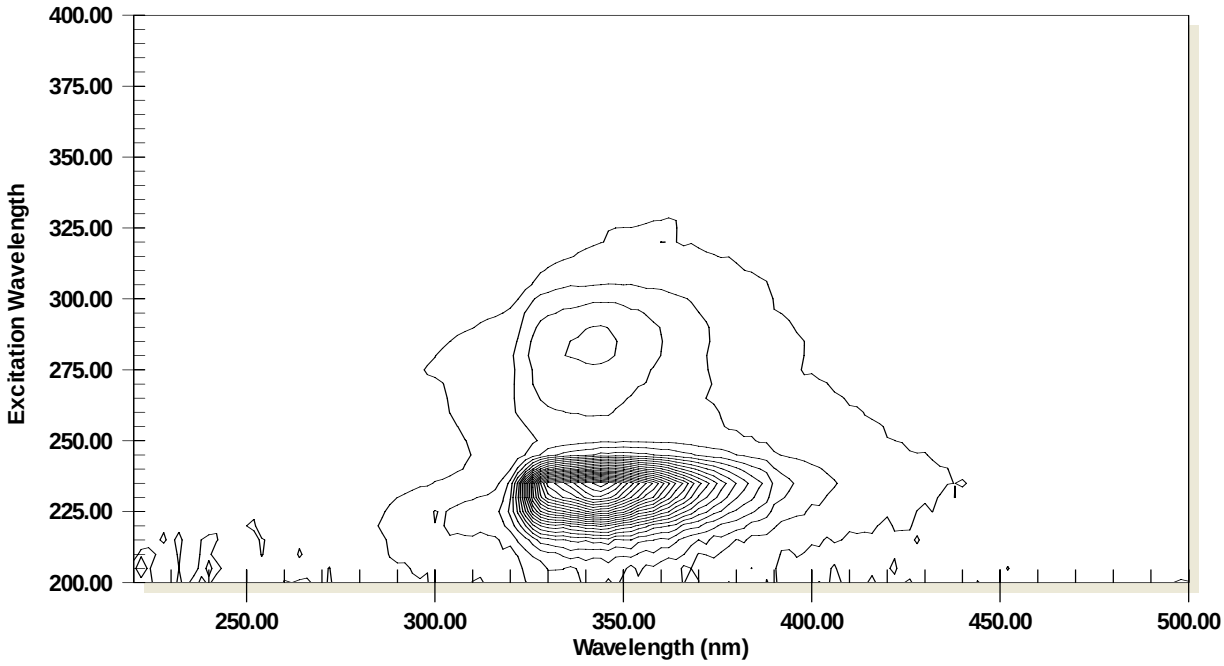
400.00
375.00
350.00
325.00
300.00
275.00
250.00
225.00
200.00
Excitation Wavelength
250.00
300.00
350.00
400.00
450.00
500.00
Wavelength (nm)

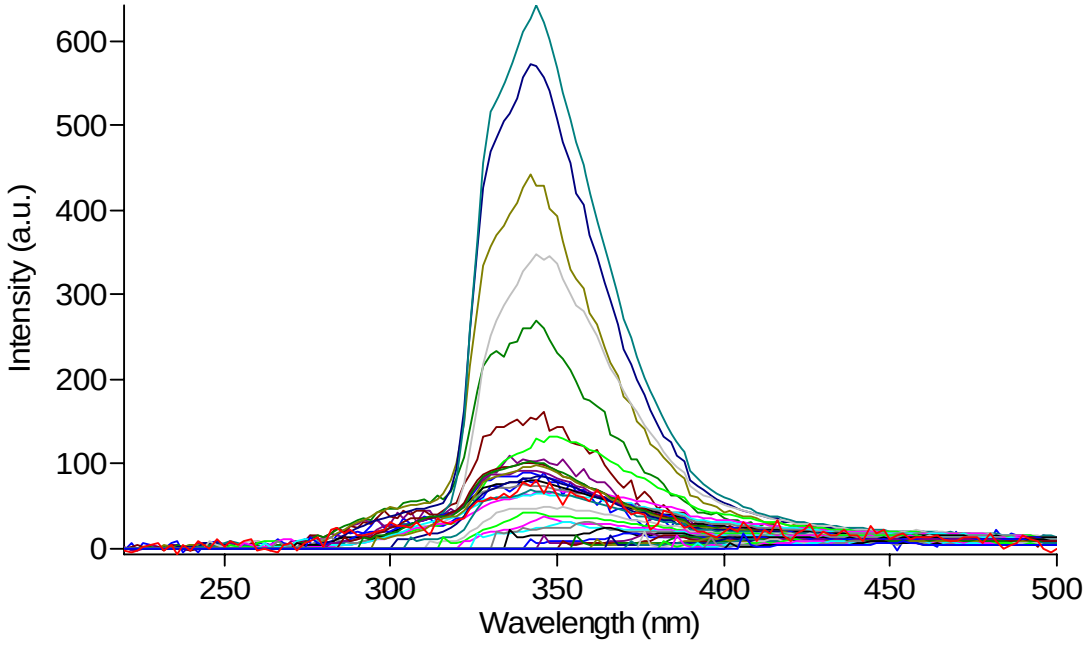
600
500
400
300
200
100
0
Intensity (a.u.)
250
300
350
400
450
500
Wavelength (nm)

14By

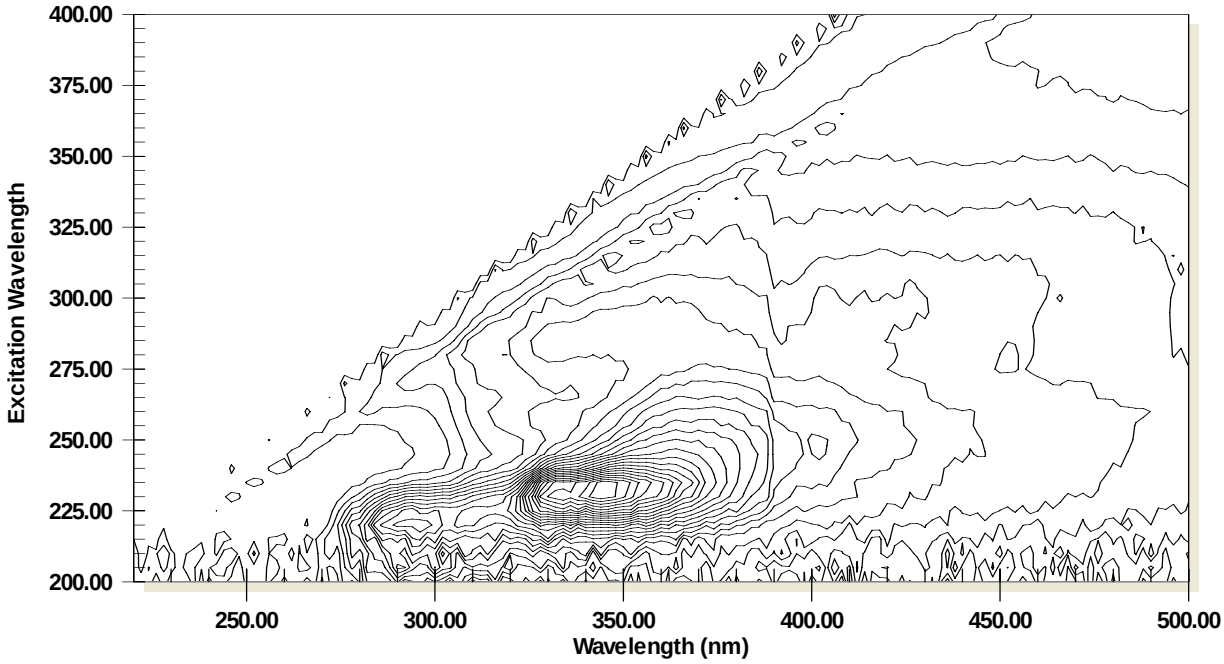
Excitation Wavelength
400.00
375.00
350.00
325.00
300.00
275.00
250.00
225.00
200.00
250.00
300.00
350.00
400.00
450.00
500.00
Wavelength (nm)

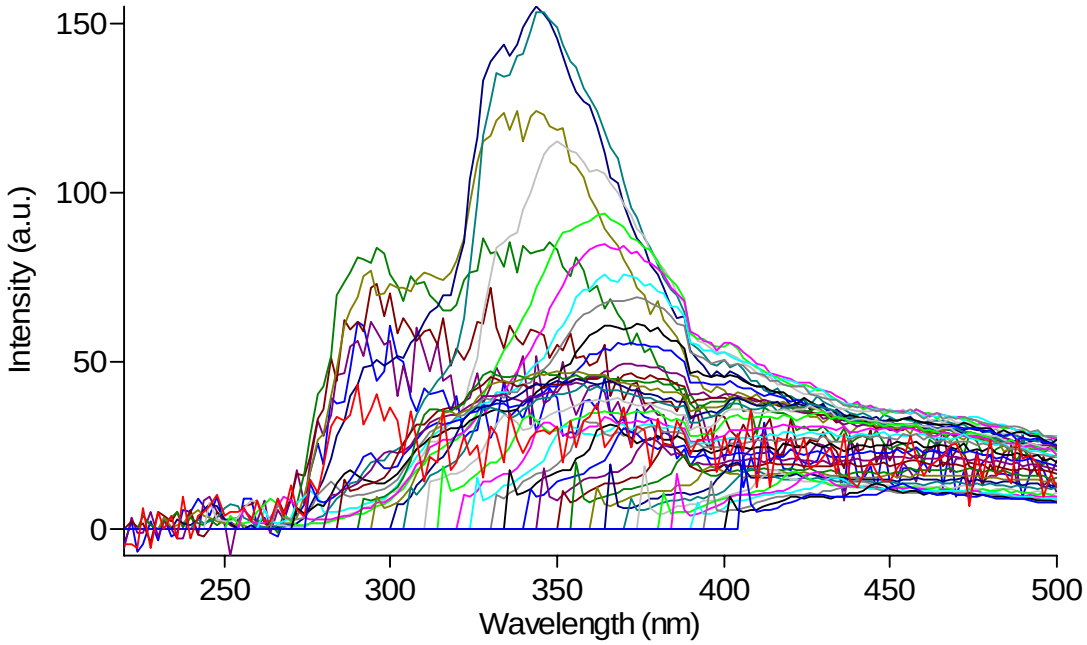
Intensity (a.u.)
150
100
50
0
250
300
350
400
450
500
Wavelength (nm)

15By

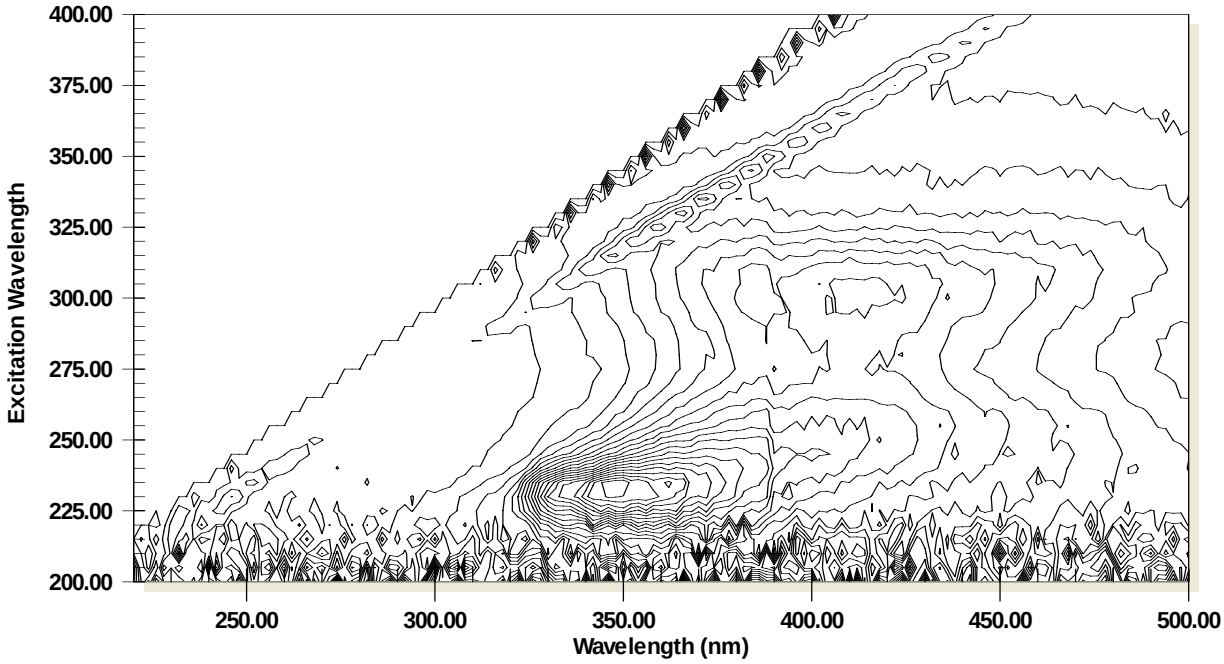
400.00
375.00
350.00
325.00
300.00
275.00
250.00
225.00
200.00
Excitation Wavelength
250.00
300.00
350.00
400.00
450.00
500.00
Wavelength (nm)

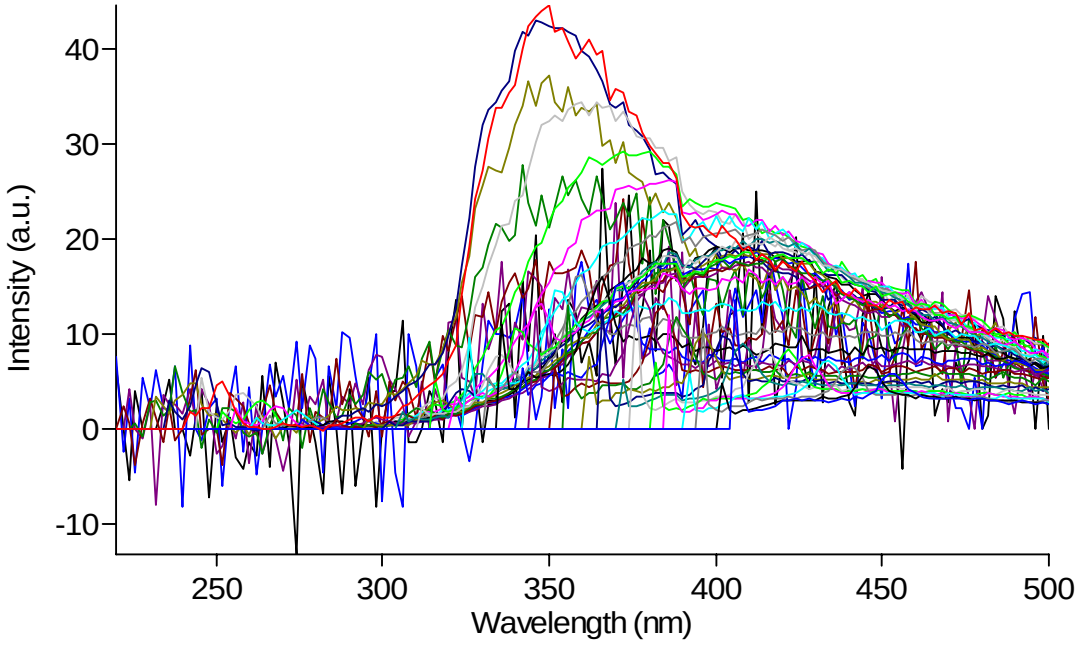
40
30
20
10
0
-10
Intensity (a.u.)
250
300
350
400
450
500
Wavelength (nm)

21By

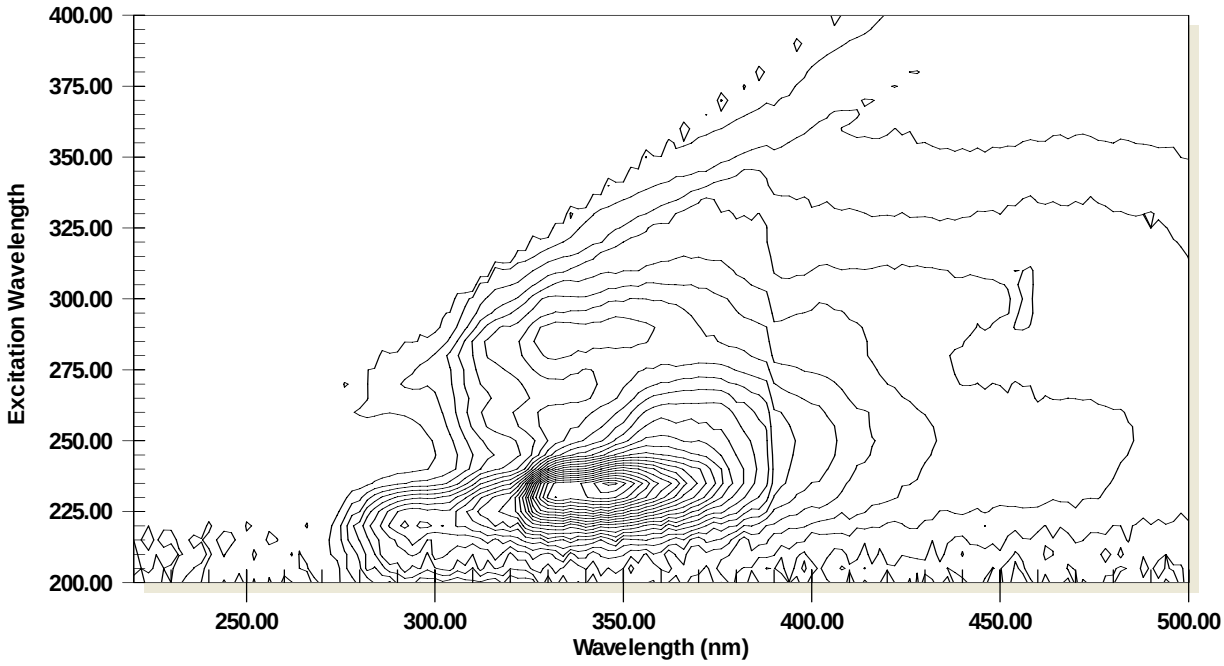
400.00
375.00
350.00
325.00
300.00
275.00
250.00
225.00
200.00
Excitation Wavelength
250.00
300.00
350.00
400.00
450.00
500.00
Wavelength (nm)

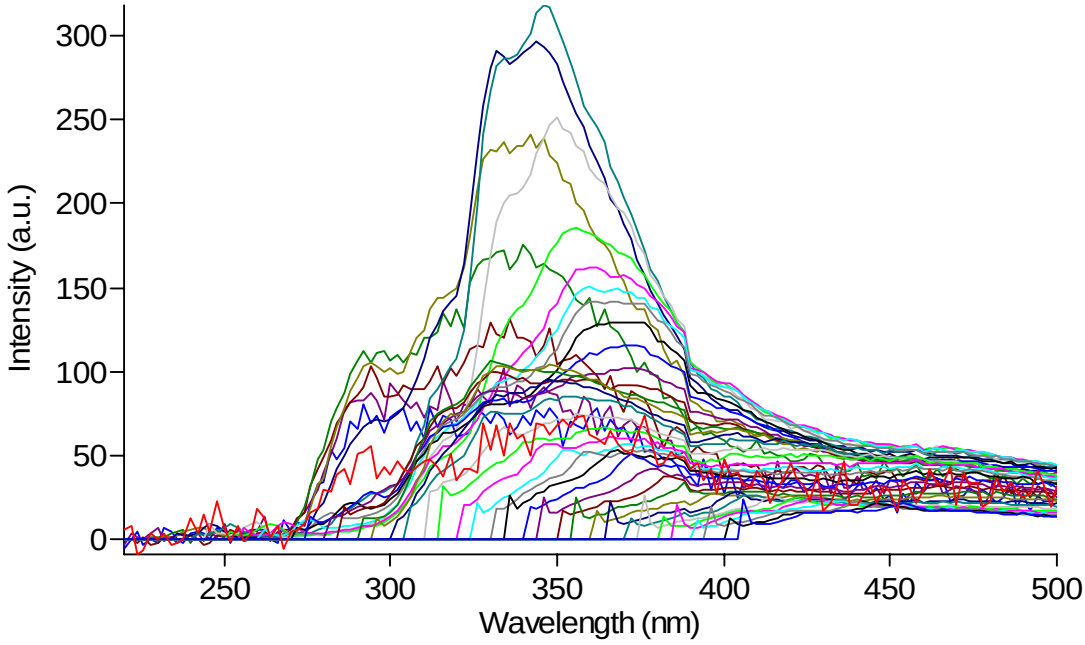
300
250
200
150
100
50
0
Intensity (a.u.)
250
300
350
400
450
500
Wavelength (nm)

22Ay

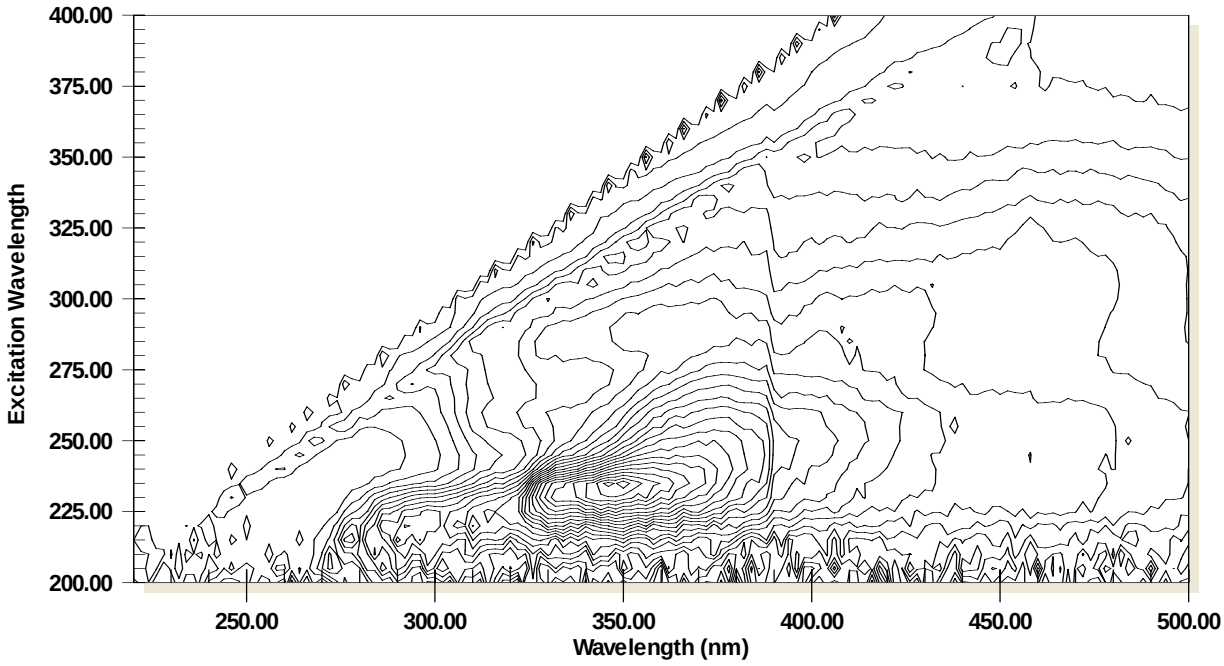
Excitation Wavelength
400.00
375.00
350.00
325.00
300.00
275.00
250.00
225.00
200.00
250.00
300.00
350.00
400.00
450.00
500.00
Wavelength (nm)

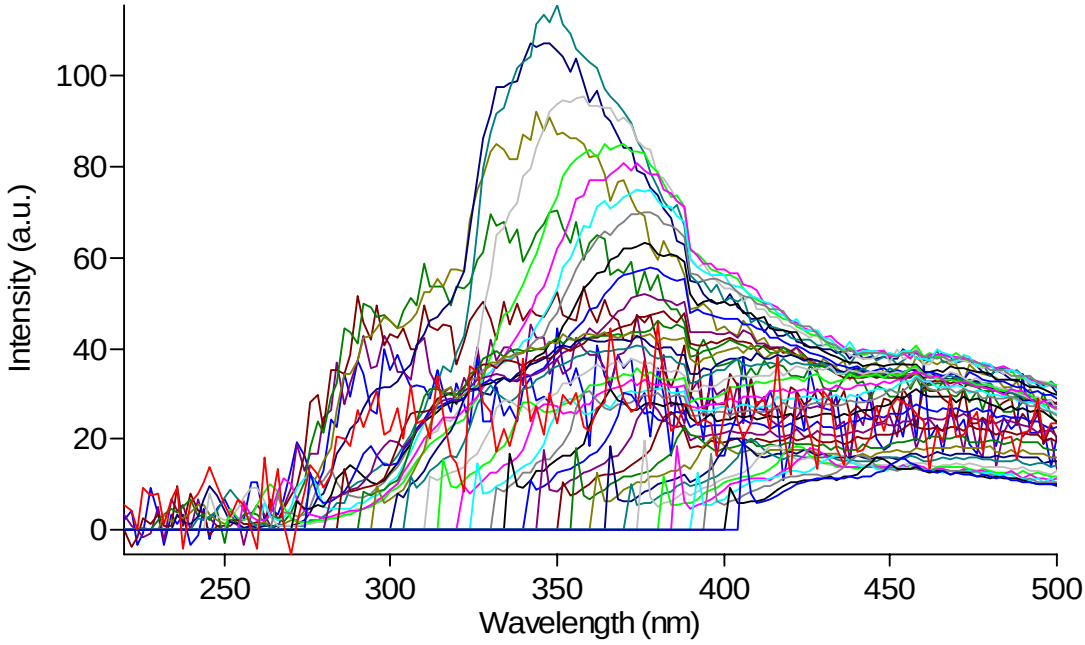
Intensity (a.u.)
100
80
60
40
20
0
250
300
350
400
450
500
Wavelength (nm)

23Ay

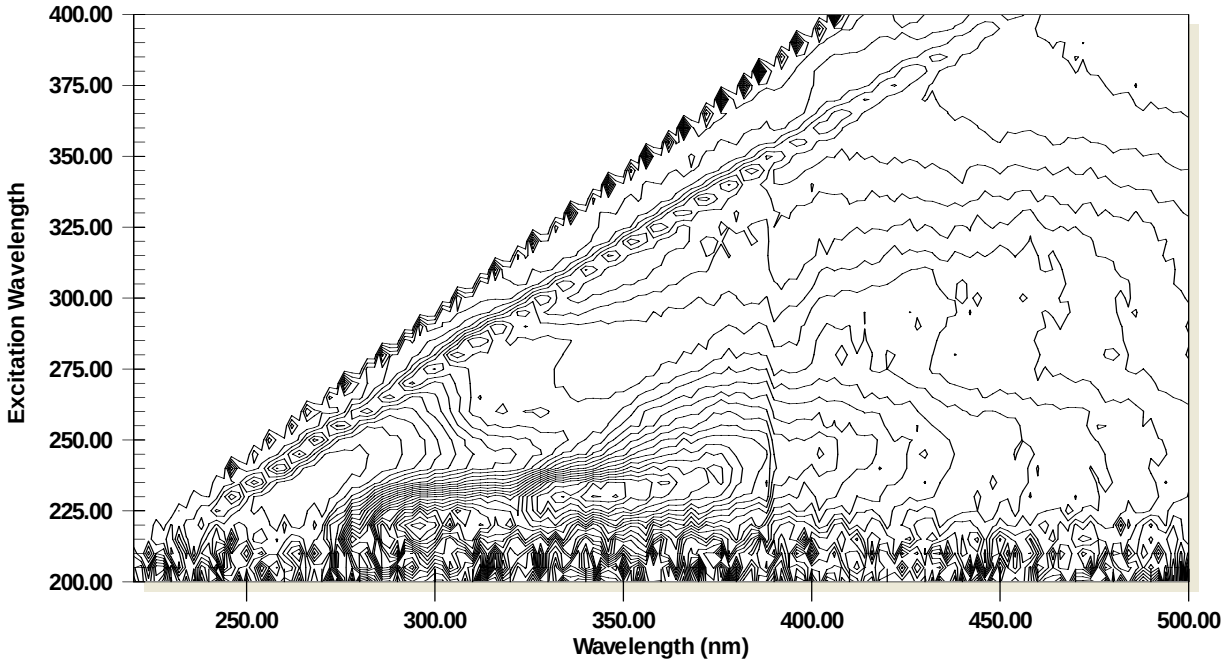
Excitation Wavelength
400.00
375.00
350.00
325.00
300.00
275.00
250.00
225.00
200.00
250.00
300.00
350.00
400.00
450.00
500.00
Wavelength (nm)

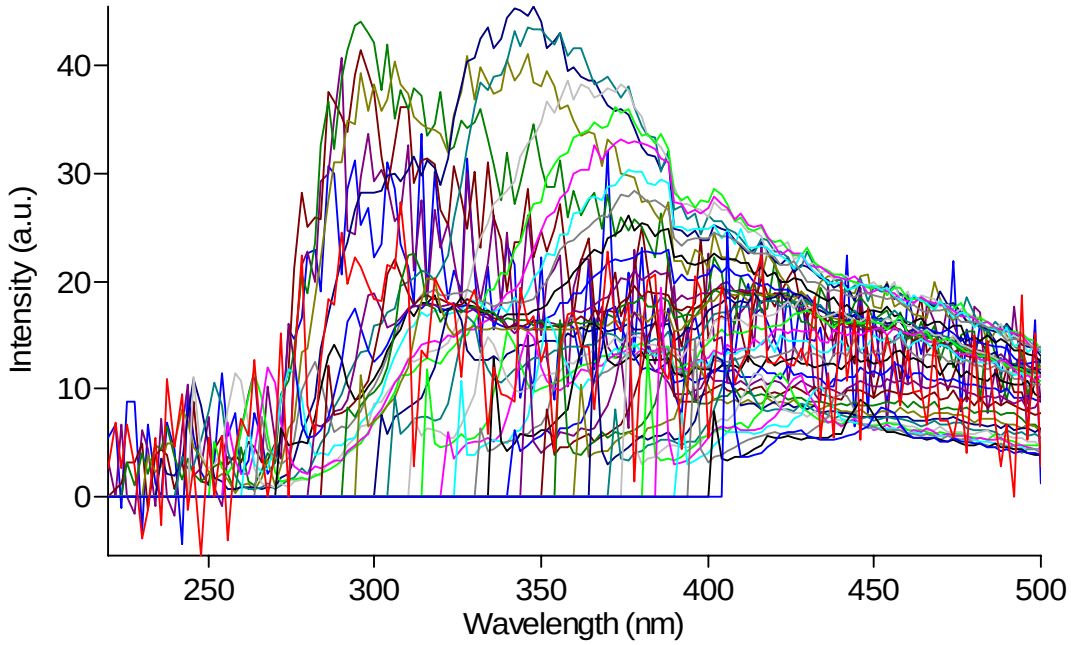
Intensity (a.u.)
40
30
20
10
0
250
300
350
400
450
500
Wavelength (nm)

24Cy

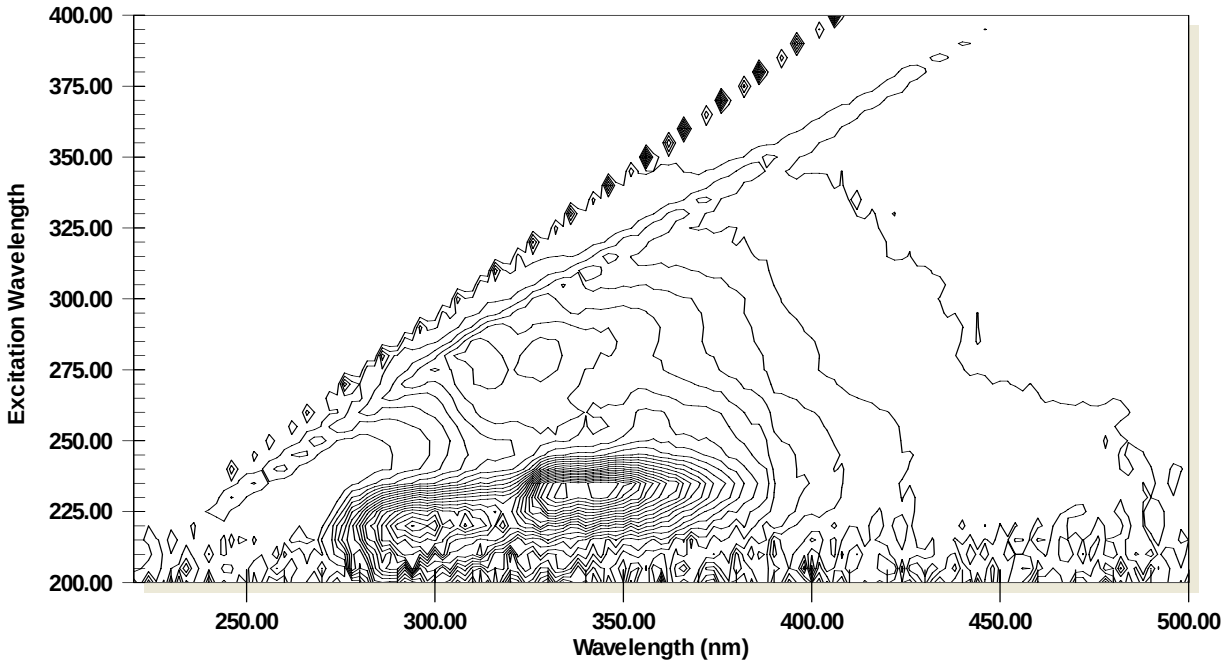
Excitation Wavelength
400.00
375.00
350.00
325.00
300.00
275.00
250.00
225.00
200.00
250.00
300.00
350.00
400.00
450.00
500.00
Wavelength (nm)

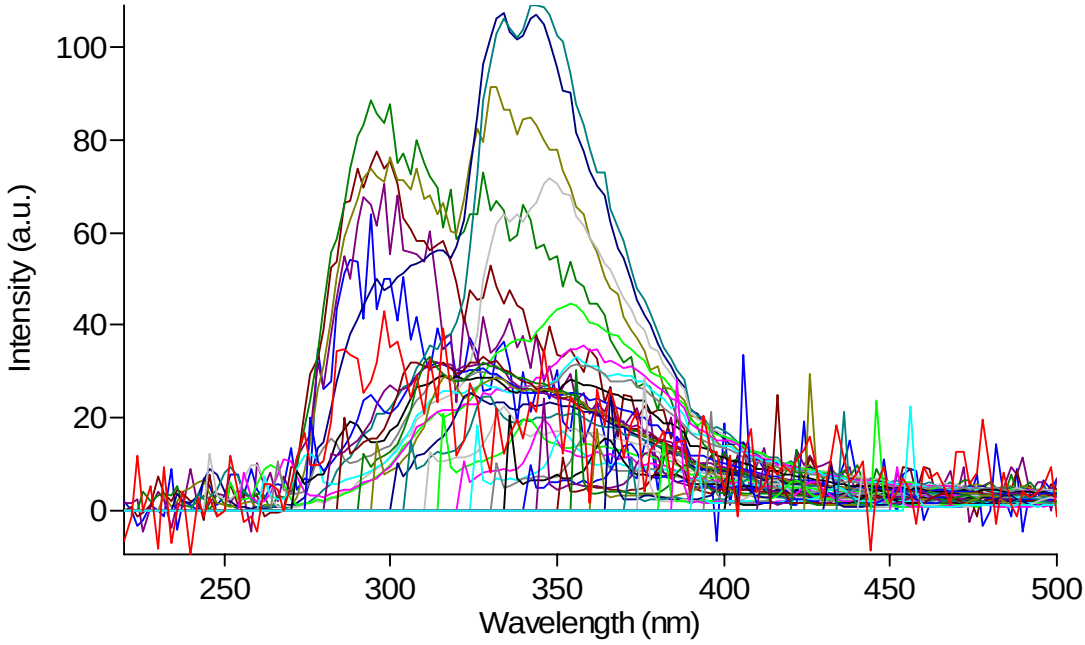
Intensity (a.u.)
100
80
60
40
20
0
250
300
350
400
450
500
Wavelength (nm)

25Cy

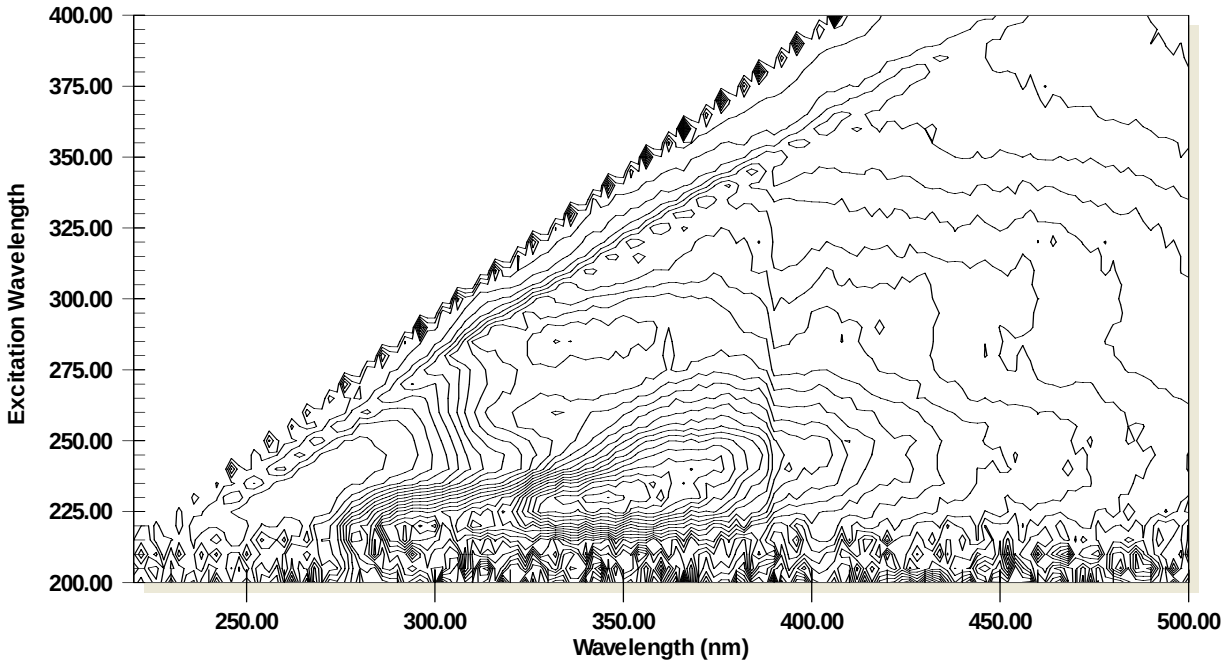
Excitation Wavelength
400.00
375.00
350.00
325.00
300.00
275.00
250.00
225.00
200.00
250.00
300.00
350.00
400.00
450.00
500.00
Wavelength (nm)

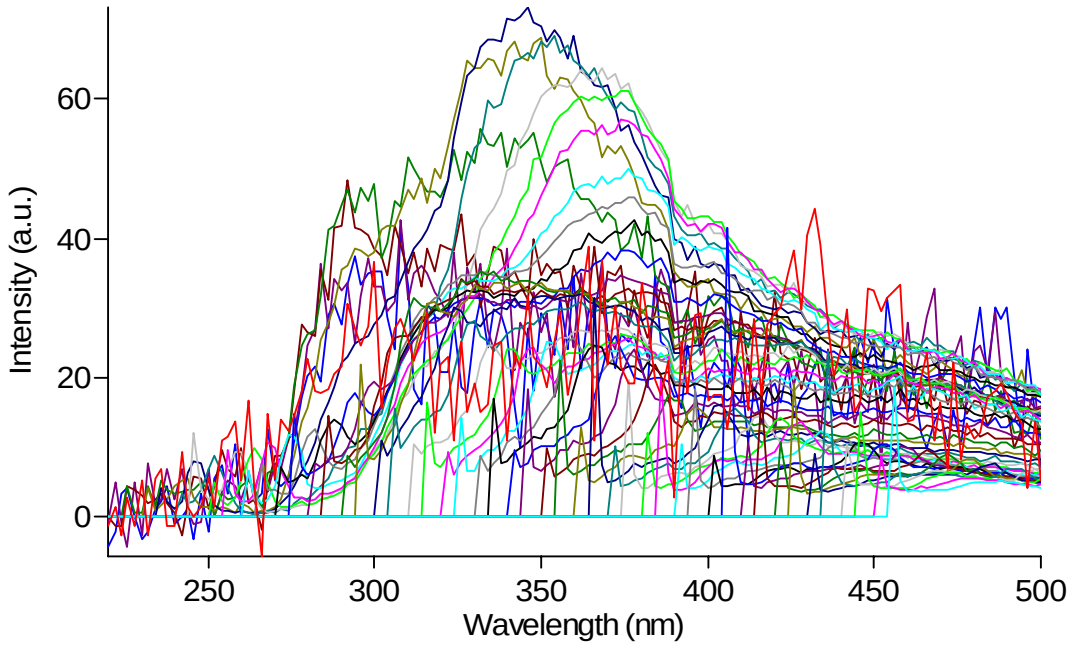
Intensity (a.u.)
60
40
20
0
250
300
350
400
450
500
Wavelength (nm)

31Cy

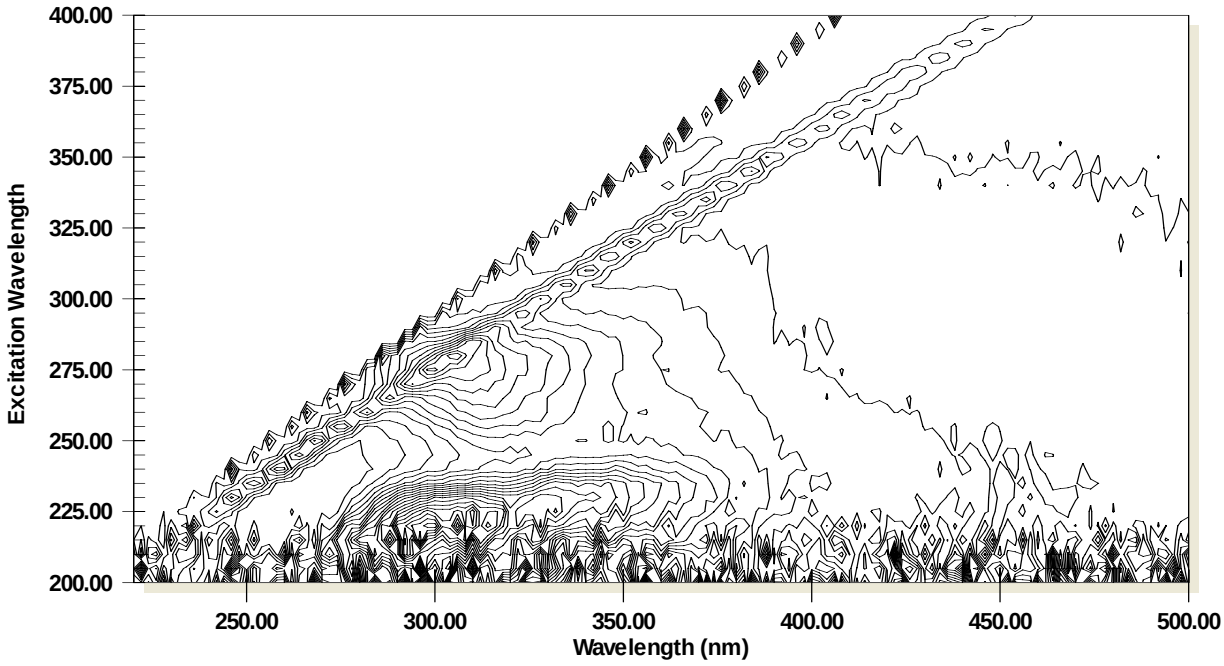
400.00
375.00
350.00
325.00
300.00
275.00
250.00
225.00
200.00
Excitation Wavelength
250.00
300.00
350.00
400.00
450.00
500.00
Wavelength (nm)

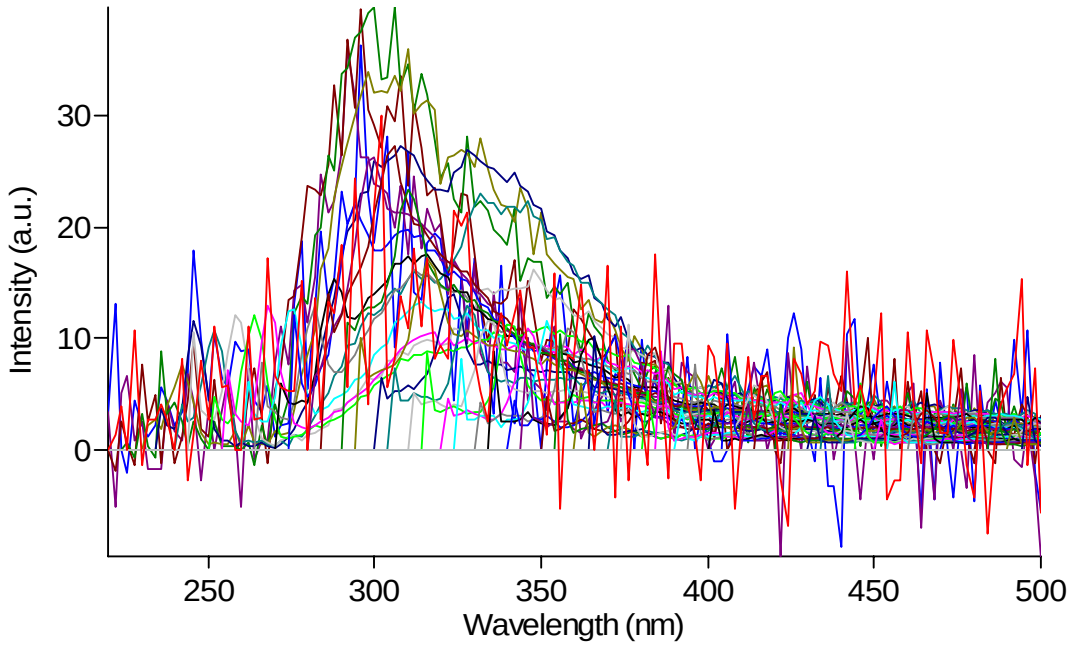
30
20
10
0
Intensity (a.u.)
250
300
350
400
450
500
Wavelength (nm)

32Cy

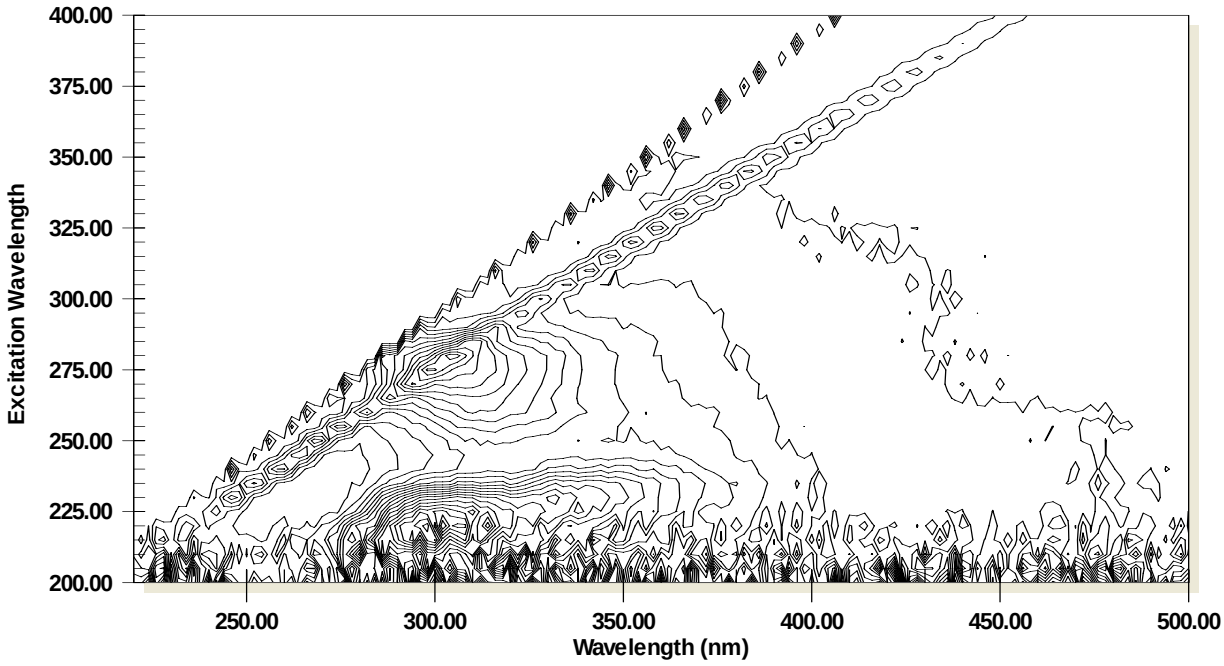
400.00
375.00
350.00
325.00
300.00
275.00
250.00
225.00
200.00
Excitation Wavelength
250.00
300.00
350.00
400.00
450.00
500.00
Wavelength (nm)

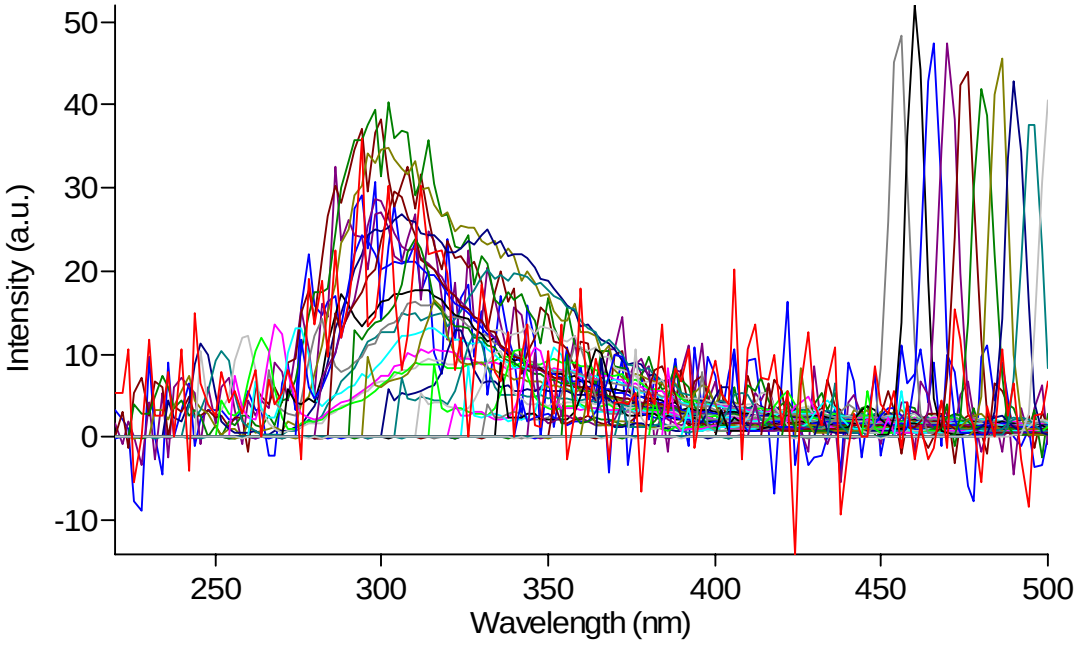
50
40
30
20
10
0
-10
Intensity (a.u.)
250
300
350
400
450
500
Wavelength (nm)

33Ay

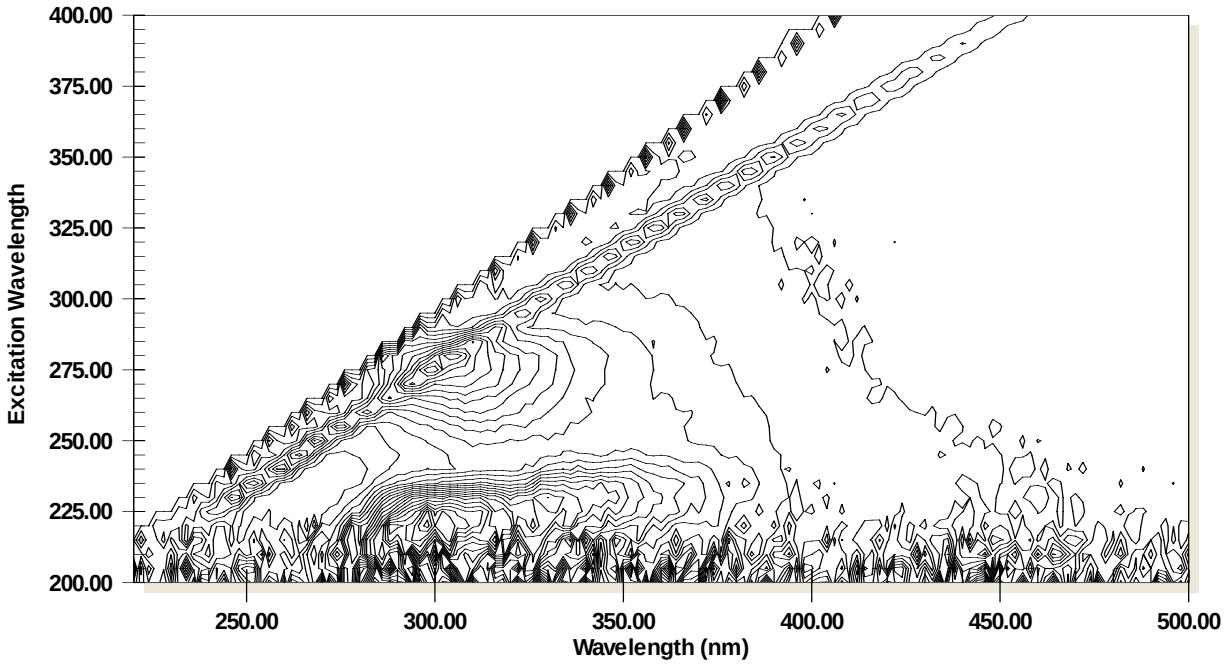
Excitation Wavelength
400.00
375.00
350.00
325.00
300.00
275.00
250.00
225.00
200.00
250.00
300.00
350.00
400.00
450.00
500.00
Wavelength (nm)

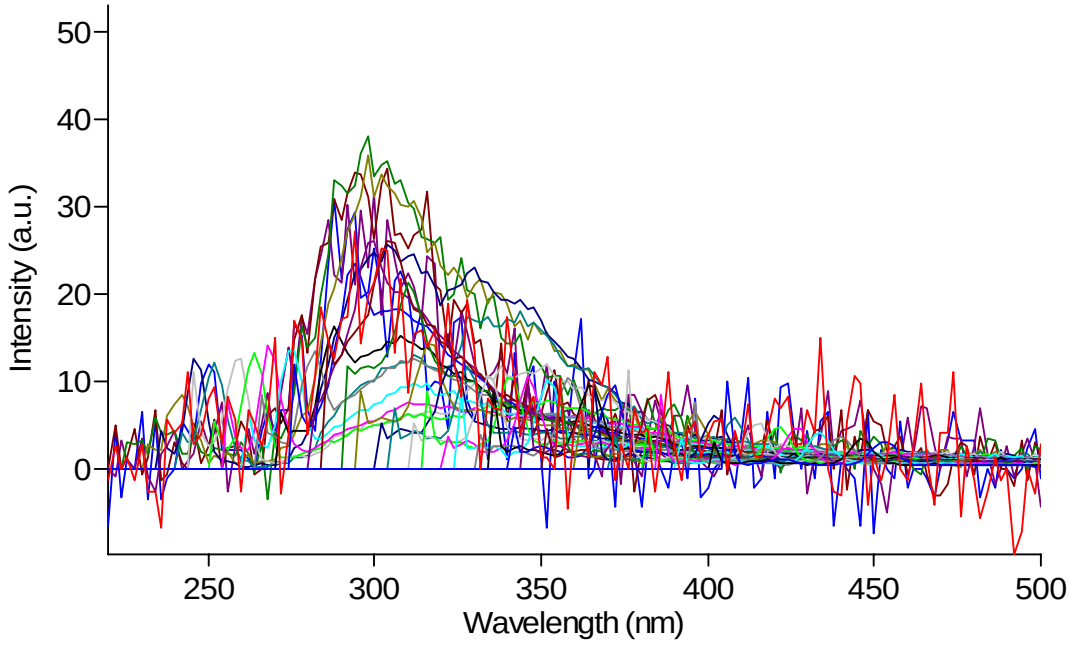
Intensity (a.u.)
50
40
30
20
10
0
250
300
350
400
450
500
Wavelength (nm)

34By

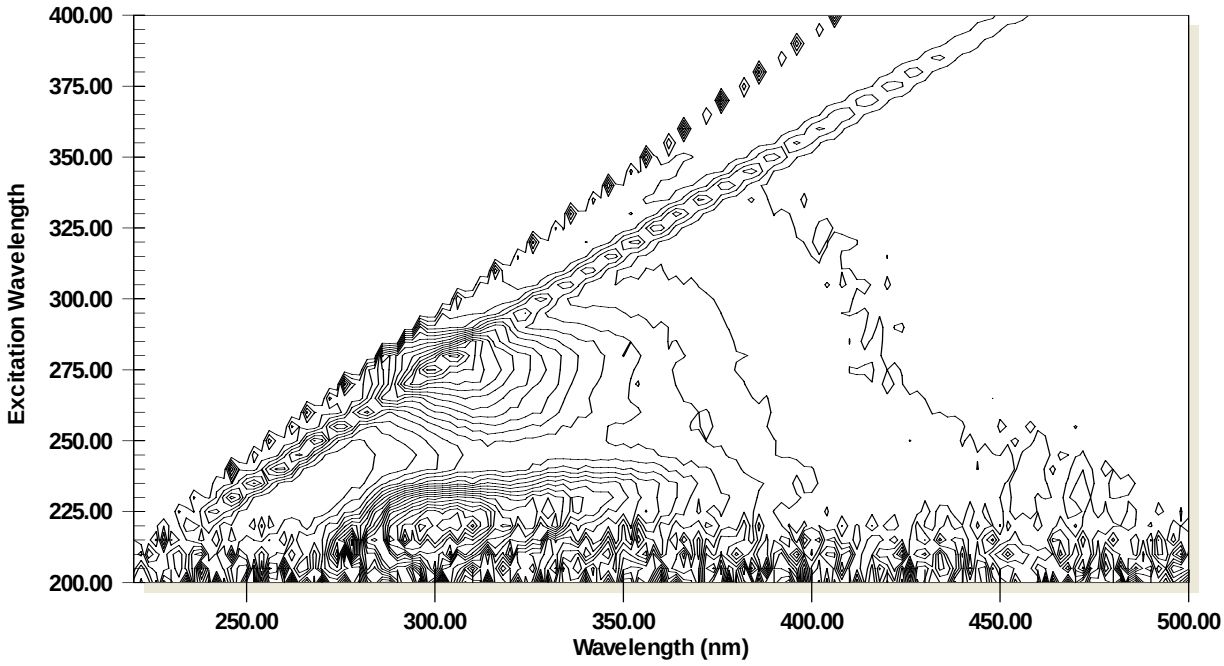
400.00
375.00
350.00
325.00
300.00
275.00
250.00
225.00
200.00
Excitation Wavelength
250.00
300.00
350.00
400.00
450.00
500.00
Wavelength (nm)

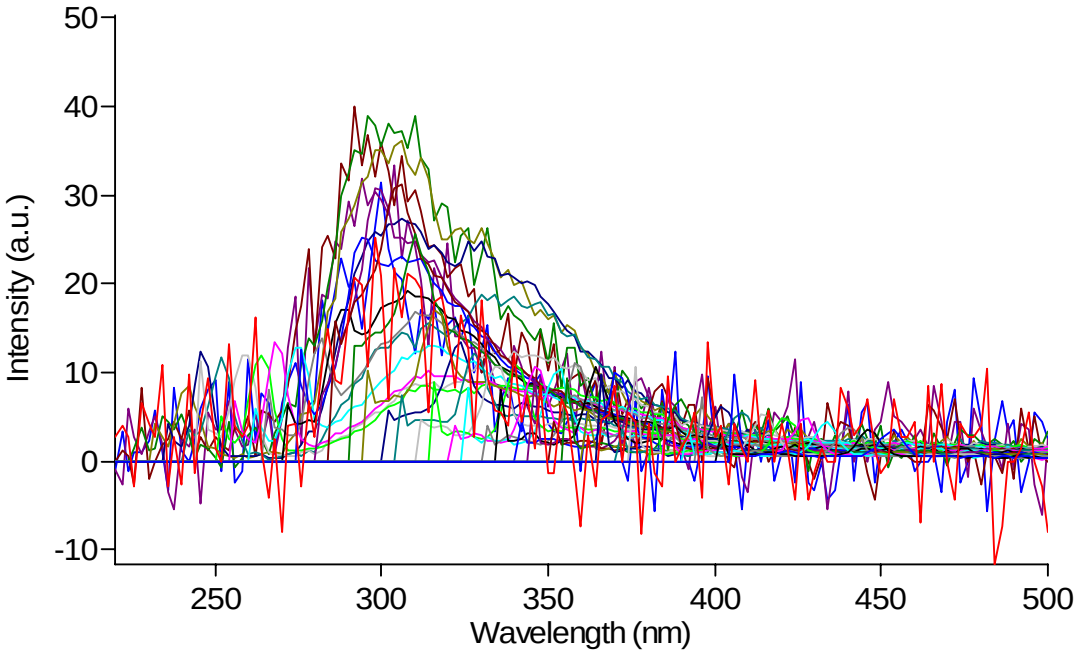
50
40
30
20
10
0
-10
Intensity (a.u.)
250
300
350
400
450
500
Wavelength (nm)

35Cy

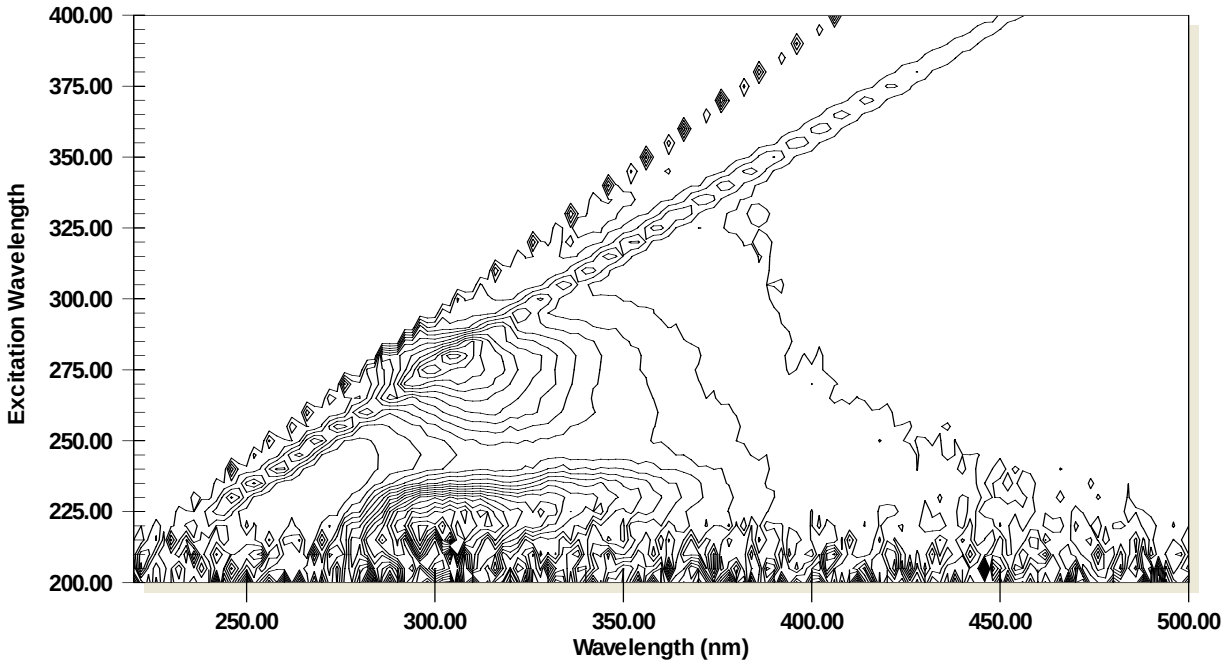
Excitation Wavelength
400.00
375.00
350.00
325.00
300.00
275.00
250.00
225.00
200.00
250.00
300.00
350.00
400.00
450.00
500.00
Wavelength (nm)

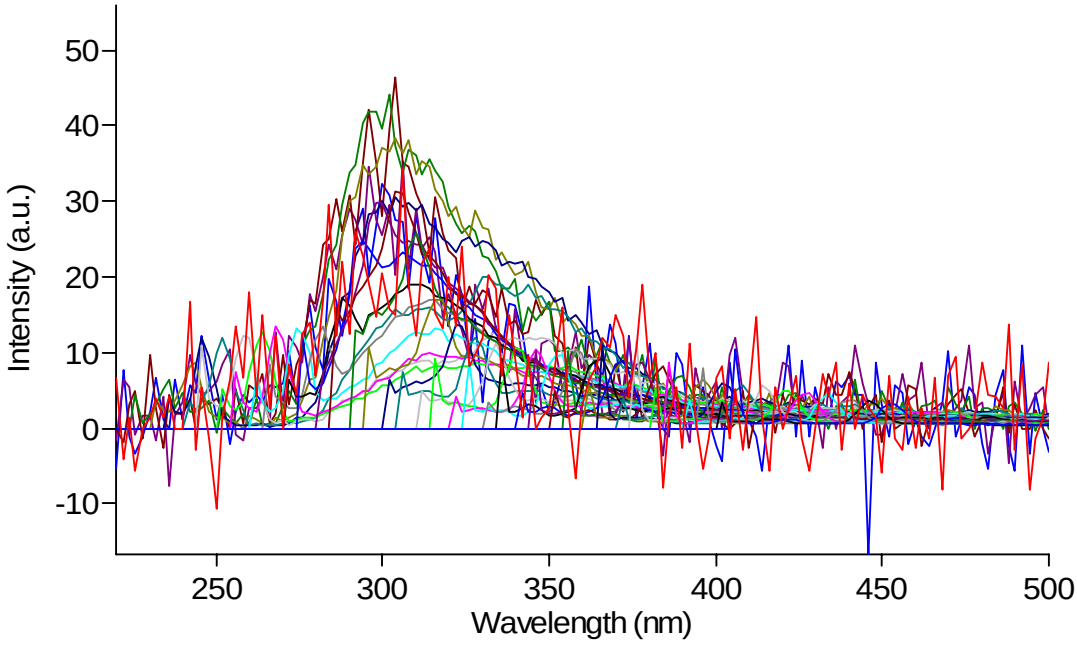
Intensity (a.u.)
50
40
30
20
10
0
-10
250
300
350
400
450
500
Wavelength (nm)

41Cy

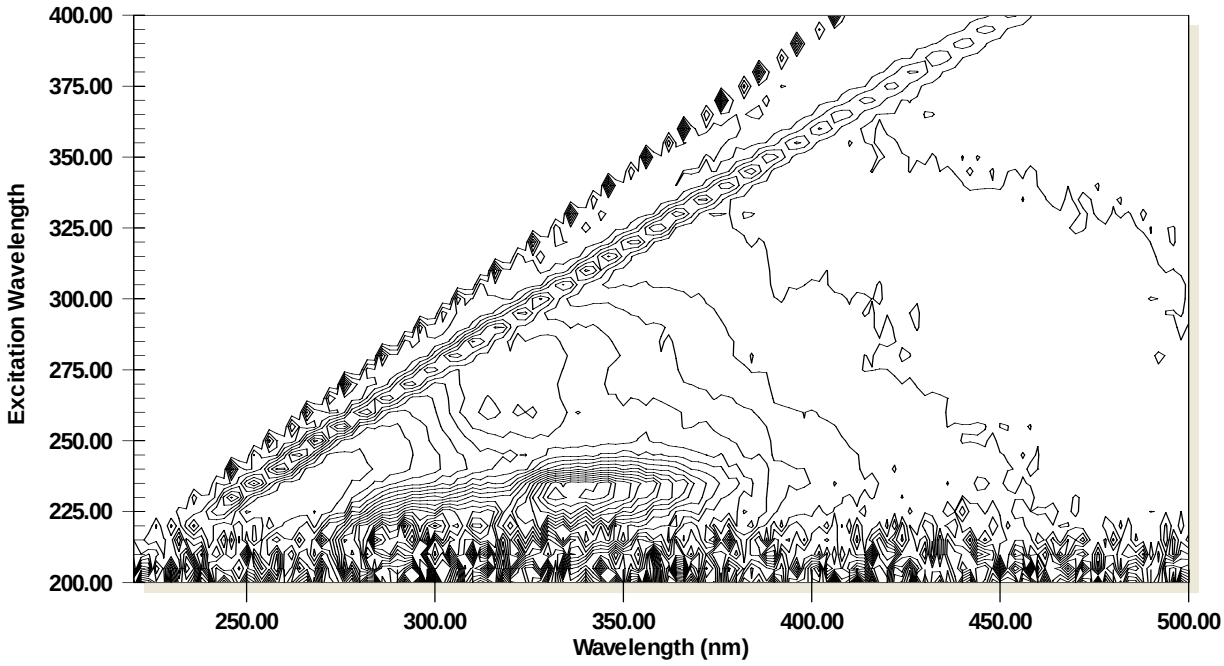
Excitation Wavelength
400.00
375.00
350.00
325.00
300.00
275.00
250.00
225.00
200.00
250.00
300.00
350.00
400.00
450.00
500.00
Wavelength (nm)

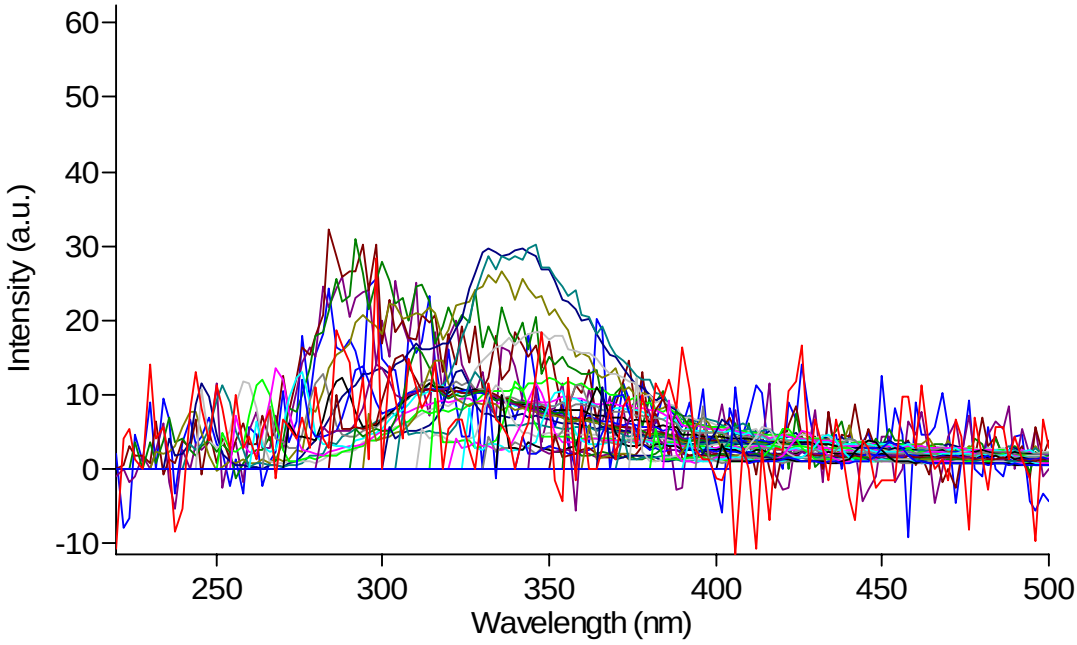
Intensity (a.u.)
60
50
40
30
20
10
0
-10
250
300
350
400
450
500
Wavelength (nm)

42By

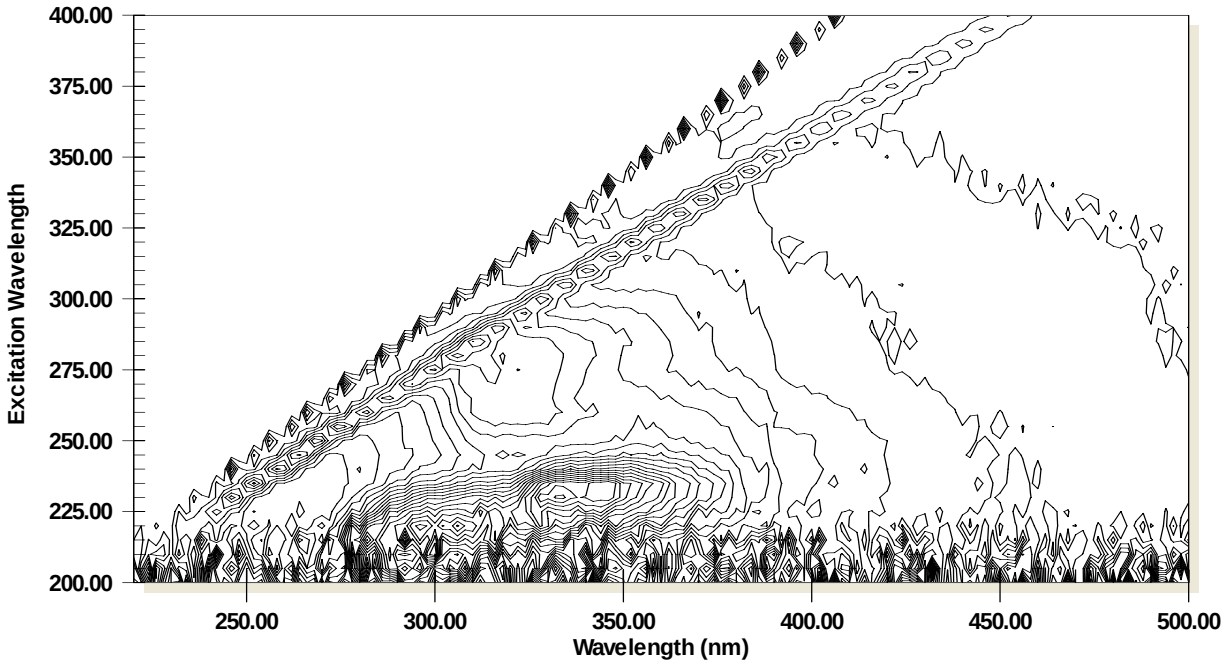
400.00
375.00
350.00
325.00
300.00
275.00
250.00
225.00
200.00
Excitation Wavelength
250.00
300.00
350.00
400.00
450.00
500.00
Wavelength (nm)

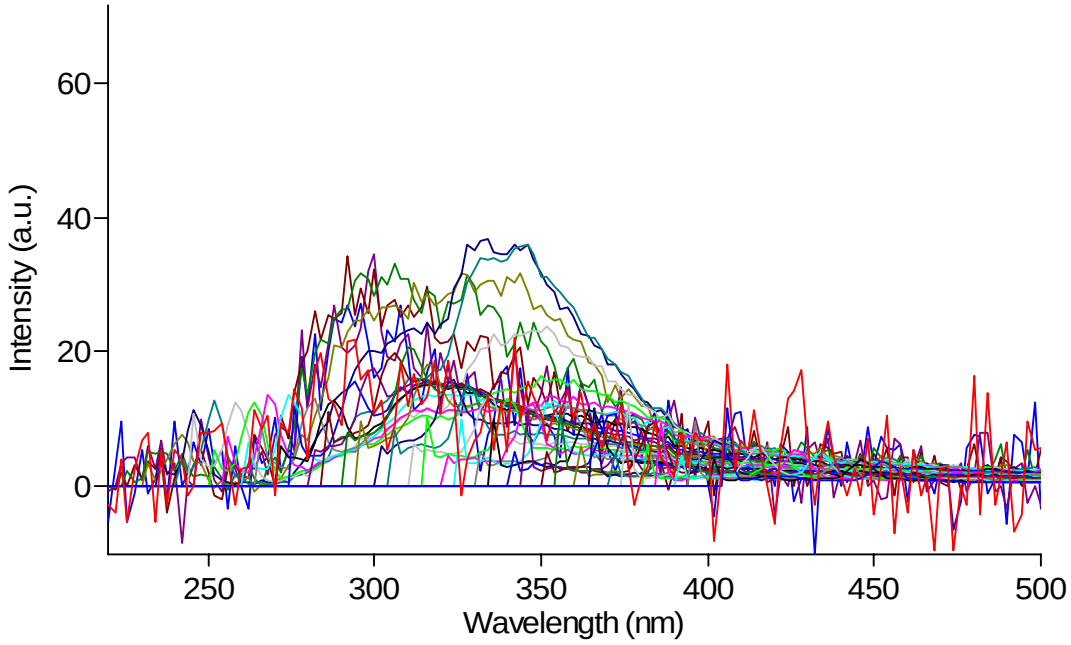
60
40
20
0
Intensity (a.u.)
250
300
350
400
450
500
Wavelength (nm)

43Ay

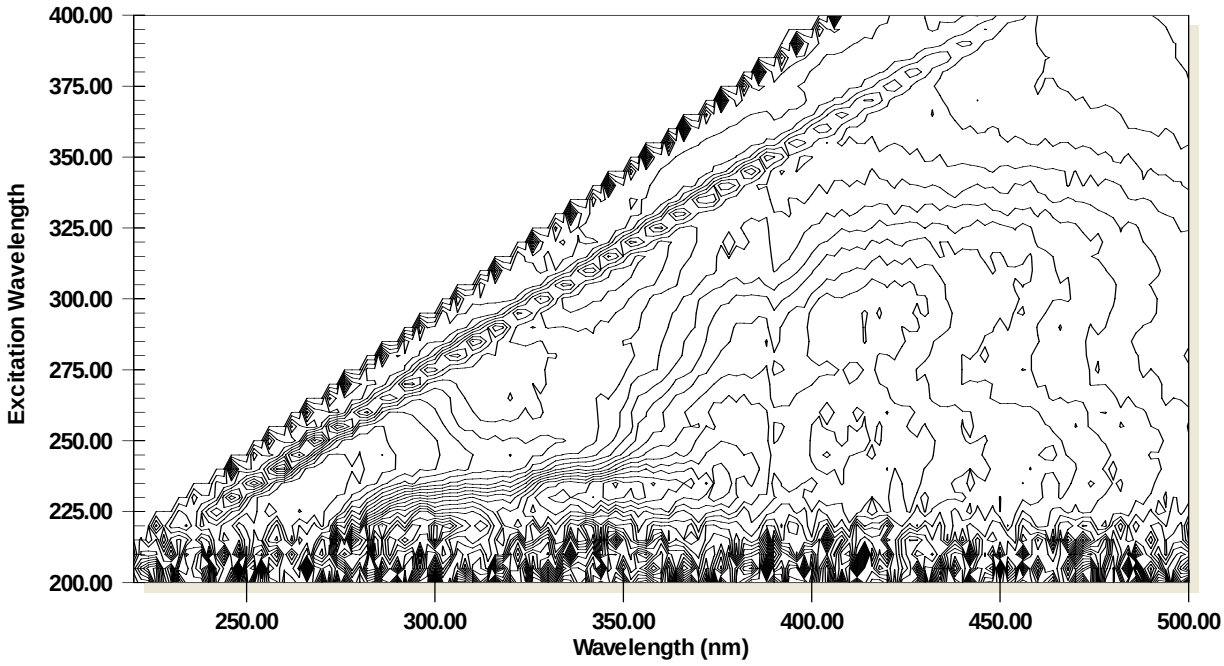
400.00
375.00
350.00
325.00
300.00
275.00
250.00
225.00
200.00
Excitation Wavelength
250.00
300.00
350.00
400.00
450.00
500.00
Wavelength (nm)

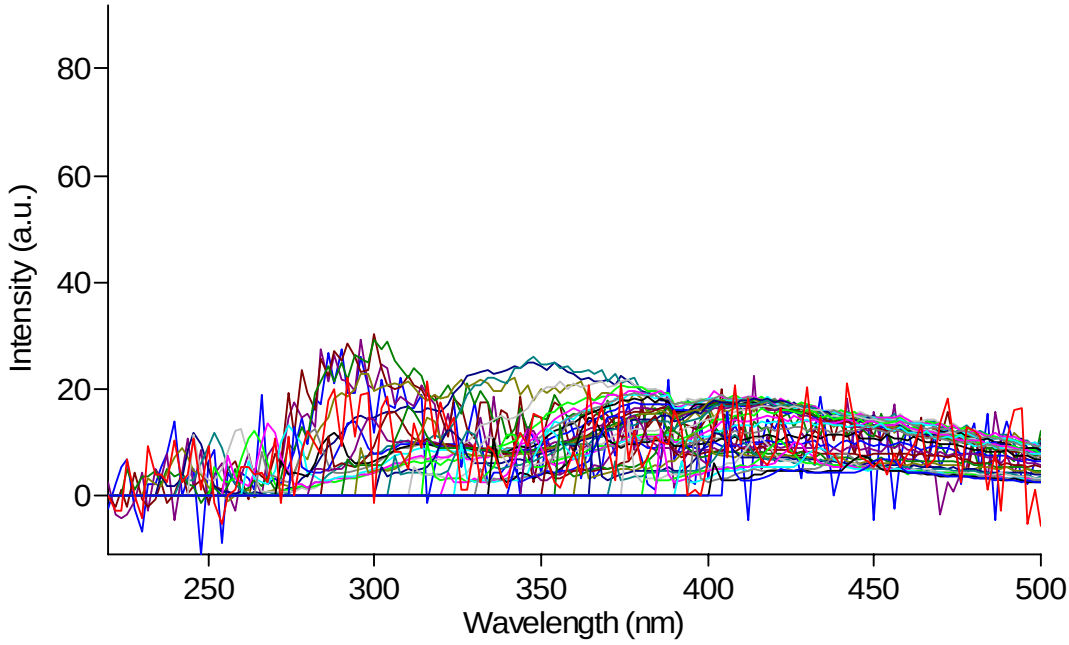
80
60
40
20
0
Intensity (a.u.)
250
300
350
400
450
500
Wavelength (nm)

44Ay

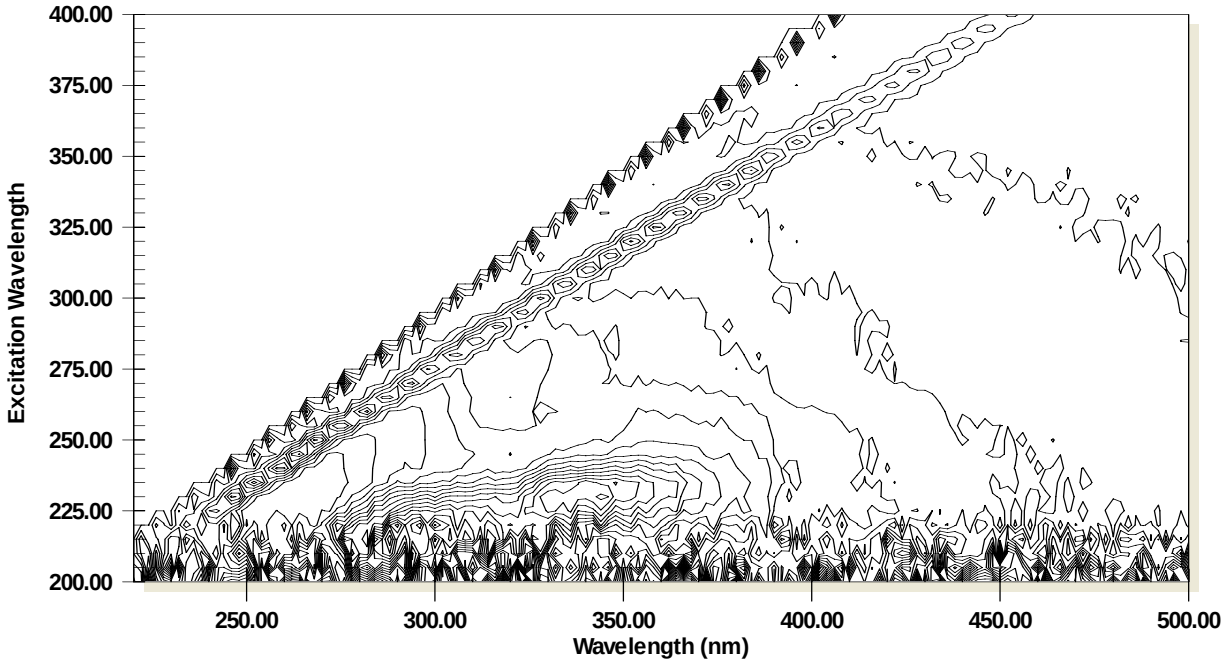
400.00
375.00
350.00
325.00
300.00
275.00
250.00
225.00
200.00
Excitation Wavelength
250.00
300.00
350.00
400.00
450.00
500.00
Wavelength (nm)

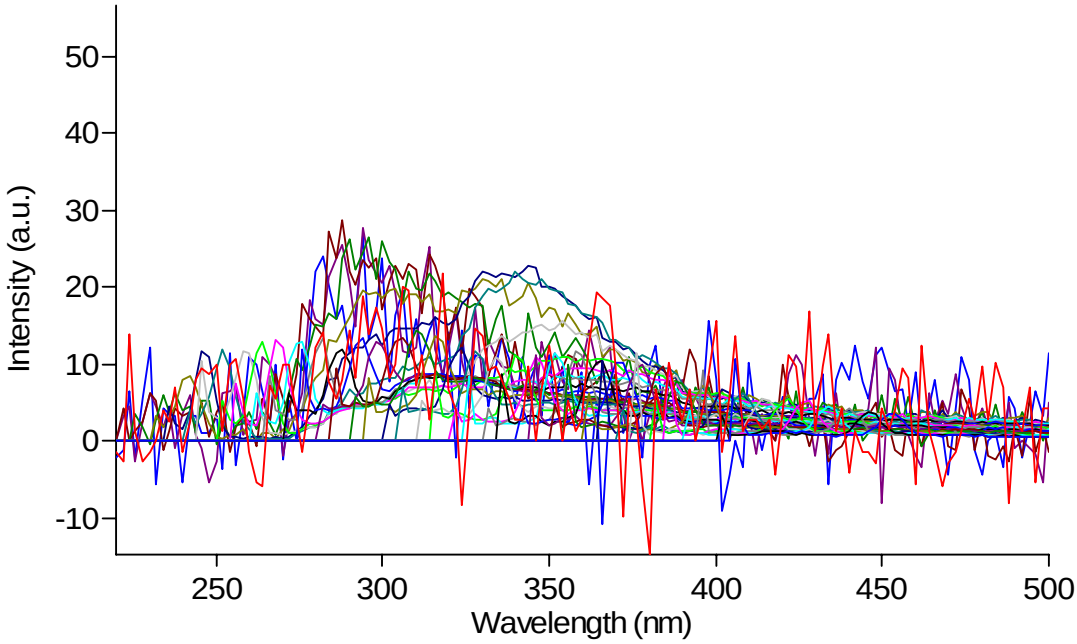
50
40
30
20
10
0
-10
Intensity (a.u.)
250
300
350
400
450
500
Wavelength (nm)

45Cy

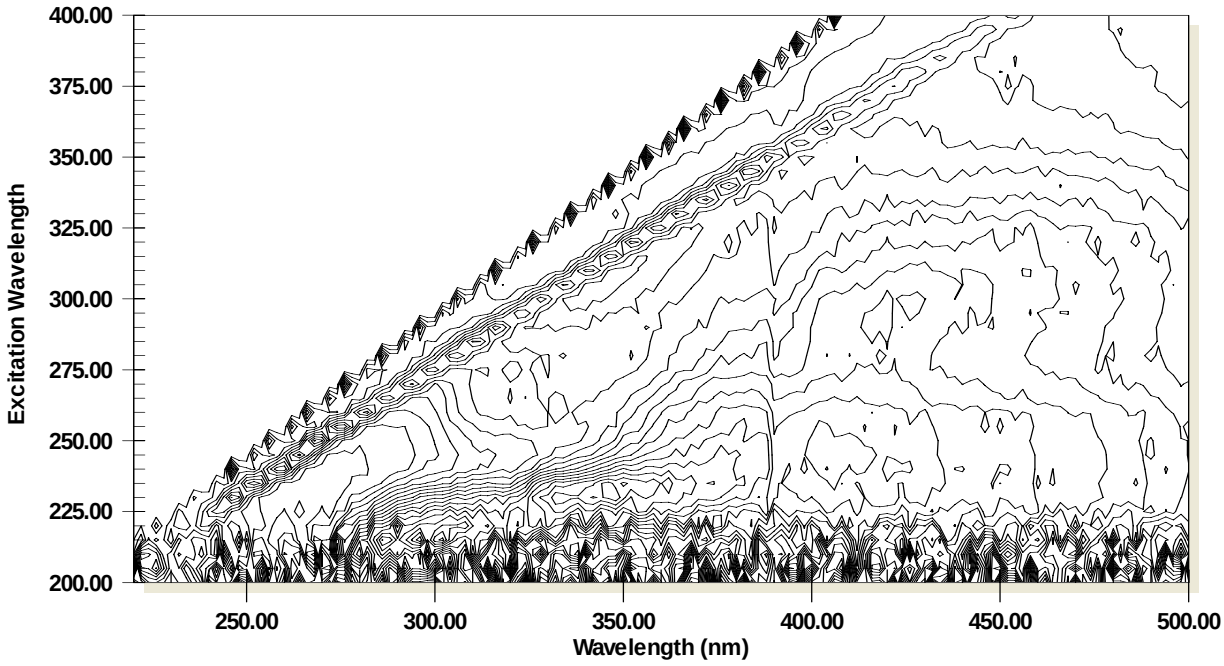
Excitation Wavelength
400.00
375.00
350.00
325.00
300.00
275.00
250.00
225.00
200.00
250.00
300.00
350.00
400.00
450.00
500.00
Wavelength (nm)

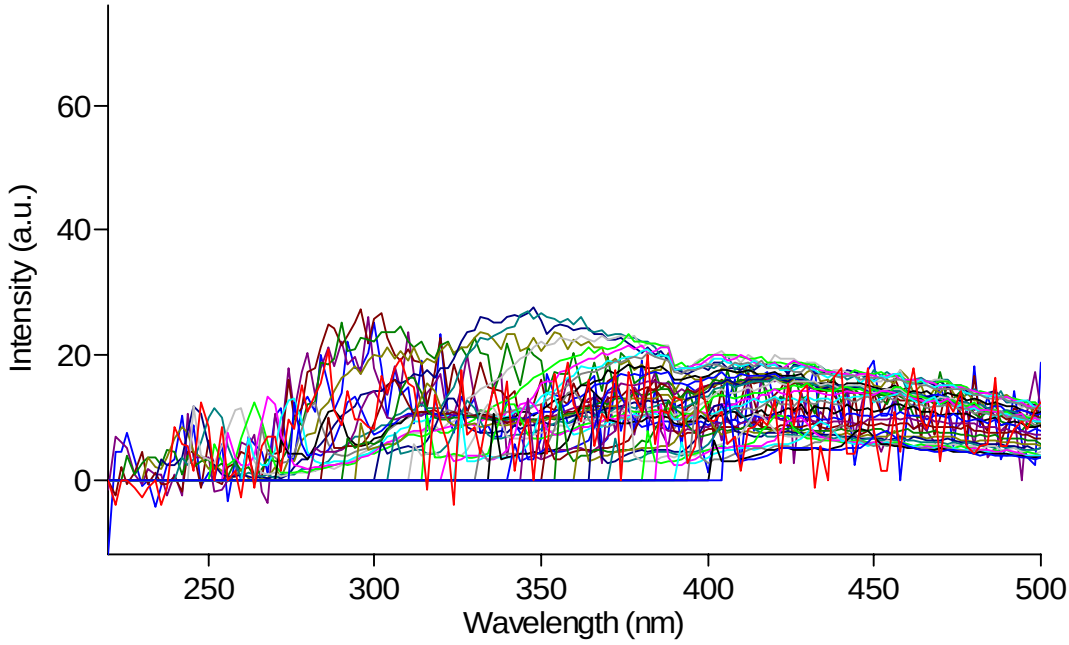
Intensity (a.u.)
60
40
20
0
250
300
350
400
450
500
Wavelength (nm)

51Cy

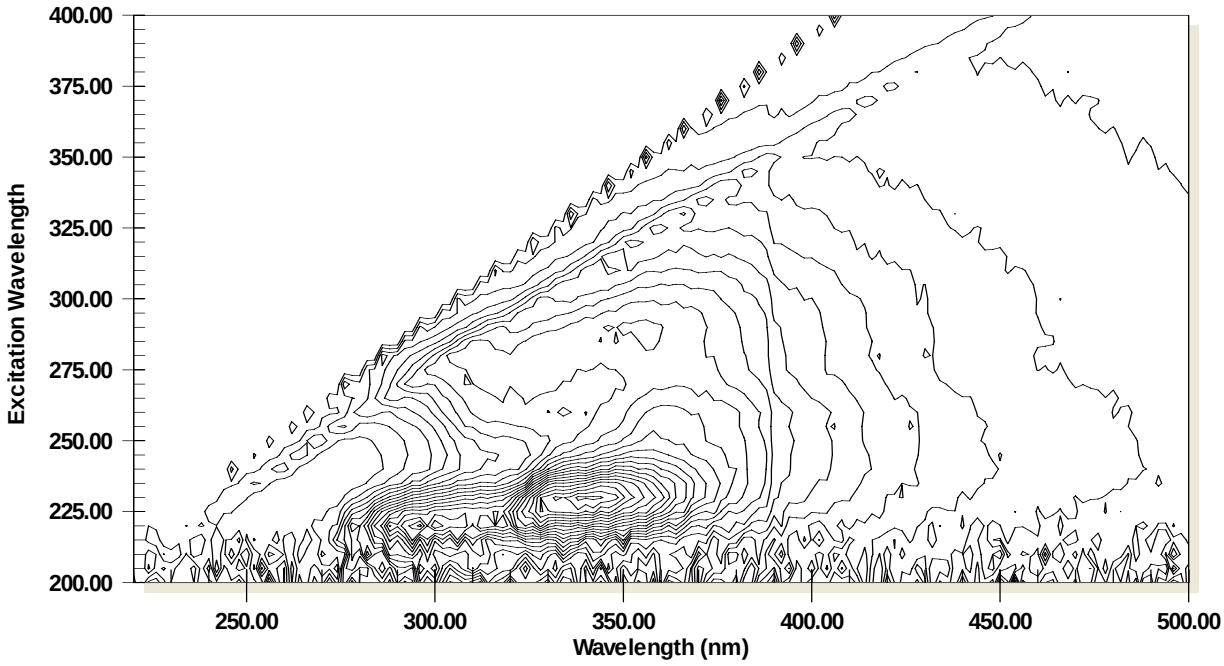
Excitation Wavelength
400.00
375.00
350.00
325.00
300.00
275.00
250.00
225.00
200.00
250.00
300.00
350.00
400.00
450.00
500.00
Wavelength (nm)

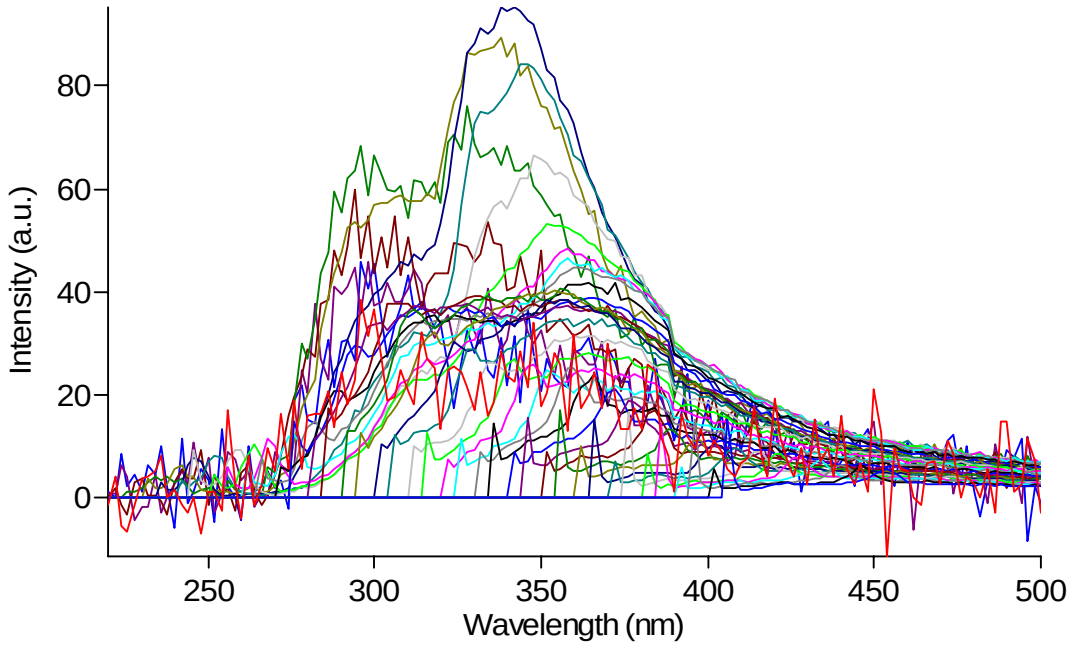
Intensity (a.u.)
80
60
40
20
0
250
300
350
400
450
500
Wavelength (nm)

52By

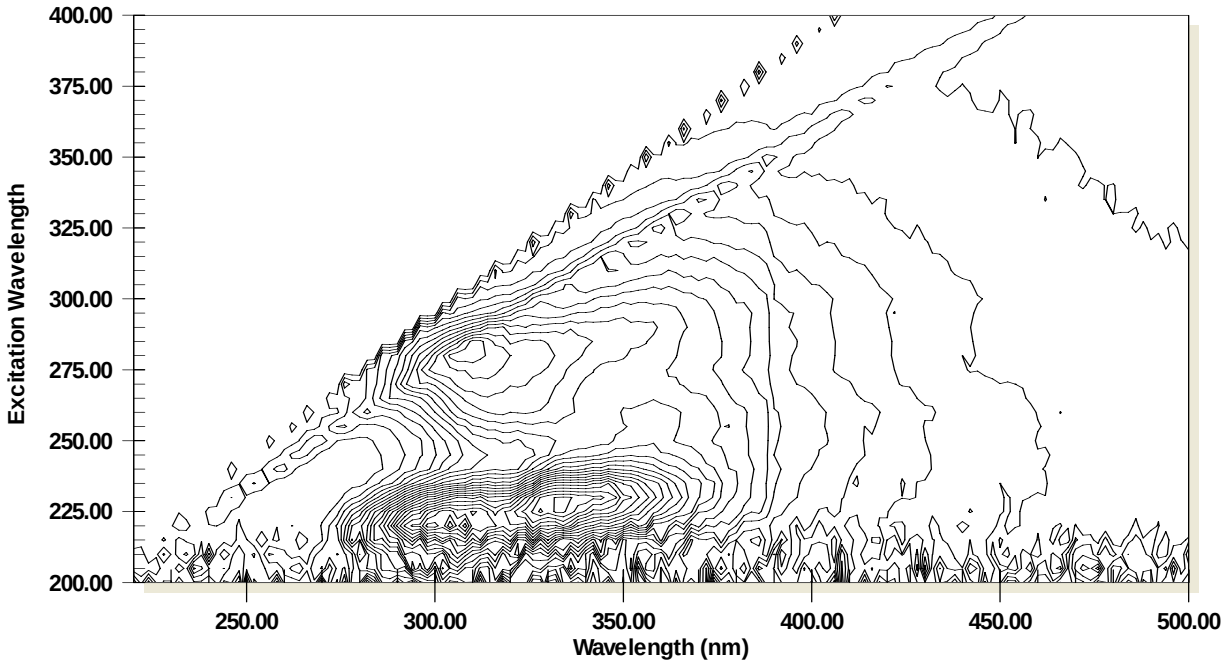
400.00
375.00
350.00
325.00
300.00
275.00
250.00
225.00
200.00
Excitation Wavelength
250.00
300.00
350.00
400.00
450.00
500.00
Wavelength (nm)

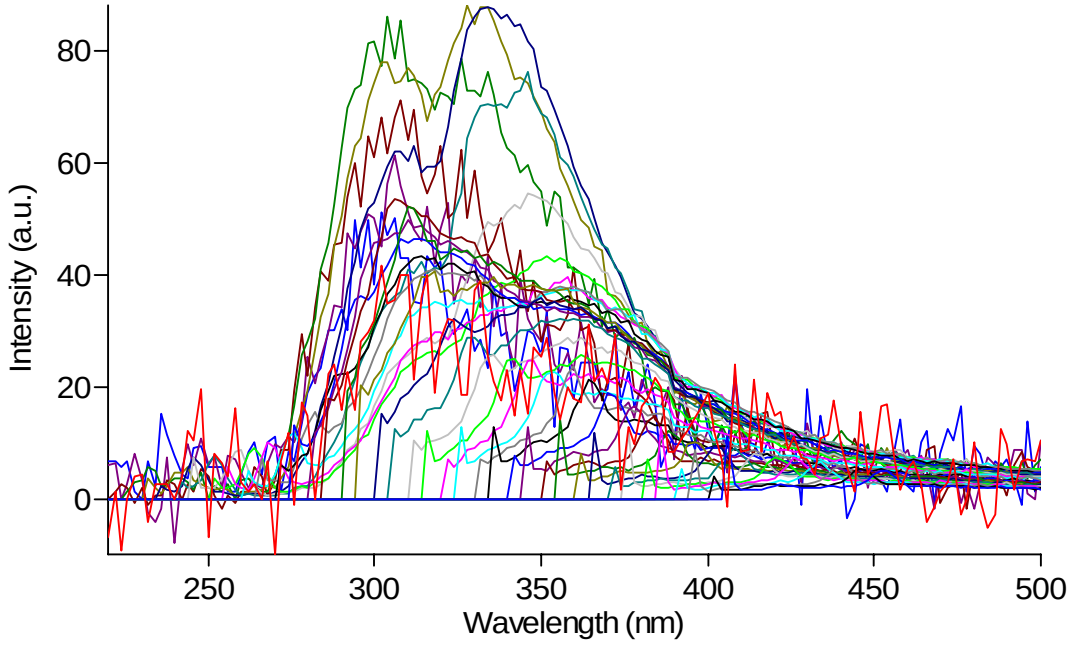
80
60
40
20
0
Intensity (a.u.)
250
300
350
400
450
500
Wavelength (nm)

53Ay

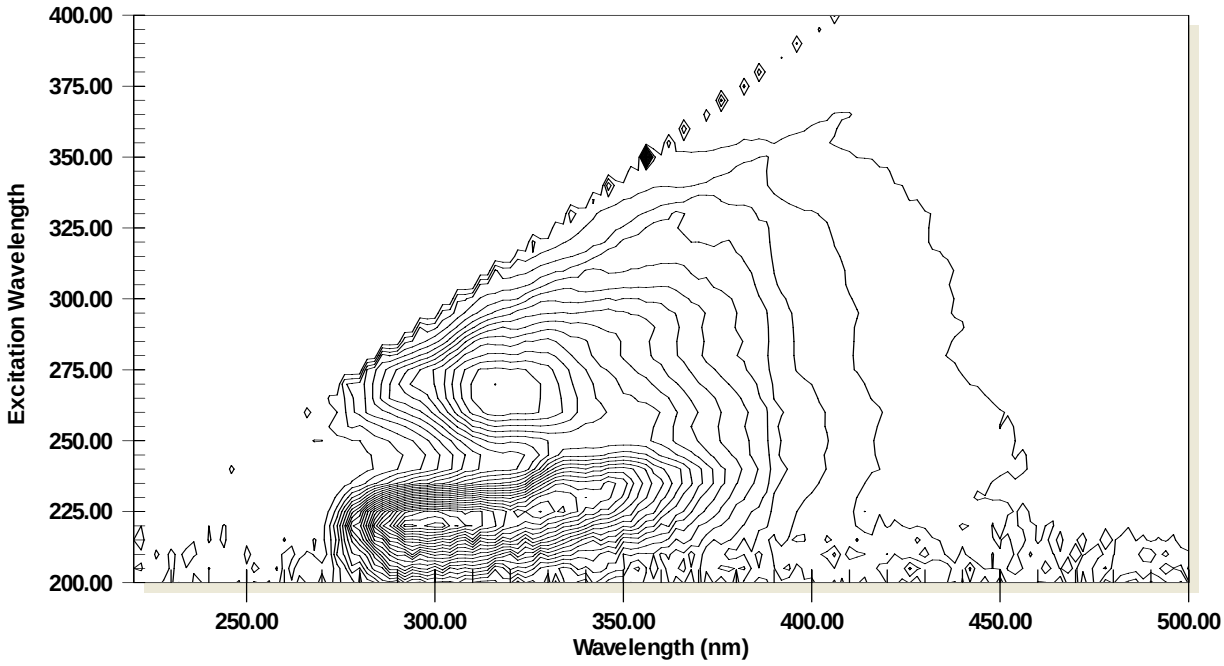
400.00
375.00
350.00
325.00
300.00
275.00
250.00
225.00
200.00
Excitation Wavelength
250.00
300.00
350.00
400.00
450.00
500.00
Wavelength (nm)

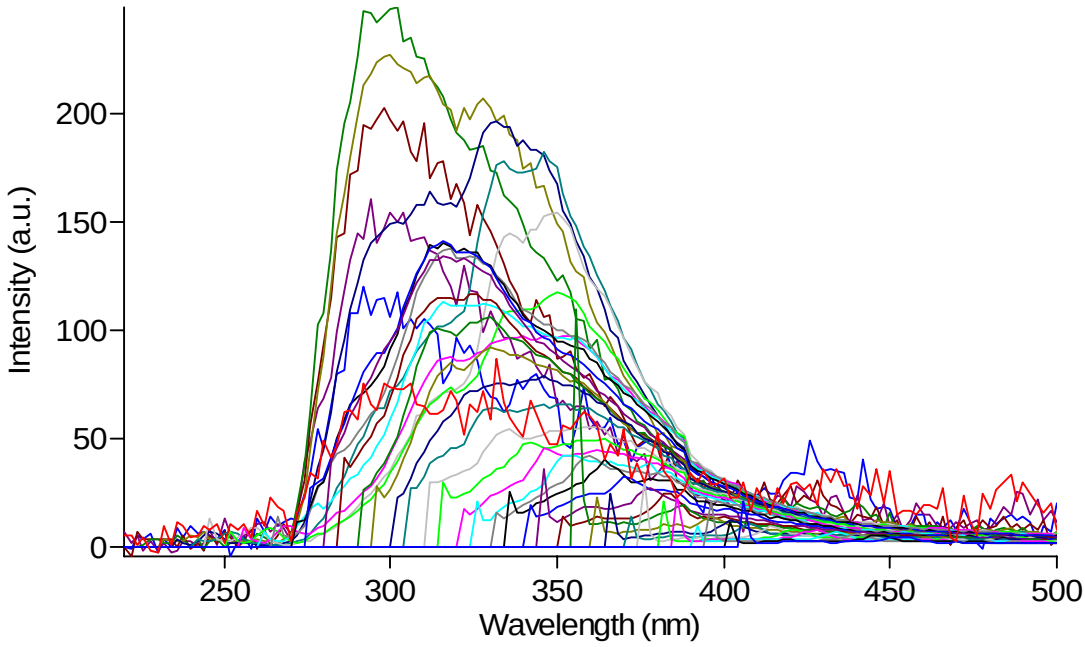
200
150
100
50
0
Intensity (a.u.)
250
300
350
400
450
500
Wavelength (nm)

54By

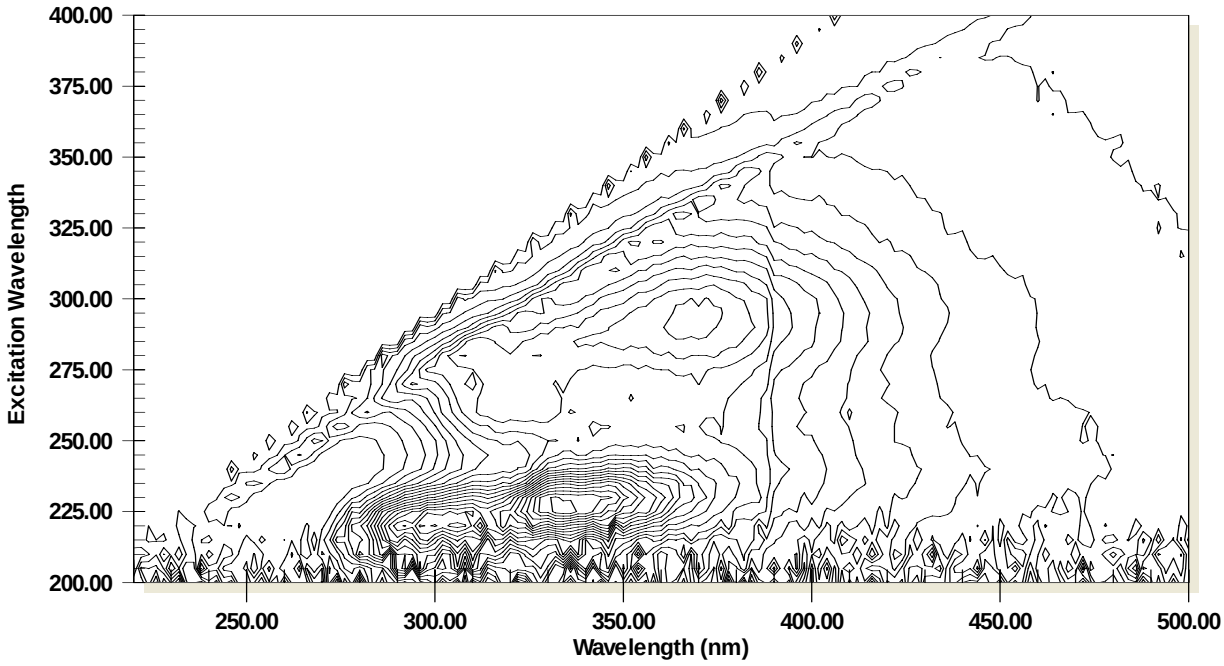
400.00
375.00
350.00
325.00
300.00
275.00
250.00
225.00
200.00
Excitation Wavelength
250.00
300.00
350.00
400.00
450.00
500.00
Wavelength (nm)

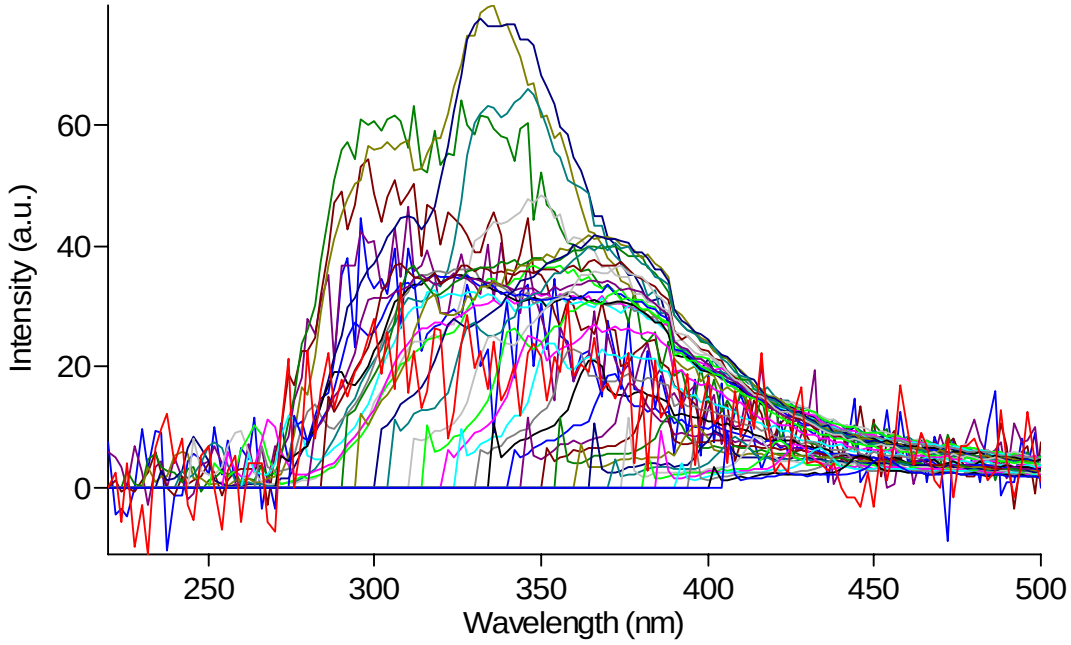
60
40
20
0
Intensity (a.u.)
250
300
350
400
450
500
Wavelength (nm)

55Cy

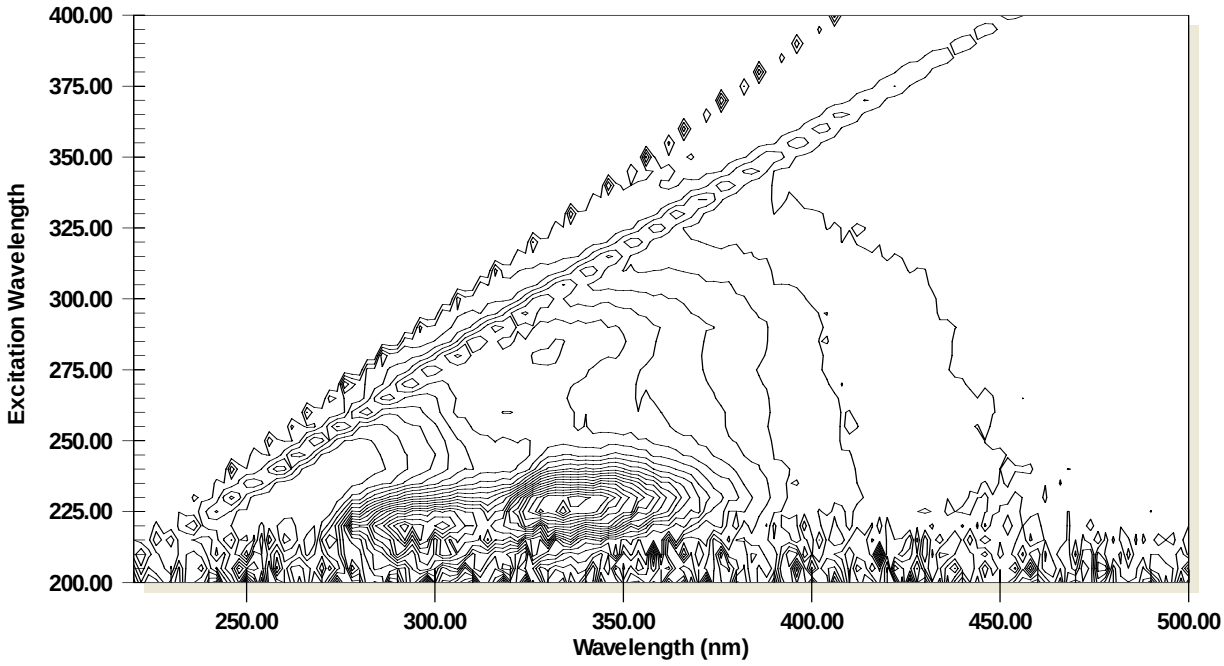
400.00
375.00
350.00
325.00
300.00
275.00
250.00
225.00
200.00
Excitation Wavelength
250.00
300.00
350.00
400.00
450.00
500.00
Wavelength (nm)

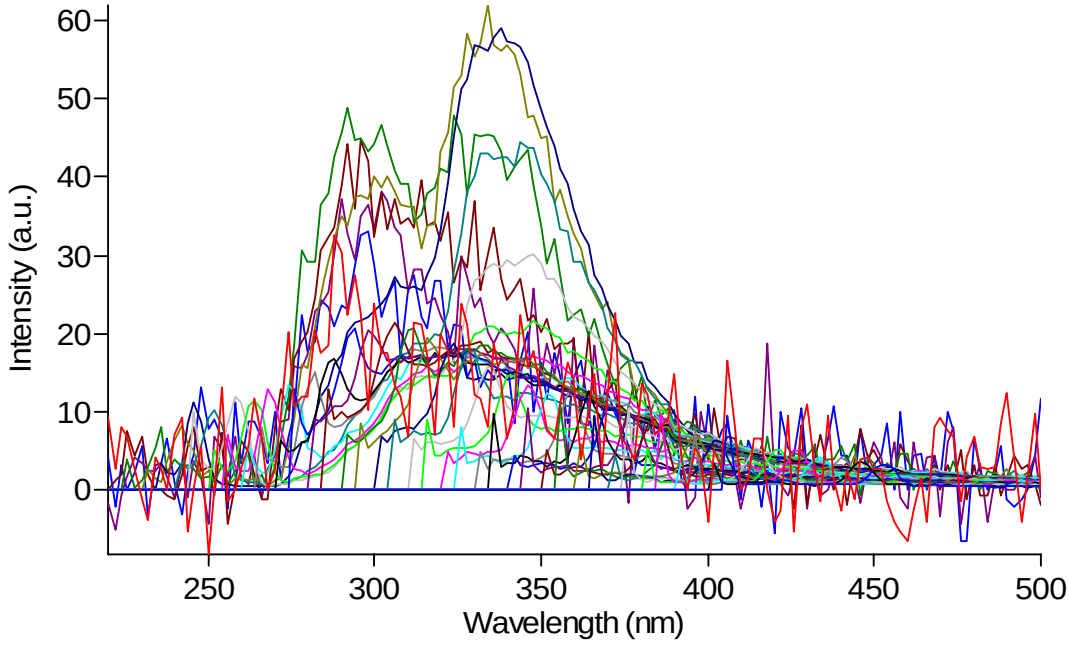
60
50
40
30
20
10
0
Intensity (a.u.)
250
300
350
400
450
500
Wavelength (nm)

61Ay

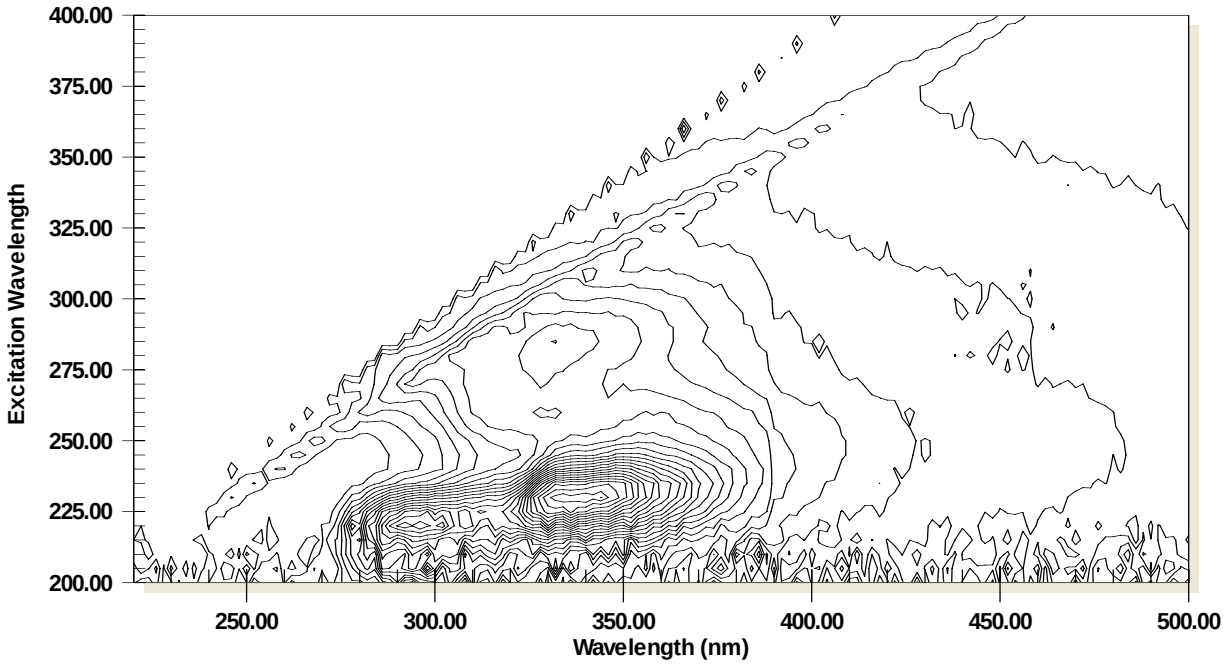
400.00
375.00
350.00
325.00
300.00
275.00
250.00
225.00
200.00
Excitation Wavelength
250.00
300.00
350.00
400.00
450.00
500.00
Wavelength (nm)

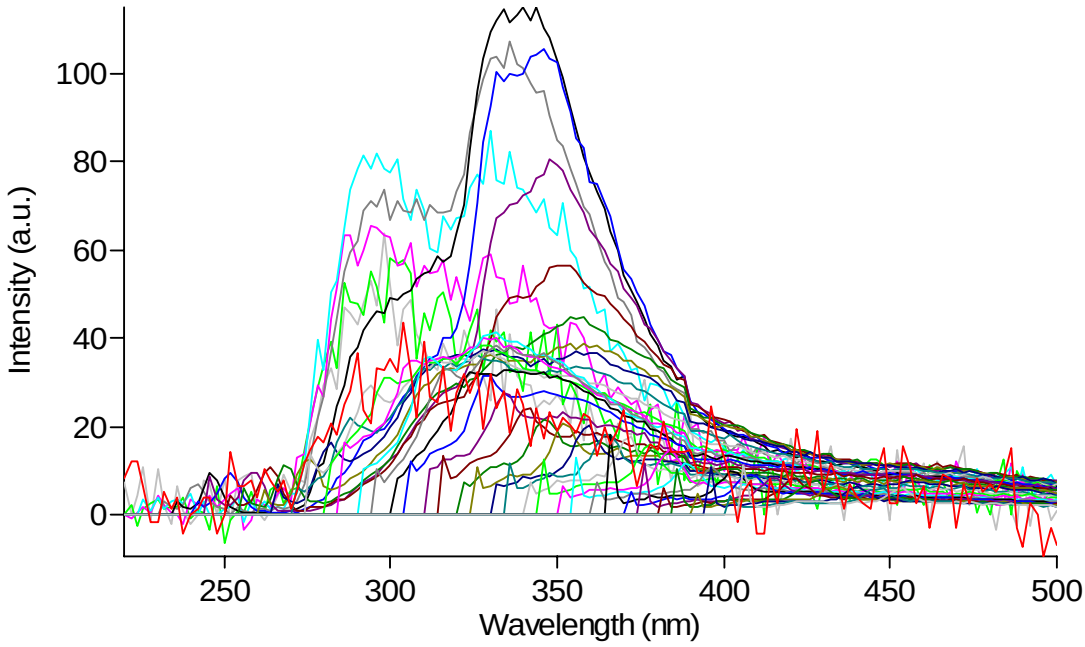
100
80
60
40
20
0
Intensity (a.u.)
250
300
350
400
450
500
Wavelength (nm)

62Cy

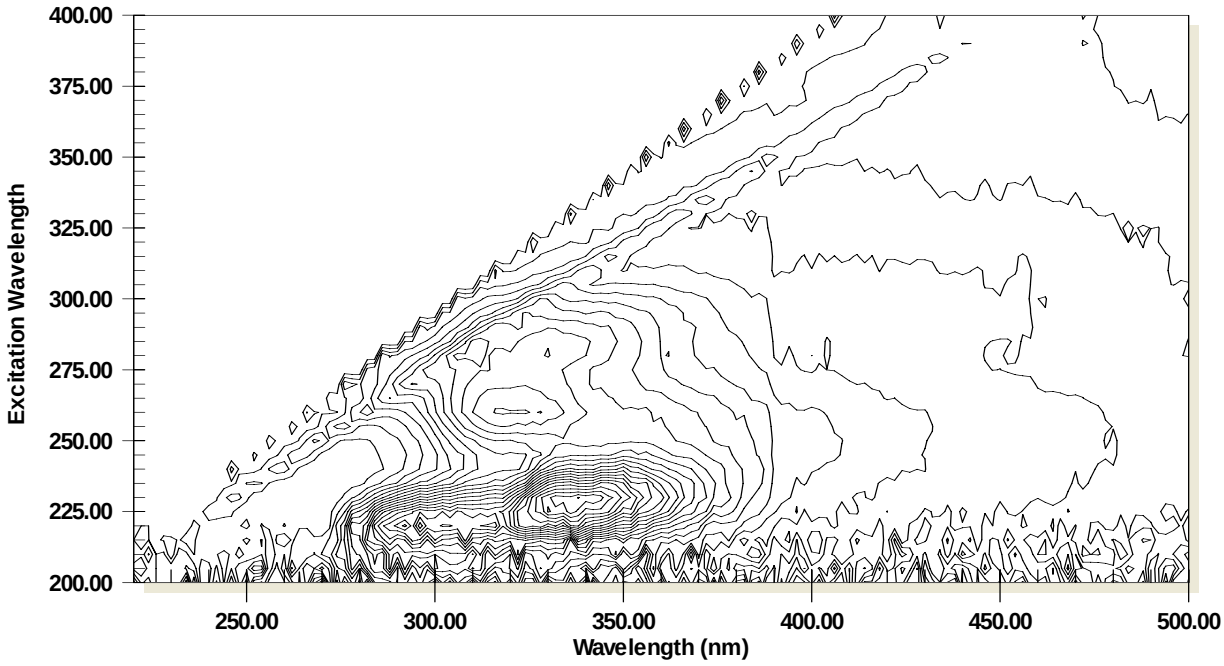
400.00
375.00
350.00
325.00
300.00
275.00
250.00
225.00
200.00
Excitation Wavelength
250.00
300.00
350.00
400.00
450.00
500.00
Wavelength (nm)

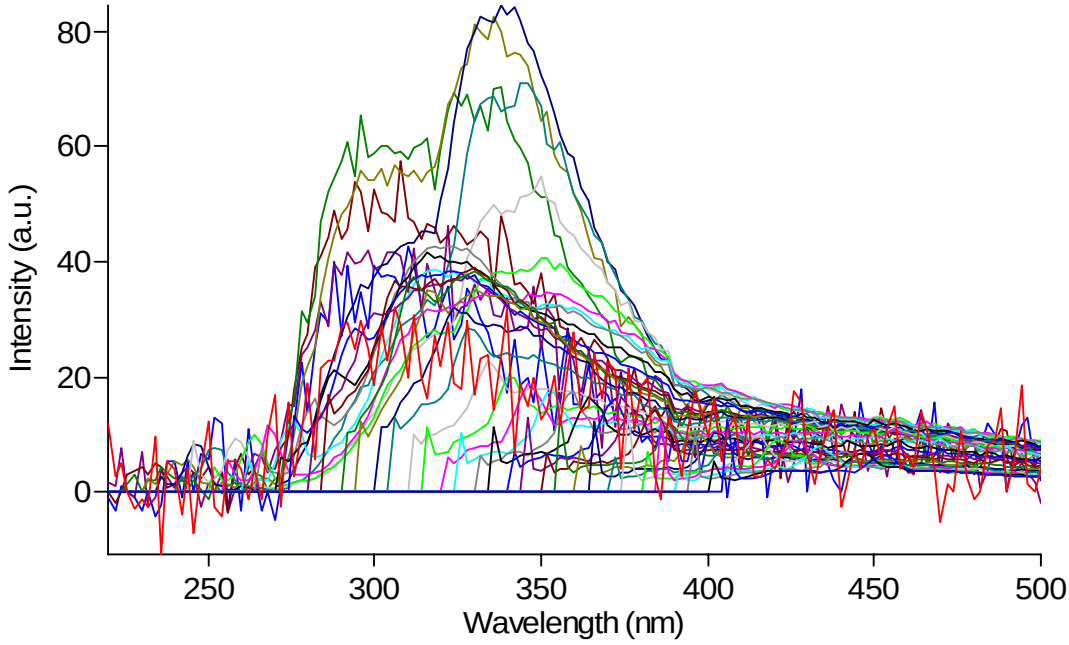
80
60
40
20
0
Intensity (a.u.)
250
300
350
400
450
500
Wavelength (nm)

63By

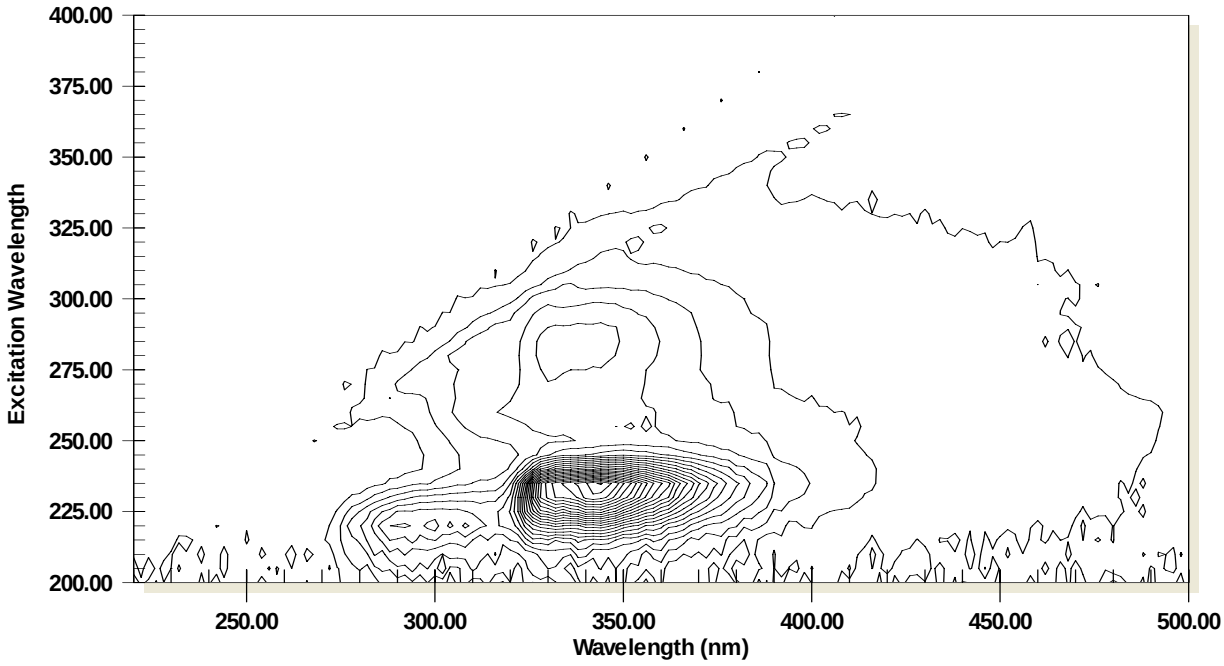
Excitation Wavelength
400.00
375.00
350.00
325.00
300.00
275.00
250.00
225.00
200.00
250.00
300.00
350.00
400.00
450.00
500.00
Wavelength (nm)

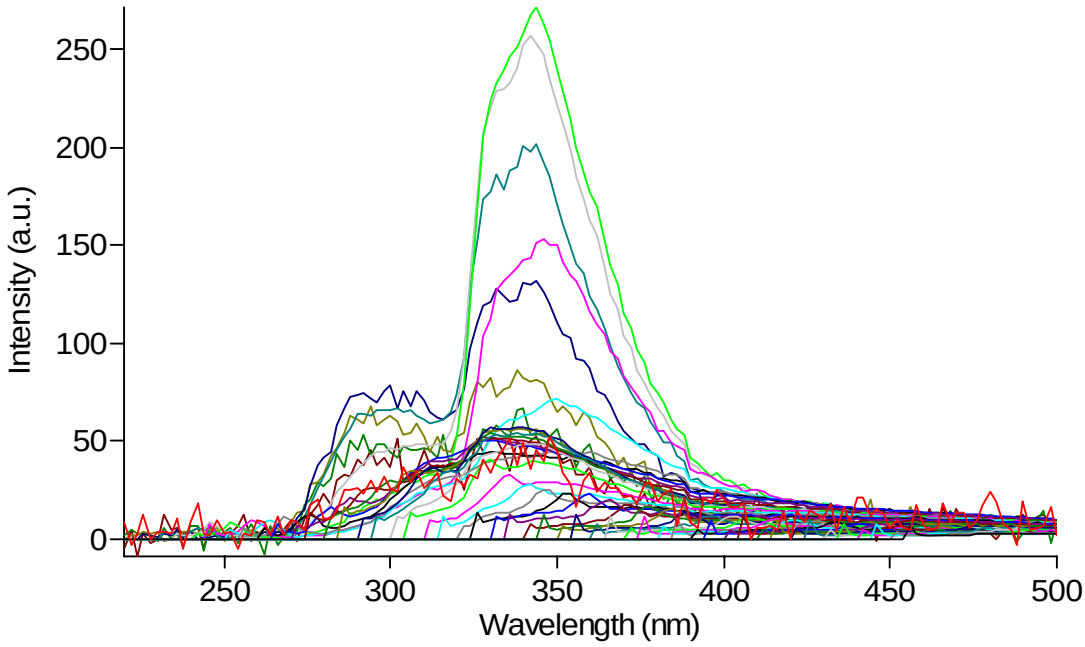
Intensity (a.u.)
250
200
150
100
50
0
250
300
350
400
450
500
Wavelength (nm)

64Ay

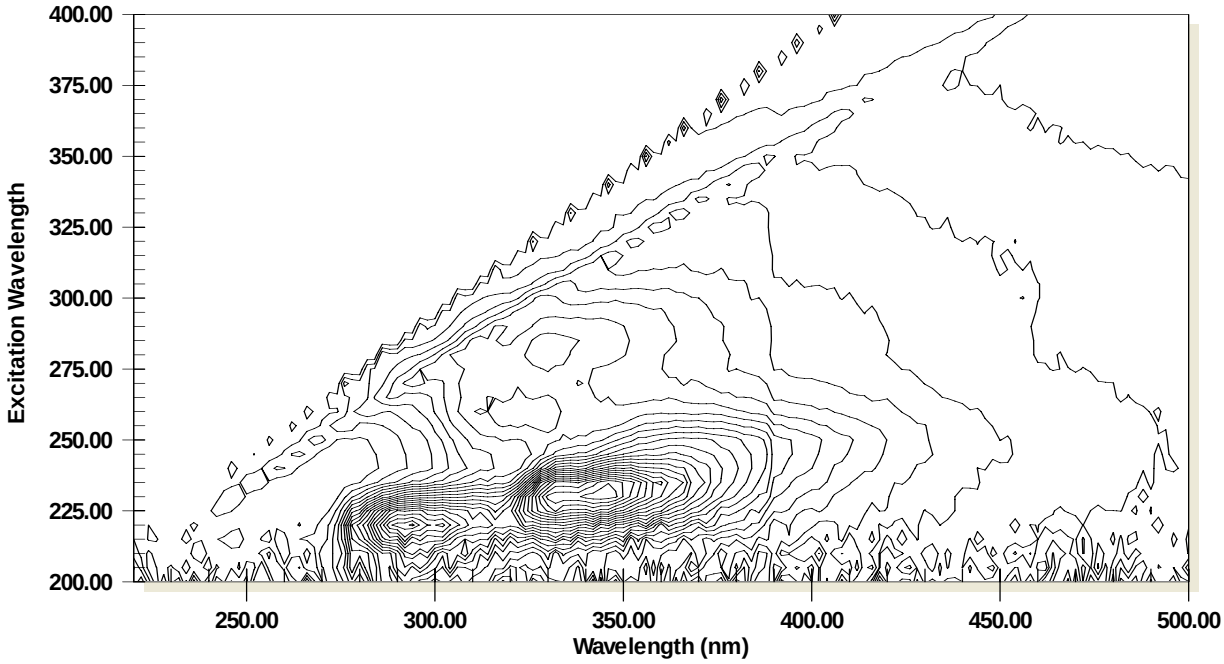
Excitation Wavelength
400.00
375.00
350.00
325.00
300.00
275.00
250.00
225.00
200.00
250.00
300.00
350.00
400.00
450.00
500.00
Wavelength (nm)

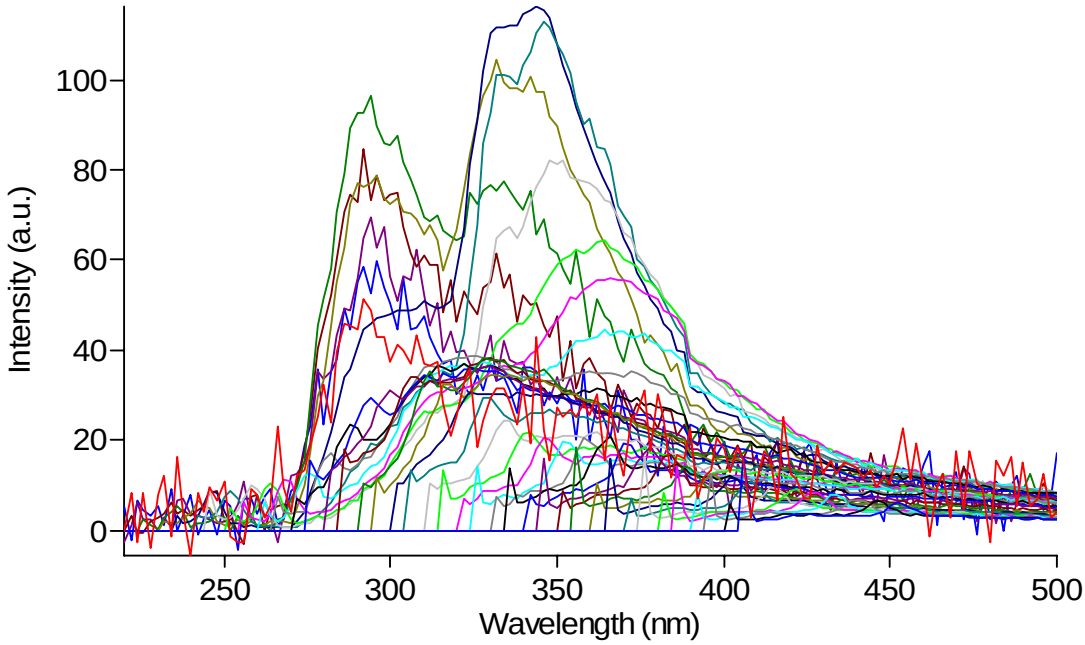
Intensity (a.u.)
100
80
60
40
20
0
250
300
350
400
450
500
Wavelength (nm)

65By

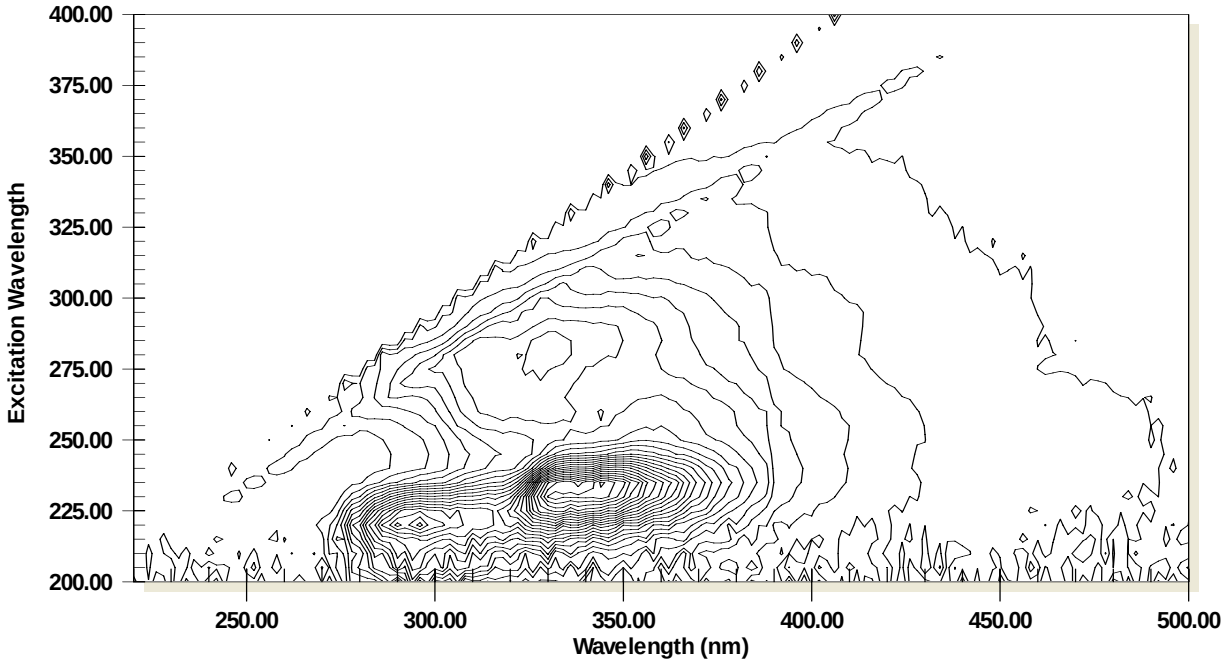
400.00
375.00
350.00
325.00
300.00
275.00
250.00
225.00
200.00
Excitation Wavelength
250.00
300.00
350.00
400.00
450.00
500.00
Wavelength (nm)

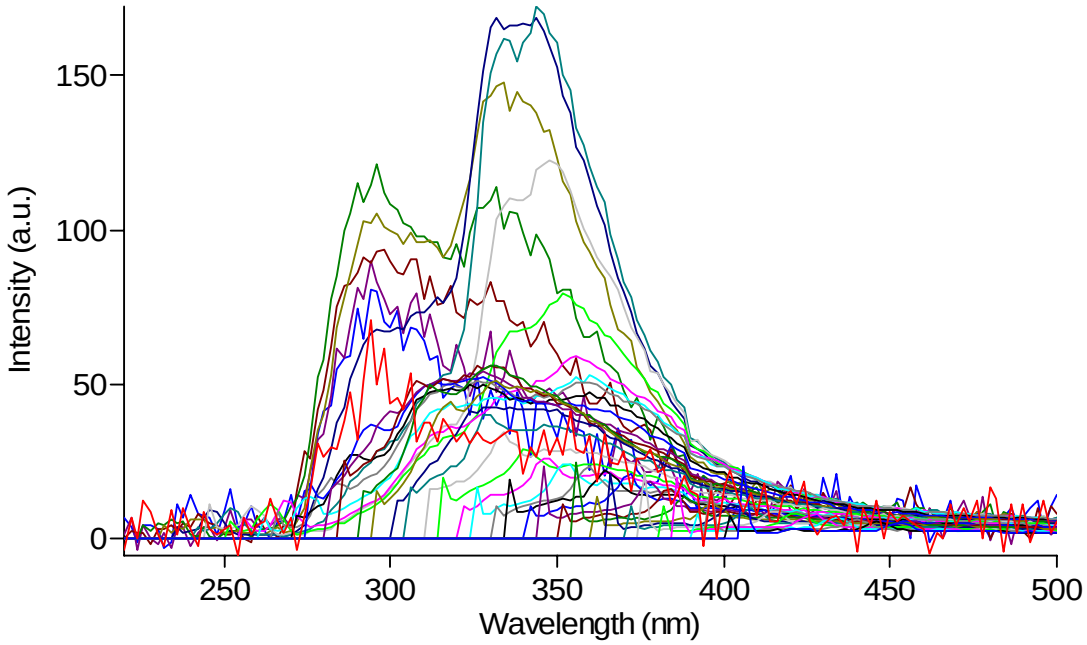
150
100
50
0
Intensity (a.u.)
250
300
350
400
450
500
Wavelength (nm)

71By

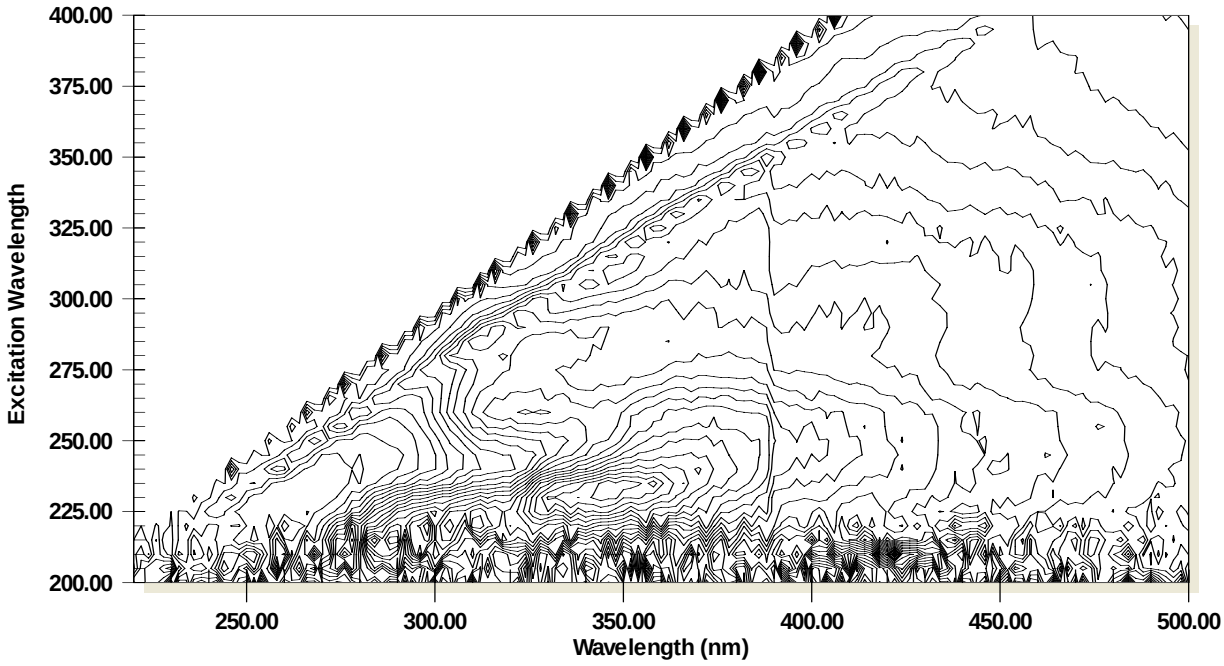
400.00
375.00
350.00
325.00
300.00
275.00
250.00
225.00
200.00
Excitation Wavelength
250.00
300.00
350.00
400.00
450.00
500.00
Wavelength (nm)

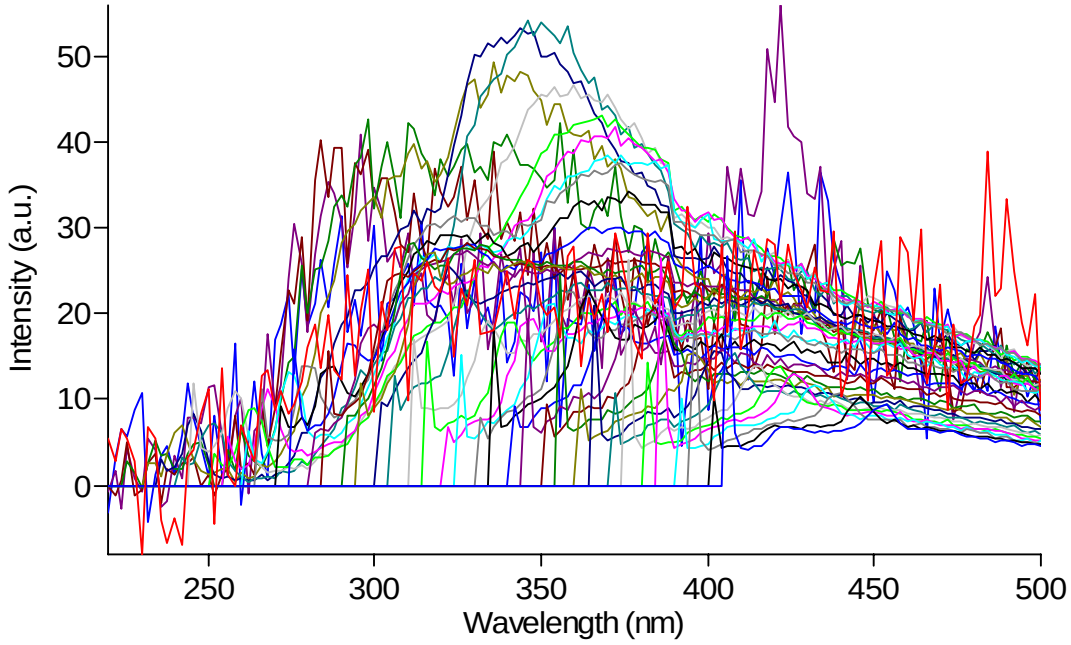
50
40
30
20
10
0
Intensity (a.u.)
250
300
350
400
450
500
Wavelength (nm)

72Ay

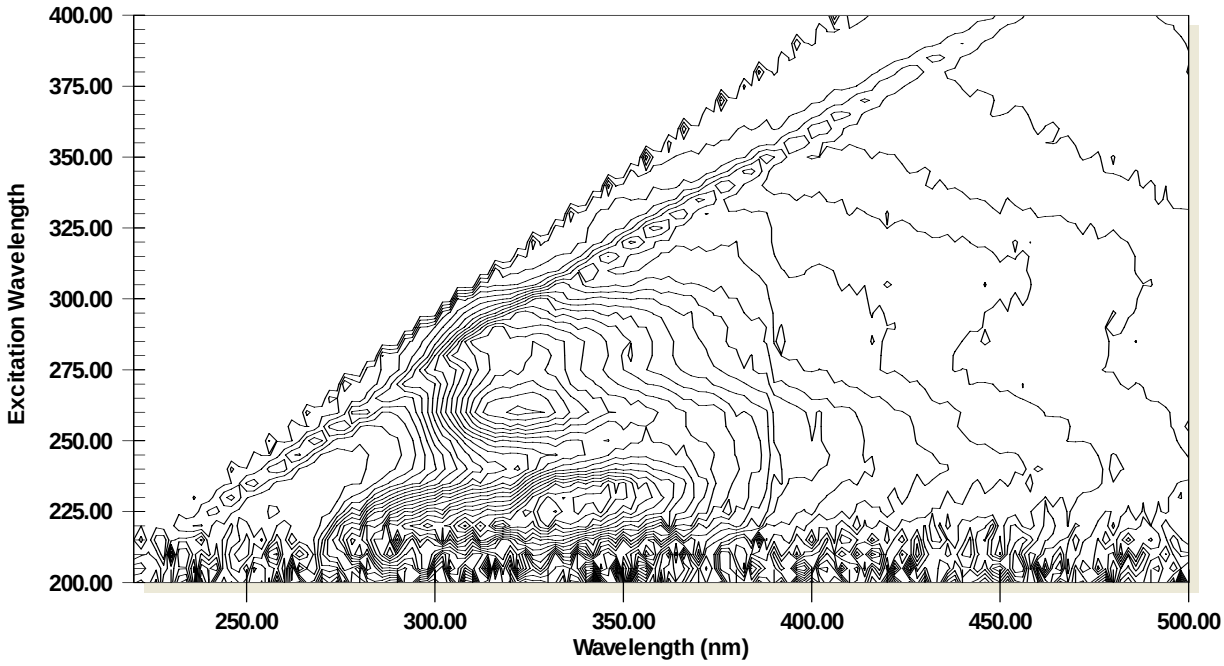
Excitation Wavelength
400.00
375.00
350.00
325.00
300.00
275.00
250.00
225.00
200.00
250.00
300.00
350.00
400.00
450.00
500.00
Wavelength (nm)

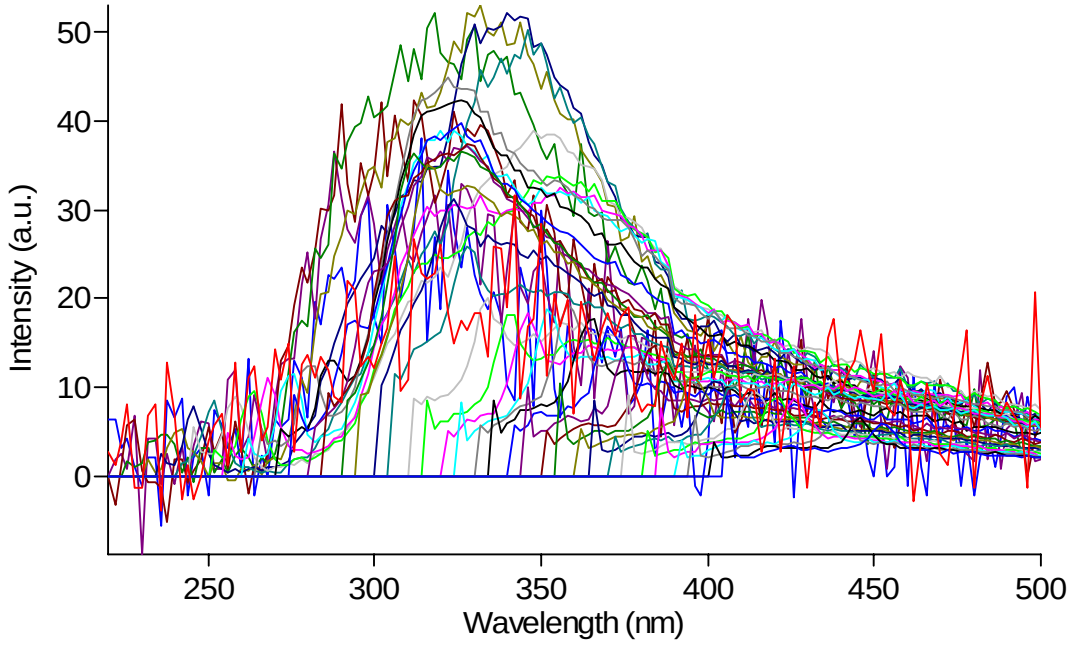
Intensity (a.u.)
50
40
30
20
10
0
250
300
350
400
450
500
Wavelength (nm)

73Cy

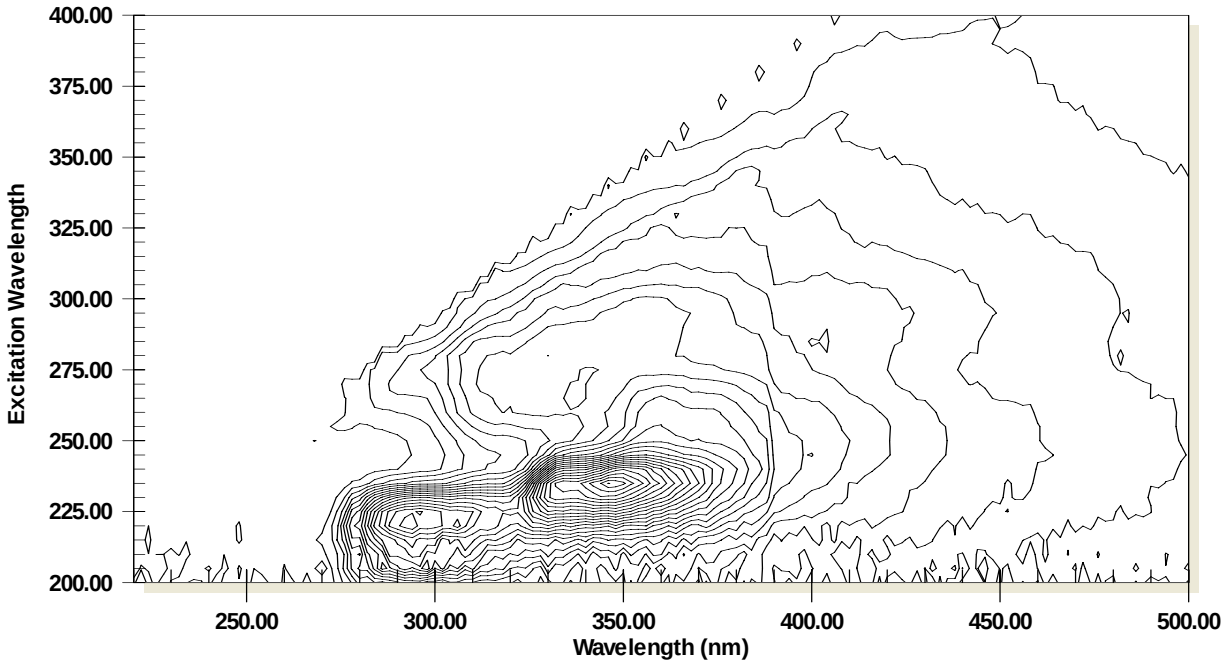
400.00
375.00
350.00
325.00
300.00
275.00
250.00
225.00
200.00
Excitation Wavelength
250.00
300.00
350.00
400.00
450.00
500.00
Wavelength (nm)

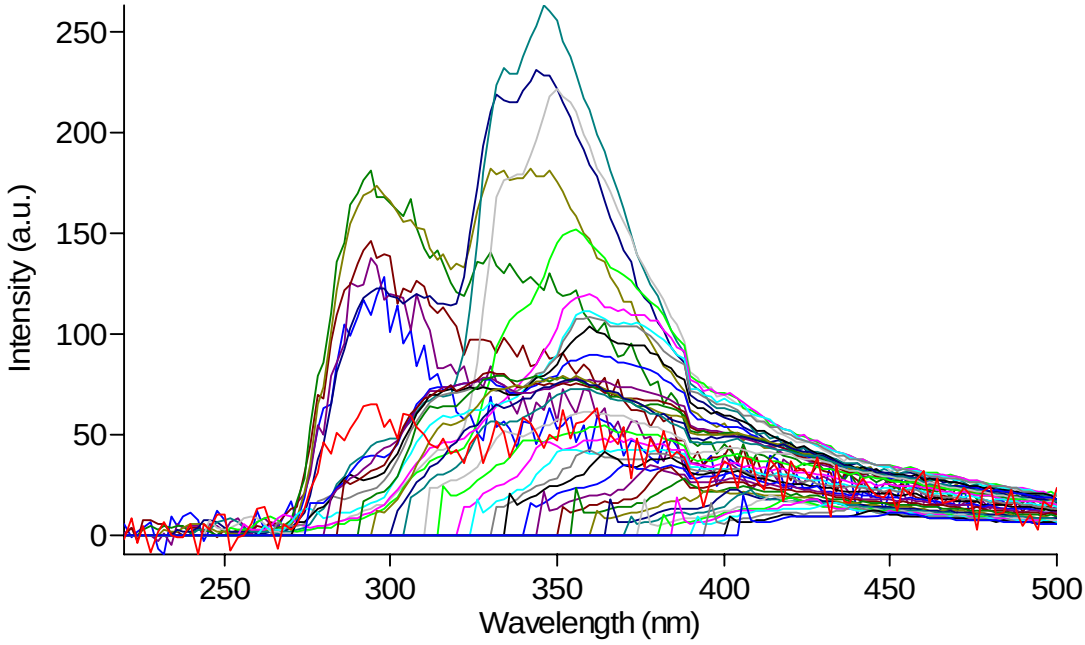
250
200
150
100
50
0
Intensity (a.u.)
250
300
350
400
450
500
Wavelength (nm)

74Ay

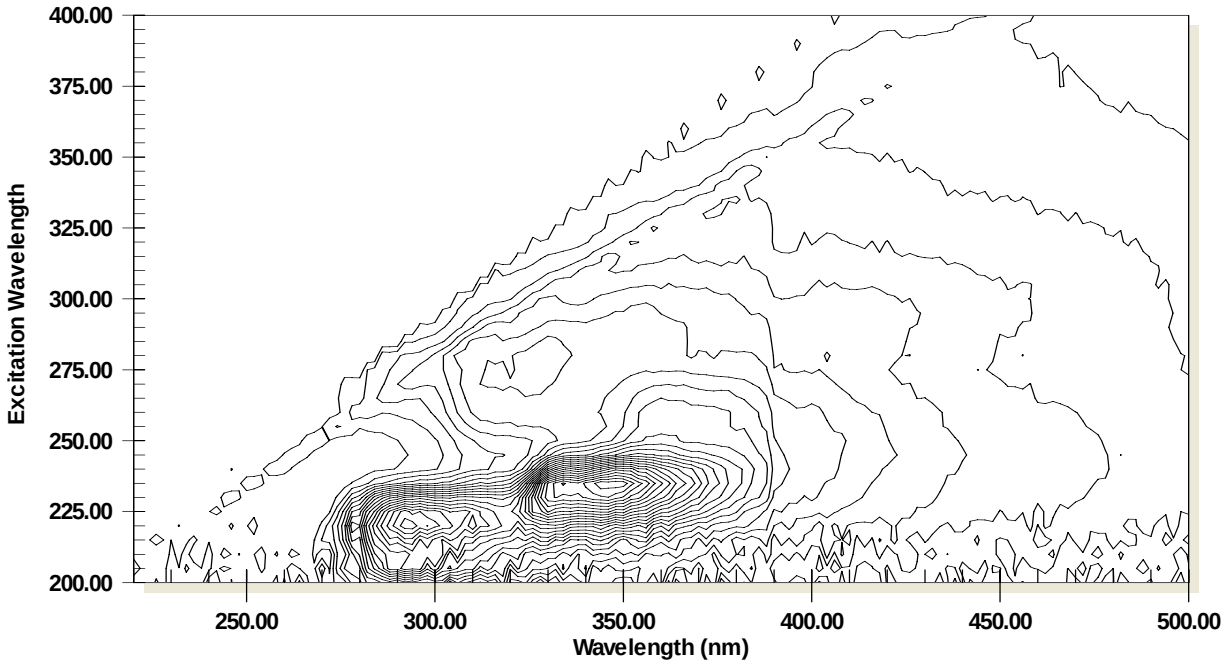
400.00
375.00
350.00
325.00
300.00
275.00
250.00
225.00
200.00
Excitation Wavelength
250.00
300.00
350.00
400.00
450.00
500.00
Wavelength (nm)

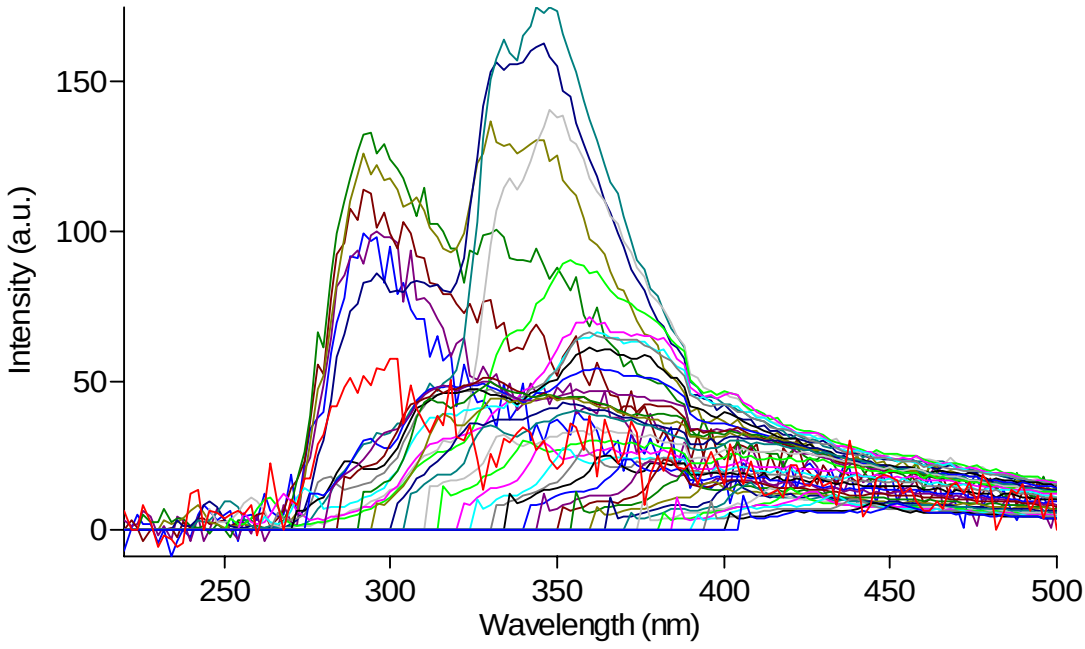
150
100
50
0
Intensity (a.u.)
250
300
350
400
450
500
Wavelength (nm)

75Ay

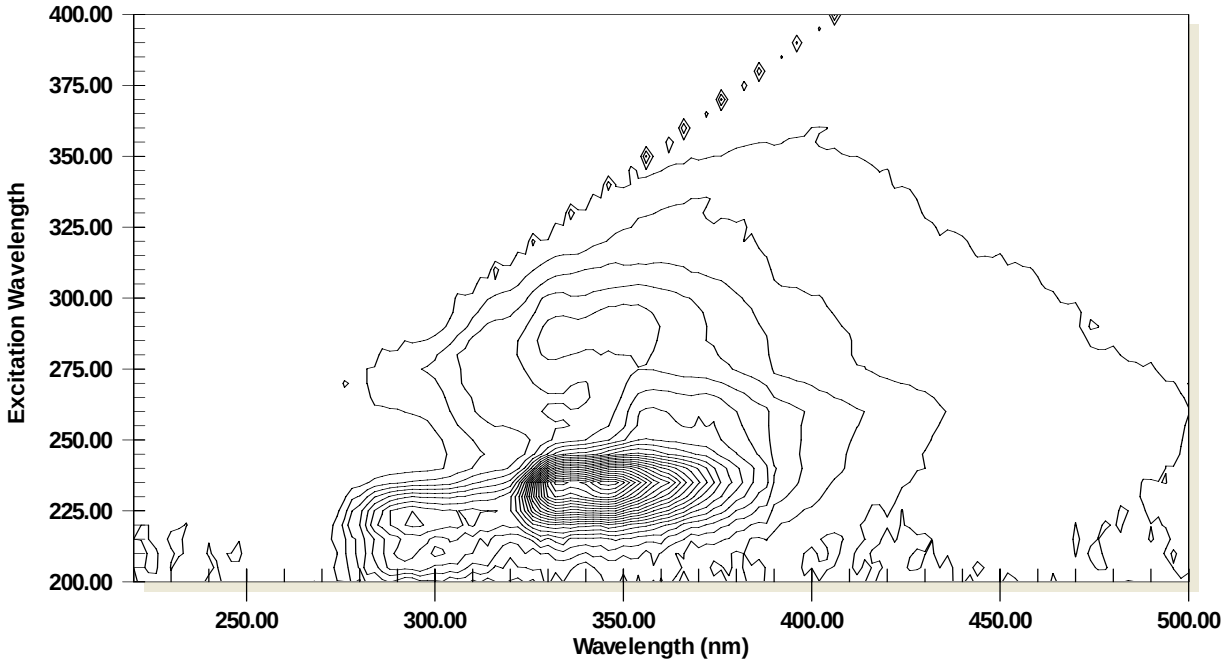
Excitation Wavelength
400.00
375.00
350.00
325.00
300.00
275.00
250.00
225.00
200.00
250.00
300.00
350.00
400.00
450.00
500.00
Wavelength (nm)

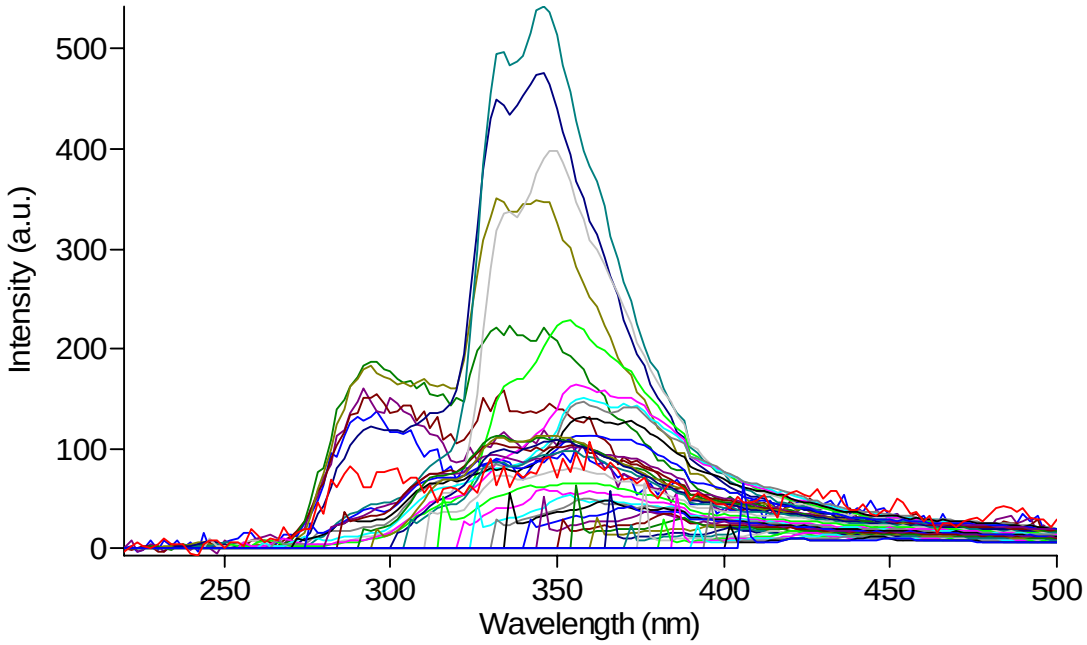
Intensity (a.u.)
500
400
300
200
100
0
250
300
350
400
450
500
Wavelength (nm)

81Ay

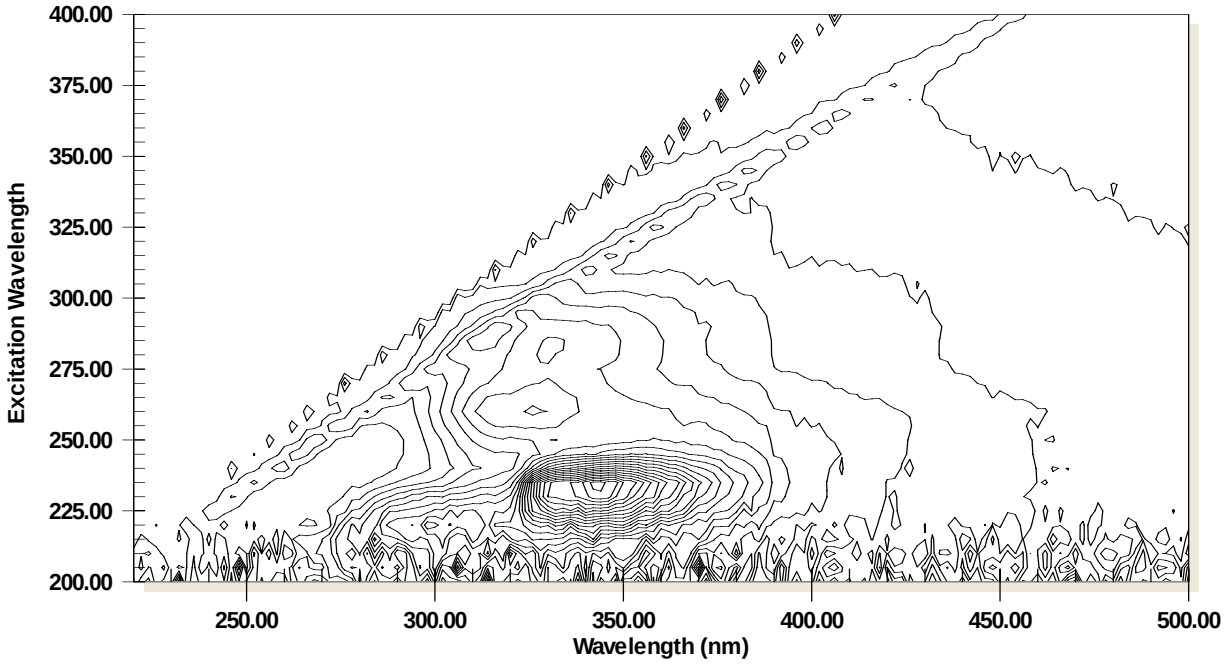
Excitation Wavelength
400.00
375.00
350.00
325.00
300.00
275.00
250.00
225.00
200.00
250.00
300.00
350.00
400.00
450.00
500.00
Wavelength (nm)

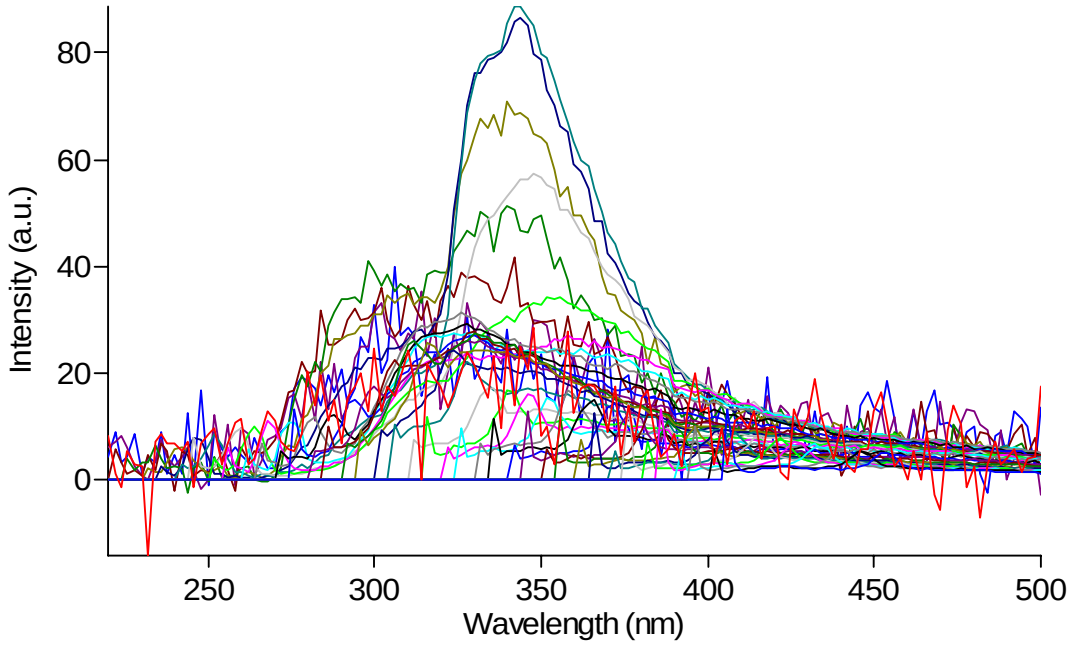
Intensity (a.u.)
80
60
40
20
0
250
300
350
400
450
500
Wavelength (nm)

82By

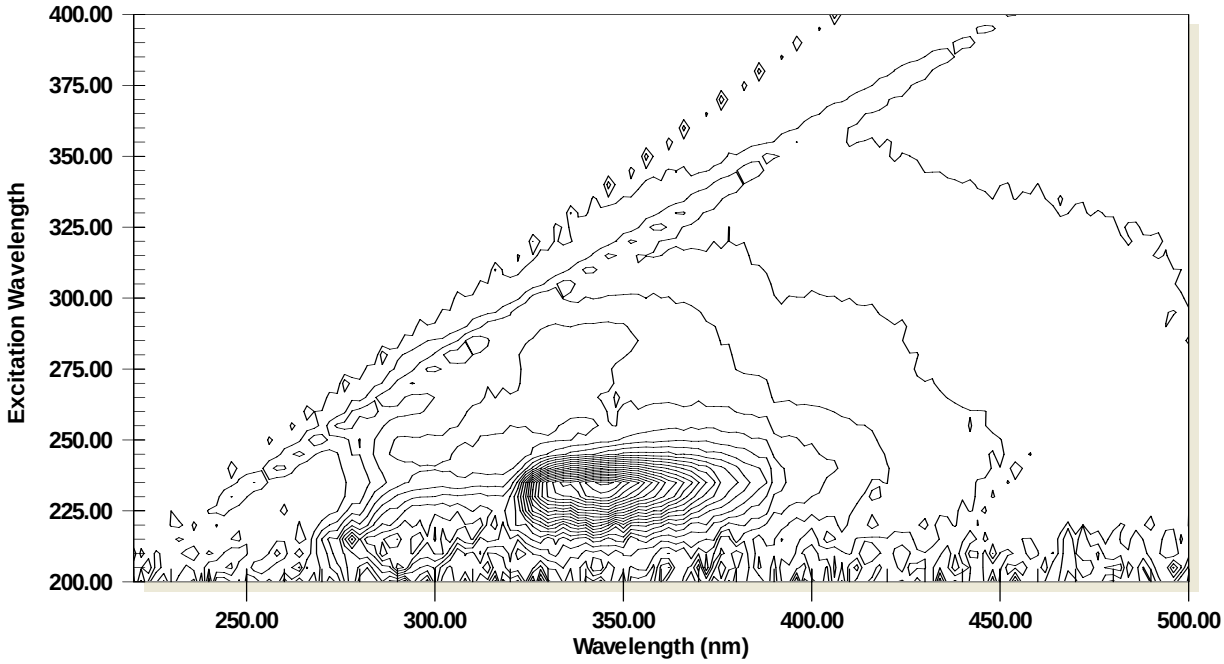
Excitation Wavelength
400.00
375.00
350.00
325.00
300.00
275.00
250.00
225.00
200.00
250.00
300.00
350.00
400.00
450.00
500.00
Wavelength (nm)

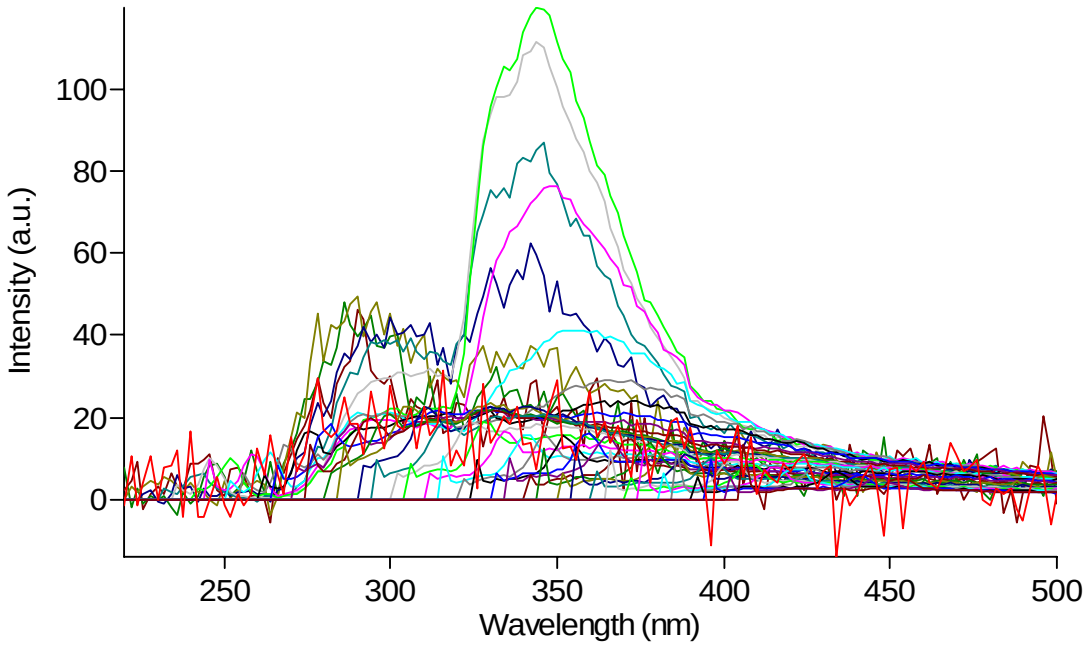
Intensity (a.u.)
100
80
60
40
20
0
250
300
350
400
450
500
Wavelength (nm)

83By

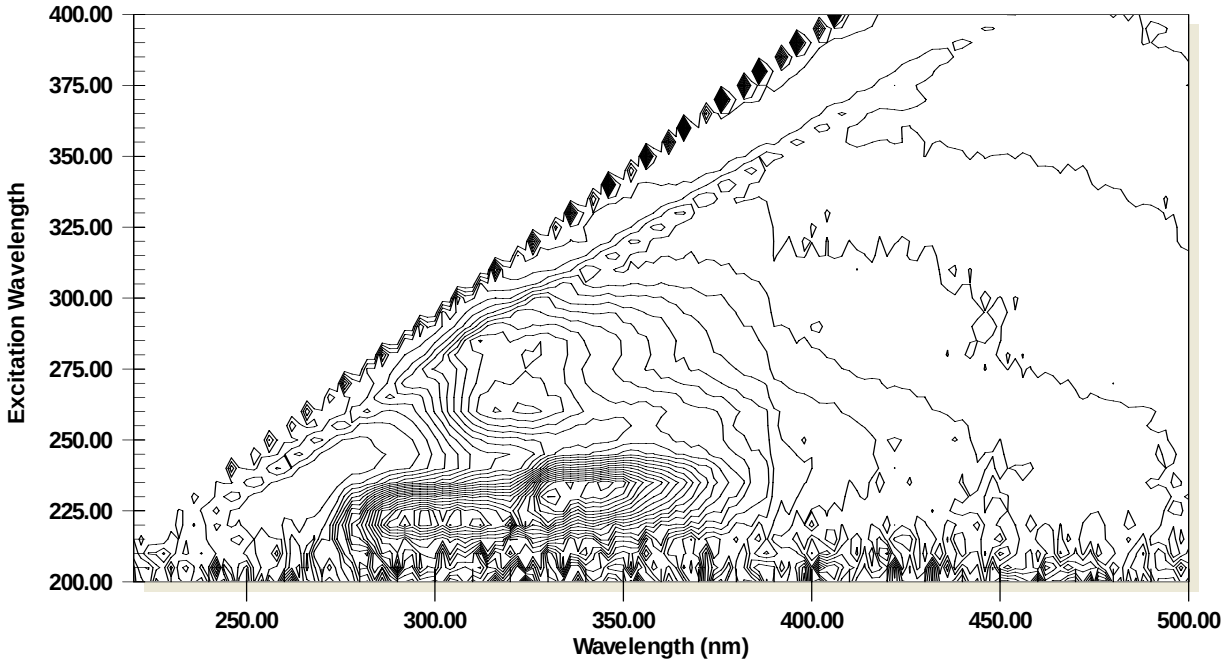
Excitation Wavelength
400.00
375.00
350.00
325.00
300.00
275.00
250.00
225.00
200.00
250.00
300.00
350.00
400.00
450.00
500.00
Wavelength (nm)

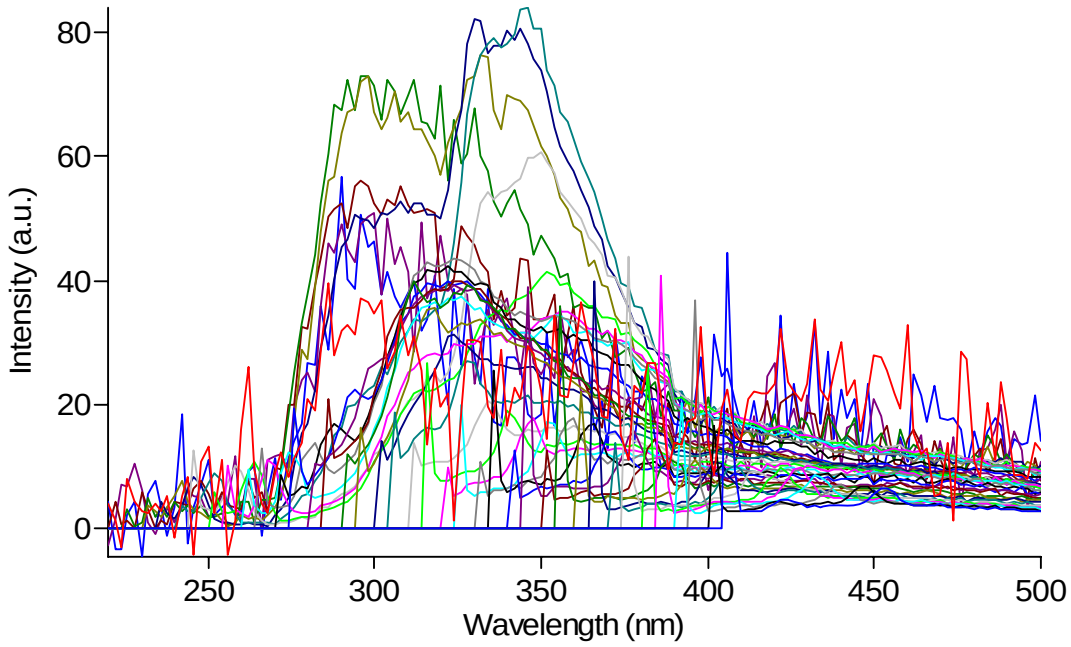
Intensity (a.u.)
80
60
40
20
0
250
300
350
400
450
500
Wavelength (nm)

84By

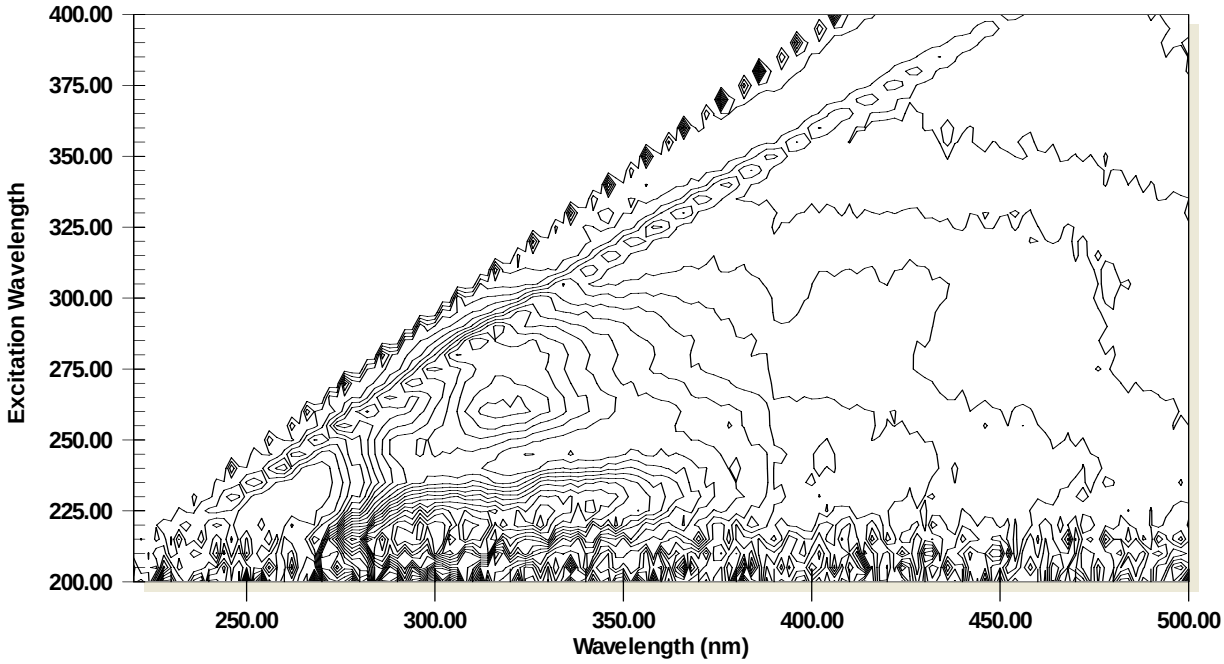
400.00
375.00
350.00
325.00
300.00
275.00
250.00
225.00
200.00
Excitation Wavelength
250.00
300.00
350.00
400.00
450.00
500.00
Wavelength (nm)

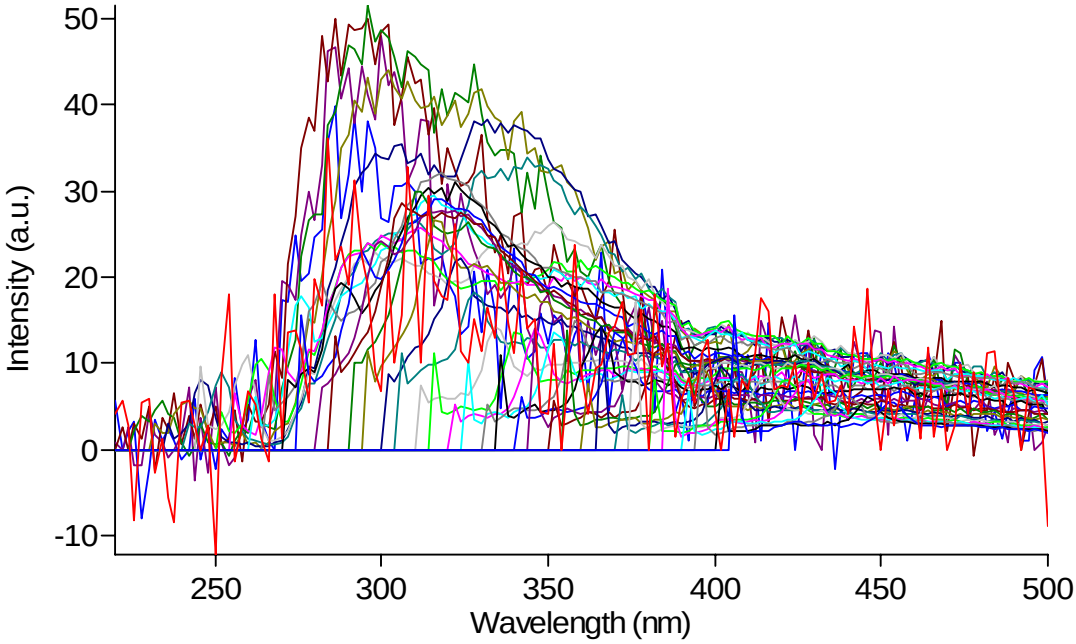
50
40
30
20
10
0
-10
Intensity (a.u.)
250
300
350
400
450
500
Wavelength (nm)

85Ay

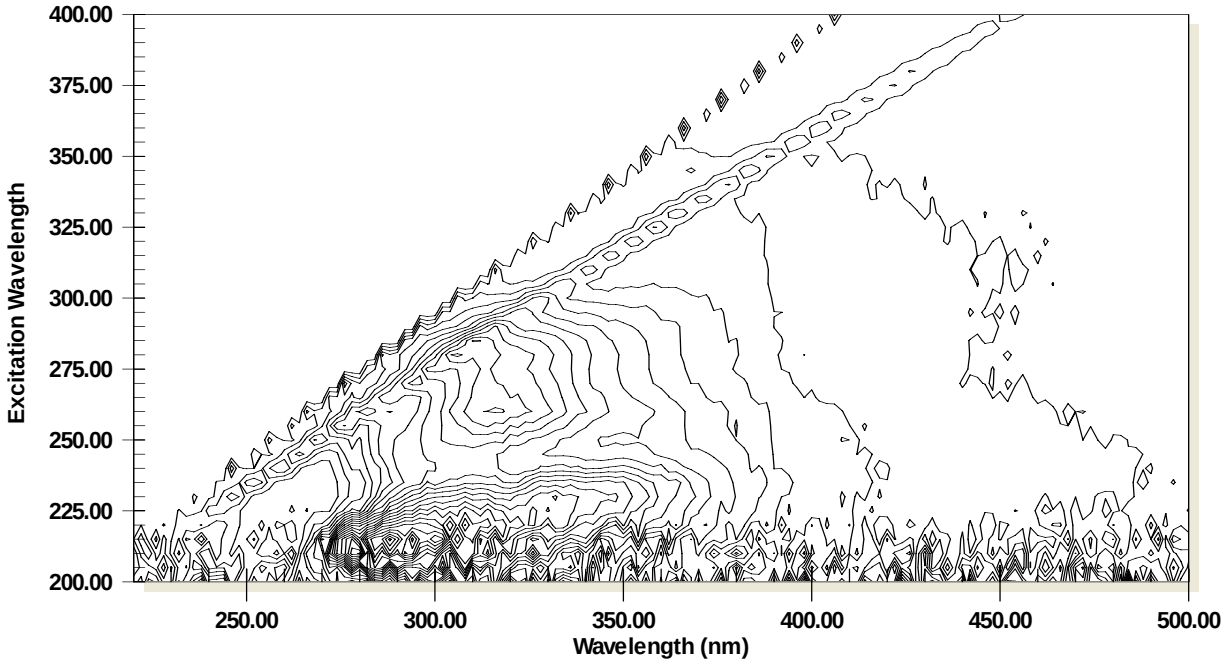
Excitation Wavelength
400.00
375.00
350.00
325.00
300.00
275.00
250.00
225.00
200.00
250.00
300.00
350.00
400.00
450.00
500.00
Wavelength (nm)

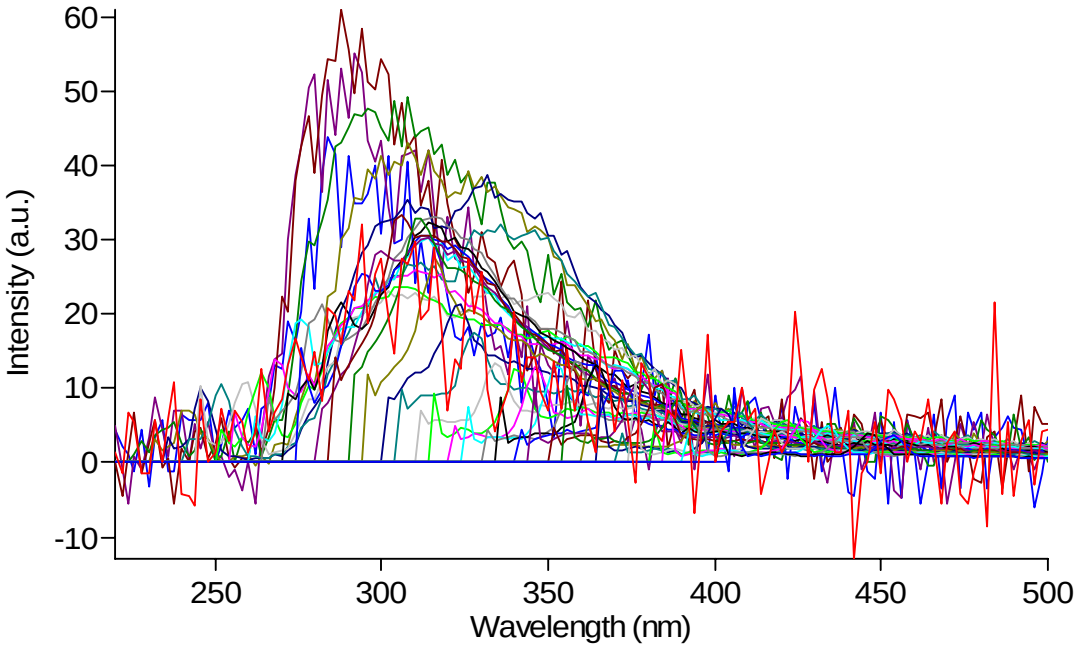
Intensity (a.u.)
60
50
40
30
20
10
0
-10
250
300
350
400
450
500
Wavelength (nm)

91Ay

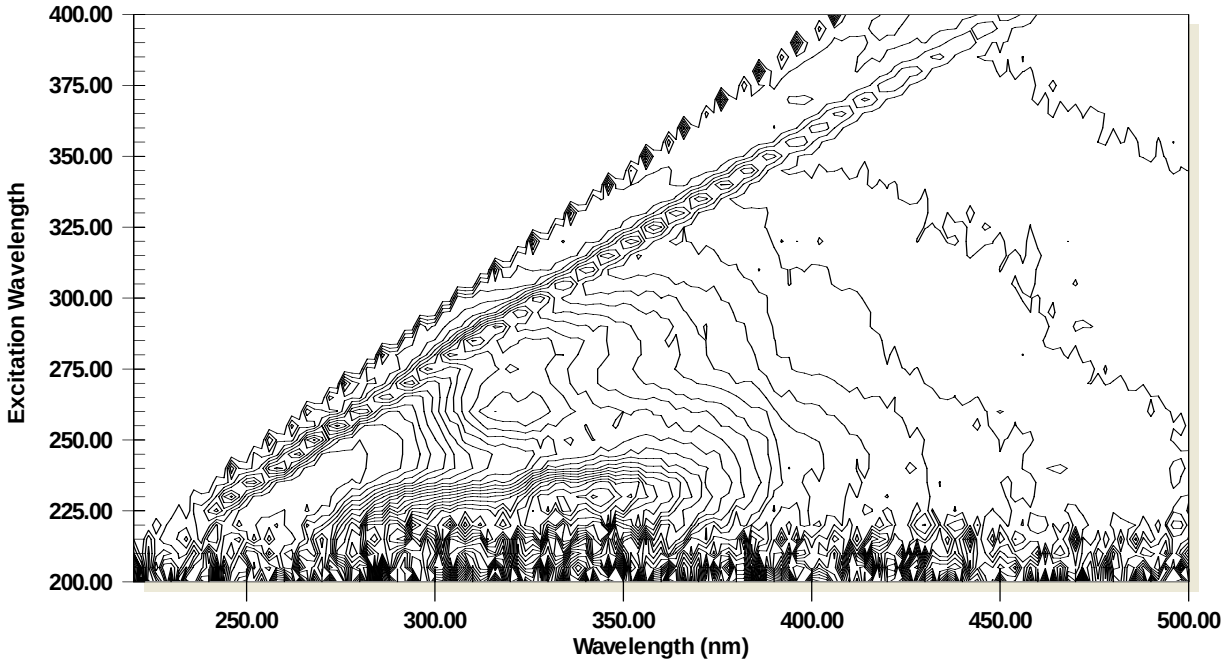
400.00
375.00
350.00
325.00
300.00
275.00
250.00
225.00
200.00
Excitation Wavelength
250.00
300.00
350.00
400.00
450.00
500.00
Wavelength (nm)

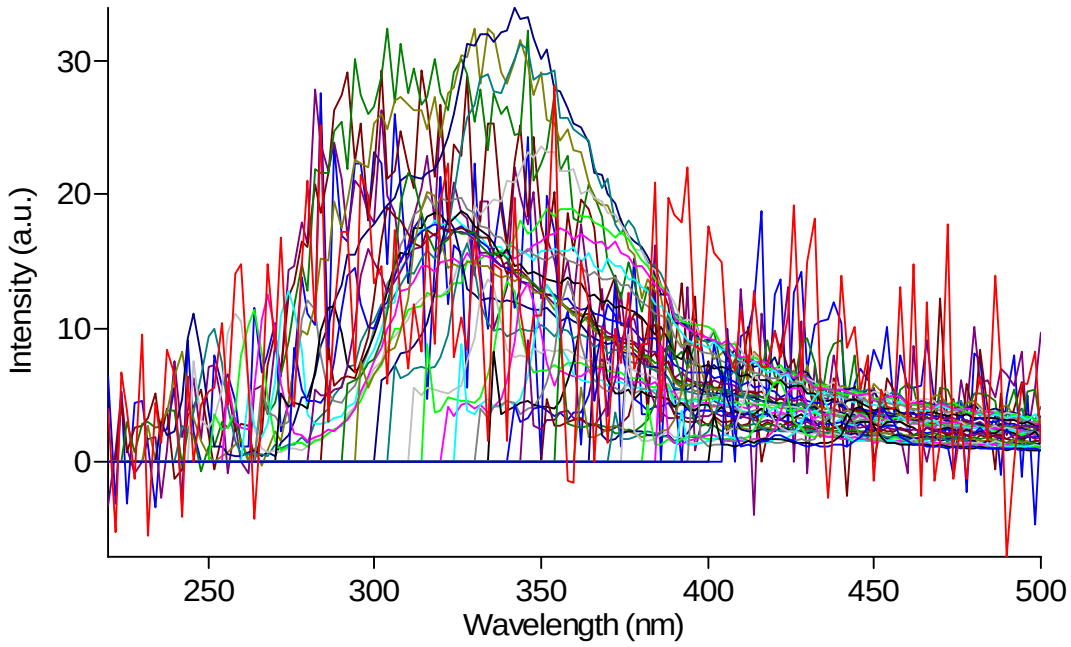
30
20
10
0
Intensity (a.u.)
250
300
350
400
450
500
Wavelength (nm)

92Ay

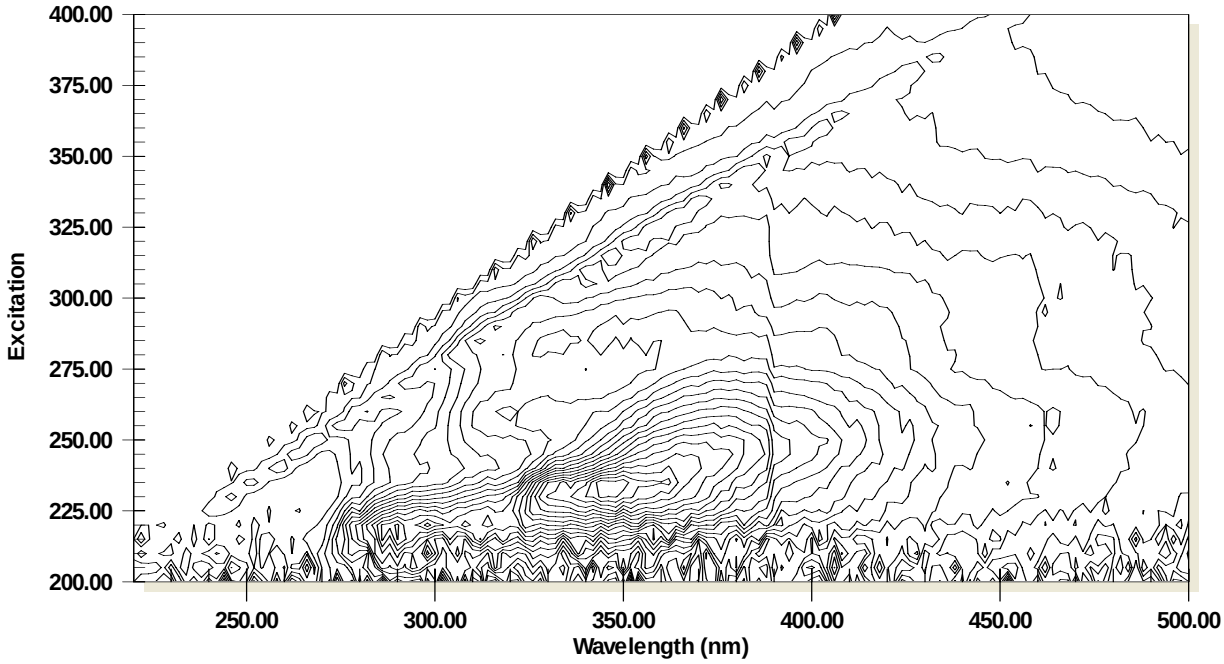
400.00
375.00
350.00
325.00
300.00
275.00
250.00
225.00
200.00
Excitation
250.00
300.00
350.00
400.00
450.00
500.00
Wavelength (nm)

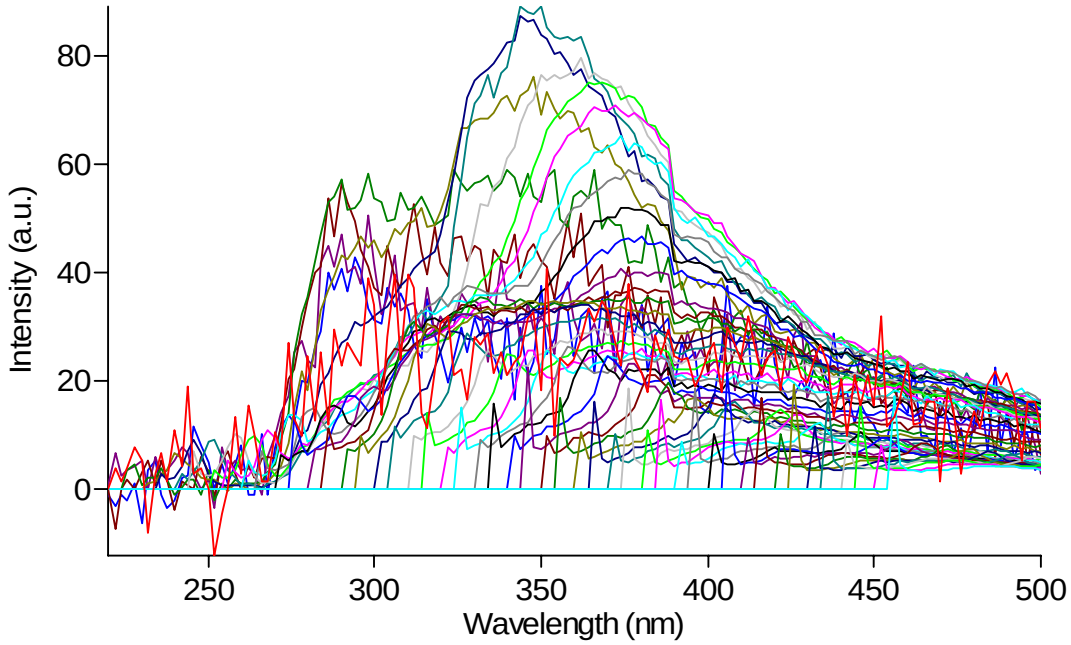
80
60
40
20
0
Intensity (a.u.)
250
300
350
400
450
500
Wavelength (nm)

93Ay

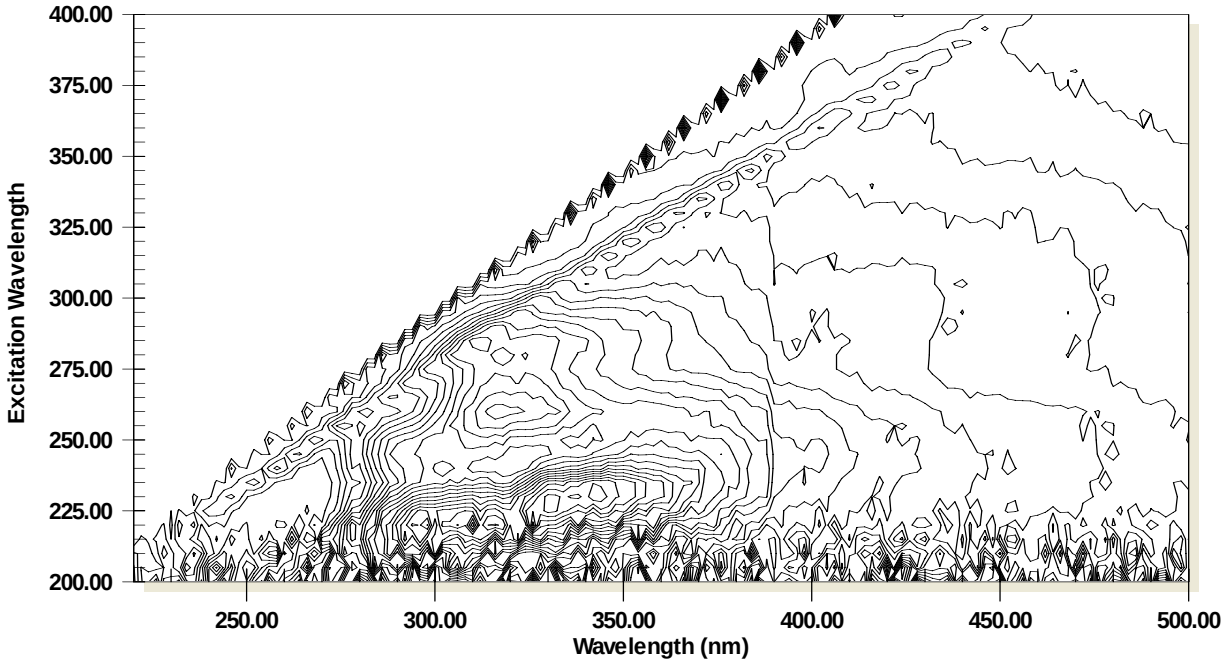
Excitation Wavelength
400.00
375.00
350.00
325.00
300.00
275.00
250.00
225.00
200.00
250.00
300.00
350.00
400.00
450.00
500.00
Wavelength (nm)

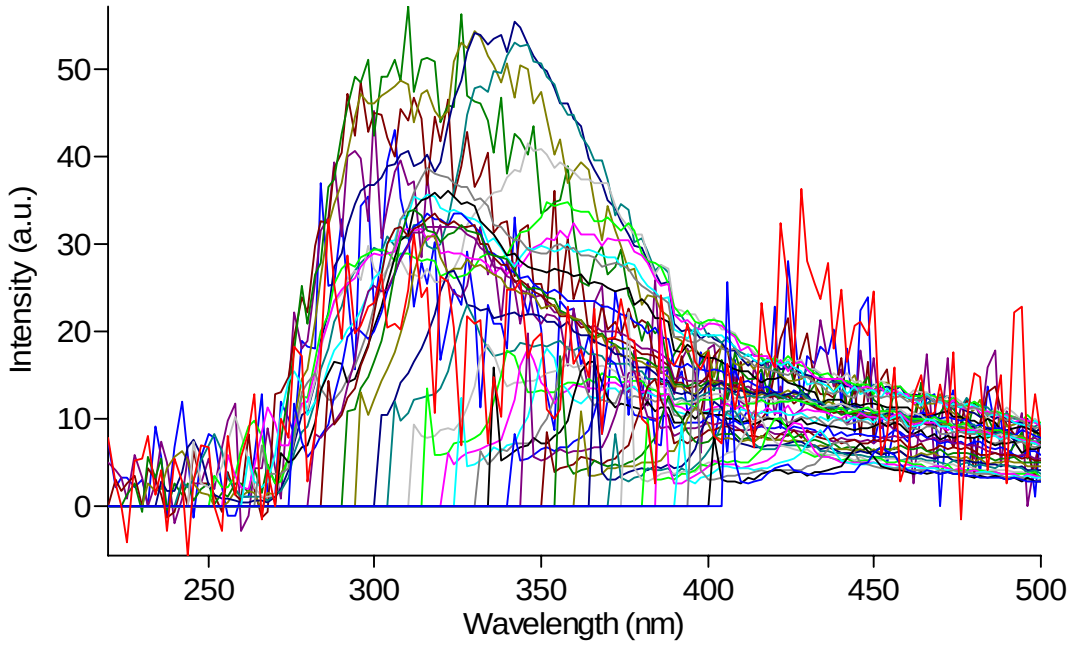
Intensity (a.u.)
50
40
30
20
10
0
250
300
350
400
450
500
Wavelength (nm)

94By

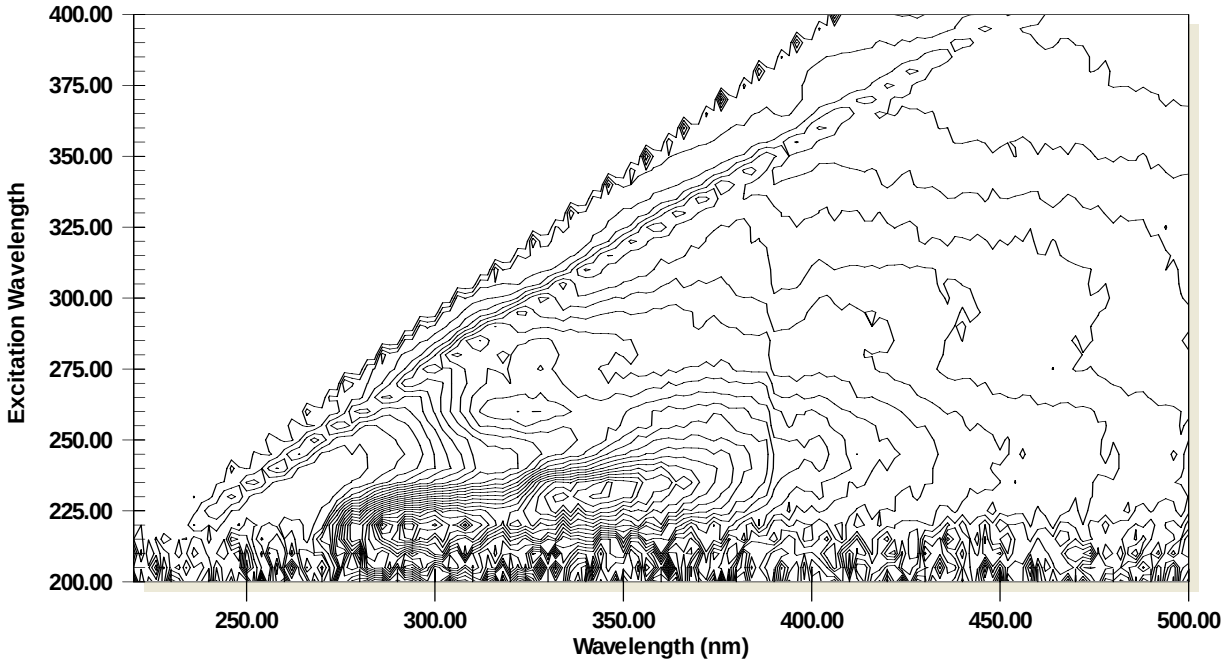
400.00
375.00
350.00
325.00
300.00
275.00
250.00
225.00
200.00
Excitation Wavelength
250.00
300.00
350.00
400.00
450.00
500.00
Wavelength (nm)

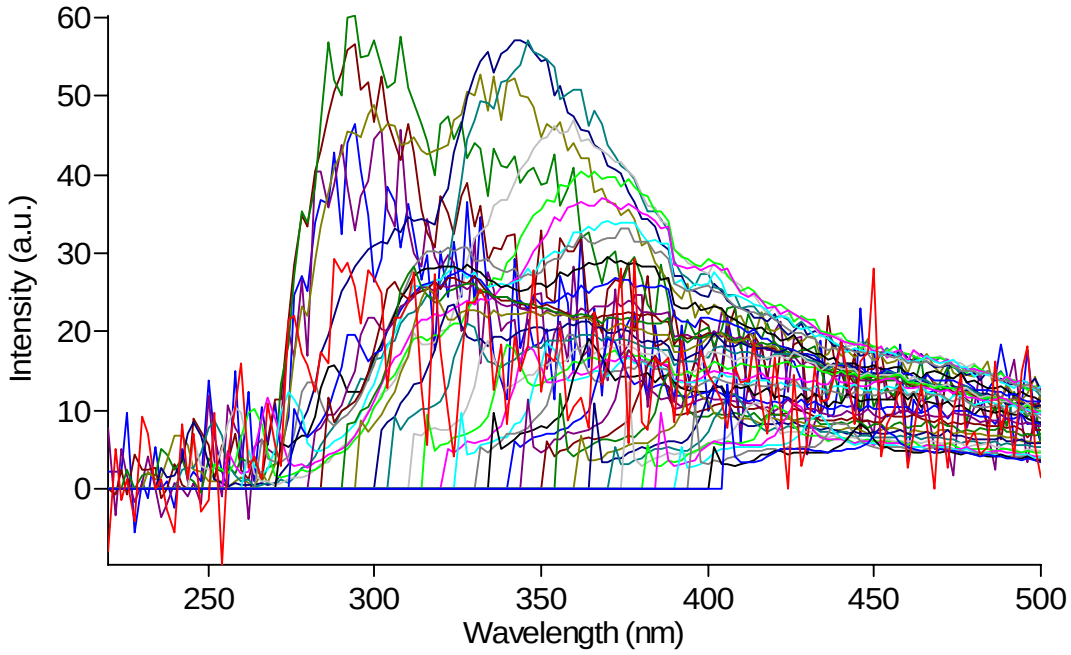
60
50
40
30
20
10
0
Intensity (a.u.)
250
300
350
400
450
500
Wavelength (nm)

95By

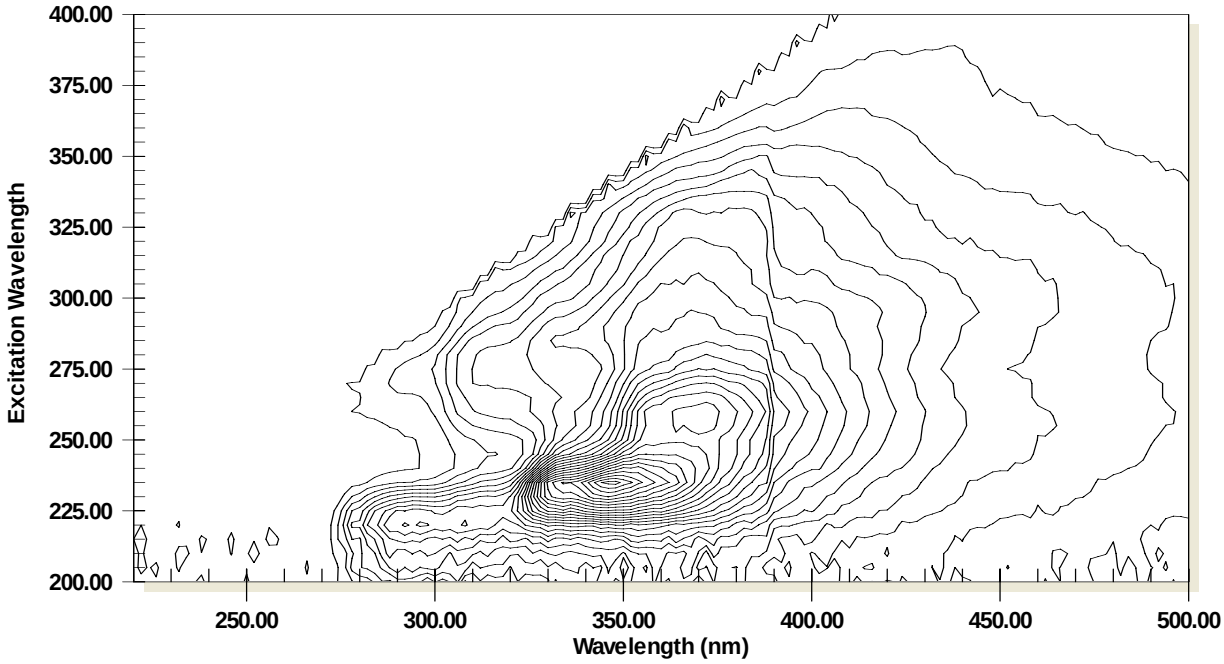
Excitation Wavelength
400.00
375.00
350.00
325.00
300.00
275.00
250.00
225.00
200.00
250.00
300.00
350.00
400.00
450.00
500.00
Wavelength (nm)

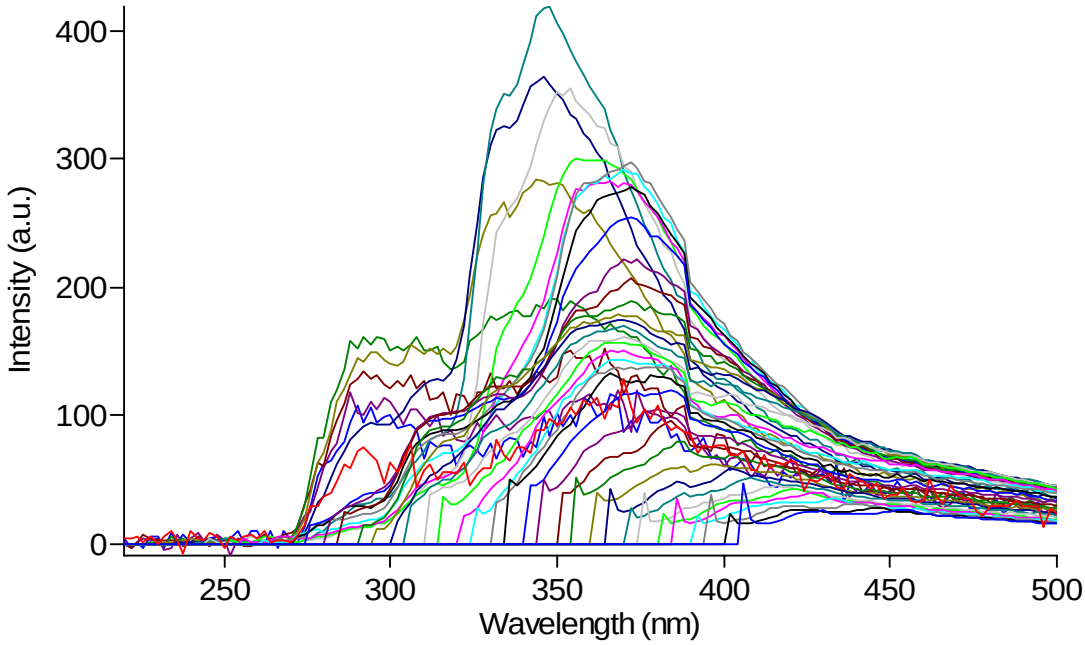
Intensity (a.u.)
400
300
200
100
0
250
300
350
400
450
500
Wavelength (nm)

101Ay

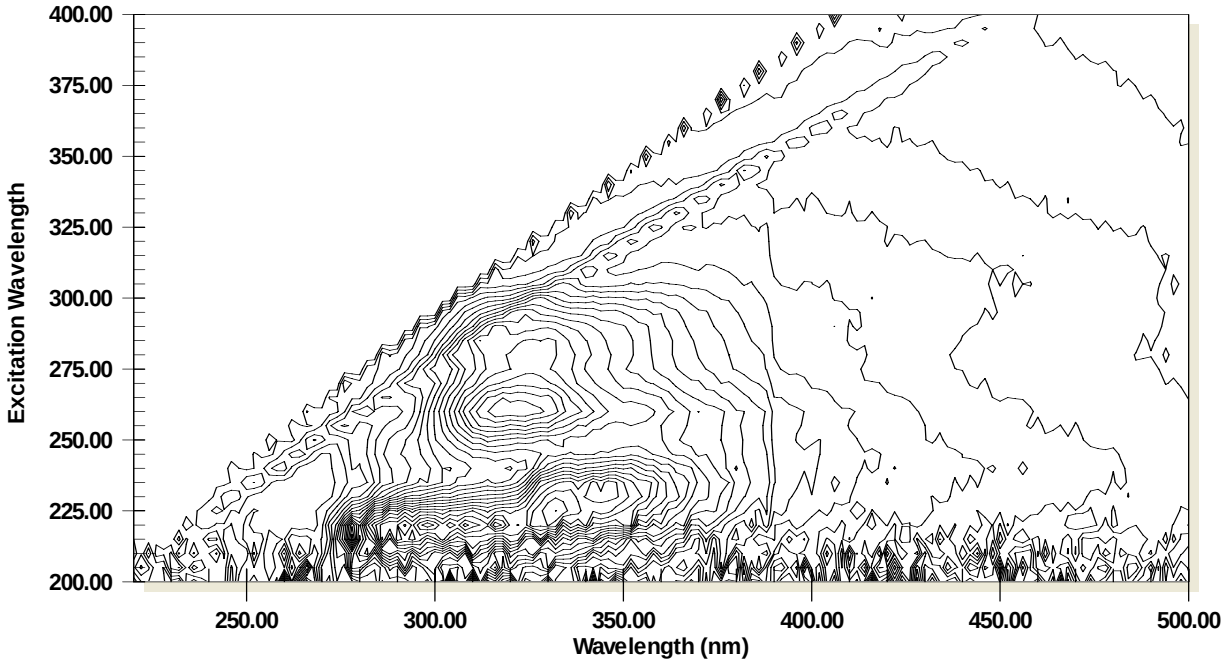
Excitation Wavelength
400.00
375.00
350.00
325.00
300.00
275.00
250.00
225.00
200.00
250.00
300.00
350.00
400.00
450.00
500.00
Wavelength (nm)

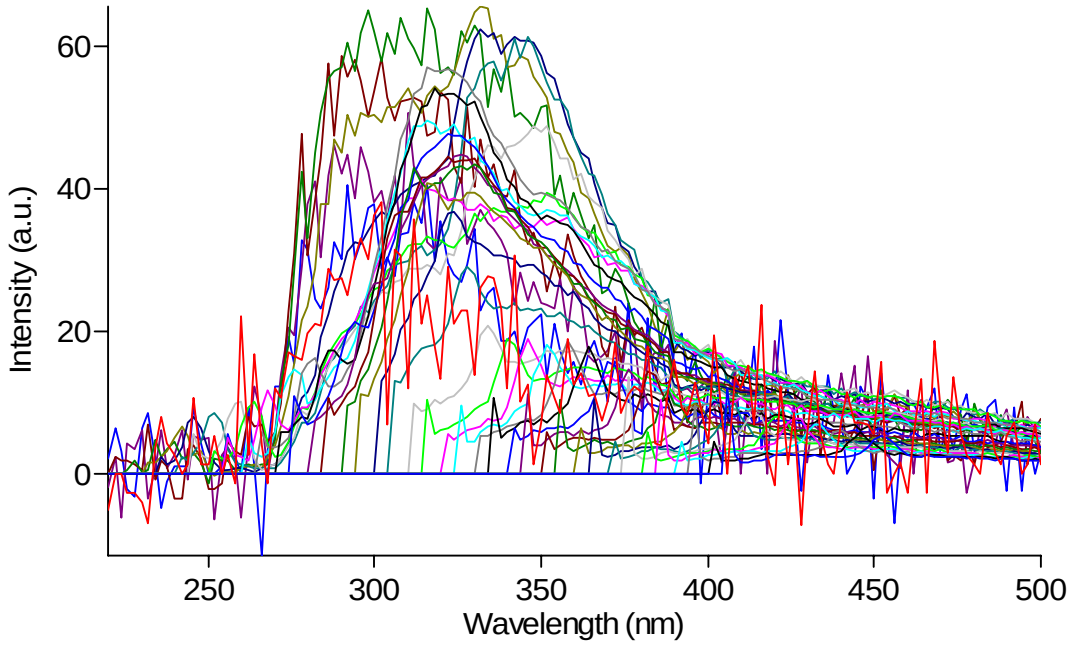
Intensity (a.u.)
60
40
20
0
250
300
350
400
450
500
Wavelength (nm)

102Ay

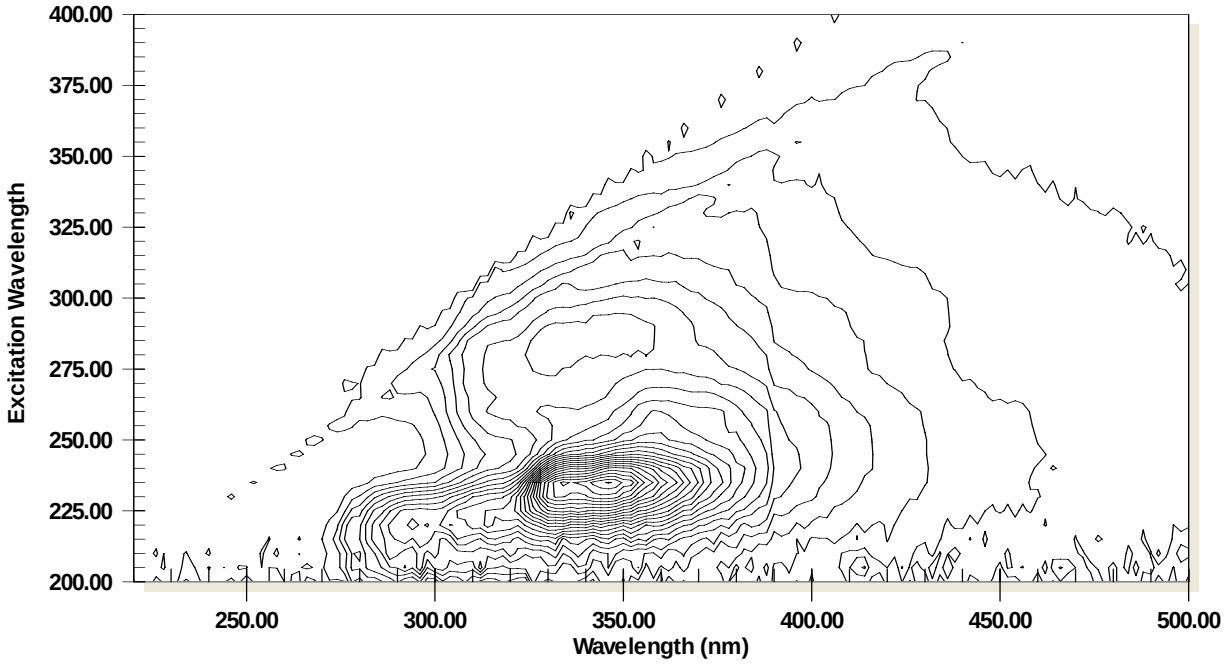
Excitation Wavelength
400.00
375.00
350.00
325.00
300.00
275.00
250.00
225.00
200.00
250.00
300.00
350.00
400.00
450.00
500.00
Wavelength (nm)

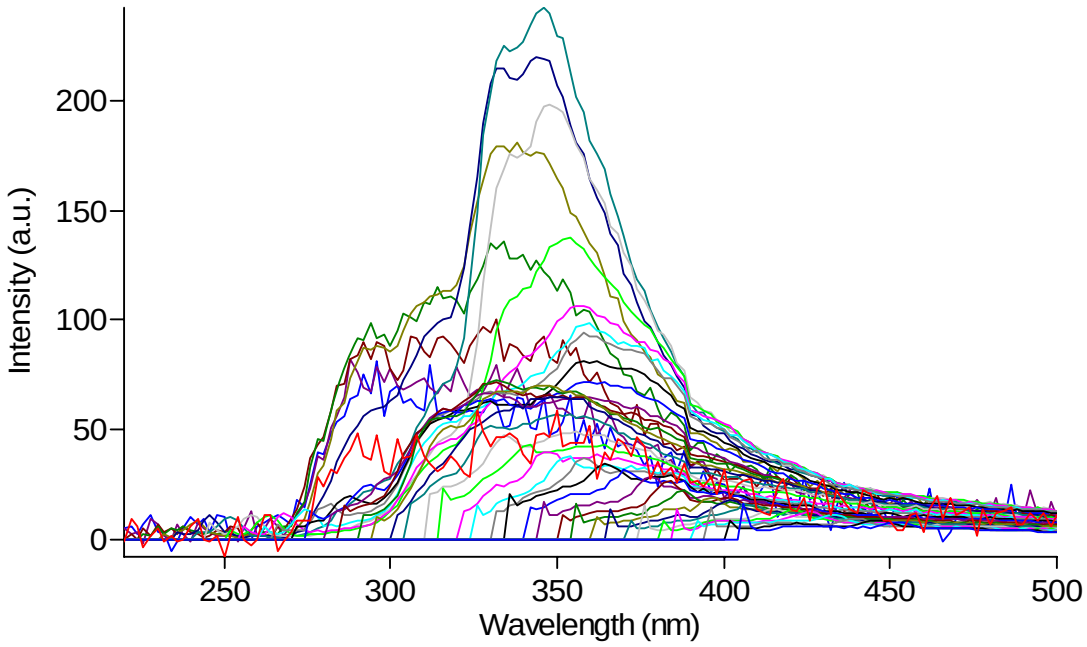
Intensity (a.u.)
200
150
100
50
0
250
300
350
400
450
500
Wavelength (nm)

103By

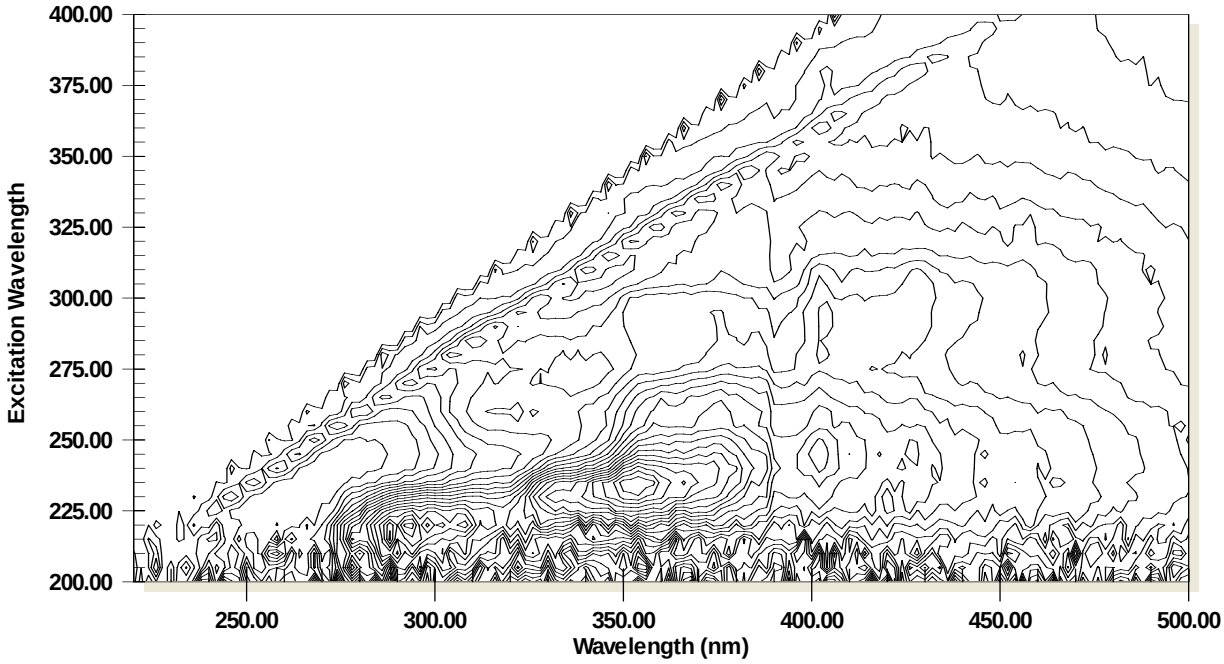
Excitation Wavelength
400.00
375.00
350.00
325.00
300.00
275.00
250.00
225.00
200.00
250.00
300.00
350.00
400.00
450.00
500.00
Wavelength (nm)

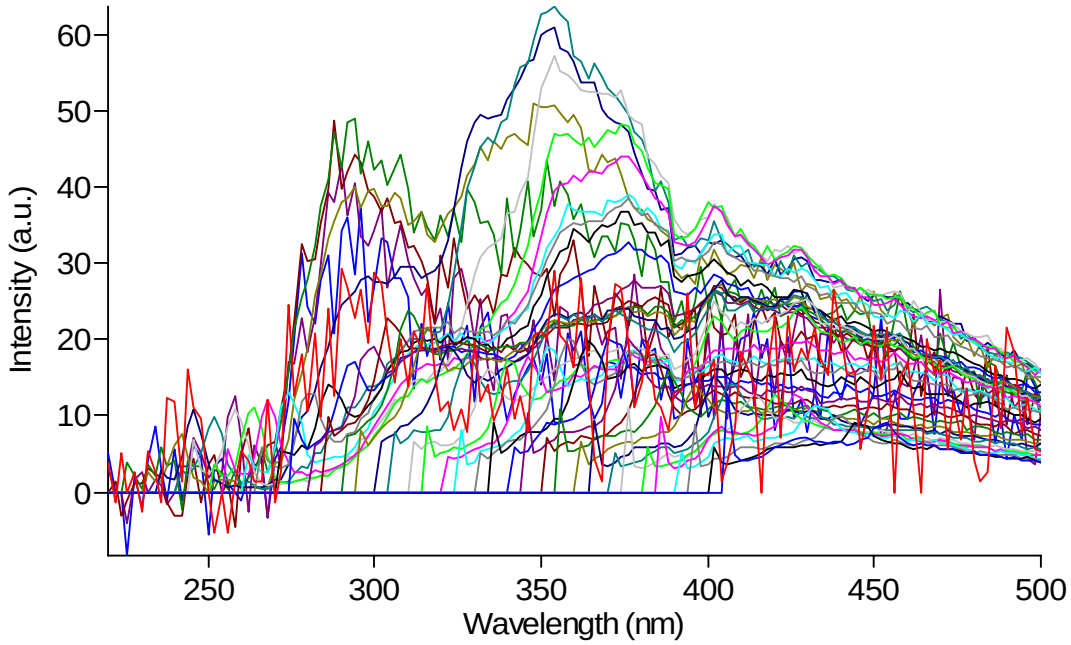
Intensity (a.u.)
60
50
40
30
20
10
0
250
300
350
400
450
500
Wavelength (nm)

104Cy

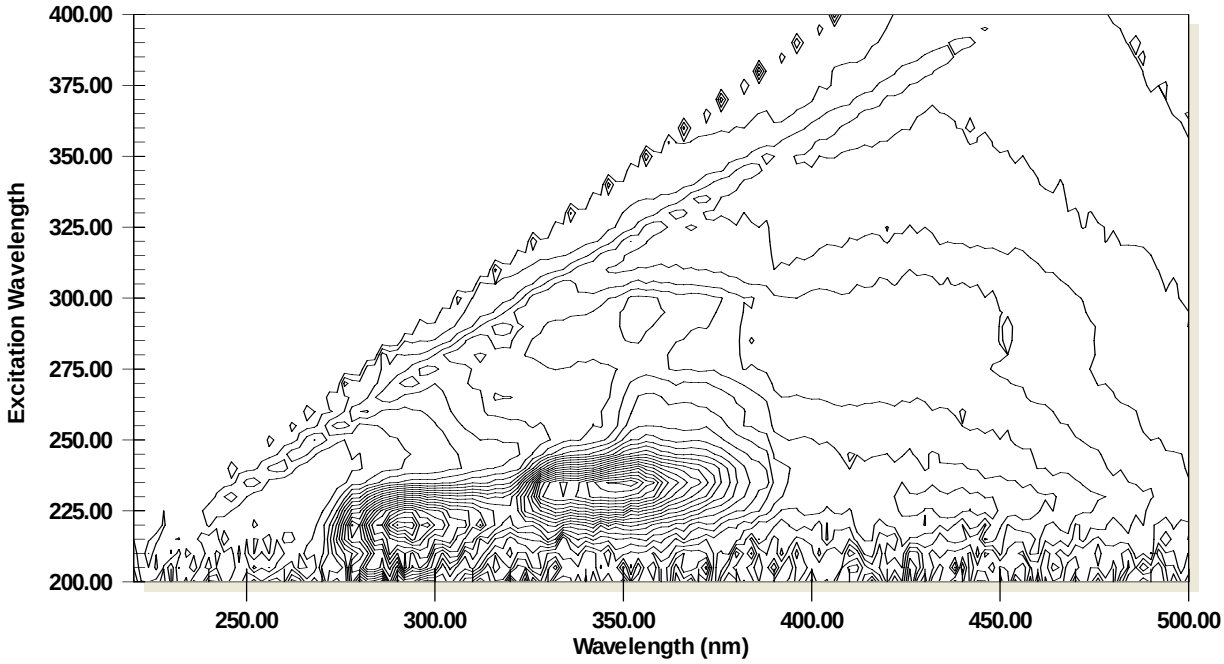
Excitation Wavelength
400.00
375.00
350.00
325.00
300.00
275.00
250.00
225.00
200.00
250.00
300.00
350.00
400.00
450.00
500.00
Wavelength (nm)

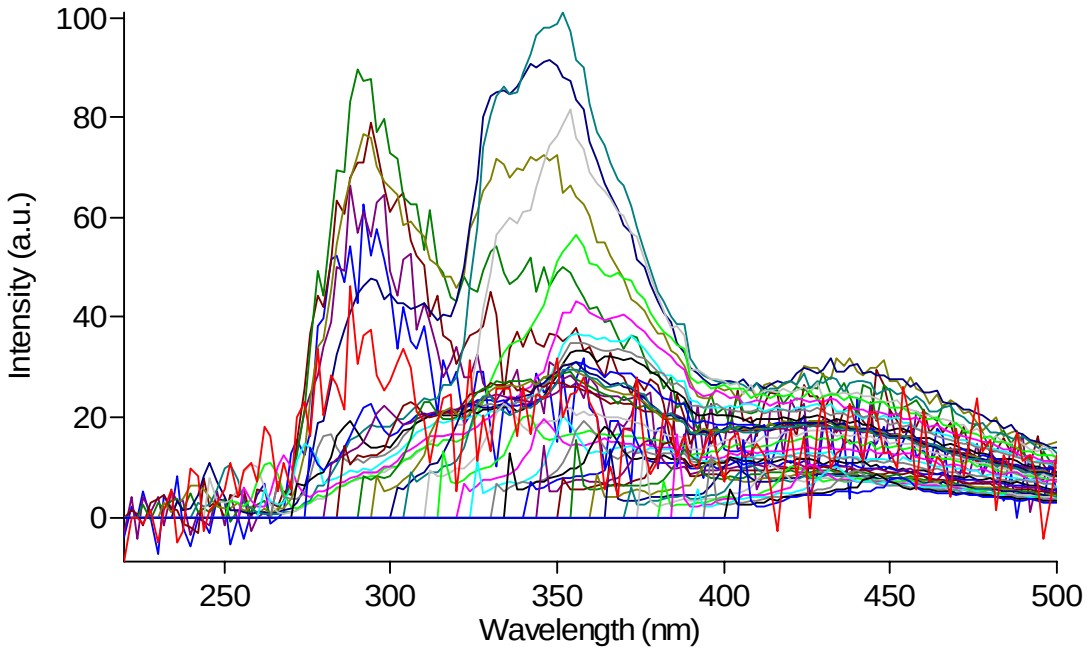
Intensity (a.u.)
100
80
60
40
20
0
250
300
350
400
450
500
Wavelength (nm)

105Cy

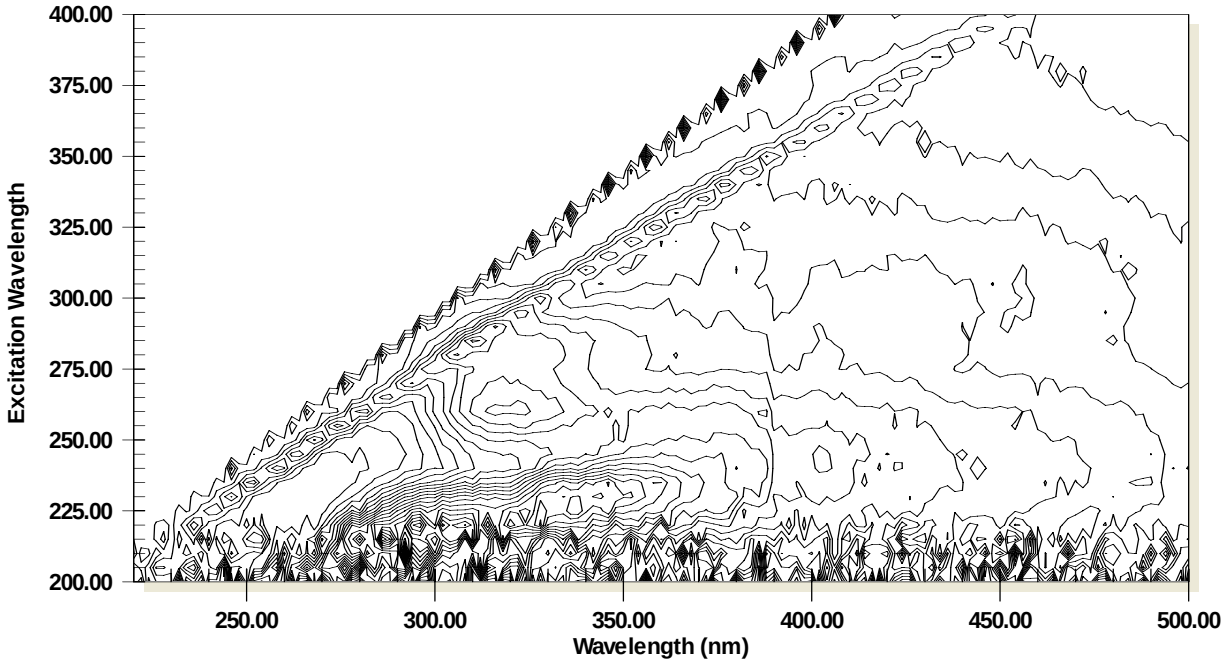
Excitation Wavelength
400.00
375.00
350.00
325.00
300.00
275.00
250.00
225.00
200.00
250.00
300.00
350.00
400.00
450.00
500.00
Wavelength (nm)

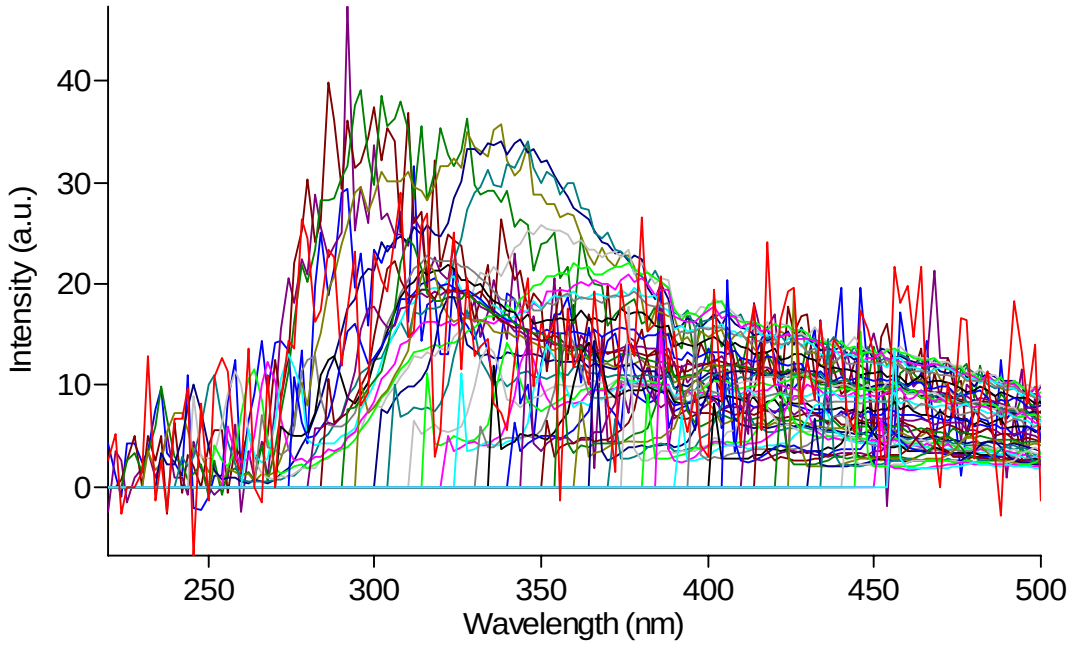
Intensity (a.u.)
40
30
20
10
0
250
300
350
400
450
500
Wavelength (nm)

M06y

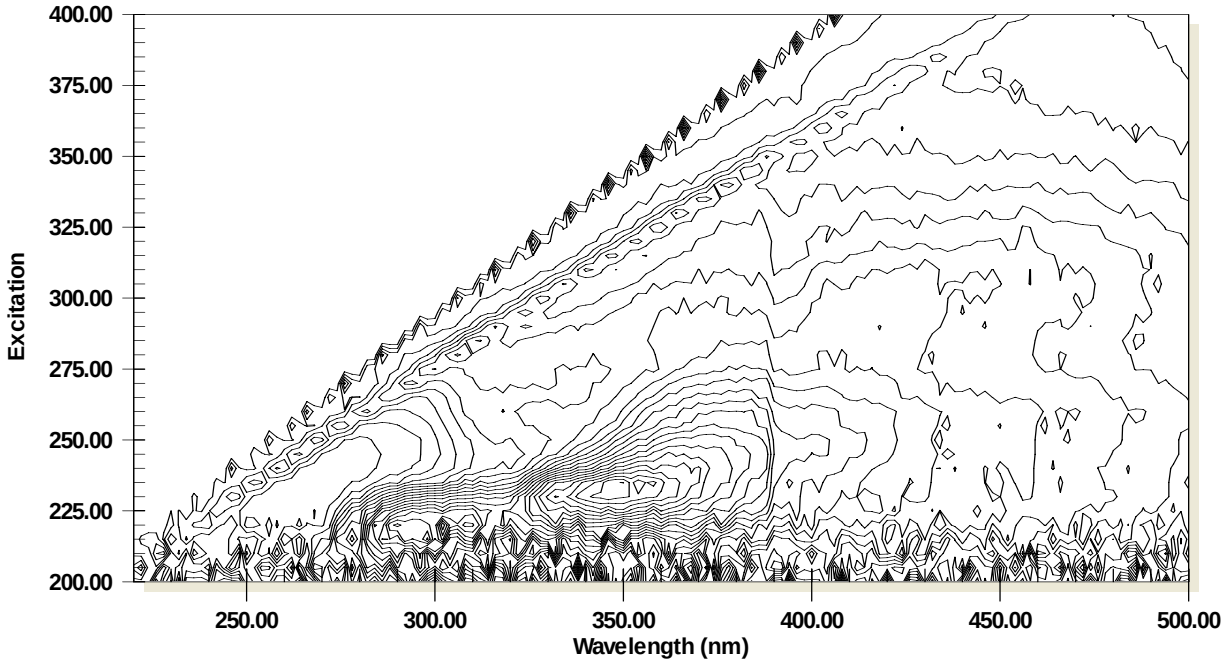
400.00
375.00
350.00
325.00
300.00
275.00
250.00
225.00
200.00
Excitation
250.00
300.00
350.00
400.00
450.00
500.00
Wavelength (nm)

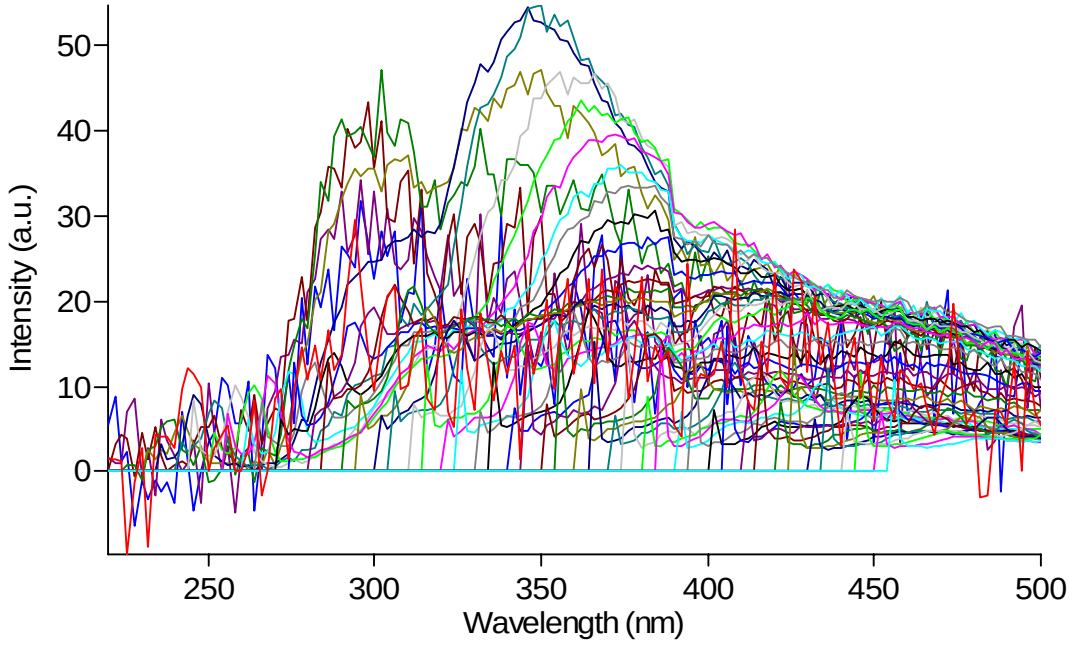
50
40
30
20
10
0
Intensity (a.u.)
250
300
350
400
450
500
Wavelength (nm)

M10y

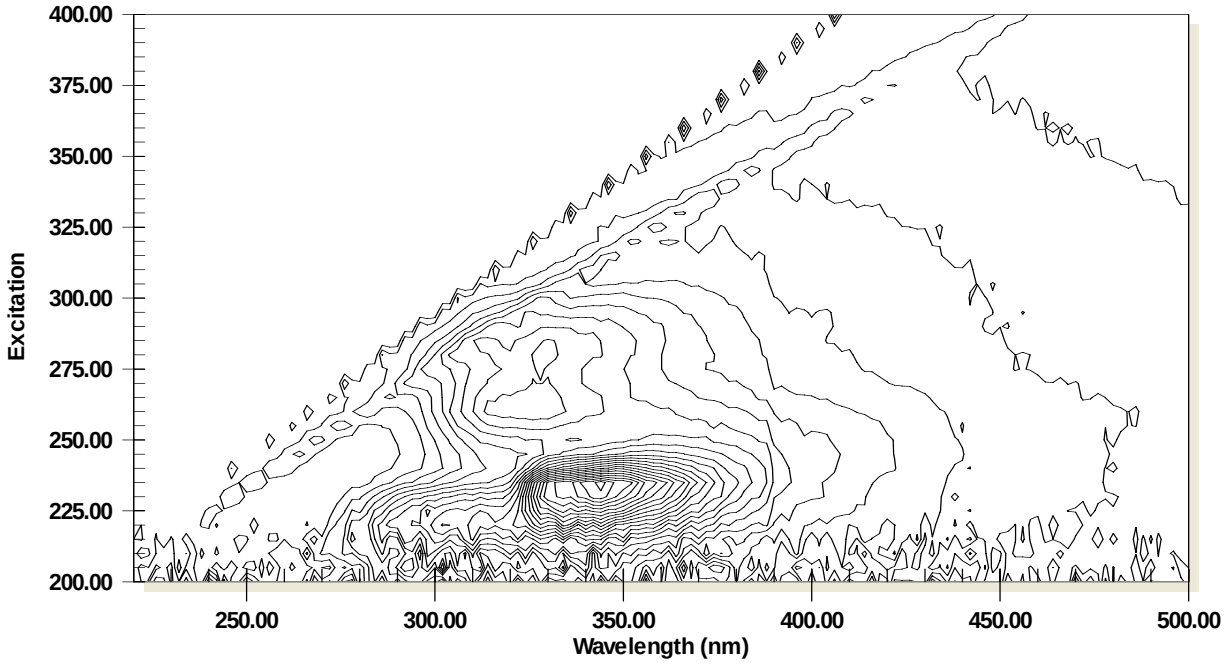
400.00
375.00
350.00
325.00
300.00
275.00
250.00
225.00
200.00
Excitation
250.00
300.00
350.00
400.00
450.00
500.00
Wavelength (nm)

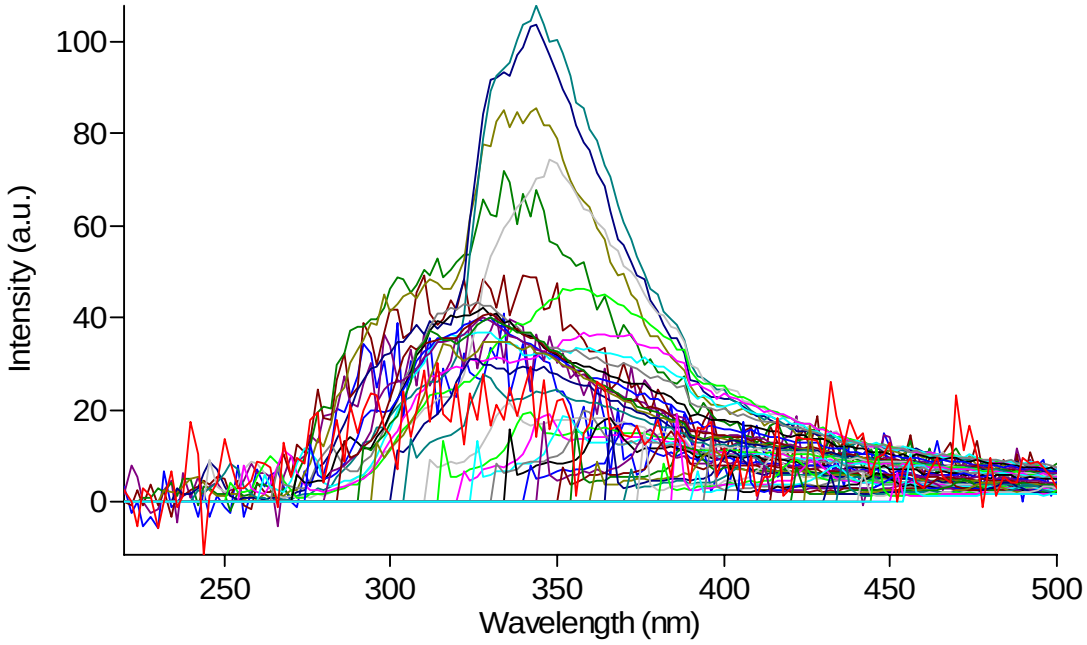
100
80
60
40
20
0
Intensity (a.u.)
250
300
350
400
450
500
Wavelength (nm)

M12y

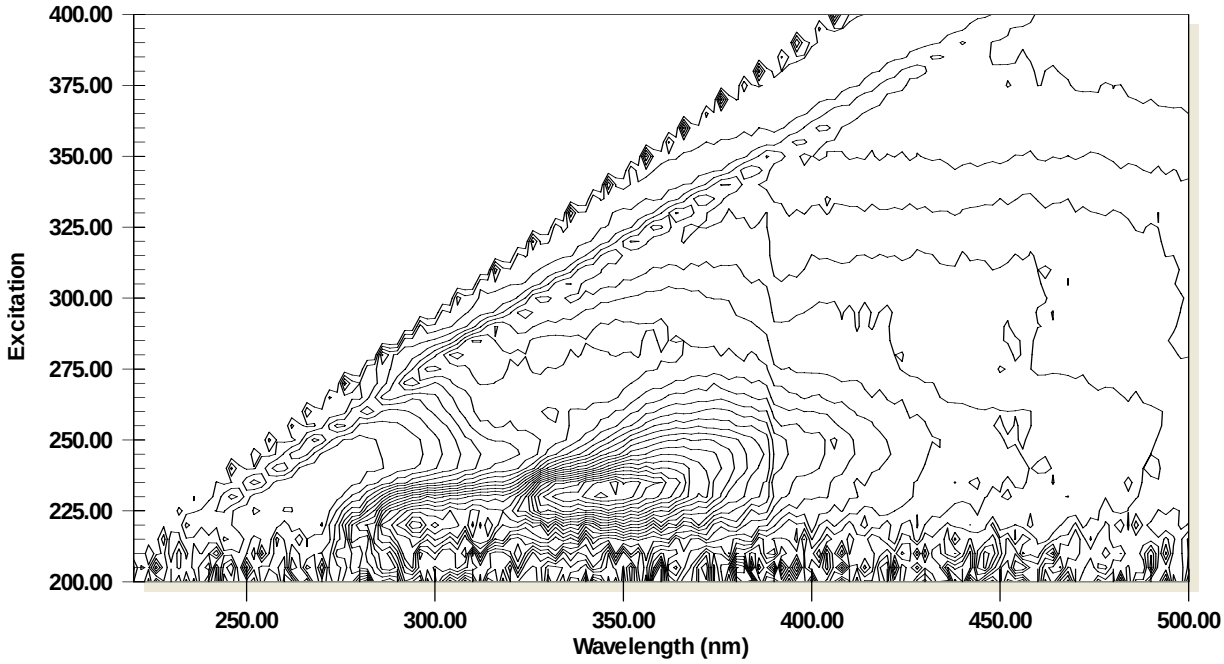
400.00
375.00
350.00
325.00
300.00
275.00
250.00
225.00
200.00
Excitation
250.00
300.00
350.00
400.00
450.00
500.00
Wavelength (nm)

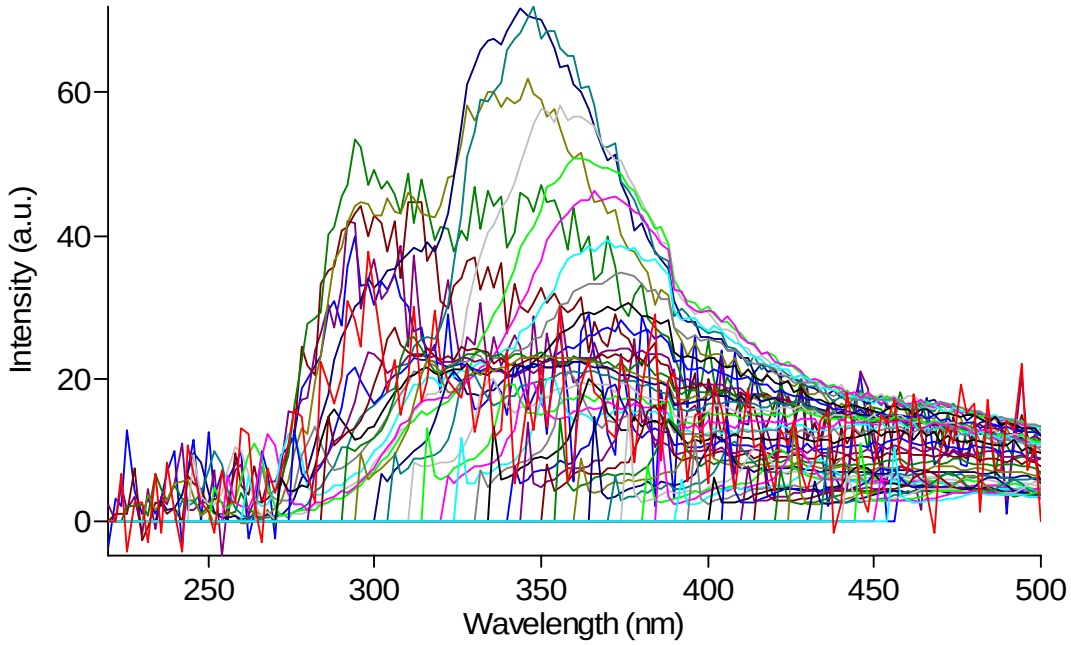
60
40
20
0
Intensity (a.u.)
250
300
350
400
450
500
Wavelength (nm)

M19y

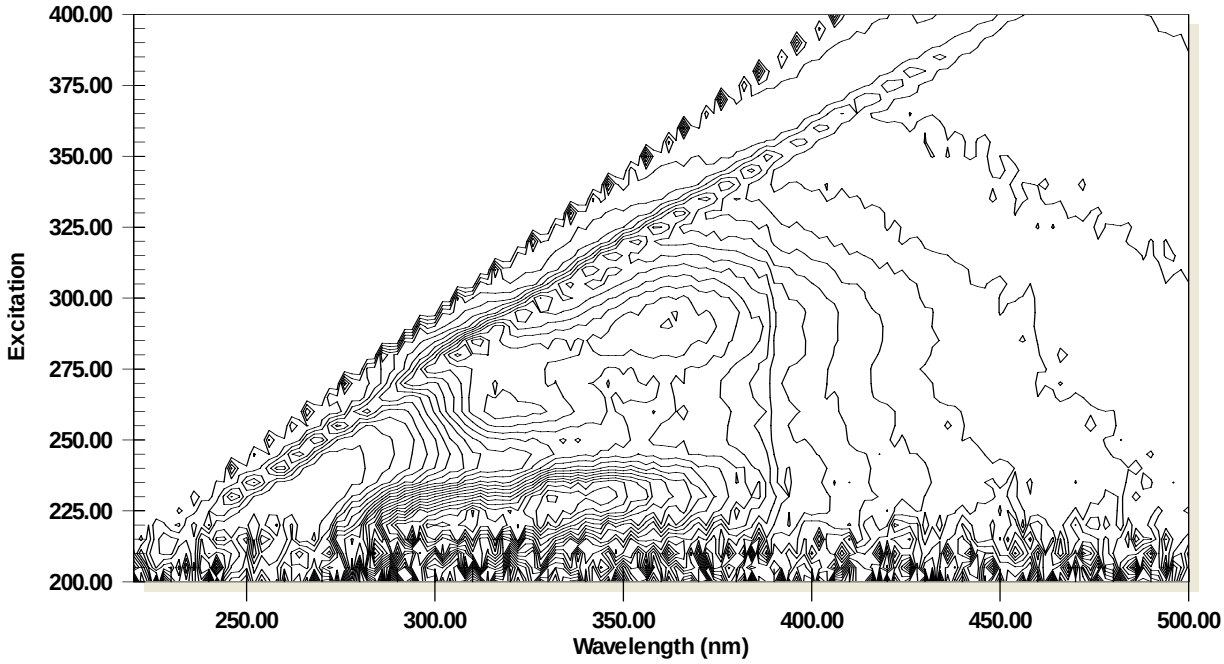
400.00
375.00
350.00
325.00
300.00
275.00
250.00
225.00
200.00
Excitation
250.00
300.00
350.00
400.00
450.00
500.00
Wavelength (nm)

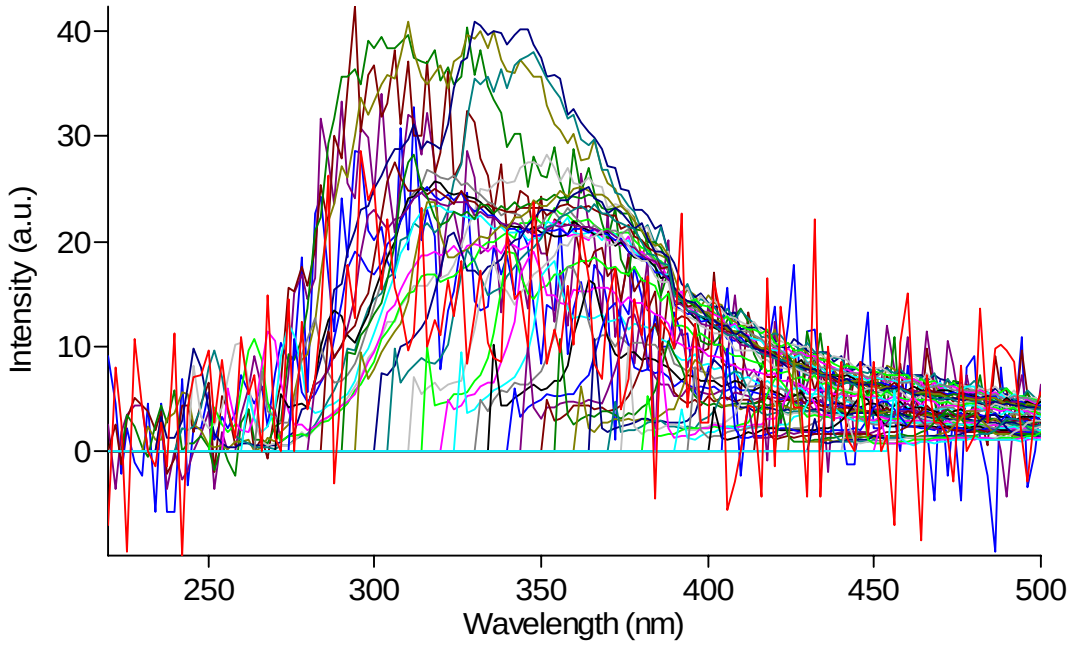
40
30
20
10
0
Intensity (a.u.)
250
300
350
400
450
500
Wavelength (nm)

M24y

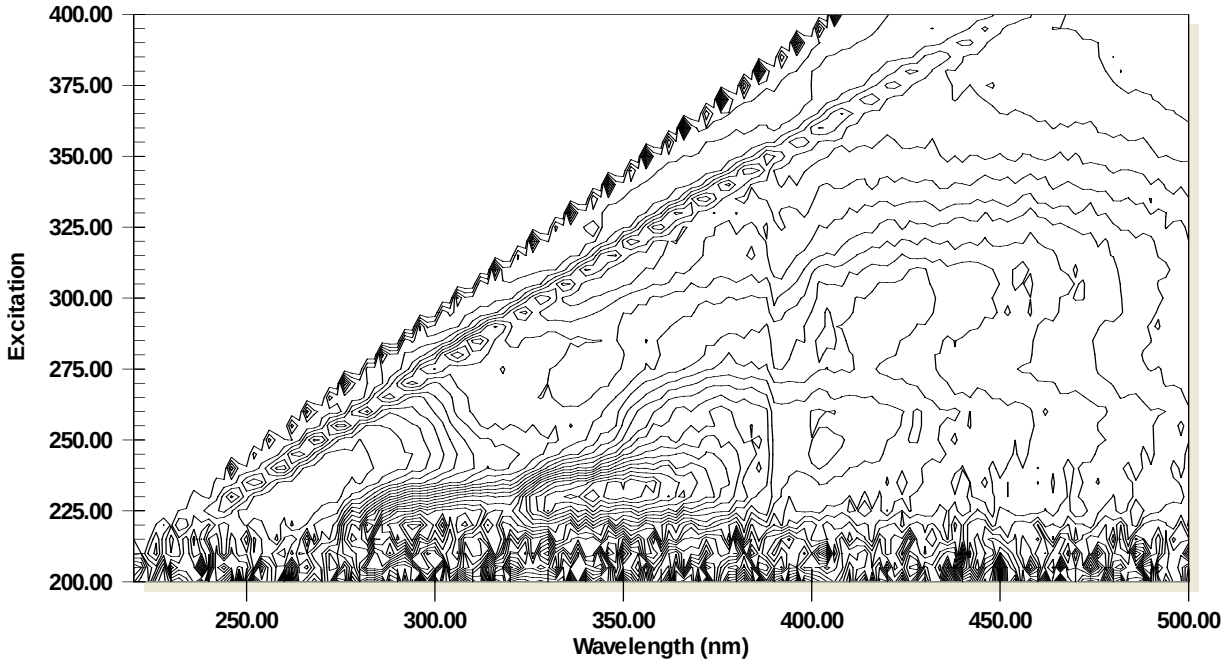
400.00
375.00
350.00
325.00
300.00
275.00
250.00
225.00
200.00
Excitation
250.00
300.00
350.00
400.00
450.00
500.00
Wavelength (nm)

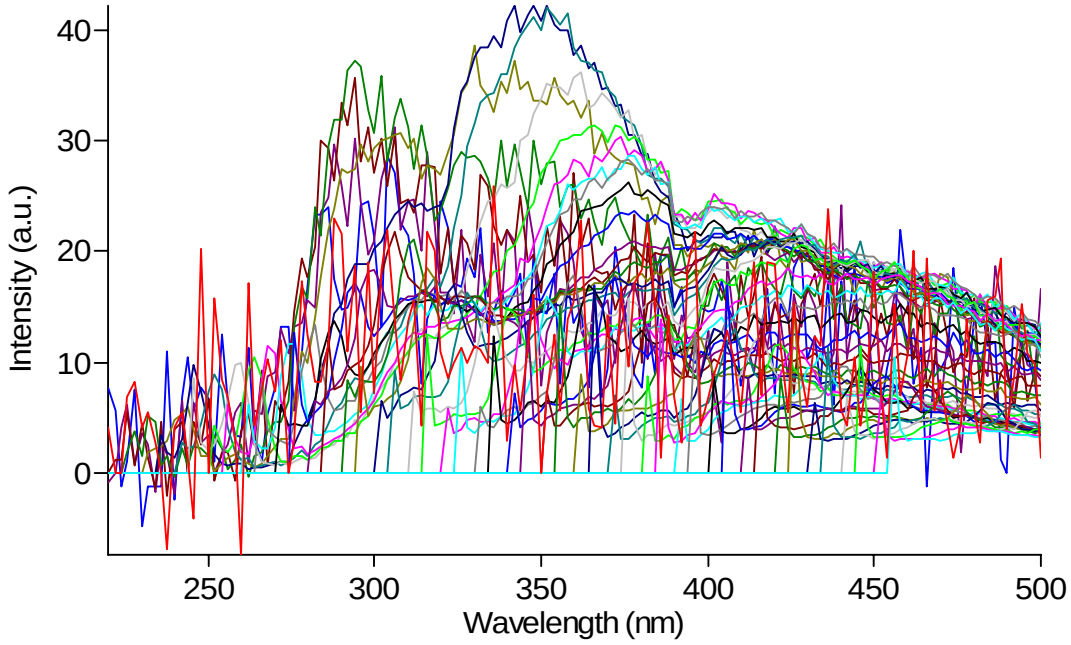
40
30
20
10
0
Intensity (a.u.)
250
300
350
400
450
500
Wavelength (nm)

M28y

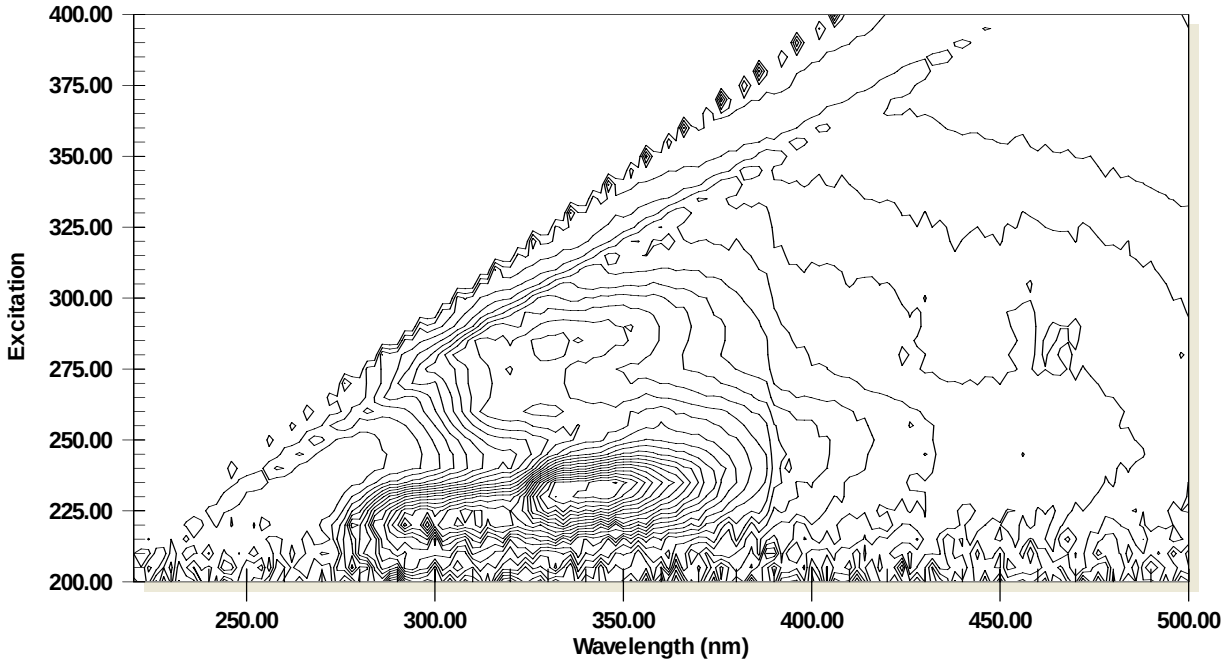
400.00
375.00
350.00
325.00
300.00
275.00
250.00
225.00
200.00
Excitation
250.00
300.00
350.00
400.00
450.00
500.00
Wavelength (nm)

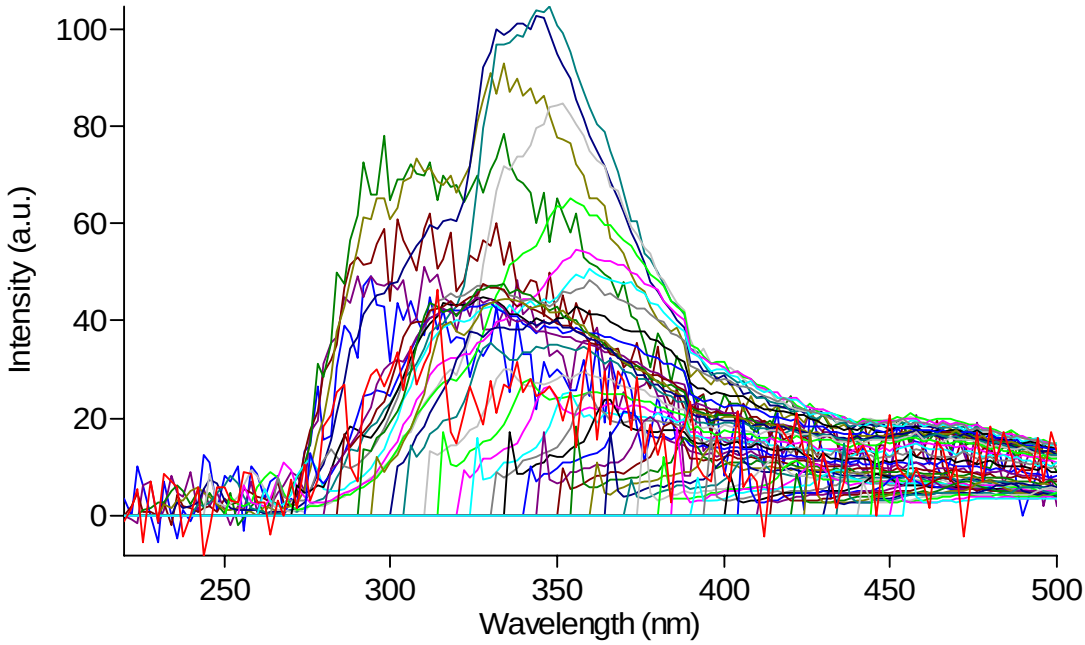
100
80
60
40
20
0
Intensity (a.u.)
250
300
350
400
450
500
Wavelength (nm)

M29y

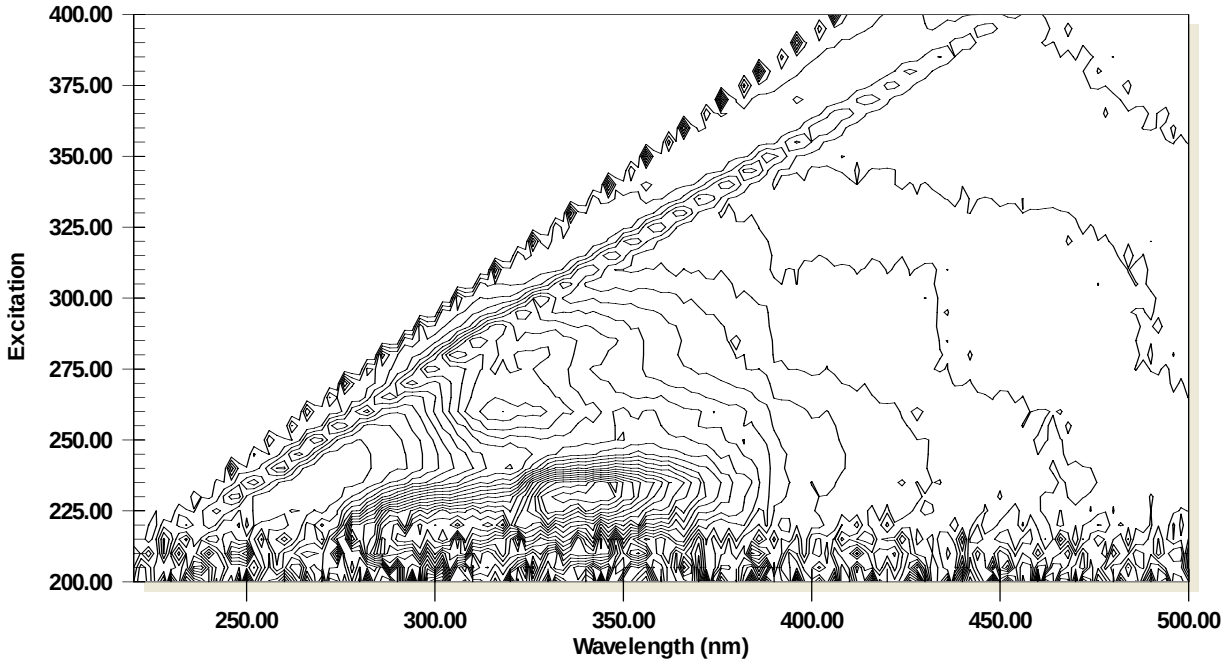
400.00
375.00
350.00
325.00
300.00
275.00
250.00
225.00
200.00
Excitation
250.00
300.00
350.00
400.00
450.00
500.00
Wavelength (nm)

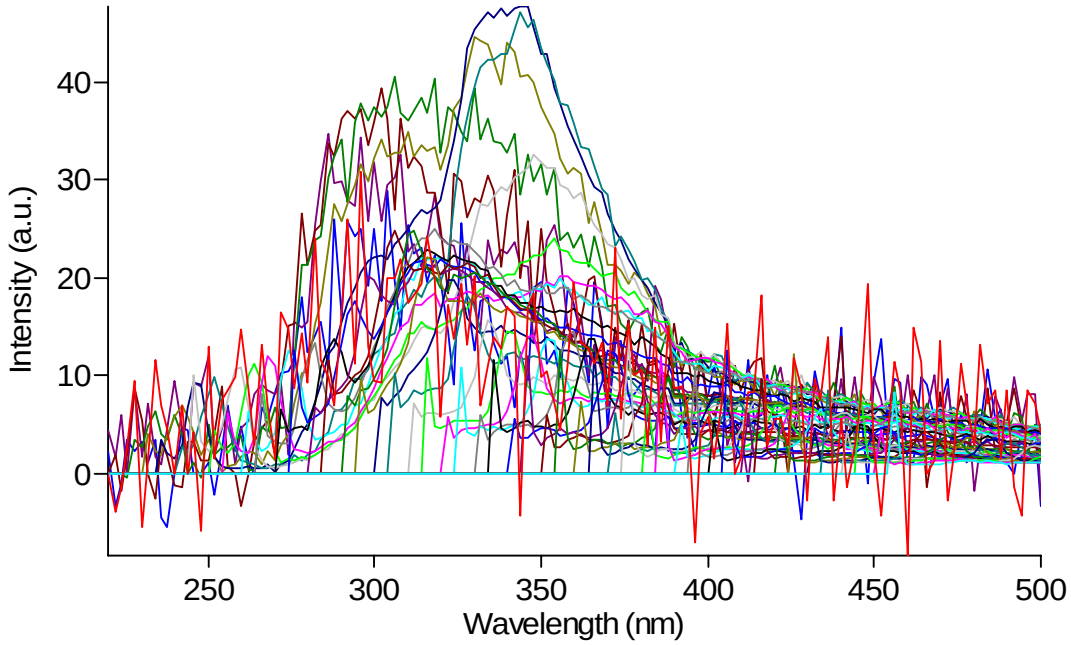
40
30
20
10
0
Intensity (a.u.)
250
300
350
400
450
500
Wavelength (nm)

M36y

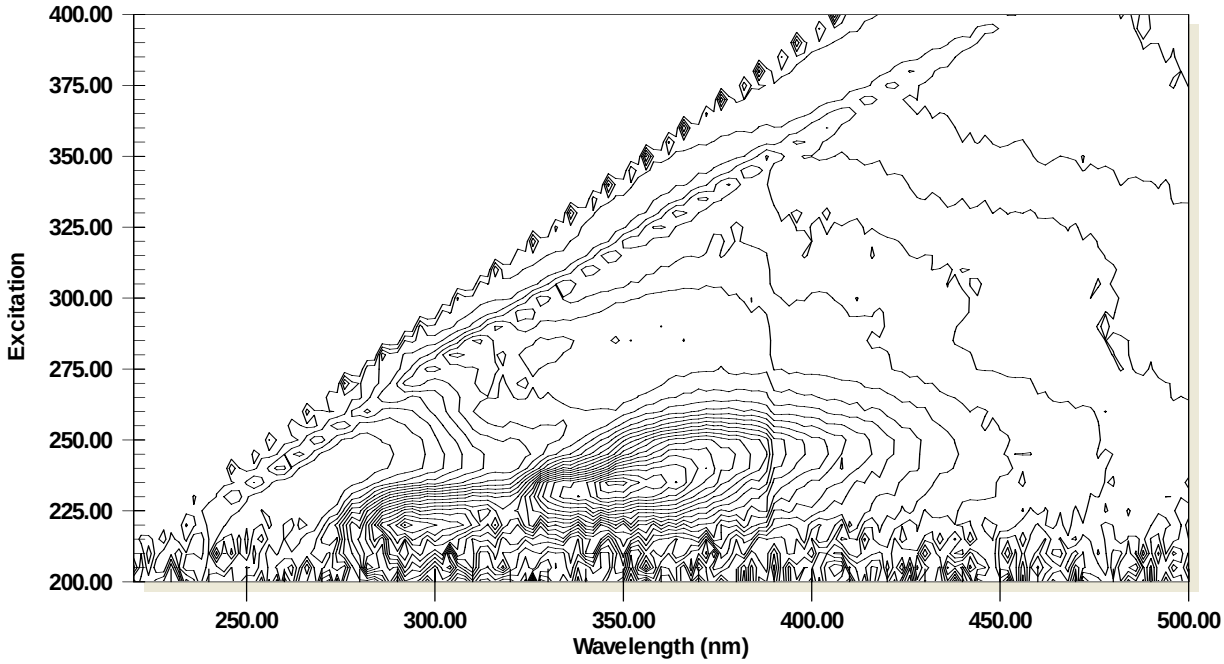
400.00
375.00
350.00
325.00
300.00
275.00
250.00
225.00
200.00
Excitation
250.00
300.00
350.00
400.00
450.00
500.00
Wavelength (nm)

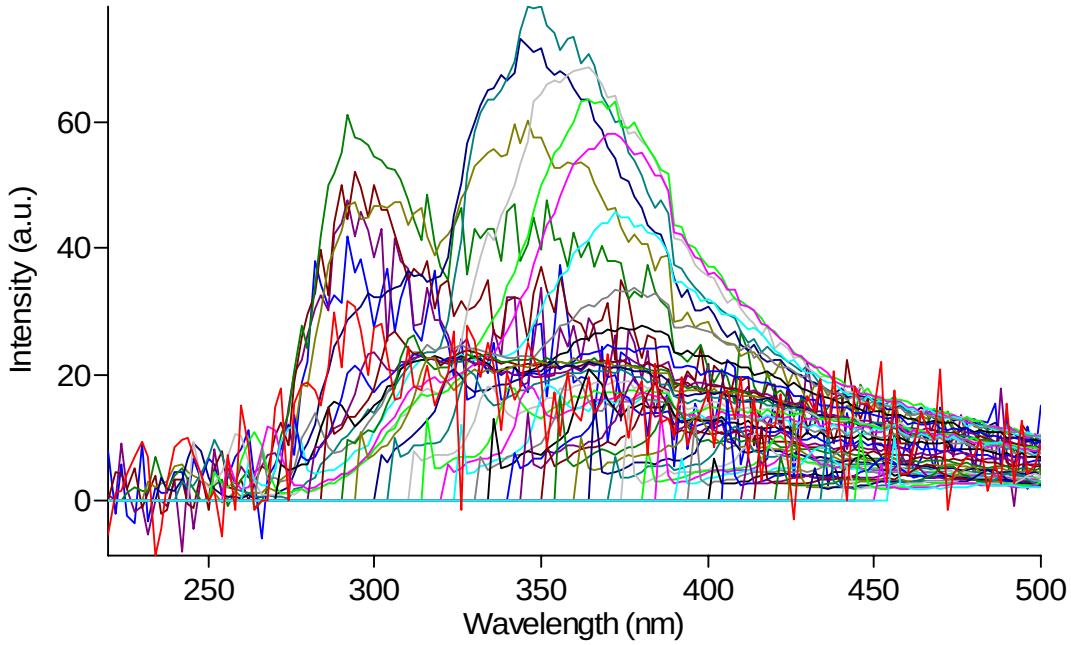
60
40
20
0
Intensity (a.u.)
250
300
350
400
450
500
Wavelength (nm)

M40y

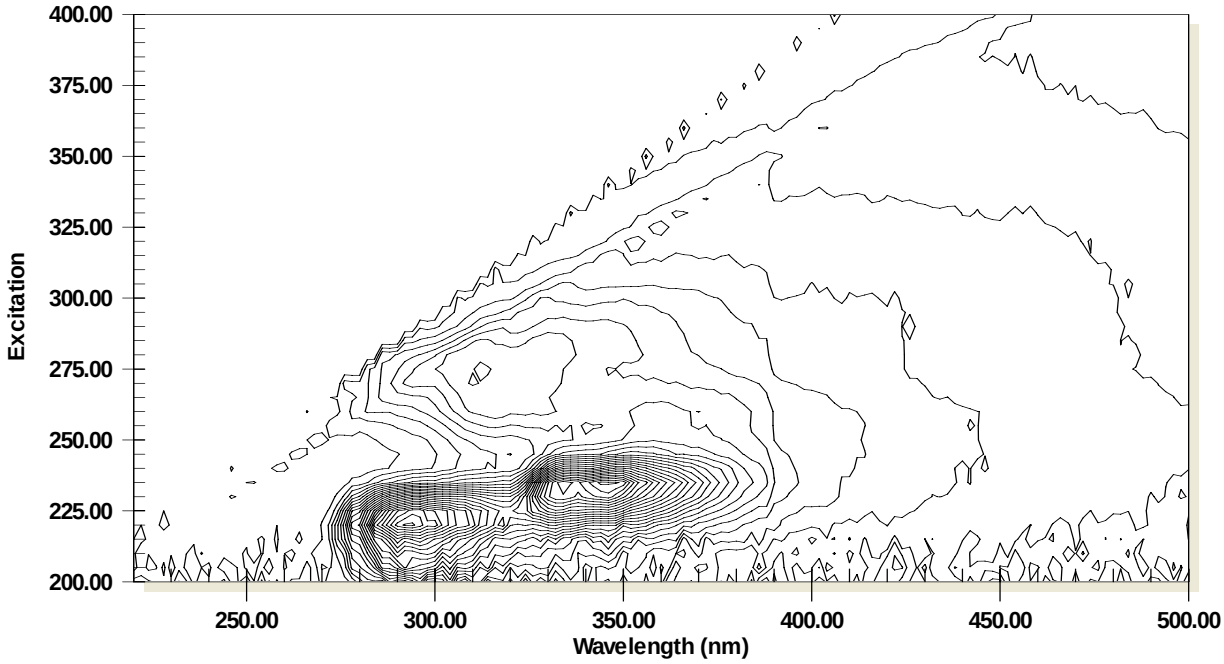
400.00
375.00
350.00
325.00
300.00
275.00
250.00
225.00
200.00
Excitation
250.00
300.00
350.00
400.00
450.00
500.00
Wavelength (nm)

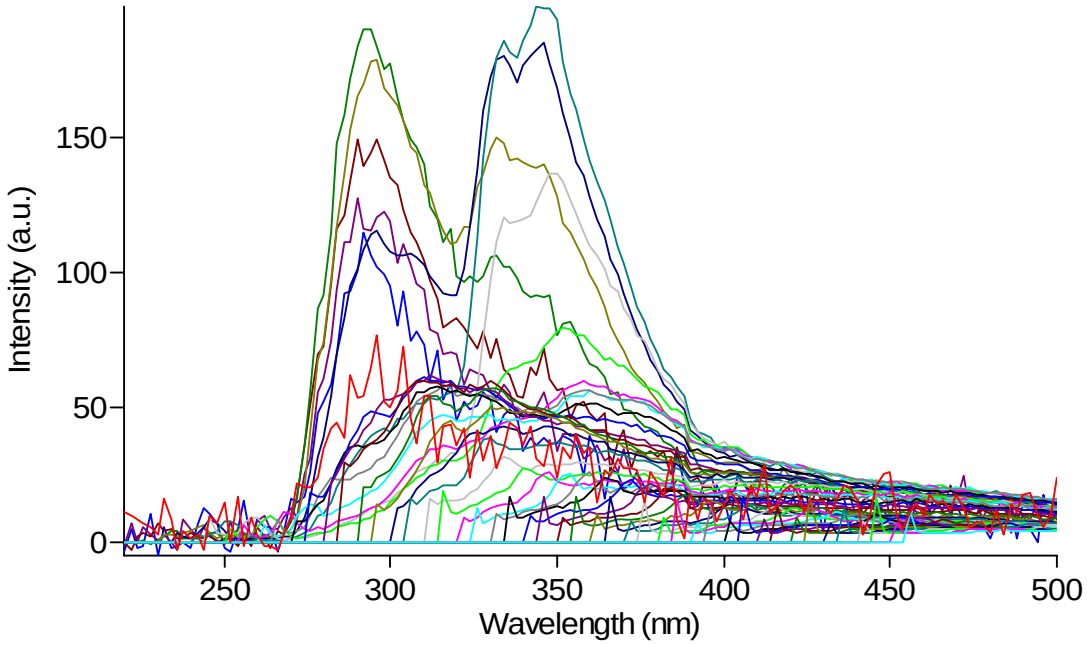
150
100
50
0
Intensity (a.u.)
250
300
350
400
450
500
Wavelength (nm)

M46y

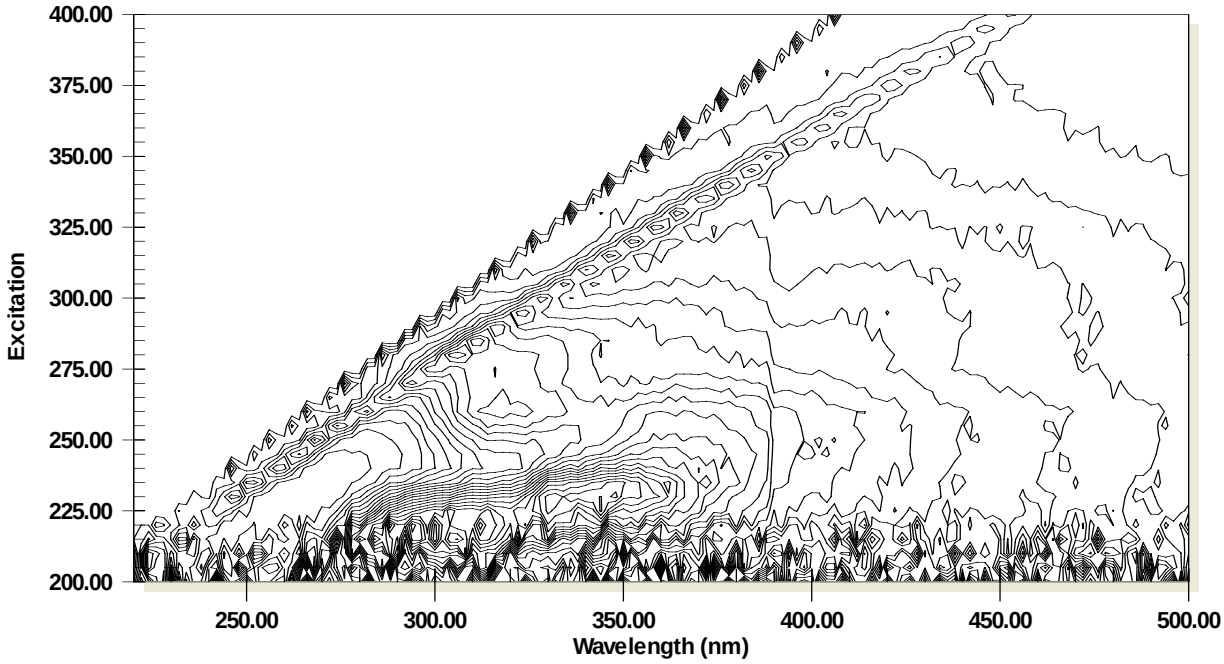
400.00
375.00
350.00
325.00
300.00
275.00
250.00
225.00
200.00
Excitation
250.00
300.00
350.00
400.00
450.00
500.00
Wavelength (nm)

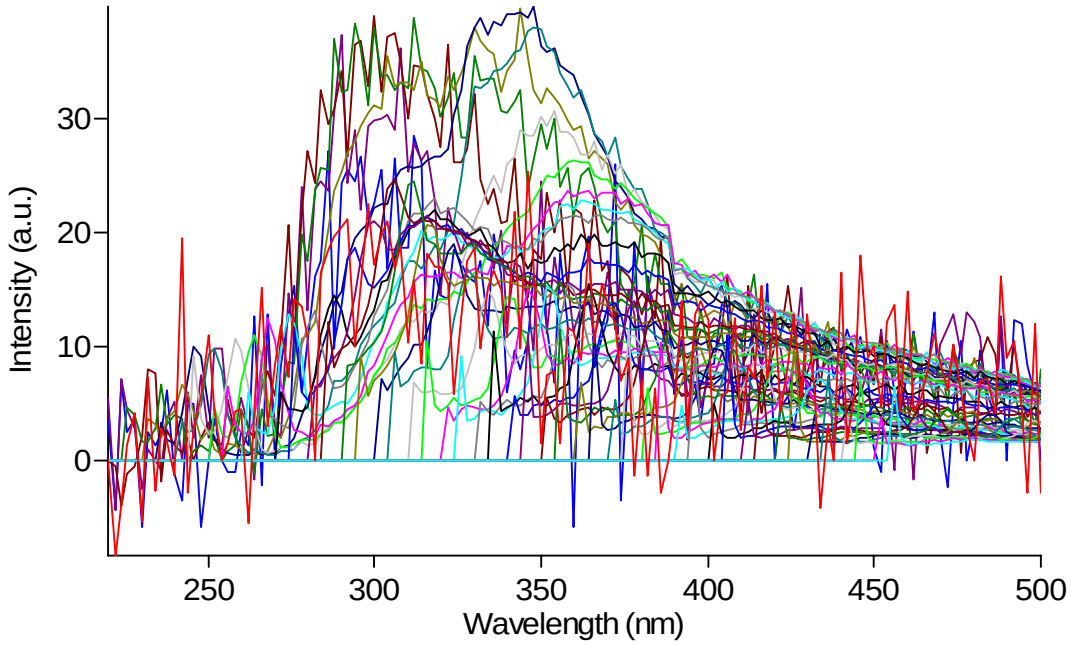
30
20
10
0
Intensity (a.u.)
250
300
350
400
450
500
Wavelength (nm)

Bibliography

Blackledge R. D., (1980) Examination of Automobile Rubber Bumper Guards by Synchronous Excitation Spectrofluorometry. Journal of Forensic Sciences. 25(3), 582-588.

Blackledge, R. D., (1983) Examination for Petroleum Based Lubricants in Evidence from Rapes and Sodomies. Journal of Forensic Sciences. 28(2), 451-462.

Butcher, J. B., Gauthier, T. D., Garvey, E. A. (1997) Use of Historical PCB Aroclor Measurements: Hudson River Data. Environmental Toxicology and Chemistry., 16, (8) 1618-1623.

Caragena v. Jersey Paper Company et. al. Docket No: MID-L-11650-01

Curtis, M. L, (1977) Use of Pattern Recognition Techniqus for Typing and Identification of Oil Spills. U.S. Coast Guard Research and Development Center. Report CG-D-38-77. Washington, D. C.

Durose., M. R., 2008. Census of Publicly Funded Forensic Crime Laboratories, 2005. U.S. Department of Justice, Office of Justice Programs, Bureau of Justice Statistics. Available at www.ojp.usdoj.gov/bjs/pub/pdf/cpffcl05.pdf.

Eastwood, D., Fortier, S., Hendrick, M., (1978) Oil Identification: Recent developments in fluorescence and low temperature luminescence. American Laboratory. 10 (3), 45-55.

Fletcher, K. A., Fakayode, S. O., Lowry, M., Tucker, S. A., Neal, S. L., Kimaru, I. W., McCarroll, M. E., Patoney, G., Oldham., P. B., Rusin, O., Strongin, R. M., Warner, I. M., (2006) Molecular Fluorescence, Phosphorescence and Chemiluminescence Specttrometry. Analytical Chemistry. 78, 4047-4068.

Fortier, S. H., Eastwood, D., (1978) Identification of Fuel Oils by Low Temperature Luminescence Spectrometry. Analytical Chemistry. 50(2), 334-338.

Freegarde, M., Hatchard, C., G., Parker, C., A., (1971) Oil Spilt at Sea: Its Identification, Determination, and Ultimate Fate. Laboratory Practice 20(1), 35-40.

Guilbault, G. G., (1990) Practical Fluorescence. 2nd Ed. Marcel Dekker, Inc. CRC Press

Holbrook R. D., DeRose, P. C., Leigh, S. D., Rukhin, A. L., and Heckert, N. A., (2006) Excitation–Emission Matrix Fluorescence Spectroscopy for Natural Organic Matter Characterization: A Quantitative Evaluation of Calibration and Spectral Correction Procedures," Applied Spectroscopy 60, 791-799.

Houck, M. Mute Witnesses: Trace Evidence Analysis. 2001. Academic Press.
Ingle, J. D., Crouch, S. R., (1988) Spectrochemical Analysis. Englewood Cliffs NJ; Prentice Hall.

Kershaw, J. R., Fetzer, J. C., (1995) The Room Temperature Fluorescence Analysis of Polycyclic Aromatic Compounds in Petroleum and Related Materials. Polycyclic Aromatic Compounds. 7, 253-268.

Kubic, T. A., Lasher., C. M., Dwyer, J., (1983) Individualizaiton of Automobile Engine Oils I: The Introduction and Variable Separation Synchronous Excitation Fluorescence to Engine Oil Analysis. Journal of Forensic Sciences. 28(1), 186-199.

Kubic, T. A., Sheehan, F. X., (1983) Individualization of Automobile Engine Oils II: Application of Variable Separation Synchronous Excitation Fluroscence to the Analysis of Used Automobile Engine Oils. Journal of Forensic Sciences. 28(2), 345-350.

Lloyd J. B. F., (1971) The Nature and Evidential Value of the Luminescence of Automobile Engine Oils and Related Materials, Part I: Synchronous Excitation of Fluorescence Emission. Journal of Forensic Science Society. 11(2), 83-94.

Lloyd, J. B. F., (1971) The Nature and Evidential Value of the Luminescence of Automobile Engine Oils and Realted Material, Part III: Separated Luminescence. Journal of the Forensic Science Society. 11(4), 235-252.

Lloyd, J. B. F., (1971) The Nature and Evidential Value of the Luminescence of Automobile Engine Oils and Related Materials, Part II: Aggregated Luminescence. Journal of the Forensic Science Society. 11(3), 153-170.

Motor Oil Guide (1971) American Petroleum Institute. Lubrication Subcommittee. Washington D. C.

National Academies of Science Strengthening Forensic Science in the United States: A Path Forward. 2009. National Research Council. Nation Academies Press.

NYC DEP 2007 Annual Report.

Patra, D., Mishra, A. K., (2001) Concentration dependent red shift: qualitative and quantitative investigation of motor oils by synchronous fluorescence scan. Talanta. 53, 783-790.

Pharr, D. Y. (1992) Fingerprinting Petroleum Contamination Using Synchronous Scanning Fluorescence Spectroscopy. Ground Water. 30 (4), 484-489.

Pineiro-Iglesias, M., Lopez-Mahia, P., Vazquez-Blanco, E., Mniategui-Lorenzo, S., Prada-Rodriguez, D., (2002) Problems in the Extraction of Polycyclic Aromatic

Hydrocabons form Diesel Particulate Matter. Polycyclic Aromatic Compounds. 22, 129-146.

Pornile, N. T., (1987) Modern University Chemistry. Orlando: Harcourt Brace Jovanovich, Inc.

Petraco, N. D. K., Gil, M., Pizzola, P., Kubic, T. A., (2008) Statistical Discrimination of Liquid Gasoline Samples from Casework. Journal of Forensic Sciences. 53 (5), 1092-1101.

Purcell, D., (2002) Three-dimensional spectrofluorometric fingerprinting of automobile undercarraige petroleum products. Thesis. (M.S.) John Jay College of Criminal Justice.

Reardon, M., Allen, L., Bender, E. C., Boyle, K., (2007) Comparison of Motor Oils Using High Temperature Gas Chromatography-Mass Spectrometry. Journal of Forensic Sciences. 52(3), 656-663.

Rogge, W. F., Hildemann, L. M., Mazurek, M. A., Cass, G. R., (1993) Sources of Fine Organic Aerosol. 3. Road Dust, Tire Debris, and Organometallic Brake Lining Dust: Roads as Sources and Sinks. Environmental Science and Technology. 27, 1892-1904.

Schenk, G. H., Absorption of Light and Ultraviolet Radiation: fluorescence and phosphorescence emission. 1973. Allen and Bacon Inc, Boston.

Sharma A., Schulman S. G., (1999) Introduction to Fluorescence Spectroscopy. New York: Wiley Interscience.

Siddiqui, K. J., Eastwood, D., (2005) Classification of Synchronous Fluorescence Petroleum Oils. SPIE. Vol. 5993.

Siegel, J. A., Cheng, N., (1989) Fluorescence of Petroleum Products III: Three Dimensional Fluorescence Plots of Petroleum-Based Products. Journal of Forensic Sciences. 34(5), 1128-1155

Soper, S. A., Warner, I. M., McGown, L. B., (1998) Molecular Fluorescence, Phosphorescence and Chemiluminescence Spectrometry. Analytical Chemistry. 70, 477R-494R

Taroni,F., Bozza, S. Biedermann, A. (2010) Data Analysis in Forensic Science: A Bayesian Decision Perspective. Wiley and Sons.

U.S. Department of Transportation, National Highway Traffic Safety Administration, Traffic Safety Facts 2005 Early Edition, Washington, DC: 2006

Wilkinson, T., (1992) Understanding What's In Your Car's Motor Oil. Consumer's

Research. 75, 20-23.

Zieba, J., (1985) Examination of Lubricating Oils by Infrared Spectroscopy. Forensic Science International. 27, 31-39.